UNCLASSIFIED

AD NUMBER

ADB067554

NEW LIMITATION CHANGE

TO

Approved for public release, distribution unlimited

FROM

Distribution limited to U.S. Gov't. agencies only; Test and Evaluation; Jul 82. Other requests for this document must be referred to Naval Sea Systems Command, Washington, DC 20362.

AUTHORITY

NSWC ltr., 506 Ser 94, 19 Nov 1998

THIS PAGE IS UNCLASSIFIED

DAVID W. TAYLOR NAVAL SHIP
RESEARCH AND DEVELOPMENT CENTER

Bethesda, Maryland 20084

SUMMARY REPORT OF THE CONTROLLABLE
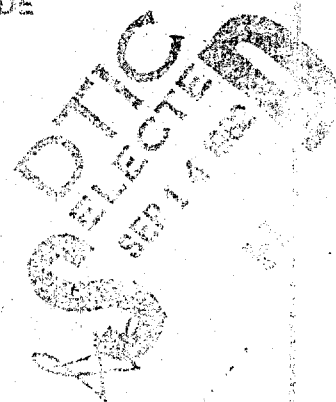## PITCH PROPELLER RESEARCH PROGRAM

RESEARCH AND DEVELOPMENT REPORT

July 1982

MAJOR DTNSRDC ORGANIZATIONAL COMPONENTS

```
                        ┌─────────────────────┐
                        │      DTNSRDC         │
                        │    COMMANDER     00  │
                        │  TECHNICAL DIRECTOR  │
                        │                  01  │
                        └─────────────────────┘

┌─────────────────────┐                      ┌─────────────────────┐
│  OFFICER-IN-CHARGE   │                      │  OFFICER-IN-CHARGE   │
│  CARDEROCK       05  │                      │  ANNAPOLIS       04  │
└─────────────────────┘                      └─────────────────────┘

┌─────────────────────┐
│      SYSTEMS         │
│   DEVELOPMENT        │
│   DEPARTMENT     11  │
└─────────────────────┘

┌─────────────────────┐                      ┌─────────────────────┐
│  SHIP PERFORMANCE    │                      │   AVIATION AND       │
│   DEPARTMENT         │                      │  SURFACE EFFECTS     │
│                  15  │                      │   DEPARTMENT     16  │
└─────────────────────┘                      └─────────────────────┘

┌─────────────────────┐                      ┌─────────────────────┐
│    STRUCTURES        │                      │   COMPUTATION,       │
│   DEPARTMENT         │                      │  MATHEMATICS AND     │
│                  17  │                      │ LOGISTICS DEPARTMENT │
└─────────────────────┘                      │                  18  │
                                             └─────────────────────┘

┌─────────────────────┐                      ┌─────────────────────┐
│   SHIP ACOUSTICS     │                      │   PROPULSION AND     │
│   DEPARTMENT         │                      │  AUXILIARY SYSTEMS   │
│                  19  │                      │   DEPARTMENT     27  │
└─────────────────────┘                      └─────────────────────┘

┌─────────────────────┐                      ┌─────────────────────┐
│   SHIP MATERIALS     │                      │     CENTRAL          │
│   ENGINEERING        │                      │  INSTRUMENTATION     │
│   DEPARTMENT     28  │                      │   DEPARTMENT     29  │
└─────────────────────┘                      └─────────────────────┘
```

REPORT DOCUMENTATION PAGE	READ INSTRUCTIONS BEFORE COMPLETING FORM

1. REPORT NUMBER	2. GOVT ACCESSION NO.	3. RECIPIENT'S CATALOG NUMBER
DTNSRDC-81/065	AD-B067 554L	

4. TITLE (and Subtitle)	5. TYPE OF REPORT & PERIOD COVERED
SUMMARY REPORT OF THE CONTROLLABLE PITCH PROPELLER RESEARCH PROGRAM	Final
	6. PERFORMING ORG. REPORT NUMBER

7. AUTHOR(s)	8. CONTRACT OR GRANT NUMBER(s)
Chapter IV E. Czyryca Chapter I A. Reed Chapter V R. Rockwell Chapter II C. Noonan Chapter VI J. Allen Chapter III R. Boswell Chapter VII R. Rockwell et al.	

9. PERFORMING ORGANIZATION NAME AND ADDRESS	10. PROGRAM ELEMENT, PROJECT, TASK AREA & WORK UNIT NUMBERS
David W. Taylor Naval Ship Research and Development Center Bethesda, Maryland 20084	(See reverse side)

11. CONTROLLING OFFICE NAME AND ADDRESS	12. REPORT DATE
Naval Sea Systems Command Washington, D.C. 20362	July 1982
	13. NUMBER OF PAGES
	485

14. MONITORING AGENCY NAME & ADDRESS(If different from Controlling Office)	15. SECURITY CLASS. (of this report)
	UNCLASSIFIED
	15a. DECLASSIFICATION/DOWNGRADING SCHEDULE

16. DISTRIBUTION STATEMENT (of this Report)

DISTRIBUTION LIMITED TO U.S. GOVERNMENT AGENCIES ONLY; TEST AND EVALUATION; JULY 1982. OTHER REQUESTS FOR THIS DOCUMENT MUST BE REFERRED TO NAVSEA CODE 52B.

17. DISTRIBUTION STATEMENT (of the abstract entered in Block 20, If different from Report)

18. SUPPLEMENTARY NOTES

19. KEY WORDS (Continue on reverse side if necessary and identify by block number)

Bearing materials, blade attachments, bolt preload, bolted joints, bolts, cold-rolling, controllable pitch propeller, corrosion fatigue, crank rings, fatigue, finite elements, fracture toughness, friction, galvanic corrosion, loads, lubrication, maneuvering, marine propeller, nonmetalic coatings,
(Continued on reverse side)

20. ABSTRACT (Continue on reverse side if necessary and identify by block number)

This report is a summary of the controllable pitch (CP) propeller blade attachment investigations which were conducted by the David W. Taylor Naval Ship Research and Development Center subsequent to the failure of the CP propeller on the USS BARBEY (FF-1088). Analysis of the BARBEY failures revealed that there was insufficient information available concerning design loads, structural response, and material selection for CP propeller hub components. Serious fundamental questions were raised concerning the adequacy
(Continued on reverse side)

DD FORM 1473 EDITION OF 1 NOV 65 IS OBSOLETE
1 JAN 73
S/N 0102-LF-014-6601

(Block 10)

Program Element 63508N
Project S0379SL
Task Area S0379SL001

Task 19977		Task 19978		Task 19979	
Work Units:	1524-567	Work Units:	1725-441	Work Unit:	2814-181
	1524-607		1720-578		
	1524-612		1720-585		
	1524-641		1720-608		
	1524-684		1720-630		
	1544-296				
	1544-317	SCN Funds for CG-47 Project			
	1544-330	Work Unit:	1720-620		
	1544-339				
	1544-350				
	1962-133				
	1962-151				
	1962-156				
	1962-171				

SCN Funds for DD-963 Project		SCN Funds for FFG-7 Project	
Work Units:	1725-442	Work Units:	1725-444
	1725-445		1720-574
	1720-645		1720-596
	1720-649		1962-162
	1962-140		

(Block 19 continued)

notch sensitivity, numerical methods, propeller blade instrumentation, propeller bronzes, propulsion, propeller strength, steels, wear, unsteady loads, scale-model experiments.

(Block 20 continued)

of the CP propellers then being procured for the USS SPRUANCE (DD-963) and USS OLIVER HAZARD PERRY (FFG-7) Classes, and of those which would be required eventually in future gas turbine propelled ships. The Naval Sea Systems Command, therefore, initiated a program to determine the adequacy of the CP propellers then under production for SPRUANCE and OLIVER HAZARD PERRY Classes and also undertook a research and development program to improve the technology base in design loads, strength analysis, and material selection of CP propeller blade attachment components for future procurements. The entire effort, both the research and development portion and the portion which was directed specifically to support the ongoing ship construction projects, made important contributions to the resolution of the CP propeller problems. The investigations included:

    1. Sea trials on USS BARBEY, USS SPRUANCE, and R/V ATHENA to measure blade loads and resultant attachment stresses;
    2. Sea trials on USS OLIVER HAZARD PERRY to measure blade bolt stresses;
    3. Analytical and laboratory experimental investigations to develop a substantially improved load and stress prediction capability;
    4. Investigations of the suitability of potential blade attachment materials; and
    5. The evolution of a rationale and criteria for the evaluation of new CP propeller designs, with similarly configured blade attachments and the proposed materials. The report summarizes the work which was accomplished in each major area, and provides references to the many more detailed reports which were prepared in the investigations.

TABLE OF CONTENTS

ABSTRACT

This report is a summary of the controllable pitch (CP) propeller blade attachment investigations which were conducted by the David W. Taylor Naval Ship Research and Development Center subsequent to the failure of the CP propeller on the USS BARBEY (FF-1088). Analysis of the BARBEY failures revealed that there was insufficient information available concerning design loads, structural response, and material selection for CP propeller hub components. Serious fundamental questions were raised concerning the adequacy of the CP propellers then being procured for the USS SPRUANCE (DD-963) and USS OLIVER HAZARD PERRY (FFG-7) Classes, and of those which would be required eventually in future gas turbine propelled ships. The Naval Sea Systems Command, therefore, initiated a program to determine the adequacy of the CP propellers then under production for SPRUANCE and OLIVER HAZARD PERRY Classes and also undertook a research and development program to improve the technology base in design loads, strength analysis, and material selection of CP propeller blade attachment components for future procurements. The entire effort, both the research and development portion and the portion which was directed specifically to support the ongoing ship construction projects, made important contributions to the resolution of the CP propeller problems. The investigations included:

1. Sea trials on USS BARBEY, USS SPRUANCE, and R/V ATHENA to measure blade loads and resultant attachment stresses;

2. Sea trials on USS OLIVER HAZARD PERRY to measure blade bolt stress;

3. Analytical and laboratory experimental investigations to develop a substantially improved load and stress prediction capability;

4. Investigations of the suitability of potential blade attachment materials; and

5. The evolution of a rationale and criteria for the evaluation of new CP propeller designs, with similarly configured blade attachments and the proposed materials. The report summarizes the work which was accomplished in each of the major areas and provides references to the many more detailed reports which were prepared in the investigations.

ADMINISTRATIVE INFORMATION

EXECUTIVE SUMMARY

TABLE OF CONTENTS

SCOPE OF REPORT

This report is a summary of the controllable pitch (CP) propeller blade attachment investigations which were conducted by the David W. Taylor Naval Ship Research and Development Center (DTNSRDC) subsequent to the failures of the CP propeller on the USS BARBEY. These investigations included:

1. Sea trials on USS BARBEY (FF-1088), USS SPRUANCE (DD-963), and R/V ATHENA to measure blade loads and resultant attachment stresses.

2. Sea trials on USS OLIVER HAZARD PERRY (FFG-7) to measure blade bolt stresses.

3. Analytical and laboratory experimental investigations to develop a substantially improved load and stress prediction capability.

4. Investigations of the suitability of potential blade attachment materials.

5. The evolution of a rationale and criteria for the evaluation of proposed new CP propeller designs, with similarly configured blade attachments and the proposed materials.

ORGANIZATION OF THE REPORT

The report is divided into seven chapters: Introduction, Trials, Loads, Materials, Strength, Specifications, and Guidelines and Procedures for Evaluation. Chapter I (Introduction) provides a brief description of the CP propeller blade attachment geometry, a history of the CP propeller, a summary of failure histories in both merchant and naval application, and a summary of the chapters in the report.

Chapter II (Trials) reports on the sea trials on USS BARBEY, USS SPRUANCE, USS OLIVER HAZARD PERRY, and R/V ATHENA. It also includes related information from trials on USS FRANKLIN D. ROOSEVELT (CVA-42), USS DOUGLAS (PG-100), and USCG POLAR STAR (WAGB-10). It describes the scope of the trials, how they were carried out, the key information which was obtained, and the important conclusions which were made directly on the basis of the experimental data.

Chapter III (Loads) reports on the development of a major improvement in blade load predictions (time average, transient, periodic, and peak loads) with allowances for sea states and maneuvers. It includes guidelines for minimizing the loads.

4

Chapter IV (Materials) reports on material investigations which were conducted, primarily concerning crank rings, blade bolts, and bearing rings. They considered strength, ductility, fracture toughness, fatigue, stress corrosion cracking, corrosion, mechanical and galvanic compatibility, and bearing integrity. It includes guidelines on material selection.

Chapter V (Strength) reports on the development of various analytical and experimental techniques for predicting blade attachment stresses and guidelines for minimizing them. A strength assessment process is described for determining the structural adequacy of blade attachments.

Chapter VI (Specifications) reports on the rigid versus flexible approaches to specification. It then comments on Military Specification DOD-P-24562, the currently governing specification, pointing out where the present program has already had impact on the specification, and those areas, namely stress calculation and fatigue analyses, where further improvements will be made.

Chapter VII (Guidelines and Procedures for Evaluation) describes the strength evaluation process as it now exists for blade attachments of U.S. Navy CP propellers. The necessary guidelines for appropriately using the several load and stress prediction methods are provided along with guidelines for examining material properties. Details for use of each method are given in the appendix or are available in specified references.

SUMMARY OF WORK PERFORMED

The major objective of the Naval Sea Systems Command (NAVSEASYSCOM) CP propeller research and development (R and D) program was to develop the technology which would allow the correction of the design deficiencies in the CP propellers of existing ship classes and to improve the specification and verification of future CP propeller designs. A specification (Military Specification DOD-P-24562) was issued on 28 December 1977 early in the CP propeller R&D program, and therefore it does not incorporate all of the knowledge gained in the program. However, the specification does include several requirements based on the preliminary results from the R and D program:

1. Charpy impact strength requirements for propeller blade attachment components.

2. Minimum fatigue life requirements for propeller blade attachments.

3. Requirements to torque propeller blade bolts under controlled conditions.

4. Requirements to calculate stresses in the propeller blade attachment assuming that 90 percent of the forces on the blade are transmitted through any bolt in tension, that fatigue studies be prepared, and that blade alternating stresses shall be a minimum of 40 percent (specification sections 3.22.1 and 3.22.1.1).

At the beginning of the CP propeller R and D program, the status of the technology of CP propeller design and analysis could be summarized as follows:

1. Mean blade loads could be predicted in a satisfactory fashion.

2. Errors of 40 to 60 percent existed in the prediction of unsteady loads in uniform motion in calm water.

3. No measurements of loads during transient maneuvers such as crashahead, crashback, or turns existed.

4. No wake data for a ship in a turn existed.

5. No detailed structural analysis of the propeller blade-propeller hub interface had been performed.

6. No fatigue analysis of a CP propeller or its components had been carried out.

The following sections contain a summary of the work which was carried out under the CP propeller R and D program in the areas of trials, loads, materials, and strength. This work was aimed at alleviating the deficiencies in the CP propeller technology base.

FULL-SCALE MEASUREMENT

CP propeller system loads and stresses could not be reliably predicted at the beginning of the program. Full-scale, underway trials were undertaken to obtain the required data. The following is a short summary of the ships tested under this program. All were fitted with CP propellers.

6

Results from Trials on USS BARBEY (FF-1088)

The BARBEY is a KNOX (FF-1052) Class fast frigate. This ship experienced trouble and then failure of the CP propeller unit which had been installed for test and evaluation. Trials were run to determine the cause of this failure as well as to provide experimental guidance to the propeller design programs.

Drydock tests proved quite enlightening in a number of areas, the first of these being bolt preload. It is generally recognized that if the preload characteristics (induced stress versus some measurable parameter) and the external loads can be defined, an appropriate bolt preload can be applied which will minimize cyclic bolt stresses, thereby reducing the possibility of bolt fatigue. Although the concept of how this is accomplished is relatively simple, the variables associated with a complex installation (such as a CP propeller) make the actual determination of preload difficult. Drydock test results for bolt preload tests, show that the preload which existed on the bolts which failed in fatigue could, at best, be only estimated. It was also found that a bending stress was induced into the bolt on installation. This stress averaged 15 percent of the installed preload stress.

The next phase of drydock tests was the application of known static loads to the propeller blades. Measured response of the propeller blade for these tests indicated that a reasonable estimate of static blade "loads" can be obtained by using the measured principal stress and the calculated section properties.

Measured results on the blade bolts and crank disk showed that unlike the propeller blade, the accountability of stresses for these components was considerably more difficult. These tests showed that the CP propeller components (bolts and crank disk) exhibited a nonuniform, nonlinear response to a linear load.

Analysis of full-power data showed that the qualitative and quantitative mean response of the propeller blades correlated well with both drydock and standardization results. Propeller blade "loads" were calculated by using the measured stress at the root and the known geometric properties. The blade response was linear with load.

During full-power steady-ahead maneuvers alternating blade stresses were found to be of a periodic and complex nature. The harmonic content of this complex signal was primarily shaft frequency with a large number of higher frequency components. The average (percent of mean) alternating stress over the entire blade was approximately 45 percent. The mean response of the blade bolts for full-power underway operation showed similar characteristics to those seen in the drydock tests. The hydrodynamic loads were not distributed to the bolts in a uniform fashion, with both the mean and alternating strains increasing nonlinearly. In addition, the mechanism which was inducing a bending load into the bolt was more pronounced, such that bending and axial stresses were approximately equal.

Crank disk stress showed a corresponding skew to produce higher fillet stresses next to the most highly loaded bolt (Bolt 6).

Maneuvering operations produced surprising results in that the maximum measured stresses occurred during full-power turns, rather than the crashback maneuvers as were predicted. Full-power turns resulted in stresses which exceeded the accepted trial criteria.

Results from Trials on USS SPRUANCE (DD-963)

Trials were run because the experience on the BARBEY left considerable doubt as to the structural adequacy of this new CP propeller, and because of the design differences, hull characteristics, and twin screw versus single screw configuration. As a result, it was not possible to predict the loads or response of the SPRUANCE CP system with confidence. The objectives of the trial were to define the system stresses and contribute experimental information to the propeller design technique.

Test objectives included the determination of the structural adequacy of the CP propeller system components (blade, bolts, and crank disk) and also comparison of the performance of different material properties and designs.

Dry dock tests determined the bolt preload characteristic (stress versus elongation) for both K-Monel and steel blade bolts. It was seen that this system also experienced bolt bending during installation, the bending stress being higher at the bolt head.

Static blade load tests showed similar results as those on BARBEY (i.e., linear blade response and nonlinear, nonuniform bolt response).

Underway tests on SPRUANCE, demonstrated the recurring theme of higher than predicted alternating blade loads (approximately 40 percent of the mean) and maximum stresses were developed during high speed turns with alternating loads increasing to more than $\pm$ 80 percent of the mean.

Results from Trials on USS OLIVER HAZARD PERRY (FFG-7)

Trials were run because of continued concern for the structural adequacy of the CP propeller system. This system was similar to that installed on the SPRUANCE except for a different propeller blade design and a different hull and propulsion system configuration. Trial objectives were to define the CP propeller bolt stresses and to contribute to the propeller design program. Ship builder contractual obligations restricted trial instrumentation to the measurement of blade bolt stresses only. Drydock tests were limited to the determination of bolt preload characteristics which turned out to be similar to those on the SPRUANCE (K-monel), to the measurement of bolt preload, and to dynamic blade bolt characteristics. No blade load measurements were performed and no dockside tests were done.

Underway tests produced the same nonuniform bolt response as seen before on SPRUANCE and BARBEY, with the highest stresses occurring in high speed turns. Unlike the SPRUANCE, however, the most highly loaded bolt was at the leading edge, pressure face (Bolt 5) rather than at the trailing edge, pressure face (Bolt 8). This bolt load distribution was unexpected. Actually the leading and trailing edge bolts tended to "share" the load, resulting in a lower overall bolt stress picture. This was due to different blade shape (lower fluctuating propeller blade loads), and changes in the propeller blade fillet and palm geometry.

Results from Trials on R/V ATHENA

The R/V ATHENA is an ASHEVILLE Class ship which has been reassigned to DTNSRDC for use as an high speed test vehicle. Trials were run on the ATHENA for purely R and D information.

Underway trials and laboratory tests on the ATHENA have recently been completed.

Dry dock test results indicate that bolt bending was lower than on the other CP propellers measured.

Underway test results showed patterns similar to other CP propellers, except that the maximum loads were not developed during turns, but rather during crash-back maneuvers.

PROPELLER LOADING

Blade loading is defined as the forces on a propeller blade. The detailed distribution of the incremental forces over the blade is generally required for determination of the stresses in the blade; however, for determination of the the stresses in the blade fillet components of the propeller hub, it is generally sufficient to know the force and moment components of the total loading on the blade along three arbitrary noncoplanar axes. The strength of components inside the hub rather than the strength of the blades was the primary concern of the CP propeller R and D program, because blade loads and stresses had been satisfactorily defined previously.

In general, blade loads vary as a function of time. It is convenient to represent this time-dependence as follows:

1. Mean loads, or time-average loads over some specified length of time equal to or greater than the time of one revolution of the propeller, under steady-state conditions.

2. Transient loads, or the variation of the mean load in a maneuver.

3. Periodic loads, or cyclic variation of loads with a repeating function such as blade angular position or wave velocities or ship motions in a sea state. These periodic loads are superimposed on the pertinent mean loads or transient loads.

4. Peak load is the designation used in this chapter for the largest instantaneous load including contributions from mean loads, transient loads, and periodic loads.

Blade loading arises from the distribution of hydrodynamic, centrifugal, and gravitational forces over the blade. The total centrifugal load, which is a

10

function only of the blade geometry, blade density, and propeller rotational speed, has only time average and transient components and can be readily calculated. The net gravitational loading, which is a function only of blade geometry and blade and water density, occurs only as a first harmonic of blade angular position and can be readily calculated. In almost all underway situations the largest component of blade loading is the hydrodynamic load. Further, the hydrodynamic load is much more complex and difficult to predict than are centrifugal or gravitational loads. Therefore, this report addresses primarily the hydrodynamic loads.

The work on blade loading under the CP propeller R and D program consisted of developing improved methods of predicting blade loads. This was achieved through various model experiments, development of improved analytical procedures full scale measurements, and their correlation. Most of the analytical work and a major portion of the model experimental program were directed toward developing a rational and generally reliable method for calculating the periodic blade loads arising from the inclination of the inflow relative to the propeller shaft, which is the primary cause of periodic blade loads.

At the beginning of the R and D program on CP propellers the best available analytical method for calculating the periodic blade loads due to circumferentially nonuniform inflow, underpredicted the periodic loads due to operation in inclined flow by from 40 to 80 percent. This method was erroneously thought to be reliable in inclined flow because it worked reasonably well in axial flow, and there existed no reliable experimental data in inclined flow with which to compare this analytical method.

During the course of the present R and D program analytical and experimental methods were developed which yield substantially improved predictions of the periodic blade loads due to operation in inclined flow. However, correlation of the analytical method with the extensive experimental data developed during the present R and D program shows that this improved analytical method still underpredicts the periodic blade loads by from 10 to 20 percent; thus, an empirical factor is required to compensate for the underprediction of the analytical procedure. Therefore, for a new propeller-hull configuration the periodic blade

11

loads in inclined flow can be predicted by model experiments using the procedures
developed under the present R and D program, or by the analytical procedure with
appropriate empirical factors, developed under the present R and D program.

It is obviously more difficult to calculate the blade loads during maneuvers
for an operation in a sea state than it is for steady ahead operation in a calm
sea. Any method for calculating loads under these conditions is, of necessity,
more approximate than for steady ahead operation in a calm sea; therefore, there
is a greater need for systematic reliable experimental blade loading data to
serve as a check for guidance, to provide empirical factors. Before the current
R and D program there existed no such experimental data. There also existed no
known systematic controlled experimental measurements of the transient or periodic
blade loads in crash-ahead or crash-astern maneuvers, and no known measurements
of the mean or periodic blade loads due to operation in a sea state. Further,
there existed no known measurements of the wake patterns in a turn, which is
necessary for making a rational prediction of the mean and periodic loads in a
turn.

Rational procedures for predicting blade loads during maneuvers and for opera-
tion in a sea state were developed during the present R and D program. These
include the development of experimental procedures for measuring these loads on
model scale, and measuring blade loads over a systematic range of parameters during
crash-ahead and crash-astern maneuvers and for operation in a sea state. Further,
wake patterns during turns were measured on two model hulls. Engineering procedures
were developed for calculating blade loads during maneuvers and for operation in
a sea state using the experimental data as a check, for guidance to provide any
necessary empirical factors.

MATERIALS

The R and D program on materials for CP propeller blade attachment components
assessed related CP propeller damage and failure experience in order to identify
material problem areas and assist in determining guidelines for selection of
materials for Navy CP propeller components. The following material areas were of
concern:

12

Blade and hub materials

Blade bolt materials

Blade carrier materials

Pitch change bearing materials

Studies were conducted in each of the identified problem areas, and the results
and findings are summarized in the following discussion.

Controllable Pitch Propeller Damage and Failure Experience

The majority of CP propeller problems have been in control systems and
hydraulics, not in blade attachment components. In the category of blade attachment
failures of CP propeller systems, propeller blade failures were most prevalent;
the majority in cast stainless steel blades. Failure rates increased with increased
power (shp). Increased number of blades compounded reliability problems. With
experience in designing for a given power level, failure rates in CP propeller hub
and mechanisms dropped, but blade failure rates remained the same and similar to
that of fixed pitch propellers of the same material.

Blade and Hub Materials

Cast Ni-Al-bronze (MIL-B-21230A, Alloy 1) is the best available material for
large CP propeller blades and hubs. Corrosion fatigue properties for the alloy
are well established for design against fatigue. The fatigue notch sensitivity
of cast Ni-Al bronze was demonstrated to be low. Cast stainless steels for large
propellers involve a risk of cracking and distortion in the casting process, a
heat treatment requirement, a requirement of intentional and maintained cathodic
protection for corrosion resistance, and stringent repair procedures with post
repair heat treatment required. They are not recommended for large Navy CP
propellers.

Blade Carrier Materials

Blade carriers for high-powered, large CP propeller mechanisms require the
use of high yield strength alloys. A fracture toughness level, optimum for the
strength and thickness of the component, must be specified and controlled to

13

prevent brittle fracture. High strength, high toughness steels were evaluated. These alloys require special melting and processing and contain high alloy content. Conventional low alloy, quenched and tempered steels may not obtain sufficient toughness in heavy sections to render a high-powered CP propeller immune to brittle fracture and tolerant of small cracks and defects from service.

Fatigue properties for large high strength forgings were examined. Endurance strength was between 40 percent and 45 percent of tensile strength, decreasing to the lower value as strength increased, emphasizing the need for detailed design against fatigue in high performance systems. Seawater contamination of hub oil, even at low levels, reduces the fatigue strength of steels to low levels.

Surface treatment by cold rolling delays initiation of corrosion fatigue cracks but shot peening was ineffective. Surface coating of critical areas with epoxy coatings, urethane, or vulcanized rubber can prevent corrosion fatigue cracking if coatings remain intact.

Inconel 718 was selected as a candidate corrosion resistant alloy having strength and toughness comparable to the high strength steels considered for the application but resistant to corrosion fatigue. Evaluation of an Inconel 718 forging showed that fatigue strength was not comparable to those steels (only 25 percent of the tensile strength) due to the large grain size developed in the item. Use of the alloy was not considered cost effective.

Blade Bolt Materials

In most applications CP propeller designers and producers use blade bolts of corrosion resistant alloys (bronzes, nickel alloys, stainless steels) compatible with blade and hub alloys. Use of low alloy steels requires complicated capping and sealing arrangements which may be unreliable in preventing corrosion and corrosion fatigue.

The fatigue and corrosion fatigue properties of several high performance bolt alloys were investigated. Nickel alloys, Inconel 718 and K-monel, and titanium 6Al4V showed superior fatigue and corrosion fatigue strength relative to tensile strength. However, the fatigue of the Ni alloys was dependent upon section size (grain size) of the stock.

Notch sensitivity of the alloys in fatigue increased with strength levels. Machined threads (K_t=3 to 4), therefore, reduce the intrinsic fatigue strength of high strength alloys to levels not different than lower strength materials.

Cold roll forming of threads after all thermal treatments offers the best option for fatigue and corrosion fatigue strength in a threaded fastener. Studies determined that compressive residual stresses at the root of the thread result from the roll forming operation and inhibit fatigue crack initiation. Root rolling of partially cut machined threads offers the same or greater benefits in fatigue strength as full roll forming in difficult, work hardening high strength alloys.

Exposed bolt heads constitute a small exposed area in relation to blade and hub area. Any alloy near or more noble than the propeller alloy in the galvanic series in seawater should perform satisfactorily. The cathodic protection applied in the stern area to protect the hull from galvanic corrosion from the propeller also protects the propeller from selective attack when more noble blade bolts attach the blade.

Pitch Change Bearing Materials

Severe wear of pitch change bearings has only occurred in highly loaded CP propeller systems or in instances where seawater has entered the hub and contaminated the oil. A small-scale tester was developed to evaluate the tribological characteristics of sliding couples of the materials used in CP propeller bearings; primarily bronze bearing surfaces against steel or bronze crank rings.

A large-scale tester was constructed to simulate performance of the bearing pairs under service type loadings. The results for both testers were correlated and gave similar ranking, frictional, and wear performance for the same materials.

For steel surfaces against bronze at high bearing stresses, four stages of wear were identified. However, the most important was a final steady-state achieved after transference of bronze to the steel surface. This stage showed a low wear rate and friction coefficient similar to bronze against bronze. Surface finish and hardness of steel surfaces were found only to influence initial, break-in stages and not the steady-state characteristics. High tin bronze (CDA 911) was found to be the best of the bronzes in friction and wear performance. Composite materials

DU(B) and Karon may be applied to bronze backing and offer very low friction and wear characteristics. These materials may be back-fitted if problems with conventional bronzes have occurred.

Additives in the oil exert a minor influence on the friction and wear properties of the bronze against steel sliding couple. Seawater contamination of the oil causes increased friction and high wear rates.

PROPELLER STRENGTH

The propeller strength chapter addresses the strength assessment of the blade attachment. The limiting structural problem areas have been identified as the blade attachment oolts and crank ring to which the blade is attached. Stress analyses of the blade attachment are complicated by their involvement with preloaded parts in contact and the complex deformation patterns of the blade palm, crank ring, and hub which make rigorous analyses difficult and expensive. Simplifying assumptions can be made, but the subsequent limitations in results must be recognized and evaluated.

Stress analysis methods described in the chapter include model and full-scale experiments in the laboratory as well as the numerical methods of three-dimensional and two-dimensional finite elements (FE) along with closed form equations. The accuracy of the stress analysis methods is determined wherever possible by comparison with results from measurements at sea.

Experimental methods on a model scale are much less costly than full-scale experiments, at the expense of accuracy. However, one-third scale metal models have provided a good simulation for determining stress levels and the effect of design changes on the SPRUANCE Propeller.

The numerical methods have been applied singly and in combination to predict stresses in the crank ring and blade attachment bolts. In all cases, involvements of the more expensive FE methods increases accuracy of the results. For example, use of a semiempirical closed form equation provided an indication of the average tensile stress in the most highly loaded bolt within about 30 percent of experimental data. Improved predictions, within about 15 percent were found by combining two-dimensional FE analyses with closed-form equations. The best numerical stress predictions are made using three-dimensional FE analysis, but the total blade

16

attachment including part of the hub must be included in order to properly account for the bolted joint nonlinearities. At this time, this full three-dimensional analysis is very time consuming and expensive. An attempt to reduce the costs by replacing the crank ring and hub with an elastic foundation of "equivalent spring stiffness" was limited by uncertainties in the determination of "equivalent spring stiffness" and because crank ring deformations under load, which affect bolt bending, were not included.

Methods to reduce stress levels have been identified including modifying the shape of the blade fillet and palm, changing the magnitude of bolt preload, and increasing radii in way of stress concentrations. The geometry of the blade fillet and palm has been shown to directly affect the distribution of forces in the blade attachment bolts. The severly skewed distribution which caused fatigue problems in the BARBEY CP propeller can be much improved by changing blade fillet shape. Increasing bolt preload decreases unsteady bolt stresses at the expense of increased mean stress in the bolt and in the blade palm counterbore area under the bolt head. While lower unsteady bolt stresses improve bolt fatigue performance, higher mean stress degrades it. Also, as preload is increased, the problem of yielding in the low strength bronze propeller blade under _he bolt head must be faced.

Two stress criteria must be satisfied at all times during the useful life of a CP propeller in order for the bolts and crank ring to be considered adequate. The maximum stress must be less than the material's yield stress (except at the thread roots, a special case, and under bolt heads) and the spectrum of fatigue stresses must be within the material's endurance capacity for a ship life. Examination of these criteria is referred to as the strength assessment process. Uncertainites in input to the process include the areas of blade load and blade stress prediction and the characterization of material properties. The amount of uncertainty can be reduced in each area by using more sophisticated and more expensive methods to obtain the desired data. The choice of margins of safety are dependent upon which methods are used. It is desirable for any new CP propeller that strength criteria be satisfied with as small a hub as possible, but it is also desirable that costs and time associated with analyses and experiments required to demonstrate adequacy be limited.

The approach described herein to the strength assessment process is intended to eliminate the need for expensive, large-scale testing in the laboratory and at sea. Such tests were necessary for assessing the SPRUANCE and PERRY Class propellers, but the analytical methods developed during that process and the lessons learned should provide a suitable basis for determining structural adequacy in future CP propellers.

CONCLUSIONS AND RECOMMENDATIONS

TRIALS

Blade Loads

1. For steady-ahead operation, there is reasonable agreement between predicted and measured time average blade response.

2. For steady-ahead operations, shaft frequency propeller forces are approximately $\pm$ 50 percent of the mean.

3. Maximum total (mean plus alternating) forces on most CP propellers occurred during high speed, full-power turns. The USS ASHEVILLE PG-84 Class appears to be the exception to this.

4. There is no indication that the natural frequency of the propeller blade or propulsion system influence the propeller forces.

Blade Attachment Strength

1. "Beam theory" reasonably predicts the roo stress of the blades.

2. There is no appreciable increase in blade stress due to blade vibrations with the possible exception of brief transients generated during crash-back maneuvers.

3. Accurate bolt preload cannot be predicted for a given installation procedure without establishing the bolted joint characteristics experimentally.

4. Former CP propeller design assumptions concerning the load transfer from the propeller blade palm to the crank ring were invalid.

5. The CP propeller blade palm stiffness distribution acts as a nonuniform loading mechanism on the blade bolts.

6. In general, the determination of actual stresses in the blade attachment requires strain measurements at sea where the many factors such as friction,

18

tolerances, vibrations, load and structure interaction, blade loads, etc., which directly affect structural response are all included.

7. The problems identified in the BARBEY CP propeller design were common to the SPRUANCE and PERRY CP propeller designs which are or will be used in many ships of the U.S. Navy.

Miscellaneous

1. The use of vulcanized rubber patches for waterproofing protection of propeller instrumentation provides excellent long-term results.

2. Spray urethane can be used for waterproofing for short-term applications.

3. The cost of measuring propeller parameters could be considerably reduced by the use of a hydrotelemetry system. Such a system is feasible but still highly developmental at this point.

Recommendations

1. Development of the hydrotelemetry system should continue on a planned basis in order to reduce the cost of future trials of this type.

LOADS

Full-Power Steady Motion

1. The modified loads theory by Kerwin agrees with experiments within 20 percent.

2. The tangential velocity component measured full-scale on the R/V ATHENA is much larger than that measured model scale. This is in conflict with the model and full-scale load measurements which correlate well.

Acceleration and Deceleration

1. The Taylor wake fraction during acceleration or deceleration maneuvers can be substantially different from the values under steady-ahead self-propulsion conditions. Therefore, reasonably accurate estimates of the Taylor wake fractions are necessary in order to calculate the transient loads during acceleration or deceleration maneuvers.

2. The transient and peak blade loads tend to be larger during acceleration maneuvers than during deceleration maneuvers.

19

3. The transient and peak blade loads during acceleration maneuvers can be substantially larger than the time-average and maximum blade loads, respectively, maneuvers than during deceleration maneuvers.
during full-power steady-ahead operation.

4. The transient and periodic loads are controlled predominantly by the instantaneous values of the ship speed V, propeller rotational speed n, and the propeller pitch ratio P/D. The periodic and transient loads are not sensitive to the time rates of change of these quantities. Therefore, the transient and periodic blade loads during acceleration and deceleration maneuvers can be adequately estimated in a quasisteady manner.

5. During acceleration and deceleration maneuvers the variation of loads with blade angular position retain the same basic form as for steady-ahead operation.

6. The periodic blade loads during acceleration and deceleration maneuvers vary in a nearly linear manner with the product of ship speed V, propeller rotational speed n, and a function of propeller pitch ratio P/D. Therefore, these loads can be readily estimated for an acceleration or deceleration maneuver with a known time history of V, n, and P/D from the periodic loads under steady-ahead operation.

7. The periodic blade loads during acceleration and deceleration maneuvers, are, in general, less than the periodic blade loads during full-power steady ahead operation.

Ship Motions in Waves

1. Hull pitching (in calm water) substantially increases the maximum periodic blade loads over the corresponding periodic loads without hull pitching. The primary controlling parameter is the ratio of the vertical velocity of the propeller resulting from the hull pitching to the ship speed. The maximum periodic loads occur when the velocity of the propeller and stern are maximum downward.

2. Hull pitching increases the maximum time-average loads per revolution by only a small amount over the time-average loads per revolution without hull pitching.

3. The maximum values of the periodic variation of loads with angular position and the time-average loads per angular position occur near the same point in the pitch cycle.

20

4. Waves (without ship motions) substantially increase the maximum periodic blade loads over the corresponding periodic loads in calm water. The primary controlling parameter is the ratio of the vertical component of the orbital wave velocity in the propeller plane to the ship speed. The maximum periodic loads occur when the vertical component of the orbital wave velocity in the propeller plane is maximum upward.

5. Waves (without hull pitching) substantially increase the maximum time-average loads per revolution over the corresponding time-average loads in calm water. The primary controlling parameter is the change in effective advance coefficient due to the longitudinal component of orbital wave velocity.

6. The maximum values of the periodic variation of loads with angular position and the time-average loads per angular position occur near the same point in the wave cycle.

7. For given amplitudes of waves and pitching, the maximum values of the time-average loads per revolution, peak loads, and the periodic variation of loads with with angular position vary substantially depending upon the difference in phase between the hull pitch and the wave at the propeller. The time-average loads, peak loads, and periodic loads are near their respective largest values for any difference in phase whereby the crest of the wave reaches the propeller between 0.3 and −0.1 of the period of encounter before the maximum stern-up position.

8. Linear superposition of the increases in blade loads due to pitching in calm water and due to waves without hull pitching, taking into account the phase between the waves and the pitching, gives a good, or slightly conservative, estimate of the net increase in blade loads due to operation in waves with hull pitching.

Turns

1. The circumferential variation of the wake into the propeller plane is dominated by the drift angle at the propeller.

Summary Conclusion

If the time-history of the maneuver is predicted by the best available methods, then the maximum values of the blade forces and moments, except for spindle torque, during acceleration and deceleration maneuvers car   predicted by theoretical

21

calculations plus an empirical factor to an accuracy of approximately ± 25 percent. Similarly, the maximum values of the these forces and moments during turning maneuvers can be calculated to an accuracy of approximately ±30 percent if model wake surveys during simulated turns are conducted, and to an accuracy of approximately ± 40 percent if the wake patterns during the turns are approximated from the drift angle and the wake data during steady ahead operation or the statistical wake data in the literature. The deviations from the true values for the spindle torque are approximately twice the percentages for the other components.

Recommendations

1. For a new propeller-hull configuration which is significantly different from an existing configuration, it is recommended that blade loads be predicted by both model measurements of the six components of blade loading and by the unsteady lifting surface theoretical method of Kerwin supplemented by the appropriate empirical factor. This provides two independent predictions which can be cross-checked. These predictions should be further checked by comparison with the existing statistical database.

2. To estimate the effects of ship motions on loads, the absolute values of the maximum increases in time-average, peak, and periodic loads due to the separate influences of waves and hull pitching should be added without regard to the relative phase between wave and hull pitching.

3. To minimize the propeller blade loads, the following two rules should be followed:

a. Use balanced skew (skew forward at the inner radii and skew back at the outer radii) and forward rake. This is desirable from consideration of bending moments due to centrifugal force. Balanced skew is also desirable for producing a small time-averaged spindle torque which tends to increase pitch under steady-ahead operation. Skew also has advantages unrelated to blade loading, such as reduced propeller induced unsteady hull forces, reduced blade frequency bearing forces and moments, and improved cavitation performance. However, practical amounts of skew do not measurably reduce the periodic hydrodynamic blade loads arising from the inclination of the flow.

22

b. Unload the blade tips. This pushes the radial centers of the time-averaged hydrodynamic loads closer to the hub and thereby reduces the moment arms and moments in the hub. This may reduce the time-averaged moments by, approximately, eight percent relative to an optimum radial distribution of loading. Unloading the blade tips has other advantages unrelated to blade loading, such as reducing propeller-induced unsteady hull forces and suppressing tip vortex cavitation.

MATERIALS

Blade and Hub Material

1. Cast Ni-Al bronze (MIL-B-21230A, Alloy 1) remains the best alloy for large CP propeller blades and hubs. The selection of another alloy must be shown to be equal or superior to Ni-Al bronze in properties, castability, and ease of repair.

2. Cast stainless steels of the high Cr-Ni-Mo types require deliberate cathodic protection to prevent crevice corrosion, stress corrosion cracking of repairs, and to raise corrosion fatigue strength. It is recommended that these alloys not be used for Navy CP propeller blades.

3. Detailed analysis should be performed in CP propeller blade and hub design. Sufficient fatigue data, stress trials data, and load prediction capability exist for highly refined designs against blade and hub fatigue without overly conservative safety factors.

4. U.S. Navy propeller repair guidance should be revised to include CP propeller blades and hubs, defining critical regions.

Blade Carrier Materials

1. A material fracture toughness requirement should be determined for blade carriers of high-strength steels to be part of the material specification.

2. Detailed fatigue analysis of the blade carrier should be performed based on data for the material used and conservative factors that are applied.

3. The full theoretical stress concentration factor should be used as the fatigue notch reduction factor in fatigue design.

4. Protection of steel blade carriers by nonmetallic coatings applied in high stress areas such as fillets and grooves is recommended for corrosion fatigue resistance.

Blade Bolt Materials

1. Corrosion-resistant alloys with properties documented for the stock size intended for bolt manufacture should be used.

2. For maximum fatigue strength, the bolts should be manufactured with rolled threads and head fillet. Roll forming of the threads must be performed after all strengthening and stress relieving heat treatments are complete.

3. Root rolling of partially cut machined threads should be used for the manufacture of blade bolts of difficult to work materials. The manufacturing techniques and details, however, need to be developed and properties demonstrated for each particular case of material and fastener size.

4. The alloy should have corrosion fatigue strength in seawater.

5. The alloy should be near to or more noble than the alloy used as blade and hub in the galvanic series in seawater.

6. Alloys susceptible to galling should not be used in blade bolt applications.

Pitch Change Bearing Materials

1. A limiting bearing pressure should be established for the sliding couples involved in the pitch change bearing and calculation criteria should be established.

2. Of the bearing bronzes evaluated, tin bronze (CDA 911) is recommended where separate bearing rings are used.

3. Composite materials DU(B) and Karon offer a means of reducing friction and wear in highly loaded systems. These materials are recommended for facing the bronze bearings in such systems to reduce maintenance required to refinish surfaces after bronze transfer and buildup.

4. Seawater intrusion into the hub can cause degradation of the blade carrier, bearings, hydraulic, and control components. Indicators which warn of seawater leakage into the hub should be considered to prevent prolonged operation with seawater within the hub.

STRENGTH

1. The limiting structural problem areas are the blade attachment bolts and crank ring to which the blade is attached. Stress analyses of the blade attachment are complicated by their involvement with preloaded parts in contact and the complex deformation patterns of the blade palm, crank ring, and hub which make rigorous analyses difficult and expensive.

2. One-third scale metal models provided a good simulation for determining stress levels and the effect of design changes on the SPRUANCE propellers.

3. Numerical methods, applied singly and in combination, can predict stresses in the crank ring and blade attachment bolts. In all cases, involvement of the more expensive finite element methods increases accuracy of the results.

4. The best numerical stress predictions were made using three-dimensional finite element analyses, but the total blade attachment including part of the hub must be included in order to properly account for the bolted joint nonlinearities and hub and crank ring deformations. At this time, this full three-dimensional analysis is very time consuming and expensive.

5. A method for predicting crank ring fillet stresses, which is based on closed-form equations, provides reasonable accuracy if the minimum distance between the bolt threads and fillet is large enough to keep the effect of bolt thread loading on fillet stress to an insignificant level. A crude empirical method for determining this distance is described.

CHAPTER I

INTRODUCTION

TABLE OF CONTENTS

Page

LIST OF FIGURES

SCOPE

This report is a summary of the controllable pitch (CP) propeller blade attachment investigations which were conducted by the David W. Taylor Naval Ship Research and Development Center (DTNSRDC) subsequent to the failures of the CP propeller on the USS BARBEY. These investigations included:

1. Sea trials on USS BARBEY, USS SPRUANCE and R/V ATHENA to measure blade loads and resultant attachment stresses.

2. Sea trials on USS OLIVER HAZARD PERRY to measure blade bolt stresses.

3. Analytical and laboratory experimental investigations to develop a substantially improved load and stress prediction capability.

4. Investigations of the suitability of potential blade attachment materials.

5. The evolution of a rationale and the criteria for the evaluation of new CP propeller designs, with similarly configured blade attachments and the proposed materials.

BACKGROUND

The advent of the large aircraft type gas turbine as a prime mover for naval ships has had a profound impact on the design of marine propulsion systems. Because no reversing gas turbine of equal capacity exists, because the technology to build satisfactory reversing gears does not exist, and because of the extreme weight penalties associated with existing electrical propulsion systems, CP propellers are now required on all gas turbine powered ships.

The origins of the CP mechanism can be traced to the work of Hooke in 1683. The concept was initially incorporated into marine propellers in the middle 1800's possibly to feather propellers on early steam ships when they were under sail. Table 1 lists the CP propeller applications in the U.S. Navy and U.S. Coast Guard since World War II, including a comparison of increasing power level with some of their overall physical characteristics and some remarks of interest concerning their applications.

The newest ships to employ gas turbines as their prime movers are the USS SPRUANCE (DD-963) and the USS OLIVER HAZARD PERRY (FFG-7) Classes. The SPRUANCE Class is equipped with two 40,000 shp* CP propeller systems, and the PERRY Class

---

*Power levels are given on a per shaft basis.

is equipped with a single 40,000 shp system. These 40,000 shp systems represent a significant increase in power over 6650 shp of the USS ASHEVILLE (PG-84) Class patrol gunboats, and the 7900 shp of the USS NEWPORT (LST-1179) Class, the largest system in previous classes of U.S. Navy ships to be equipped with CP propellers.

When it became apparent that the Navy would probably use gas turbines in the SPRUANCE Class, a program was undertaken to obtain early experience with comparable CP propellers in order to develop confidence in a potential design for the new class. Two experimental systems were developed for test and evaluation; one system, jointly developed by the Baldwin-Lima-Hamilton (BLH) Corporation and the U.S. Navy, was installed on the USS PATTERSON (FF-1061). The other, a Liaaen design constructed by Propulsion Systems, Inc (PSI), was installed on the USS BARBEY (FF-1088). Both ships use conventional steam turbine power plants. Both systems were designed for 35,000 shp operation.

The BARBEY CP propeller system was installed in November 1973. In April 1974, after approximately 1,000 hours of operation, an investigation of an oil leak in the system led to the discovery of a failure: the complete fracture of one propeller blade bolt and cracks in six other bolts. The surfaces of the bolt that fractured indicated a fatigue failure, which was attributed to higher than predicted cyclic loading. The solution was to modify the bolt design in order to obtain a more even thread load distribution.

In August 1974 BARBEY suffered the second CP propeller failure. All five propeller blades, all bolts, and most of the crank disks were lost when the crank disks failed in fast fracture during a crashback maneuver. When this second failure occurred, the main propulsion system had approximately 1,000 hours of operation with the modified bolts and approximately 2,000 hours of total operation with the CP propeller.

Examination of the failed parts after drydocking showed that the crank disk material had a very low fracture toughness, making the disk susceptible to catastrophic brittle fracture at a general stress level less than yield stress in the presence of a critical crack in the structure. Because fatigue cracks were found in the crank disk, it was speculated that a growing crack weakened the crank disk to the point where a fast fracture occurred.

29

As a result of these two failures, the d. ion was made to conduct full-scale experiments on an assembled SPRUANCE Class propeller at DTNSRDC. Simultaneously, redesigned crank disks with improved blade bolts were installed on BARBEY and instrumented sea trials were conducted during which unacceptable high stresses were recorded in high-speed turns. Both the BARBEY and PATTERSON CP propellers were then removed and replaced with fixed pitch propellers.

It had become apparent that there was insufficient information available concerning design loads, structural reponse, and material selection for CP propeller hub components, thereby raising serious fundamental questions concerning the adequacy of the CP propellers then being procured for the SPRUANCE and PERRY Classes, and of those which would be required eventually in future gas turbine propelled ships. The Naval Sea Systems Command (NAVSEA), therefore, initiated a program to determine the adequacy of the CP propellers then under production for SPRUANCE and PERRY Classes and also undertook a research and development program to improve the technology base in design loads, strength analyses, and material selection of CP propeller blade attachment components for future procurements. The entire effort, both the research and development portion and the portion which was directed specifically to support the ongoing ship construction projects, made important contributions to the resolution of the CP propeller problems in the SPRUANCE, PERRY, and TICONDEROGA (CG-47) Classes.

The two basic questions in the blade attachment structural problem were: what are the forces imposed by the blades during the variety of ship operating conditions, and how does the extremely complex hub structure respond to the pulsating and multibladed forces in a "ship-at-sea" environment? Answers to these questions were uired in order to be confident of judgments which could be reached on the basis o .aboratory experiments and analysis.

At that time: (1) only mean blade loads could be predicted in a satisfactory fashion; (2) gross errors of 40 to 60 percent existed in the prediction of unsteady loads at design speed in calm water; (3) no measurements of loads during transient mane vers such as crash-ahead, crashback, or turns existed; (4) no wake data for a ship in a turn existed; (5) no detailed structural analysis of the propeller blade-propeller hub interface had been performed; (6) no fatigue analysis of a CP propeller or its components had been performed; (7) no Charpy impact strength

requirements for propeller blade attachment components were specified; (8) no fatigue
life requirements for propeller blade attachments were specified; (9) no requirements
to torque propeller blade bolts under controlled conditions in order to have assured
preload were specified; and (10) no special requirements concerning stress calcula-
tions in the propeller blade attachments were specified.

The NAVSEA program was divided into four parts: (1) full-scale load and stress
determination, (2) load prediction, (3) strength assessment, and (4) material
investigations.

DESIGN CONSIDERATIONS FOR CONTROLLABLE PITCH
PROPELLER BLADE ATTACHMENTS

A controllable pitch propeller consists primarily of a large hollow hub assembly
containing the pitch changing mechanism, the supports for the blades and their
bearings, and lastly, the blades themselves.

There are basically three types of blade attachment: (1) blades connected by
bolts to a crank ring (in BARBEY called a crank disk), Figures 1 and 2; (2) blades
which have a threaded extension which is screwed into a crank ring inside the hub,
Figure 1; and (3) the trunnion type in which the blade has a trunnion-shaped blade
carrier supported in the hub by journal bearings. Three versions of the third type,
the trunnion suspension, are shown in Figures 3, 4, and 5; a trunnion integral with
the blade; a semi-integrated blade attachment where long, slender bolts carry only
the blade centrifugal load; and a blade bolted to a separate trunnion piece. This
latter method is essentially a bolted-on blade because it provides the capability for
emergency replacement of blades underwater. The crank rings are sealed to prevent
water entry into the hydraulic actuating system when the blades are removed. Presum-
ably the same feature could be provided with a bolted-on trunnion arrangement but no
such design is known to have been used in either military or civilian applications;
therefore, it was not considered in this investigation. The strength of the screwed
in-crank ring attachment was evaluated. It was judged that the screwed in-crank
ring would probably be adequate structurally but that a substantial test program
would be required to demonstrate adequacy. No further consideration was given to
that type--again because of the desired capability for underwater blade replacement
and also because the subject program was successfully developing the basis for a
satisfactory bolted-on five-bladed CP propeller design in the sizes of interest.

31

Several factors must be considered in sizing the CP propeller hub and blade palms: (a) from the aspects of propulsive efficiency and shaft size, the hub should be as small as possible. Excessively large hub size requires an unnecessarily larger shaft diameter to bear the overhung weight; (b) the mean and unsteady operating forces applied to a blade, stresses the blade, the blade root, the blade palm, the blade bolts and the hub. The maximum size of the blade palm for a given number of blades on a hub is governed within small limits by the diameter of the hub. The blade palm must be of sufficient diameter to accommodate the blade root and an adequate blade bolting arrangement. Blade flange ports in the hub must match the palm. Small blade palm diameter forces the use of: (1) short, thick blade root sections for sufficient strength; (2) an overhang of blade root sections beyond the blade palm, especially the leading edge, in order to achieve an acceptable hydrodynamic section shape of the blade at short radii; and (3) blade bolts which are closely spaced in a small bolt circle and, therefore, highly stressed in supporting the blade overturning moments.

Thus, propulsive efficiency, cost, and weight drive CP hub size reduction while hub strength considerations drive hub size increase. The CP propeller designer must strive to balance these factors in the achievement of an optimum design.

FAILURE EXPERIENCE OF CONTROLLABLE PITCH PROPELLER BLADE ATTACHMENTS

A review of the various types of damage and failures which have occurred in CP propellers in service is important in determining the source of potential problems. The majority of recent CP propeller installations in either merchant or naval service were designed, developed, and built by several firms in western Europe or licensee's of these firms. Thus, the database related to operational experience of CP propeller systems was primarily gathered from these sources, and from Det Norske Veritas, a European classification society, which continually examines surveyors' reports in a statistical manner searching for problem areas. Experience in the Navy with CP propeller systems has also been reviewed.

The vast majority of the problems in CP propeller systems occurred in the hydraulic systems: pitch control system malfunctions, sealing problems, pump or pump drive malfunctions, corrosion, and oil contamination. Except for the consideration

of water contamination which finds its way into the hub, these problems are neither influenced by nor effect the strength or integrity of the blade attachment. Those which involve cracking, fracture or deterioration in the blade attachment are important in setting design criteria. These problems are reviewed.

MERCHANT SERVICE EXPERIENCE

Several thousand CP propeller installations have been or are regularly in merchant service in plants of less than 500 shp and experience with those plants provided the bulk of reliability failure statistics through to the early 1970's. The development and use of larger power CP propeller installations (5,000 to 20,000 shp) in merchant service dramatically increased in the past decade. Their reliability experience has been similar to the experience with the smaller plants.

1. Propeller blade failure and cracking by fatigue in blade bolt holes, blade palm, and blade root was the most significant and prevalent problem, occurring in cast 13 percent Cr stainless steel alloy usually found in the higher power systems or in the Mn-Ni-Al bronze in the lower powered systems. These are the alloys most used in European practice. These failures resulted primarily from material problems: where material soundness (production process), repair procedures, quality control, and inspections were unsatisfactory. They were similar to blade failure incident rates in fixed-pitch propellers made of the same materials. This experience cannot be related to U.S. Navy practice, in which Ni-Al bronze is used specifically to minimize the possibility of such problems, in accepting its lower strength.

2. Initially, damage incidents and failures increased rapidly with increasing horsepower.

3. As design and service experience within a power range grew, hub and CP blade attachment mechanism damage (crank rings, blade bolts, bearings) decreased; but blade failure problems did not.

4. Hub and CP blade attachment mechanism damages were considered to be related to design rather than to material deficiency.

5. Blade bolt fatigue failures were attributed to lack of proper preload in the assembly unless occurring with other damage which indicated an inadequate design.

33

6. In some highly loaded merchant ship CP propeller systems, broken blade bolts, fatigue cracking in crank rings, and wear in bearings resulted from cyclic overstressing in inadequate designs.

7. Some manufacturers have gone to the effort of protecting highly stressed internal parts from corrosion fatigue, indicating that seawater leakage and intrusion have occurred and caused concern.

NAVAL SERVICE EXPERIENCE

The U.S. Navy has had experience with CP propeller installations for many years, but that experience was with plants 8,000 shp or less until the development of the 35,000 to 40,000 shp range plants for current gas-turbine powered frigates and destroyers. A reliability study of the smaller CP propeller systems indicated that hydraulic systems and control systems were the prevalent problem areas; however, the CP propeller equipped vessels were primarily minesweepers and amphibious ships (LST) where required performance is similar to the merchant service previously reviewed.

The first class of warships with CP propellers in the U.S. Navy were the gas-turbine powered ASHEVILLE Class patrol gunboats (6,650 shp). This class of vessels experienced extensive propeller blade failures (fracture and cracking) in early service when cast titanium alloy blades were used. The blade material was changed and no more blade problems were experienced.

There have been no blade attachment failures other than those on the BARBEY which led to the investigations being reported herein. It is apparent that the CP propeller blade attachment problem became critical with the major increase in horsepower and the simultaneous increase in the number of blades to five, thereby reducing the relative strength of the blade attachment. Bearing distress in the form of bronze transfer from the bearing ring to the steel crank ring bearing surface was observed on inspection of the SPRUANCE and BARBEY Class crank rings after instrumented trials. Similar observations had been made occasionally on inspections of crank rings in NEWPORT Class CP propeller systems.

The service experience in major allied warships involves CP propeller systems of less than 30,000 shp and no blade attachment failures or damage are known.

34

ORGANIZATION OF REPORT

The following chapters present a summary of the work which was accomplished in each of the major areas which were investigated and also provide references to the many more detailed reports which were prepared in the investigation.

Chapter II (Trials) reports on the sea trials on BARBEY, SPRUANCE, OLIVER HAZARD PERRY, and R/V ATHENA. It also includes related information from trials on USS ROOSEVELT (CVA-42), USS DOUGLAS (PG-100), and USCG POLAR STAR (WAGB-10). It describes the scope of the trials, how they were carried out, the key information which was obtained, and the important conclusions which were made directly on the basis of the experimental data.

Chapter III (Loads) reports on the development of a major improvement in blade load predictions (time average, transient, periodic, and peak loads) with allowances for states of sea and maneuvers. It includes guidelines for minimizing the loads.

Chapter IV (Materials) reports on material investigations which were conducted, primarily concerning crank rings, blade bolts, and bearing rings. They considered strength, ductility, fracture toughness, fatigue, stress corrosion cracking, corrosion, mechanical and galvanic compatibility, and bearing integrity. It includes guidelines on material selection.

Chapter V (Strength) reports on the development of various analytical and experimental techniques for predicting blade attachment stresses and guidelines for minimizing them. A strength assessment process is described for determining the structural adequacy of blade attachments.

Chapter VI (Specifications) reports on how the results of the program have affected or will likely affect the basic military specifications for purchase of CP propellers.

Chapter VII (Guidelines and Procedures for Evaluation) reports on the strength evaluation process for U.S. Navy CP propellers which has resulted from the program. Guidelines are provided for appropriate use of load and stress prediction methods and for examining material properties.

Each chapter includes a summary section and a short statement of conclusions and, as appropriate, recommendations.
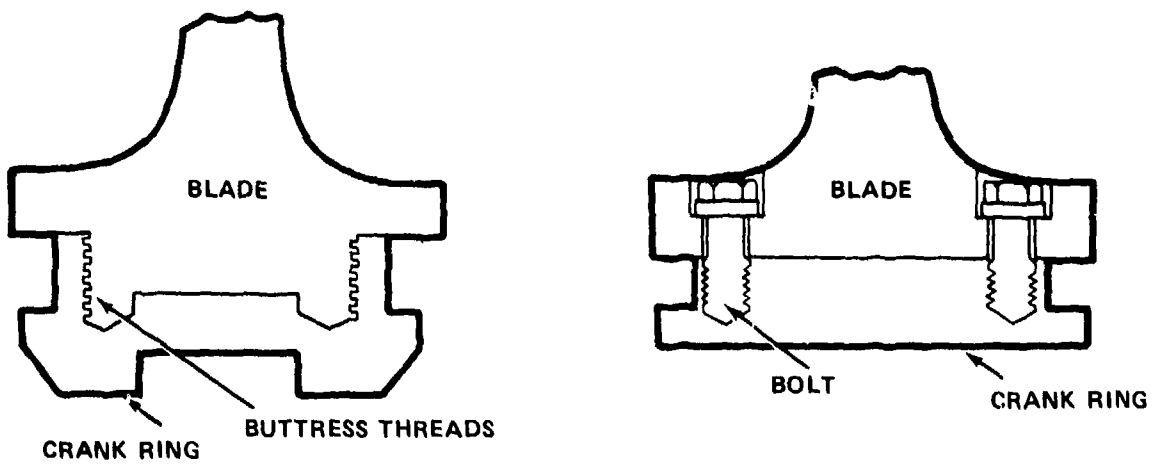
Figure 1 - Two Methods of Attaching Blade to
Blade Carrier

	DESCRIPTION	MATERIAL
1	BLADE SEAL BASE RING	CAST BRONZE
2	SPRING, COMPRESSION	STEEL
3	PIN, DOWEL	STEEL AISI C 1042
4	CAP SCREW	SILICON BRONZE
5	COVER, BLADE PORT	Ni-Al-BRONZE MIL-B-21230A
6	PROPELLER BLADE	Ni-Al-BRONZE MIL-B-21230A
7	BOLT-PROPELLER BLADE	K-MONEL
8	BEARING RING	DU BEARING ON AISI 4130
9	HUB BODY ASSEMBLY	Ni-Al-BRONZE MIL-B-21230A
10	BEARING RING LOCK PIN	DRILL ROD (STEEL) AISI SAE
11	CRANK PIN RING	A471-70 CLASS 6 STEEL

Figure 2 - Typical Bolted Blade Attachment Assembly

Figure 3 – Controllable Pitch Propeller with
Trunnion–Mounted Blade (Integral Trunnion)
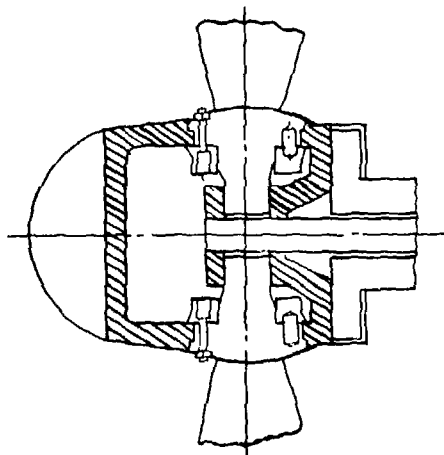
Figure 4 – Controllable Pitch Propeller with
Semi-Integrated Trunnion
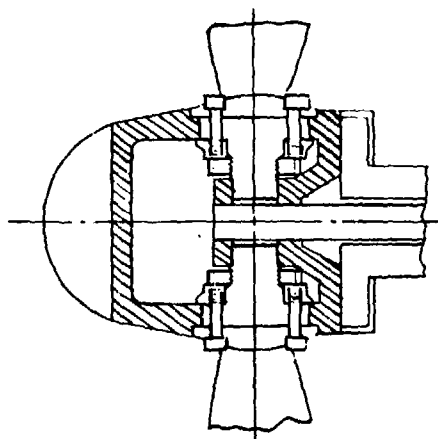
Figure 5 – Controllable Pitch Propeller with
Blade Bolted to Trunnion in Hub

TABLE 1 - CONTROLLABLE PITCH PROPELLER DATA

November 1980

CPP Class	Mfg'r.	Shaft Horsepower	Number of Blades	Hub Dia. to Propeller Dia.	Propeller Dia. (in.)	RPM	Year Placed in Service	Remarks
SC 497	GM	400	3	—	46	915	1942	Numerous failures, scrapped
MHC 43	BJCO	600	3	0.308	60	400	1956	
LSIL/LSSL	GM	660	3	—	46	—	1942	
MSO 428	Navy	800	4	0.244	84	267	1953	Good, working 24.4% hub
MSO 522	BJCO	800	3	0.274	84	267	1958	
AGOR 21	PSI	850	—	—	78	350	1973	
PT 812	EBDiv.	900	3	0.256	38	1,000	1955	Bolt fatigue problems
MSO 422	Navy	1,200	4	0.244	84	325	1953	
MSO 519	Navy	1,400	4	0.264	87	325	1958	
IFS 1	Navy	1,550	4	0.244	84	325	1955	
MSO 421	Navy	1,600	4	0.244	84	325	1956	
YTB 752*	PSI	1,800	4	0.267	129	180	1959	
T-AGOR 16	Lips	2,560	4	0.273	144	139	1971	
ATS 1	EW	3,000	4	0.279	141	150	1971	
ASR 21	EW	3,000	4	0.252	156	130	1972	
LST 1156	Navy	3,200	4	0.269	104	300	1952	
T-AGS 29	EW	3,400	4	0.300	108	190	1970	
T-ATF 166	PSI	3,600	4	—	108	227	1979	
PGH 1*	kaMeWa	3,600	3	0.315	45	1,115	1967	
LST 1176	Navy/BLH	4,800	4	0.291	117	290	1958	
PG 84	PSI	6,650	4	0.328	72	670	1966	
SES 100B	PSI	6,750	6	0.429	42	2,650	1973	
LST 1179	BJCO	8,000	4	0.291	138	226	1969	
PGG 1	EW	11,500	4	0.321	81.6	640	1981	
PuG 1	EW	11,500	4	0.310	108	350	1981	
T-AOT 168*	BJCO	14,000	4	0.261	258	90	1974	
WHEC 715	PSI	18,000	4	—	156	235	1967	
WHEC 719	EW	18,000	4	—	156	235	1968	
WAGB 10**	EW	20,000	4	—	192	175	1976	
FF 1061*	Navy/BLH	35,000	5	0.289	180	240	1972	Troublesome
FF 1088*	PSI	35,000	5	0.288	180	240	1973	Failed in Service
FFG 7*	BJCO	40,000	5	0.309	198	180	1977	
DD 963	BJCO	40,000	5	0.300	204	168	1975	
CG 47	BJCO	40,000	5	0.300	204	168	1982	

* Single screw.   All others are twin screw, unless otherwise noted.
** Triple screw.

CHAPTER II

FULL SCALE TRIALS

TABLE OF CONTENTS

LIST OF FIGURES

LIST OF TABLES

46

LIST OF TABLES

INTRODUCTION

This chapter reports on tests which were conducted on the blade attachments of the controllable pitch (CP) propellers of the USS BARBEY (FF-1088), USS SPRUANCE (DD-963), and USS OLIVER HAZARD PERRY (FFG-7) preparatory to and during sea trials which were held during the 1975 and 1978 time period. The tests were triggered by the two previously described failures of the blade attachments on the five-bladed CP propeller on BARBEY.[1*] The BARBEY trials were intended to determine the cause of those failures. They revealed the inadequacy of design information concerning the blade loads, and concerning the structural response of, and material selection for, the blade attachment. Trials were, therefore, run on SPRUANCE and OLIVER HAZARD PERRY to obtain information concerning the adequacy of their blade attachments and also to obtain information which would be used in improving the technical basis for predicting the hydrodynamic loads on and the structural response of future CP propeller blade attachments and for their material selection.

Each of those three trials is covered in this chapter: their scope, how they were carried out, the key information which was obtained, and the important conclusions which were made directly on the basis of the test data. The results of subsequent analyses of the data are included in succeeding chapters.

This chapter also reports on the four other underway trials of propellers which were conducted by the U.S. Navy in order to present a complete background concerning all such tests.**

The seven trials reported, the parameters measured, and the trial dates are listed in Table 1. The propulsion machinery and propeller characteristics are listed in Table 2.

USS FRANKLIN D. ROOSEVELT (CVA-42)

Although the ROOSEVELT trial was not part of the CP propeller program, it is included in this summary report because it was the vehicle on which the basic techniques of propeller stress measurements were developed at DTNSRDC. The ROOSEVELT*** was a USS MIDWAY (CVA-41) Class attack aircraft carrier. Work on the

---

*A complete listing of references is given on page 163.

**Great Britain and the Netherlands have also conducted similar tests.

***CVA-42 has since been decommissioned.

TABLE 1 - SUMMARY OF U.S. NAVY SHIPS ON WHICH FULL-SCALE, UNDERWAY PROPELLER TRIALS HAVE BEEN PERFORMED BY THE DAVID W. TAYLOR NAVAL SHIP RESEARCH AND DEVELOPMENT CENTER

Ship	Type	Trial Date	Measured Parameters					Type Propulsion System
			Stress			Blade		
			Blade	Bolt	Crank	Pressure	Accel-eration	
USS FRANKLIN L. ROOSEVELT (CVA-42)	Aircraft Carrier	1967	X					Conv.[1]
USS DOUGLAS (PG-100)	Patrol Gunboat	1971	X					CP[2]
USS BARBEY (FF-1088)	Destroyer Escort	1975	X	X	X	X	X	CP[2]
USS SPRUANCE (DD-963)	Destroyer	1976	X	X	X	X	X	CP[2]
USS OLIVER HAZARD PERRY (FFG-7)	Frigate	1977	X	X				CP[2]
USCG POLAR STAR (WAGB-10)	Icebreaker	1977-1980	X	(3)	(3)			CP[4]
R/V ATHENA[5]	Research Vessel	1979	X	X		X		CP[2]

Notes:

(1) Conventional (Fixed Pitch) Propeller.
(2) Controllable Pitch Propeller (Bolted Blade, Crank Disk, and Hydraulic Cylinder).
(3) Propeller Blade Trunnion and Link Stress.
(4) Controllable Pitch Propeller (Trunnion Blade, Link, and Hydraulic Cylinder).
(5) Formerly the USS CHEHALIS (PG-94).

49

TABLE 2 - HULL, PROPULSION MACHINERY AND PROPELLER CHARACTERISTICS FOR SHIPS ON WHICH FULL-SCALE, UNDERWAY PROPELLER TRIALS HAVE BEEN PERFORMED BY THE DAVID W. TAYLOR NAVAL SHIP RESEARCH AND DEVELOPMENT CENTER

Characteristic	USS FRANKLIN D. ROOSEVELT (CVA-42) Aircraft Carrier	USS DOUGLAS (PG-100) Patrol Gunboat	USS BARBEY (FF-1088) Fast Frigate	USS SPRUANCE (DD-963) Destroyer	USS OLIVER HAZARD PERRY (FFG-7) Frigate	USCG POLAR STAR (WAGB-10) Icebreaker	R/V ATHENA[1] High Speed Research Vessel
Hull:							
Overall Length, ft	979	165	438	563	440	399	165
Extreme Beam, ft	238	24	47	54	45	84	24
Max. Draft, ft	36	5	25	28	25	28	5
Full Load Displacement, tons	63,600	240	4,100	7,800	3,400	13,000	240
Machinery:							
Main Engine Type[2]	ST	GT	ST	GT	GT	GT	GT
Number of Shafts	4	2	1	2	1	3	2
Max. Shaft Horsepower	53,000	6,500	35,000	40,000	41,000	20,000	6,500
Max. Shaft Speed, rpm	160	670	240	168	180	175[3]	670

Notes:

(1) R/V ATHENA was formally the USS CHEHALIS (PG-94).
(2) ST Steam Turbine, GT Gas Turbine.
(3) 175 Max. rpm (on centerline shaft), 160 Max. rpm (on wing shafts).

TABLE 2 (Continued)

Characteristic	USS FRANKLIN D. ROOSEVELT (CVA-42) Aircraft Carrier	USS DOUGLAS (PG-100) Patrol Gunboat	USS BARBEY (FF-1088) Fast Frigate	USS SPRUANCE (DD-963) Destroyer	USS OLIVER HAZARD PERRY (FFG-7) Frigate	USCG POLAR STAR (WAGB-10) Icebreaker	R/V ATHENA[1] High Speed Research Vessel
Propellers:[4]							
Type[5]	FP	CP	CP	CP	CP	CP	CP
Number of Propellers	4	2	1	2	1	3	2
Number of Blades/Prop.	5(I)/4(O)	4	5	5	5	4	4
Diameter, ft	18.25	6	15	17	16.5	16	6
Expanded Area Ratio	0.643[6]	0.771	0.566[6]	0.730	0.739	0.540	0.771
Hub/Dia. Ratio	0.21	0.33	0.29	0.30	0.30	0.36	0.33
Rotation[7]	OB	OB	RH	IB	RH	RH[8]	OB
Design Pitch at 0.7R, in.	228.5	77.52	181.47	314.00	280.01	164.32	77.52
Pitch Ratio at 0.7R	1.04	1.08	1.01	1.54	1.42	0.86	1.08
Blade Material[9]	Mn-Br	SS	Ni-Al-Br	Ni-Al-Br	Ni-Al-Br	SS	SS

Notes:

(1) R/V ATHENA was formally the USS CHEHALIS (PG-94).

(4) Propeller data on CAV-2 refers to starboard outboard propeller only, (I) ≡ Inboard, (0) ≡ Outboard.

(5) FP ≡ Fixed Pitch Propeller, CP ≡ Controllable Pitch Propeller.

(6) Developed Area Ratio.

(7) OB ≡ Outboard, RH ≡ Right Hand, IB ≡ Inboard.

(8) Centerline Shaft Rotation, Wing Shaft Rotate Outboard.

(9) Mn-Br ≡ Manganese-Bronze, SS ≡ Stainless Steel, Ni-Al-Br ≡ Nickel-Aluminum-Bronze.

ROOSEVELT was initiated by a propeller blade facture on the starboard, outboard propeller. Trial data were taken to evaluate methods of estimating blade loads and stresses.

USS DOUGLAS (PG-100)

The DOUGLAS is a USS ASHEVILLE (PG-84) Class, aluminum hull, patrol gunboat designed for high speed operation. The first boats of this class were fitted with titanium propeller blades which experienced failures in service. The failures were attributed to poor fatigue and stress-corrosion characteristics of the titanium blade material in seawater. Trials were run using the replacement blades which were made of stainless steel. The purpose of the trials was to verify the blade loading by comparison of predicted and measured blade-root stresses.*

USS BARBEY (FF-1088)

The BARBEY is a USS KNOX (FF-1052) Class fast frigate. As noted in the Introduction, this ship experienced CP propeller failures. Trials were run to determine their causes. They also provided full-scale experimental information to the propeller blade and blade attachment technology program.[1]

USS SPRUANCE (DD-963)

The SPRUANCE is the first of its class of new destroyers, gas turbine powered which were designed to replace the World War II destroyers. Trials were run because the experience on the BARBEY showed that it was not possible to adequately predict the blade loads or structural response of the blade attachment, leaving considerable doubt as to the structural adequacy on this new CP propeller. The objectives** of the trial were to determine the system loads and stresses and to contribute experimental information to the blade and blade attachment technology program. Attempts were also made to run "simulated frigate" tests to estimate the magnitude and distribution of loads and stresses on the PERRY Class CP propeller components.

---

*Reported informally by C. Noonan as Enclosure (Agenda for Propeller Stress Trials on the PG-100) to DTNSRDC Letter 964:CJN, 9870.1 of 7 Apr 1970.

**Reported informally by G. Antonides as Enclosure (Test Plan for Underway CP Propeller Stress Trials on USS SPRUANCE (DD-963)) to DTNSRDC Letter 1962:AZ, 9073/ Noise of July 1976.

USS OLIVER HAZARD PERRY (FFG-7)

The OLIVER HAZARD PERRY is the first of its class of new guided missile frigates designed to replace World War II destroyers and postwar-built fast frigates. As for SPRUANCE, trials were run because of concern for the structural adequacy of their CP propeller blade attachments. The blade attachment was identical to that installed on the SPRUANCE, except for a different propeller blade and blade root design and slightly relocated bolt holes. These changes, together with a different hull and propulsion control system made it impossible to reasonably predict the loads on and response of the CP propeller. Trial objectives were to determine the CP propeller bolt stresses and to contribute to the blade and blade attachment technology program.

USCG POLAR STAR (WAGB-10)

The POLAR STAR is the first of a class of the world's most powerful icebreakers. The STAR experienced failure of the link between the crank ring and crosshead of the pitch-changing mechanisms on both outboard propellers on its maiden voyage into arctic ice.* Trials were run to determine blade attachment stresses for both openwater and icebreaking activities.

R/V ATHENA

ATHENA, like DOUGLAS, is an ASHEVILLE Class gunboat which has been reassigned to DTNSRDC for use as a high speed test vehicle. Although the ASHEVILLE Class had experienced propeller blade failures, these failures were not related to the CP system. Trials were run on the ATHENA for purely research and development information on blade loads and blade attachment responses.**

---

*Antonides, G., "Test-Plan Underway Propeller Stress Trials USCG POLAR STAR WAGB-10," Unpublished report, 30 April 1977.

**Noonan, C., "Test Agenda for Propeller Parameter Trials on R/V Athena," Unpublished DTNSRDC Technical Note, March 1979.

INSTRUMENTATION

To achieve the objectives of the CP propeller full-scale trials program, an approach was developed to satisfy both short-term and long-term goals. This approach basically involved development of a suitable instrumentation package and a test plan to record the blade attachment stresses as well as to provide a reasonable indication of the propeller forces. Measurements were used to determine the suitability of the design actually under test, to check the validity of the contractors' design analyses of the blade attachment and to develop design modifications and ship operational restrictions, if necessary. The information from the CP propeller trials was also used in the related research and development work in the areas of propeller loads, blade attachment design, and material selection. (See also Chapters III, IV, and V of this report.) Figure 1 shows one of the ship instrumentation arrangements.

Considering the structural complexity and the undefined loading mechanism of a CP propeller hub assembly, all the structural components from the propeller blades to the line shaft should, ideally, have been instrumented with a large number and variety of gages. However, as usual, pragmatic considerations limited the number of gages which were installed. Gage locations were selected mostly on the basis of engineering judgment. The various types of gages, the reasons for their selections, as well as where they were generally located are described next.

PROPELLER BLADE GAGES

Instrumentation on the propeller blades, Figures 2 and 1b, included strain gages (except on OLIVER HAZARD PERRY), pressure gages (on BARBEY, SPRUANCE, and ATHENA), and accelerometers (on BARBEY and SPRUANCE). Strain gages were located at identical locations on the face* and back of the propeller blades. Generally the strain gages were rectangular rosettes located where the 30 and/or 40 percent radial arcs intersect the 25, 50, and 75 percent chord lines. Because there was no concern for the structural integrity of the propeller blade, the strain gage placements were not selected to indicate maximum blade stress, but rather to determine a single load vector (resultant) which, if applied to the blade at 0.7 radius, would produce the same stresses near the blade root as did the distributed hydrodynamic differential pressure. On the POLAR STAR, which uses stainless steel blades (not the Ni-Al Bronze

---

*Propeller blade face is the pressure side of the propeller for ahead operation.

54

Figure 1 – Instrumentation Arrangement for Propeller
Measurements on USS BARBEY

— — INSTRUMENTATION CABLE

* CENTRAL INSTRUMENTATION LOCATION
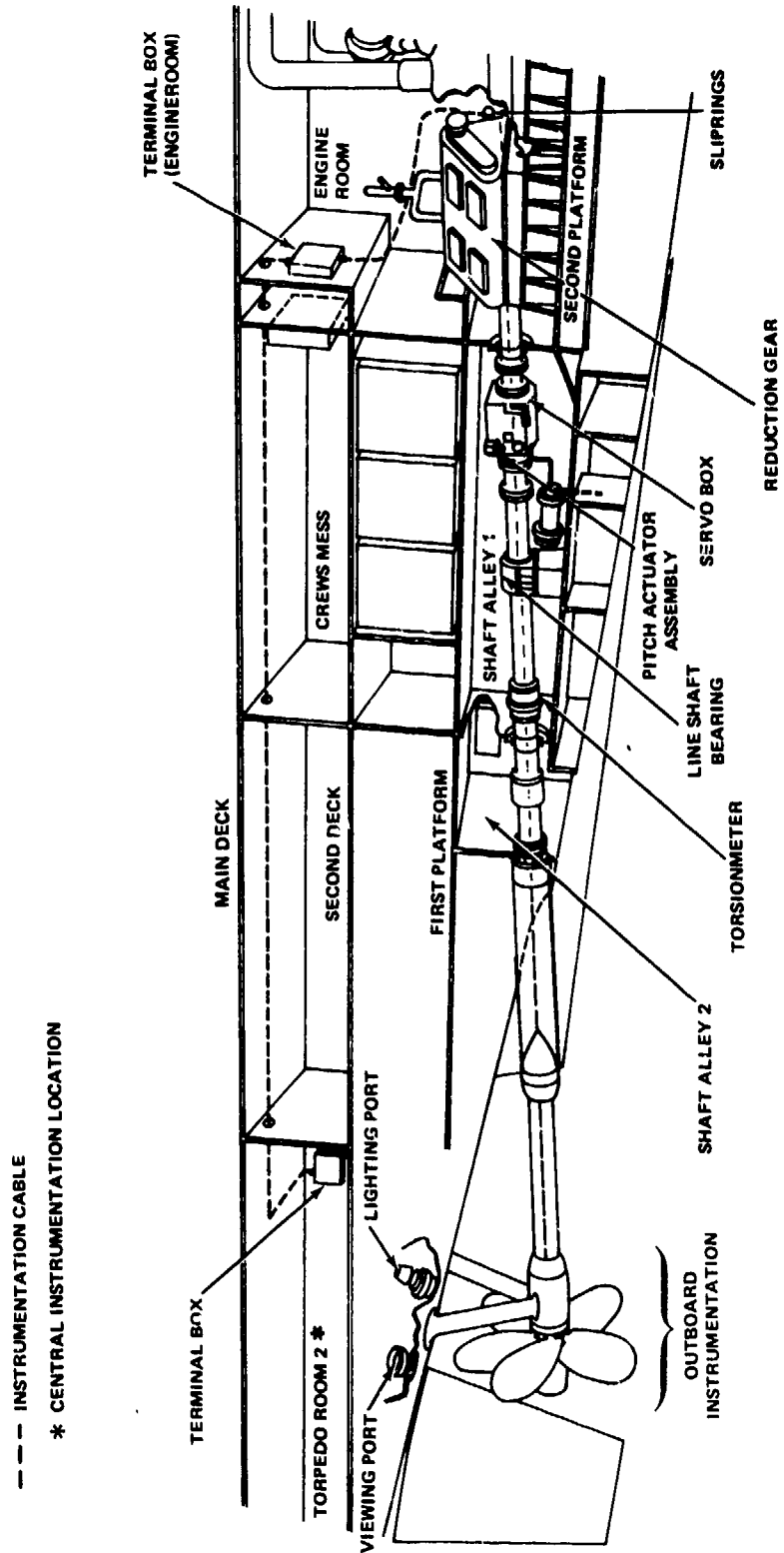
Figure 1a – Overall View of Propulsion System and Instrumentation

55

Figure 1 (Continued)

MECHANICAL VIBRATION
GENERATOR (DRYDOCK AND
DOCKSIDE TESTS ONLY)

UNDERWATER
TELEMETRY LEADWIRE
CONDUIT

AFT TERMINAL
BOX (HUB SWITCHING)

STRAIN GAGES, PRESSURE GAGES,
AND ACCELEROMETERS ON PROPELLER
BLADES, BOLTS, CRANK DISK, AND HUB

Figure 1b – Overall View of Outboard Gages on USS BARBEY

Figure 2 - Propeller Blade Gages

Figure 2a - Blade Strain Rosette Location (Matrix) on
USS BARBEY

Figure 2 (Continued)

EPOXY BONDED NEOPRENE PATCH (REFERENCE SYSTEM)

ACCELEROMETERS

PRESSURE GAGE

SPRAY URETHANE TEST PATCHES (WITH BONDING TEST CUTS)

BLADE HANDLING SLING
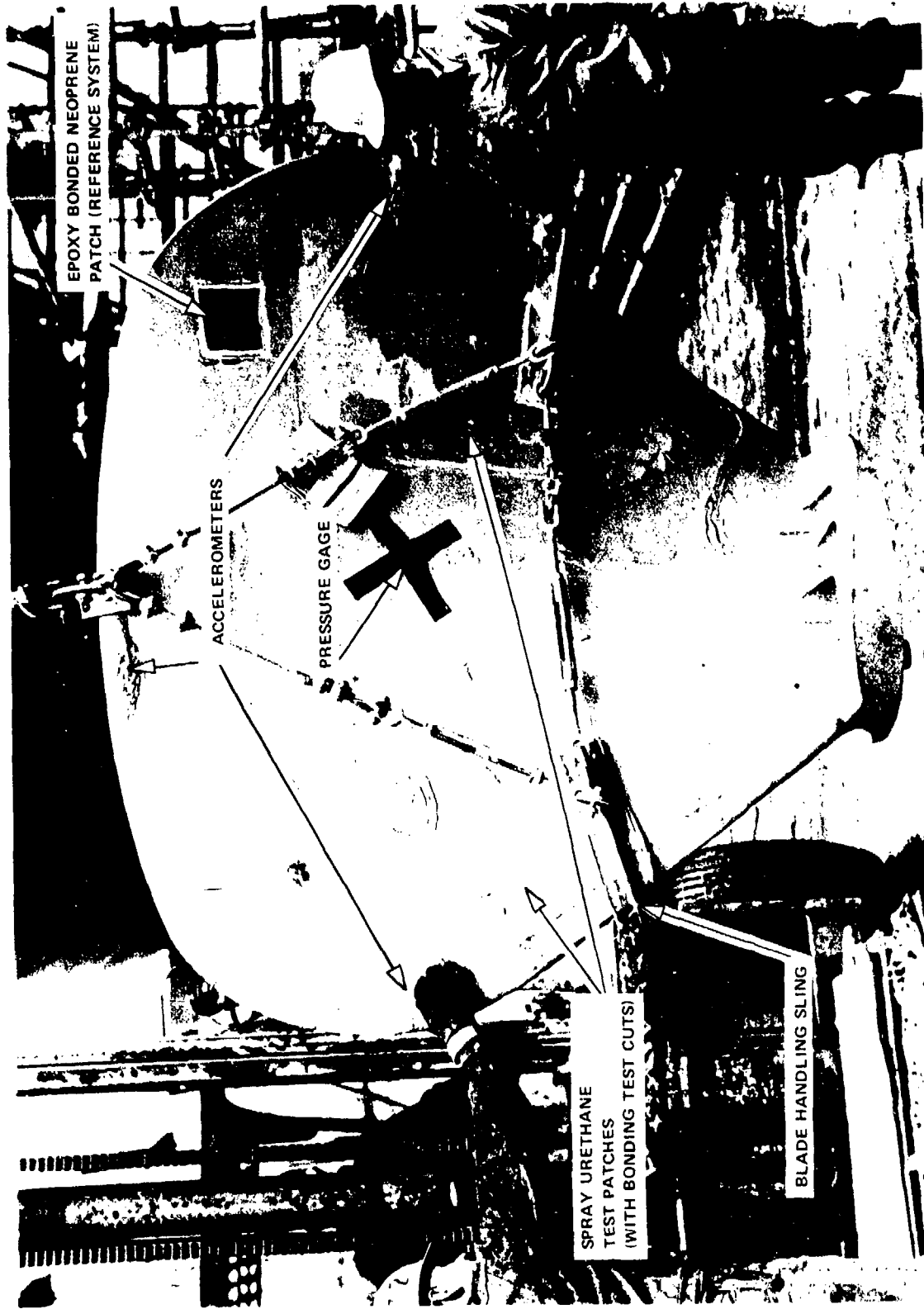
Figure 2b – Accelerometer on USS BARBEY

blades of naval CP propellers) with integral trunnions, strain gages were also used to determine the torsional and bending stress on the blade trunnions, Figure 3.

Full-Scale, underway propeller blade pressures had never been measured prior to the BARBEY trials. This work indicated that such measurements were feasible[2] and led to a more extensive effort on the SPRUANCE. Trial results were encouraging, Figure 4, but problems remained. The foremost problem was the need to develop a suitable transducer which would provide sufficient sensitivity to measure the pressures associated with the hydrodynamic propeller forces and yet be able to withstand the high transient pressures induced by cavitation.* These conflicting requirements, together with others (size, etc.) placed the ideal gage well outside the state of the art of gage manufacturing techniques. Specifications were written at DTNSRDC for the development of suitable gages which were eventually manufactured and installed on the propeller blades of the R/V ATHENA (Table 3). These gages were positioned to measure the spanwise and chordwise distribution of pressure.

Accelerometers were placed on the BARBEY and SPRUANCE blades to record blade vibratory motions. These gages were used to complement the information of the blade strain gages.

The accelerometers and strain gages were standard, commericially available transducers. Typical gage characteristics are given in Tables 4 and 5.

PROPELLER BLADE BOLT GAGES

The arrangement of strain gages as used to measure midshank strains on the propeller blade bolts is shown in Figure 5. Gages were configured at 90 deg around the bolt midshank in order to determine the static and dynamic states of stress which the bolt experiences in that plane. From these gages it is possible to calculate the average axial stress, the maximum bending stress, the maximum stress, and the orientation of the maximum stress relative to some reference. All bolts were instrumented in order to define the bolt load distribution over all tested operating conditions. In some cases additional gages were installed to determine the stresses near bolt heads and threads.

---

*Published as DTNSRDC Ship Acoustics Department Technical Memorandum TM-13-1901 (Jan 1977).

3 ROSETTES ON EACH SIDE OF BLADE

OUTLINE OF RUBBER AND 1/8-in. PLATE FOR PROTECTION

TRAILING EDGE

LEADING EDGE

15 in. — 15 in.

HOLE FOR WIRES

2 TORSION AND 2 BENDING STRAIN GAGE BRIDGES

CONNECTOR

43 in. RADIUS

WIRES

GAGE

RUBBER

CENTER OF HUB

BENDING BRIDGES MEASURE BENDING ABOUT EACH AXIS

"A" TRUNNION GAGES

TRAILING

LEADING

3

2

1

EDGE

4

5

6

EDGE

"B" TRUNNION GAGES

CODE FOR BLADE GAGES:

BB45C ◄— ORIENTATION:
  A TOWARD LEADING EDGE
  B RADIAL
  C TOWARD TRAILING EDGE

GAGE ROSETTE NUMBER:
  1, 6 NEAR LEADING EDGE
  2, 5 ON SPINDLE AXIS
  3, 4 NEAR TRAILING EDGE

BLADE NUMBER, 2 OR 4

**NOTE: FOR PORT (L.H.) BLADES, ROS. 1, 2, 3 ON AFT FACE: 1, 5, 6 ON FWD FACE
FOR STBD (R.H.) BLADES, ROS. 4, 5, 6 ON AFT FACE: 1, 2, 3 ON FWD FACE**

Figure 3 — USCG POLAR STAR Propeller Blade Strain Gage Locations

Figure 4 - Underway Propeller Blade Pressure Measurements on
USS BARBEY

TABLE 3 - PROPELLER BLADE PRESSURE GAGE CHARACTERISTICS ON
R/V ATHENA

Manufacturer: KULITE

Type: Diaphragm/Strain Gage

Range: 100 psi

Calibration Data:

Pressure, psig	Output, mV
0.18	-0.60113
-12.88	-8.21075
0.15	-0.90523
20.46	10.37482
40.10	21.28006
50.11	26.65488
0.18	-0.63648

Sensitivity: 0.552 mV/psi at 9.876 volts
excitation or 0.0559 mV/psi/
volt excitation.

TABLE 4 - TYPICAL PROPELLER BLADE PRESSURE GAGE CHARACTERISTICS

Gage Factor	2.04 ± 1 percent
Resistance, ohms	1000.0 ± 2.0
Excitation, volts	10.0 ± 0.1

TABLE 5 - TYPICAL PROPELLER BLADE STRAIN GAGE CHARACTERISTICS

Voltage Sensitivity	9 mV/g, nominal
Mounted Resonance Frequency	42,000 Hz, nominal
Frequency Response	±5 percent, 2 to 8000 hz
Transverse Sensitivity	3 percent maximum
Amplitude Linearity, Range	1 percent per 400g, 0 to 2500g

CRANK RING GAGES

The remains of the crank rings which survived the catastrophic failure on the BARBEY (see Introduction) indicated that fatigue cracks had been initiated in the fillet adjacent to the aft bolts holes. Strain gages were placed in this area on BARBEY in order to define the magnitude and orientation of the principal stress as well as the stress distribution along the fillet; see Figure 6. Additional gages were placed around the crank ring to define the distribution of stress for all conditions of operation. A similar pattern of strain gages was used on the crank ring on the SPRUANCE.

OTHER CONTROLLABLE PITCH COMPONENTS

Critical locations on the BARBEY propeller hub were gaged to determine web stress and hub vibrations; see Figure 7. On the POLAR STAR, the links which position the pitch of the blades were gaged; see Figure 8. Two independent bridges are used on each link, one with the gages in line with the link pins on the ends and the other 90 deg from that. In addition, link bending was measured in both directions with two more bridges. Even though normal operation should result in negligible bending, the failed links showed some indication of bending. This could be caused by the bearings at the ends seizing, so the link bending measurements were intended as indicators of bearing failure.

MISCELLANEOUS GAGES

A number of channels of pertinent propulsion system and ship's information were also recorded, Figure 9 and Table 6. The total number of information channels used on the trials have ranged from 50 to 300.

63

STRAIN GAGE LEADWIRES

VULCANIZED RUBBER COATING
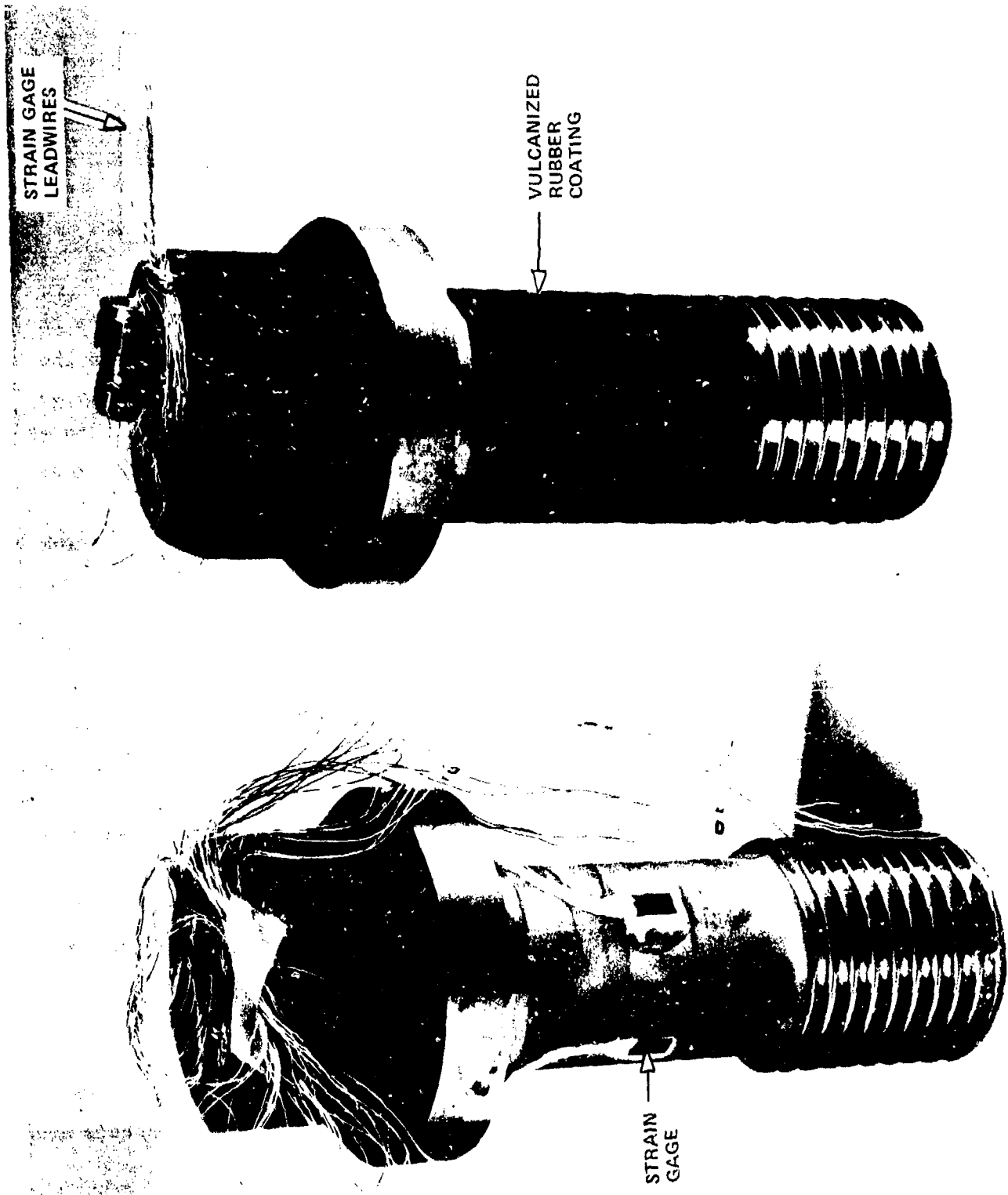
STRAIN GAGE

Figure 5 - Propeller Blade Bolt Gages on R/V ATHENA

64
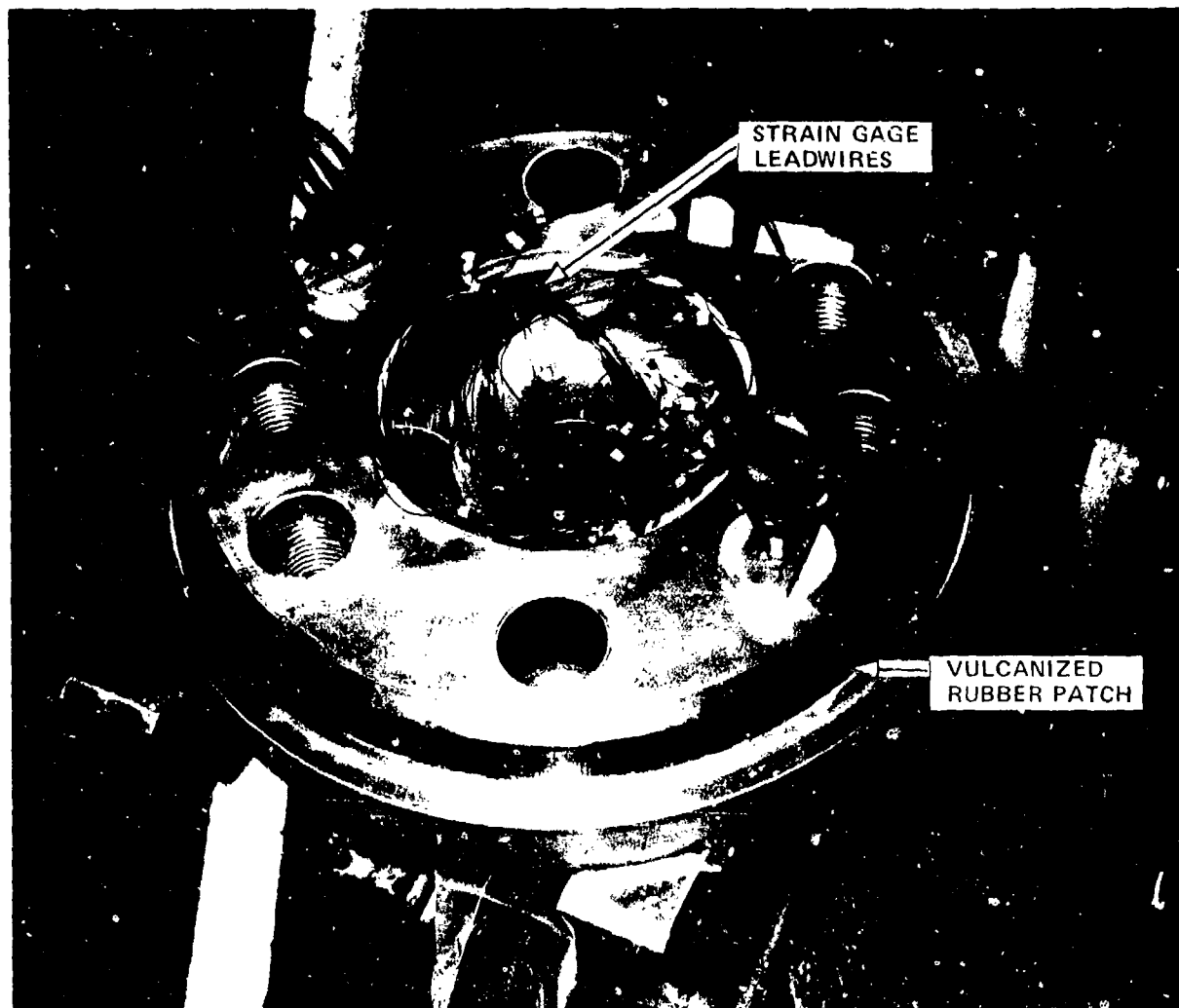
Figure 6 - Crank Ring Gages on USS BARBEY
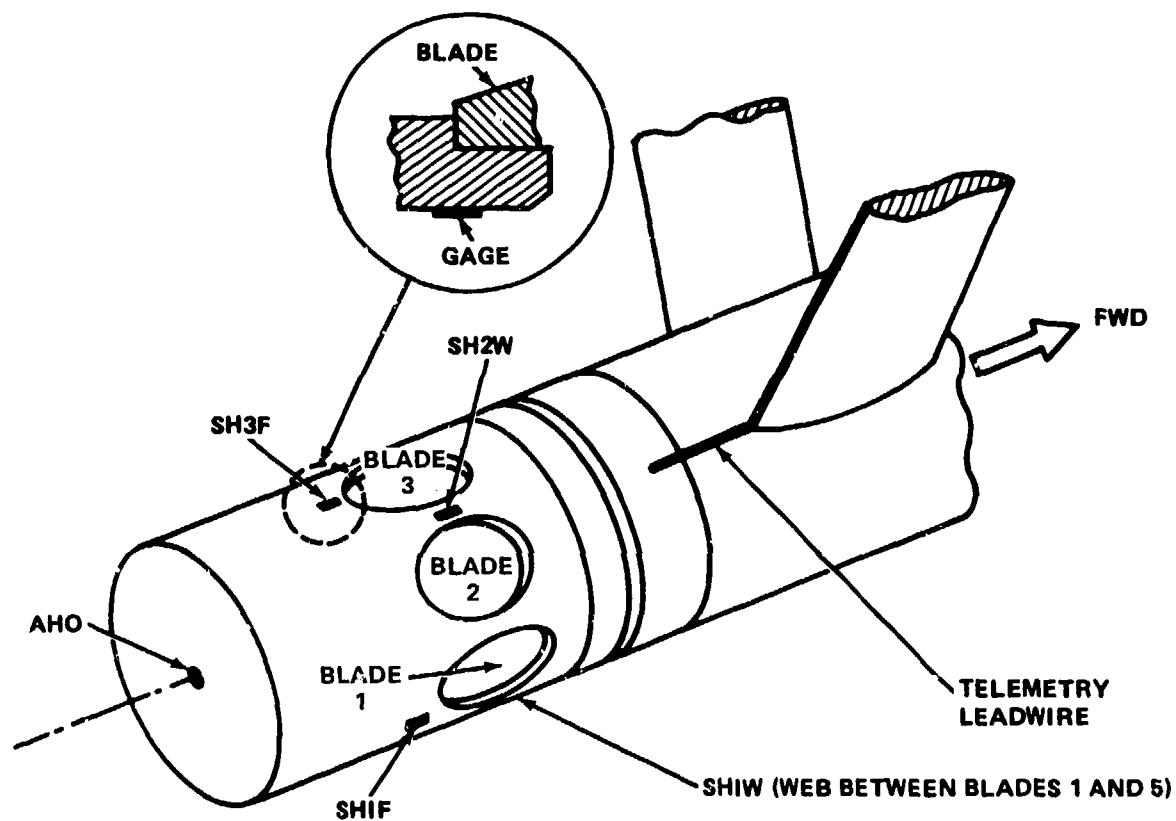
AHO = ACCELEROMETER HUB ₵ (IN AFT TERMINAL BOX)

SH1F ⎫
SH3F ⎬ = HUB STRAIN GAGE ON CRANK DISK BEARING FLANGE

SH1W ⎫
SH2W ⎬ = HUB STRAIN GAGE ON WEB BETWEEN PROPELLER BLADE HOLES

TELEMETRY LEADWIRE WAS IN 1/4-inch STAINLESS STEEL TUBE FROM
STRUT BEARING TO HULL PENETRATION

Figure 7 – Hub Gages on USS BARBEY

66

METAL STRAPS   CONNECTOR AND BRACKET

BENDING BRIDGE   AXIAL BRIDGE

VULCANIZED RUBBER COVERING

RUBBER
COVERING   CONNECTOR

*LINK CONNECTS
CRANKHEAD TO
CRANK RING

BENDING MEASURED
ABOUT THESE AXES
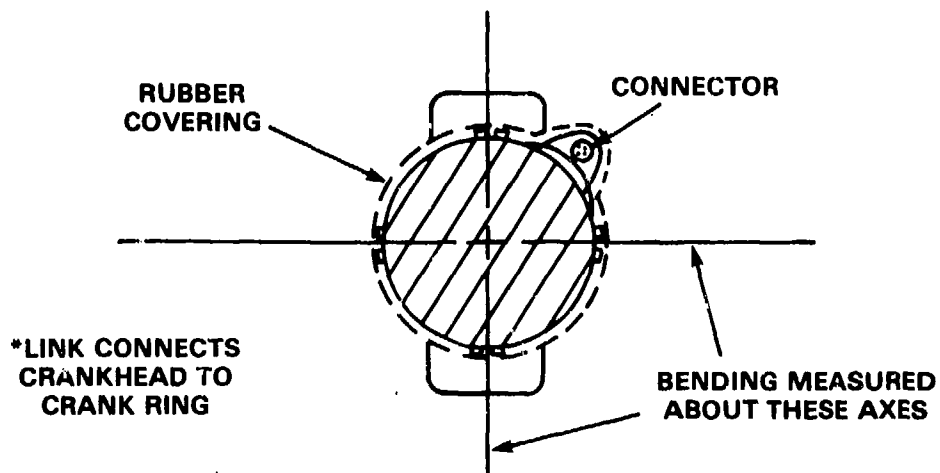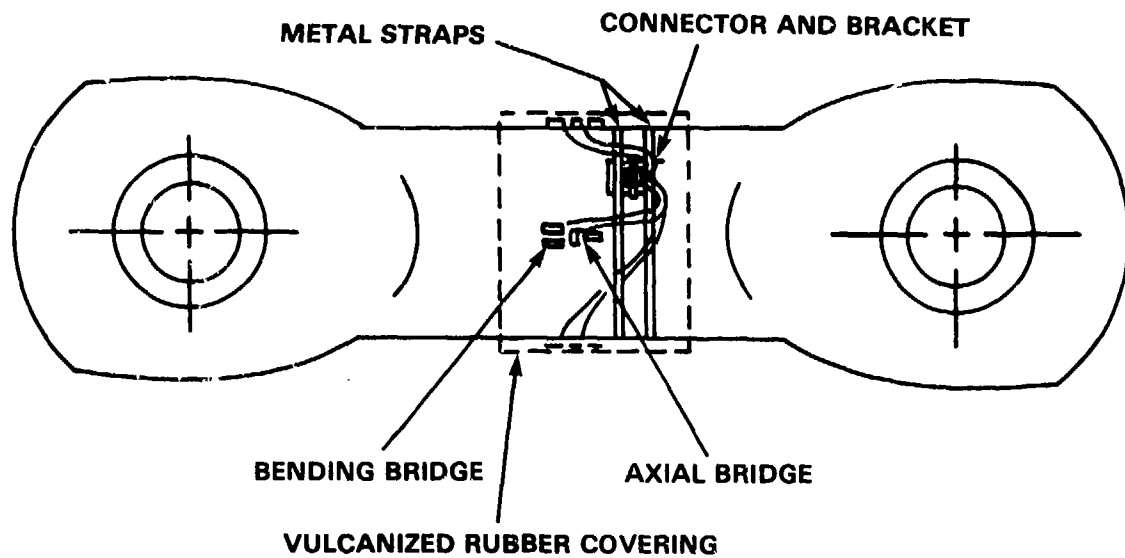
Figure 8 - Arrangement of Strain Gages on Links on
USCG POLAR STAR

67

SERVO SPOOL SHAFT   SERVO BOX

T1 T2 T3 Q   FWD

STRAIN
GAGES

RPM

TELEMETRY
AND BATTERIES   ANTENNA

P
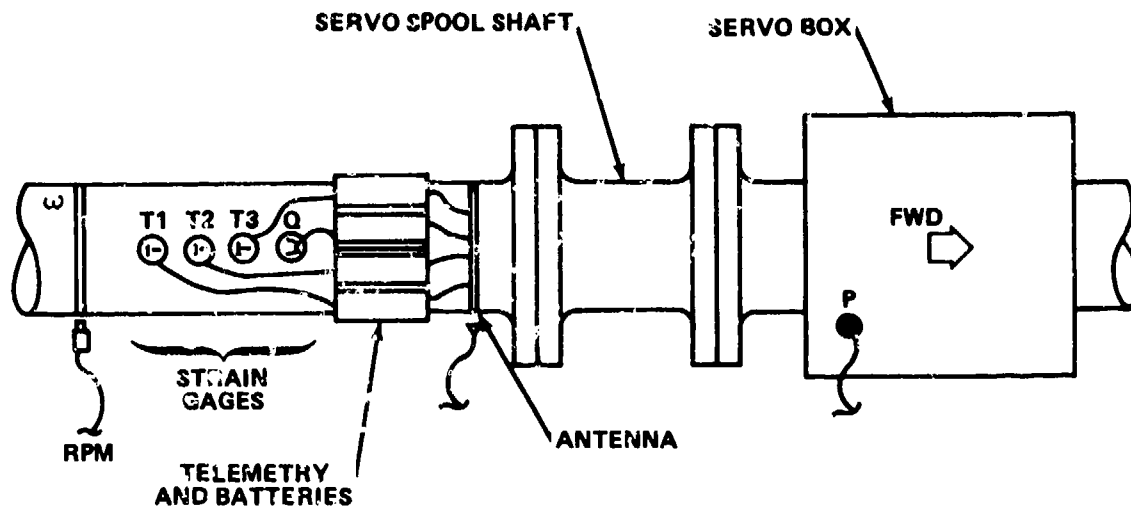
QUANTITIES MEASURED

Q — MEAN AND ALTERNATING TORQUE
T1 — MEAN AND ALTERNATING THRUST
T2 — MEAN AND ALTERNATING THRUST
T3 — MEAN AND ALTERNATING THRUST
W — SHAFT RPM (INDEX PROP. BLADE 1 AT 12 O'CLOCK POSITION)
P — PROPELLER PITCH

Figure 9 — Typical Inboard Shaft Gages

68

TABLE 6 - SHIP'S TYPICAL INFORMATION GAGES

Parameter	Location
Torque	Line Shaft
Thrust	Line Shaft
RPM	Line Shaft
Pitch	Shaft Alley
Rudder	Steering Room
Speed	Bridge
Hull Motions	Main Deck
Wind	Bridge

Inboard and outboard gages on the propeller and line shafts were linked to conditioning, monitoring, and recording electronics in the trial room via slip rings or telemetry, Figures 1, 9, 10, 11* and Table 6. All other ship's information channels were hard wired directly to the trial room electronics, Figures 13 and 14. The electronics instrumentation used for conditioning, monitoring and recording the trial information were all standard commercially available items.

SYSTEM CALIBRATION

All gages were electronically shunt calibrated before, during and after trials. Electronic calibrations were routinely scheduled into the trial agenda. With few exceptions, variations in the shunt calibrations were approximately ±1 percent. In addition to electronic calibration, physical calibrations (known loads, pressures, displacements, etc.) were applied where possible. Physical calibrations are discussed in another section of this chapter (see Test Conditions).

GAGE PROTECTION

Although certain experimental tools, such as strain gages, have been available to the technical community for a number of years[3] the lack of adequate gage protection has hampered their use in measuring strains, vibrations, and pressures on a marine propeller.

---

*More detail on this system is given in "Signal Transmission" Section.
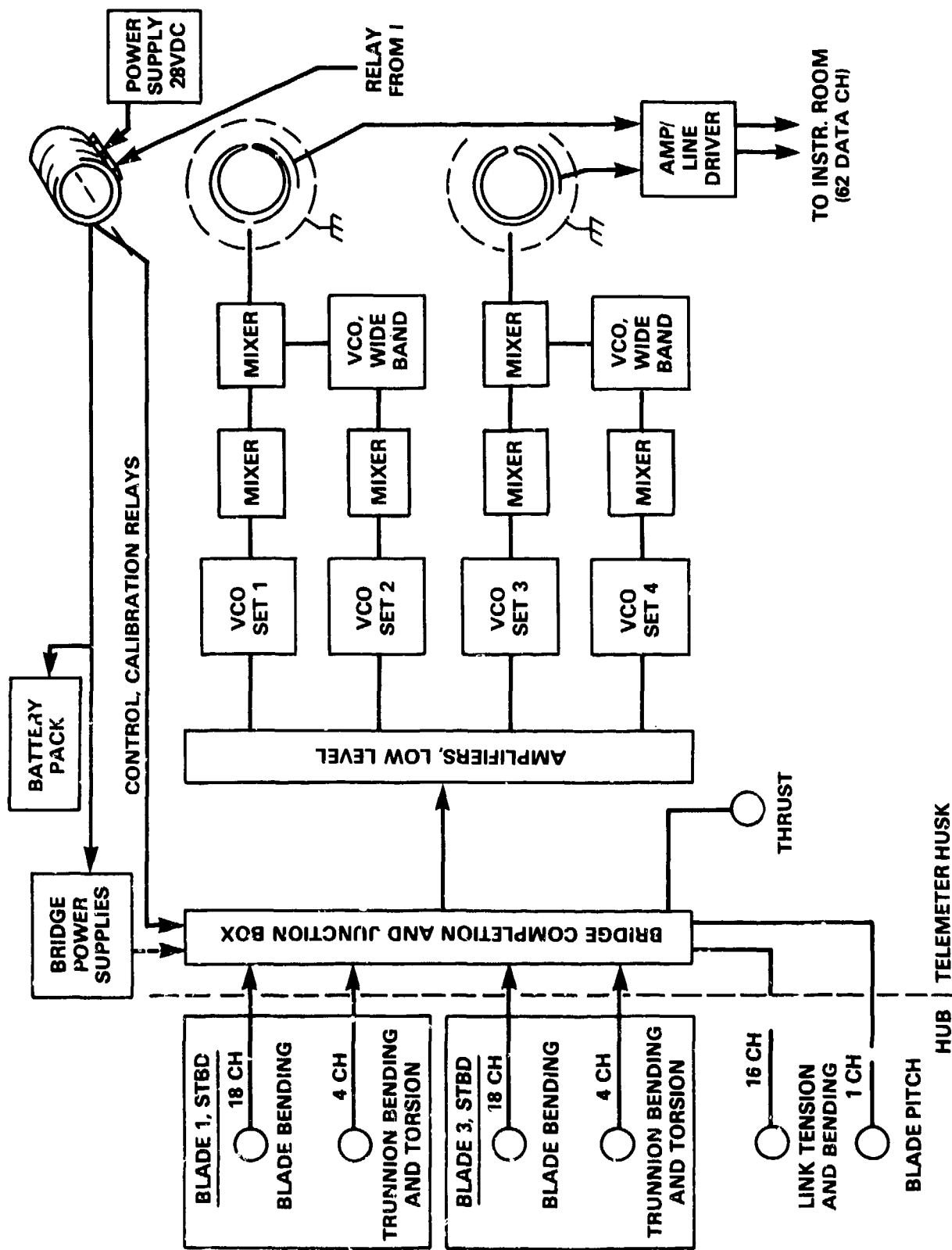
Figure 10 – Instrumentation in Hub and on Shaft on
USCG POLAR STAR

70
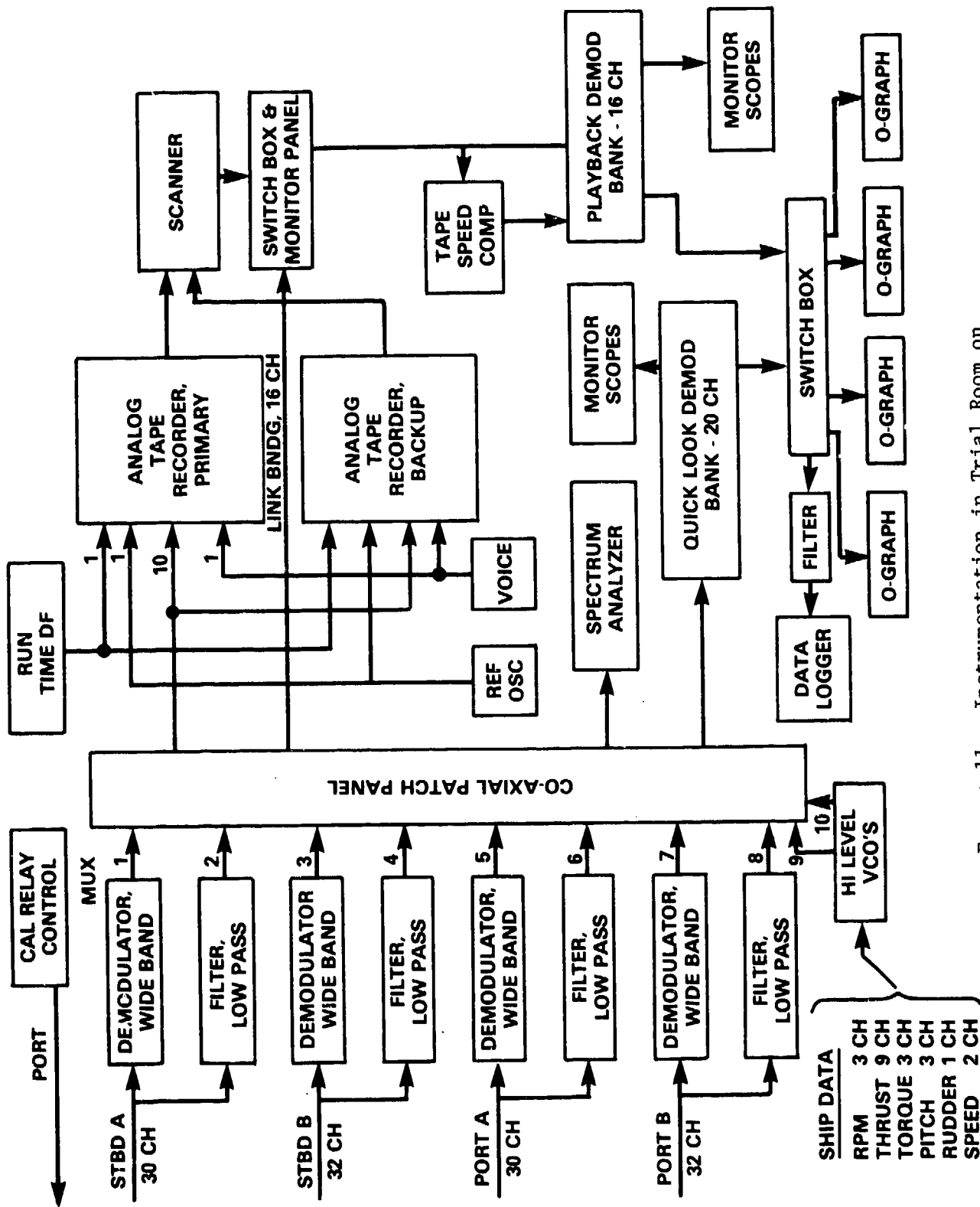
Figure 11 – Instrumentation in Trial Room on USCG POLAR STAR

71

An ideal protective coating for gages located on a marine propeller should have the following characteristics:

1. Resist water absorption for long periods.

2. Survive hydrodynamic flow forces including cavitation.

3. Not adversely affect the transducer characteristics.

4. Not change the hydrodynamic characteristics of the propeller blade.

Early experience at DTNSRDC led to an extensive evaluation of epoxy-bonded neoprene rubber coatings in underwater applications of strain gages. As part of the ROOSEVELT and DOUGLAS trials, a systematic series of static and dynamic tests were performed to evaluate various combinations of epoxies and elastomeric materials.[4,5] Although successful trials were conducted with this type of coating, they were found to be difficult and laborious to apply. In addition, it was not possible to determine their long term suitability in actual use. For trials on BARBEY[1] two other coating systems were evaluated; the primary system was a vulcanized rubber[6] and the secondary system was a spray polyurethane. These were selected on the basis of laboratory tests which showed them to have superior durability to the epoxy-bonded neoprene system. Although the vulcanized and polyurethane systems were used for gage protection on the BARBEY propeller blades, one epoxy-bonded neoprene patch was applied on one blade to serve as the basis for judgment of the comparative performance of these systems. The performance of the various protection systems was monitored periodically in order to evaluate the long-term effects of submersion and cavitation. A final evaluation was made when BARBEY was drydocked. The results are tabulated in Table 7. It is obvious from this table that virtually all gages under the primary system (vulcanized rubber) were intact and operational; the rubber on the propeller blade showed no wear or damage after 287 days of submersion and approximately 1400 hours of main propulsion plant operation. It is noted that the spray polyurethane provided good protection during the trial periods but did not survive the long-operation period, thereafter.

The epoxy-bonded neoprene patch (reference system) which was placed on the 80 percent radius (3/4 chord, back side) of the propeller was partially intact at the final evaluation.

72

TABLE 7 – LONG-TERM EFFECTS OF SUBMERSION AND CAVITATION ON
OUTBOARD INSTRUMENTATION ON USS BARBEY

Period	Surviving Gages								Total Number of Days Submerged	Operation Total Number of Main Propulsion Plant** Hours
	Number and Percent of Surviving Gages									
	Vul. Rubber		Spray Methane		Total					
	Number	Percent	Number	Percent	Number	Percent				
Original Flooding (4/25/75)	96	100	24	100	120	100			0	0
Completion of Sea Trials (4/12/75)	96	100	18	75	114	95			11	100
Dockside (8/8/75)	96	100	0	0	96	80			125	700
Drydocking to Remove CP Propeller System (1/13/76)	80*	83	0	0	80	67			287	1371

*Gages lost inboard at sliprings: further investigation showed gages to be good at installed location.

**Total operating time for CP propeller system since original installation (November 1973) was 3439 hr.

73

After the BARBEY work, the vulcanized rubber technique was used exclusively on all trials, Table 8. The longest and most demanding test for this system was on the POLAR STAR trials. This gage protection system was originally installed on the propeller blades and trunnion links in 1977, Reference 7. From that time to the present (1980), the POLAR STAR has logged approximately 100,000 nautical miles in two trips to the South Pole. While at the South Pole each time the POLAR STAR was involved in extensive ice breaking activity. After each deployment, the propulsion system was disassembled, modified, and reassembled. The vulcanized rubber protection which was originally installed has survived all of this activity and is still being used on the ship which is currently deployed to Alaska for further ice breaking activities. Additional propeller blade data have been taken during these trials (April 1980). Details of the vulcanizing process are given in References 1 and 5. Basically the process included:

1. Machining of blades to provide for gages and leadwires,

2. Preparation of blades (cleaning, priming, etc.) and specialized handling and layout of equipment,

3. Installation of gages and leadwires (Figure 12a),

4. Installation (vulcanization) of the coating (Figure 12b), and

5. Coating adhesion tests, instrumentation checkout, and calibrations.

Steps 1 through 3 and 5 are usually done at DTNSRDC. The vulcanization has been done either at Rohr Industries in Riverside, California or at Martin-Marietta in Baltimore, Maryland. Both locations have the large autoclaves necessary to vulcanize a full-scale propeller blade. In summary, it can be concluded that underway propeller measurements can be made with the assurance that when used with a vulcanized rubber protection system, the instrumentation will survive the adverse environment of the propeller for extended periods. In cases where vulcanization is not practical, epoxy-bonded neoprene or spray polyurethane can be used on a short-term (one- or two-week) basis.

Vulcanized rubber was also used on the other CP propeller components which are instrumented; see Table 8. In all these cases, a synthetic rubber was used because these components are internal to the hub and therefore are exposed to lubricating oil.

TABLE 8 - SUMMARY OF GAGE PROTECTION TECHNIQUES USED ON PROPELLER
PARAMETER TRIALS AT THE DAVID W. TAYLOR NAVAL SHIP
RESEARCH AND DEVELOPMENT CENTER

Propulsion System Component	Ship [1]						
	CVA-42	PG-100	FF-1088	DD-963	FFG-7	WAGB-10	R/V
Blades	E[2]	E	E,V,P*	V	[2]	V	V
Bolts	--[2]	--[2]	V	V	V	V[3]	V
Crank Disk	--[2]	--[2]	V	V	--[2]	--[3]	--[2]
Trial Data	5/67	1/70	4/75	8/76	4/79	12/77[4]	4/79

*E = epoxy-bonded neoprene rubber; V = vulcanized rubber; and
P = polyurethane.

Notes: (1) For list of specific ships, see Table 1.

(2) Component not instrumented (or not applicable to propulsion system).

(3) WAGB-10 was the only controllable pitch propulsion system tested which did not have bolted blades. Blade trunnion and pitch changing links were instrumented.

(4) Date of original trial installation. The most recent trial (5/80) has just been completed using the same instrumented components.

Figure 12 – Instrumented Propeller Blade Before and
After Vulcanization

GAGES
(TYPICAL)

LEADWIRES
(TYPICAL)
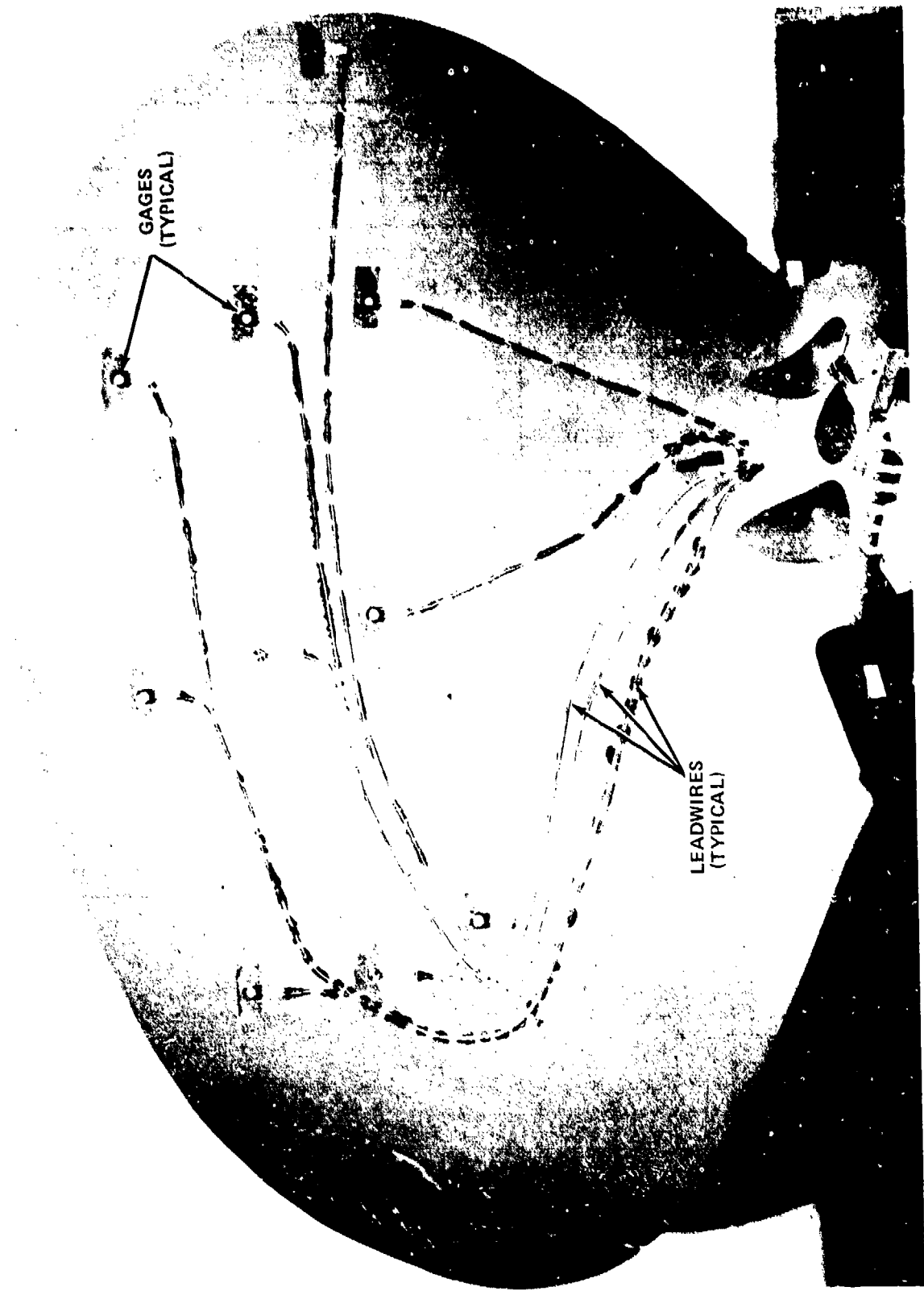
Figure 12a – Instrumented Blade Prior to Vulcanization

76

PRESSURE GAGE
LOCATION
(TYPICAL)

Figure 12 (Continued)

Figure 12b – Instrumented Blade After Vulcanization

SIGNAL TRANSMISSION

Transducer signals are transferred from the propeller to conditioning electronics via a signal transmission system similar to that shown in Figure 1. The transmission path can be divided into:

1. Propeller blade to hub junction.

2. Propeller hub and shaft.

3. Rotating or stationary interface to trial room.

Details of these systems on a conventional (fixed pitch) propeller and the DOUGLAS CP propeller are shown in Figures 13 and 14. Variations include both internal and external wiring between blades and hub to allow pitching of the blades. Propeller line shaft transmissions are accomplished by a specially constructed conduit within the hollow bore of the shafting. Rotating or stationary interfacing has been accomplished by both slip-ring and telemetry transfer techniques. From this point the transducer signals are cabled to a central location (trial room) where they are electronically conditioned for monitoring and recording purposes; see Figures 11 through 15.

The signal transmission system represents a major expenditure in the overall cost of full-scale trial data acquisition. Because propulsion systems for different ship classes are different, each transmission system has to be individually designed and each ship's propulsion system on which it is to be installed must be modified to accept it. The installation and removal of these systems involve multiple drydockings and propulsion system disassemblies and reassemblies. After trials the transmission systems are usually discarded because they cannot be reused or modified for ships of different classes.

The DTNSRDC proposed to develop an Underwater Telemetry system (Hydrotelemetry) which could considerably reduce the cost of these trials.* Some work has been done at DTNSRDC to develop this system. Its availability would eliminate much of the propulsion system modifications and drydock costs. A prototype system was installed on the SPRUANCE. Results indicate that the transmission of transducer intelligence directly, as shown conceptually in Figure 16, is possible. However, more work is needed to make this system suitable for full-scale trial measurements.

---

*Reported informally as Enclosure to DTNSRDC Letter 964:CJN,987D.1 of 5 Feb 1970.
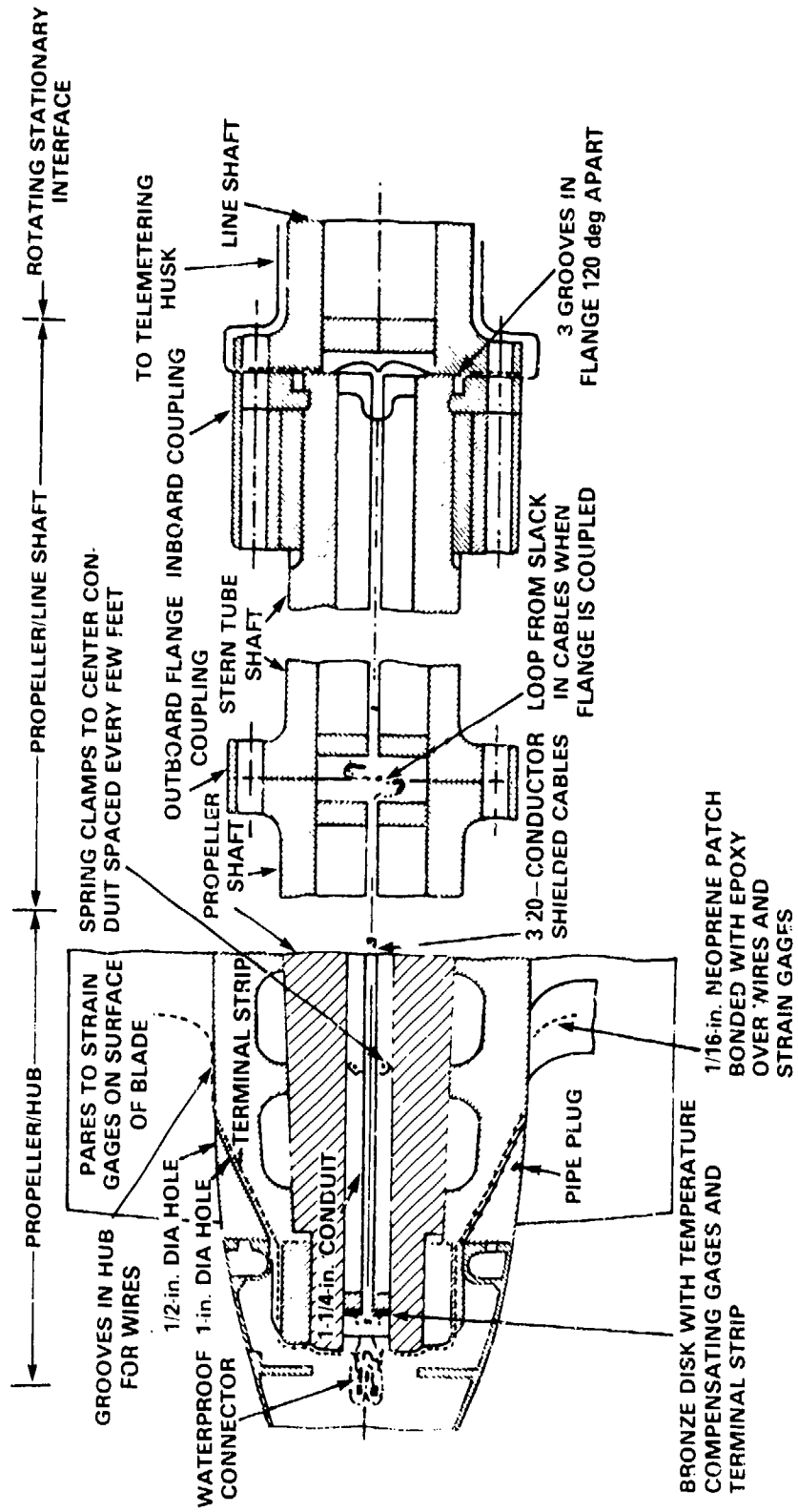
Figure 13 – Signal Transmission System on a Conventional (Fixed Pitch) Propeller on USS FRANKLIN D. ROOSEVELT

79

Figure 14 – Signal Transmission System on a Controllable Pitch
Propeller on USS DOUGLAS

PROTECTIVE COATING

DRILLED HOLE FOR LEAD WIRES

ROTATING JOINT
ACCOMODATES PITCH CHANGE

PROPELLER
SHAFT

LEAD WIRES FROM
STRAIN GAGES ON BLADES

STRAIN
GAGE

CRANK PIN

CRANK DISK

PLUG

HUB

U-TUBE WITH
LEAD WIRES
1/4" DIA-M.

72 LEADWIRE BUNDLE ROUT'D IN
CENTER WIRE TUBE TO SLIPR'NG ASSEMBLY

DRY TERMINAL COMPARTMENT

AFT TERMINAL BOARDS

PISTON

INNER OIL TUBE

SERVO OIL

CYLINDER

HUB
OIL

COVER PLATE

Figure 14a – Propeller and Hub Detail (Internal Wiring)
USS DOUGLAS

80

Figure 14 (Continued)
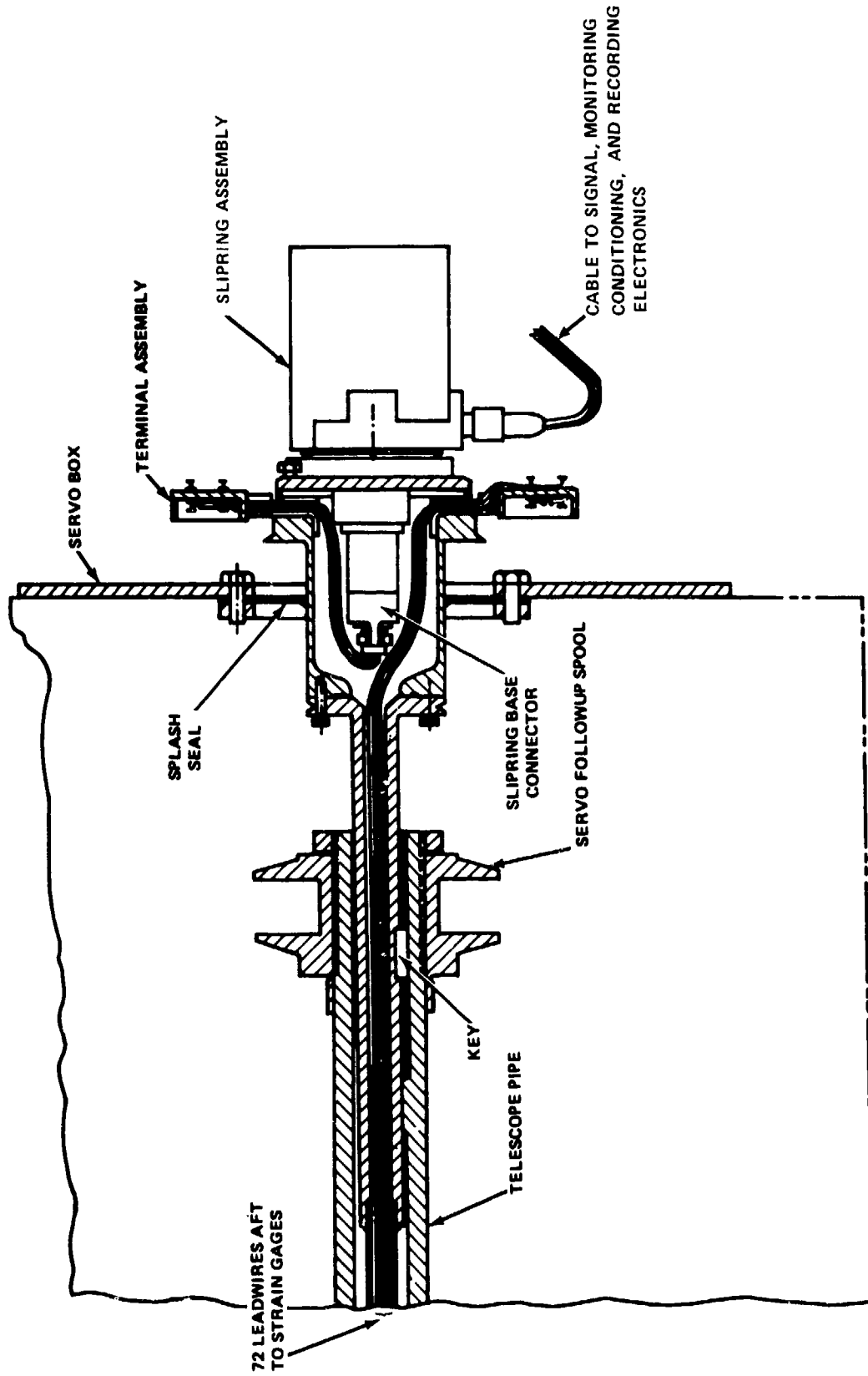
Figure 14b — Rotating/Stationary Transfer Detail
(Slip Ring Technique)

81
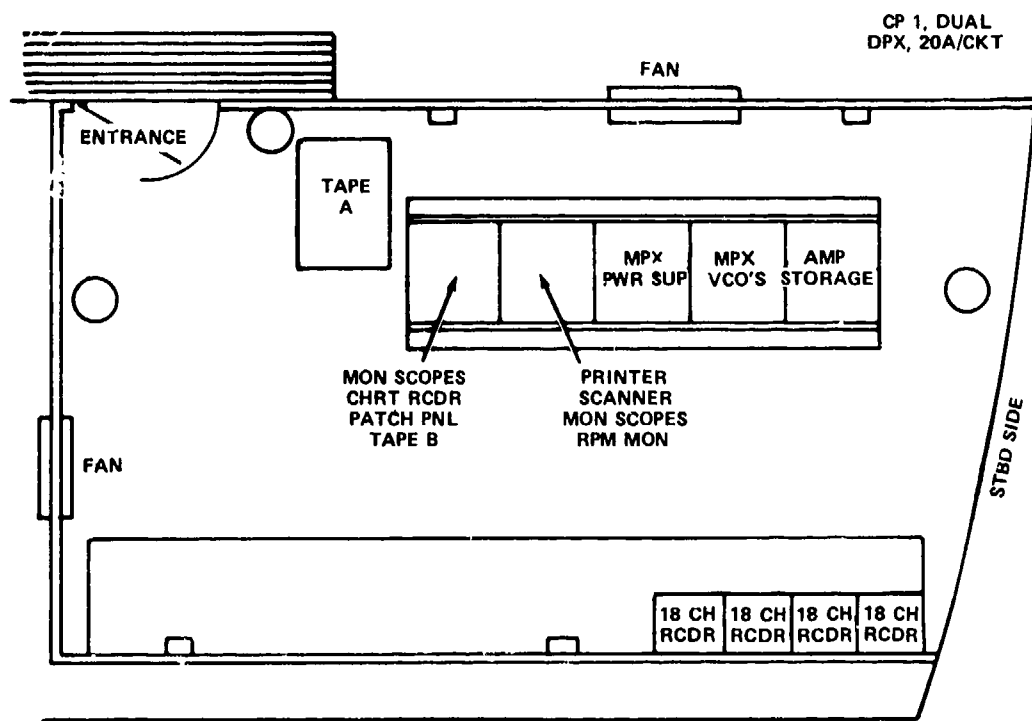
Figure 15a - Trial Room of USCG POLAR STAR
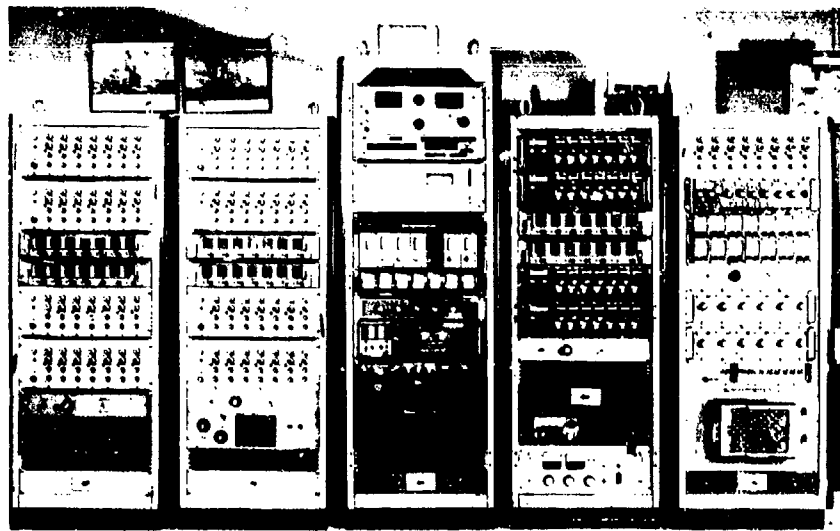
Figure 15b - Trial Room of R/V ATHENA

Figure 15 - Layout of Trial Room
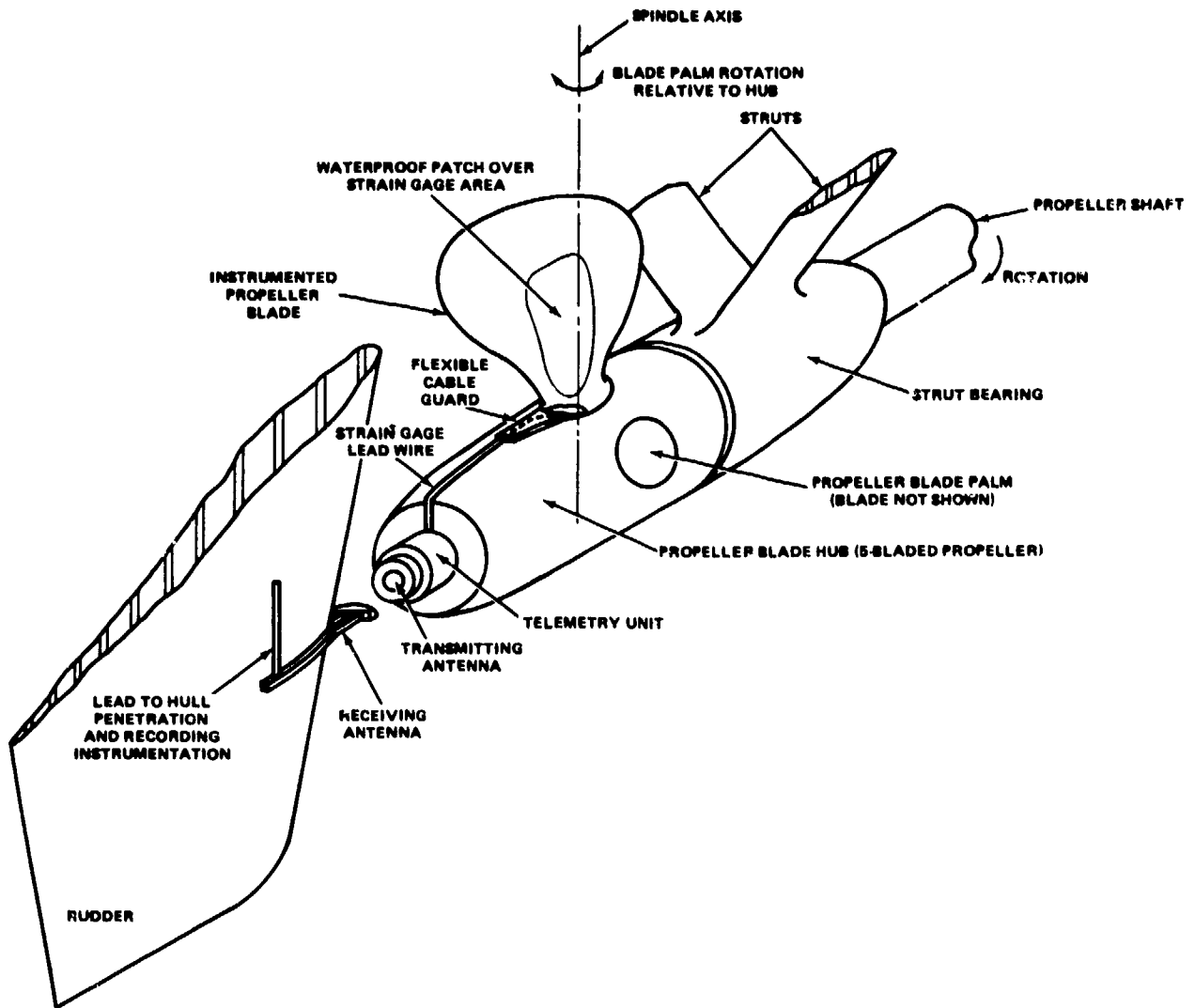
Figure 16 – Conceptual View of Underwater Telemetry System

RECORDING AND MONITORING

After the electronic signals were taken off the propeller line-shaft inboard the ship, they were cabled to a central location (trial room) for further processing. Figure 15 shows one of the trial room layouts. In addition to the propeller data, any number of channels of "ship's information" (e.g., both mean and alternating shaft torque and thrust, rpm, propeller pitch and position, rudder angle, ship speed, wind direction and speed, etc.) were also measured and cabled to the trial room for processing. Of the up to 300 channels of information which were brought into the trial rooms, several dozen were closely monitored (analog data were converted to engineering units) and plotted against failure criteria. This was done to prevent damage or failure of the propulsion system. The failure criterion which seemed most appropriate to the propeller components under test was that of fatigue failure. Therefore, the fatigue characteristics of the components in question were considered in setting the limits of stress that should not be exceeded during trials, as shown in Figure 17.

Critical measurements were plotted on the graph as the trial progressed. Any test condition which exceeded the criteria was not repeated and the agenda was subsequently modified to avoid conditions which data extrapolation indicated would also exceed the trial criteria

Analysis of the test data was done using both manual (oscillograph) and automated (computer) techniques,[8] Figures 18 and 19 and Table 9. All data channels were visually monitored on oscilloscopes before and after recording on magnetic tapes.

TEST CONDITIONS

The CP propeller trials programs involved a series of laboratory, drydock, dockside, and underway tests. The laboratory, drydock, and dockside tests provided calibration and response to known loads as well as a general system checkout. Underway tests, provided information under actual conditions of operation.

LABORATORY TESTS

Blade bolts and trunnion links were calibrated in the laboratory at DTNSRDC using 100,000 and 800,000 pound load test machines; see Figure 20. In addition to providing calibrations, these tests provided data to check the value of the elastic modulus of the bolt material and the effective area of the links.

84
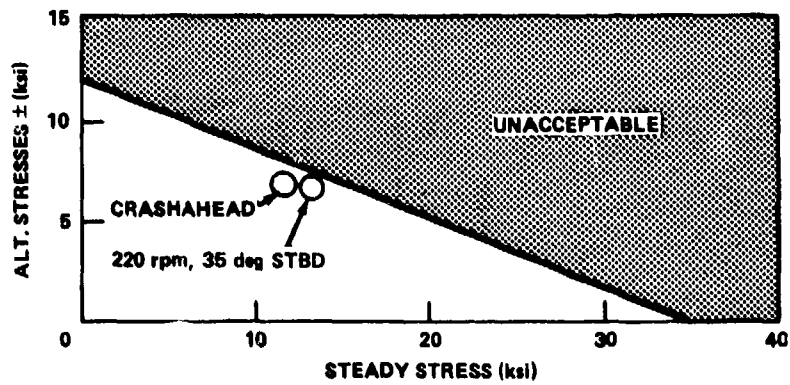
Figure 17a - Propeller Blades (Ni-Al-Bronze)
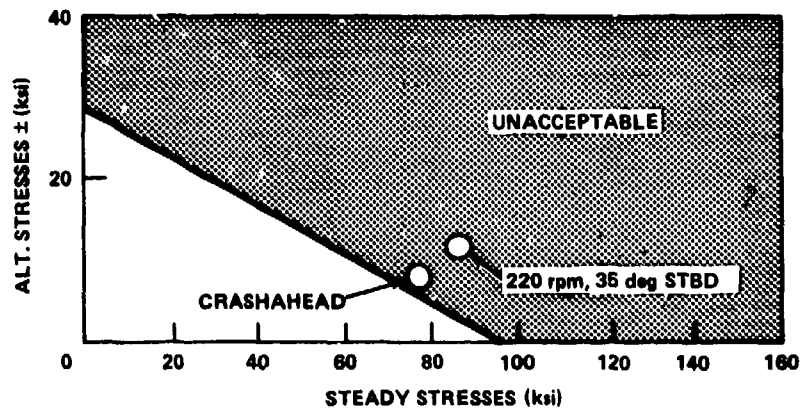
Figure 17b - Propeller Bolts (17-4 Ph)
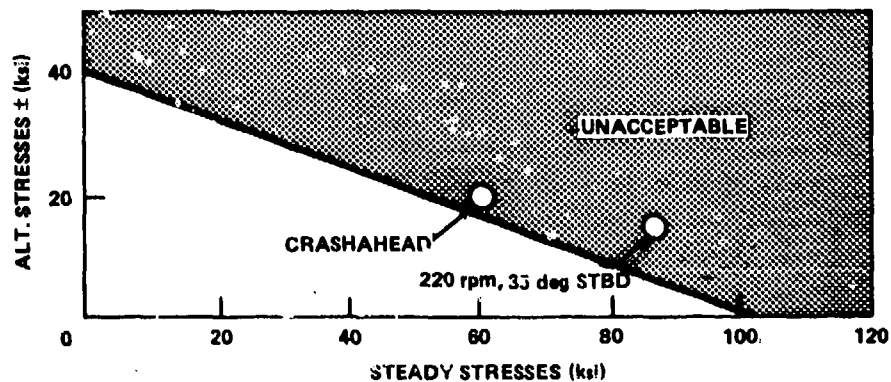
Figure 17c - Crank Disks (HY-100)

Figure 17 - General Controllable Pitch Propeller Stresses versus Limits
for Propeller Blades, Bolts, and Crank Disks for
USS BARBEY Trials
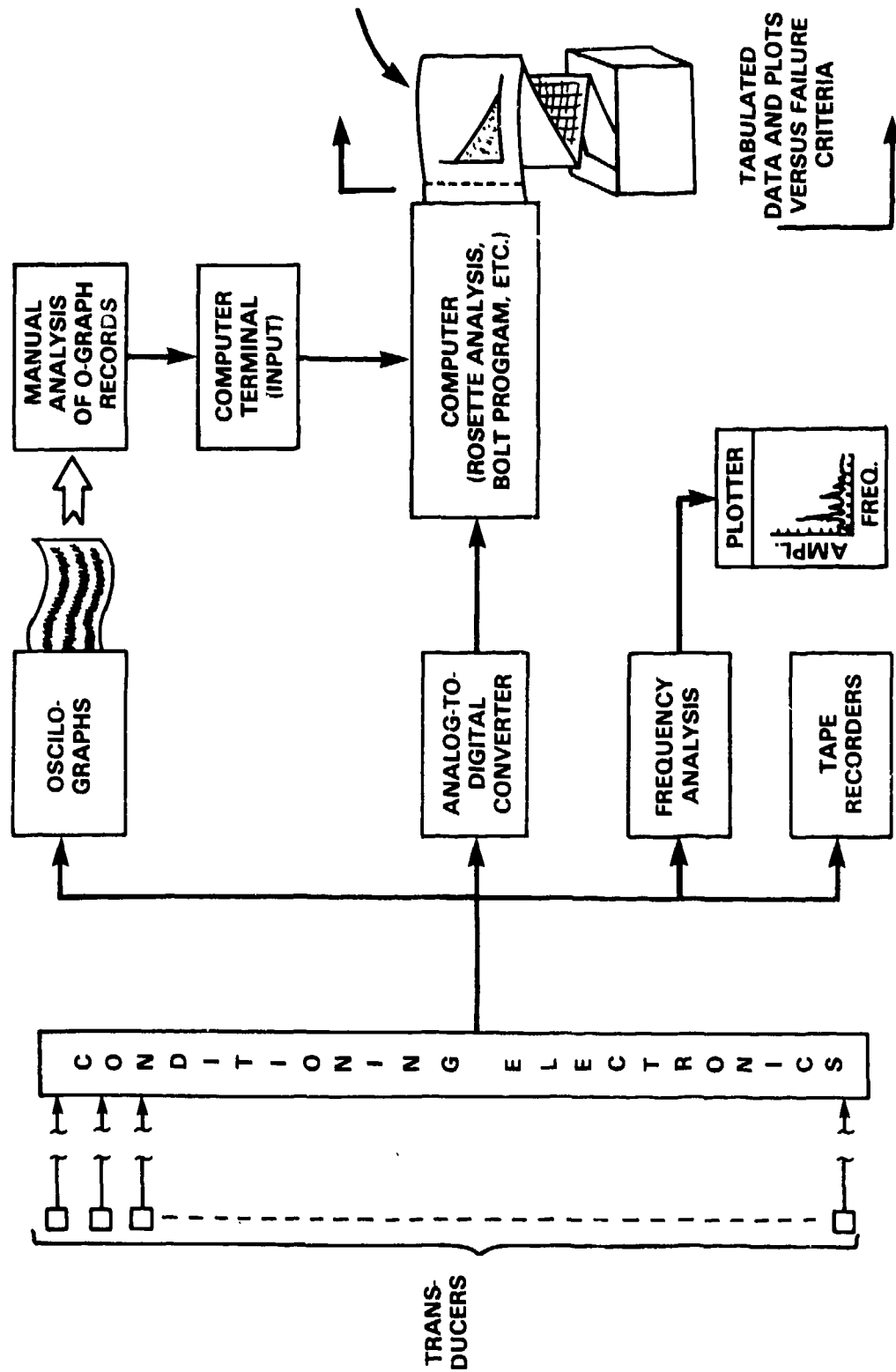
Figure 18 – Onboard Data Monitoring and Analysis

Figure 19 – Typical Computer Output

TODAYS DATE: 2-7-80
TIME= 16 HRS 13 MINS

PIVOT AXIS

L.E.

MTL

1

2

3

C.L.PROP
HUB

ROSETTE LOCATIONS:
1: 40%RAD 25%CHORD
   PRIN. STRESS=7684.PSI
2: 40%RAD 50%CHORD
   PRIN. STRESS=9953.PSI
3: 40%RAD 75%CHORD
   PRIN. STRESS=14840.PSI
FS=10000 PSI

MTL=MAX THICKNESS LINE
L.E.=LEADING EDGE

R.V.ATHENA
PROPELLER LOAD TEST
(UNDERWAY) MEAN STRESSES
BLADE NUMBER: 4
RUN: 48 AT 655 RPM
LOOKING AT PRESSURE SIDE
PROPELLER MATERIAL:
STAINLESS STEEL
MODULUS(E)=27.6(10*6)PSI
POISSONS RATIO(U)=0.305

Figure 19a – Physical Orientation of Measured Propeller Blade Stress Vectors

Figure 19 (Continued)

RESULTS OF ROSETTE STRESS CONVERSION PROGRAM (ROSE), ROSETTE P-8
PROJECT: R V ATHENA RUN NUMBER=48   TODAYS DATE: 2-5-80
SYSTEM: GAGE (A)=101 GAGE (B)=100 GAGE (C)=99   TIME= 12 HRS 43 MINS

YOUNGS MODULUS (E)= 27.6
POISSONS RATIO (U)= .30

STRAIN (A)= 152.5 MICROINCHES
STRAIN (B)= 325.   MICROINCHES
STRAIN (C)= 178.   MICROINCHES

STRESS (A)= 4.81 KSI
STRESS (B)= 8.97 KSI
STRESS (C)= 4.91 KSI

MAX SHEAR=3387. PSI

MAX STRESS=9953. PSI
AT ANGLE OF=47.27 DEG
FROM STRAIN (A)
FROM STRAIN (B)2.268 DEG
MIN STRESS=3177. PSI
AT ANGLE OF=137.2 DEG
FROM STRAIN (A)
POS. ANGLE IS COUNTERCLOCKWISE

PERIMETER=300 USTRAIN
INPUT-MEAN STRAINS

PERIMETER=10000 PSI
OUTPUT-MEAN STRESSES

Figure 19b – Details of Rosette Analysis (Input and Output)

88

Figure 19 (Continued)
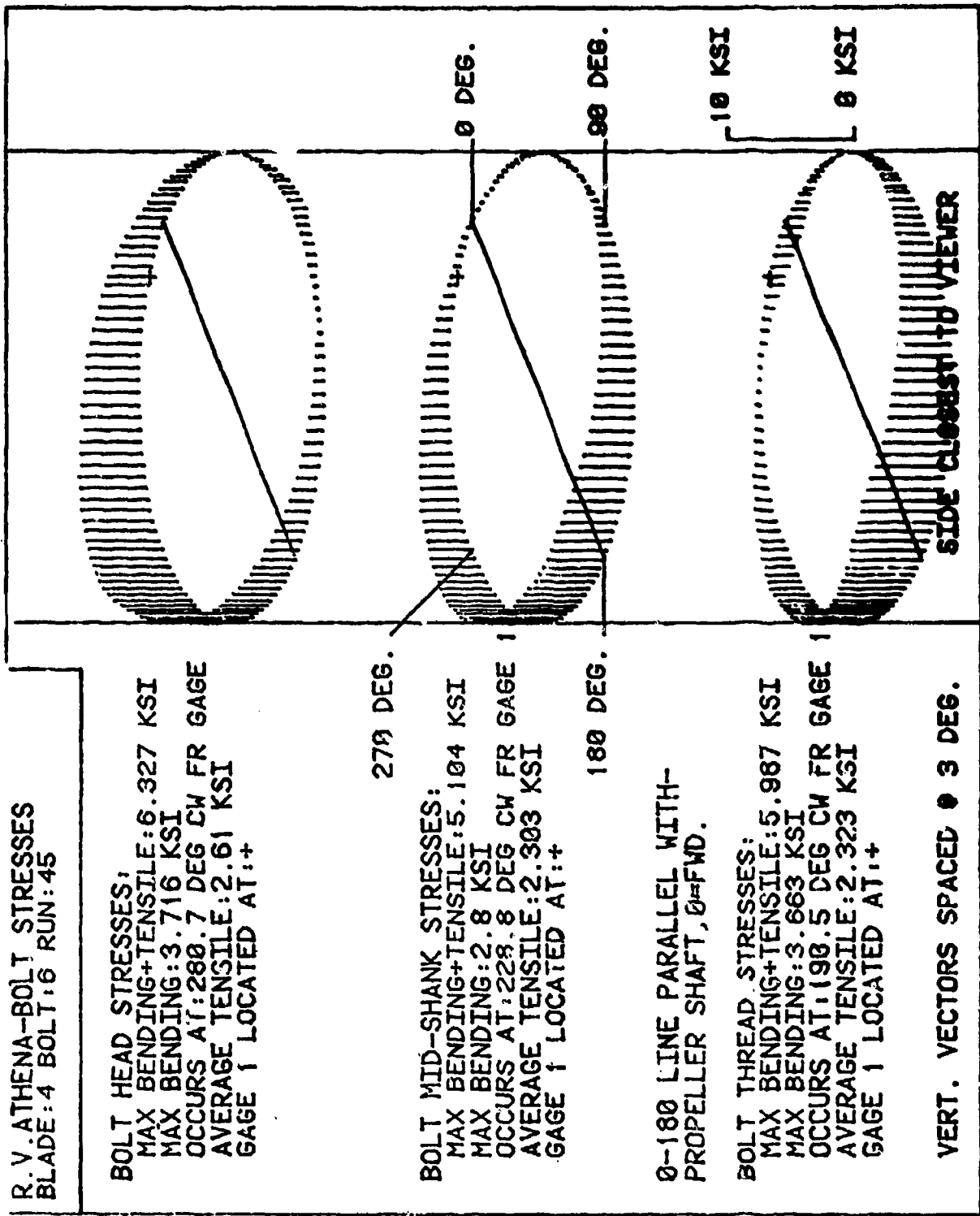
Figure 19c – Bolt Stresses on R/V ATHENA

89

Figure 19 (Continued)

USS SPRUANCE FULL SCALE TRIAL DATA

RUN NUMBER   222
POINT NUMBER   477
PHASE   B
DATE AND TIME OF RUN   04-JUN-77   01:45:21
RUN ID FILTER 50 HZ×ZERO-RUN 219×   100% PITCH   150 RPM   35 DEG LEFT TURN
DATE OF PLOT   26-JUL-77
GAGE   GAGE #   BLADE #   BOLT #
A   62   4   0

Figure 19d - Computer Generated Fatigue Diagram
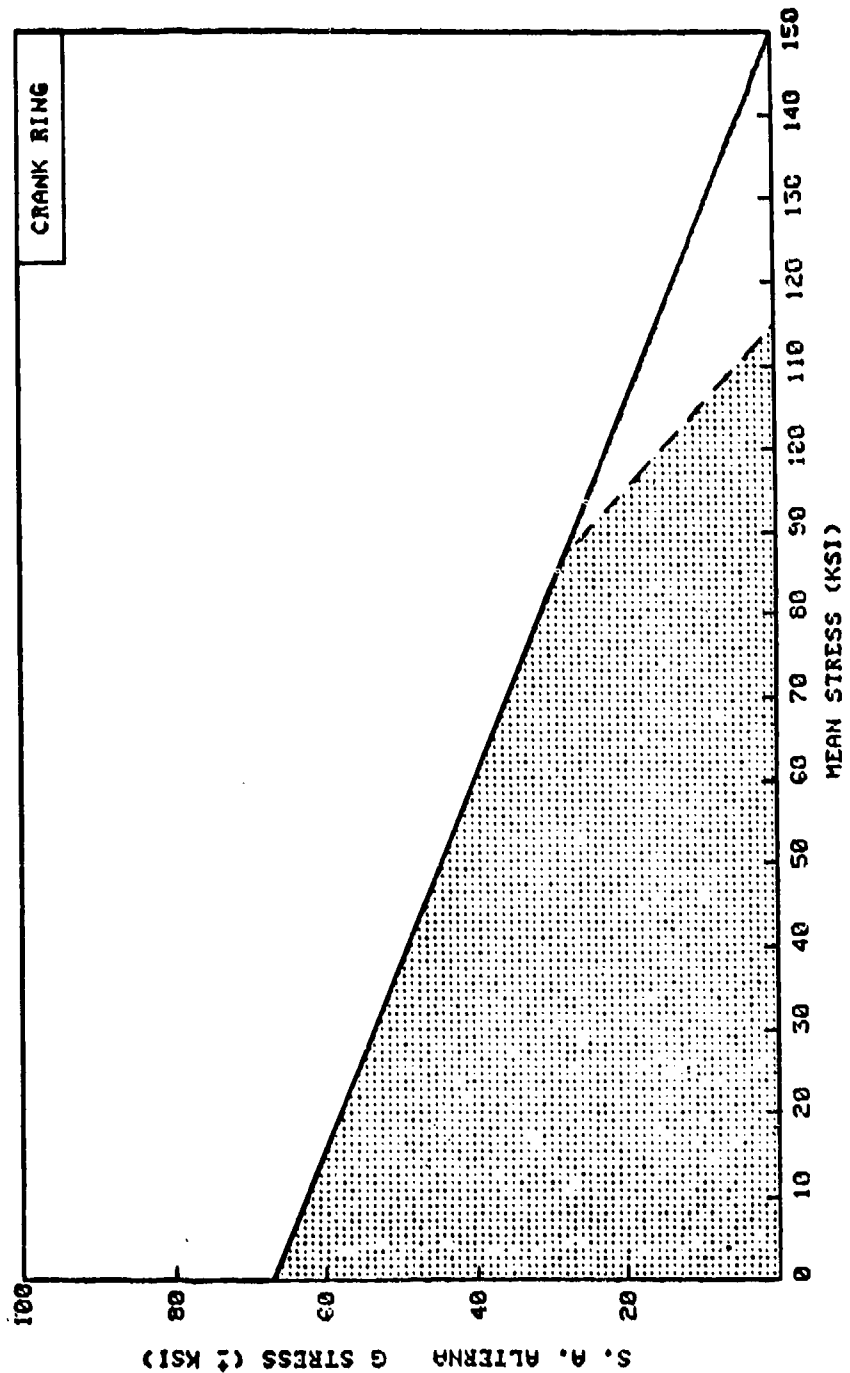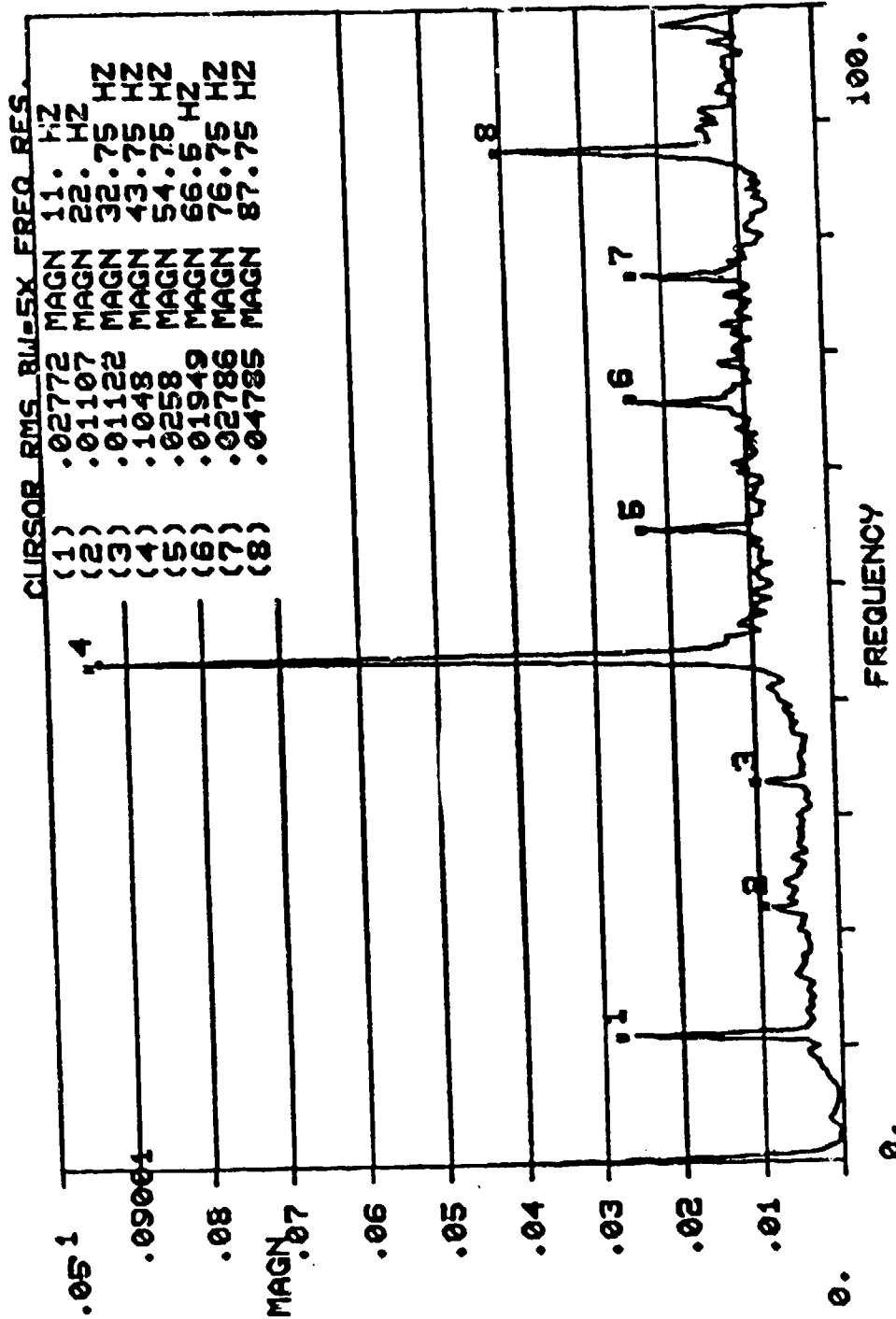
NOTES: 1 = GAGE A WITH PRESTRESS

90

Figure 19 (Continued)

Figure 19e – Frequency Analysis of Data (Accelerometer)

TABLE 9 – USS SPRUANCE COMPUTER DATA OUTPUT

| GAGE IDENTIFIER | | | | | | GAGE DATA | | | STRESSES WITHOUT PRESTRESS | | | | | | ALTERNATING | | | | PRE STRS |
| | | | | | | KSI/ | | | M E A N | | | EXTREME | | | | | | | |
CH	GAGE	B	TYPE	ID	LOCATION	VOLT	GAIN	ZERO	AVG	MAX	MIN	MAX	MIN	RMS	AVG	H10	MAX	
1	1	1	BOLT	8A	HEAD	-65.1	5	-2.2	0.3	-1.2	0.7	-3.0	3.6	1.4	2.1	2.6	3.1	34.6
2	2	1	BOLT	8B	HEAD	-65.3	10	-1.2	0.7	0.4	2.0	-3.2	5.4	1.7	2.9	3.4	4.0	32.3
3	3	1	BOLT	8C	HEAD	-65.9	20	-0.1	10.1	9.7	10.6	3.1	19.8	3.7	6.3	7.1	7.5	34.0
4	4	1	BOLT	8D	HEAD	-65.6	20	-0.9	11.0	8.4	12.1	3.3	21.0	3.5	5.8	6.8	7.1	35.8
5	5	1	BOLT	7A	HEAD	-66.2	20	-2.7	-4.0	-4.5	-3.7	-6.9	-1.3	0.8	1.3	1.6	2.0	36.8
6	6	1	BOLT	7B	HEAD	-65.7	20	-1.4	-6.1	-7.3	-2.9	-10.4	0.6	1.8	2.7	3.8	4.6	35.0
7	7	1	BOLT	7C	HEAD	-66.2	5	0.8	5.2	5.0	5.8	2.7	9.1	1.5	2.5	2.9	3.0	37.0
8	8	1	BOLT	7D	HEAD	-66.5	10	-0.4	6.8	5.8	7.8	-0.1	12.5	2.4	3.7	4.6	5.3	39.4
9	9	1	BOLT	6A	HEAD	-66.2	20	-0.5	7.3	6.9	7.7	3.6	13.9	1.7	2.9	3.4	3.8	40.9
10	10	1	BOLT	6B	HEAD	-66.4	10	-0.5	4.7	-1.4	5.6	-2.4	8.9	2.0	3.2	4.2	5.3	41.5
11	11	1	BOLT	6C	HEAD	-65.3	10	-2.0	-3.9	-4.1	-3.6	-6.9	-0.9	0.8	1.3	1.6	1.6	33.4
12	12	1	BOLT	6D	HEAD	-66.4	10	-0.7	-4.0	-5.1	-0.4	-8.1	2.5	1.7	2.7	4.0	5.1	34.6

PROPELLER BOLT STRESSES   RUN   73 PHASE A

| GAGE ID | | | | PRE-STRES | NO PRESTRESS | | | MEAN AND EXTREME STRESSES WITH PRESTRESS | | | S.A. ALTERNATING | | |
NO	BL	ID	TYPE		AVGMEAN	MAXIMEAN	EXTREME	AVGMEAN	MAXIMEAN	EXTREME	AVG	H10	MAX
1	1	8A		34.6	0.3	-1.2	3.6	34.9	33.4	38.2	2.1	2.6	3.1
2	1	8B		32.3	0.7	2.0	5.4	33.0	34.3	37.7	2.9	3.4	4.0
3	1	8C		34.0	10.1	10.6	19.8	44.1	44.6	53.8	6.3	7.1	7.5
4	1	8D		35.8	11.8	12.1	21.0	46.8	47.9	56.8	5.8	6.8	7.1
++++		MAX STRESS		36.0	12.7	13.7	23.7	48.0	48.9	58.9	6.8	7.8	8.1
-+++		TEN STRESS		34.2	5.5	5.9	12.4	39.7	40.8	46.6	4.3	5.0	5.4
-+++		BEN STRESS		1.8	7.1	7.8	11.2	8.3	8.8	12.3	2.5	2.8	2.7
++++		% BENDING		5.2	129.2	132.4	90.5	20.9	22.0	26.5	58.6	57.1	49.5
		1-(T1/T2)		0.7	11.1	33.2	11.5	1.0	5.1	2.7	3.4	5.0	5.5
		THETA		279.7	226.1	220.2	224.0	236.0	230.2	230.8	214.6	216.5	215.2
5	1	7A		36.8	-4.0	-4.5	-6.9	32.8	32.3	29.9	-1.3	1.6	2.0
6	1	7B		35.0	-6.1	-7.3	-10.4	29.5	28.3	25.2	-2.7	3.8	4.6
7	1	7C		37.0	5.2	5.8	9.1	42.2	42.8	46.1	2.5	2.9	3.0
8	1	7D		39.4	6.8	7.8	12.5	46.2	47.2	51.9	3.7	4.6	5.3
--++		MAX STRESS		39.1	8.4	9.6	15.0	47.3	46.5	53.9	3.3	4.0	4.4
--++		TEN STRESS		37.2	0.5	0.5	1.1	37.7	37.7	38.3	2.5	3.2	3.7
--++		BEN STRESS		1.9	7.9	9.1	13.9	9.6	10.8	15.6	0.8	0.8	0.6
--++		% BENDING		5.1	1625.0	1939.5	1299.5	25.5	28.7	40.7	30.4	24.0	16.5
		1-(T1/T2)		1.6	68.7	119.5	6.9	8.9	0.7	1.4	40.5	45.5	48.9
		THETA		267.0	234.7	235.6	235.1	240.8	240.9	238.8	218.2	214.5	214.7

TEST MACHINE (RAM)

BOLT

SOCKET
(USED TO EVENLY DIS-
TRIBUTE LOAD AND
PROVIDE CLEARANCE
FOR LEADWIRES)

STEEL
BLOCK

STEEL
BLOCK

TEST MACHINE (TABLE)
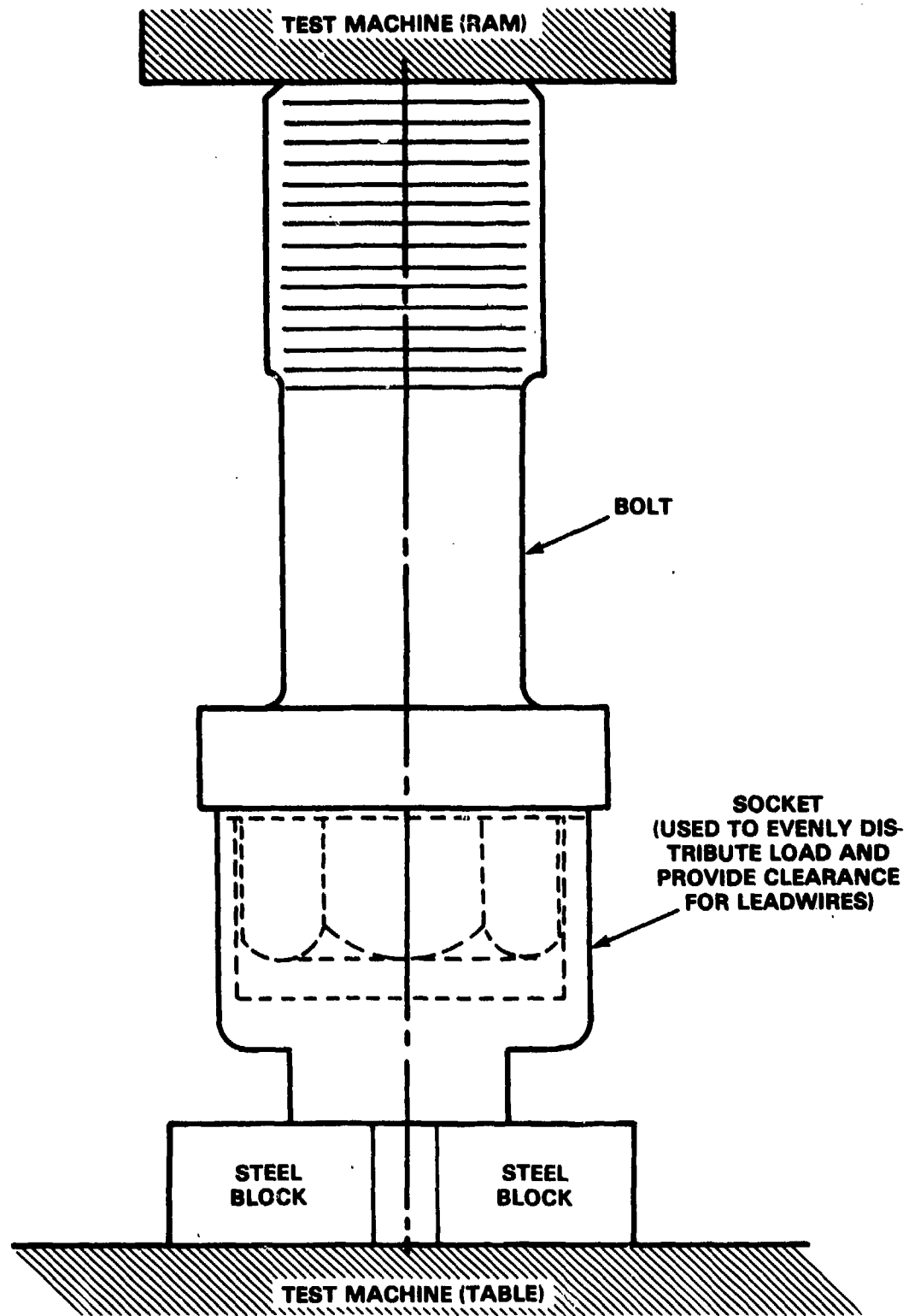
Figure 20 - Calibration of Controllable Pitch Propeller Components

DRYDOCK TESTS

Objectives of the drydock tests, as appropriate to the specific ships tested, were to:

1. Measure both pretrial and post trial bolt preload.

2. Measure induced stresses in the crank ring which result from bolt preloading.

3. Measure the static response of the instrumented CP propeller blade attachment to a known load.

4. Determine the natural frequencies of the propeller blades and the resulting effect on system response.

5. Provide an accurate pressure calibration for the blade pressure gages as installed in the ship.

Objectives 1 and 2 were accomplished during assembly of the propeller blades on the hub. Tests involved evaluation of a variety of techniques* recommended by manufacturers to determine bolt preloads.

Objective 3 was a system calibration to a known load. On BARBEY, SPRUANCE, and POLAR STAR the load was applied to the propeller blades using a hydraulic blade loader designed by DTNSRDC; Figure 21 and Table 10. The loader has nine hydraulic rams supplied by a single hydraulic pump, but with individual cutoff valves. The positions of the rams on the blades are shown in Figure 22. Loads were applied simultaneously to all rams in increments of 1000 pounds per ram up to 7000 pounds per ram. Ad hoc arrangements were used on the other ships.

Dynamic tests on the propeller blades, objective 4, included impulse tests to identify natural frequencies, and on BARBEY vibration generator tests to determine the forced response; see Figure 4.

All pressure transducers were calibrated using the propeller blade pressure gage calibrator shown in Figure 23. Characteristics of this system are given in Table 11.

---

*Various bolt installation techniques include "slugging up," torque measurements, angular rotation measurements, bolt stretch measurements, etc.

SHUT-OFF VALVES

RAMS (9)

PRESSURE CONTROL VALVE

HYDRAULIC PUMP

— — 0.7R

— 0.8R

— 0.9R

MOUNTING BASE

DRYDOCK FLOOR
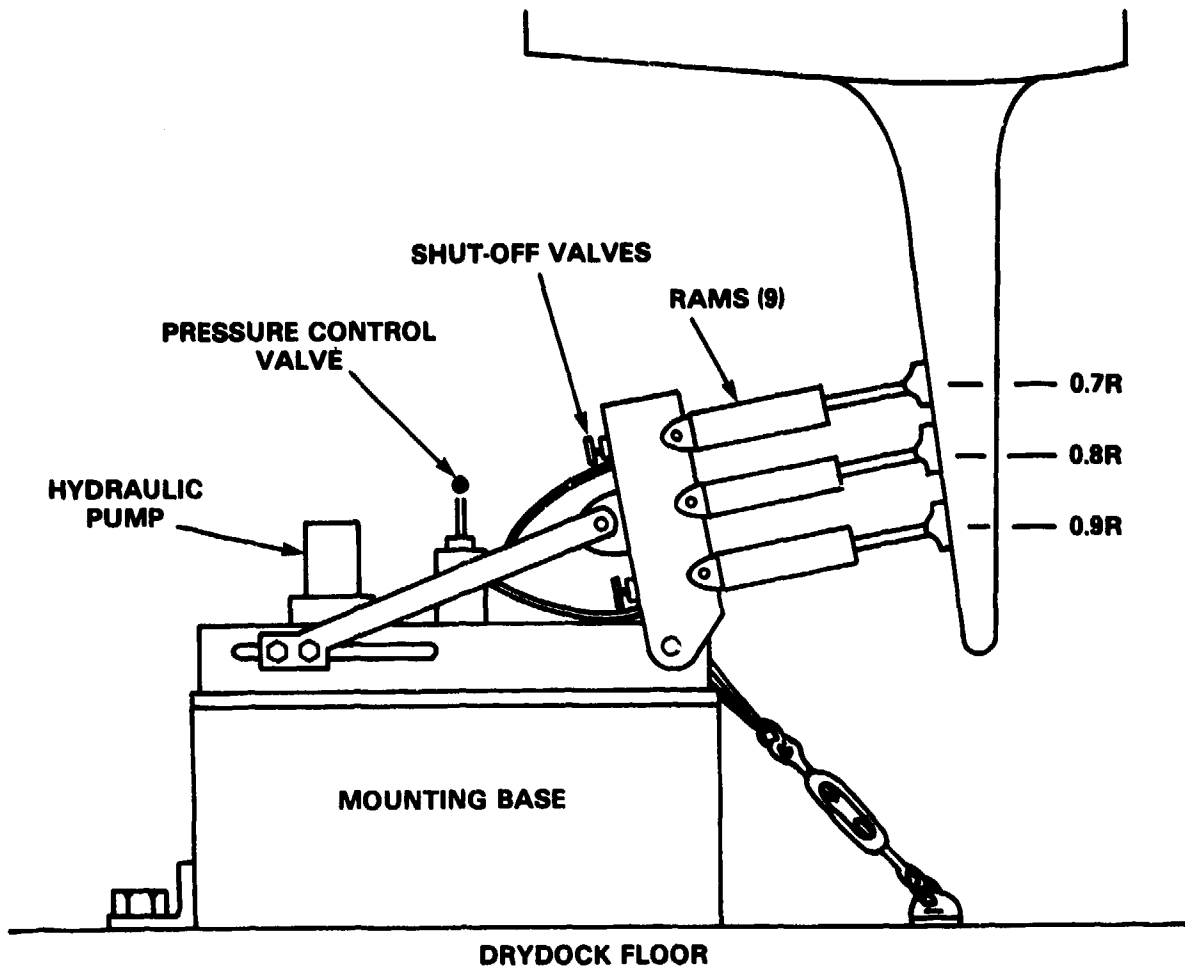
Figure 21 – David W. Taylor Naval Ship Research and Development Center
Propeller Blade Loader on USS SPRUANCE, USS BARBEY, and
USCG POLAR STAR

TABLE 10 - CHARACTERISTICS OF THE DAVID W. TAYLOR NAVAL SHIP RESEARCH AND
DEVELOPMENT CENTER HYDRAULIC BLADE LOADER

Number of Rams....................................	9
Ram Locations (on Propeller Blade):	
Percent Radius................................	60,70,80
Percent Chord (from leading edge).............	25,50,75
Maximum Ram Pressure, psi......................	1,000
Maximum Force Ram, lb..........................	8,000
Maximum Total Loader Force (9 Rams), lb........	72,000

TABLE 11 - CHARACTERISTICS OF THE DAVID W. TAYLOR NAVAL SHIP
RESEARCH AND DEVELOPMENT CENTER PROPELLER BLADE
PRESSURE GAGE CALIBRATOR

Pressure Range (regulated)	0 to +50 psig
Vacuum Range	0 to -13.2 psig (27 inches of mercury)
Convertible Compressor and Vacuum Pump	1/2 hp
Two Reservoirs (Pressure and Vacuum)	9 gal
Secondary Standard	
Range	100 psia
Type	Diaphragm and Strain Gage

- HYDRAULIC RAM LOCATIONS
- STRAIN-GAGE LOCATIONS (PRESSURE FACE)
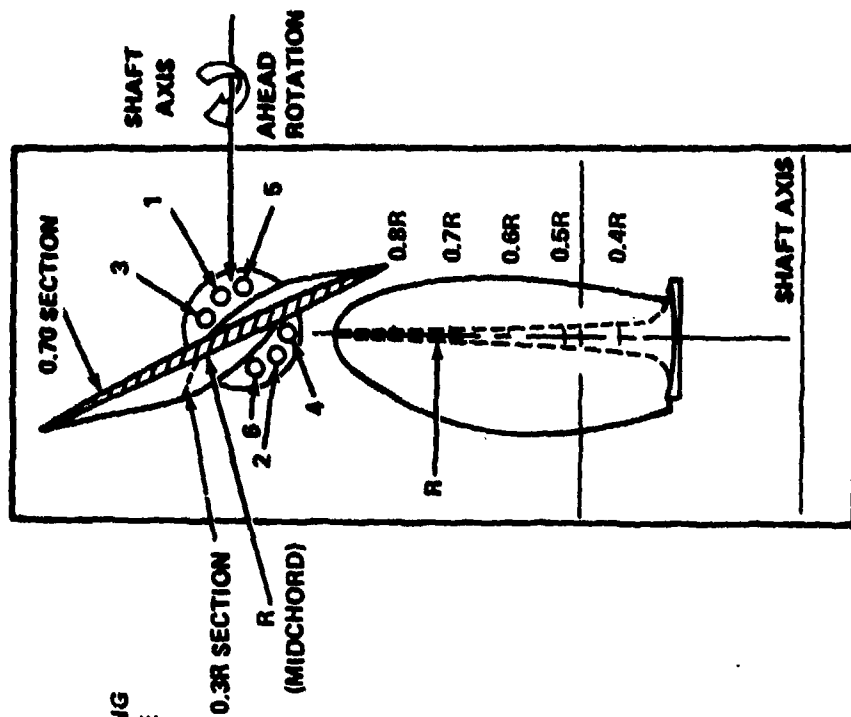
Figure 22b — Resultant Load Vector for Nine-Ram Loading

Figure 22a — Hydraulic Loader Matrix

Figure 22 — Load Matrix for David W. Taylor Naval Ship Research and Development Center Nine-Ram Hydraulic Propeller Blade Loader on USS BARBEY

97
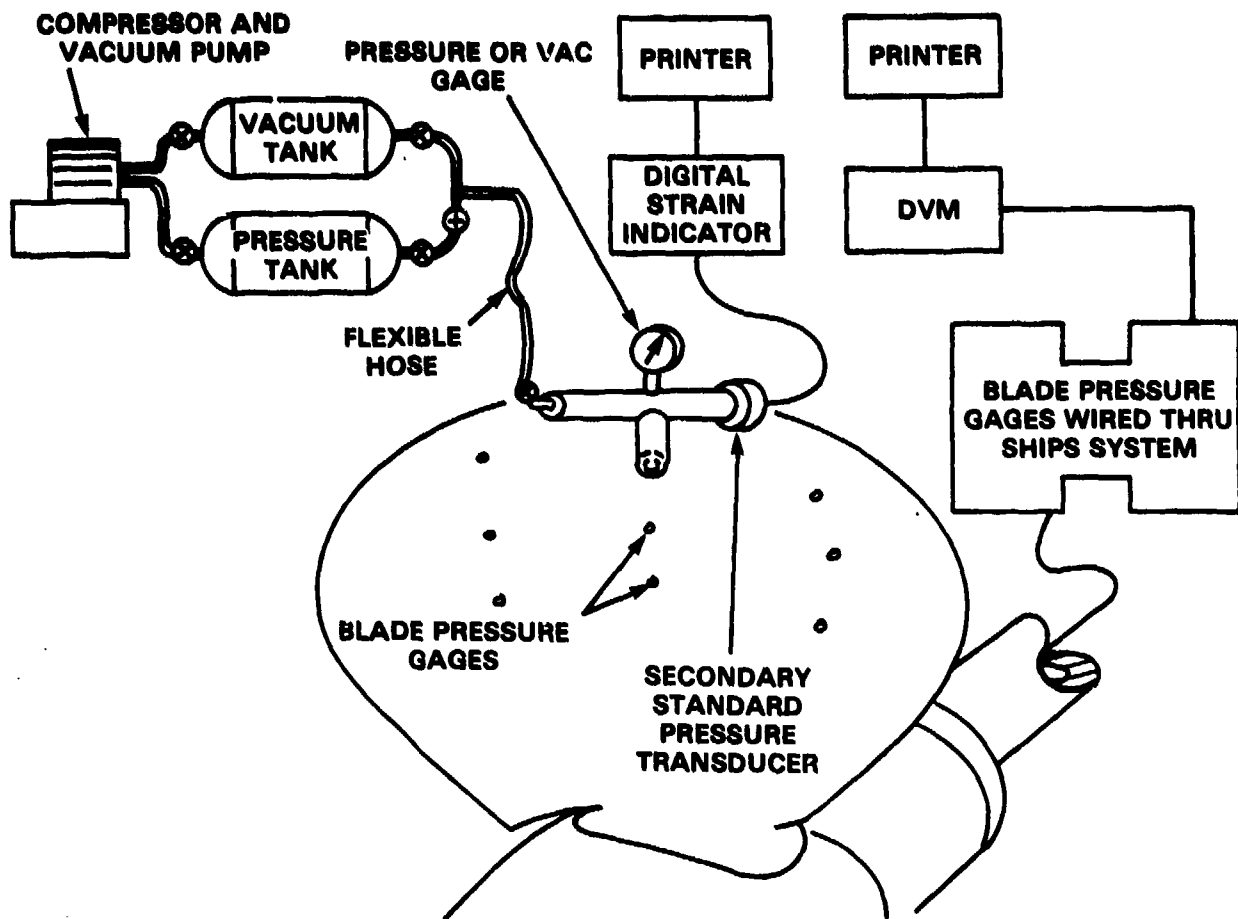
Figure 23 - Propeller Blade Pressure Gage
Field Calibration System

DOCKSIDE TESTS

After the drydock had been flooded, the dynamic test on the propeller blades
(except on ROOSEVELT) was repeated to determine the effects of the added mass and
damping of the water on the blade characteristics. Tests were done while blades were
not rotating. In addition to this the static pressure head as seen by each propeller
blade pressure gage was recorded on magnetic tape as the propeller was slowly
(approximately 0.07 rpm) rotated with the jacking motor. This information was used
as additional calibration as well as for future data analysis input.

UNDERWAY TESTS

Prior to initial underway tests, care was exercised in arriving at the selected
test site to ensure that the outboard instrumentation was not damaged. For the open
water trials, the site was free of vehicular traffic to allow for sufficient room
for high speed operation and maneuvering. Water depth was adequate ($6\times$ draft) to
avoid bottom effects. On arrival at the test site, the ship was brought to a
complete stop and kept dead in the water for measuring system calibration. Tests
were run in a calm (State 3) sea* with the ship ballast in the full load design
condition.

Except for ROOSEVELT the typical underway trial program consisted initially of
a gradual buildup to the full power condition at design pitch. Incremental speed
runs were made at selected rpm's, and included port and starboard turns with various
left and right rudder (up to maximum rudder angle), crashbacks, and crashaheads at
50, 75, and 100 percent of full power. Less extensive maneuvers were conducted at
other selected pitch settings. Occasionally specialized runs or maneuvers were
included in the test agenda. A sample trial run schedule is given in Table 12.
Figure 24 shows the execution of sample trial maneuvers. During some trials,
photographs were taken through the propeller viewing ports to document the condition
of the instrumentation protective coating system and the nature of the cavitation.
Environmental tests conditions were periodically (approximately every four hours)
recorded during testing. The average propeller trial required three to five days of
ship operation at the test site.

---

*These conditions refer to "open water" tests, in contrast refer to the section
on Ice Trials.

TABLE 12 – USS BARBEY SAMPLE TRIAL RUN SCHEDULE

Run	Type	Run	Type	Run		Type	Run		Type
1	Exp, Bolt 1 Torque Test	26	Design Ahead Pitch	53	(103)	120 rpm	87	(813)	240 in P 140 rpm
2	Bolt 1 Torque Test	27	Design Ahead Pitch Start Load Blade 2	54	(106)	150 rpm	88	(814)	240 in P 160 rpm
3	Bolt 2 Torque Test	28	Design Ahead Pitch Start Load Blade 2	55	(110)	180 rpm/Turns	89	(815)	240 in P 180 rpm
4	Bolt 3 Torque Test	29	Design Ahead Pitch Start Load Blade 2	56	(118)	Crashback Ahead / 220 rpm/turns / Crashback	90	(186)	240 in P 180 rpm Turns / Phase A 35 deg
5	Bolt 4 Torque Test	30	Design Ahead Pitch Start Load Blade 2	57	(115)	Not Run / Boiler Problems 190 in Man. Mode	91	(817)	240 in P 180 rpm Turns / Phase B 35 deg
6	Bolt 5 Torque Test	31	Neutral Pitch	58	(415)	100 rpm	92	(818)	240 in P 180 rpm Turns / Incl. Crashback A 5 deg
7	Bolt 6 Torque Test	32	Neutral Pitch	59	(414)	110 rpm	93	(819)	240 in P 180 rpm Turns / Incl. Crashback B 5 deg
8	Torque Release on Crank 2	33	Neutral Pitch Start Load Blade 4	60	(413)	120 rpm	94	(822)	240 in P 180 rpm Turns / Prog. Mode Ahead Pitch 'A'
9	Bolt 1 Torque Test	34	Design Ahead Pitch Start Load Blade 5	61	(412)	130 rpm	95	(823)	Crashback/back / Prog. Mode Ahead Pitch 'B'
10	Bolt 2 Torque Test	35	Neutral Pitch Fwd Side Start Load Blade 5	62	(411)	140 rpm	96	(609)	Crashback/back / 299 rpm 100 Turns & Crashback
11	Bolt 3 Torque Test	36	Neutral Pitch Fwd Side Start Load Blade 5	63	(410)	150 rpm	97	(610)	170 in Pitch - Phase A
12	Bolt 4 Torque Test	37	Neutral Pitch Fwd Side Start Load Blade 5	64	(409)	160 rpm	98	(611)	170 in Pitch - Phase B
13	Bolt 5 Torque Test	38	Neutral Pitch Fwd Side Start Load Blade 2	65	(408R)	170 rpm (Razoroed)	99	(612)	170 in Pitch Phase A / 170 in Pitch Phase B
14	Bolt 6 Torque Test	39	Design Ahead Start Load Blade 2	66	(408)	170 rpm Phase A Only	100	(118R)	220 rpm 35 deg Turns / 190 in Pitch A-B
15	Cal	40	Design Astern Fwd Side Start Load Blade 2	67	(407)	180 rpm	101	(301)	Drag Blade from
16	Shaker Sweep in Air Blade 4	41	Design Astern Fwd Side Start Load Blade 4	68	(407R)	180 rpm	102	(302)	80 rpm Phase A / Drag Blade from
17	Shaker Sweep in Air Blade 4	42	Design Astern Fwd Side Start Load Blade 5	69	(406)	190 rpm	103	(303)	120 rpm Phase A / Drag Blade from
18	Shaker Sweep in Air Blade 4	43	Neutral Pitch Trans. Excit by Diver Blade 4 Underwater	70	(405)	200 rpm	104	(304)	160 rpm A-B / Drag Blade from
19	Shaker Sweep in Air Blade 2	44	Shaker Sweep Blade 4	71	(403)	220 rpm	105	(305)	202 rpm A-B / Drag Blade from
20	Shaker Sweep in Air Blade 5	45	Underway 40-55 rpm	72	(801)	200 rpm 5 deg Turns	106	(701)	150 rpm Phase A / 20 in Pitch (DIW)
21	Trans Excit Blade 5	46	Underway 98 rpm	73	(802)	Crashback/Ahead Phase A / 200 rpm 5 deg Turns	107	(702)	100 rpm A-B / 7 in Pitch (DIW)
22	Trans Excit Blade 5	47	Underway 122 rpm	74	(803)	Crashback/Ahead Phase B / 200 rpm 10 deg Turns	108	(703)	140 rpm A-B / 7 in Pitch (DIW)
23	Re-Null Values	48	121 rpm	75	(804)	Crashback/Ahead Phase A / 200 rpm 10 deg Turns	109	(704)	180 rpm A-B / 7 in Pitch (DIW) / 220 rpm A-B
24	Static Load Test Blade 2	49	50 rpm	76	(805)	Crashback/Ahead Phase B / 200 rpm 20 deg Turns			
25	Design Ahead Pitch Start Load Blade 2	50	Razoroed Zero Level	77	(806)	Crashback/Ahead Phase A / 200 rpm 20 deg Turns			
		51	On Jack Gear from Jack Shaft to Mar	78	(807)	Crashback/Ahead Phase B / 200 rpm 30-35 deg Turns			
		52	Rpm to Zero	79	(808)	Crashback/Ahead Phase A / 200 rpm 30-35 deg Turns			
				80	(402)	Crashback/Ahead Phase B / 225 rpm			
				81	(809)	223 rpm 190 deg Pitch / Phase A F.P. Crashback			
				82	(820)	Accel. from DIW to F.P.			
				83	(810)	Phase A / F.P. Crashback			
				84	(821)	Phase B / F.P. Accel.			
				85	(811)	Phase B / 240 in P 100 rpm			
				86	(812)	240 in P 120 rpm			

NOTE: DD = DRYDOCK TESTS
       DS = DOCKSIDE TESTS
        U = UNDERWAY TESTS

100

Figure 24a - Incremental Run Sequence
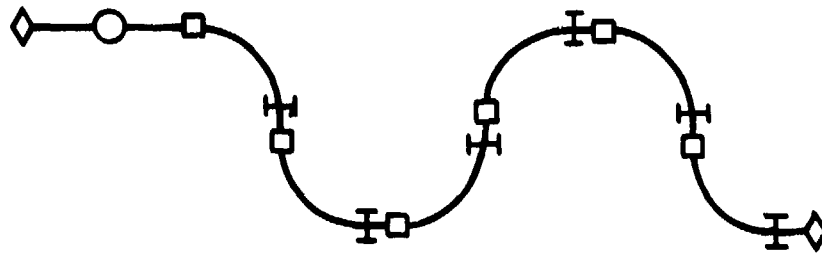
Figure 24b - Turns

LEGEND

◇   ZERO

◯   INCREMENTAL RUN

▢   TURN

△   CRASHBACK

▽   CRASHAHEAD

⬡   DEAD IN THE WATER

I   STEADY-UP
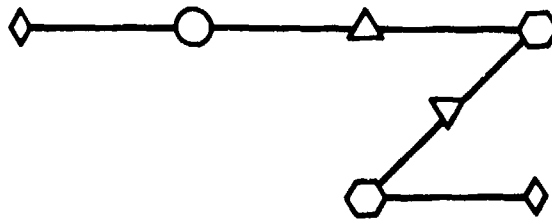
Figure 24c - Crashback and Crashahead

Figure 24 - Sample Run Sequence

ICE TRIALS ON USCG POLAR STAR

During ice operation in Operation Deep Freeze 1978, a number of different conditions were encountered. Briefly, the first few runs were in thin ice and involved various speeds, turns, and backing. It became necessary to back and ram as the ship progressed into ice of greater thickness.* After the first pass which opened a channel to McMurdo Station, the ship added two more modes of operation:

1. Running the already broken channel clogged with ice chunks
2. Scarfing

Scarfing is paralleling the existing channel about 300 ft away. This causes large floes to be broken off between the two channels. In order to avoid being drawn into the old channel, the ship has to head 10 deg to 30 deg away from it, thereby crabbing somewhat and exposing one of the outboard propellers to large quantities of ice.

TEST RESULTS

The number of ships (total of seven) included in this summary, the large number of gage locations (>1000), and trial test conditions (>2000), together with the large variety of data processing and presentation techniques, make it impractical to review here all of the recorded material. Therefore, only representative data are presented. Generally they concern the steady-ahead condition, with limited information on maneuvers. The data are presented under the subheadings: Laboratory Tests, Drydock Tests, Dockside Tests, and Underway Tests. Discussion of the data, particularly where the full-scale test results have confirmed, enlightened, or questioned the basis which was used in the development of the blade attachment, is covered in the Evaluation of Data, Section of this chapter. The discussion of the results of gage protection systems is covered under the previous section (Instrumentation). More details of most of the data presented in this report can be found in References 1, 9, and 10.

---

*The snow cover on the ice increased the hull drag.

LABORATORY TESTS

Laboratory tests provided static loads for purposes of calibration and response analysis. Sample test results are given in Figure 25 and Table 13.
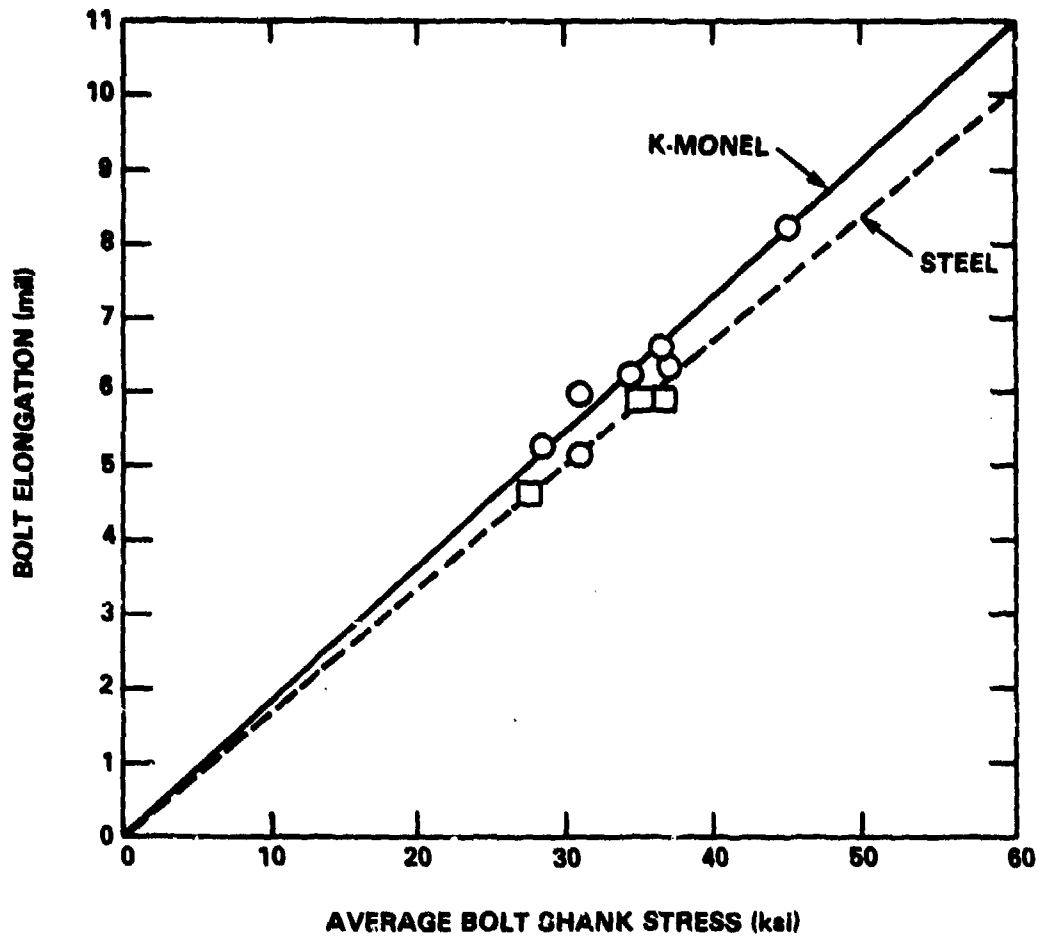
Figure 25 – Midshank Stress and Elongation Relationship for
USS SPRUANCE Propeller Bolts

TABLE 13 – MEAN STRESS IN BOLTS OF PROPELLER BLADE 3
AFTER PRELOADING ON R/V ATHENA

Location	Bolt Number		Bolt Stress (ksi)				Percent Bending Stress[2] σ_B
			$\sigma_{Max.}$	$\sigma_{Min.}$	$\sigma_{Avg.}$[3]	σ_B	
Blade Face	6	H[4]	+50.1	+45.7	+47.9	±2.2	5
		M	+45.6	+40.3	+43.0	±2.7	6
		T	+46.4	+41.2	+43.8	±2.6	6
	2M		+47.0	+37.4	+42.2	±4.6	11
	4M		+49.7	+31.7	+40.7	±9.0	22
Blade Back	5M		+60.1	+28.1	+44.1	±16.0	36
	1M		+58.6	+27.6	+43.1	±15.5	36
	3M		+53.2	+39.4	+46.3	±6.9	15

Notes:

[1] No load on propeller blade (bolt preload only)

[2] Bending Stress $(\sigma_B) = (\sigma_{Max} - \sigma_{Avg})$; percent $\sigma_B = (\sigma_B/\sigma_{Avg})$ 100

[3] Four-gage average

[4] H = Head, M = Midshank, T = Thread

FWD.

BLADE BOLT LOCATIONS

104
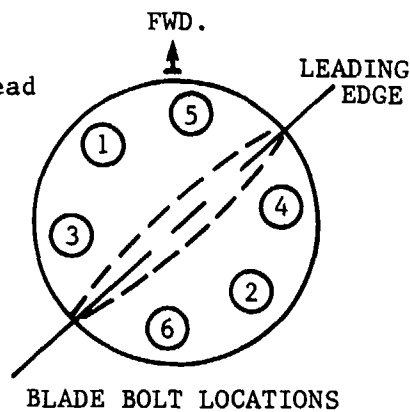
DRYDOCK TESTS

These tests provided information pertinent to the evaluation of bolt preloading techniques, elastic characteristics for both steel and K-Monel bolts, the qualitative and quantitative nature of preload bolt stresses, and the effects of bolt-preload on crank ring stresses. Sample bolt preload test results are shown in Figures 26 through 29 and Tables 14 through 20. In addition, sample data for static blade loader tests and dynamic tests are given in Table 21 and Figure 30.

DOCKSIDE TESTS

Dockside tests provide information on the dynamic response of the CP propeller in air and in water (nonrotating). Sample test results are given in Tables 22 thru 25.

UNDERWAY TESTS

Some of the more significant results for underway operations are given in Figures 31 through 51 and Tables 26 through 29.

EVALUATION OF DATA

Most of the enormous quantity of data which has been recorded in the full-scale, underway test program (as previously mentioned, it included over a thousand channels of information and over two thousand test conditions on a variety of ships ranging from aircraft carriers to patrol gunboats) has not been analyzed. This is because emphasis has been put on analysis of data which would: (1) explain failures which had occurred; (2) prevent failures which might occur by modifying existing propellers for safe operation; and (3) to provide inputs for the development of a technology base on blade hydrodynamic loads, CP propeller structural response, and material characteristics which would support the future design of reliable propellers. As a summary report then, this section on the evaluation of the data will review what the full-scale, underway trials phase of the CP propeller program has produced directly in the way of confirmation, clarification, or questioning of the design assumptions which were used when the blade attachments were developed.
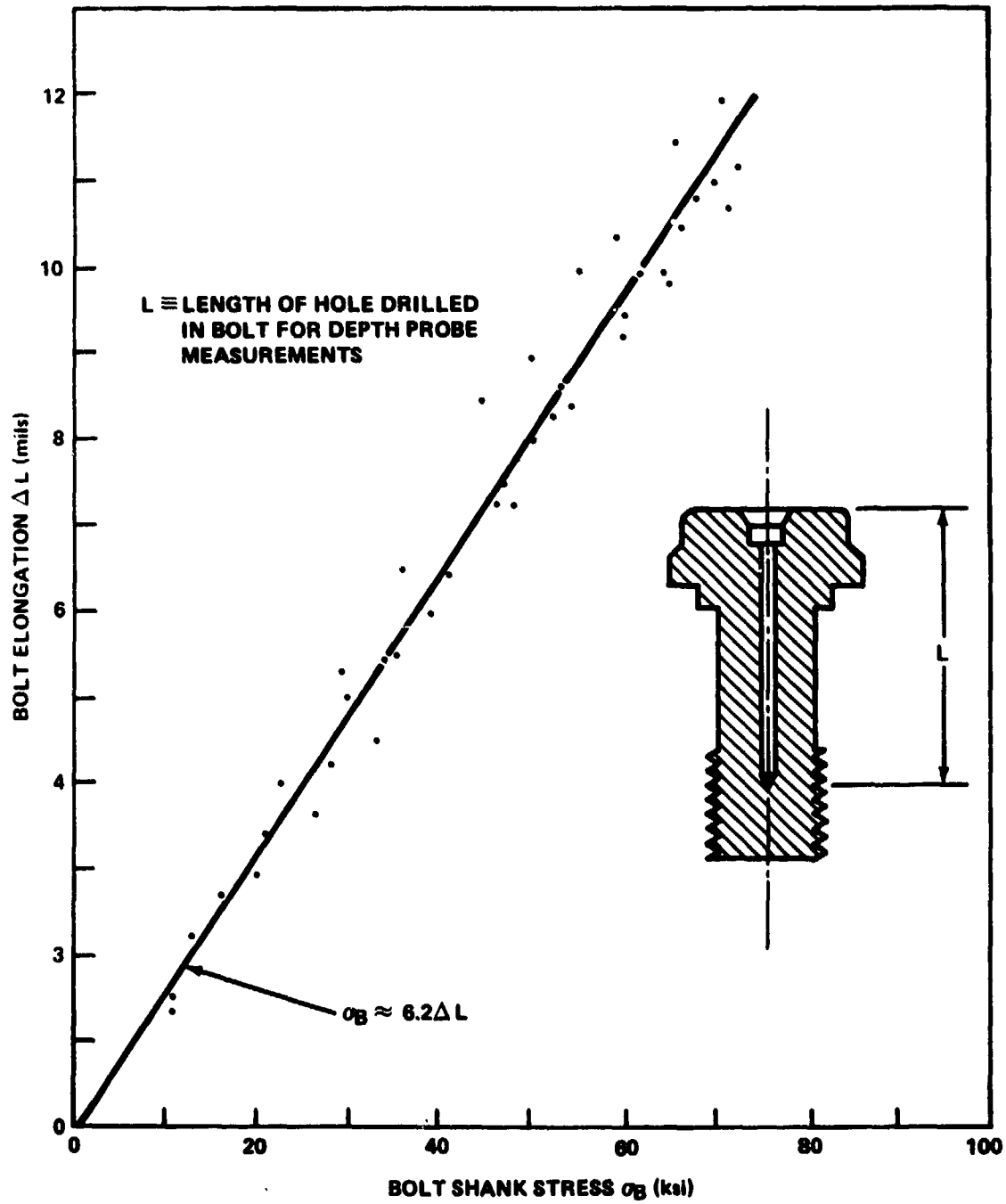
Figure 26 – Average Midshank Bolt Stress versus Elongation for
As-Installed Conditions on USS BARBEY
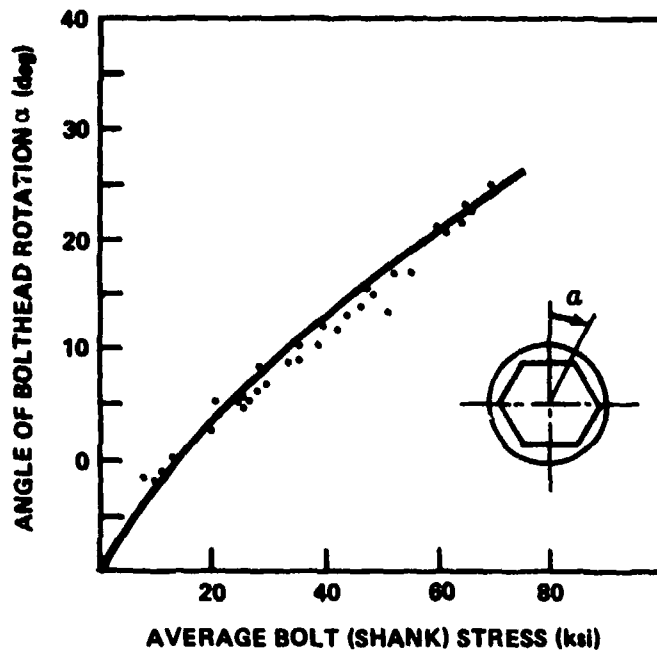
Figure 27 - Average Bolt Midshank Stress versus Angular Rotation
for As-Installed Conditions on USS BARBEY
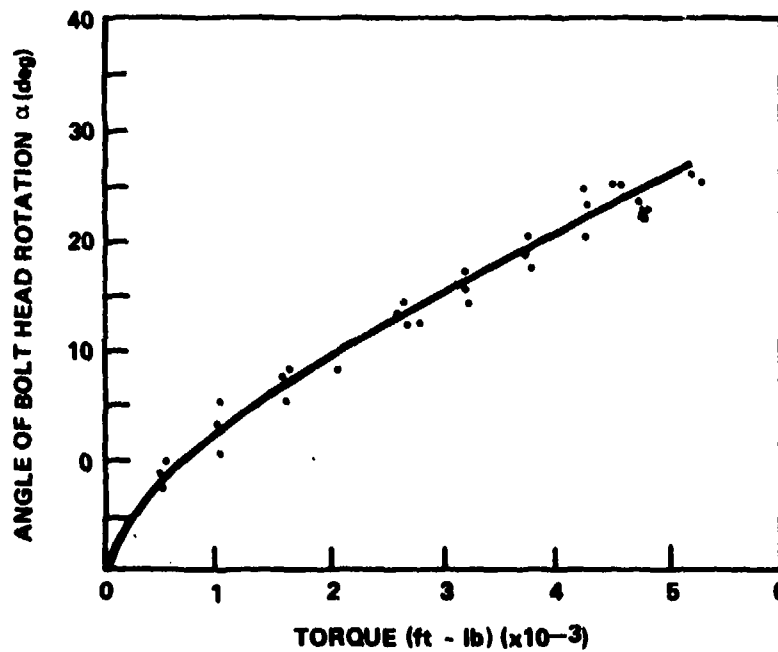
Figure 28 - Propeller Bolt Rotation versus Installation Torque
for As-Installed Conditions on USS BARBEY

Figure 29 – Measured Response of Controllable Pitch Propeller
Components for Drydock Static Load Tests on USS BARBEY
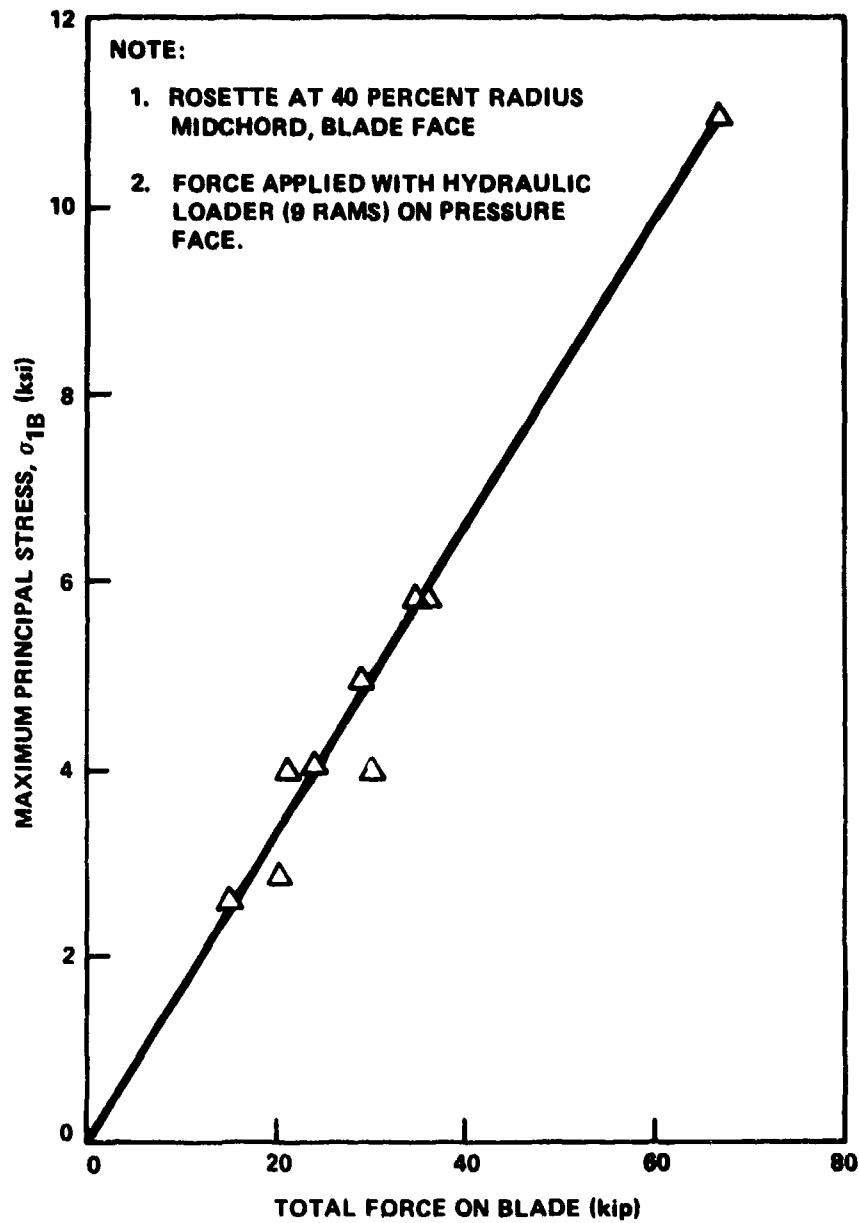
Figure 29a – Principal Stress on Propeller Blade 2

Figure 29 (Continued)
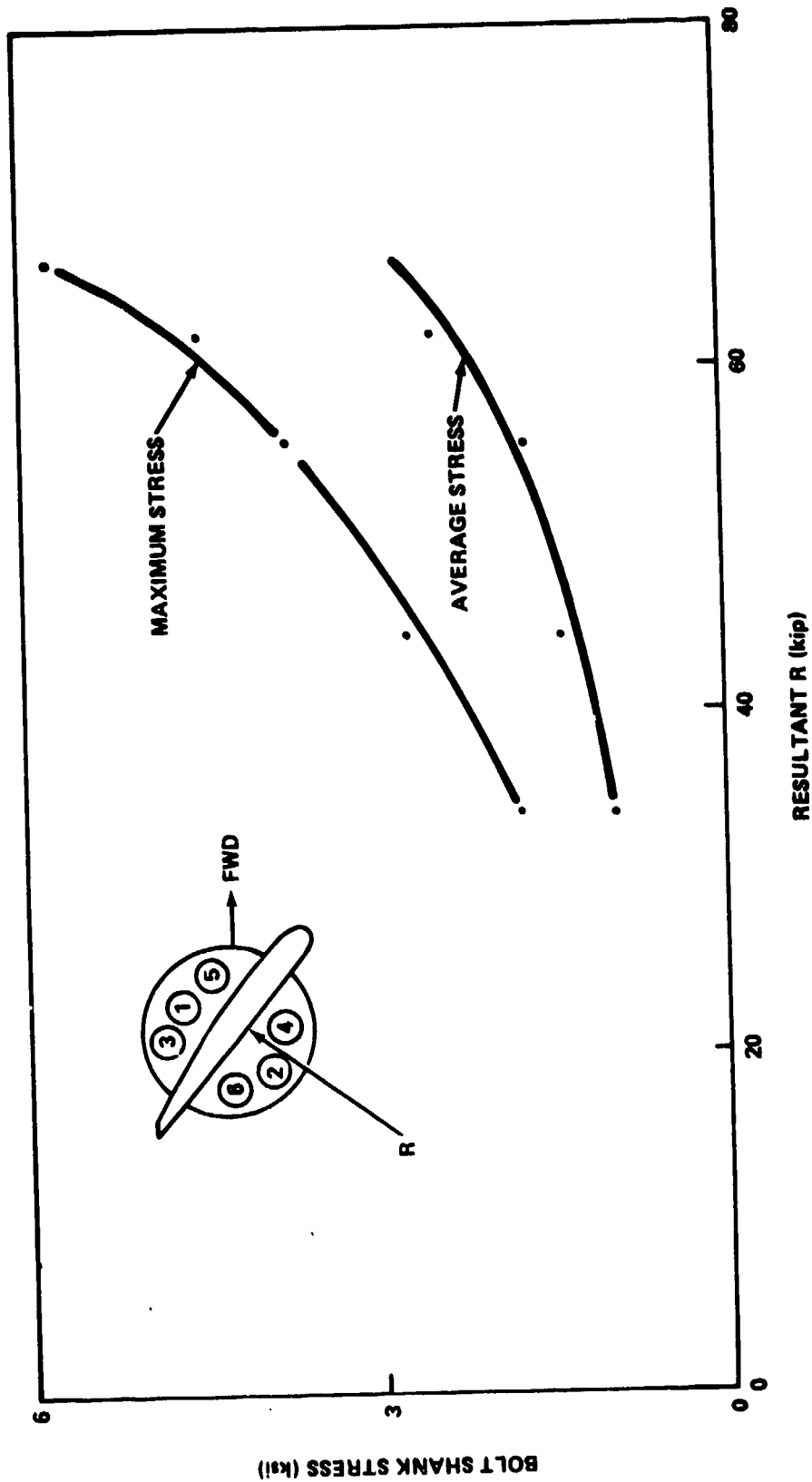
Figure 29b – Propeller Blade Bolt 6 Midshank Stress Variation for Static (Ahead)
Loading at Design Pitch (Stresses above Prestress)

Figure 29 (Continued)
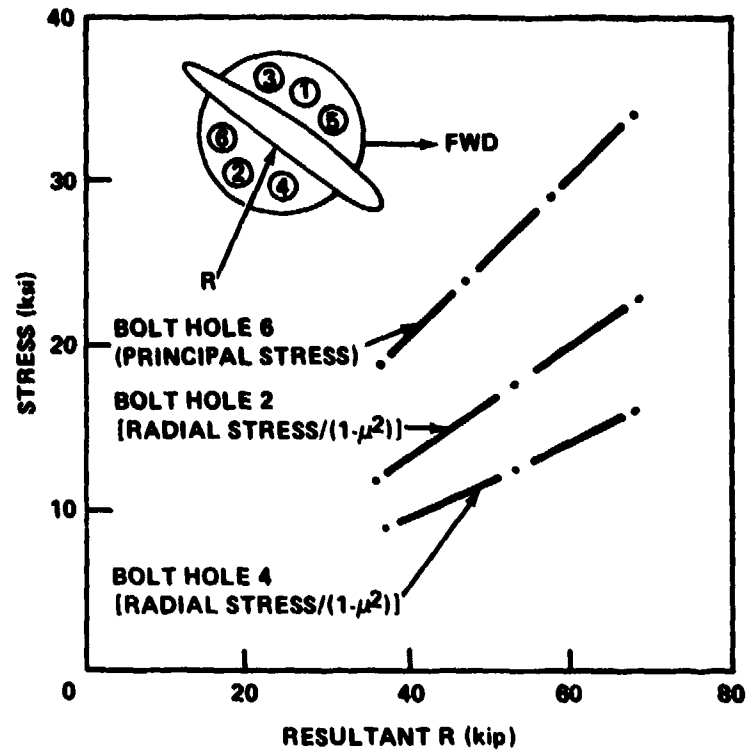
Figure 29c – Crank Disk 2 Stress versus Static (Ahead)
Loading at Design Pitch
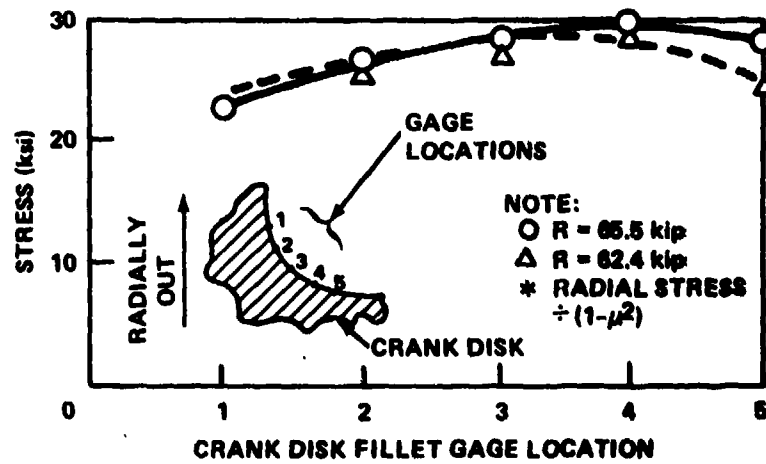
Figure 29d – Radial Stress Distribution in Crank Disk Fillet Juxtaposition
Bolt Hole 6 for Static Ahead Loading at Design Pitch

Figure 29 (Continued)
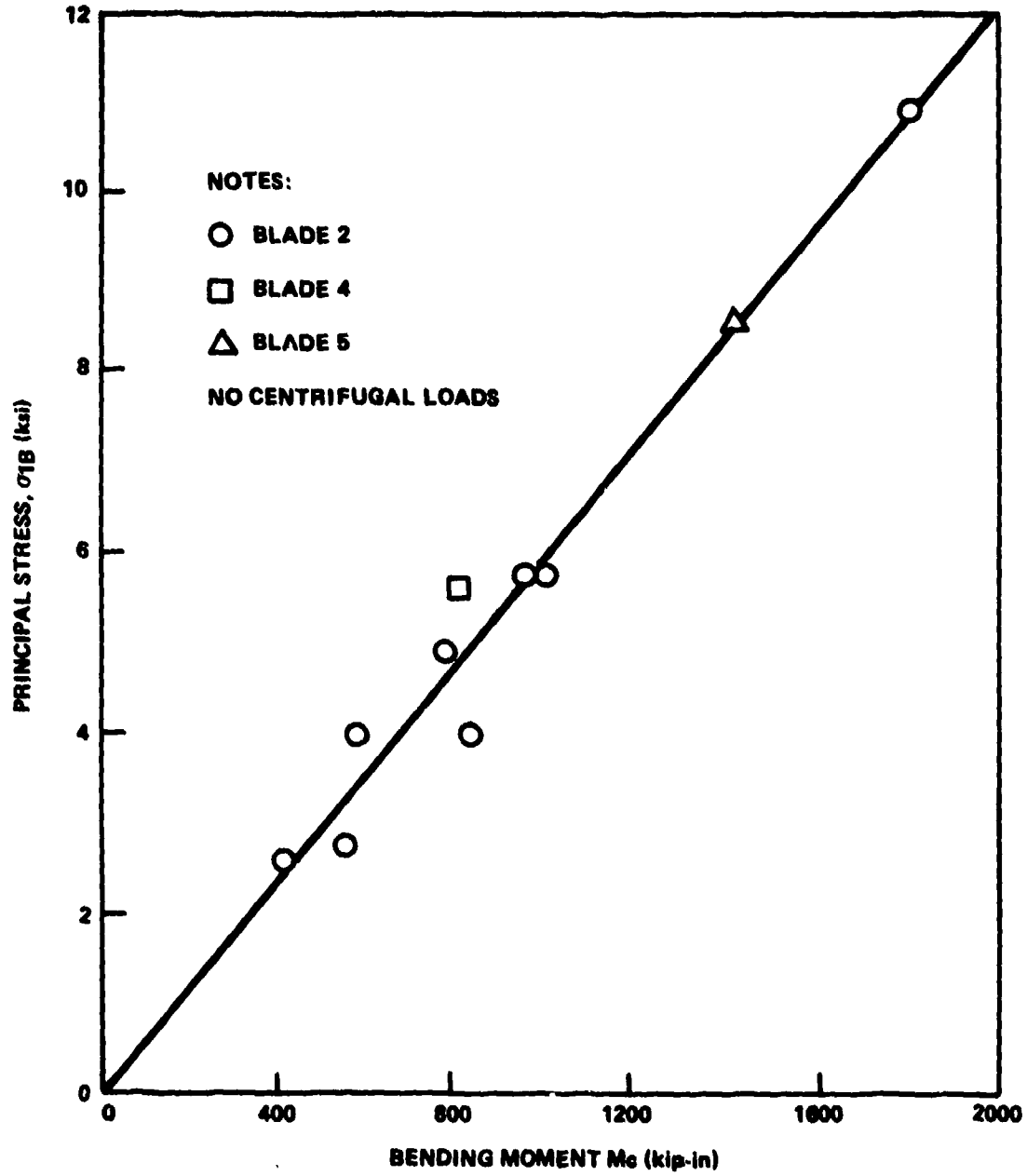
Figure 29e – Principal Stress Measured at Maximum Thickness,
40-Percent Radius, Pressure Face

Figure 29 (Continued)

TABLE 14 – MEAN MIDSHANK STRESS IN BOLTS OF PROPELLER BLADE 2
AFTER PRELOADING ON USS BARBEY

Location	Bolt Number	Bolt Stress[1] (ksi)				Percent Bending Stress[2] S_B
		$S_{Max.}$	$S_{Min.}$	S_{Avg}[3]	S_B	
Blade Face	6	+67.2	+46.1	+56.6	±10.6	19
Blade Face	2	+63.3	+48.4	+55.9	±7.4	14
Blade Face	4	+66.1	+43.2	+54.7	±11.4	21
Blade Back	5	+61.3	+47.8	+54.6	±6.8	13
Blade Back	1	+61.6	+53.3	+57.5	±4.1	7
Blade Back	3	+63.9	+46.9	+55.4	±8.5	16

NOTES:
1. No load on propeller blade (bolt preload only).
2. Bending Stress $(S_B) = (S_{Max} - S_{Avg})$; percent $S_B = (S_B/S_{Avg})$ 100.
3. Four-gage average.

TABLE 15 – SUMMARY OF PROPELLER BLADE BOLT ELONGATION AND MIDSHANK STRESS DUE TO PRELOAD ON USS BARBEY

Propeller Blade Number	Blade Bolt Number	Bolt Elongation* (in. x 10⁻³)		Average Bolt Shank** Stress (ksi)	
		Mar 1975***	Jan 1976†	Mar 1975***	Jan 1976†
1	1	8.2	2.5	50.46	15.5
	2	8.5	6.5	52.31	40.3
	3	8.5	10.0	52.31	62.0
	4	9.0	8.0	55.38	49.6
	5	8.5	8.0	52.31	49.6
	6	9.0	5.0	55.38	31.0
2	1	9.3	8.6	57.45	52.87
	2	9.1	8.8	55.88	54.23
	3	9.0	9.0	55.41	55.58
	4	8.9	8.9	54.68	54.65
	5	8.9	8.5	54.58	52.09
	6	9.2	8.4	56.60	51.95
3	1	8.0	6.0	49.23	37.2
	2	9.0	7.5	55.38	46.5
	3	8.2	7.8	50.46	48.4
	4	8.5	11.5	52.31	71.3
	5	8.5	8.0	52.31	49.6
	6	8.8	8.0	54.15	49.6
4	1	7.8	7.5	48.00	46.5
	2	8.6	8.0	52.92	49.6
	3	8.5	9.5	52.31	58.9
	4	9.3	8.0	57.23	49.6
	5	8.5	8.0	52.31	49.6
	6	8.5	8.5	52.31	52.7
5	1	8.2	8.0	50.46	49.6
	2	9.0	7.0	55.38	43.4
	3	8.7	8.0	53.54	49.6
	4	9.0	8.0	55.38	49.6
	5	9.0	8.0	55.38	49.6
	6	9.0	8.5	55.38	52.7

*Bolt Elongations were measured on propeller Blades 1, 3, 4, and 5. Bolt shank stresses for these bolts were calculated from the emperical relationship established in Figure 25.

**Bolt shank stresses were measured on propeller Blade 2. Bolt elongations for these bolts were calculated from the emperical relationship established in Figure 25.

***Date of original installation prior to sea trial.

†Date of drydocking for removal of CP propeller system.

TABLE 16 - PRELOAD CHARACTERISTICS FOR K-MONEL AND STEEL BOLTS ON USS SPRUANCE

Bolt Material	Stress Elongation (ksi/mil)
K-Monel	5.5
Steel	6.0

TABLE 17 - PRINCIPAL STRESSES INDUCED IN CRANK RING 2 BY BOLT PRELOADING ON USS BARBEY

	Parameter / Location	Radial Stress* σ_r ksi	Angle θ deg	Principal Stress σ_1 ksi	σ_2 ksi	Maximum Shear Stress τ ksi
Aft Side (Ahead Operation)	Locator Pin	−1.8	+108	+0.9	−1.6	+1.2
	Bolt Hole 6	**	**	**	**	**
	6/2	−6.8	+88	−2.4	−6.9	+2.3
	Bolt Hole 2	−10.1	***	***	***	***
	2/4	−5.7	***	***		***
	Bolt Hole 4	−8.9	***	***	***	***
Fwd Side (Ahead Operation)	Bolt Hole 5	−11.0	+90	+12.6	−6.2	+9.4
	5/1	−6.3	***	***	***	***
	Bolt Hole 1	−7.0	***	***	***	***
	Bolt Hole 3	−7.6	***	***	***	***
	Crank Pin	+2.7	−27	+3.4	+1.2	+1.1

* $\sigma_r = E\,\epsilon_r/(1\cdot\mu^2)$, where ϵ_r is strain measured on single radial gage

** Record gains not recorded

*** Radial gage only (no rosette)

TABLE 18 - USS SPRUANCE BOLT[1] PRELOAD SUMMARY
PROPELLER BLADE 2

Bolt Number		Stress			Elongation (mil)	
		Avg. (ksi)	Max. (ksi)	Percent Bending	Measured [2]	Calculated [3]
2-1		38.0	43.2	13.7	6.4	6.3
2-2		37.1	41.9	12.9	5.7	6.2
2-3		43.3	46.9	8.3	6.6	7.2
2-4		34.3	37.7	10.2	5.7	5.7
2-5		34.9	38.5	10.3	5.0	5.8
2-6		42.6	-[4]	-[4]	7.1	-[4]
2-7[6]	H	34.4	39.4	14.6	6.3	5.9 [7]
	T	-[5]	-[5]	-[5]		
2-8[6]	H	37.3	50.3	34.9	6.1	6.4 [7]
	T	39.0	50.4	29.2		

Notes:

1   All bolts on propeller blade number 2 were steel (4140).
2   Measured with dial indicator.
3   Calculated from experimental stress-to-elongation relationship for steel
     bolts (6.0 ksi/mil).
4   Bolt number 2-6 was not instrumented.
5   Not measured.
6   All bolt gages were at midshank except on bolts 2-7 and 2-8:
     H indicates gage location ½ in. below head
     T indicates gage location ½ in. above thread.
7   Assumes midshank stress average of head and thread stress.

TABLE 19 - USS SPRUANCE BOLT[1] PRELOAD SUMMARY
PROPELLER BLADE 4

Bolt Number		Stress			Elongation (mils)	
		Avg. (ksi)	Max. (ksi)	Percent Bending	Measured[2]	Calculated[3]
4-1		44.7	48.7	8.9	8.2	8.1
4-2		40.7	44.5	9.3	6.8	7.4
4-3		34.0	37.9	11.7	-[4]	6.2
4-4		37.1	40.4	8.9	6.4	6.7
4-5		36.5	40.1	10.0	-[4]	6.6
4-6		36.8	40.8	9.8	6.6	6.7
4-7[5]	H	33.6	36.7	9.2	6.2	6.2[6]
	T	35.1	37.6	7.1		
4-8[5]	H	36.3	42.2	16.3	6.4	6.7[6]
	T	37.6	42.3	12.5		

Notes:

[1] All bolts on propeller blade number 4 were K-Monel.

[2] Measured with dial indicator.

[3] Calculated from experimental stress-to-elongation relationship for K-Monel bolts (5.5 ksi/mil).

[4] Not measured.

[5] All bolt gages were at midshank except on bolts 4-7 and 4-8:
H indicates gage location ½ in. below head
T indicates gage location ½ in. above thread.

[6] Assumes midshank stress average of head and thread stress.

TABLE 20 - USS OLIVER HAZARD PERRY BOLT PRELOAD SUMMARY
BEFORE AND AFTER TRIALS

Prop. Blade	Bolt[1]	Stress						
		Installed Average (ksi)	Removal Average (ksi)	Change in Average (ksi)	Installed Max. (ksi)	Removal Max. (ksi)	Installed[2] Percent Bend	Removal[2] Percent Bend
1	5H	29.2	27.4	-1.8	31.8	36.0	8.9	31.5
	6H	37.6	34.6	-3.0	42.7	47.9	13.6	38.5
	7H	37.2	34.6	-2.6	39.1	46.1	5.1	33.3
	8H	34.2	31.0	-3.2	36.0	41.0	5.3	32.3
2	4H	32.0	29.0	-3.0	32.5	33.8	1.6	16.5
	8H	35.5	30.2	-5.0	35.8	42.2	6.9	39.7
	8M	33.6	-	-	35.4	-	5.4	-
	8T	37.1	-	-	35.8	-	4.6	-
3	5H	30.2	37.7	+7.5	34.1	49.7	12.9	31.7
	6H	30.3	28.5	-1.8	31.6	38.2	4.3	33.8
	7H	31.5	29.6	-1.9	34.4	42.2	9.2	42.8
	8H	31.8	31.0	-0.8	33.0	42.5	3.8	37.3
	4H	34.6	32.8	-1.8	37.0	38.7	6.9	17.8
	8H	35.3	31.8	-3.5	36.4	44.3	3.1	39.0
	8M	37.4	-	-	38.5	-	2.9	-
	8T	37.1	-	-	38.0	-	2.4	-
5	8H	30.5	27.5	-3.0	34.8	37.5	14.1	34.9
	8M	30.2	29.5	-0.7	33.7	35.6	11.6	20.7
	8T	34.4	28.4	-6.0	36.7	34.8	6.7	22.7

NOTES:

1. H = Head, M = Midshank, T = Thread.
2. Percent bending = [(Max-Avg)/Avg] × 100.

Location / Parameter	Radial Stress σ_{rB} ksi	Angle θ_B deg	Principal Stress σ_{1B} ksi	σ_{2B} ksi	Radial Stress σ_{rB} ksi	Angle θ_B deg	Principal Stress σ_{1B} ksi	σ_{2B} ksi	Radial Stress σ_{rB} ksi	Angle θ_B deg	Principal Stress σ_{1B} ksi	σ_{2B} ksi
Propeller Blade 4:												
40 — Percent Chord from Leading Edge	← 25 →				← 50 →				← 75 →			
40 Face	+4.5	–11	+4.5	+0.8	+5.7	–2	+5.6	+1.2	+4.1	+3	+3.8	+0.1
40 Back	←			No Stress Gages on Back (Suction Face)								→
50 — Percent Chord from Leading Edge	← 25 →				← 50 →				← 75 →			
50 Face	+4.9	–8	+4.7	+0.5	+5.4	+3	+5.4	+1.3	+4.4	+5	+4.1	+0.2
50 Back	←			No Stress Gages on Back (Suction Face)								→
Propeller Blade 5:												
40 — Percent Chord from Leading Edge	← 25 →				← 50 →				← 75 →			
40 Face	*	*	*	*	+8.5	**	**	**	+6.4	**	**	**
40 Back	*	*	*	*	*	*	*	*	–4.5	+101	–1.3	–4.7
50 — Percent Chord from Leading Edge	← 25 →				← 50 →				← 75 →			
50 Face	+8.2	**	**	**	+7.4	+2	+7.6	+2.5	+6.4	**	**	**
50 Back	–7.9	+87	–1.4	–7.7	–8.6	+94	–2.4	–8.6	–5.5	+98	–1.1	–5.5

* No gages recorded
** Radial gage only

Load Matrix (kips)

	Percent Radius	Percent Chord from L.E. 25	50	75	Total Load	Blade Pitch (in)
Blade 4	80 (Bl. Face)	7.4	7.4	7.4	22.2	190
Blade 5	70 (Bl. Face)	7.4	7.4	7.4	44.4	191
	80 (Bl. Face)	7.4	7.4	7.4		
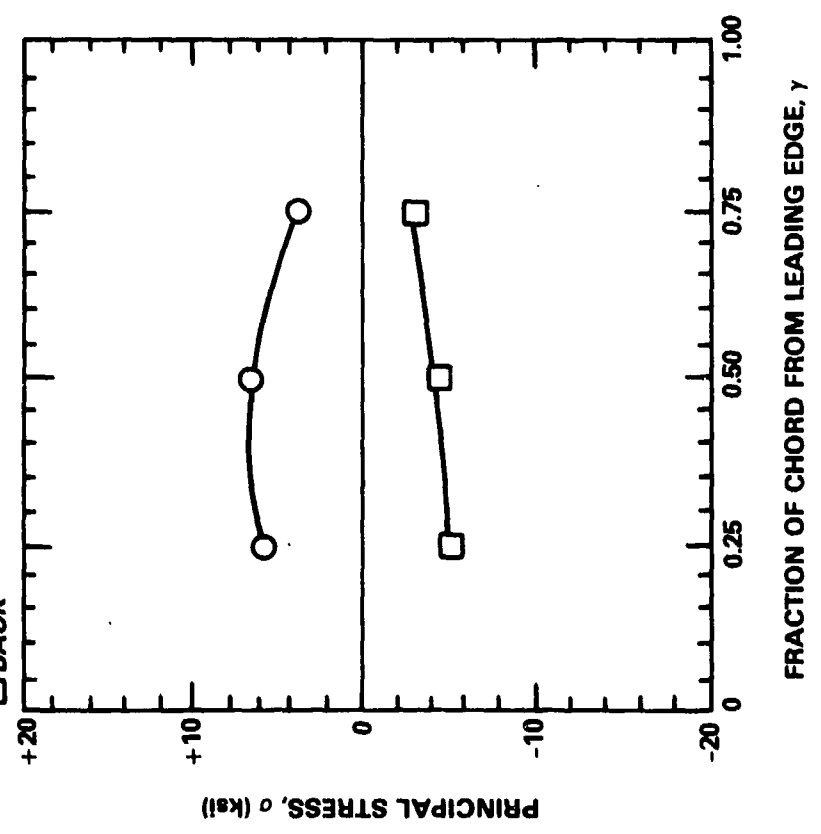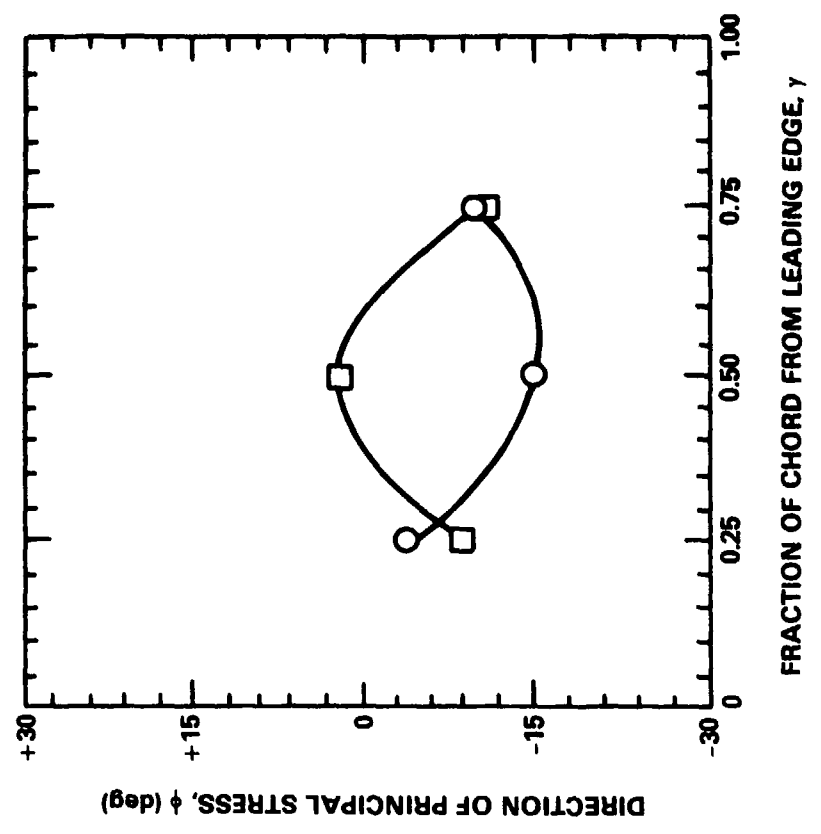
Figure 30 – Principal Stress Distribution on R/V ATHENA Propeller Blade 4
(40 Percent Radius)

119

TABLE 22 – NATURAL FREQUENCIES OF PROPELLER BLADE ON
USS BARBEY

Frequency Hz			Ratio	Comments
Mode	In-Air(fa)	In-Water(fw)	fa/fw	
First Bending	31	19	1.6	Node line approx. on 0.4 radius
First Torsional	127	80	1.6	Node line approx. on 50-percent chord

TABLE 23 – NATURAL FREQUENCIES OF PROPELLER BLADE IN AIR AND
IN WATER ON USS SPRUANCE

Mode	Frequency (Hz)	
	In-Air	In-Water
1st Bending	31	19
1st Torsional	67	42

TABLE 24 - USS OLIVER HAZARD PERRY PROPELLER BLADE NATURAL
FREQUENCIES (IN-AIR) DRYDOCK TESTS

Mode Shape	Natural Frequencies (Hz)
1st Bending	33.0
1st Torsional	50.5
*	87.0
*	114.0
*	137.0
*Mode shape could not be identified.	

TABLE 25 - PROPELLER BLADE FREQUENCIES (IN AIR)
ON R/V ATHENA

| Mode | Frequency (Hz) | |
	Experimental	Theory
1st Bending	112	133 $\pm$ 10
1st Torsional	202	190 $\pm$ 19
--	262	300 $\pm$ 10
--	346	375 $\pm$ 10
--	477	482 $\pm$ 48
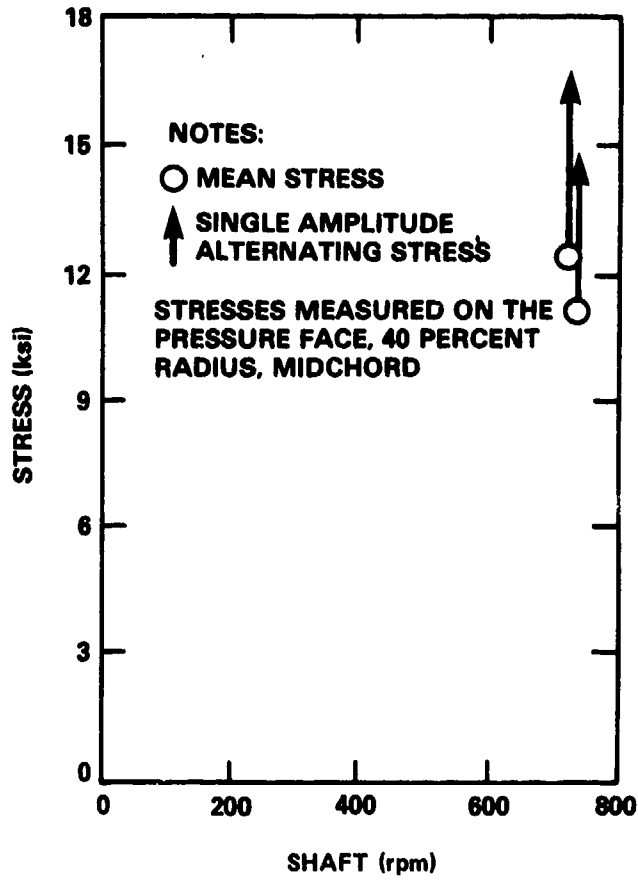
Figure 31 - Measured Combined (Static and Dynamic) Radial
Stress at 0.4R (Maximum Thickness Line) on
USS DOUGLAS

122

35 SECONDS

STEADY-AHEAD FULL-POWER OPERATION (1X670 RPM)

ZERO STRESS LEVEL

TURBINE OVERSPEED OPERATION (670→870→670 rpm)

REVERSE PITCH OPERATION (670 rpm)

STEADY FULL ASTERN OPERATION (670 rpm)

CRASHBACK MANEUVER

(1) (2) (3) (4) (5) (6) (7)
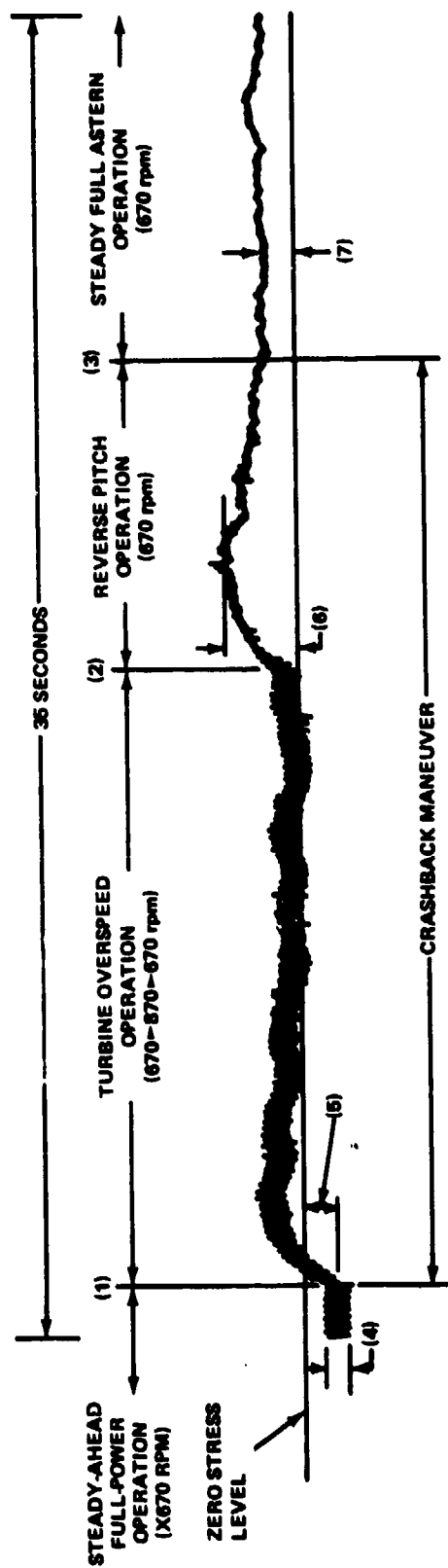
NOTES:
(1) EXECUTE CRASHBACK (FULL AHEAD PITCH TO ZERO PITCH, TURBINE OVERSPEEDS, GOVERNOR PREVENTS FURTHER PITCH CHANGE UNTIL SYSTEM IN CONTROLLED TO APPROX 670 rpm
(2) REVERSE PITCH OPERATION
(3) STEADY FULL ASTERN OPERATION
(4) STEADY FULL POWER ALTERNATING STRESS (±3,700 psi) SHAFT FREQ.

(5) STEADY FULL POWER MEAN STRESS (12,400 psi)
(6) MAXIMUM CRASHBACK MEAN STRESS (26,900 psi)
(7) AVERAGE STEADY ASTERN MEAN STRESS (10,900 psi)
(8) STRESSES INCLUDE HYDRODYNAMIC AND CENTRIFUGAL LOADS

Figure 32 - Radial Stress Measured on USS DOUGLAS Propeller Blade at
40 Percent Radius (Midchord)

123
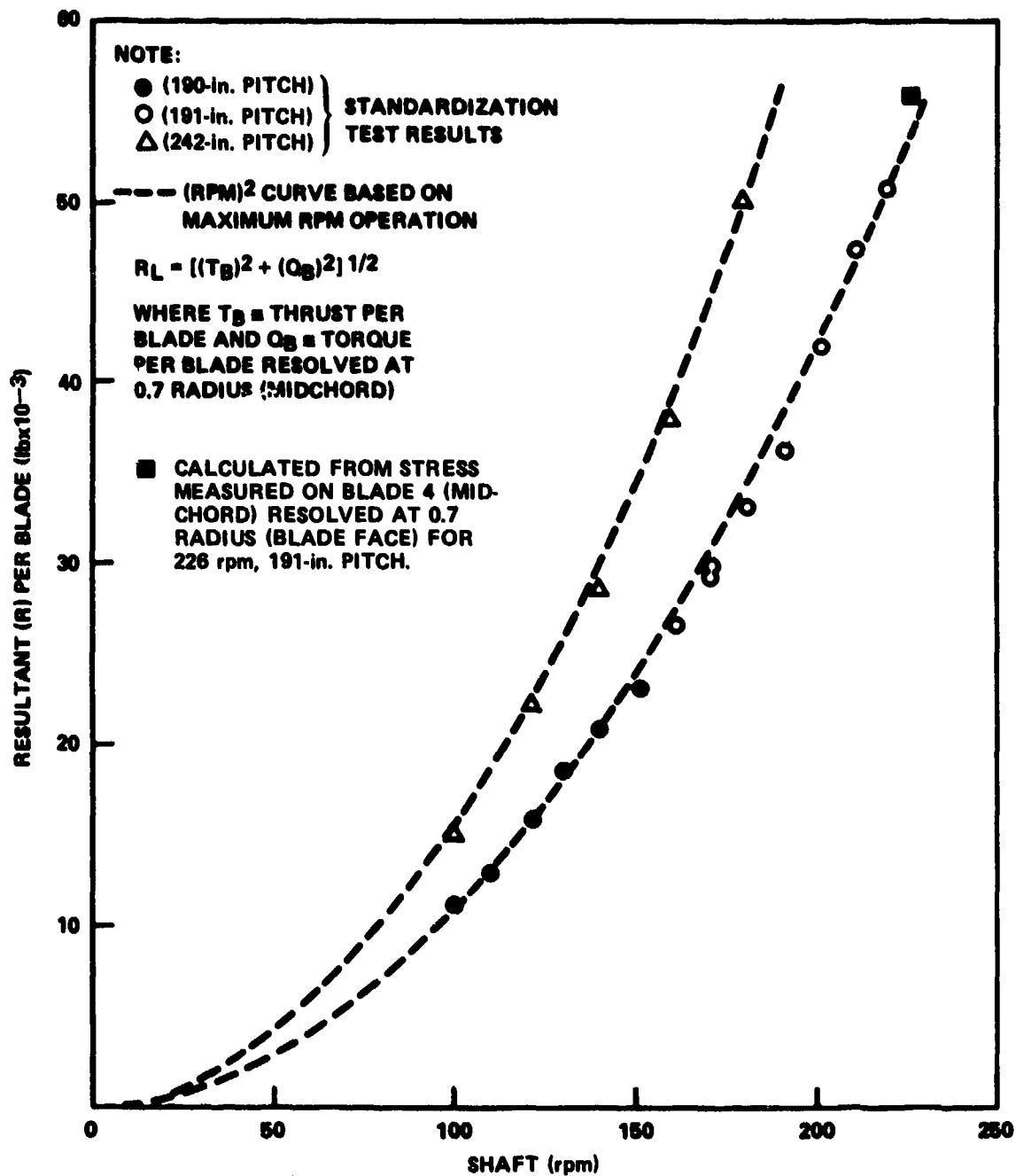
Figure 33 – Propeller Blade Resultant (R_L) versus Shaft
Revolutions per Minute on USS BARBEY

124
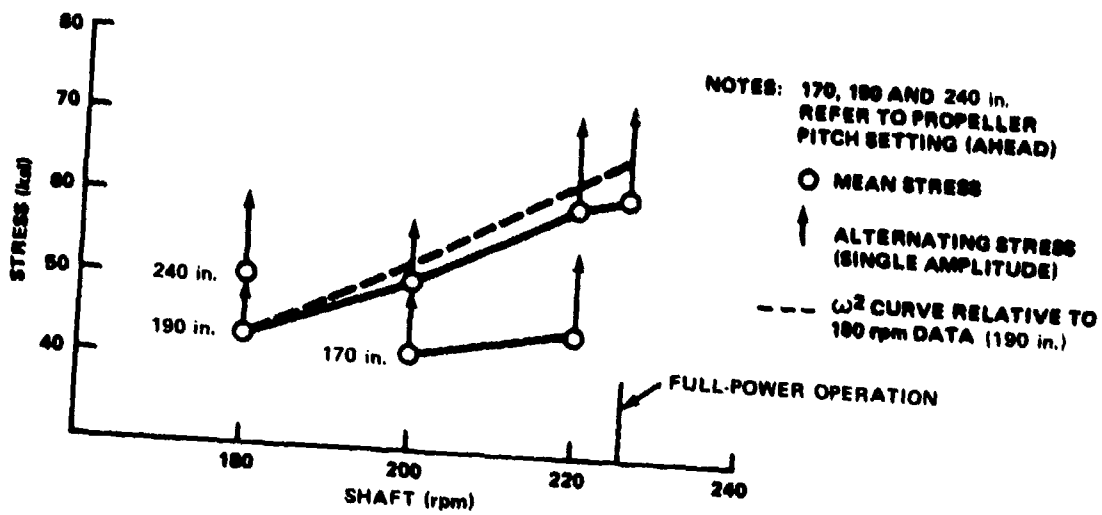
Figure 34a – Principal Stresses on Crank Disk 4
Juxtaposition Bolt Hole 6
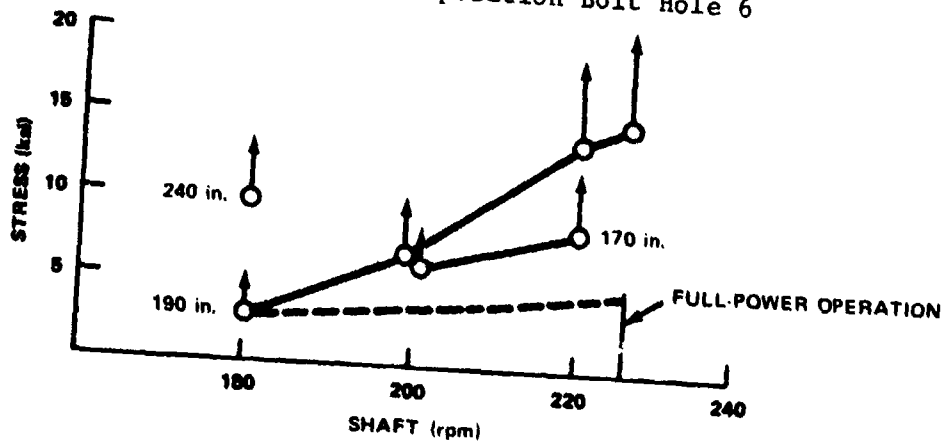
Figure 34b – Maximum Stress (above Prestress) on
Blade Bolt 6
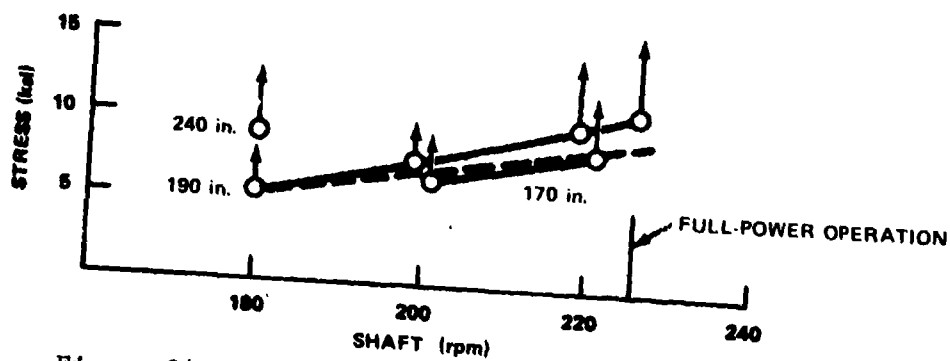
Figure 34c – Principal Stress on Blade 5 at 40 Percent Radius,
Midchord (Blade Face)

Figure 34 – Stress in the Controllable Pitch Propeller Components for
Various Pitch Settings and Shaft Revolutions per Minute on
USS BARBEY
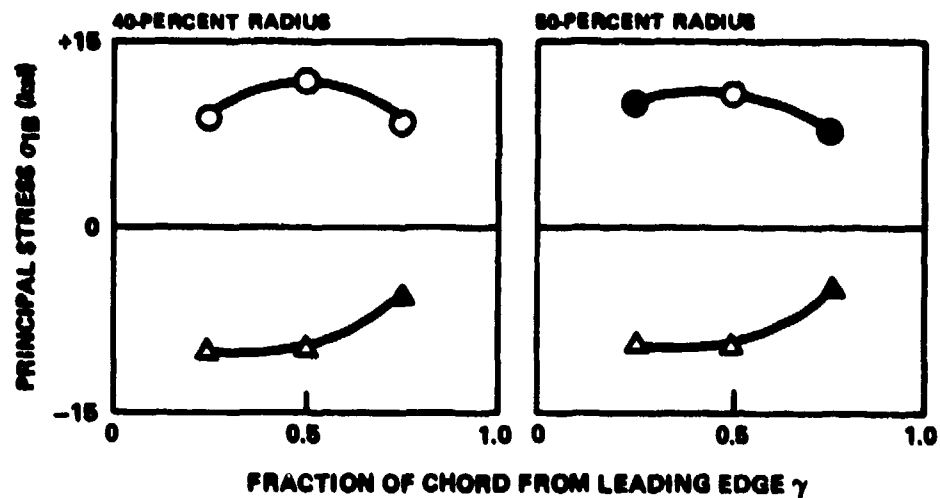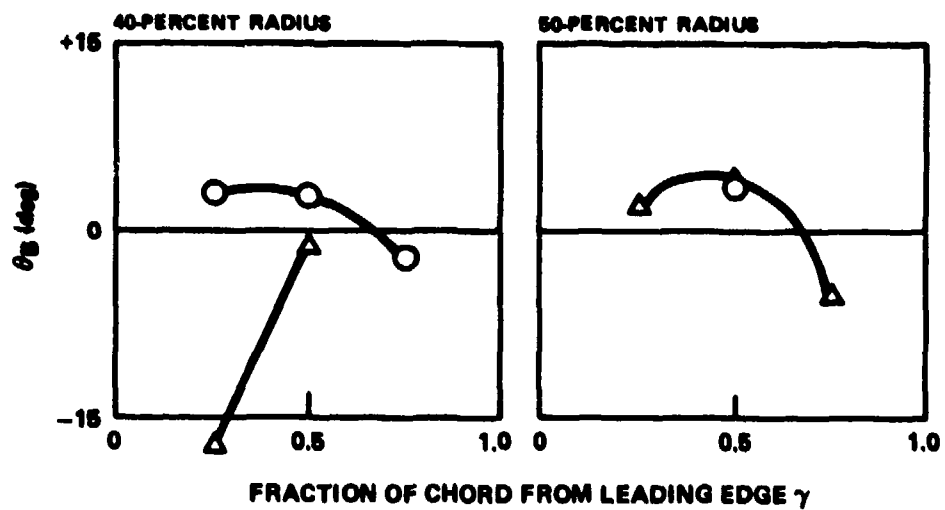
125

Figure 35 – Mean Principal Stress on Propeller on USS BARBEY

126
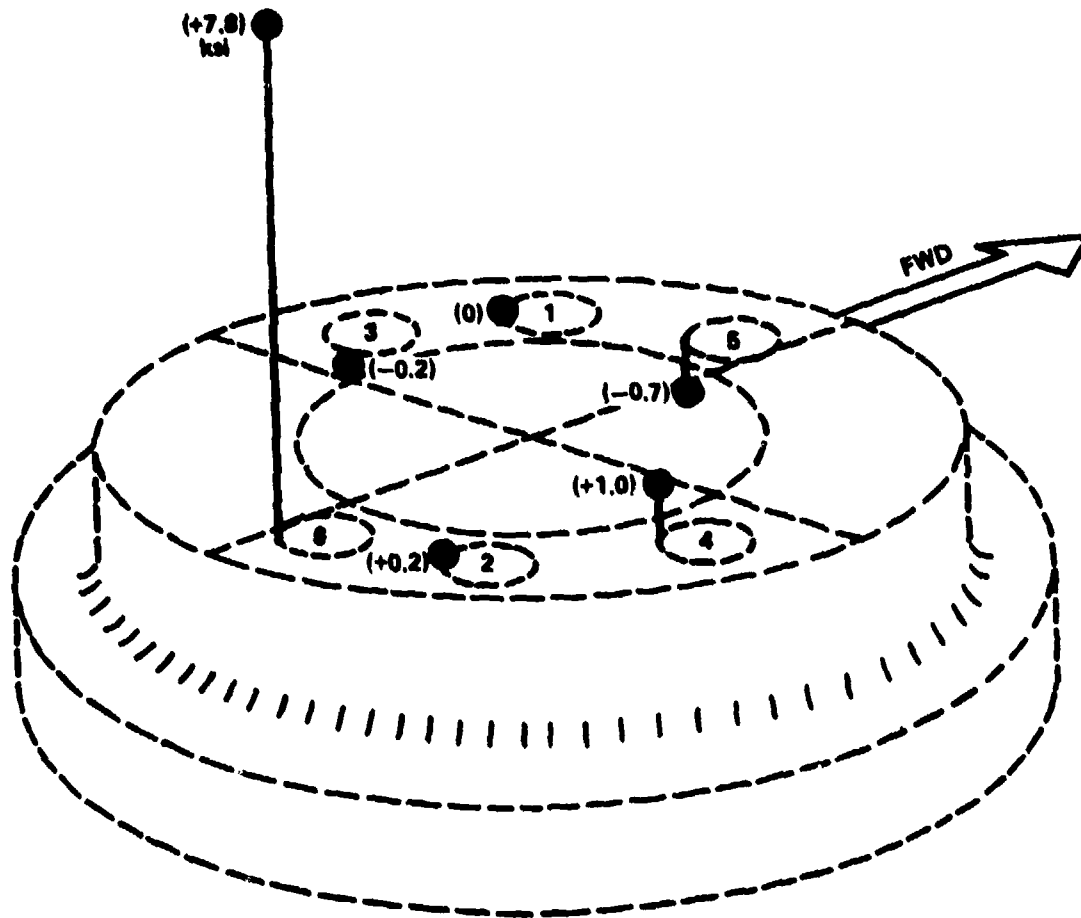
Figure 36 – Average Midshank Mean Stress (above Prestress)
in Blade Bolts, Propeller Blade 2, for Full-Power,
Underway Operation on USS BARBEY
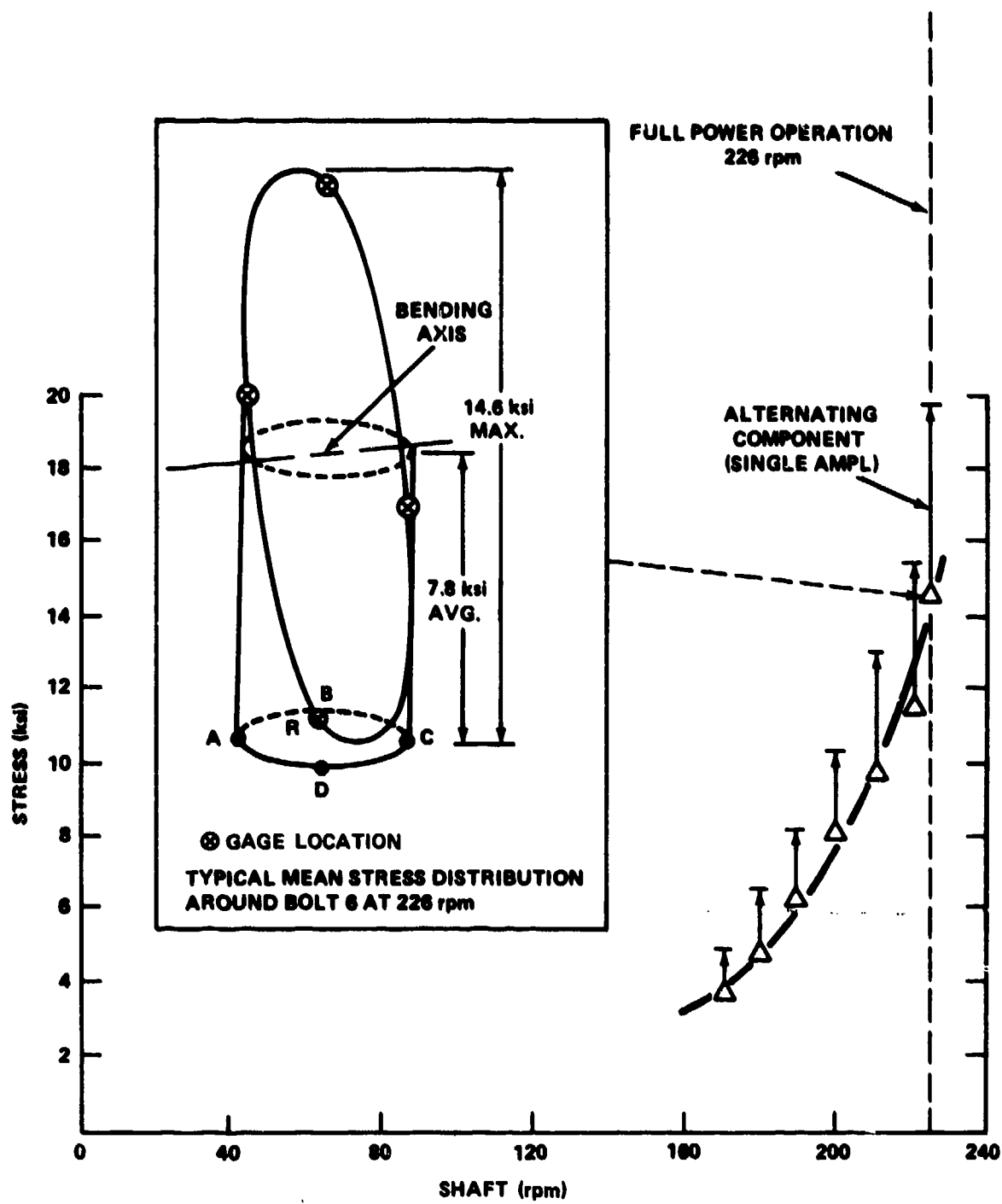
Figure 37 – Maximum Stress (above Prestress) in Midshank of
Blade Bolt 6, Propeller Blade 2, for Full-Power,
Underway Operation on USS BARBEY

128
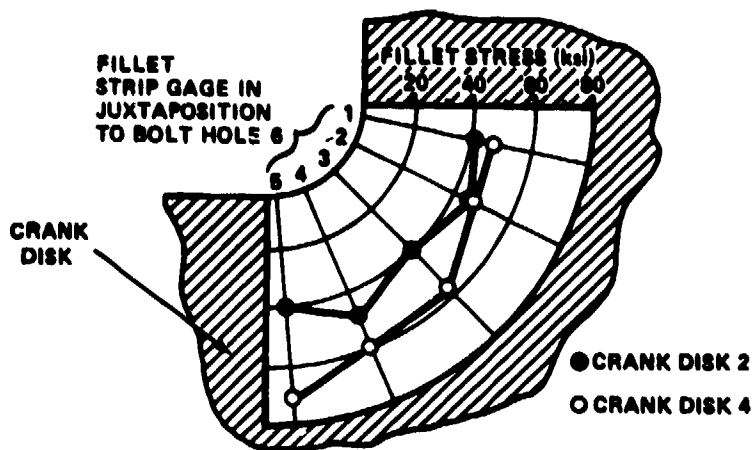
Figure 38a – General Stress Distribution in Fillet Including
Maximum Values for Crank Disk 4
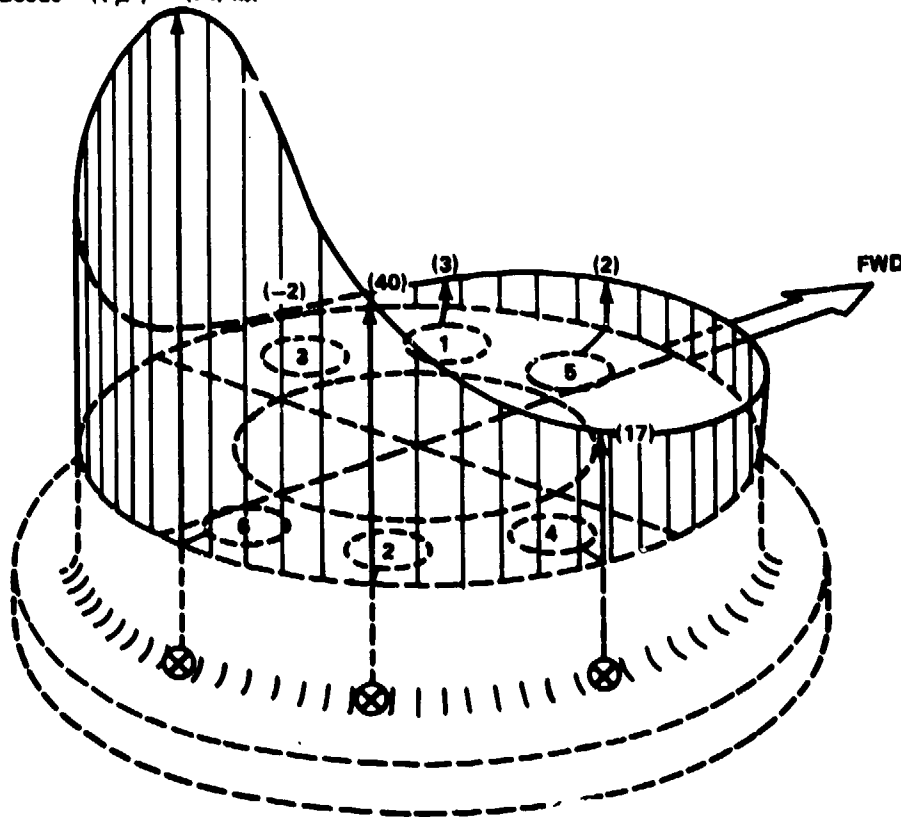
Figure 38b – Crank Disk Fillet Stress Distribution
Juxtaposition Bolt Hole 6

Figure 38 – Radial Stresses in Fillets of Crank Disks 2 and 4 for Full-Power,
Underway Operation (Condition of 266 Revolutions per Minute and
191-Inch Pitch) on USS BARBEY

129
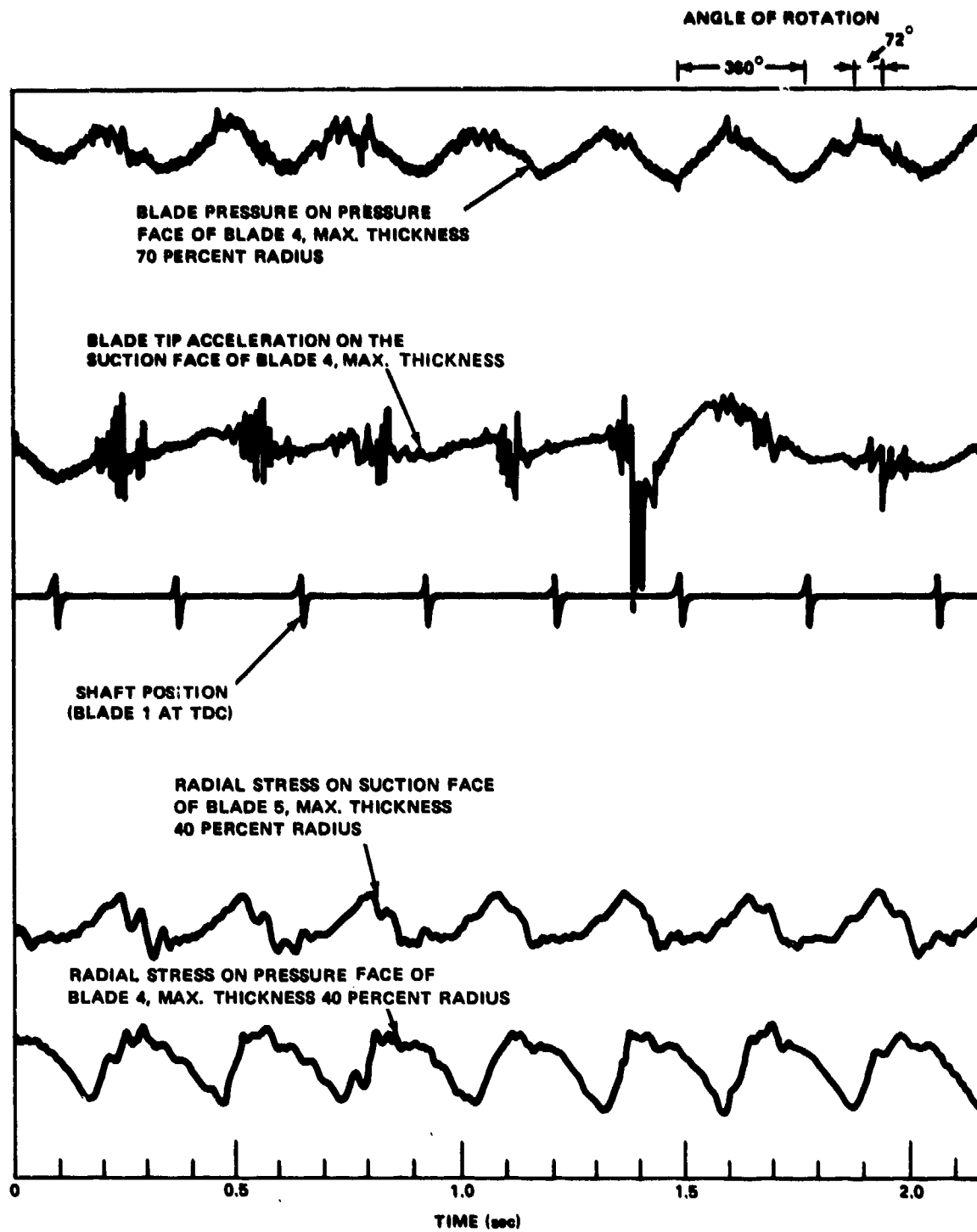
Figure 39 - Variation of Propeller Blade Pressure, Acceleration Strain with
Blade Position at 210 Revolutions per Minute on USS BARBEY

130
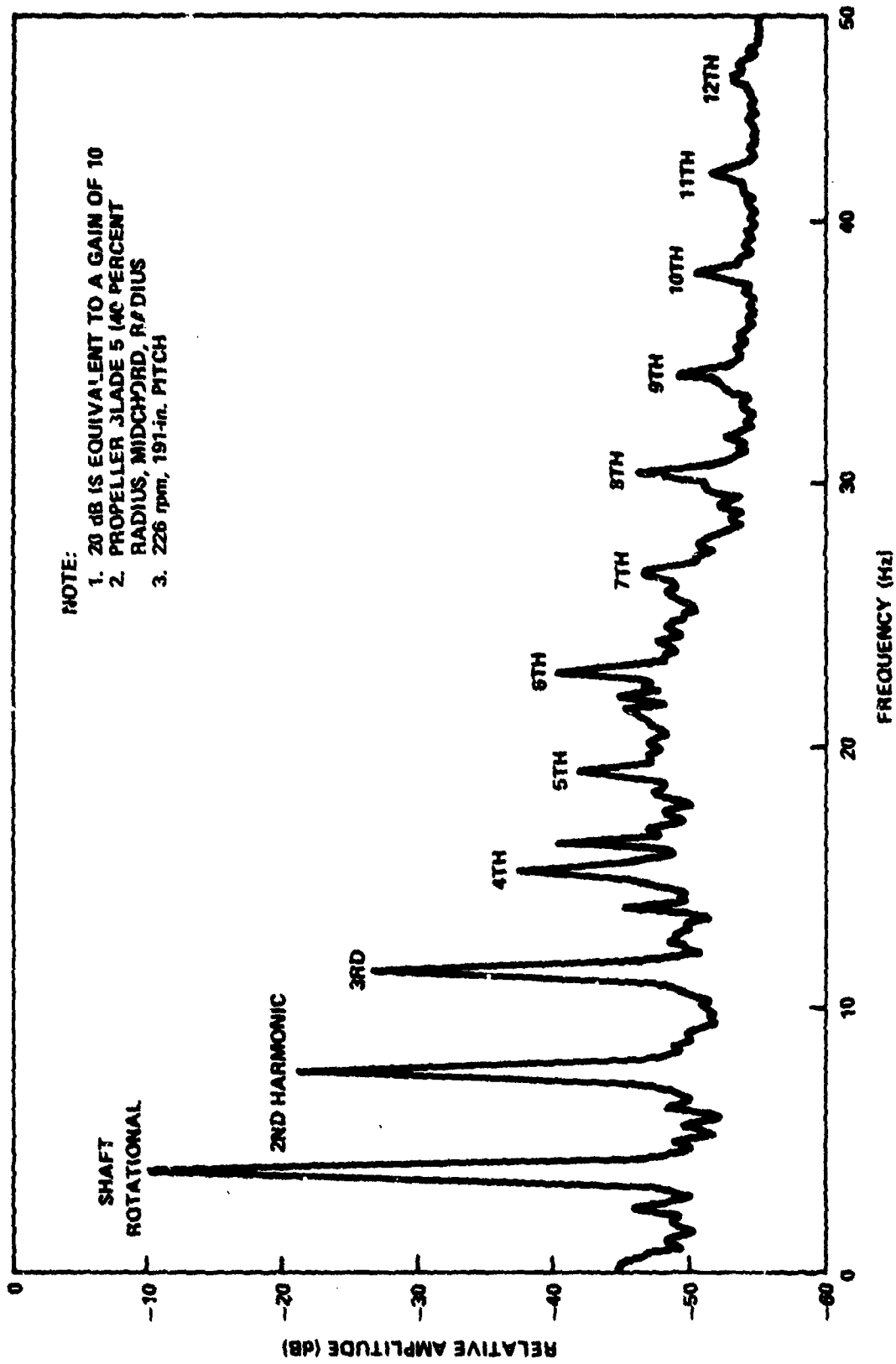
Figure 40 – Frequency Content of Propeller Blade Strain for Full-Power, Underway Operation on USS BARBEY

131
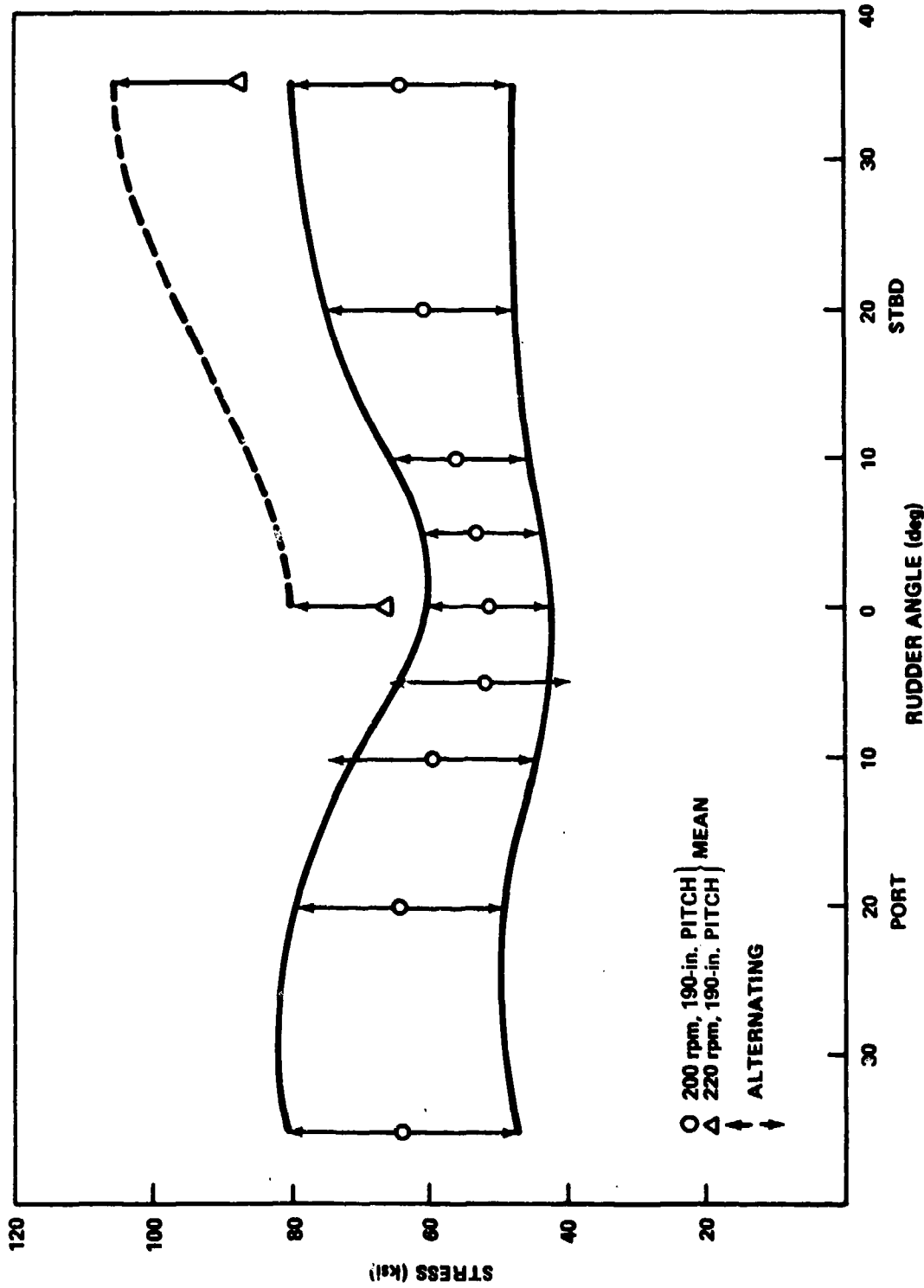
Figure 41 – Effect of Turns on Crank Disk Stresses in Juxtaposition to Bolt Hole 6

(Disk Stresses = Radial Stress $\div$ $(1-\mu^2)$) on USS BARBEY

132
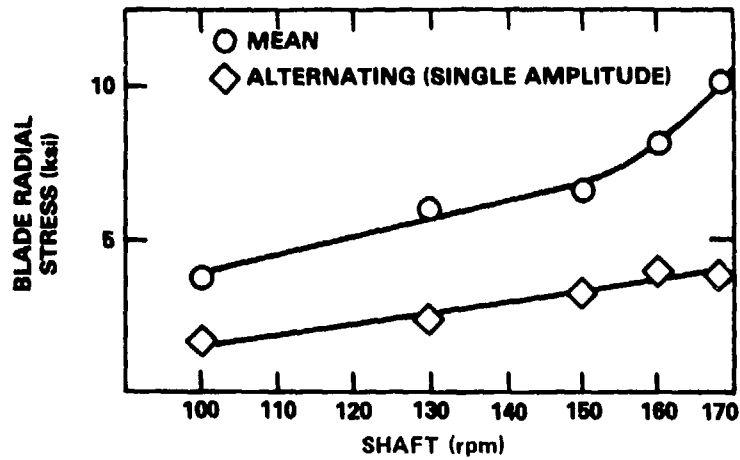
Figure 42a – Blade Stress at 0.35R, 1/2 Chord versus Revolutions per Minute (Pressure Face)
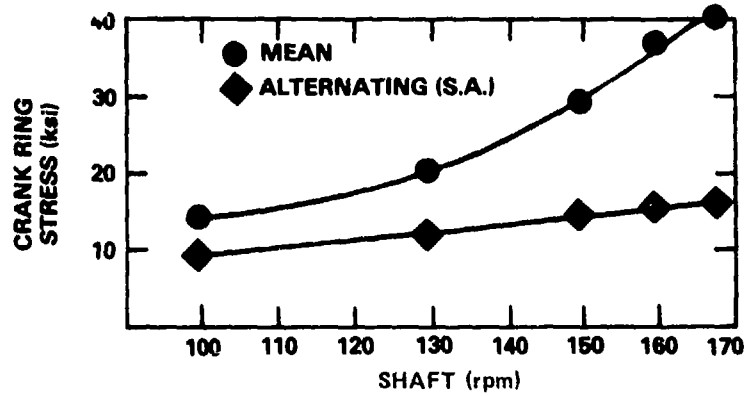
Figure 42b – Crankring Stress Between Holes 7 and 8 versus Revolutions per Minute
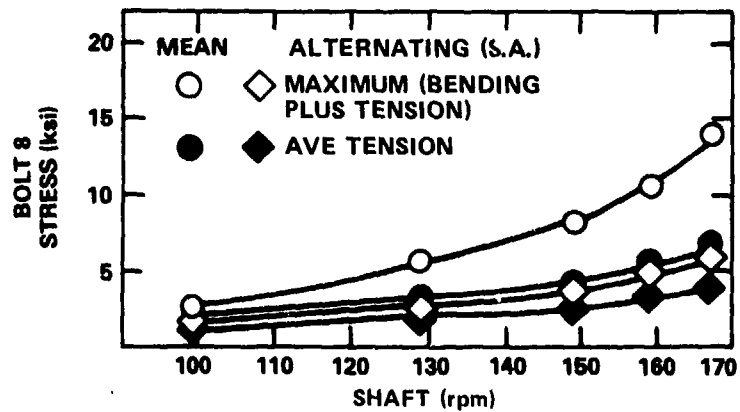
Figure 42c – Bolt (Head) Stress in Steel Bolt 8, Blade 2 versus Revolutions per Minute

Figure 42 – Measured Underway Controllable Pitch Component Stresses on USS SPRUANCE
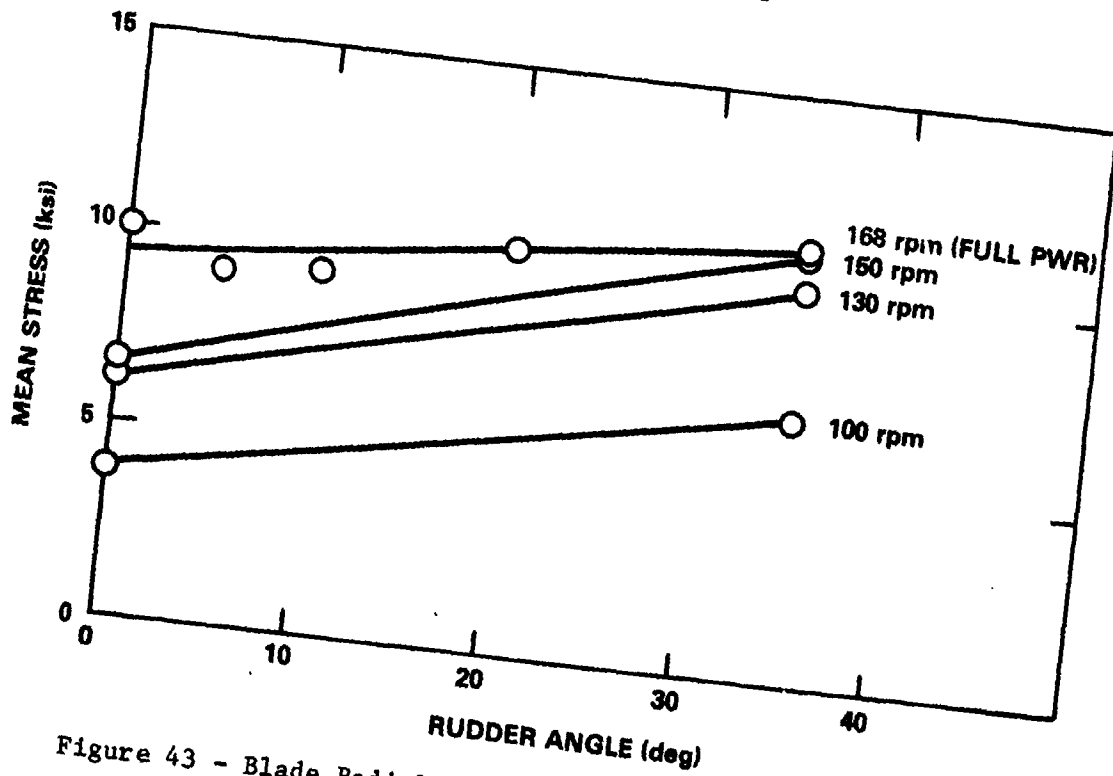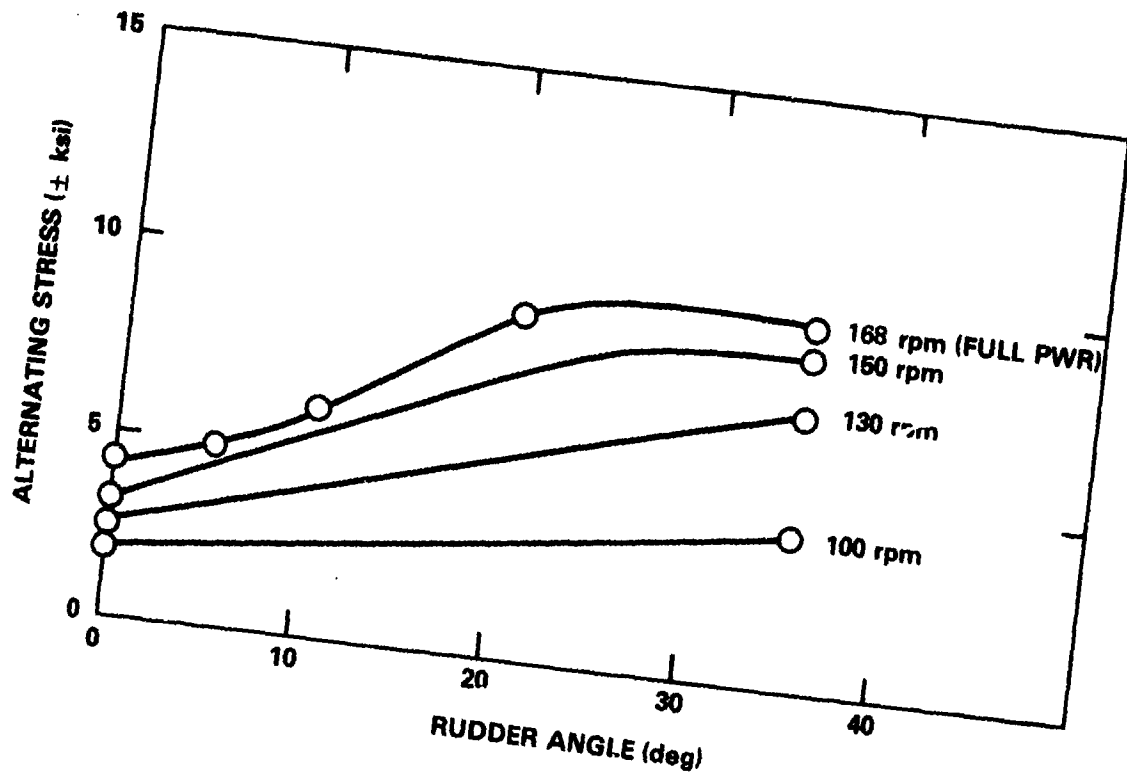
Figure 43 - Blade Radial Stress at 0.35R, 1/2 Chord versus
Rudder Angle--Design Propeller Pitch on
USS SPRUANCE

134
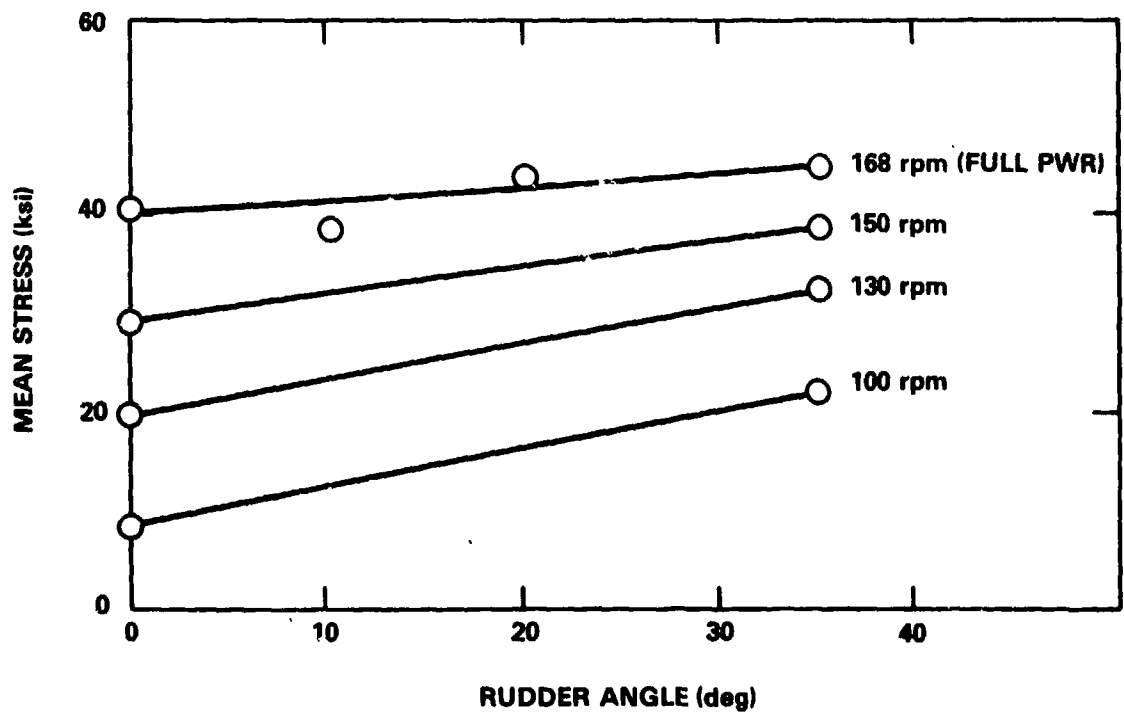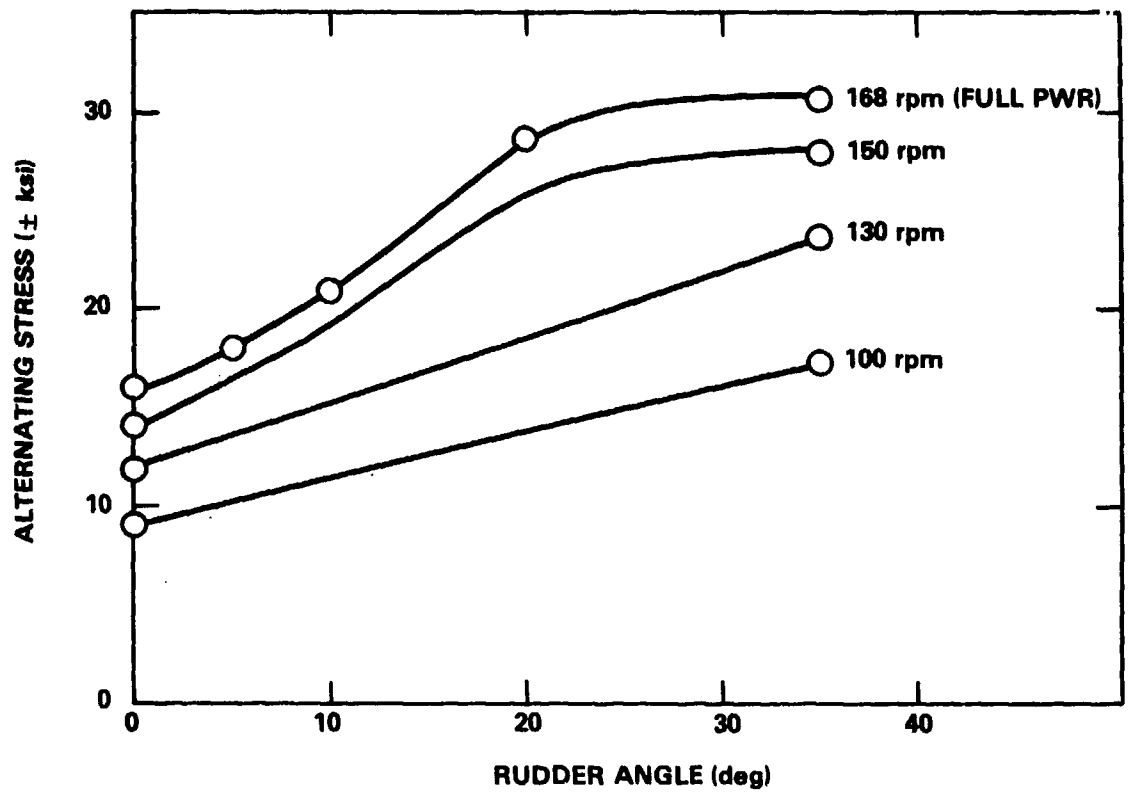
Figure 44 – Crank Ring Stress Between Holes 7 and 8 (Blade 2)
versus Rudder Angle--Design Propeller Pitch on
USS SPRUANCE

135
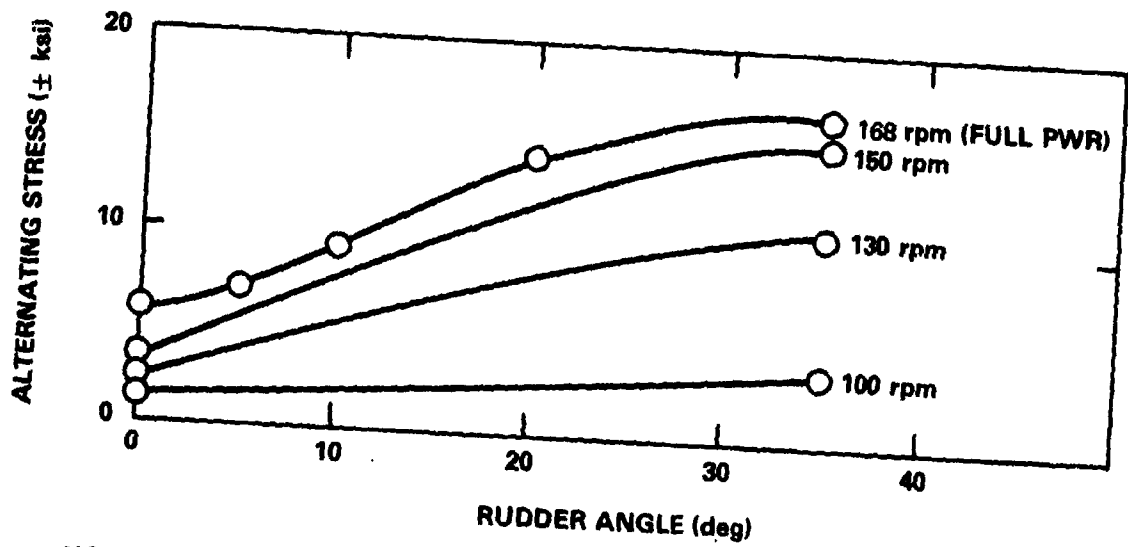
NOTE - STRESSES SHOWN ARE AVERAGES OF THE MAXIMUM BOLT STRESSES (TENSION AND BENDING) OCCURING DURING PORT AND STARBOARD TURNS
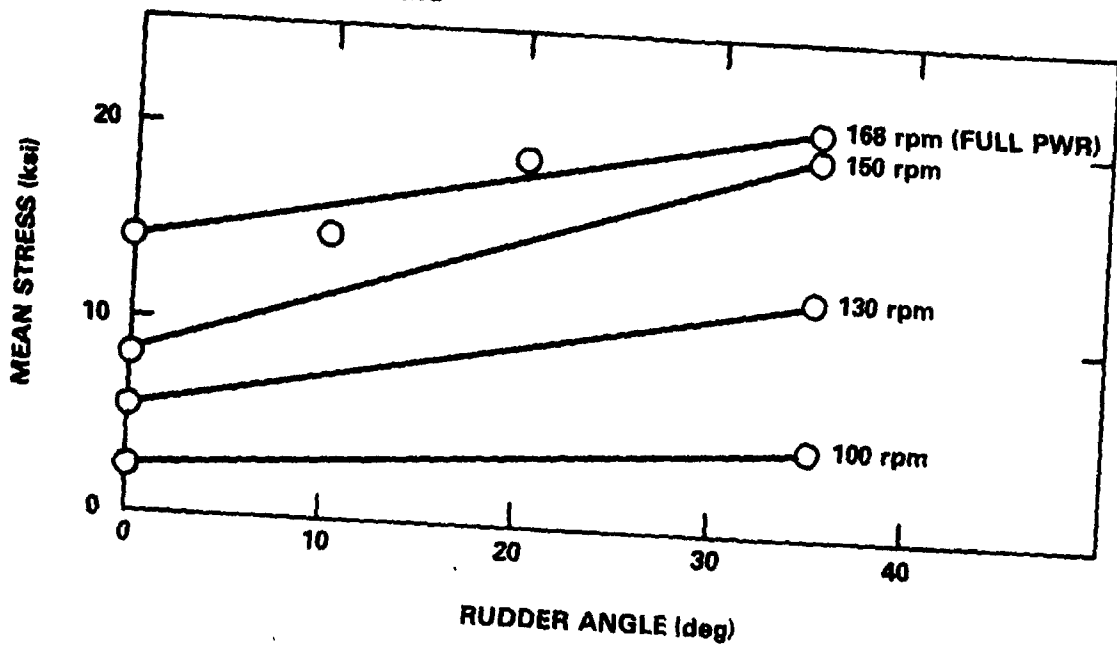
Figure 45 - Bolt (Head) Stress in Steel Bolt 8, Blade 2 versus
Rudder Angle--Design Propeller Pitch on
USS SPRUANCE

136
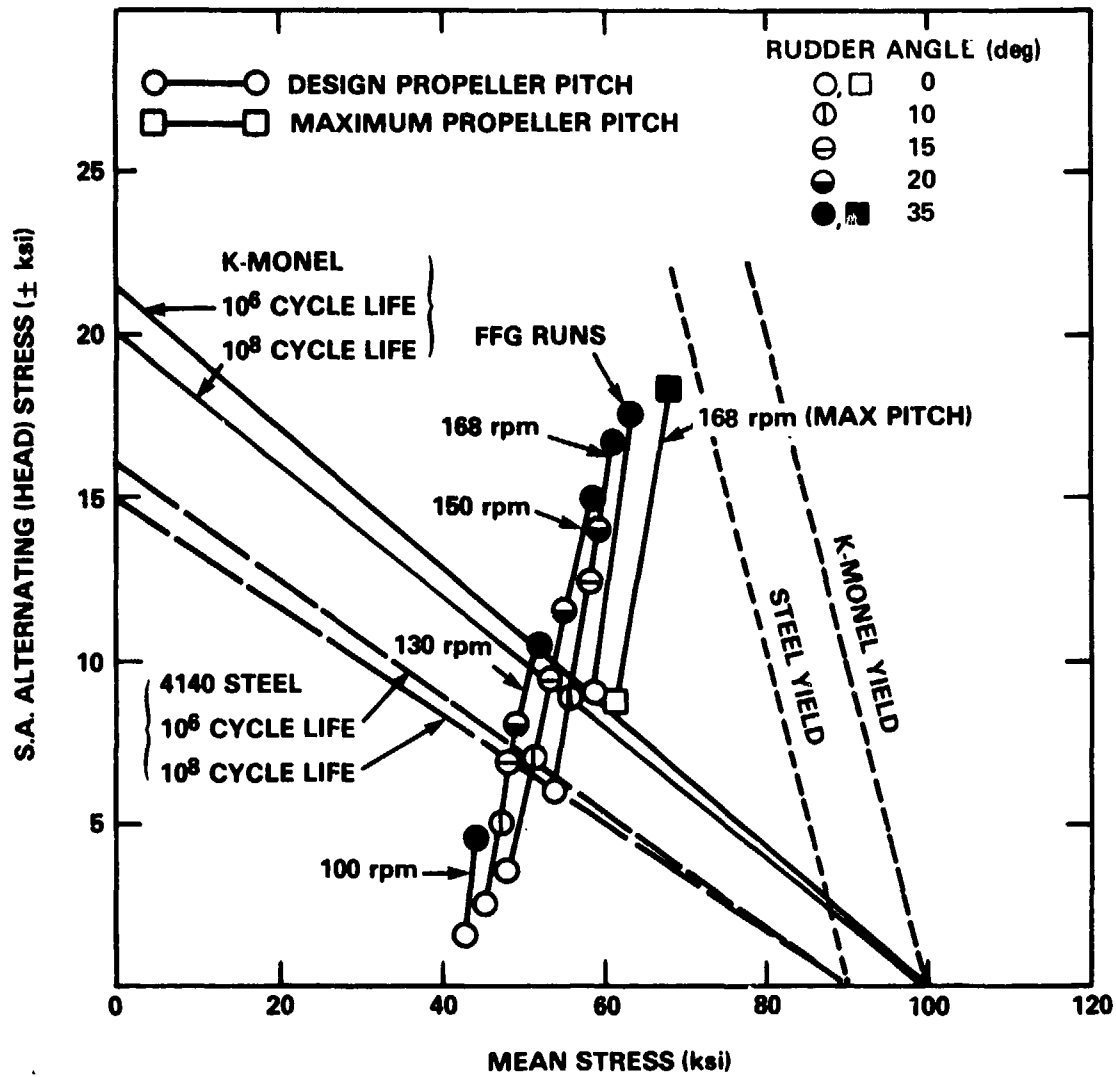
Figure 46 - Fatigue Diagram (Soderberg Line) for
Steel Bolt 8, Blade 2 on USS SPRUANCE

137
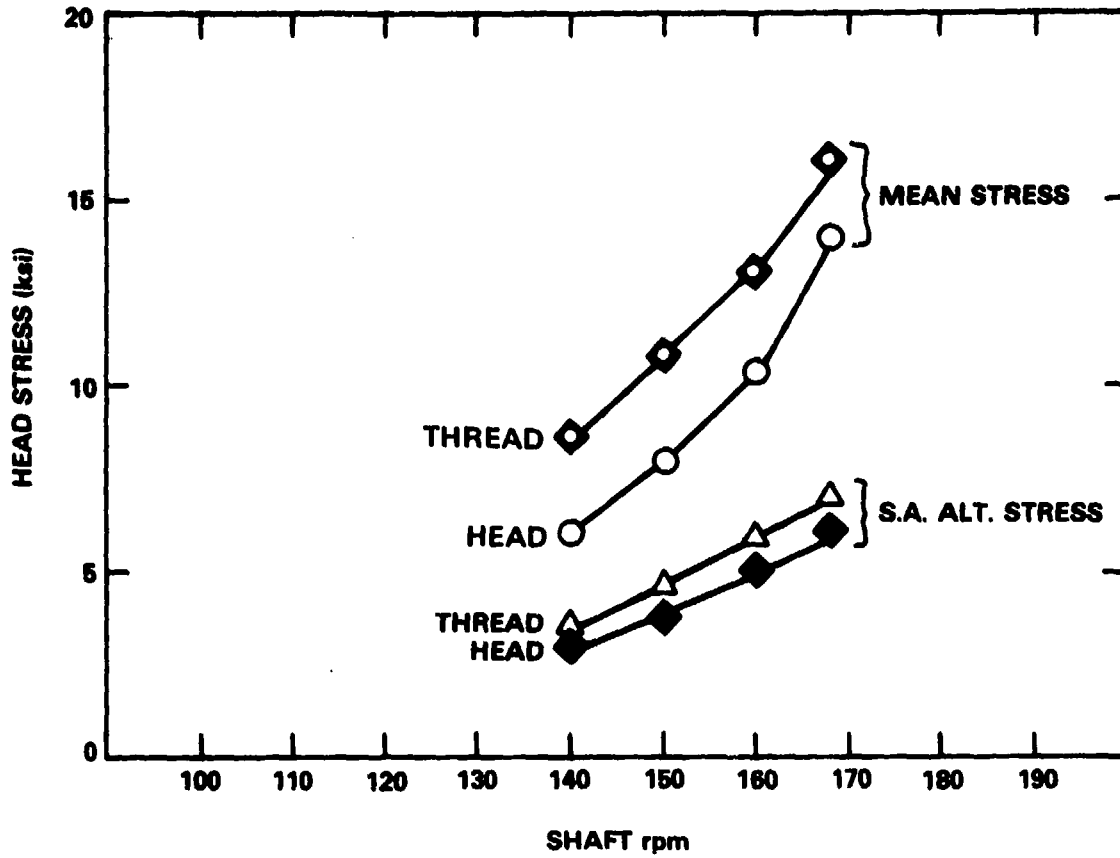
Figure 47 - Maximum Stress (Bending and Tension) Steel Bolt 8,
Blade 2 for Steady-Ahead Operation on USS SPRUANCE

Figure 48 - Propeller Bolt (Head) Stress Distribution at Full-Power
Steady-Ahead and 35 Degree Turn Conditions for
USS OLIVER HAZARD PERRY
(180 Revolutions per Minute)
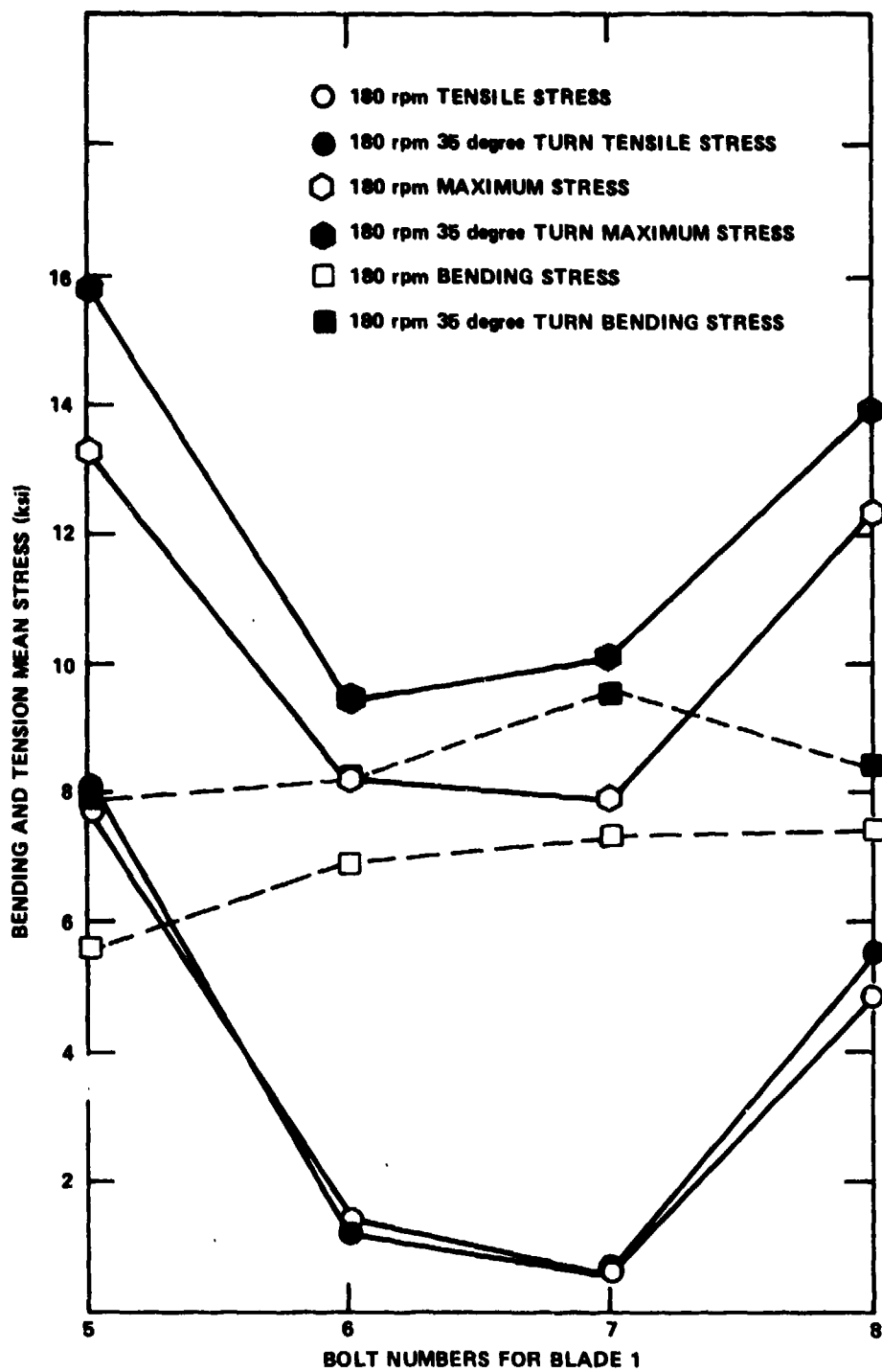
Figure 48a - Mean Stress

Figure 48 (Continued)
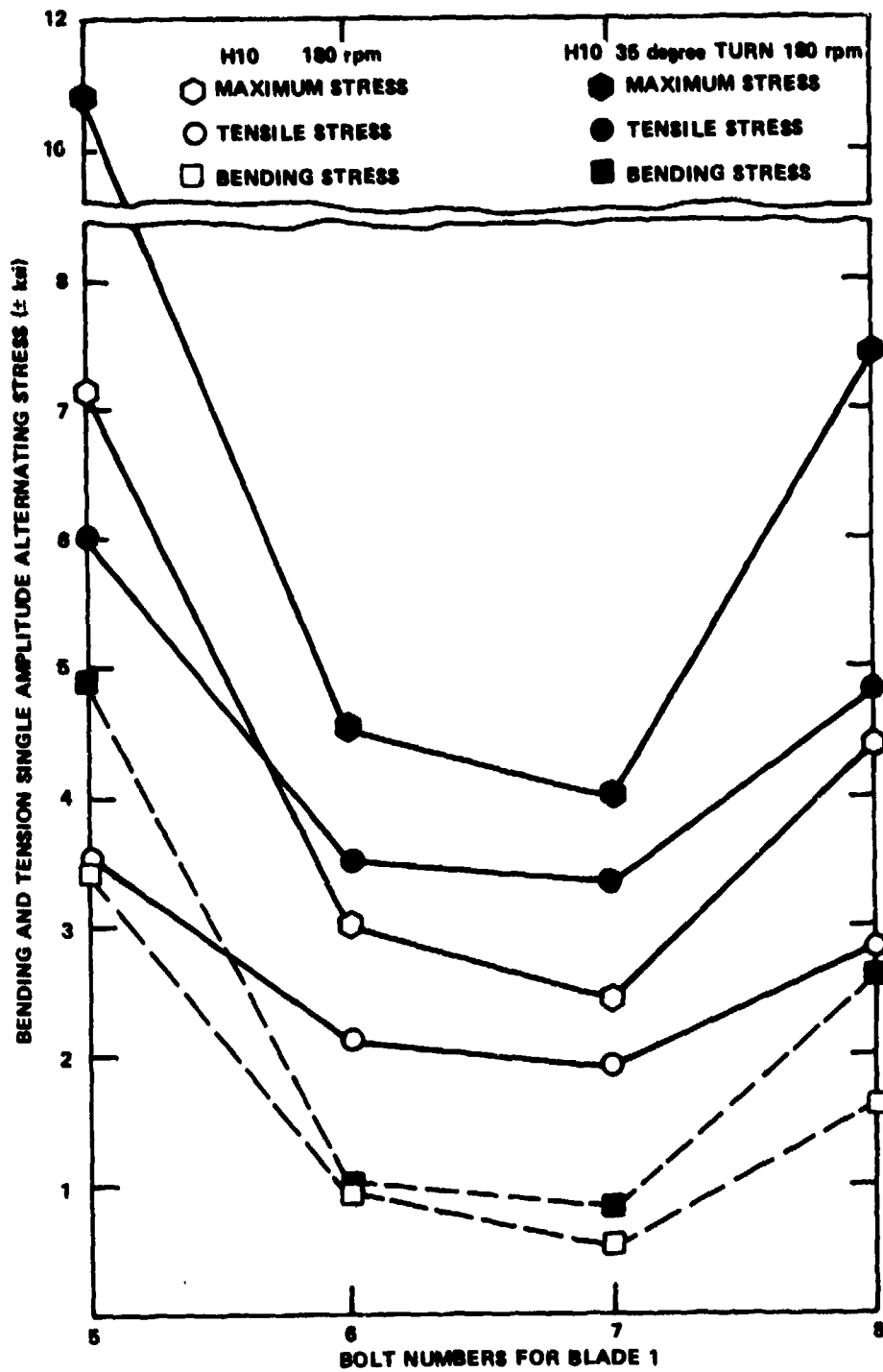
Figure 48b - Single Amplitude Alternating Stress

140
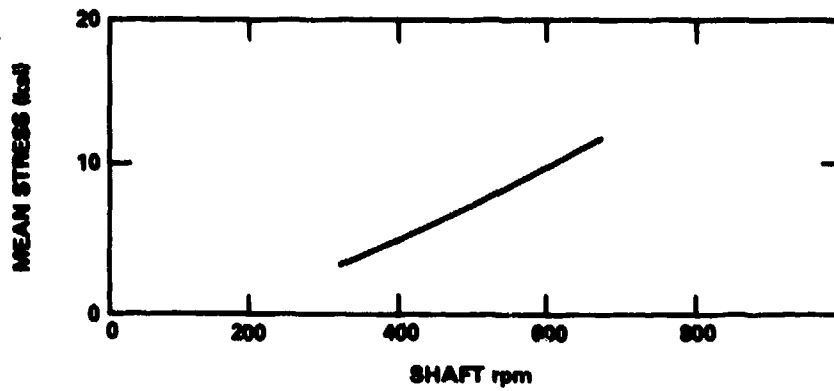
Figure 49a – Propeller Blade 4
(0.4 Radius, Midchord, Pressure Face)
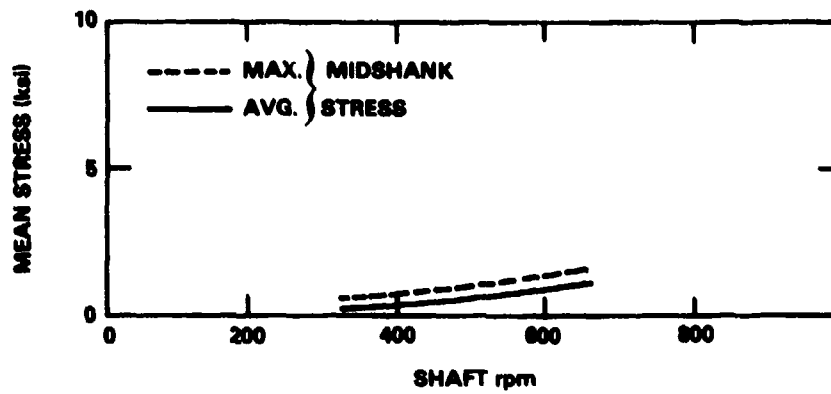
Figure 49b – Bolts 2 and 4
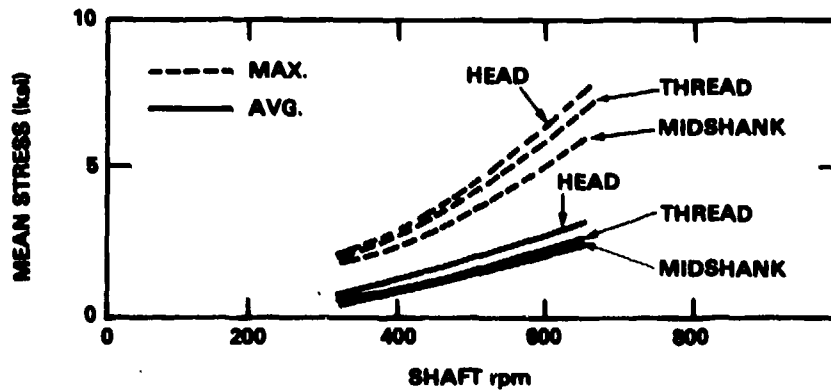
Figure 49c – Bolt 6

Figure 49 – Response of Controllable Pitch Propeller
Component Measured on R/V ATHENA
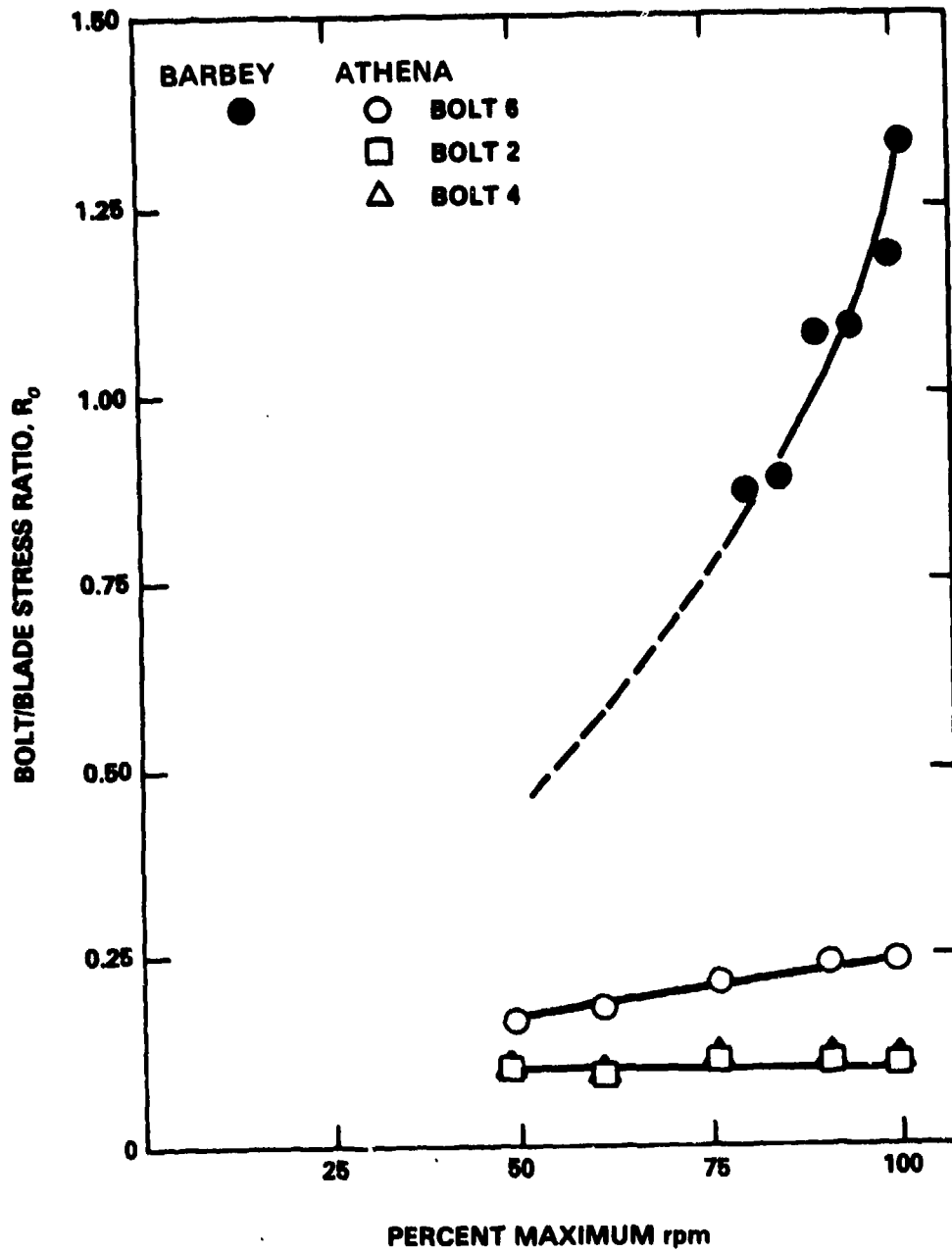
Figure 50 – Comparison of Average Midshank Bolt Stress on USS BARBEY and R/V ATHENA

142
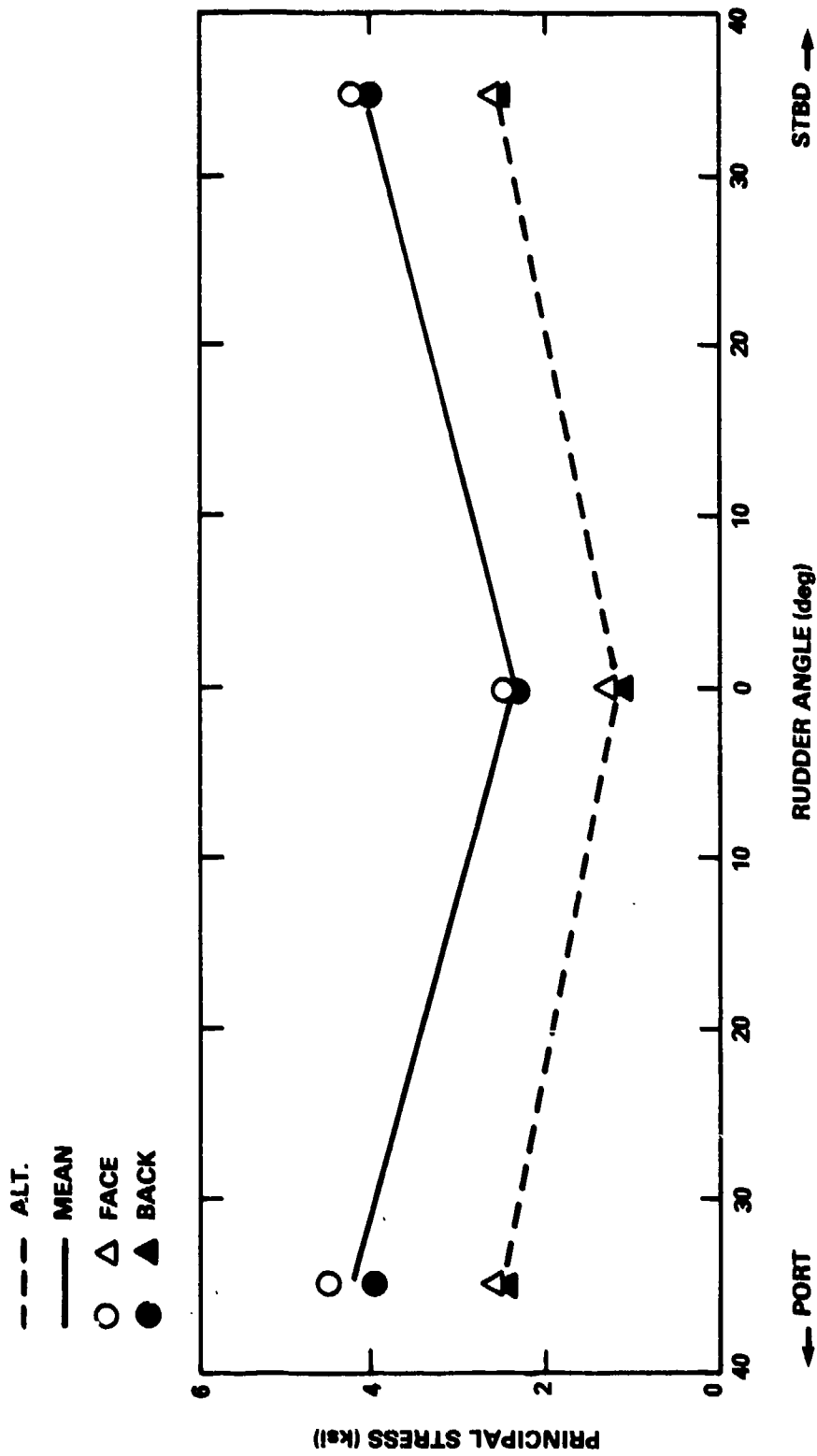
Figure 51 - Effect of Turns of Propeller Blade Stress
(40 Percent Radius, 50 Percent Chord),
Blade 4 on R/V ATHENA at 15.3 Knots

TABLE 26 - PERCENT ALTERNATING PRINCIPLE STRESS ON PROPELLER BLADES
FOR FULL-POWER, AHEAD OPERATION ON USS BARBEY

(226 rpm and 191-in. Pitch)

Blade Number	Percent Alternating Stress*		
	Face	Back	Total**
4	±43	•••	•••
5	±42	±47	±45

*Percent alternating stress = (Alt Stress/Mean Stress) x 100
**Total = average of face and back (roughly compensates for centrifugal load)
***No gages on back of Blade 4.

144

TABLE 27 – MEAN, MIDSHANK STRESS IN BOLTS OF BLADE 2 FOR FULL-POWER, UNDERWAY OPERATION ON USS BARBEY

TABLE 27A – INCLUDING PRESTRESS

| Location | Bolt Number | Mean Bolt Stress (ksi) | | | | Percent Bending Stress (σ_b)*** |
		$\sigma_{Max.}$	$\sigma_{Min.}$	$\sigma_{Avg.}$	σ_b*	
Blade Face	6	+80.8	+48.2	+64.5	±16.3	±25
Blade Face	2	†	†	+56.1	†	†
Blade Face	4	†	†	+55.8	†	†
Blade Back	5	†	†	+53.6	†	†
Blade Back	1	†	†	+57.2	†	†
Blade Back	3	†	†	+55.8	†	†

TABLE 27B – ABOVE PRESTRESS

| Location | Bolt Number | Mean Bolt Stress (ksi) | | | | Percent Bending Stress (σ_b)*** |
		$\sigma_{Max.}$	$\sigma_{Min.}$	$\sigma_{Avg.}$	σ_b**	
Blade Face	6	+14.6	+1.1	+7.8	±6.8	±87
Blade Face	2	†	†	+0.2	†	†
Blade Face	4	†	†	+1.1	†	†
Blade Back	5	†	†	−0.8	†	†
Blade Back	1	†	†	−0.0	†	†
Blade Back	3	†	†	−0.2	†	†

*Mean stress includes both hydrodynamic and centrifugal loads. Centrifugal bolt stress is complicated because of propeller palm distortion at full-power ahead operation. Based on unpublished test results at DTNSRDC on the full-scale SPRUANCE model, it is estimated that centrifugal bolt stress on the most heavily loaded bolt was < 1.0 ksi; conditions of 226 rpm and 191-in. pitch.

** $\sigma_b = (\sigma_{Max.} - \sigma_{Avg.})$

*** Percent $\sigma_B = (\sigma_B / \sigma_{Avg.})\, 100$

†Underway trial instrumentation was limited to two diametrically opposed gages on Bolts 1, 2, 3, 4 and 5.

TABLE 28 - MEAN PRINCIPAL STRESS DISTRIBUTION ON PROPELLER BLADE 4 FOR FULL-POWER, UNDERWAY OPERATION ON R/V ATHENA

Parameter		Percent Chord from Leading Edge								
		25			50			75		
		Angle θ_B (deg)	Principal Stress (ksi)		Angle θ_B (deg)	Principal Stress (ksi)		Angle θ_B (deg)	Principal Stress (ksi)	
			σ_{1B}	σ_{2B}		σ_{1B}	σ_{2B}		σ_{1B}	σ_{2B}
L O C A T I O N	Face	+2	+9.0	+1.0	-1	+11.2	+4.0	-	-	-
	Back	-15	-0.6	-6.5	-25	-2.3	-10.5	-17	-2.9	-8.6

Note: $\theta_B \equiv$ angle between σ_1 (principal stress) and radial stress, positive towards trailing edge.

146

TABLE 29 - RELATIVE EFFECT OF TURNS AT 15.3 KNOTS ON
PROPELLER BLADE STRESS ON R/V ATHENA

Quantity Measured		Percent Increase (+) or Decrease (-) Due to Turns Relative to Straight Ahead Operation — Rudder Angle						Ratio of (Alt/Mean) Stress During Run in Percent — Rudder Angle		
		35 deg port		0 deg		35 deg stbd		35 deg port	0 deg	35 deg stbd
		Mean	Alt	Mean	Alt	Mean	Alt			
Principal Stress	Face	+75	+96	0	0	+70	+103	56	50	60
	Back	+72	+112	0	0	+73	+117	61	49	60
Shaft rpm		-3.6		0		-1.7				

*Propeller Blade 4 (40 Percent Radius, 50 Percent Chord)

147

DISCUSSION

This interpretation of the test results assumes some knowledge on the part of the reader of the details of design of propellers in general and of CP propellers in particular. The discussion of data will concentrate only on the major findings and on other contributions which each trial has made. Then a summary of the trends which the data has established, and the significance of these trends on propeller theory and CP propeller design will be presented.

Results from Trials on USS ROOSEVELT

It was determined that the propeller blade failure on the ROOSEVELT resulted from fatigue[11] in the manganese-bronze blades (the BARBEY, SPRUANCE and OLIVER HAZARD PERRY used Ni-Al-Bronze blades). It was also determined that the alternating stresses were higher (approximately ± 40 percent of the mean) than were allotted for in the design. The effects of turns on this ship were minimal.

Results from Trials on USS DOUGLASS

Presentation of the preliminary tests results* met the needs of the sponsor, NAVSEA. It was determined that the blade failures were caused by degraded metallurgical characteristics of the titanium propeller blades in a saltwater environment. It was also determined that the alternating blade stresses were higher (approximately ± 33 percent of the mean) than the ± 20 percent which was then normally allowed in design (Figure 31). It was also found that turns had little effect on blade stresses but that the mean stress was doubled in a crashback maneuver (Figure 32).** Note that of all the trials conducted by DTNSRDC, the DOUGLAS has had the least data analyzed.

---

*Reported informally by C. Noonan as Enclosure (Preliminary Report on Propeller Stress and Hull) Superstructure Vibration Measured on USS DOUGLAS (PG-100) to DTNSRDC letter 962:CJN, 9870.1 of 10 Mar 1971.

**Based on analysis of one channel only.

Results from Trials on USS BARBEY

As noted in the Introduction the BARBEY was one of two ships to have a high power, prototype CP propeller installed for test and evaluation. The problems encountered on this system initiated the CP propeller program reported here. The test results analyzed on BARBEY represent the most extensive analysis to date. They revealed many design problem areas and provided much of the data upon which the work presented in the other chapters was based. A detailed discussion of BARBEY test data is contained in Reference 1. Because that discussion is well over 100 pages in length, only a brief summary will be given here.

The drydock tests proved quite enlightening in a number of areas. Consider bolt preload. The theory of bolt preload has been covered by many authors.[12-17] It is generally recognized that preloading a bolted joint which is subjected to variable tensile forces will minimize cyclic bolt stresses, thereby reducing the possibility of bolt fatigue. Although the concept is relatively simple, assurance of the amount of preload obtained at installation may not be simple to obtain. Table 14 shows that with the preloading technique used in the tests, consistency in the amount of preload was quite good. The amount of preload on the bolts which failed in fatigue during prior operations is, or course, unknown. Bolt preload characteristics for this installation were determined, Figures 26 through 28, but there was still the problem of the proper amount of preload to be applied. An arbitrary value of preload stress of 55 ksi* was used and the preload was applied by stressing the bolts to 70,000 psi, thereby yielding the blade palm and then backing off to 55 ksi. It was also found that a bending stress was induced into the bolt on installation. This stress averaged 15 percent of the installed preload stress. It could have been induced by inconsistencies within the assembly (e.g., allowable manufacturing tolerances in specified parallelisms, perpendicularity, etc.) or the design of the joint (e.g., contoured stiffness of the propeller blade palm, bearing rigidity of the clamped surfaces, etc.). Bolt removal in drydock after trials showed little or no change in preload (Table 15).

---

*All bolt stresses on the BARBEY were measured at the middle of the bolt shank (midshank), see Figure 5.

The effect of bolt preloading was seen, as expected, to induce a relatively small stress in the crank ring fillet adjacent to the bolts (Table 17).

The next phase of drydock tests was the application of known static loads to the propeller blades, Figure 29a and Table 21. Measured response of the propeller blade for these tests indicated that a reasonable estimate of static blade "loads" can be obtained by using the measured principle stress (40 percent radius, midchord) and the calculated section properties.

Measured results on the blade bolts and crank ring (Figures 29c and 29d) showed that unlike the propeller blade, the accountability of stresses for these components was considerably more difficult because the load path is far more complex. These tests showed that the bolts exhibited a nonuniform response as well as a nonlinear response to a linear load as is characteristic of preloaded bolts. As dicsussed in Reference 1 and Chapter V, this is caused by distortion of the blade palm and by separation of the palm and crank ring interface.

The final phase of drydock tests examined the natural frequencies of the blade as attached to the hub (Table 22). It was found that the fundamental blade bending and torsional modes (in air) were 31 Hz and 127 Hz, respectively.

Dockside tests determined the (nonrotating) natural frequencies of the CP propeller system in water. As predicted by theory, the added mass effect of the water lowers the two fundamental modes to 19 Hz (bending) and 80 Hz (torsional). These characteristics were noted in order to aid in underway evaluation of the measured stresses because the first bending mode was very close to full-power blade frequency excitation (approximately 20 Hz).

The objective of the underway tests was to determine actual operational stresses on the blades, bolts, and crank ring. A considerable number of underway test conditions were run to determine the magnitude of blade loads and the stresses induced under a variety of operating conditions. Selected tests were analyzed in order to present a comprehensive picture of system response. Most of the emphasis was on the design-ahead condition (steady state operation) in order to directly correlate the propeller design assumptions with experimental results. In addition, maneuvering test results were analyzed to determine the effects of off-design operation.

During all underway runs, standardization data were recorded and certain parameters monitored to avoid overloading the propulsion plant. Some of this information was used to calculate blade loads. A single blade hydrodynamic resultant (R_L) was determined by using the measured torque, thrust, and rpm. See Figure 33 for the input forcing function on each blade at 0 deg rudder. This function follows a frequency square (ω^2) law. The magnitude of the resultant for full-power (226 rpm) steady operation is approximately 54,000 lb/blade.*

Reponse of the propeller blade, bolts, and crank ring to steady, incremented steps in powering are shown in Figure 34. This figure presents an overall view of both the mean and alternating stresses for steady-state operation. Details of the mean and alternating stress response of the individual CP propeller components at full power (226 rpm, 190 in pitch) operation are shown in Figures 35 through 38. Figure 39 shows typical transducers' time history responses relative to angular rotation of the propeller at 210 rpm. Analysis of this information showed that the qualitative and quantitative mean response of the propeller blades correlated well with both drydock and standardization results. Propeller blade "loads" at 0.7R were calculated using the measured stress at the root (40 percent radius, midchord) and the previously determined geometric properties. The calculated resultant (R_L) was 56,000 lb. This is shown in Figure 33 together with standardization data. The blade response was linear with load.**

Fluctuating blade stresses are seen to be of a periodic, complex nature. The harmonic content of this complex signal is seen in Figure 40 to be primarily shaft frequency with a large number of higher frequency components. The average (percent of mean) alternating stress over the entire blade is shown in Table 26. The value is approximately 45 percent. The mean response of the blade bolts for full-power underway operation, Figure 34, showed similar characteristics to those seen in the drydock tests. The hydrodynamic loads were not distributed among the bolts as was assumed in the design. Bolt 6 (on the pressure face of the blade towards the

---

*Design calculated 120 percent of R_L was 74,300 lb at 240 rpm. Extrapolation of the measured R_L at 226 rpm to 240 showed that agreement between calculated and measured results was within 2 percent.

**Dashed curves in Figure 34 are presented in order to compare the measured CP propeller component responses with that of one which is proportional to ω^2 (arbitrarily referenced to data at 180 rpm, 191 in pitch).

trailing edge, Figure 52) was subjected to an inordinately large mean stress (Figure 36) and both mean and alternating strains increased nonlinearily (Figure 37). In
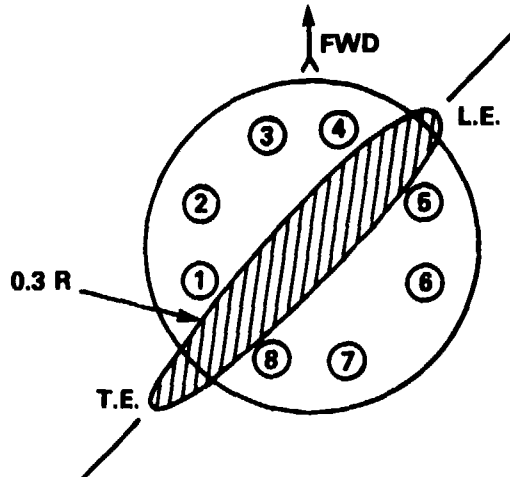
Figure 52a – Bolt Pattern for USS SPRUANCE and
USS OLIVER HAZARD PERRY Propellers
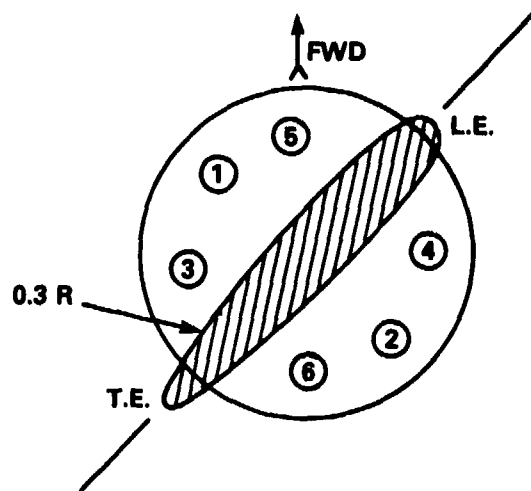
Figure 52b – Bolt Pattern for USS BARBEY, USS DOUGLAS and
R/V ATHENA Propellers

Figure 52 – Controllable Pitch Propeller Bolt Patterns

addition, the mechanism which was inducing a bending load into the bolt was more
pronounced, such that bending and axial stresses in the most highly loaded bolt
(Bolt 6) were approximately the same, Figure 37. The crank ring stress, Figure 38,
showed a corresponding skew to produce higher fillet stresses next to the most
highly loaded bolt (Bolt 6).

Maneuvering operations produced surprising results in that the maximum measured
stresses occurred during full-power turns, Figure 41, rather than the crashback
maneuvers as were predicted, Table 30. These turns result in stresses which exceeded
the accepted trial criteria, Figure 17.

TABLE 30 - PREDICTED MEAN HYDRODYNAMIC PROPELLER LOADS ON
USS BARBEY

Load Condition	Bending Moment* Due to Torque and Thrust ft - lb	Percent of Full Power
Design Full Power Ahead (No Alt Loads)	220,500	100
Crash Astern (No Alt Loads)	378,750	172
Full-Power Turn (No Alt Loads)	297,850	135
*Bending moment at crank disk fillet		

Results from Trials on USS SPRUANCE

Underway tests on the SPRUANCE represent one of the most extensive instrumentation efforts undertaken at DTNSRDC. Test objectives included the determination of the structural adequacy of the CP propeller system components (blade, bolts and crank ring), a comparison of the performance of different material and designs, and the obtainment of experimental data to aid in understanding blade loads and the response of the blade attachment to those loads.

Drydock tests were used to determine the linear bolt preload characteristic (stress and elongation) for both K-Monel and steel blade bolts, Figure 53 and Tables 16, 18 and 19. This system also experienced bolt bending during installation, the bending stress being higher at the bolt head.

Static blade load tests showed results similar to those on BARBEY (i.e., linear blade response and nonlinear, nonuniform bolt response).

In-air (drydock) and in-water (dockside) natural frequencies of the propeller blades were determined, Table 23.

Underway tests on SPRUANCE, Figures 42 through 47, demonstrated the recurring theme of higher than predicted alternating blade loads (approximately ± 40 percent of the mean for steady-ahead operation), maximum stresses occurring during high speed turns with alternating loads increasing to more than ± 80 percent of the mean and high stresses in one blade bolt; propeller blade pressure measurements have been made but have not been analyzed.

Results from Trials on USS OLIVER HAZARD PERRY

The CP propeller system installed on the OLIVER HAZARD PERRY was identical to that on SPRUANCE with the exception of the propeller blade which was more highly skewed, with a different blade root and a slight relocation of blade bolts. In spite of these similarities and the added benefit of "FFG" trial runs during SPRUANCE testing, there still was concern for the structural adequacy of the CP propeller system because of different hydrodynamic environments and control systems. Ship builder contractural obligations restricted trial instrumentation to measurement of blade bolt stresses only. Drydock tests were limited to the determination of bolt preload characteristics (which were the same as the K-Monel bolts on SPRUANCE), the bolt preload (Figure 53 and Table 20), and dynamic blade characteristics in-air (Table 24). Neither blade loader tests nor dockside tests were performed.

154

Figure 53 - Stress-Elongation Relationship
for K-Monel Bolts

155

Underway tests produced the same type of nonuniform, nonlinear bolt response as seen before on SPRUANCE and BARBEY, with the highest stresses occurring in high speed turns. Unlike the SPRUANCE however, the most highly loaded bolt (Bolt 5) was at the leading edge, pressure face rather than at the trailing edge, pressure face (Figure 48). This bolt-load distribution was unexpected and not predicted. Actually the leading and trailing edge bolts tended to "share" the load, resulting in a lower overall bolt stress picture. The reasons for this behavior are related to the shape of the blade and are discussed in Chapter V.

Results from Trials on USCG POLAR STAR

Work on the POLAR STAR involves extensive instrumentation of her three CP propeller systems as well as an elaborate series of drydock and underway tests. Testing is still being conducted at this time. Open water, underway testing showed low (as expected) stress levels on the CP components on this four-bladed propeller with stainless steel blades and integral trunnions designed for ice breaking forces which far exceed propulsion forces. The unique nature of the ice breaking data requires special computerized data processing and analysis which is currently being developed. Preliminary results indicate that instantaneous ice impact loads on each blade can be as high as 1,000,000 lb.

Results from Trials on R/V ATHENA

Underway trials on the ATHENA have recently been completed. Laboratory tests are currently being conducted at DTNSRDC.

Drydock test results indicate that preload bolt bending was lower than on the other CP propeller units (Table 13). Measured propeller blade frequencies are given in Table 25. Underway test results, Figures 49 through 51, show patterns similar to other CP propellers, but data analysis is not complete and no conclusions are made at this time. Blade pressure measurements were made and analysis of the data is planned.

It can be seen from this synopsis of the full-scale, underway tests that a number of trends were established. These data have confirmed that the propeller hydrodynamic theory that was current when the propellers were designed predicted reasonably well mean loads on the propeller blades for steady, full-power operation.

156

However, the experiments also showed that satisfactory methods were not available at that time for predicting fluctuating and off-design blade loads (e.g., fluctuating loads for steady-ahead operation were underpredicted by 100 percent). It was shown that shaft order fluctuating loads for steady-ahead operation in a calm sea were approximately 50 percent of the mean as they are on a wide variety of ships (Table 31). The current improved approach for determining hydrodynamic design loads is discussed in Chapter III.

The measured structural response of these CP propeller blade attachments also revealed a number of weaknesses in the strength design of the blade bolts, inadequate crank ring fillets, lack of consideration for the effects of fatigue, and examples of use of improper materials. Detailed discussions of each of these problems, of the related investigations which were conducted by DTNSRDC, and of the resulting design and material selection processes are contained in Chapters IV and V.

The data obtained in the full-scale trials program have produced much information that had previously been unavailable to the propeller designer. Knowledge of both the hydrodynamic and strength characteristics have been improved. The test data demonstrated that the design assumptions which presumably had been used successfully for the blade attachments on relatively low power three- and four-bladed propellers were inadequate for use with relatively high power five-bladed propellers with their inherently weaker blade attachments. The trials provided much of the information which was necessary to develop solutions for the SPRUANCE and OLIVER HAZARD PERRY CP propellers and to support the reliable design of future CP propellers.

CONCLUSIONS

The conclusions drawn from the full-scale, underway trials program are summarized here:

1. Blade loads

a. For steady-ahead operation, there is reasonable agreement between predicted and measured time average blade response.

b. For steady-ahead operations, the best available propeller theory existing prior to these tests, underpredicted shaft frequency propeller forces by a factor of 2 (100 percent).

c. For steady-ahead operations, shaft frequency propeller forces are approximately ± 50 percent of the mean.

157

TABLE 31 – COMPARATIVE SUMMARY OF FULL-SCALE, UNDERWAY PROPELLER BLADE STRESS MEASUREMENTS ON A VARIETY OF SHIPS

Ship	Source	Average Stress tons/in² (kg/mm²)	Fluctuation in Stress ton/in² (kg/mm²)	Percent Fluctuation	Remarks
VLANA	Wereldsma – International Shipbuilding Progress 133, 1964	2.93 (4.61)	±0.84 (1.32)	±29	42,000 ton Tanker
USS FRANKLIN D. ROOSEVELT	Antonides, DTNSRDC Report 2562, 1968	3.88 (6.11)	±1.61 (2.54)	±47*	Aircraft Carrier, quadruple screw
NEUENFELS	Keil et al., Journal of Hydronautics, 1972	1.79 (2.82)	±1.50 (2.36)	±84	Cargo ship (two failures in class)
FLINDERS BAY	Chirila, Shipping World and Shipbuilder, 1971	1.91 (3.01)	±0.76 (1.12)	±40	Containership
MICHIGAN	Brewer, J.SESA, 1971	4.68 (7.37)	±2.61 (4.11)	±56	Fast cargo ship (five failures in class)
GOLER NICHU	Sontvedt et al., RINA Symp., 1973	4.00 (6.30)	±1.40 (2.20)	±35	Ducted propeller
SEIUN MARU	Ueta et al., Mar. Eng. Soc., Japan, 3/74	5.85 (9.21)	±2.76 (4.35)	±46	Training ship
HEKANO MARU	Nakano, Shipbuilding Research Assoc. R.A. Japan 172, 1972	3.62 (5.70)	±1.33 (2.09)	±37	Containership

*Test results have been modified to exclude centrifugal loads.

158

TABLE 31 (Continued)

Ship	Source	Average Stress tons/in² (kg/mm²)	Fluctuation in Stress tons/in² (kg/mm²)	Percent Fluctuation	Remarks
USS DOUGLAS	Noonan, C.J., DTNSRDC, 1971	5.64 (8.88)	±1.68 (2.65)	±33*	Patrol gunboat, twin-screw
**	Conolly, Trans. Royal Inst. of Naval Architects, 1960	-	-	±43	Destroyer, twin-screw
USS BARBEY	Noonan, C.J. et al., DTNSRDC, 1975	4.80 (7.56)	±1.90 (2.99)	±45*	Frigate, single-screw
USS SPRUANCE	Antonides, G.P., DTNSRDC, 1976	4.68 (7.38)	±1.77 (2.79)	±45*	Destroyer, twin-screw
R/V ATHENA	Noonan, et al., DTNSRDC 1977, 1978	-	-	±50***	Twin-screw research vessel
USCG POLAR STAR	Hagen, A., DTNSRDC 1979	-	-	>±50***	Triple-screw icebreaker

*Test results have been modified to exclude centrifugal loads.

**Ship name not given.

***Preliminary data, analysis of test results incomplete.

159

d. Maximum total (mean plus alternating) forces on most CP propellers occurred during high speed, full-power turns. The ASHEVILLE Class appears to be the exception to this.

e. There is no indication that the natural frequency of the propeller blade or propulsion system influence the propeller forces.

2. Blade Attachment Strength

a. "Beam theory" reasonably predicts the root stress of the blades.

b. There is no appreciable increase in blade stress due to blade vibrations with the possible exception of brief transients generated during crashback maneuvers.

c. Accurate bolt preload cannot be predicted for a given installation procedure without establishing the bolted joint characteristics experimentally.

d. Bolt preloading is accompanied by a certain amount of bending. Bolt bending also occurs under applied loads.

e. The basic CP propeller design assumptions concerning the load transfer from the propeller blade palm to the crank ring were invalid.

f. The CP propeller blade palm stiffness distribution acts as a nonuniform loading mechanism on the blade bolts.

g. The then current blade attachment design assumptions could not adequately predict stresses induced by blade hydrodynamic and centrifugal forces.

h. In general the determination of actual stresses in the blade attachment requires strain measurements at sea where the many factors such as friction, tolerances, vibration, load-structure interaction, blade loads, etc., which directly affect structural response, are all included.*

i. The problems identified in the BARBEY CP propeller design were common to the SPRUANCE and PERRY CP propeller designs which are or will be used in many ships of the U.S. Navy.

3. BARBEY Failure

a. The most heavily loaded bolt (Bolt 6) was subjected to higher loads than the other bolts because of the various mechanism described above.

b. Periodic blade loads were higher than expected.

---

*Rockwell, R., "Controllable Pitch Propeller Blade Attachment Strength," Unpublished Paper, Jan 1978.

c. The combination of Items a and b perhaps aggravated by less than desired preload, resulted in the fatigue damage suffered in the first BARBEY failure.

d. The nonuniform bolt load distribution was reflected in the crank ring stress distribution and, in conjunction with a locally inadequate bolt hole wall thickness, resulted in fatigue cracks in the crank rings.

e. The material properties of the crank ring were found to be susceptible to catastrophic "brittle" fracture at less than yield strength when accompanied by a crack of critical size in the structure.

f. Crank ring failure was imminent on all blades and had no particular relation to the crashback maneuver.

4. Miscellaneous

a. The use of vulcanized rubber patches for waterproofing protection of propeller instrumentation provides excellent long-term results.

b. Spray urethane can be used for waterproofing for short-term applications.

c. Propeller blade pressure measurements are feasible, but the experimental technique needs further development.

d. The cost of measuring propeller parameters could be considerably reduced by the use of a hydrotelemetry system. Such a system is feasible, but still highly developmental at this point.

RECOMMENDATIONS

Development of the hydrotelemetry system should continue on a planned basis in order to reduce the cost of future trials of this type.

REFERENCES

1. Noonan, C. et al., "The BARBEY REPORT - An Investigation into Controllable Pitch Propeller Failures from the Standpoint of Full-Scale, Underway Propeller Measurements," DTNSRDC 77-0080 (Aug 1977).

2. Dean, M., "Miniature Pressure Gage (for use in Aerodynamic and Hydrodynamic Research Investigation)," presented at 8th Transducer Workshop, St. Louis, Mo (22-24 Apr 1975).

3. Tatnall, F. G., "Tatnall on Testing," American Society of Metals Publication, Metals Park, Ohio (1966).

4. Hanson, D., "Development of Strain Gage Protection System for Marine Propellers and Application to USS FRANKLIN D. ROOSEVELT (CVA-42)," United Aircraft Corporation, Hamilton-Standard Division Report HSER 4704 (25 Aug 1967).

5. Valentine, R., "Marine Propeller Strain Gage and Signal Transmission System for the USS DOUGLAS (PG-100)," United Aircraft Division, Hamilton-Standard Division Report HSER 5829 (16 Mar 1971).

6. Dean, M., "Vulcanized-Rubber Protection for Strain Gages in a Seawater Environment," Experimental Mechanics, Vol. 17, No. 8, pp. 303-307 (Aug 1977).

7. "Fatigue Study on the Propellers of the USCG POLAR STAR (WAGB-10) Preliminary Report," NKF Engineering Assoc., Inc., Report 7801-23 (19 Oct 1979).

8. Davies, J. C., "POLAR STAR Software," DTNSRDC Central Instrumentation Department Report CID-80/2 (Dec 1980).

9. Antonides, G. et al., "Full-Scale Underway CP Propeller Stress Trials on the USS SPRUANCE (DD-963)," DTNSRDC Evaluation Report SAD-164E-1962 (Jan 1977).

10. Schauer, R. E. and C. Noonan, "Full-Scale, Underway Controllable Pitch Propeller Stress Trials on USS OLIVER HAZARD PERRY (FFG-7)," DTNSRDC Report 80/114 (Dec 1980).

11. Antonides, G., "Propeller-Stress Trials on USS FRANKLIN D. ROOSEVELT (CVA-42)," DTNSRDC Report 2562 (Apr 1968).

12. Faires, V., "Design of Machine Elements," Collier-MacMillan Canada, Ltd. (1965).

13. Meyer, G., "Simple Diagrams Aid in Analyzing Forces in Bolted Joints," Assembly Engineering, Vol. 15, No. 1 (Jan 1972).

14. Motosh, N., "Determination of Joint Stiffness in Bolted Connections," J. Eng. for Indust. (Aug 1976).

15. Fazekas, G., "On Optimal Bolt Preload," J. Eng. for Indust. (Aug 1976).

16. Thompson, J. et al., "The Interface Boundary Conditions for Bolted Flanged Connections," J. Pressure Vessel Technol. (Nov 1976).

17. Landt, R., "Criteria for Evaluating Bolt Head Design," J. Eng. for Indust. (Nov 1976).

CHAPTER III

BLADE LOADS

TABLE OF CONTENTS

Page

LIST OF FIGURES

LIST OF TABLES

NOTATION

A_E Expanded area, $Z \int_{r_h}^{R} c \, dr$

A_0 Propeller disk area, $\pi D^2/4$

A_r Fourier cosine coefficient of radial component of wake velocity

A_t Fourier cosine coefficient of tangential component of wake velocity

A_x Fourier cosine coefficient of longitudinal component of wake velocity

B_r Fourier sine coefficient of radial component of wake velocity

B_t Fourier sine coefficient of tangential component of wake velocity

B_x Fourier sine coefficient of longitudinal component of wake velocity

C_{Th} Thrust loading coefficient, $T/[(\rho/2)V_A^2 A_0]$

c Chord length

D Propeller diameter

$(F)_n$ n^{th} harmonic amplitude of F

$F_{x,y,z}$ Force components on blade in x,y,z directions

J Advance coefficient, $J = V_A/nD$

J_V Ship speed advance coefficient, $J = V/nD$

K_Q Torque coefficient, $Q/(\rho n^2 D^5)$

K_T Thrust coefficient, $T/(\rho n^2 D^4)$

k Integer; reduced frequency, $\omega c(r)/(2V_r)$

168

L	Any of the measured components of blade loading; lift of wing section
L_W	Wavelength
$M_{x,y,z}$	Moment components about x,y,z axes from loading on one blade
$(M)_n$	n^{th} harmonic amplitude of M
n	Propeller revolutions per unit time
P	Propeller blade section pitch
Q	Time average propeller torque arising from loading on all blades, $-Z\overline{M}_x$
R	Radius of propeller
r	Radial coordinate from propeller axis
S	Skew back of propeller blade section measured from the spindle axis to the midchord point of the blade section, positive towards trailing edge
T	Time average thrust of propeller, positive forward, $Z\overline{F}_x$
V	Model speed or ship speed
V_A	Propeller speed of advance
V_R	Vector sum of speed of advance and rotational velocity
$V_r(r,\theta_W)$	Radial component of wake velocity, positive towards hub
$(V_r)_n$	n^{th} harmonic amplitude of V_r
$V_t(r,\theta_W)$	Tangential component of wake velocity, positive counterclockwise looking upstream for right hand rotation, positive clockwise looking upstream for left hand rotation
$(V_t)_n$	n^{th} harmonic amplitude of V_t

169

$V_x(r, \theta_W)$ Longitudinal component of wake velocity, positive forward

$(V_x)_n$ n^{th} harmonic amplitude of V_x

V_ψ Maximum vertical velocity of propeller resulting from hull pitching motions

x, y, z Coordinate axes

z Number of blades

z_R Rake of propeller blade section measured from the propeller plane to the generator line, positive aft

θ Angular coordinate used to define location of blade and variation of loads, from vertical upward positive clockwise looking upstream for right-hand rotation, positive counter-clockwise looking upstream for left-hand rotation, $\theta = -\theta_W$

θ_S Skew angle measured from spindle axis to projection of blade section midchord into propeller plane, positive towards trailing edge

θ_W Angular coordinate of wake velocity, from upward vertical, positive counterclockwise looking upstream for right hand rotation, positive clockwise looking upstream for left hand rotation, $\theta_W = -\theta$

$\kappa_{(F)n}$ n^{th} harmonic force coefficient, $(F)_n / (\rho n V_A D^3)$

$\kappa_{(M)n}$ n^{th} harmonic moment coefficient, $(M)_n / (\rho n V_A D^4)$

ρ Mass density of water

ρ_P Mass density of propeller blade

ϕ Pitch angle of propeller blade section, $\tan^{-1} [P/(2\pi r)]$

$(\phi_{F,M})_n$ n^{th} harmonic phase angles of F,M based on a cosine series,

$$(F,M) = (\overline{F}, \overline{M}) + \sum_{n=1}^{N} (F,M)_n \cos [n\theta - (\phi_{F,M})_n]$$

170

$(\phi_{Vr}{}^*)_n$ n^{th} harmonic phase angles of V_r based on a sine series,

$$V_r = (\overline{V}_r) + \sum_{n=1}^{N} (V_r)_n \sin [n\Theta_W + (\phi_{Vr}{}^*)_n]$$

$(\phi_{Vt}{}^*)_n$ n^{th} harmonic phase angles of V_t based on a sine series,

$$V_t = (\overline{V}_t) + \sum_{n=1}^{N} (V_t)_n \sin [n\Theta_W + (\phi_{Vt}{}^*)_n]$$

$(\phi_{Vx}{}^*)_n$ n^{th} harmonic phase angles of V_x based on a sine series,

$$V_x = (\overline{V}_x) + \sum_{n=1}^{N} (V_x)_n \sin [n\Theta_W + (\phi_{Vx}{}^*)_n]$$

ω Circular frequency of encounter of periodic velocity

Subscripts:

c   Arising from centrifugal loading

Exp   Experimental value

g   Arising from gravitational loading

H   Arising from hydrodynamic loading

h   Value of hub radius

M   Model value

MAX   Maximum value

MIN   Minimum value

PEAK   Peak value including variation of both time-average value per revolution and variation with blade angular position

S   Ship value

T   Total loading from hydrodynamic, centrifugal, and gravitational components

x,y,z   Component in x,y,z direction

0.3   Value at $r = 0.3R$

0.4 Value at $r = 0.4R$

0.7 Value at $r = 0.7R$

ζ Value for operation in waves

ψ Value for operation with hull pitching motion

Superscripts:

$-$ Time-average value per revolution

$\sim$ Unsteady value, peak value per revolution minus time average value per revolution

$\cdot$ Rate of change with time

INTRODUCTION

STATEMENT OF THE PROBLEM

Extreme care must be taken to design the blades, palms, fillets, and internal hub and mechanisms of high power controllable pitch (CP) propellers so that they possess adequate strength including consideration of yield and fatigue stresses. This requires an accurate estimate of the maximum time-average or transient loads and periodic loads* under all operating conditions. High time-average or transient loads and periodic loads occur at steady full-power ahead conditions and during high-speed maneuvers including full-power crash astern, full-power crash-ahead, and full-power turns. In addition, the influence of a rough sea may substantially increase the time-average, alternating, and peak loads. In the beginning of the research and development (R and D) program on CP propellers there existed no confirmed techniques whereby the pertinent loads, other than time-averaged loads, at steady ahead calm sea conditions, could be predicted to reasonable accuracies. Boswell et al.,[1-5]** Jessup et al.,[6] and Schwanecke and Wereldsma[7] reviewed the factors affecting blade loads for propellers in general, and Rusetskiy[8] and Hawdon et al.[9] discussed some of the factors peculiar to blade loads of CP propellers.

In the past, CP propellers were generally designed by calculating only the time-average loads for full-power steady-ahead operation in calm water. Periodic loads, loads during maneuvers, and loads in a rough sea were not generally calculated, but were accounted for in the structural design of the various components by applying an appropriate factor of safety to the calculated loads for full-power steady-ahead operation in calm water.

This approach was apparently satisfactory in the past when CP propellers were limited to delivered power in the range of 20,000 hp (15 MW) or less. However, this approach is not satisfactory for CP propellers with delivered power in the range of 35,000 hp (26 MW) or more, which is the range of CP propellers on the surface combatants currently being added to the fleet, such as on the USS SPRUANCE (DD-963), USS OLIVER HAZARD PERRY (FFG-7), and USS TICONDEROGA (CG-47). The problem of designing structurally reliable CP propellers with delivered power of 35,000 hp (26 MW) or more was demonstrated by the structural failure of the crank rings to which the blades of the CP propeller on the USS BARBEY (FF-1088) were bolted.[10]

---

*The terms time-average loads, transient loads, and periodic loads are defined in the following section.

**A complete listing of references is given on page 229.

DEFINITION OF BLADE LOADS

Blade loads are defined as the magnitude and distribution of incremental forces over the propeller blade. Incremental information over the blade is generally required for determination of the local stresses in the blade; however, for determination of the stresses in the blade fillet and palm and in components of the propeller hub, it is generally sufficient to know the force and moment components of the total loads on the blade along three arbitrary noncoplanar axes. The axes shown in Figure 1 are used in the present report. The strength of the blade attachments and of components inside the hub rather than the overall strength of the blades is the primary concern in the present report; therefore, blade loads in the present chapter will refer primarily to the net blade force and moment components as shown in Figure 1.

In general, blade loads vary as a function of time. It is convenient to represent this time dependence as follows:
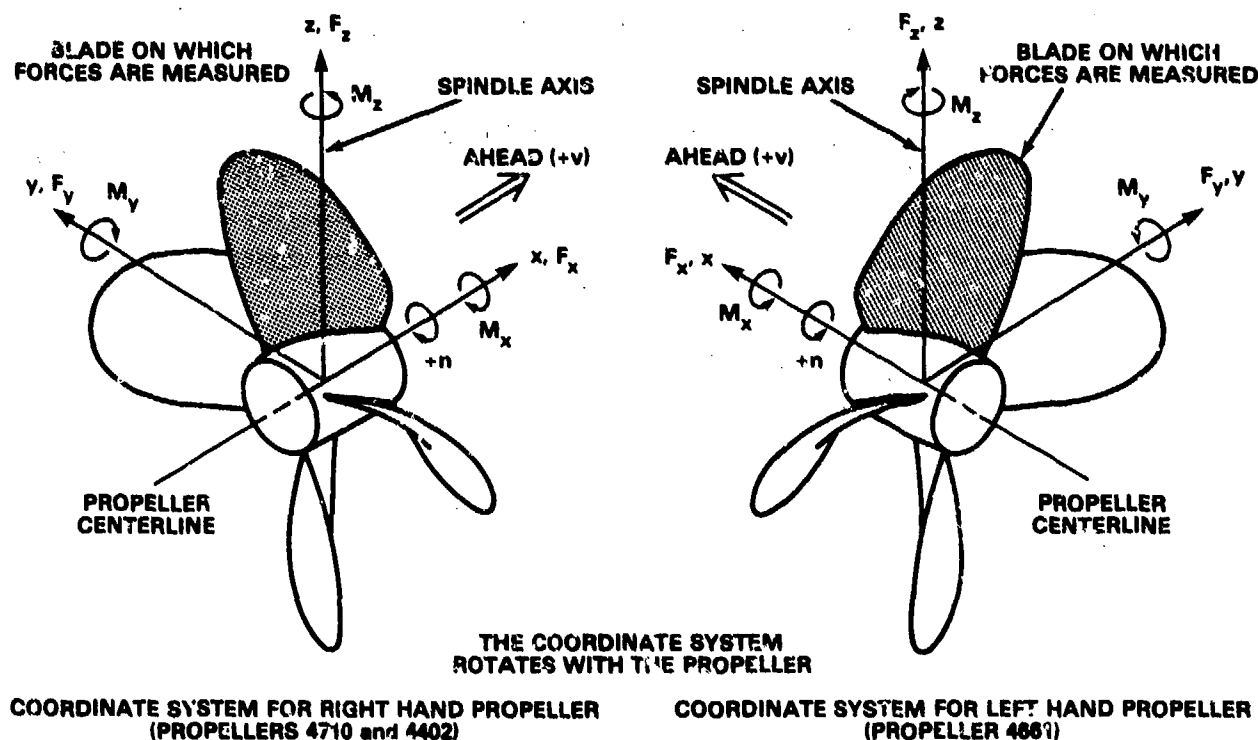
Figure 1 - Components of Blade Loading

1. Time-average loads vary over some specified length of time equal to or greater than the time of one revolution of the propeller.

2. Transient loads, or the variation of the time-average loads, vary per propeller revolution with time, such as in a maneuver or in a rough sea.

3. Periodic loads, or cyclic variation of loads with blade angular position. These periodic loads are superimposed on the pertinent time-average loads or transient loads.

4. Peak loads is the designation used in this chapter for the largest instantaneous load including contributions from time-average or transient loads and periodic loads.

Blade loads arise from the distribution of hydrodynamic, centrifugal, and gravitational forces over the blade. The total centrifugal load, which is a function only of the blade geometry, blade density, and propeller rotational speed, has only time-average and transient parts and can be readily calculated. The net gravitational load, which is a function only of the blade geometry and blade and water density, occurs only as a first harmonic of blade angular position and can be readily calculated. In almost all practical situations, the most important component of load is the hydrodynamic component. Further, the hydrodynamic loads are much more complex and difficult to predict than are centrifugal or gravitational loads. Therefore, this chapter addresses primarily the hydrodynamic loads.

BACKGROUND

In the beginning of the research and development program on CP propellers there were no confirmed methods for predicting hydrodynamic blade loads, except for time-average loads under steady-ahead operation in a calm sea.

Before the current research and development program on CP propellers, the best available analytical method for calculating the periodic blade loads (due to circumferentially nonuniform inflow) underpredicted the periodic loads as a result of operation in inclined flow of from 40 to 70 percent. This method was erroneously thought to be reliable in inclined flow because it worked reasonably well in axial flow, and there existed no reliable experimental data in inclined flow with which to compare this analytical method.

During the course of the present research and development program on CP propellers, analytical and experimental methods were developed which yield substantially

175

improved predictions of the periodic blade loads due to operation in inclined flow. However, correlation of the analytical method with the extensive model and full-scale experimental data developed during the present research and development program, shows that this improved analytical method underpredicts the periodic blade loads by from 10 to 20 percent; thus, an empirical factor is required to compensate for the underprediction of the analytical procedure. Therefore, for a new propeller-hull configuration, the periodic blade loads in inclined flow can be predicted by model experiments using the procedures developed under the present research and development program, or by the analytical procedure, with appropriate empirical factors, developed under the present research and development program.

It is more difficult to calculate the blade loads during maneuvers or for an operation in a rough sea than it is for steady-ahead operation in calm water. Any methods for calculating loads under these conditions are, of necessity, more approximate than for steady-ahead operation in a calm sea; therefore, there is a greater need for systematic reliable experimental blade load data to serve as a check for guidance, and to provide empirical factors. Before the current research and development program, no such experimental data were known to exist. There existed no known systematic controlled experimental measurements of the transient or periodic blade loads in crash-ahead or crash-astern maneuvers, and no known measurements of the time-average or periodic blade loads due to operation in a rough sea. Further, there existed no known measurements of the wake patterns in a turn, which are necessary for making a rational prediction of the periodic loads in a turn.

Rational procedures for predicting blade loads during maneuvers and for operation in a rough sea were developed during the present research and development program. These include the development of experimental procedures for measuring these loads on a model scale, and for measuring blade loads over a systematic range of parameters during crash-ahead and crash-astern maneuvers and operation in a rough sea. Further, wake patterns during turns were measured on two model hulls. Engineering procedures were developed for calculating blade loads during maneuvers and for operation in a rough sea using the experimental data as a check, for guidance and to provide any necessary empirical factors.

176

SUMMARY OF CHAPTER III

The present chapter summarizes the work on blade loads under the research and development program on CP propellers, presents methods of calculating blade loads under various operating conditions, and presents some guidelines for minimizing blade loads in future designs.

The work on blade loads under the CP propeller research and development program consisted of developing improved methods of predicting blade loads. This was achieved through various model and full-scale experiments; development of improved analytical procedures; and correlation of the results of model experiments, analytical procedures, and various full-scale measurements described in Chapter II. Most of the analytical work and a major portion of the model experimental program were directed towards developing rational and reliable methods for predicting the periodic blade loads arising from the inclination of the inflow relative to the propeller shaft, which is the primary cause of periodic blade loads behind hulls with high speed transom sterns, with exposed shafting and struts, such as surface combatants. These methods can be used for predicting periodic blade loads on surface combatants under steady-ahead operation in a calm sea.

Experiments were conducted to determine the influence of ship acceleration and deceleration, operation in a rough sea, and turns on the periodic blade loads. Using these experimental results as a guide, approximate methods were developed for predicting periodic blade loads for these operating conditions. These predictions require knowledge of the operating conditions including the time dependence of ship speed, propeller rotational speed, and propeller pitch-ratio for all maneuvers; ship drift and heel angle for turning maneuvers; and sea state characteristics and ship motions for operation in a rough sea.

The use of available techniques for predicting time-average or transient hydrodynamic blade loads and periodic hydrodynamic blade loads under various operating conditions, and their associated accuracies and costs, are summarized. These include the use of model experiments, analytical procedures, and existing statistical data. Centrifugal and gravitational loads can be accurately calculated analytically for all operating conditions.

The techniques for predicting blade loads discussed in the present chapter are applicable to fixed-pitch as well as CP propellers; however, the resulting stresses are more critical in CP propellers due to the complex mechanism inside the hub, the restricted length of the blade attachment to the palm, and the short chord lengths

177

at the inner radii. These techniques may be useful in the design of fixed-pitch propellers, especially for determining the minimum required chord lengths and thicknesses near the hub for adequate structural integrity.

Some guidelines for minimizing blade loads in future CP propeller designs are presented including consideration of the stern geometry, preliminary propeller design, detailed propeller blade design, the propulsion control system, and operating guidelines.

Specific recommendations include the following:

1. Consider the influence on propeller blade loads of the following variables during the preliminary design stage: number of propellers, propeller diameter, number of blades, and propeller rotational speed under full-power steady-ahead operation.

2. Minimize the inclination of the shaft relative to the stern. This will reduce the effective inclination of the inflow relative to the propeller shaft and, thereby, reduce the periodic blade loads for all operating conditions.

3. Use balanced skew (skew forward at the inner radii and skew backward at the outer radii) and forward rake. This is desirable for considerations of bending moments arising from centrifugal and gravitational forces, and for minimizing spindle torque arising from centrifugal and hydrodynamic forces. With this technique the net time-average blade spindle torque can be made negligible under steady-ahead operation.

4. Unload the blade tips. This moves the radial centers of the time-average hydrodynamic blade loads closer to the hub and thereby reduces time-average bending moments.

5. Design the propulsion control system with the aid of computer dynamic simulations and the associated supporting model experiments in an attempt to obtain the optimum balance between minimizing the values of peak propeller blade loads in maneuvers and maintaining superior ship maneuvering characteristics.

6. Provide guidelines to the shipboard personnel regarding manually controlled operating conditions which have a large influence on propeller blade loads, such as power reduction for operation in rough seas.

BLADE LOAD INVESTIGATIONS UNDER THE RESEARCH AND DEVELOPMENT PROGRAM ON CONTROLLABLE PITCH PROPELLERS

INTRODUCTION

The woik on blade loads under the research and development program on CP propellers consisted of developing improved methods of predicting blade loads, especially the variation of loads with blade angular position. This was achieved through various model experiments, development of improved analytical procedures, and correlation of the results of model experiments, analytical procedures, and various full-scale measurements described in Chapter II. Most of the analytical work and a major portion of the model experimental program was directed towards developing rational and reliable methods for predicting the periodic blade loads arising from the inclination of the inflow relative to the propeller shaft. This is the primary cause of periodic blade loads on ships, such as surface combatants, with high speed transom sterns and exposed shafts and struts. These methods can be used for predicting periodic blade loads on surface combatants under steady-ahead operation in a calm sea.

Experiments were conducted to determine the influence of ship acceleration and deceleration, operation in a rough sea, and turns on the periodic blade loads. Using these experimental results as a guide, approximate methods were developed for predicting periodic blade loads for these operating conditions. These predictions require knowledge of the operating conditions including the time dependence of ship speed, propeller rotational speed, and propeller pitch-ratio for all maneuvers; ship drift and heel angle for turning maneuvers; and sea state characteristics and ship motions for operation in a rough sea.

STEADY-AHEAD OPERATION IN CALM WATER

Variations of blade loads with the angular position of the blade in the wake, or periodic blade loads, are caused by the circumferential variation of the inflow velocity components in the axial, tangential, and radial directions relative to the propeller axis at the propeller.plane; see Figure 2.* These components are commonly represented by their harmonic constituents as a function of angular position.

---

*References in this report to inflow velocity components imply components in a polar coordinate system as defined in Figure 2. Note that a uniform flow inclined to the propeller shaft has tangential and radial components with a sinusoidal variation with angular position.

V_x IS IN DIRECTION OF
PROPELLER AXIS, POSITIVE
AFT RELATIVE TO THE
PROPELLER.
OTHER COORDINATES POSITIVE
AS SHOWN.
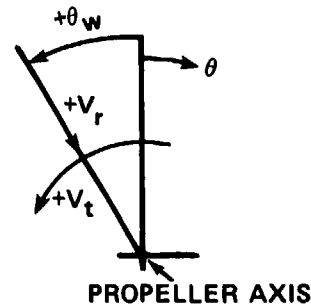
LOOKING FORWARD;
CONVENTIONS SHOWN FOR
RIGHT-HAND PROPELLER
ROTATION. FOR LEFT-
HAND ROTATION, θ, θ_W,
AND V_t ARE IN OPPOSITE
DIRECTIONS TO THOSE
SHOWN.

Figure 2a - Typical Wake Pattern of
a Given r/R for High-Speed Transom
Stern Configuration with
Exposed Shafts and
Struts

Figure 2b - Conventions

Figure 2 - Wake Components

For hulls with high-speed transom sterns with exposed shafts and struts, such
as surface combatants, the circumferential variation of the inflow is predominantly
the first harmonc of the tangential component arising from the inclination of the
inflow relative to the propeller shaft. Therefore, for these vessels, the periodic
blade loads are produced primarily by the inclination of the inflow velocity
relative to the propeller shaft.

At the beginning of the current research and development program on CP pro-
pellers, the most sophisticated method for calculating periodic blade loads under
steady-ahead operation in calm water was the method of Tsakonas et al.,[11,12] which

180

is based on linearized unsteady lifting-surface theory. This method had been developed to calculate periodic propeller shaft, or thrust and lateral bearing forces which arise from the kZ - 1, kZ, and kZ + 1 harmonics of the wake and blade loading, where k is an integer and Z is the number of blades. This method, which had correlated well with experimental data for blade frequency bearing forces, was generally assumed to predict periodic blade loads with good accuracy.

Early in the current research and development program on CP propellers the six components of blade loading (Figure 1) were measured behind the model of the BARBEY.[1-3] For this hull form the periodic blade loads are produced primarily by the inclination of the inflow relative to the propeller shaft. These model results for circumferential variation of bending moments about the nose-tail line at the 0.4 radius agreed fairly well with loads deduced from strain measurements on the full-scale propeller, as discussed in Chapter II, but they were substantially larger than values calculated by the method of Tsakonas et al.[11,12] The experimental results revealed that the periodic loads were very substantial (approximately 40 percent of the time-average loads on the BARBEY) so that they could be of paramount importance to the structural integrity of the CP propeller from consideration of fatigue. Therefore, it was concluded that the method of Tsakonas et al. was completely inadequate for calculating periodic blade loads due to the inclination of the flow relative to the propeller shaft.*

Based on these results on the BARBEY, it was decided to direct a major effort towards developing a rational and generally reliable method for calculating the periodic blade loads arising from the inclination of the inflow relative to the propeller shaft. This effort included:

1. Developing refined analytical methods, and associated computer programs, for calculating periodic blade loads due to inclined flow.

2. Developing an extensive database of reliable blade loading measurements covering a range of pertinent parameters, to serve as a basis for evaluating the refined analytical methods.

3. Evaluating the refined analytical methods developed under item 1 by correlation with the experimental data developed under item 2.

---

*This does not contradict the apparent good correlation of this method with experimental blade frequency bearing forces because the inclination of the flow to the propeller shaft produces only a shaft frequency harmonic of tangential wake, and thus loading, and does not directly influence the higher harmonics of the wake such as the kZ - 1, kZ, and kZ + 1 harmonics which produce the periodic bearing forces and moments.

181

4. Conducting fundamental experimental measurements of the blade surface pressures and propeller-induced field point velocities near the propeller for operation in uniform flow and inclined flow. The objective of these experiments was to obtain further insight into the physical mechanisms causing the periodic blade loading in inclined flow to aid in the further refinement of the analytical methods developed under item 1, if necessary.

5. Conducting fundamental studies into the manner in which wake pattern into the propeller plane scales from the model to the full-scale ship. The objective of this study is to determine whether the periodic blade loading coefficients measured in model scale, and calculated based on model wake surveys, are directly applicable to the full-scale ship, or whether they must be adjusted for wake scaling effects.

Analytical Methods

As stated previously, at the beginning of the current research and development program on CP propellers, the most sophisticated available method for calculating periodic blade loads was the method of Tsakonas, et al. This procedure is based on linearized unsteady lifting surface theory for a lightly loaded propeller using an acceleration potential. The numerical procedure uses the mode approach and collocation method in conjunction with "generalized lift operators." This procedure, which is based on the frequency domain rather than the time domain, (1) assumes that a given harmonic of blade loading depends upon the corresponding harmonic of the wake velocity normal to the blade chord line, (2) is independent of whether the normal velocity results from axial or tangential components of the wake, (3) is independent of other harmonics of the wake, (4) is independent of the radial variation of the circumferential mean wake, and (5) is independent of any time-average propeller loads. The shed and trailing vortices are assumed to lie on an "exact" helicoidal surface of constant pitch extending to infinity downstream, determined by the propeller rotational speed and a single axial inflow velocity (independent of radius), independent of time-average or periodic induced velocities. The axis of this helicoidal surface coincides with the propeller axis, independent of the inclination of the propeller shaft to the incoming flow. This method does not consider any contraction or roll-up of the propeller slipstream. All geometric characteristics of the propeller are considered, except rake, camber, and thickness, which are assumed to be zero.

182

Under the current research and development program, Valentine[13] developed a refinement to the method of Tsakonas et al. for operation in slightly inclined flow. This refinement, in effect, replaces the "exact" helicoidal wake whose axis coincides with the propeller axis with a slightly distorted helicoidal wake in the direction of the inflow velocity. This refinement, which is incorporated as a perturbation for small inclination angles, relates the unknown loading at the first harmonic of shaft frequency with the loadings at the zeroth* and second harmonics of shaft frequency evaluated without the distorted helicoidal wake. All other assumptions of the method of Tsakonas et al. are retained, including the assumption that the propeller is lightly loaded.

At the beginning of the present research and development program, methods were under development by Kerwin and his associates at MIT for predicting the time-average loading for a given propeller, wake pattern, and advance coefficient. Under the present research and development program this work was extended to include the prediction of the periodic blade loading. This extension was undertaken in two stages: in the first stage it was assumed that the axis of the propeller slipstream coincides with the propeller axis, and in the second stage it was assumed that the axis of the propeller slipstream is a function of the inclination of the propeller axis to the inflow.

The method developed by Kerwin and his associates is based on moderately loaded numerical lifting-surface theory in the time domain, using a velocity potential. The propeller blades are represented by a spanwise and chordwise distribution of discrete vortices and source elements located on the exact mean surface of the blade. Thus, the geometric complications of skew, rake, and radial variation in pitch are readily accommodated. The trailing vortex wake is permitted to contract and roll up, and the effect of vortex sheet separation from the blade tip is taken into consideration. The wake contains trailing vortices which are extensions of the chordwise vortices on the blade. The wake region close to the propeller blades (transition wake) also contains shed vortices. In the first stage, developed by Kerwin and Lee,[14] it is assumed that the axis of the propeller slipstream coincides with the propeller axis.

The second stage, developed by Kerwin,[15] is a refinement to the method of Kerwin and Lee for operation in inclined flow. This refinement entails a more

---

*This method considers the effect of blade camber and thickness only on the loading at the zeroth harmonic, i.e., the time-average loading.

realistic representation of the path of the propeller slipstream. In this method the axis of the slipstream coincides with the propeller axis immediately behind the propeller, and coincides with the direction of the free stream far downstream in the ultimate wake. A simple function, which is dependent only upon the mean flow inclination, is assumed for the wake axis in the transition wake; i.e., in the region between the propeller and the ultimate wake. Due to the asymmetry, the position of the wake relative to a blade oscillates with a once-per-revolution fundamental frequency, thus giving rise to unsteady induced velocities normal to the blade surface and thereby unsteady blade loadings of the same frequency. The strength of the vorticity in the wake, and thus the induced once-per-revolution variation of loading on the blades, is dependent upon the time-average loading of the propeller. All other characteristics of the method of Kerwin and Lee are retained, including the flexibility for the trailing vortex wake to contract and roll up, and allowance for the effect of vortex sheet separation from the blade tip.

In addition to the highly sophisticated methods for calculating periodic blade loads, such as those discussed in the preceding paragraphs, there are various simpler and approximate methods, as summarized by Boswell and Miller,[16] Schwanecke,[17] and Breslin.[18] One such method, developed by McCarthy[19] and others, is a simple quasi-steady procedure using the open water characteristics of the propeller. It is assumed that the thrust and torque developed by the propeller blade at any angular position in a circumferentially nonuniform wake is the same as would be produced by the propeller blade if it were operating continuously at the advance coefficient J and rotational speed n based on the local wake. It is further assumed that the instantaneous thrust and torque can be adequately estimated by entering the propeller open water characteristics at the values of J and n based on a weighted average over the propeller radius of the wake at the local blade angular position. Further, in order to estimate transverse forces and blade bending moments, the radial point of application of the thrust and transverse force must be assumed. For correlations presented in this report, these components of force are assumed to be applied at the 70 percent radius. This simple method can be expected to yield reasonable results only if the reduced frequency* of interest is low, the propeller

---

*The reduced frequency is $[\omega c(r)]/[2V_r(r)]$ where ω is the angular frequency of the pertinent harmonic of the wake, $c(r)$ is the chord length at radius r, and $V_r(r)$ is the resultant inflow velocity at radius r. This is a measure of the ratio of the chord length to the wavelength of the pertinent harmonic of the wake.

184

projected skew is small relative to the wavelength of the pertinent wake harmonic, and the wake harmonic corresponding to the force harmonics of interest does not vary substantially in amplitude or phase with radius. These conditions are met for calculating periodic blade loads in wakes whe the circumferential variation of the inflow velocity components arises predominantly from the inclination of the inflow to the propeller shaft, such as behind high-speed transom stern configurations with exposed shafts and struts. These conditions are not, in general, met for wakes behind full-form surface ships or submersibles.

Experimental Data

The model database, developed under the present research and development program, consists of measurements of the six components of periodic blade loading on models of the propellers on the BARBEY,[1-3] the SPRUANCE Class,[4,6] and the R/V ATHENA (formerly a member of the PG-84 Class).[5] Measurements were made on each of these propellers behind their respective model hulls at a simulated steady-ahead self-propulsion condition in calm water with no ship motions. For each of these ships, the periodic blade loads are produced primarily by the inclination of the inflow relative to the propeller shaft.

As discussed in Chapter II, full-scale trials were conducted on each of these ships. Blade strains were measured on each of these full-scale trials, and blade surface pressures were measured on SPRUANCE and R/V ATHENA. Periodic blade bending moments can be deduced from these trial data; therefore, for these three ships, a comparison of periodic blade bending moments can be made between the model experiments, full-scale trials, and the various theoretical prediction methods.

Measurements of periodic blade loads were also made on the same three model propellers (models of the propellers on BARBEY, SPRUANCE, and R/V ATHENA), each operating in various idealized flow patterns at various tip clearances from a flat plate.[20-23] These idealized flow patterns included axial wakes with a dominant first harmonic (once-per-revolution variation) component generated by variable density wire grid screens, and uniform flow with inclinations of 10, 20, and 30 degrees. The primary objectives of these experiments were to isolate influence of the circumferential variation of the axial velocity from the flow inclination, to obtain systematic data over a wide range of propeller advance coefficients, and to determine whether the periodic blade loads are sensitive to propeller tip clearance.

185

Correlation Between Experiment and Theory

The experimental results were correlated with predictions based on the follow-
ing methods:

1. The procedure developed at Davidson Laboratory by Tsakonas et al.[11,12]
based on lightly loaded unsteady lifting surface theory; Computer Program PPEXACT.
This was the most sophisticated method available at the beginning of the present
research and development program.

2. The procedure developed at MIT by Kerwin and Lee[14] based on moderately
loaded unsteady lifting surface theory; Computer Program PUF2. This is an interim
result of the method developed at MIT under the present research and development
program. This result is presented to illustrate, by comparison with the later more
refined method developed at MIT, the calculated importance of the path of the pro-
peller slipstream for operation in inclined flow.

3. A refinement of the method of Kerwin and Lee developed at MIT by Kerwin,[15]
to allow the axis of the propeller slipstream to depart from the propeller axis for
operation in inclined flow; Computer Program PUF2IS. This method, developed under
the present research and development program, is the most sophisticated method
presently available for calculating periodic propeller blade loads including the in-
fluence of inclined flow.

4. The quasi-steady procedure developed at DTNSRDC by McCarthy;[19] Computer
Program QUASI. This is a simple approximate method, which may have utility for
making quick approximations or for situations in which a large computer is not
available.

Correlations were not made between the experimental results and the modification
to the method of Tsakonas et al. as developed by Valentine[13] because calculations
made by Valentine showed that his modification to the method of Tsakonas et al. did
not significantly improve the poor correlation with experimental periodic blade
loads on the BARBEY, which are predominantly due to inclined flow, as discussed
previously. Further, with the modifications by Valentine, the disagreement in phase
between predicted and experimental blade loads on the BARBEY were even worse than
the already poor agreement obtained with the method of Tsakonas et al. Valentine
concluded that the effects of shaft inclination required a moderately loaded theory,
and could not be adequately calculated based on the lightly loaded formulation of
Tsakonas et al.

186

Figure 3 compares the variation of the bending moment about the 40 percent radius from the model of the BARBEY with the values deduced from the strains measured at the midchord of the face of the 40 percent radius in the full-scale propeller. This illustrates that the basic form of the variation of the blade loads with blade angular position agrees between model and full-scale. Chapter 11 presents more details of the variations of the measured strains and pressures on the full-scale propellers with blade angular position.
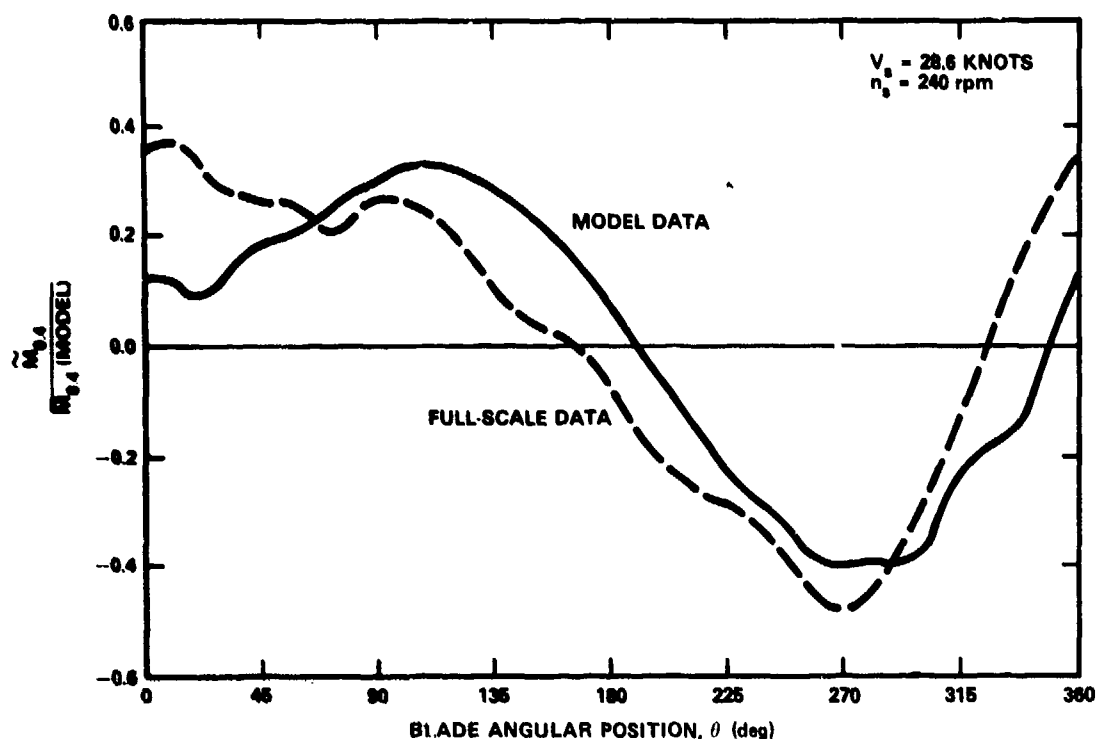
Figure 3 - Variation of Bending Moment at 40 Percent Radius
with Blade Angular Position, Comparison of Model Data
and Full-Scale Data for USS BARBEY

Figure 4 summarizes the results of the periodic blade loads behind the model BARBEY, SPRUANCE, and R/V ATHENA hulls for steady-ahead operation in calm water with no ship motions. Figure 4 shows the blade bending moments about the 40 percent radii; however, the trends for the other components are similar. It is apparent from comparing the circumferential variation of the blade bending moment with the circumferential variation of the tangential wake (see Figure 2) that the periodic loads are caused primarily by the tangential wake.

Table 1 compares the peak to peak variations of the blade bending moments for the BARBEY, SPRUANCE, and R/V ATHENA as determined from model scale experiments and

187

Figure 4 – Summary of Blade Loads from Model Experiments on the
USS BARBEY, USS SPRUANCE Class, and R/V ATHENA
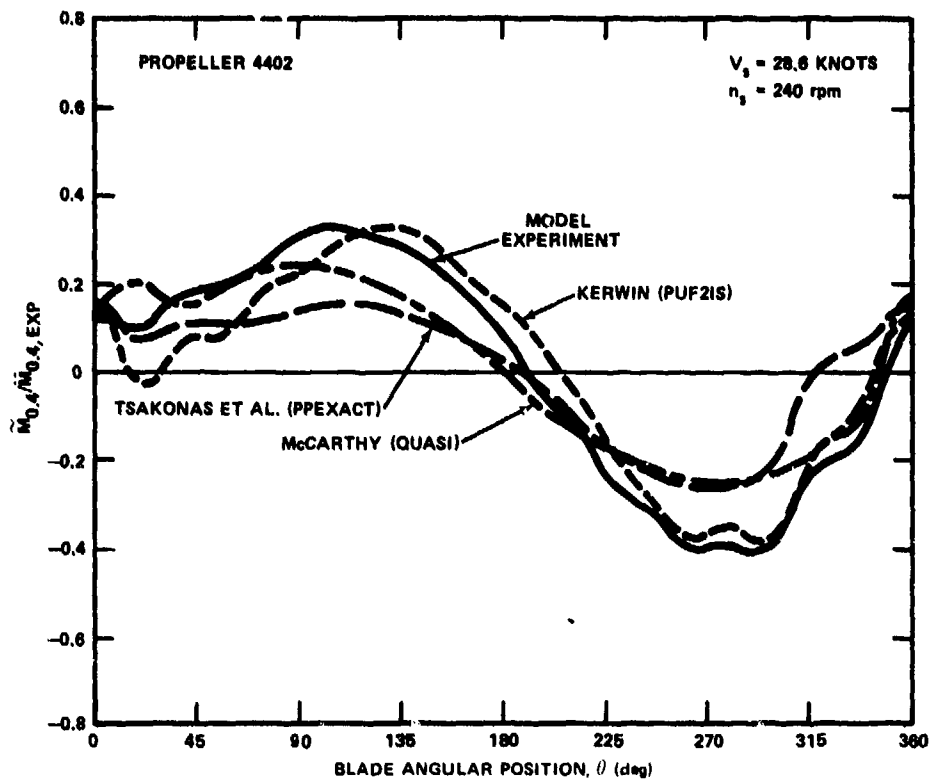
Figure 4a – USS BARBEY

Figure 4 (Continued)
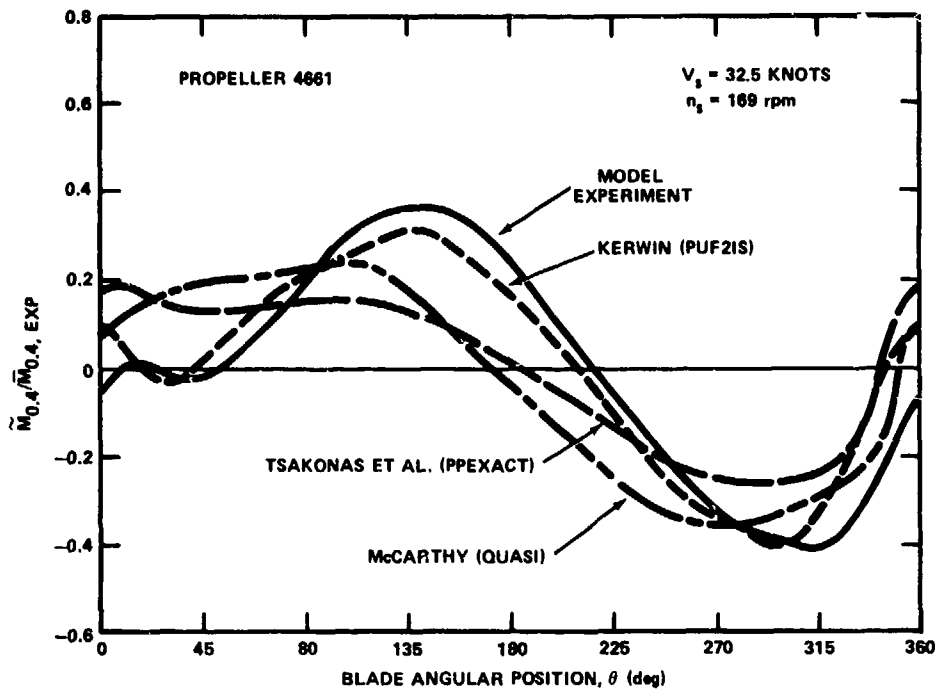
Figure 4b - USS SPRUANCE Class
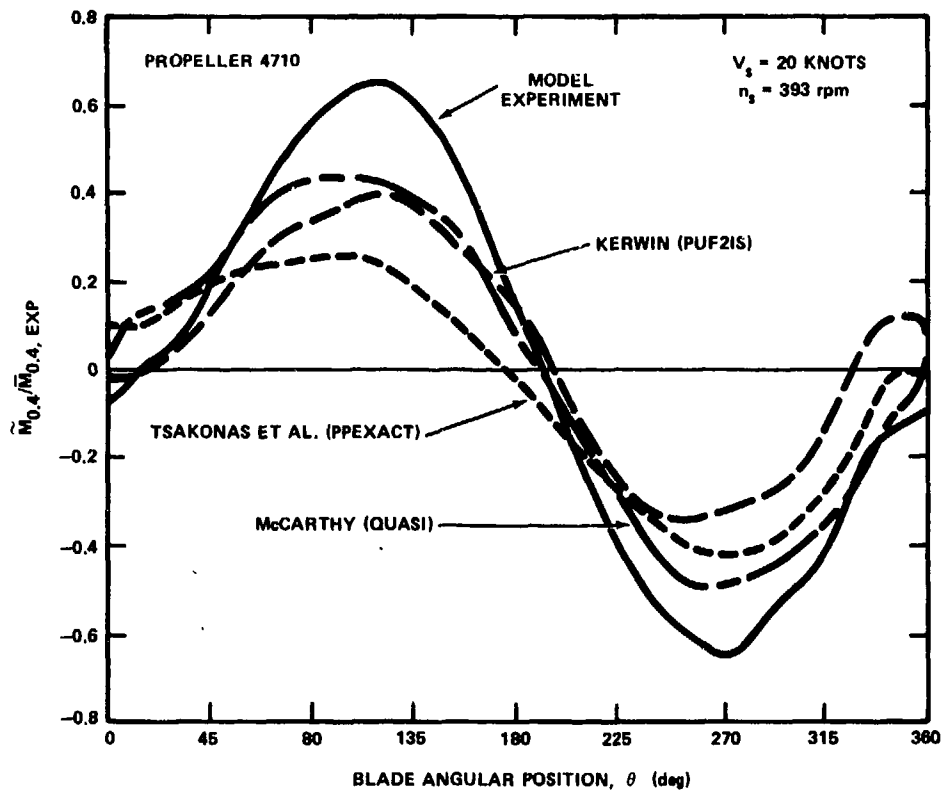
Figure 4c - R/V ATHENA

189

TABLE 1 - PERIODIC BLADE LOADS ON USS BARBEY, USS SPRUANCE, AND R/V ATHENA-- CORRELATION OF MODEL AND FULL-SCALE MEASUREMENTS

	$\left(\dfrac{M_{Max,0.3}-M_{Min,0.3}}{\overline{M}_{0.3}}\right)_{Ship*}$	$\left(\dfrac{M_{Max,0.3}-M_{Min,0.3}}{\overline{M}_{0.3}}\right)_{Model}$
USS BARBEY	0.45	0.40
USS SPRUANCE	0.40	0.45
R/V ATHENA	0.50	0.65

*The full-scale data are deduced from strain gages or pressure transducers on the blade surfaces, as discussed in Chapter II.

full-scale data.* The results presented in Table 1 and Figure 4 indicate reasonably good agreement between the model data and the full-scale data; however, the analytical methods underpredict the peak-to-peak variations in the blade bending moments. The method of Kerwin, developed under the research and development program on CP propellers, yields substantially better agreement with experiment than does the method of Tsakonas et al., the most sophisticated method at the beginning of this research and development program.

Figures 5 and 6 show the amplitudes and phases, respectively, of the first harmonic thrust coefficient $\kappa_{(Fx)1}$, for the three model propellers** in idealized wake patterns over a range of advance coefficient J. In Figure 5 the periodic thrust is nondimensionalized as follows:

$$\kappa_{(Fx)n} = (F_x)_n / (\rho n V_A D^3)$$

where n (subscript) = harmonic number

ρ = mass density of water

n = propeller rotational speed

V_A = speed of advance

D = propeller diameter

---

*The full-scale data are discussed in more detail in Chapter II.

**All three propellers were not experimentally evaluated in all of the wake patterns.

Figure 5 – Sample Results Showing Variation of Amplitudes of First
Harmonic Blade Loads with Advance Coefficient in
Idealized Wake Patterns

Figure 5b – Propeller on USS SPRUANCE with an
Inclination of 10 Degrees
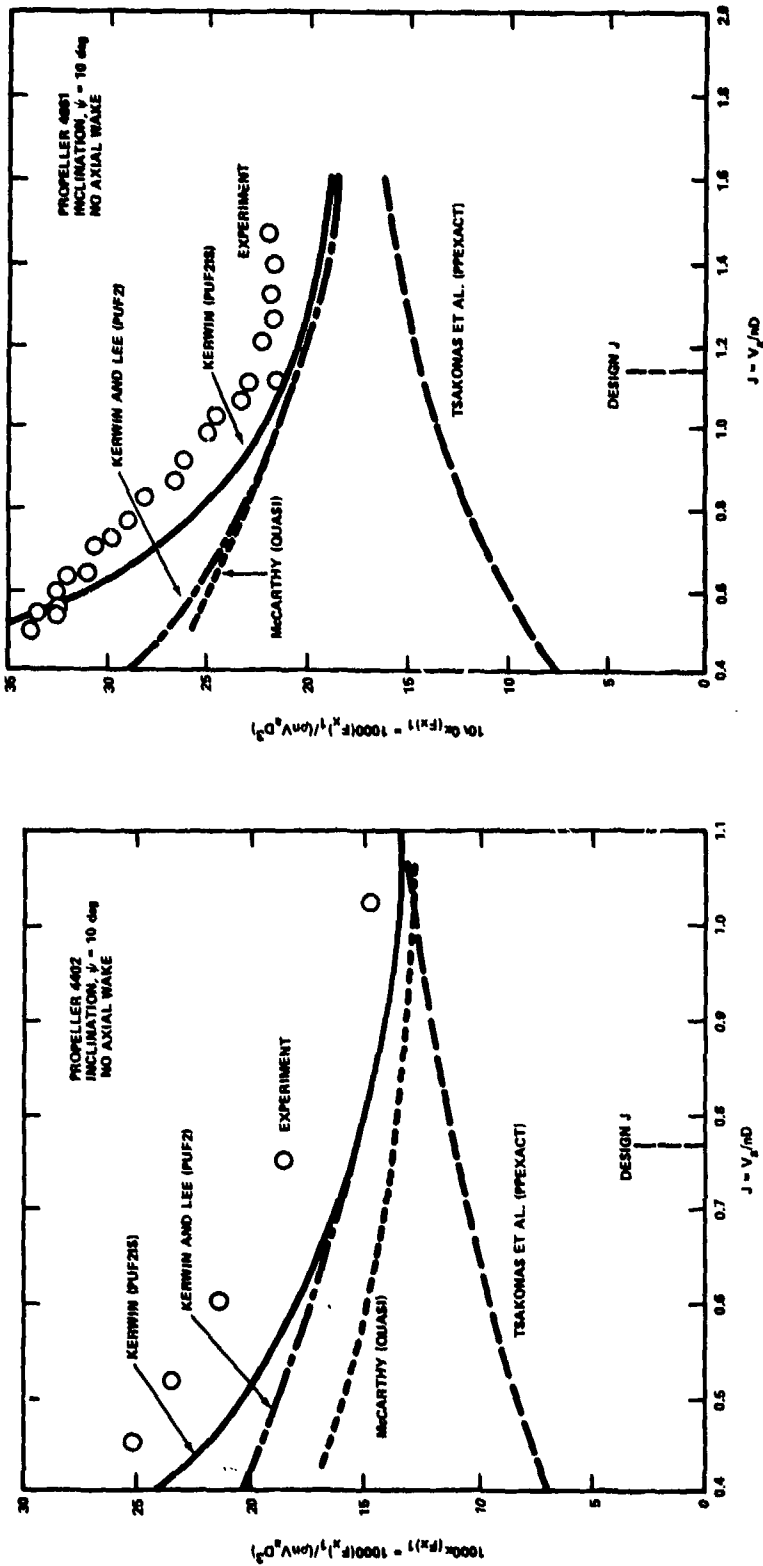
Figure 5a – Propeller on USS BARBEY with an
Inclination of 10 Degrees

Figure 5 (Continued)

Figure 5d - Propeller on USS SPRUANCE with an
Inclination of 30 Degrees

Figure 5c - Propeller on USS SPRUANCE with an
Inclination of 20 Degrees
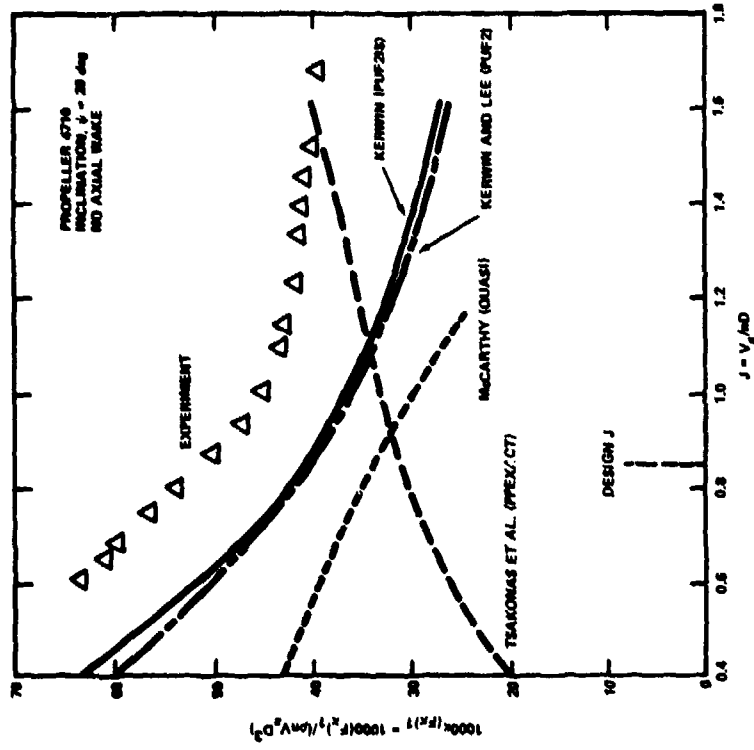
Figure 5 (continued)

Figure 5f – Propeller on R/V ATHENA with an Inclination of 20 Degrees
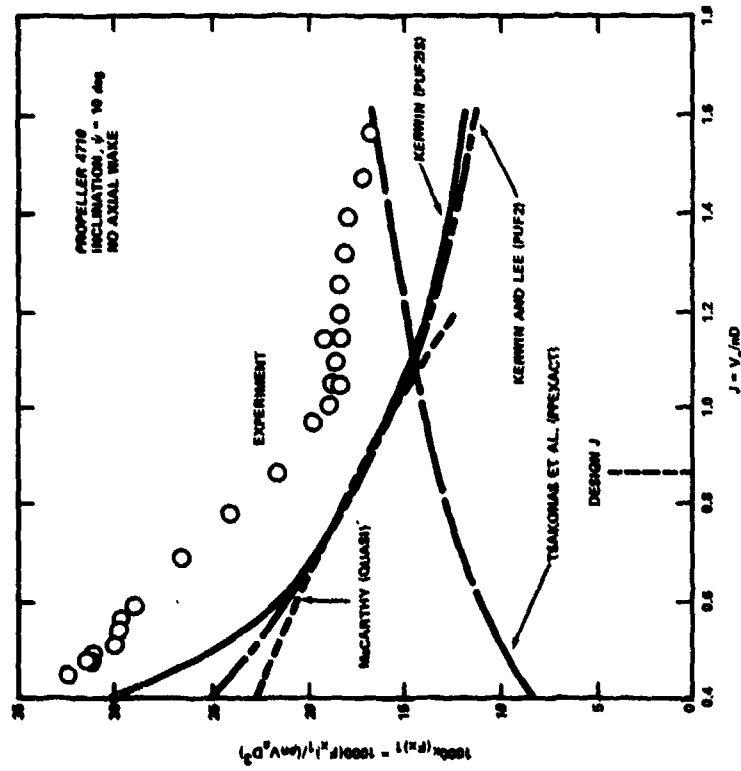
Figure 5e – Propeller on R/V ATHENA with an Inclination of 10 Degrees

193

Figure 5 (Continued)
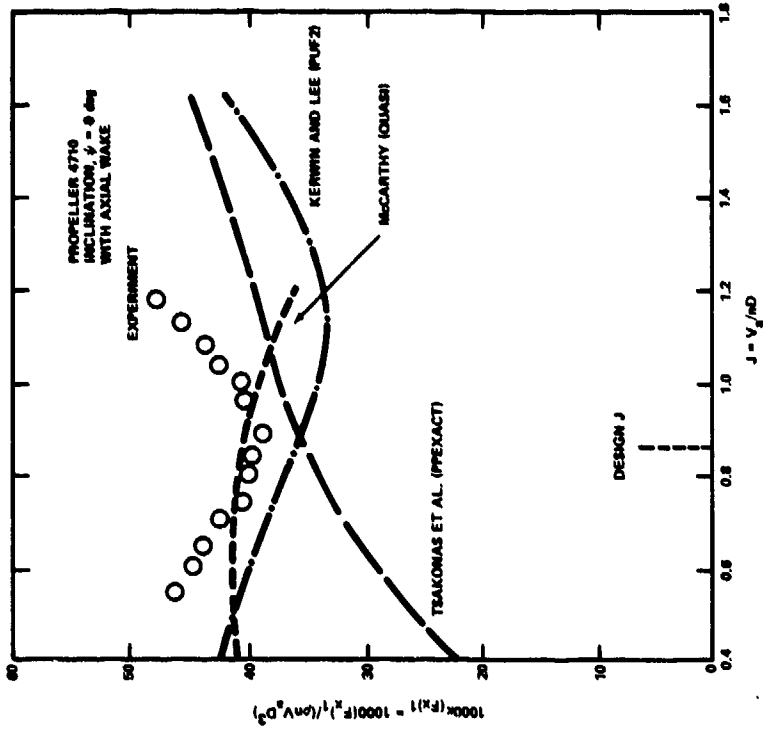
Figure 5h - Propeller on R/V ATHENA with an
Inclination of 0 Degree
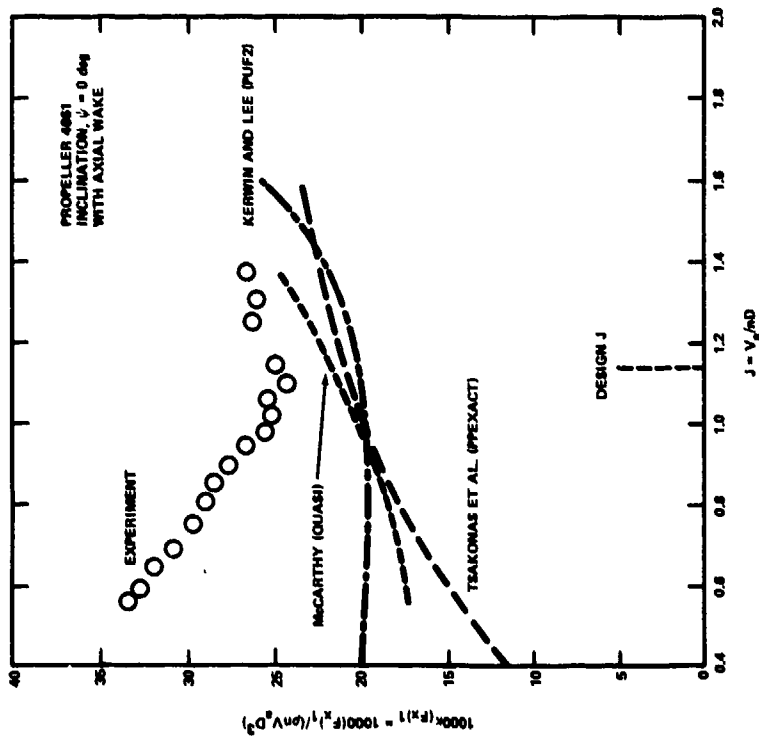
Figure 5g - Propeller on USS SPRUANCE with an
Inclination of 0 Degree

194
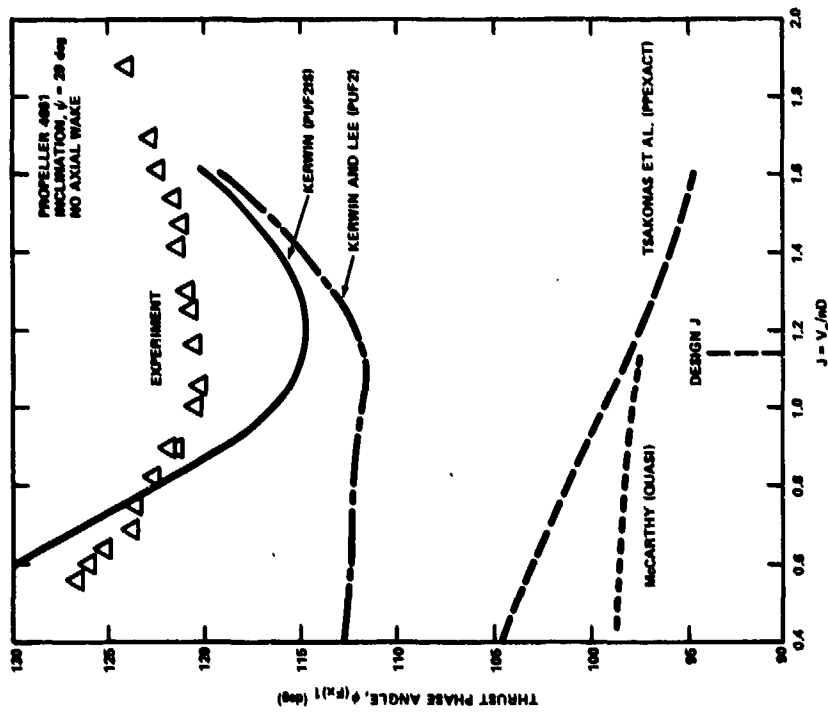
Figure 6a – Propeller on USS SPRUANCE with an
Inclination of 20 Degrees
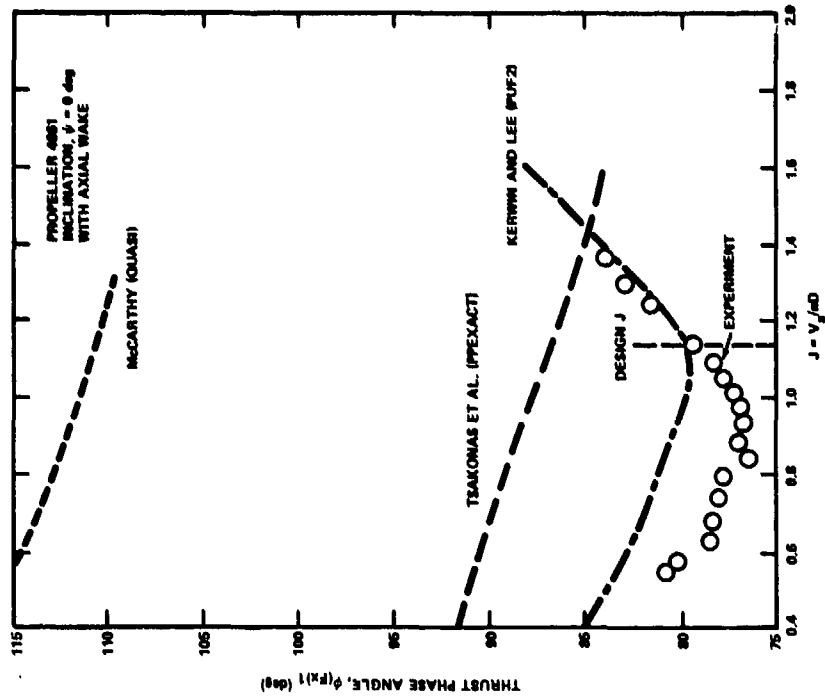
Figure 6b – Propeller on USS SPRUANCE with an
Inclination of 0 Degree

Figure 6 – Sample Results Showing Variation of Phases of First
Harmonic Blade Loads with Advance Coefficients in
Idealized Wake Patterns

This form of nondimensionalization was used because simple analysis indicates that, for a given propeller in a given wake pattern, the circumferential variation of the hydrodynamic loading varies approximately as nV_A, and for a given value of nV_A the circumferential variation of hydrodynamic loading is insensitive to J. Therefore, this simple analysis indicates that $\kappa_{(Fx)n}$ and $\kappa_{(Mx)n}$ should be insensitive to J.

The results in idealized inclined flows show that the inclination of the propeller slipstream relative to the propeller axis can significantly influence the periodic loads on the propeller blades. The importance of this inclination increases with increasing time-average loading. Of the four methods evaluated, the method of Kerwin, which was developed under the current research and development program and which accounts for the inclination of the slipstream, gives the best predictions of the amplitudes and phases of the periodic blade loads. The method of Taskonas et al., which was the most sophisticated method available at the beginning of the current research and development program, gives the worst prediction of the amplitudes of the periodic loads. Further, this method failed to predict the trend of the variation of the loading coefficients with advance coefficient.

Figure 7 presents the variation of the periodic loads with inclination angle for propeller Model 4661 near design J. These results show that the rate of increase of the periodic loads with inclination angle increases with increasing inclination angle. Figure 7 also shows that the correlation between experimental results and the analytical method of Kerwin, which considers the inclination of the propeller slipstream, is essentially independent of the angle of inclination up to 30 deg.

In the axial wake, all three* calculation procedures predicted $\kappa_{(Fx)1}$ to within 20 percent of the experimental values at design J. However, the agreement at substantially off-design J was not as good. In general, the method of Kerwin and Lee gave the best agreement with experimental results in the magnitude and trend of $\kappa_{(Fx)1}$ over a range of J. In addition, the method of Kerwin and Lee gave the best agreement with experimental results in phases and in the trends of the variation of phases with J.

Table 2 presents a comparison of the first harmonic loads on the three propellers in the wakes behind the three model hulls and in the idealized wakes in inclined flow at the same advance coefficient and shaft inclination angle

---

*In longitudinal wakes, there is no difference between the methods of Kerwin and Kerwin and Lee.
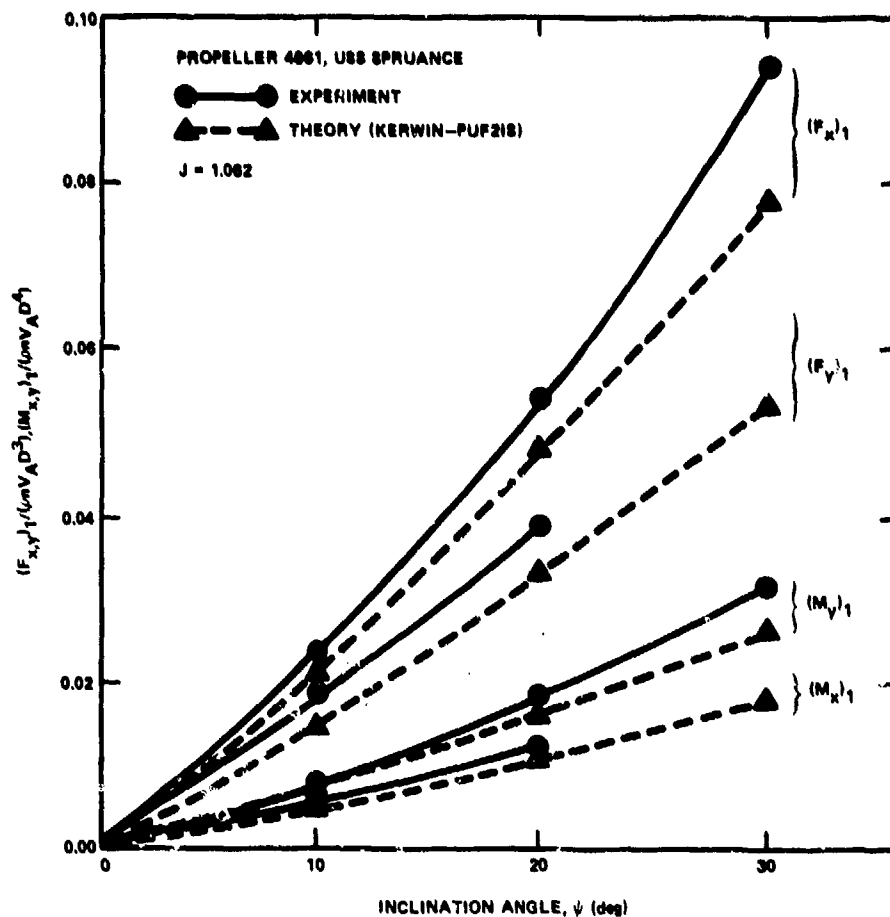
Figure 7 - Variation of Periodic Blade Loads with Shaft Inclination

(interpolated from idealized flow data). The shaft inclination angles for the experimental conditions presented in this table were approximated from the measured wake velocities. Table 2 presents experimental data and predictions by the method of Kerwin.

For propeller Models 4402 and 4661, Kerwin's method underpredicted the experimental first harmonic loads by approximately 20 to 30 percent in the wake behind hull (WBH) and 10 to 15 percent in the idealized wake (IW). For propeller Model 4710, the method of Kerwin underpredicted the experimental first harmonic loads by about 40 to 45 percent in WBH and about 20 percent in IW. More details of these correlations are given in Reference 24.

TABLE 2 - COMPARISON OF FIRST HARMONIC BLADE LOADS IN WAKES BEHIND HULL AND IN
IDEALIZED WAKES

Conditions		1000 K(Fx)1		1000 K(My)1		1000 K(Fy)1		1000 K(Mx)1	
		WBH[1]	IW[2]	WBH	IW	WBH	IW	WBH	IW
Propeller Model 4402 J = 0.731 ψ = 8.4 deg	Experiment	17.45	15.90	6.03	5.00	7.15	11.40	2.18	2.50
	Kerwin (PUF2IS)	13.41	13.40	4.24	4.30	6.29	6.60	2.19	2.30
	(PUF2IS / Experiment)	0.77	0.84	0.70	0.86	0.88	0.58	1.00	0.92
Propeller Model 4661 J = 1.062 ψ = 6.4 deg	Experiment	17.11	14.00	5.95	4.50	11.43	11.50	3.38	3.50
	Kerwin (PUF2IS)	14.03	12.70	4.71	4.20	9.79	8.80	3.11	2.80
	(PUF2IS / Experiment)	0.82	0.91	0.79	0.93	0.86	0.75	0.92	0.76
Propeller Model 4710 J = 0.817 ψ = 9.87 deg Vs = 20 knots	Experiment	30.83	22.30	10.17	7.10	16.93	15.30	5.79	4.70
	Kerwin (PUF2IS)	18.85	17.50	6.00	5.40	9.06	8.20	3.18	3.10
	(PUF2IS / Experiment)	0.61	0.79	0.59	0.76	0.54	0.54	0.55	0.66
Propeller Model 4710 J = 0.807 ψ = 9.27 deg Vs = 15 knots	Experiment	28.77	20.80	9.80	6.60	15.47	14.30	5.33	4.40
	Kerwin (PUF2IS)	16.98	16.10	5.33	5.00	8.05	7.60	2.85	2.90
	(PUF2IS / Experiment)	0.59	0.77	0.54	0.76	0.52	0.53	0.54	0.66

[1]WBH = Wake behind hull.

[2]IW = Idealized wakes.

198

Blade Surface Pressures and Field Point Velocities

Experiments were conducted to measure the blade surface pressures and propeller-induced field point velocities near the propeller for operation in uniform flow and in inclined flow. The objective of these experiments is to obtain further insight into the physical mechanisms causing the periodic blade loading in inclined flow to aid in the further refinement of the analytical method, if necessary.

The experiments have been completed and the results are described in References 25, 26, and 27; however, no further refinement to the previously described analytical methods has been attempted based on these results. Discussion of these experimental results is beyond the scope of the present report.

Wake Scaling

Model and full-scale wake surveys were conducted on the R/V ATHENA to determine the manner in which the wake pattern in the propeller plane scales from the model to the full-scale ship for hulls with high-speed transom sterns with exposed shafts and struts. The objective of this study was to determine whether the periodic blade load coefficients measured on the model scale, and those calculated based on model wake surveys, are directly applicable to the full-scale ship, for hulls with high-speed transom sterns with exposed shafts and struts, or whether they must be adjusted for wake scaling effects.

The results of these wake scaling studies are described in References 28 through 32. The important result relative to periodic blade loads is that the first harmonic of the tangential component of the wake, or the effective inclination of the inflow to the propeller, appears to be substantially larger on the full-scale ship than on the model scale. Possible reasons for this apparent difference in flow inclination between model and full-scale are discussed in References 28 and 29.

Periodic blade loads were calculated on the R/V ATHENA using the method of Kerwin[15] based on the model wake survey and the corresponding full-scale wake survey;* see Table 3. The periodic blade loads determined from model experiments and full-scale experiments are also shown in Table 3. The results of the wake scaling studies indicate that the periodic blade loading coefficients should be larger on the full-scale than on the model, which is apparently inconsistent with the results of the measurements of the blade loads on the model and full-scale propellers. The reason for these apparently inconsistent results is unknown.

---

*The calculation using the full-scale wake assumes that the nondimensional wake contours at 20 knots are the same as they are at 15 knots.

TABLE 3 – BLADE LOADS ON THE R/V ATHENA—MODEL AND FULL-SCALE MEASUREMENTS
AND CALCULATIONS BASED ON MODEL AND FULL-SCALE WAKE SURVEYS

	$\dfrac{M_{Max,0.3} - M_{Min,0.3}}{\overline{M}_{0.3}}$
Model experiment	0.65
Calculations* based on model wake	0.40
Full-scale measurement	0.50
Calculations* based on full-scale wake	0.45

*Calculations by the method of Kerwin (Computer Program PUF2IS).

ACCELERATION AND DECELERATION

The six components of blade loading (Figure 1) were measured on the models of the BARBEY and SPRUANCE Class ships to determine the periodic, transient, and peak loads during acceleration and deceleration maneuvers with specified time dependence of ship speed V, propeller rotational speed n, and propeller pitch ratio P/D. The variations of these quantities with time, which depend upon the maneuver being performed and upon the responses of the ship, propeller, turbine, and control system, must be determined from ship trials or from computer dynamic simulation of the system using specified characteristics of the hull, propeller, turbine, and control system. The hull and propeller characteristics for such a computer simulation must be obtained from systematic model experiments on the hull and propeller.

The objective of these experiments was to obtain systematic accurate experimental data showing the effects of acceleration and deceleration on periodic,* transient, and peak blade loads under carefully controlled experimental conditions so that the effects of acceleration and deceleration on blade loads could be isolated. These data serve as a basis for developing procedures for calculating periodic blade loads during general acceleration and deceleration maneuvers.

---

*The periodic blade loads were of greater interest here than the transient blade loads (the peak is simply the sum of the transient and periodic loads) because the transient blade loads can be determined from transient propeller shaft loads measured on either model or full-scale.

Before the present research and development program on CP propellers there existed no known direct measurement of periodic blade loads during controlled acceleration or deceleration maneuvers.

The following conclusions were drawn from the blade loading experiments simulating acceleration and deceleration maneuvers.

1. The Taylor wake fraction during acceleration or deceleration maneuvers can be substantially different from th. values under steady-ahead self-propulsion conditions. Therefore, reasonably accurate estimates of the Taylor wake fractions are necessary to calculate the transient loads during acceleration or deceleration maneuvers.

2. The transient and peak blade loads tend to be larger during acceleration maneuvers than during deceleration maneuvers.

3. The transient and peak blade loads during acceleration maneuvers can be substantially larger than the time-average and maximum blade loads, respectively, during full-power steady-ahead operation.

4. The transient and periodic loads are controlled predominantly by the instantaneous values of the ship speed V, propeller rotational speed n, and the propeller pitch ratio P/D, which fix the instantaneous value of the Taylor wake fraction. The periodic and transient loads are not sensitive to the time rates of change of these quantities; i.e., to V, n, and P/D. Therefore, the transient and periodic blade loads during acceleration and deceleration maneuvers can be adequately estimated in a quasi-steady manner; i.e., by calculating or measuring these loads at the proper instantaneous ship speed and propeller rotational speed, but assuming that the time rates of change of ship speed and propeller rotational speed are zero.

5. During acceleration and deceleration maneuvers the variation of loads with blade angular position retain the same basic form as for steady-ahead operation; i.e., these loads are predominantly a once-per-revolution variation produced by the inclination of the inflow for ships with high-speed transom sterns with exposed shafting and struts.

6. The periodic blade loads during acceleration and deceleration maneuvers vary in a nearly linear manner with the product of ship speed V, propeller rotational speed n, and a function of propeller pitch ratio P/D. Therefore, these loads can be readily estimated for an acceleration or deceleration maneuver with a known time history of V, n, and P/D from the periodic loads under steady-ahead operation.

7. The periodic blade loads during acceleration and deceleration maneuvers are, in general, less than the periodic blade loads during full-power steady-ahead operation.

HULL PITCHING AND WAVES

The six components of blade loading were measured on the models of the BARBEY, SPRUANCE Class, and R/V ATHENA ships to determine the influence of hull pitching and regular head waves* on periodic and time-average blade loads. The objective of these experiments was to obtain systematic accurate experimental data showing the effects of hull pitching and waves on periodic and time-average blade loads under carefully controlled experimental conditions so that the effects of ship motions and waves on periodic and time-average blade loads could be isolated. These data serve as a basis for developing procedures for calculating periodic and time-average blade loads for operation in a sea state.

These experiments did not attempt to simulate true operating conditions of the various ships. In these experiments the model speed and propeller rotational speed were held constant at the values corresponding to operation in calm water with no ship motions. In practice, when a ship operates in rough seas the ship speed and propeller rotational speed at a given delivered power decrease from the corresponding values in calm water due to increased resistance of the hull and change in the propulsion coefficients (involuntary speed loss).[33-35] Furthermore, in rough seas the delivered power is often reduced from the calm water value (voluntary speed loss).[35,36] Therefore, the difference in blade loads between operation in calm seas and operation in rough seas can be represented as being made up of two major parts:

1. Differences in loads resulting from the difference in ship speed and propeller rotational speed between calm seas and rough seas, and

2. Increases in loads due to the direct influence of waves and ship motions at a given value of ship speed and propeller rotational speed.

The changes in propeller rotational speed, ship speed, and Taylor wake fraction due to operation in rough seas can be estimated experimentally or theoretically using methods or data summarized by Oosterveld,[34] Day et al.,[35] and Lloyd and Andrew.[36] The resulting changes in periodic blade loads can be estimated based on the systematic experimental data or theoretical methods developed under the current

---

*Experiments in waves were conducted only on the model of the R/V ATHENA.

research and development program and described previously. The experiments described in the present section provide information on the direct influence of the waves and ship motions on periodic and time-average blade loads.

Before the present research and development program on CP propellers there existed no known direct measurement of periodic blade loads for operation with either hull pitching or waves.

The following conclusions were drawn from the blade loading experiments with hull pitching and in waves.

1. Hull Pitching in Calm Water

a. <u>Transient Loads</u>. Hull pitching increases the maximum transient loads, or time-average loads per revolution,* by only a small amount over the time-average loads per revolution without hull pitching. This increase can be approximated as follows:

$$\Delta\overline{L}_{max,\psi} \doteq (\overline{L})(2\psi_A) = (\overline{L}_\psi)(\psi_A)$$

where $\Delta\overline{L}_{max,\psi}$ = maximum increase in time-average loads per revolution with hull pitching over the value in calm water

$\overline{L}$ = time-average load in calm water

$\overline{L}_\psi$ = time-average load in waves

ψ_A = amplitude of the variation in hull pitch angle in radians

In practice, this maximum increase in time-average loads per revolution due to pitching is negligible relative to the corresponding increase due to waves, as discussed later.

b. <u>Periodic Loads</u>. Hull pitching (in calm water) substantially increases the maximum periodic blade loads over the corresponding periodic loads without hull pitching. The primary controlling parameter is the ratio of the vertical velocity of the propeller resulting from the hull pitching to the ship speed. The maximum periodic loads occur when the velocity of the propeller and stern are maximum downward. This downward velocity of the propeller effectively increases the inclination of the inflow relative to the propeller and thereby increases the periodic loads. Due to the displacement effect of the hull above the propeller, the vertical velocity

---

*The transient loads are periodic with the period of the hull pitching for hull pitching in regular waves.

of the propeller relative to the local fluid particles is only 60 percent or less of the vertical velocity of the propeller. Therefore, for ships with high-speed transom sterns with exposed shafts and struts, the maximum periodic blade loads due to hull pitching can be approximated from the corresponding loads without hull pitching as follows:

$$\Delta \tilde{L}_{max,\psi} = \frac{0.6 \ V_\psi}{(V_{t0.7})_1} \ \tilde{L}$$

where $\Delta \tilde{L}_{max,\psi}$ = maximum increase in periodic loads with hull pitching over the values without ship motions

$\tilde{L}$ = periodic blade load without ship motions

V_ψ = maximum vertical velocity of the propeller due to the pitching motions

$(V_{t0.7})_1$ = first harmonic of the tangential wake at the 0.7 radius without ship motions

c. <u>Peak Loads</u>. The maximum values of the periodic variation of loads with angular position and the time-average loads per angular position occur near the same point in the pitch cycle. Therefore, the increase in peak loads due to hull pitching is approximately the sum of the increases in these components:

$$\Delta L_{peak,\psi} = \Delta \overline{L}_{max,\psi} + \Delta \tilde{L}_{max,\psi}$$

2. Regular Head Waves Without Ship Motions

a. <u>Transient Loads</u>. Waves (without ship motions) substantially increase the maximum transient loads or time-average loads per revolution* over the corresponding time-average loads in calm water. The primary controlling parameter is the change in effective advance coefficient due to the longitudinal component of orbital wave velocity. The hull boundary above the propeller does not appear to significantly influence the longitudinal component of orbital wave velocity. Therefore, the maximum increase in time average loads per propeller revolution due to waves

---

*The transient loads are periodic with the wave period of encounter for operation in a regular sea.

can be adequately predicted by the use of the trochoidal wave theory neglecting the influence of the hull on the waves, and simple quasi-steady propeller theory using the open-water characteristics of the propeller.

   b. _Periodic Loads._ Waves (without ship motions) substantially increase the maximum periodic blade loads over the corresponding periodic loads in calm water. The primary controlling parameter is the ratio of the vertical component of the orbital wave velocity in the propeller plane to the ship speed. The maximum periodic loads occur when the vertical component of the orbital wave velocity in the propeller plane is maximum upward. This upward orbital velocity component effectively increases the inclination of the inflow to the propeller and thereby increases the periodic loads. Due to the hull boundary above the propeller the maximum upward orbital velocity into the propeller is only 50 percent or less of the corresponding upward orbital velocity in an unbounded fluid for ships with high-speed transom sterns and exposed shafts and struts. Therefore, for these ships the maximum periodic blade loads due to waves can be approximated from the corresponding loads without waves as follows:

$$\Delta \tilde{L}_{max,\zeta} = \frac{0.5 \ V_\zeta}{(V_{t0.7})_1} \ \tilde{L}$$

where $\Delta \tilde{L}_{max,\zeta}$ = maximum increase in periodic loads with waves over the values in calm water

   $\tilde{L}$ = periodic blade load in calm water

   V_ζ = maximum vertical component of the orbital wave velocity in the propeller plane neglecting the influence of the hull

   $(V_{t0.7})_1$ = first harmonic of the tangential wake at the 0.7 radius in calm water

   c. _Peak Loads._ The maximum values of the periodic variation of loads with angular position and the time-average loads per angular position occur near the same point in the wave cycle. Therefore, the increase in peak loads due to waves is approximately the sum of the increases in these components:

$$\Delta L_{peak,\zeta} = \Delta \overline{L}_{max,\zeta} + \Delta \tilde{L}_{max,\zeta}$$

205

3. Hull Pitching in Regular Head Waves

Experiments* with hull pitching in regular head waves with pitching frequency equal to the wave frequency of encounter showed the following:

a. For given amplitudes of waves and pitching the maximum values of the time-average loads per revolution, peak loads, and the periodic variation of loads with angular position vary substantially depending upon the difference in phase between the hull pitch and the wave at the propeller. The time-average loads, peak loads, and periodic loads are near their respective largest values for any difference in phase whereby the crest of the wave reaches the propeller between 0.3 and -0.1 of the period of encounter before the maximum stern-up position.

b. Linear superposition of the increases in blade loads due to pitching in calm water and due to waves without hull pitching, taking into account the phase between the waves and the pitching, gives a good, or slightly conservative, estimate of the net increase in blade loads due to operation in waves with hull pitching. For engineering calculations, it is recommended that the absolute values of the maximum increases in time-average, peak, and periodic loads due to the separate influences of waves and hull pitching be added without regard to the relative phase between the wave and the hull pitching.

TURNS

It would have been desirable to measure the variation of loads with blade angular position, or the periodic blade loads, behind model hulls during simulated turning maneuvers, similar to the measurements of blade loads under other operating conditions as described in the preceding sections. However, the periodic blade loads could not be measured accurately behind model hulls with exposed shafting during simulated turning maneuvers due to serious limitations of the current state-of-the-art experimental techniques.**

---

*These experiments were conducted only on a model of the R/V ATHENA.

**The model experimental procedure for measuring periodic blade loads on hulls with exposed shafting requires that the propeller be driven from a downstream body as discussed in References 1 through 6. This downstream body does not significantly influence the wake pattern into the propeller for situations in which the direction of the model velocity is parallel to the hull centerline, as is the case for the operating conditions described in the preceding sections. However, the downstream body would significantly influence the wake pattern into the propeller for situations in which there is a substantial angle between the tangent to the path of the model and the hull centerline, as is the case for turns.

206

Therefore, in order to systematically evaluate the influence of turning maneuvers on periodic blade loads, wake surveys were conducted in the propeller planes on models of the BARBEY[37] and SPRUANCE[38] Class ships during simulated turns. As discussed previously, the circumferential variation of the wake velocity components is the primary cause of the periodic blade loads. The periodic blade loads in turns were calculated based on these wake data using the refined analytical technique[15] for calculating periodic blade loads including the influence of an angle between the direction of inflow in the propeller shaft axis. This refined technique was developed under the current research and development program for CP propellers, as discussed previously.

These wake surveys were conducted in the simulated steady portions of the turns at specified values of turning radius, drift angle, heel, and ship speed. In addition, the associated calculations of blade loads were conducted at the corresponding specified values of propeller rotational speed and pitch ratio. These quantities, which depend upon the turning maneuver being performed and the responses of the ship, propeller, turbine, and control system, must be determined from ship trials or from computer dynamic simulation of the system using specified characteristics of the hull, propeller, turbine, and control system. The hull and propeller characteristics for such a computer simulation must be obtained from systematic model experiments on the hull and propeller, including experiments during turns.

The objective of these experiments and calculations was to obtain systematic accurate experimental data showing the effect of turns on wake patterns and, indirectly, on periodic blade loads under carefully controlled experimental conditions so that the effects of turning maneuvers on wake patterns and periodic blade loads could be isolated. These data serve as a basis for developing procedures for predicting periodic blade loads during general turning maneuvers.

Before the present research and development program on CP propellers, there existed no known measurements of wake surveys in simulated turns.

The following conclusion is drawn from the wake surveys in turns:

The circumferential variation of the wake into the propeller plane is dominated by the drift angle at the propeller.

SUMMARY

During the course of the research and development program on CP propellers, analytical and experimental methods were developed which yield substantially improved predictions of periodic blade loads due to operation in inclined flow, such

207

as behind hulls with high-speed transom sterns with exposed shafting and struts. These methods can be used for predicting periodic blade loads on surface combatants under steady-ahead operation in a calm sea.

Experiments were conducted to determine the influence of ship acceleration and deceleration, operation in a rough sea, and operation in turns on the periodic blade loads. Using these experimental results as a guide, approximate methods were developed for predicting periodic blade loads for these operating conditions. These predictions require knowledge of the operating conditions including (1) the time dependence of ship speed, propeller rotational speed, and propeller pitch ratio for all maneuvers; (2) ship drift angle and heel angle for turning maneuvers; and (3) sea state characteristics and ship motions for operation in a rough sea. These approximate methods will be discussed in some detail in the following sections.

METHODS OF PREDICTING BLADE LOADS

This section summarizes the available techniques for predicting blade loads under various operating conditions using, in part, the results and procedures development under the research and develop program on CP propellers. As discussed previously, the blade loading transmitted to the hub can be represented as three force components and three moment components along a set of orthogonal axes. The coordinate systems shown in Figure 1 are used in the present report. The F_x, M_y, F_y, and M_x components (see Figure 1) can also be resolved into the magnitude and direction of a force and bending moment about some reference radius such as the average radius of the crank ring. For hydrodynamic loads, the directions of these force and moment vectors are approximately perpendicular and parallel, respectively, to the blade pitch line at the 70 percent radius for all operating conditions except crashback maneuvers. The spindle torque M_z is, in general, substantially less than the bending moments M_x and M_y. Spindle torque M_z is important from considerations of controlling the blade pitch, and may, depending on the blade skew, significantly contribute to high stresses in various components of the hub mechanism. The role of skew in minimizing M_z is discussed in the section on Guidelines for Minimizing Blade Loads.

CENTRIFUGAL AND GRAVITATIONAL LOADS

The centrifugal loading, which is a function only of the blade geometry, blade density, and propeller rotational speed, has only time average and transient

components and can be readily calculated. This is generally calculated during the propeller blade design process, when the propeller blade is structurally analyzed by finite element methods.

Centrifugal loading can be represented as a concentrated radial force through the blade centroid, and transmits primarily an $F_{z,c}$* component to the hub; see Figure 1. However, depending upon the blade rake and skew, centrifugal loads can also produce substantial bending moment components $M_{y,c}$ and $M_{x,c}$. The propeller blade designer has essentially no control over the value of $F_{z,c}$ after the preliminary design state in which propeller diameter and rpm are fixed; however, the designer can control $M_{y,c}$ and, to a lesser extent $M_{x,c}$, by the proper selection of blade rake and skew. It is desirable to minimize the total (hydrodynamic plus centrifugal) values of loading components, and the hydrodynamic portion $M_{y,H}$* is inherently positive (see Figure 1 for sign convention) and is the largest moment component for all operating correlations except deceleration and backing. Therefore, it is desirable to have $M_{y,c}$ negative, which can be achieved by placing the blade centroid forward of the spindle axis. This requires negative rake or skew.

Requirements to minimize propeller-induced vibratory forces and spindle torque under steady-ahead operation dictate a balanced skew with forward skew at the inner radii and aft skew at the outer radii. This inherently places the blade centroid near the spindle axis for an unraked blade so that $M_{y,c}$ and $M_{x,c}$ are small. Blade rake has no influence on $M_{x,c}$, but $M_{y,c}$ varies directly with rake for all other parameters held constant. Therefore, it is desirable to apply as much forward (negative) rake as practical from considerations of clearances, design theory, and total blade geometry. In summary, balanced skew and forward rake are recommended from considerations of centrifugal blade loads.

The gravitational loading, which is a function only of the blade geometry and blade density, occurs primarily as a first harmonic of blade angular position and can be readily calculated.

The gravitational loads can be represented as a constant downward force (the weight of the blade in water) applied at the centroid of the blade. The magnitude and point of application of the blade weight is generally calculated during the propeller design process. The blade weight is generally an order of magnitude less than the time-average thrust under full-power steady-ahead operation. The blade

---

*The subscript c denotes centrifugal loads; H denotes hydrodynamic loads.

209

weight has a constant F_x component $F_{x,g}$* and a first harmonic component of F_y, F_z, M_x, M_y, and M_z relative to a coordinate system rotating with the propeller blade. Force component $\overline{F}_{x,g}$** is negligible relative to $\overline{F}_{x,H}$ for realistic shaft inclination angles. The amplitudes of $(M_y)_{1,g}$*** and $(M_z)_{1,g}$, which are essentially the product of the weight of the blade and the x coordinate of the blade centroid relative to the spindle axis, are negligible relative to the respective hydrodynamic components. The amplitude of $(F_z)_{1,g}$ is essentially the weight of the blade which is, in general, less than three percent of $\overline{F}_z$ which is essentially the centrifugal force on the blade. Therefore, $(F_z)_{1,g}$ can be neglected. Components $(F_y)_{1,g}$ and $(M_x)_{1,g}$ are, in general, approximately 180 degrees out of phase with and smaller than the respective components of hydrodynamic loading for wakes behind high-speed transom sterns with exposed struts and shafting; i.e., for wakes of the type encountered on surface combatants. On the SPRUANCE and R/V ATHENA these components of centrifugal loading reduced the maximum bending moment about the hub by less than seven percent of the hydrodynamic moment for steady-ahead operation. Therefore, the neglect of these components results in a slightly conservative prediction of the maximum periodic blade bending moment. In summary, the gravitational loads may be completely neglected without a significant loss in accuracy of the predicted total loads.

HYDRODYNAMIC LOADS

In this section, the use of available techniques, for determining hydrodynamic loads as they are applicable to CP propeller design, and their associated accuracies and costs, is discussed. The available techniques which were developed under the research and development program on CP propellers were discussed earlier in this chapter. The estimated accuracies and costs are summarized in Table 4.

The blade loading transmitted to the palm is represented as the three force components and three moment components shown in Figure 1. For the radial force component F_z, the hydrodynamic loads are relatively unimportant since essentially all of the time average and transient portion of F_z arises from centrifugal force, and most of the periodic portion of F_z which is quite small, arises from gravitational loads.

---

*The subscript g denotes gravitational loads.

**The subscript — denotes time-average loads.

***The notation ( )$_1$ denotes the first harmonic of ( ).

TABLE 4 – SUMMARY OF DESIGN TOOLS AND ESTIMATED ACCURACY AND COST FOR PREDICTING PROPELLER BLADE LOADS

	Time-Average and Transient Loads	Accuracy[1] ± Percent	Estimated Cost[2] ($k)	Periodic Loads[3]	Accuracy[1] ± Percent	Estimated Cost[2] ($k)
Steady-ahead in a calm sea	Design calculations	5	2	Model blade loading experiments	15	100
	Model powering experiments	8	2	Theory plus empirical factor	20	10
	Theory	10	5	Statistical data	30	3
Acceleration and deceleration in a calm sea	Computer simulation[4]	15	150	Theory plus empirical factor	25	10
	Statistical data	40	10	Statistical data	40	5
Turning maneuvers in a calm sea	Computer simulation[4]	20	150	Theory plus empirical factor with model wake survey in turn	30	30
				with estimated wake in turn	40	10
	Statistical data	40	10	Statistical data with model wake survey in turn	45	25
				with estimated wake in turn	60	5
Steady-ahead in rough water	Model experiments in rough water[5]	15	40	Semi-empirical theory[4,7]	30	5
	Statistical data[5]	25	5			
	Semi-empirical theory[4,6]	20	5			

All accuracies are ± "true" value in percent.

[1]Accuracies shown apply to the F_x, M_y, F_y, and M_x component; the deviations from "true" values for M_z are approximately twice the values shown.

[2]All estimated costs are rough approximations for conducting the work in FY 1980. It is assumed that the usual information for designing the propeller and evaluating the hull and propeller, without regard to blade loads, is available. This includes model hull and propellers, model resistance, propulsion, maneuvering, and seakeeping experiments, and steady-ahead wake surveys. The cost of special experiments, useful primarily for predicting blade loads, is included in the estimates quoted. Actual costs may vary substantially.

[3]Assumes that the most accurate method listed was used to predict time-average or transient loads.

[4]Requires same supporting model experiments.

[5]Time-average values.

[6]Transient values.

[7]Assumes that the most accurate method listed was used to predict periodic loads in calm sea.

211

Steady-Ahead in a Calm Sea

Time-Average Loads. Time average loads under steady-ahead operation in a calm sea can be predicted to a high accuracy by any one of several methods. These methods include: (1) routine model powering experiments, (2) propeller design calculations, (3) theoretical predictions based on propeller inverse theory, and (4) a combination of these methods.

1. Routine model powering experiments. Routine model powering experiments yield predictions of time-average thrust and torque over the speed range. Blade bending moments about any desired radius equal to or less than the radius of the blade palm can be calculated from these measured quantities by assuming a radial point of application of thrust $\overline{F}_x$ and transverse force $\overline{F}_y$. An estimate of the radial points of application of these force components can be obtained from propeller design or analysis calculations, or, if these are unavailable, it is reasonable to assume that these force components are applied at the 0.7 radius. The true radial centers of these force components are generally within ± 2 percent of the 0.7R; therefore, errors resulting from assuming that these radial centers are located at 0.7R can result in an error of ± 5 percent in the moment arms at the crank ring (at approximately 0.25R). These experiments predict thrust and torque to within approximately ± 3 percent, and blade bending moments at the crank ring to within approximately ± 8 percent. These experiments yield no information on spindle torque M_z. The estimated cost of these predictions is approximately $2000.00.*

2. Propeller design calculations. The distribution of hydrodynamic loads over the blade at the design condition** is specified during the process of designing the propeller blades. This yields the F_x, F_y, M_x, and M_y components to an accuracy of approximately ± 5 percent and the M_z component to an accuracy of approximately

_____

*All estimated costs are rough approximations for conducting the work in FY 1980. It is assumed that the usual information for designing the propeller and evaluating the hull and propeller, without regard to blade loads, is available. This includes model hull and propellers, model resistance, propulsion maneuvering, seakeeping experiments, and steady-ahead wake surveys. The cost of special experiments useful primarily for predicting blade loads is included in the estimates quoted. Actual costs may vary substantially.

**The design condition is defined as the steady-ahead condition in calm water at which the detailed design of the propeller blades is conducted. This condition generally corresponds to a specified speed or delivered power, and a specified propeller rotational speed.

+10 percent at an estimated cost of approximately $1000.00. The predicted spatial distributions of loading are applicable only at the design advance coefficient J; however, the radial distributions of these loads are insensitive to J over the range of J encountered by a surface combatant under steady-ahead operation in a calm sea. Therefore, the blade bending moments over the speed range can be readily calculated using the radial centers of thrust and transverse force from the design calculations, and the thrust and torque as a function of speed from routine model powering experiments, as discussed in the preceding paragraph. The estimated cost of these predictions is approximately $2000.00.

3. _Propeller inverse theory_. The distribution of time-average hydrodynamic loads over a propeller blade can be calculated by propeller lifting-surface theory[6] for given propeller geometry, radial distributions of inflow, and operating conditions. This yields the F_x, F_y, M_x, and M_y components to an accuracy of approximately ± 10 percent, and the M_z component to an accuracy of approximately ± 20 percent at an estimated cost of approximately $3000.00. The primary use of this method is for applications in which the design calculations are unavailable or unsuitable, such as off-design conditions. The predicted radial centers of F_x and F_y from this method can also be used with the thrust and torque predicted from routine powering experiments to more accurately calculate the blade bending moments, as discussed previously. The estimated cost of these predictions is $5000.00.

Periodic Loads. Periodic blade loads under steady-ahead operation in a calm sea can be predicted by one of several methods. These methods include: (1) model blade loading experiments on the propeller-hull configuration under consideration, (2) analytical calculations on the propeller-hull configuration under consideration plus an appropriate empirical factor, and (3) estimates from the existing statistical database of model and full-scale blade loading experiments.

1. _Model experiments_. The most accurate, but also the most expensive and time consuming, method of predicting periodic blade loads on a new propeller-hull configuration is to measure the six components of blade loading on a model of the propeller-hull configuration under consideration using the experimental techniques developed under the research and development program on CP propellers. This yields the periodic portions of F_x, F_y, M_x, and M_y components to an accuracy of approximately

± 15 percent of their true values, and the periodic portion of M_z to an accuracy of approximately ± 30 percent of its true value, at an estimated cost of approximately $100,000.00.

2. <u>Analytical calculations</u>. The periodic blade loads can also be analytically calculated using the method of Kerwin[7] together with an empirical factor derived from extensive correlations between this method and experimental data obtained under the research and development program on CP propellers. A wake survey conducted behind the model hull is a necessary input to this calculation. This method yields $\tilde{F}_x$, $\tilde{F}_y$, $\tilde{M}_x$, and $\tilde{M}_y$* to an accuracy of approximately ± 20 percent of their true values, and M_z to an accuracy of approximately ± 40 percent of its true value, at an estimated cost of approximately $10,000.00. This method is substantially cheaper and quicker, but somewhat less accurate than measuring the periodic blade loads behind the model hull.

3. <u>Statistical data</u>. The periodic blade loads on a new propeller-hull configuration can also be estimated directly from the existing statistical database of model and full-scale measurements of periodic blade loads. This method is substantially cheaper and quicker, but less accurate than either model experiments or analytical calculations. The accuracy of estimates using this procedure depends upon the degree of similarity between the new configuration including propeller geometry, wake, and operating conditions and the configurations in the database, and upon the physical insight of the person making the estimates. For a new configuration which is somewhat similar to the configurations in the database, a person with reasonable insight into the problem could probably estimate F_x, F_y, M_x, and M_y to an accuracy of approximately ± 30 percent of their true values, and M_z to an accuracy of ± 60 percent of its true value, at an estimated cost of $3000.00.

For a new propeller-hull configuration which is significantly different from an existing configuration, it is recommended that blade loads be predicted by both model measurements of the six components of blade loading and by the unsteady lifting surface theoretical method of Kerwin[15] supplemented by the appropriate empirical factor. This provides two independent predictions which can be cross-checked. These predictions should be further checked by comparison with the existing statistical database.

---

*Superscript ~ denotes the periodic portion of loads.

214

Maneuvers

Transient Loads

1. <u>Computer dynamic simulation</u>. Transient loads during maneuvers, including
acceleration, deceleration, and various types of turning maneuvers, depend strongly
upon the instantaneous values of ship speed, propeller rotational speed, propeller
pitch, and propeller-hull interaction coefficients. The transient loads, or time-
average loads per revolution, appear to be insensitive to the time rate of change
of the aforementioned variables, based on limited experimental data and physical
arguments. Therefore, if the time histories of the aforementioned variables through
a maneuver are known, then the time-average loads can be estimated from routine
propeller model thrust and torque characteristics in uniform flow (propeller open
water characteristics) and propeller inverse lifting surface theory[14] as described
in the preceding section for steady-ahead operation.

The time histories of ship speed, propeller rotational speed, propeller pitch,
and propeller-hull interaction coefficients during a specific maneuver depend in a
complex manner upon interactions between the characteristics of the propeller, hull,
prime mover, and control system. For a new ship design, the best method of predict-
ing the time histories of the aforementioned variables is a computer dynamic simu-
lation of the complete propulsion system and ship response, such as those described
in References 39 through 43. These dynamic simulations require accurate knowledge
of the individual characteristics of the propeller, hull, propeller-hull interaction,
prime mover, and control system.

The individual characteristics of the propeller, hull, and propeller-hull
interactions over the pertinent range of conditions likely to be encountered during
maneuvers must be obtained from systematic model experiments on the propeller and
hull under consideration. These experiments include open-water characterization of
the propeller and associated blade spindle torque measurements over a range of
conditions including ahead and astern velocities, each over a range of positive and
negative pitches, determining the pertinent maneuvering coefficients of the hull,
and determining the propeller-hull interaction coefficients over the pertinent range
of conditions likely to be encountered during maneuvers.

The accurate determination of the propeller-hull interaction coefficients over
the pertinent range of conditions is probably the most difficult and weakest part
of the simulation. There exist very few reliable measurements of these interaction

coefficients under conditions likely to be encountered during maneuvers. These interaction coefficients are inherently difficult to determine accurately, and they are very sensitive to small changes in many parameters so that it is difficult to interpolate or extrapolate them, as is necessary in the dynamic simulation process, without further loss of accuracy. This is a particularly difficult problem for turning maneuvers due to the large number of pertinent parameters in turns. In addition to those listed previously, these include roll, drift angle, rudder angle unbalances between the two propellers for twin-screw ships, and complex interactions between the various parameters.

Another problem in simulating turning maneuvers is that the path and orientation of the hull, which have a very significant influence on the loads, must be predicted. These can be predicted using four degrees of freedom maneuvering simulation programs for the hull, which use the pertinent maneuvering coefficients of the hull as determined from model experiments. Usually, four-degrees-of-freedom programs are designed to predict ship motion characteristics for constant power maneuvers with no regard to propeller thrust and torque.[44,45] Recently Carroll and Harper[46] modified the ship motion equations in the four-degrees-of-freedom simulation to include propeller thrust and torque as a function of propeller rotational speed, ship velocity, and ship orientation. With this refinement, the influence of the path and orientation of the hull can be incorporated into the dynamic simulation of the system including the propeller, hull, propeller-hull interaction, prime mover, and control system.

The use of computer dynamic simulations, supported by the necessary model experiments on the propeller and hull under consideration, yields predictions of the maximum transient values of the F_x, F_y, M_x, and M_y components of blade loading to an accuracy of approximately ±15 percent for acceleration and deceleration maneuvers, and to an accuracy of approximately ±20 percent for turning maneuvers, at an estimated cost of approximately \$150,000.00. The deviations from the true values for M_z are approximately twice the percentages for the other components. If the computer dynamic simulations use propeller, hull, or propeller-hull interaction coefficients approximated from hulls or propellers which are different from the final configuration, then the inaccuracies in predicting the blade loads become somewhat greater.

216

2. _Statistical data_. The transient blade loads on a new propeller-hull con-
trol system configuration can also be estimated directly from the existing statisti-
cal database of full-scale measurements and computer dynamic simulations on previous
ships. This method is substantially cheaper and quicker, but less accurate than the
use of computer dynamic simulations, supported by the necessary model experiments,
on the control system, hull, and propeller under consideration. The accuracy of
estimates using this procedure depends upon the degree of similarity between the new
configuration including propulsion control system, stern geometry, propeller geome-
try, and types of maneuvers and the configurations in the database, and upon the
physical insight of the person making the estimates. For a new configuration, which
is somewhat similar to the configurations in the database, a person with reasonable
insight into the problem could probably estimate the maximum values of F_x, F_y, M_x,
and M_y to an accuracy of approximately ± 40 percent of their true values, and the
maximum value of M_z to an accuracy of ± 100 percent of its true value for acceler-
ation, deceleration, and turning maneuvers, at an estimated cost of approximately
$10,000.00. For a new configuration, which is significantly different from an
existing configuration, the inaccuracies in predicting transient blade loads from
the statistical database become somewhat greater.

Periodic Loads

1. _Analytical calculations_. The periodic loads during maneuvers, including
acceleration, deceleration, and various types of turning maneuvers, depend upon the
same parameters as discussed in the preceding paragraphs for transient loads,
except that the dependence upon the propeller-hull interaction coefficients may not
be as strong. However, unlike the transient loads, the periodic loads depend
critically upon the spatial distribution of the wake velocity components in the
propeller at a given time in a maneuver. Therefore, two basic inputs are required
for predicting periodic blade loads in a maneuver:

a. A time-history of the maneuver which may be estimated as described in the
preceding paragraphs, and

b. An estimate of the wake velocity components in the propeller plane at a
given time in the maneuver.

For acceleration and deceleration maneuvers, the nondimensional wake velocity
components for ahead speed $V > 0$ is approximately the same as it is for steady-ahead

operation.[2,11] For astern speed V < 0, the periodic loads are, in general, sma'!
due to the relatively low magnitudes of V and rotational speed n under these con-
ditions so that it is not usually necessary to accurately estimate the wake velocity
components. If desirable, model wake surveys can be conducted under astern ope.-
ation simulated in a quasi-steady manner; i.e., V < 0 and $\dot{V}$ = 0.

For turning maneuvers the circumferential variation of the wave velocity compo-
nents in the propeller becomes more severe than it is for steady-ahead operation
due to the large drift angle; i.e., the angle between the local undistributed
direction of motion and the hull centerline. This drift angle is, in principle,
equivalent to the inclination angle of the flow relative to the propeller shaft for
steady-ahead operation, except that it occurs in the horizontal plane. Therefore,
this drift angle produces a large first harmonic tangential wake, and thereby
produces large first harmonic periodic loads.

Wake surveys conducted on models of the SPRUANCE[37] and BARBEY[38] during simu-
lated steady turns showed that the circumferential variation of the wake is dominated
by the drift angle at the propeller plane. Further, these wake surveys indicated
that the peak-to-peak circumferential variation of the velocity components of the
wake of a high-speed transom stern configuration with exposed shafting and struts in
a turning maneuver can be estimated within approximately ±20 percent from the known
wake velocity components under steady-ahead operation, the drift angle at the pro-
peller plane, and the location of the propeller in the turn; i.e., inboard, out-
board, or centerline.

Alternatively, a more accurate estimate of the wake velocity components can be
obtained from a model wake survey conducted on a model of the hull of interest at
the conditions existing at a given time in the maneuver simulated in a quasi-steady
manner; i.e., constant values of ship speed, drift angle, turning radius, roll, etc.
This model wake survey would be run for conditions at which nearly maximum values of
periodic loads are predicted based on more approximate wake velocity components.
The estimated cost of conducting a model wake survey in turns is $20,000.00.

Once the time-history of the maneuver, including the wake velocity components,
is estimated, the periodic loads at any time during the maneuver can be calculated
using the same procedures as for steady-ahead operation as described in a preceding
section. For preliminary estimates to determine at what conditions the largest

218

peak and periodic loads occur, the periodic loads can be estimated from the calcu-
lated or measured periodic loads under steady-ahead operation, adjusted for
operating conditions and wake patterns using trends of the data presented in
References 1 through 6, 21, and 22 as a guide.

If the time-history of the maneuver is predicted by the best available methods
as discussed in the preceding section, then the maximum values of the $\tilde{F}_x$, $\tilde{F}_y$, $\tilde{M}_x$,
and $\tilde{M}_y$ components during acceleration and deceleration maneuvers can be predicted
by theoretical calculations[15] plus an empirical factor to an accuracy of approxi-
mately ± 25 percent at an estimated cost of approximately \$10,000.00. Similarly, the
maximum values of the $\tilde{F}_x$, $\tilde{F}_y$, $\tilde{M}_x$, and $\tilde{M}_y$ components during turning maneuvers can be
calculated to an accuracy of approximately ± 30 percent if model wake surveys during
simulated turns are conducted, and to an accuracy of approximately ± 40 percent if
the wake patterns during the turns are approximated from the drift angle and the
wake data during steady-ahead operation or the statistical wake data in the litera-
ture. The estimated cost is approximately \$30,000.00 if a model wake survey in
turns is conducted, and \$10,000.00 if no such wake survey is conducted. The de-
viations from the true values for the M_z component are approximately twice the per-
centage for the other components.

2. _Statistical data._ The periodic blade loads on a new propeller-hull configu-
ration can also be estimated directly from the existing statistical database of
model and full-scale measurements and theoretical calculations of periodic blade
loads. This method is somewhat cheaper but less accurate than analytical calcu-
lations. The accuracy of estimates using this procedure depends upon the degree of
similarity between the new configuration including propeller geometry, wake, and
operating conditions and the configurations in the database and upon the physical
insight of the person making the estimates. If the time-history of the maneuver is
predicted by the best available methods, as discussed in the preceding section, then,
for a new configuration which is somewhat similar to the configurations in the
database, a person with reasonable insight into the problem could probably estimate
the maximum values of F_x, F_y, M_x, and M_y to an accuracy of ± 40 percent of their
true values for acceleration and deceleration maneuvers, to an accuracy of ± 45 per-
cent for turning maneuvers using measured wakes on the configuration under con-
sideration in simulated turns, and to an accuracy of ± 60 percent for turning

219

maneuvers using estimated wakes in turns. The deviations from the true values for the M_z component are approximately twice the percentages for the other components. The estimated cost of predicting these periodic loads in maneuvers based on the statistical data is approximately $5000.00.

Influence of Rough Seas

When a ship operates in rough seas the ship speed and propeller rotational speed at a given delivered power decrease from the corresponding values in calm water due to increased resistance of the hull and change in the propulsion coefficients (involuntary speed loss).[33-35] Furthermore, in rough seas the delivered power is often reduced from the calm water value (voluntary speed loss).[34,36] Therefore, the difference in blade loads between operation in calm seas and operation in rough seas can be represented as being made up of two major parts:

1. Differences in loads resulting from the difference in ship speed and propeller rotational speed between calm seas and rough seas, and

2. Increases in loads due to the direct influence of waves and ship motions at a given value of ship speed and propeller rotational speed.

Time-Average-Loads. The changes in the time-average* propeller rotational speed, speed of advance, thrust, and torque at a given delivered power due to operation in rough seas can be estimated experimentally or theoretically using methods or data summarized by Oosterveld,[34] Day et al.,[35] and Lloyd and Andrew.[36] The most accurate approach is to conduct model experiments on the propeller-hull configuration of interest using the experimental procedures summarized by Day et al.[35]

For a given operating condition and time-average thrust and torque, the time-average values of the various components of blade loading can be calculated using the pertinent procedures as described previously for steady-ahead operation in a calm sea.

Using these procedures based on a model experiment on the propeller-hull configuration of interest, the F_x, F_y, M_x, and M_y components can be calculated to an

---

*Time-average quantities are defined here as quantities averaged over a length of time which is much greater than the period of any significant component of the wave or ship motion of interest.

accuracy of ± 15 percent and the M_z component can be calculated to an accuracy of ± 30 percent at a cost of approximately $40,000.00 including the model experiment.

Alternatively, using these procedures, based on statistical data, the F_x, F_y, M_x, and M_y components can be calculated to an accuracy of ± 25 percent, and the M_z component to an accuracy of ± 50 percent at a cost of approximately $5000.00.

Transient and Periodic Loads. For given time-average ship speed and propeller rotational speed, the increase in transient and periodic loads* due to the influence of waves and ship motions can be estimated from the experimental data obtained under the research and development program on CP propellers as discussed previously. It is reasonable to disregard any transient variation in ship speed and propeller rotational speed n. In practice, there is a small transient variation in V and n, the variation in n for a gas turbine propulsion system being dependent upon the propulsion control system.

As discussed previously, the increase in transient loads is controlled primarily by the axial component of the orbital wave velocity at the propeller, and the increase in the periodic loads is controlled primarily by the vertical component of the orbital wave velocity at the propeller, as modified by the presence of the hull, and by the vertical velocity of the propeller due to ship motions.

For a given sea spectrum, the orbital wave velocities can be calculated directly from orbital wave theory.[47,48] McCarthy et al.[47] gives equations for averaging the orbital wave velocities over the propeller disk. However, this refinement is not justified in light of the various approximations that are required for predicting loads in a rough sea. Therefore, it is recommended that the orbital wave velocities be calculated at the depth of the propeller centerline.

The vertical velocity of the propeller due to ship motions depends upon the sea spectrum and the response of the hull in the pitch, heave, and roll modes. The response of the hull is best predicted by seakeeping experiments on a model of the hull under consideration. These experiments give information on the amplitudes and phases of the various components of hull response as functions of the lengths and orientations of the various wave components.

---

*Transient portion of quantities are defined here as the variations of time-average values per propeller revolution with local sea conditions and ship motions, and the periodic portion is defined as the variation with blade angular position.

Therefore, the maximum transient loads in a rough sea $\overline{L}_{max,\zeta,\psi}$* for ships with high-speed transom sterns and exposed shafts and struts may be calculated as follows:

1. Calculate the minimum axial velocity at the shaft centerline from orbital wave theory for the assumed or specified sea spectrum, $V_A + V_{\zeta A,min}$, where V_A is the time-average axial velocity of advance derived from a thrust identity from the predicted powering performance in a rough sea, and $V_{\zeta A,min}$ is the minimum axial velocity due to the waves ($V_{\zeta A,min}$ is negative so that $V_A + V_{\zeta A,min} < V_A$).

2. Calculate the maximum transient loads $\overline{L}_{max,\zeta,\psi}$ from quasi-steady theory[19] based on $V_A + V_{\zeta A,min}$ and the time-average n that is predicted in a rough sea.

The maximum periodic loads in a rough sea $\tilde{L}_{max,\zeta,\psi}$ for ships with high-speed transom sterns and exposed shafts and struts may be calculated as follows:

1. Calculate the periodic blade $\tilde{L}$ that would occur if the ship were operating in a calm sea at the values of V and n that are predicted to occur in a rough sea. This may be estimated from the values calculated for steady-ahead operation in a calm sea, with adjustment for the differences in V and n between operation in a calm sea and in a rough sea, using the trends of the data in Reference 22.

2. Calculate the maximum upward orbital wave velocity component V_ζ at the shaft centerline from orbital wave theory in the absence of the hull for the assumed or specified sea spectrum.

3. Calculate the maximum increase in periodic blade loads due to wave velocities from the corresponding loads that would occur if the ship were operating in calm water without ship motions at the same V and n as follows:

$$\Delta\tilde{L}_{max,\zeta} = \frac{0.5\,V_\zeta}{(V_{t0.7})_1}\,\tilde{L}$$

where $\Delta\tilde{L}_{max,\zeta}$ = maximum increase in periodic loads with waves over the values in calm water at the values of V and n that occur in a rough sea

$\tilde{L}$ = periodic blade loads in calm water at the values of V and n that occur in a rough sea

V_ζ = maximum vertical component of the orbital wave velocity in the propeller plane neglecting the influence of the hull

---

*The subscript ζ denotes the direct influence of the waves, and the subscript ψ denotes the influence of ship motions.

222

$(V_{t0.7})_1$ = first harmonic of the tangential wake at the 0.7 radius in calm water at the values of V and n that occur in a rough sea

The 0.5 is an empirical factor to account for the influence of the hull boundary in reducing the upward orbital velocity to below its calculated value in the absence of of the hull.

4. Calculate the maximum downward vertical velocity of the propeller from the pitch, heave, and roll modes of ship motions for operation in the assumed or specified sea spectrum.

5. Calculate the maximum increase in periodic blade loads due to ship motions from the corresponding loads that would occur if the ship were operating in calm water without ship motions at the same V and n as follows:

$$\Delta \tilde{L}_{max,\psi} = \frac{0.6 \, V_\psi}{(V_{t0.7})_1} \, \tilde{L}$$

where $\Delta \tilde{L}_{max,\psi}$ = maximum increase in periodic loads with ship motions over the values in calm water without ship motions at the values of V and n that occur in a rough sea

$\tilde{L}$ = periodic blade loads in calm water without ship motions, at the values of V and n that occur in a rough sea

V_ψ = maximum vertical velocity of the propeller due to ship motions

$(V_{t0.7})_1$ = first harmonic of the tangential wake at the 0.7 radius in calm water without ship motions at the values of V and n that occur in a rough sea

The 0.6 is an empirical factor to account for the displacement effect of the hull above the propeller. This displacement effect induces a velocity at the propeller so that the velocity of the propeller relative to the local fluid particles is only 60 percent or less of the vertical velocity of the propeller.

6. Calculate the maximum periodic blade loads assuming that the increases in periodic loads due to wave velocities and due to ship motions occur simultaneously and, therefore, add in phase as:

$$\tilde{L}_{max,\zeta,\psi} = \tilde{L} + \Delta \tilde{L}_{max,\zeta} + \Delta \tilde{L}_{max,\psi}$$

The assumption that these two increases add directly in phase is justified by results from the research and development program on CP propellers as discussed previously, and any error in this assumption is conservative.

The maximum value of the peak loads, including both transient and periodic contributions, may then be calculated assuming that the maximum values of the periodic loads and transient loads occur simultaneously and, therefore, add in phase as:

$$L_{peak,\zeta,\psi} = \overline{L}_{max,\zeta,\psi} + \tilde{L}_{max,\zeta,\psi}$$

The assumption that these two values add directly in phase is justified by the results from the research and development program on CP propellers as discussed previously, and any error in this assumption is conservative.

If ship motions and time-average conditions and loads in a rough sea are predicted, based on experiments on a model of the hull and propeller under consideration, and if loads under steady-ahead motion in a calm sea are predicted by the best available methods, then the maximum values of $\overline{F}_x$, $\overline{F}_y$, $\overline{M}_x$, and $\overline{M}_y$ due to operation in a rough sea can be predicted to an accuracy of approximately ±20 percent using the procedures described here. Similarly, the maximum values of $\tilde{F}_x$, $\tilde{F}_y$, $\tilde{M}_x$, and $\tilde{M}_y$ can be predicted to an accuracy of ±30 percent, and the maximum values of $\overline{F}_x + \tilde{F}_x$, $\overline{F}_y + \tilde{F}_y$, $\overline{M}_x + \tilde{M}_x$, and $\overline{M}_y + \tilde{M}_y$ can be predicted to an accuracy of ±25 percent. The deviations from the true values for the M_z components are approximately twice the percentages for the other components. If ship motions or time-average conditions and loads in a rough sea are estimated from hulls or propellers which are different from the final configuration, then the inaccuracies in predicting transient and periodic blade loads in a rough sea become somewhat greater. The estimated cost of calculating the influence of a rough sea on blade loads is approximately $5000.00.

Summary

The use of available techniques for predicting time-average or transient hydrodynamic blade loads and periodic hydrodynamic blade loads under various operating conditions, and their associated accuracies and costs, are summarized in

$(V_{t0.7})_1$ = first harmonic of the tangential wake at the 0.7 radius in calm water at the values of V and n that occur in a rough sea

The 0.5 is an empirical factor to account for the influence of the hull boundary in reducing the upward orbital velocity to below its calculated value in the absence of of the hull.

4. Calculate the maximum downward vertical velocity of the propeller from the pitch, heave, and roll modes of ship motions for operation in the assumed or specified sea spectrum.

5. Calculate the maximum increase in periodic blade loads due to ship motions from the corresponding loads that would occur if the ship were operating in calm water without ship motions at the same V and n as follows:

$$\Delta \tilde{L}_{max,\psi} = \frac{0.6 \, V_\psi}{(V_{t0.7})_1} \tilde{L}$$

where $\Delta \tilde{L}_{max,\psi}$ = maximum increase in periodic loads with ship motions over the values in calm water without ship motions at the values of V and n that occur in a rough sea

$\tilde{L}$ = periodic blade loads in calm water without ship motions, at the values of V and n that occur in a rough sea

V_ψ = maximum vertical velocity of the propeller due to ship motions

$(V_{t0.7})_1$ = first harmonic of the tangential wake at the 0.7 radius in calm water without ship motions at the values of V and n that occur in a rough sea

The 0.6 is an empirical factor to account for the displacement effect of the hull above the propeller. This displacement effect induces a velocity at the propeller so that the velocity of the propeller relative to the local fluid particles is only 60 percent or less of the vertical velocity of the propeller.

6. Calculate the maximum periodic blade loads assuming that the increases in periodic loads due to wave velocities and due to ship motions occur simultaneously and, therefore, add in phase as:

$$\tilde{L}_{max,\zeta,\psi} = \tilde{L} + \Delta \tilde{L}_{max,\zeta} + \Delta \tilde{L}_{max,\psi}$$

223

The assumption that these two increases add directly in phase is justified by results from the research and development program on CP propellers as discussed previously, and any error in this assumption is conservative.

The maximum value of the peak loads, including both transient and periodic contributions, may then be calculated assuming that the maximum values of the periodic loads and transient loads occur simultaneously and, therefore, add in phase as:

$$L_{peak,\zeta,\psi} = \overline{L}_{max,\zeta,\psi} + \tilde{L}_{max,\zeta,\psi}$$

The assumption that these two values add directly in phase is justified by the results from the research and development program on CP propellers as discussed previously, and any error in this assumption is conservative.

If ship motions and time-average conditions and loads in a rough sea are predicted, based on experiments on a model of the hull and propeller under consideration, and if loads under steady-ahead motion in a calm sea are predicted by the best available methods, then the maximum values of $\overline{F}_x$, $\overline{F}_y$, $\overline{M}_x$, and $\overline{M}_y$ due to operation in a rough sea can be predicted to an accuracy of approximately ±20 percent using the procedures described here. Similarly, the maximum values of $\tilde{F}_x$, $\tilde{F}_y$, $\tilde{M}_x$, and $\tilde{M}_y$ can be predicted to an accuracy of ±30 percent, and the maximum values of $\overline{F}_x + \tilde{F}_x$, $\overline{F}_y + \tilde{F}_y$, $\overline{M}_x + \tilde{M}_x$, and $\overline{M}_y + \tilde{M}_y$ can be predicted to an accuracy of ±25 percent. The deviations from the true values for the M_z components are approximately twice the percentages for the other components. If ship motions or time-average conditions and loads in a rough sea are estimated from hulls or propellers which are different from the final configuration, then the inaccuracies in predicting transient and periodic blade loads in a rough sea become somewhat greater. The estimated cost of calculating the influence of a rough sea on blade loads is approximately $5000.00.

Summary

The use of available techniques for predicting time-average or transient hydrodynamic blade loads and periodic hydrodynamic blade loads under various operating conditions, and their associated accuracies and costs, are summarized in

224

$(V_{t0.7})_1$ = first harmonic of the tangential wake at the 0.7 radius in calm water at the values of V and n that occur in a rough sea

The 0.5 is an empirical factor to account for the influence of the hull boundary in reducing the upward orbital velocity to below its calculated value in the absence of of the hull.

4. Calculate the maximum downward vertical velocity of the propeller from the pitch, heave, and roll modes of ship motions for operation in the assumed or specified sea spectrum.

5. Calculate the maximum increase in periodic blade loads due to ship motions from the corresponding loads that would occur if the ship were operating in calm water without ship motions at the same V and n as follows:

$$\Delta \tilde{L}_{max,\psi} = \frac{0.6 \, V_{\psi}}{(V_{t0.7})_1} \, \tilde{L}$$

where $\Delta \tilde{L}_{max,\psi}$ = maximum increase in periodic loads with ship motions over the values in calm water without ship motions at the values of V and n that occur in a rough sea

$\tilde{L}$ = periodic blade loads in calm water without ship motions, at the values of V and n that occur in a rough sea

V_{ψ} = maximum vertical velocity of the propeller due to ship motions

$(V_{t0.7})_1$ = first harmonic of the tangential wake at the 0.7 radius in calm water without ship motions at the values of V and n that occur in a rough sea

The 0.6 is an empirical factor to account for the displacement effect of the hull above the propeller. This displacement effect induces a velocity at the propeller so that the velocity of the propeller relative to the local fluid particles is only 60 percent or less of the vertical velocity of the propeller.

6. Calculate the maximum periodic blade loads assuming that the increases in periodic loads due to wave velocities and due to ship motions occur simultaneously and, therefore, add in phase as:

$$\tilde{L}_{max,\zeta,\psi} = \tilde{L} + \Delta \tilde{L}_{max,\zeta} + \Delta \hat{L}_{max,\psi}$$

223

The assumption that these two increases add directly in phase is justified by results from the research and development program on CP propellers as discussed previously, and any error in this assumption is conservative.

The maximum value of the peak loads, including both transient and periodic contributions, may then be calculated assuming that the maximum values of the periodic loads and transient loads occur simultaneously and, therefore, add in phase as:

$$L_{peak, \zeta, \psi} = \overline{L}_{max, \zeta, \psi} + \tilde{L}_{max, \zeta, \psi}$$

The assumption that these two values add directly in phase is justified by the results from the research and development program on CP propellers as discussed previously, and any error in this assumption is conservative.

If ship motions and time-average conditions and loads in a rough sea are predicted, based on experiments on a model of the hull and propeller under consideration, and if loads under steady-ahead motion in a calm sea are predicted by the best available methods, then the maximum values of $\overline{F}_x$, $\overline{F}_y$, $\overline{M}_x$, and $\overline{M}_y$ due to operation in a rough sea can be predicted to an accuracy of approximately ± 20 percent using the procedures described here. Similarly, the maximum values of $\tilde{F}_x$, $\tilde{F}_y$, $\tilde{M}_x$, and $\tilde{M}_y$ can be predicted to an accuracy of ± 30 percent, and the maximum values of $\overline{F}_x + \tilde{F}_x$, $\overline{F}_y + \tilde{F}_y$, $\overline{M}_x + \tilde{M}_x$, and $\overline{M}_y + \tilde{M}_y$ can be predicted to an accuracy of ± 25 percent. The deviations from the true values for the M_z components are approximately twice the percentages for the other components. If ship motions or time-average conditions and loads in a rough sea are estimated from hulls or propellers which are different from the final configuration, then the inaccuracies in predicting transient and periodic blade loads in a rough sea become somewhat greater. The estimated cost of calculating the influence of a rough sea on blade loads is approximately $5000.00.

Summary

The use of available techniques for predicting time-average or transient hydrodynamic blade loads and periodic hydrodynamic blade loads under various operating conditions, and their associated accuracies and costs, are summarized in

224

this section. These include the use of model experiments, analytical procedures, and existing statistical data. Centrifugal and gravitational loads can be accurately calculated analytically for all operating conditions.

GUIDELINES FOR MINIMIZING BLADE LOADS

There are many variables that influence propeller blade loads. Blade loads in future designs may be reduced if the influences of these variables on propeller blade loads are considered in the design process.

Some guidelines for minimizing blade loads in future CP propeller designs are presented in this section including consideration of the stern geometry, preliminary propeller design, detailed propeller blade design, the propulsion control system, and operating guidelines.

STERN GEOMETRY

Several variables relating to the stern geometry of a high-speed transient stern configuration with exposed struts and shafting have a significant influence on blade loads. However, these variables will be controlled by many criteria other than blade loads.

The general influence of the more important variables are as follows:

1. Number of propellers: for a given total delivered power and required thrust, increasing the number of propellers decreases the time-average loads per propeller. For all other parameters held constant, which is unrealistic, the number of propellers or time-average load per propeller does not have a first order influence on the periodic blade loads.

2. Inclination of the shaft: the periodic blade loads increase monotomically with the inclination of the shaft relative to the stern. The time-average loads are not sensitive to the shaft inclination. Therefore, from consideration of blade loads, the inclination of the shaft to the stern should be minimized. Decreasing the shaft inclination may result in reduced tip clearances which tend to increase the propeller-induced periodic forces on the hull.

PRELIMINARY PROPELLER DESIGN

Variables set in the preliminary design of the propeller, such as propeller diameter D, rotational speed n, and number of blades Z may have a significant influence on blade loads. However, these variables will be controlled by many criteria other than blade load.

The general influence of the more important variables are as follows:

1. Diameter D: reducing the diameter reduces the moment arms to the hub and, thereby, reduces the bending moments.

2. Number of blades Z: increasing the number of blades reduces the time-average and periodic loads per blade. However, this advantage tends to be offset by the reduced space per blade on and inside the hub.

3. Pitch-diameter ratio P/D (controlled by the rotational speed and diameter): lower values of P/D tend to reduce the time-average transverse force per unit of thrust, and, thereby, reduce the time-average blade bending moments for a given thrust. Changing values of P/D changes several factors such as rotational speed and blade pitch angle, which influence periodic blade loads in different ways; therefore, it is difficult to generalize on the influence of P/D on periodic blade loads.

DETAILED PROPELLER BLADE DESIGN

Once the preliminary design of the propeller is completed, so that the propeller diameter D, rotational speed n, and number of blades Z are fixed, there is relatively little that the designer of the propeller can do to minimize blade loads, with the exception of the M_z component.

Specific recommendations are as follows:

1. Use balanced skew (skew forward at the inner radii and skew back at the outer radii) and forward rake.[49-54] This is desirable from consideration of bending moments due to centrifugal and gravitational forces as discussed previously. Balanced skew is also highly desirable for producing a small time-average blade spindle torque.[53] With proper selection of skew and rake, the net time-average spindle torque M_z arising from hydrodynamic and centrifugal loads can be made vanishingly small under steady-ahead operation in a calm sea. Skew also has advantages unrelated to blade loading,[55-61] such as reduced propeller-induced unsteady hull forces, reduced blade frequency bearing forces and moments, and improved

226

cavitation performance. However, practical amounts of skew do not measurably reduce the periodic hydrodynamic blade loads arising from the inclination of the flow.

2. Unload the blade tips. This moves the radial centers of the time-average hydrodynamic loads closer to the hub and, thereby, reduces the moment arms and moments in the hub. This may reduce the time-average moments by approximately eight percent relative to an optimum radial distribution of loading. Unloading the blade tips has other advantages unrelated to blade loading, such as reducing propeller-induced unsteady hull forces and suppressing tip vortex cavitation.[55-57]

PROPULSION CONTROL SYSTEM

The propulsion control system of a gas turbine powered ship has a dominant influence on the propeller blade loads during maneuvers including accelerations, decelerations, and turning maneuvers. The propulsion control system controls the variation of the propeller rotational speed and pitch during a maneuver and may limit the maximum time-average torque per revolution to the propeller. Further, during turning maneuvers, the propulsion control system may control the different propellers of a multipropeller ship independently from one another.

A computer dynamic simulation of the complete propulsion system and ship response is an effective tool for establishing control system characteristics to obtain a good balance between values of peak propeller blade loads in maneuvers and ship maneuvering characteristics. Work of this nature is underway in an attempt to reduce the maximum transient propeller blade loads likely to be encountered during maneuvers on the SPRUANCE without significantly reducing the performance of the SPRUANCE.*

Therefore, it is recommended that for future CP propellers the propulsion control system be designed with the aid of computer dynamic simulations and the associated supporting model experiments in an attempt to obtain the optimum balance between minimizing the values of peak propeller blade loads in maneuvers and superior ship maneuvering characteristics.

OPERATING GUIDELINES

In addition to the automated operating conditions during maneuvers, which are controlled by the propulsion control system as discussed in the preceding section,

---

*By Propulsion Dynamics, Inc.

there are manually controlled operating conditions which may have a large influence on propeller blade loads. One important example of this is voluntary speed reduction (power reduction) for operation in rough seas. The transient and periodic blade loads in rough seas vary approximately in proportion to the square of the propeller rotational speed. Therefore, it is recommended that guidance be provided to shipboard personnel regarding manually controlled operating conditions which have a significant influence on propeller blade loads.

SUMMARY

Some guidelines for minimizing blade loads in future CP propeller designs were presented in this section including consideration of the stern geometry, preliminary propeller design, detailed propeller blade design, the propulsion control system, and operating guidelines.

RECOMMENDATIONS

1. The blade pressure and strain data obtained on the full-scale CP propeller trials described in Chapter II should be more completely reduced and analyzed. These data should be correlated with the pertinent results from model experiments and theory. If these correlations reveal specific deficiencies in the prediction methods, then further refinements to these prediction methods should be undertaken.

2. The model experimental blade surface pressures and field point velocities should be correlated with theoretical predictions using the method of Kerwin. If these correlations reveal specific deficiencies in the theory, then further refinements to the theory for predicting periodic propeller blade loads should be undertaken.

3. Blade loads should be predicted using the currently available methods, as described in this chapter, for the conditions for which the full-scale measurements were made on BARBEY, SPRUANCE, OLIVER HAZARD PERRY, and R/V ATHENA. These predicted loads should be correlated with the loads deduced from measurements made during these trials.

REFERENCES

1. Boswell, R.J. et al., "Experimental Determination of Mean and Unsteady Loads on a Model CP Propeller Blade for Various Simulated Modes of Ship Operation," The Eleventh Symposium on Naval Hydrodynamics, Sponsored Jointly by the Office of Naval Research and University College, London, Mechanical Engineering Publication Limited, London and New York, pp. 789-823, 832-834 (Apr 1976).

2. Boswell, R.J. et al., "Mean and Unsteady Loads on a CP Propeller Blade on a Model of the FF-1088 for Simulated Modes of Operation (U)," David W. Taylor Naval Ship Research and Development Center Report SPD-C-011-17 (Jun 1976) CONFIDENTIAL.

3. Boswell, R.J. et al., "Experimental Unsteady and Mean Loads on a CP Propeller Blade of the FF-1088 for Simulated Modes of Operation," DTNSRDC Report 76-0125 (Oct 1976).

4. Boswell, R.J. et al., "Experimental Time Average and Unsteady Loads on the Blades of a CP Propeller Behind a Model of the DD-963 Class Destroyer," presented at the Propellers 78 Symposium, The Society of Naval Architects and Marine Engineers, Publication S-6 (1978).

5. Boswell, R.J. et al., "Experimental Unsteady and Time-Average Loads on the Blades of the CP Propeller on a Model of the R/V ATHENA (PG-84 Class) for Simulated Modes of Operation," DTNSRDC Report 81/086 (in preparation).

6. Jessup, S.D. et al., "Experimental Unsteady and Time Average Loads on the Blades of the CP Propeller on a Model of the DD-963 Class Destroyer for Simulated Modes of Operation," DTNSRDC Report 77-0110 (Dec 1977).

7. Schwanecke, H. and R. Wereldsma, "Strength of Propellers Considering Steady and Unsteady Shaft and Blade Forces, Stationary and Nonstationary Environmental Conditions," Proceedings of the Thirteenth International Towing Tank Conference, Report of the Propeller Committee, Appendix 2B, Vol. 2 (1972).

8. Rusetskiy, A.A., "Hydrodynamics of Controllable Pitch Propellers," Shipbuilding Publishing House, Leningrad (1968).

9. Hawdon, L. et al., "The Analysis of Controllable-Pitch Propeller Characteristics at Off-Design Conditions," Transactions of the Institute of Marine Engineers, Vol. 88 (1976).

10. Angelo, J.J. et al., "U.S. Navy Controllable Pitch Propeller Programs," presented at a Joint Session of the Chesapeake Section of the Society of Naval Architects and Marine Engineers and the Flagship Section of the American Society of Naval Engineers, Bethesda, Maryland (19 Apr 1977).

11. Tsakonas, S. et al., "Documentation of a Computer Program for the Pressure Distribution, Forces and Moments on Ship Propellers in Hull Wakes," (in four volumes), Stevens Institute of Technology, Davidson Laboratory Report SIT-DL-76-1863 (Jan 1976). Revised (Apr 1977).

12. Tsakonas, S. et al., "An Exact Linear Lifting Surface Theory for Marine Propeller in a Nonuniform Flow Field," Journal of Ship Research, Vol. 17, No. 4, pp. 196-207 (Dec 1974).

13. Valentine, D.T., "Linearized Unsteady Lifting Surface Theory of a Lightly Loaded Propeller in an Inclined Flow," Stevens Institute of Technology, Davidson Laboratory Report SIT-DL-79-9-2064 (Aug 1979).

14. Kerwin, J.E. and C.S. Lee, "Prediction of Steady and Unsteady Marine Propeller Performance by Numerical Lifting Surface Theory," Transactions of the Society of Naval Architects and Marine Engineers, Vol. 86, pp. 218-253 (1978).

15. Kerwin, J.E., "The Effect of Trailing Vortex Asymmetry on Unsteady Propeller Blade Forces," Massachusetts Institute of Technology Report on contract N0014-77-C-0810, MIT OSP 85871 (May 1979).

16. Boswell, R.J. and M.L. Miller, "Unsteady Propeller Loading - Measurement, Correlation with Theory, and Parametric Study," Naval Ship Research and Development Center Report 2625 (Oct 1968).

17. Schwanecke, H., "Comparative Calculations on Unsteady Propeller Blade Forces," Proceedings of the Fourteenth International Towing Tank Conference, Report of Propeller Committee, Appendix 4, Vol. 3, pp. 357-397 (1975).

18. Breslin, J.P., "Propeller Excitation Theory," Proceedings of the Thirteenth International Towing Tank Conference, Report of the Propeller Committee, Appendix 2c, Vol. 2, pp. 527-540 (1972).

19. McCarthy, J.H., "On the Calculation of Thrust and Torque Fluctuations of Propellers in Nonuniform Wake Flow," David Taylor Model Basin Report 1533 (Oct 1961).

230

20. Boswell, R.J. and S.D. Jessup, "Experimental Determination of Periodic Propeller Blade Loads in a Towing Tank," Presented to the 18th American Towing Tank Conference, U.S. Naval Academy, Annapolis, Maryland (Aug 1977).

21. Jessup, S.D. and R.J. Boswell, "Experimental Unsteady and Time-Average Loads on the Blades of DTNSRDC Propellers 4402 and 4661 Operating in Simulated Tangential Longitudinal Wakes," DTNSRDC Report 81/085 (Nov 1981).

22. Boswell, R.J. et al., "Single Blade Loads on Propellers in Inclined and Axial Flows," DTNSRDC Report 81/034 (in preparation).

23. Boswell, R.J. et al., "Periodic Single-Blade Loads on Propellers in Tangential and Longitudinal Wakes," Propellers 81 Symposium, the Society of Naval Architects and Marine Engineers Publication S-7, pp. 181-202 (May 1981); DTNSRDC Report 81/054 (Jun 1981).

24. Kim, K.-H., "Unsteady Blade Loads on Propellers Behind High Speed Hulls with Transom Sterns," ORI, Inc. Technical Report 1866 (Feb 1981).

25. Boswell, R.J., "Exploratory Measurements of the Pressure Distribution on DTNSRDC Model Controllable Pitch Propeller 4679," DTNSRDC Report SPD-0834-01 (in preparation).

26. Jessup, S.D., "Measurement of the Pressure Distribution on Two Model Propellers," DTNSRDC Report 81/080 (in preparation).

27. Santelli, N. et al., "Experimental Determination of Two Components of Field Point Velocities Around a Model Propeller in Uniform and Inclined Flow," DTNSRDC Report SPD-0921-01 (Feb 1980).

28. Reed, A.M. and W.G. Day, "Wake Scale Effects on a Twin Screw Displacement Ship," Twelfth ONR Symposium on Naval Hydromechanics, Washington, D.C. (Jun 1978).

29. Reed, A.M. and W.G. Day, "Full-Scale Propeller Disk Wake Survey and Boundary Layer Velocity Propeller Measurements on the 154-Foot Ship R/V ATHENA," DTNSRDC Report SPD-0833-01 (in preparation).

30. Hurwitz, R.B. and L.B. Crook, "Analysis of Wake Survey Experimental Data for Model 5365 Representing the R/V ATHENA in the DTNSRDC Towing Tank," DTNSRDC Report SPD-0833-04 (Oct 1980).

31. Crook, L.B., "Powering Predictions for the R/V ATHENA (PG 94) Represented by 'odel 4950-1 with Design Propellers 4710 and 4711," DTNSRDC Report SPD-0833-05 (Jan 1981).

32. Hurwitz, R.B. and L.B. Crook, "Analysis of Wake Survey Experimental Data for Model 5365 Representing the R/V ATHENA with and without the BASS Dynamometer Boat," DTNSRDC Report SPD-0833-06 (Jan 1981).

33. Tasaki, R., "Propulsion Factors and Fluctuating Propeller Loads in Waves," Proceedings of the Fourteenth International Towing Tank Conference, Report of Seakeeping Committee, Appendix 7, Vol. 4, pp. 224-236 (1975).

34. "Report of the Seakeeping Committee," Edited by M.W.C. Oosterveld, Fifteenth International Towing Tank Conference, The Netherlands Ship Model Basin, Wageningen, pp. 55-114 (1978).

35. Day, W.G. et al., "Experimental and Prediction Techniques for Estimating Added Power Requirements in a Seaway," Proceeding of the Eighteenth American Towing Tank Conference, U.S. Naval Academy, Annapolis, Maryland, Vol. I, pp. 121-141 (1977).

36. Lloyd, A.R.J.M. and R.N. Andrew, "Criteria of Ship Speed in Rough Weather," Proceedings of the Eighteenth American Towing Tank Conference, U.S. Naval Academy, Annapolis, Maryland, Vol. II, pp. 541-565 (1977).

37. Day, W.G., "Propeller Disk Wake Survey Data for Model 4989 Representing the FF-1052 Class Ship in a Turn and with a BASS Dynamometer Boat," DTNSRDC Report SPD-0011-21 (Dec 1980).

38. Remmers, D.D. and A.L. Hendrican, "Analyses of Wake Surveys in the Port Propeller Plane During Starboard and Port Turns for the DDG-47 Class Destroyer Represented by odel 5265-1B (U)," DTNSRDC Report SPD-C-558-05 (Jun 1976) CONFIDENTIAL.

39. Rubis, C.J., "Acceleration and Steady State Propulsion Dynamics of a Gas Turbine Ship with Controllable-Pitch Propeller," Transactions of the Society of Naval Architects and Marine Engineers," Vol. 80, pp. 329-360 (1972).

40. Rubis, C.J., "CRP Propeller Ship-Propulsion Dynamics," DTNSRDC Report 3238 (Feb 1971).

41. Rubis, C.J. and T.R. Harper, "Propulsion Dynamics Simulation of the DD-963 Class Destroyer," Propulsion Dynamics, Inc. Report 74RDIB (Jan 1975).

42. Rubis, C.J. and T.R. Harper, "Gas Turbine Ship Propulsion Control Systems Research, Phase I," Propulsion Dynamics, Inc. Report 443-1, Vol. II, Propulsion and Control System Dynamics (Oct 1977).

43. Rubis, C.J. and T.R. Harper, "Reversing Dynamics of a Gas Turbine Ship with Controllable-Pitch Propeller," Proceedings of the Fifth Ship Control Systems Symposium, Sponsored by DTNSRDC, Annapolis, Maryland (Oct-Nov 1978).

44. Abkowitz, M.A., "Stability and Motion Control of Ocean Vehicles," The MIT Press (1972).

45. "A Digital Computer Technique for Prediction of Standard Maneuvers of Surface Ships," DTMB Report 2130 (Dec 1965).

46. Carroll, L.C. and T.R. Harper, "DD-963 Class Destroyer Four Degree-of-Freedom Maneuvering Simulation," Propulsion Dynamics, Inc. Report 4443-3 (Jul 1979).

47. McCarthy, J.H. et al., "The Performance of a Fully Submerged Propeller in Regular Waves," David Taylor Model Basin Report 1440 (May 1961).

48. Lewis, E.V., "Motion of Ships in Waves," Chapter IX, Principles of Naval Architecture, Edited by J.P. Comstock, The Society of Naval Architects and Marine Engineers, pp. 607-717 (1967).

49. Themak, H. et al., "Hydrodynamic Design of a Controllable-Pitch Propeller for the Patrol Frigate (U)," DTNSRDC Report SPD-C-495-H-16 (Apr 1974) CONFIDENTIAL.

50. Denny, S.B. et al., "Hydrodynamic Design Considerations for the Controllable-Pitch Propeller for the Guided Missile Frigate," Naval Engineers Journal, pp. 72-81 (Apr 1975).

51. Bjorheden, O., "Highly Skewed Controllable Pitch Propeller," 73rd Annual Meeting of the German Ship Technical Society, STG, Berlin, Germany (Nov 1978).

52. Salminen, R. and M. Kanewa, "Design of Baltic Ferries for the Eighties, Propeller and Aft End Vibrations," Propellers 81 Symposium, the Society of Naval Architects and Marine Engineers, Publication S-7, pp. 67-92 (May 1981).

53. Boswell, R.J. and G.P. Platzer, "The Design of the Blades of a Controllable-Pitch Propeller for a Dock Landing Ship (LSD-41) (U)," DTNSRDC Report SPD-0049-07 (Sep 1978) CONFIDENTIAL.

54. Boswell, R.J. et al., "Experimental Spindle Torque and Open-Water Performance of Two Skewed Controllable-Pitch Propellers," DTNSRDC Report 4753 (Dec 1975).

55. Cumming, R.A. et al., "Highly Skewed Propellers," Transactions of the Society of Naval Architects and Marine Engineers, Vol. 80 (1972).

56. Cox, G.G. and W.B. Morgan, "The Use of Theory in Propeller Design," Marine Technology, Vol. 9, No. 4, pp. 419-429 (Oct 1972).

57. Boswell, R.J. and G.G. Cox, "Design and Model Evaluation of a Highly-Skewed Propeller for a Cargo Ship," Marine Technology, Vol. 11, No. 1, pp. 73-89 (Jan 1974).

58. Teel, S.S. and S.B. Denny, "Field Point Pressures in the Vicinity of a Series of Skewed Marine Propellers," NSRDC Report 3278 (Aug 1970).

59. Hammer, N.O. and L.F. McGinn, "Highly-Skewed Propellers - Full-Scale Vibration Test Results and Economic Considerations," Ship Vibration Symposium, SNAME, Publication SY-8, pp. R-1 to R-41 (1978).

60. Kerwin, J.E. et al., "Systematic Experiments to Determine the Influence of Skew and Rake on Hull Vibratory Excitation Due to Transient Cavitation," Ship Vibration Symposium, SNAME Publication SY-8, pp. Q-1 to Q-18 (1978).

61. Bjorheden, O., "Vibration Performance of Highly Skewed CP Propellers," Proceedings of the Symposium on Propeller Induced Ship Vibration, The Royal Institute of Naval Architects, London, England, pp. 103-119 (Dec 1979).

CHAPTER IV

MATERIALS

TABLE OF CONTENTS

Page

235

LIST OF FIGURES

LIST OF TABLES

INTRODUCTION

Damage and failure of critical components have occurred during the service experience with high horsepower controllable pitch (CP) propeller systems in both merchant and naval service. Although serious failures have been considered to be design rather than material problems, in many instances the selection of more suitable materials for the components might have precluded failures. In order to provide a reliable CP propeller blade attachment with low maintenance requirements, it is necessary to select optimum materials and to base the design on the characteristics of the selected materials in their operational environment. The general objective for this section is to provide a summary of investigations of materials for the various components of CP propeller blade attachments following the failure of the BARBEY CP propeller. The optimum materials to provide strength, ductility, fracture toughness, fatigue, corrosion fatigue, and stress-corrosion cracking resistance in the various CP propeller components were considered. In addition, the various aspects of corrosion resistance, mechanical and galvanic compatibility, and bearing integrity in the complex CP propeller mechanism were addressed.

A review of the various types of damage and failures which have occurred in CP propeller development and service was undertaken[1]* to determine materials related problems and their extent. The results of that review are summarized in the following. The majority of CP propeller installations in either merchant or naval service are designed and built by several firms in Western Europe and Scandinavia, licensee's of these firms, or developments from their designs. Thus, the database related to operational experience of CP propeller systems was primarily gathered from these sources, and from a European classification society, Det Norske Veritas (DNV), which continually examines surveyors reports in a statistical manner searching for problem areas. Experience in the U.S. Navy and Royal Navy with CP propeller systems was also reviewed.

In general, the majority of the problems occurred in the control and hydraulic systems. Except for the consideration of the effects of sea water intrusion into the hub, these problems were not materials related or of consequence to the strength or integrity of the propeller. Failures which involved cracking, fracture, or

---

*A complete listing of references is given on page 319.

240

deterioration in vital parts of the CP propeller system (blades, hub, blade bolts, crank disks or rings, and bearings) were reviewed, because these were important in setting material selection criteria.

MERCHANT SERVICE CONTROLLABLE PITCH PROPELLER DAMAGE EXPERIENCE

Several thousand CP propeller installations have been or are regularly in merchant service in plants of less than 5000 shp, and experience with these plants provided the bulk of reliability failure statistics. The development and use of larger power CP propeller installations (5000 to 20,000 shp) in merchant service dramatically increased in the past decade and patterned the experience with the smaller plants as outlined in the following:

1. Propeller blade cracking and failure by fatigue in blade bolt holes, blade palm, and blade roots were the most significant and prevalent problems.

2. As design and service experience within a power range grew, hub and blade attachment damages (i.e., crank rings and disks, blade carriers, blade bolts, bearings) decreased; but blade failure problems did not.

3. Initial damage incidents and failures increased rapidly with increasing horsepower.

4. Hub and blade attachment damages were considered in retrospect to be design related; over-stressed and insufficient material girth.

It should be noted that a majority of the blade failures in merchant service were in cast stainless steel alloy blades. The propeller blade failures were primarily material problems; where material soundness (production process), repair procedures, quality control and inspection were unsatisfactory. Controllable pitch propeller blade failure rates were similar to blade failure incident rates in fixed-pitch propellers of the same material.

Blade bolt fatigue failures were attributed to lack of proper preload in assembly unless occurring with other damages which indicated a marginal design. In some highly loaded merchant ship CP propeller systems, broken blade bolts, fatigue cracking in crank rings, and wear in bearings all resulted from inadequate design against cyclic load. The practice by some manufacturers of protecting highly stressed internal parts from corrosion indicated that leakage and sea water intrusion have occurred and cause concern.

NAVAL SERVICE CONTROLLABLE PITCH PROPELLER DAMAGE EXPERIENCE

The U.S. Navy has had experience with CP propeller installations for many years, but that experience was with plants under 8000 shp until the development of the 35,000 to 40,000 shp plants for USS BARBEY (FF-1088), USS PATTERSON (FF-1061), and the current gas-turbine powered frigates and destroyers.[2,3*] A reliability study[4] of the smaller CP propeller systems indicated that hydraulic systems and control systems were the prevalent problem areas.

The first true class of high-speed warships with CP propellers in the U.S. Navy was the gas-turbine powered USS ASHEVILLE (PG-84) Class patrol gunboat (6650 shp). This class of vessels experienced extensive propeller blade failures (fracture and cracking) in early service when cast titanium alloy blades were used. The blade material was changed to stainless steel and no more blade problems were experienced.

The subject research and development program was undertaken after serious failures occurred in the BARBEY CP propeller system and the adequacy of the CP propellers for the USS SPRUANCE (DD-963) and USS OLIVER HAZARD PERRY (FFG-7) classes was questioned.[2,3] Briefly, the CP propeller blade attachment of BARBEY suffered two failures after short service. The blade bolts failed by fatigue in the first casualty, initially thought to be due to insufficient preload. In the second casualty, the crank disks which hold the blades in the hub all failed in catastrophic brittle fracture. A fatigue crack which had propagated from an internal bolt hole was identified in the crank disk remnants. Concern was also focused on bearing performance because bearing distress in the form of bronze transfer from the bearing ring to the steel crank ring bearing surface was observed on inspection of the SPRUANCE and BARBEY crank rings after laboratory tests and instrumented sea trials. Similar observations have been made on inspections of crank rings in USS NEWPORT (LST-1179) class CP propellers.[4]

The service experience in major allied warships involves CP propellers of less than 30,000 shp and no blade attachment failures are known.

MATERIAL PROBLEM AREAS FOR INVESTIGATION

The prevalent mode of failure and damage influencing the strength of the CP propeller blade attachment has been fatigue or corrosion fatigue cracking in the

---

*These propellers also required an increase in the number of blades from 4 to 5 resulting in a more difficult blade attachment design.

blade, hub, blade bolts, and blade carriers of high power installations or those
inadequately designed against dynamic loading. When increased power is required,
the higher loads must be borne by the options of increased hub size or the use of
higher strength materials. The former results in a propeller weight increase as
well as decreased propulsive efficiency; however, the latter option must be ap-
proached with caution. Careful detailed design analyses and material selection are
required because high strength alloys are typically more notch sensitive, lower in
toughness and ductility, and not proportionately higher in fatigue strength. The
material selection problem is further complicated by the consideration of seawater
intrusion into highly-stressed areas of the CP propeller mechanism.

The following components are the major problem areas where material selection
and properties required investigation.

Blade and Hub Materials

The U.S. Navy has had no problems with the cast nickel-aluminum (Ni-Al) bronze
(MIL-B-21230) Alloy 1 used exclusively for large ship propellers including CP
propellers; but some problems have occurred in commercial fixed-pitch and CP pro-
pellers where other alloys are typically used. The selection of this alloy was
examined with regard to failure experience, mechanical properties, fatigue charac-
teristics, and welding repair procedures in comparison with other propeller alloys.

Blade Carrier Materials

The crank rings, disks, or trunnions which change pitch and carry the blade
have suffered fatigue, corrosion fatigue, and brittle fracture. For these critical
hub internals, material selection was examined with regard to toughness criteria
for high strength crank ring forgings and the improvement of corrosion fatigue
resistance. The properties of inherently corrosion-resistant alloys as candidates
for blade carrier applications were also investigated.

Blade Bolt Materials

Blade bolts typically fail from fatigue or corrosion fatigue. Because total
elimination of cyclic loading and seawater at the bolt attachment may not be
practically achievable, bolts of corrosion-resistant alloys and of fatigue-resistant

geometries and processing were investigated. The galvanic compatibility of exposed
blade bolt alloy with the blade and hub material, and the frictional characteristics
of the blade bolt-crank ring threaded joints (mechanical compatibility) were also
investigated.

Pitch Change Bearing Materials

Bearing distress in the form of bronze transfer from hub or bearing ring onto
steel crank ring surfaces has been observed in highly loaded CP propellers. Design
data on the friction and wear characteristics of material combinations under the
high load and low speed bearing of the pitch change mechanism were developed.

BLADE AND HUB MATERIALS

The review of CP propeller damage and failure experience indicated that few
blade or hub problems had occurred with the cast Ni-Al bronze; the alloy which is
used by the Navy for large propellers. An investigation[5] of the problem area was
undertaken, however, based on the prevalent failures in other alloys. These fail-
ures were primarily due to fatigue cracking, either from stress raisers (blade bolt
holes, hub bridge, etc.) or improper weld repairs in cast stainless steels and
manganese-aluminum (Mn-Al) bronzes which are higher in strength than Ni-Al bronze.
The results of the study concerning three areas relevant to the development of larger,
high-power CP propellers are summarized briefly in this section. These areas are (1)
higher strength propeller alloys, (2) corrosion fatigue strength and fatigue notch
sensitivity of Ni-Al bronze, and (3) weld repair procedures for Ni-Al bronze com-
pared to the other alloys.

PROPELLER ALLOYS

The alloys most widely used for large, fixed-pitch ship propellers worldwide
are three copper base alloys: Mn bronze; Ni-Al bronze; and Mn-Al bronze. As
copper-base alloys they have moderate melting temperatures, beneficial in terms of
cost and difficulty of producing large castings; good machinability; fair corrosion
resistance; and inherent resistance to fouling by marine organisms. Because of the
higher mechanical properties of the two Al bronze alloys, they are used in about
three-quarters of the current marine propeller production.[6] The case for CP propeller

hubs and blades, however, is quite the opposite. A majority of the CP propeller installations in worldwide service have blades and hubs of cast stainless steels.[5] Primarily the 13 percent chromium (Cr) type alloys are used which require hardening and tempering heat treatments. The casting of single blades and seperate hub boss does not involve pouring large tonnage heats nor the cracking and distortion problems which would be present in producing a monobloc propeller the same diameter as a CP propeller. As previously noted, the majority of CP propeller installations in service are built by firms in Western Europe and Scandinavia where steel founders are predominant.

Blade failure was the most common failure mode in these CP propellers, usually resulting from improper weld repair and postweld heat treatment. Crevice corrosion problems have also been encountered in CP propellers made of various compositions of stainless steels.[7] Had local economics not dictated the material selection it is expected that bronzes would have been used and these problems minimized. Adequate crevice corrosion, corrosion fatigue, and stress corrosion crack initiation resistance in cast stainless steel propellers is provided by a well-maintained cathodic protection system in the propeller vicinity.

In summary, cast stainless steels may be attractive alloys for large, high power CP propeller blades and hubs, but the following must be recognized:

1. The risk of high distortion and cracking increase with casting size and thickness;

2. Heat treatment, hardening and tempering, or solution annealing and quenching of the casting is required to attain required properties;

3. Resistance to pitting corrosion, crevice corrosion, corrosion fatigue, and stress corrosion crack initiation require an effective cathodic protection system with the propeller as cathode;

4. Either stress relief or full heat treatment is required after weld repair depending on extent of repair (faulty repairs and lack of proper heat treatment were the primary cause of blade failure).

Both Ni-Al bronze and Mn-Al bronze are used in large, high-power CP propellers in both merchant and naval service. Performance has been satisfactory as might be expected from their successful experience in fixed-pitch propellers. Although Mn-Al bronze has better castability, strength, and weldability; it has some

susceptibility to stress corrosion cracking so that stress relief is required after straightening operations and weld repair, and corrosion fatigue properties are lower than Ni-Al bronze. Ni-Al bronze is not susceptible to stress corrosion; and stress relief heat treatment is not required, resulting in reduced maintenance costs.

An example of poor material selection resulting in CP propeller blade failures was that of the early USS ASHEVILLE (PG-84) Class gunboats of the USN. These were the first Navy warships using a combined diesel or gas turbine powerplant. The original propeller material was cast titanium alloy (Ti-6Al-4V) to take advantage of that material's superior corrosion and cavitation-erosion resistance, high strength (over 100,000 psi yield strength), and lower density. The first two vessels were so equipped. After 743 hours of operation, PG-84 had a propeller blade failure; Figure 1. Subsequent analysis concluded that the failure, cracks on other blades, and cracks on the sister ship's blades, USS GALLUP (PG-85), originated at defective casting repairs.[8] The castings contained numerous sharp defects; inclusions, porosity, shrinkage cavities; and were high in oxygen content rendering them unweldable. The repairs which were made contaminated (embrittled) the material, and the high residual stresses developed the cracks. These extended by stress corrosion cracking and fatigue . Stress-corrosion resistance, fatigue strength, and impact toughness are very low in high oxygen cast titanium alloys.[8] Thus, cast titanium alloy had been selected for the service without sufficient recognition of the engineering properties of the material.

Patrol gunboats PG-84 to PG-101 were subsequently fitted with cast CF-8M stainless steel blades (20Cr-10Ni austenic stainless steel) of lower design stress and larger section. Two ship sets of forged Inconel 625, Ni-Cr-Mo alloy were fitted on PG-94 and PG-100 in 1971 for increased performance (higher design stress) and are still in service on the R/V ATHENA I (ex-PG-94) and R/V ATHENA III (ex-PG-100).

CORROSION FATIGUE AND FATIGUE NOTCH SENSITIVITY

The problems of propeller blade unsteady loading, cavitation, and erosion exist for both fixed-pitch and CP propellers, but are amplified for the latter.[9] In general, the blade shapes are wide in the tip region and narrow at the root with thick blade root sections for strength purposes. The combination of small blade chord and large blade root thickness produces blade root sections with high thickness-to-chord ratios which are subject to cavitation and erosion. Controllable

Figure 1 - Failed Port Propeller Blade of USS GALLUP (PG-85)

pitch propeller installations in high speed ships are generally at a sizable shaft angle, and this angle, plus the hull slope in the region of the propeller, produces considerable upwash in the inflow to the propeller plane. The result of these factors is a tendency to vary blade loading considerably during a propeller revolution, i.e., large unsteady blade loads.[10] Thus, from the standpoints of vibration, blade stress, and fatigue, CP propeller blades and hubs for high-speed hull forms are at a distinct disadvantage.

Fatigue cracking has been experienced in the hub bridge area[1] and the Det Norske Veritas "Guidance Manual for Inspection and Repair of Steel Propellers," Reference 11, assigns this area a "Severity Zone A"; highest in degree of harmfulness of defects; in recognition of the high state of stress in that area. Because CP propeller blade shapes must reduce to narrow width and necessarily thick root sections for which large blade fillets are required blade attachment may require bolt hole recesses which cut into the blade root fillet. Controllable pitch propeller blades have experienced fatigue cracking in the bolt hole recesses, the area between bolt holes, and the blade fillet where bolt holes penetrate, but cracks in the bolt hole recess are most common.[1,5] These usually occurred where the fillet of the recess was too small in radius; however, in highly stressed designs, cracks have occurred in the walls between the bolt holes. In recognition of the criticality of the blade flange, Reference 11 also assigns the flange "Severity Zone A."

No failures have been experienced in the screwed-in blade attachment used in the Navy, but the only high power version (PATTERSON, 35,000 shp) saw only 6500 hours of service.[2] Subsequent analysis of the blade attachment using improved loads definition concluded that the blade attachment had a limited fatigue life with possible failure in the Ni-Al bronze buttress thread.[12]

Fatigue tests of cast Ni-Al bronze conducted by the Center[13] and by the LaQue Center for Corrosion Technology[14] used similar procedures and tests of rotating cantilever-beam fatigue specimens. Specimens with weldments in the tapered test length or with a circumferential V-notch in a uniform test length were included. The source materials were cast plates, bars, or blocks of several hundred pounds. Included for comparison in the present were specimens removed from the CP propeller hub which had been removed after service on the PATTERSON.[5]

The results for smooth bar tests in air, seawater, and Severn River water are given in Figure 2. Note the reduction in fatigue strength due to the saltwater
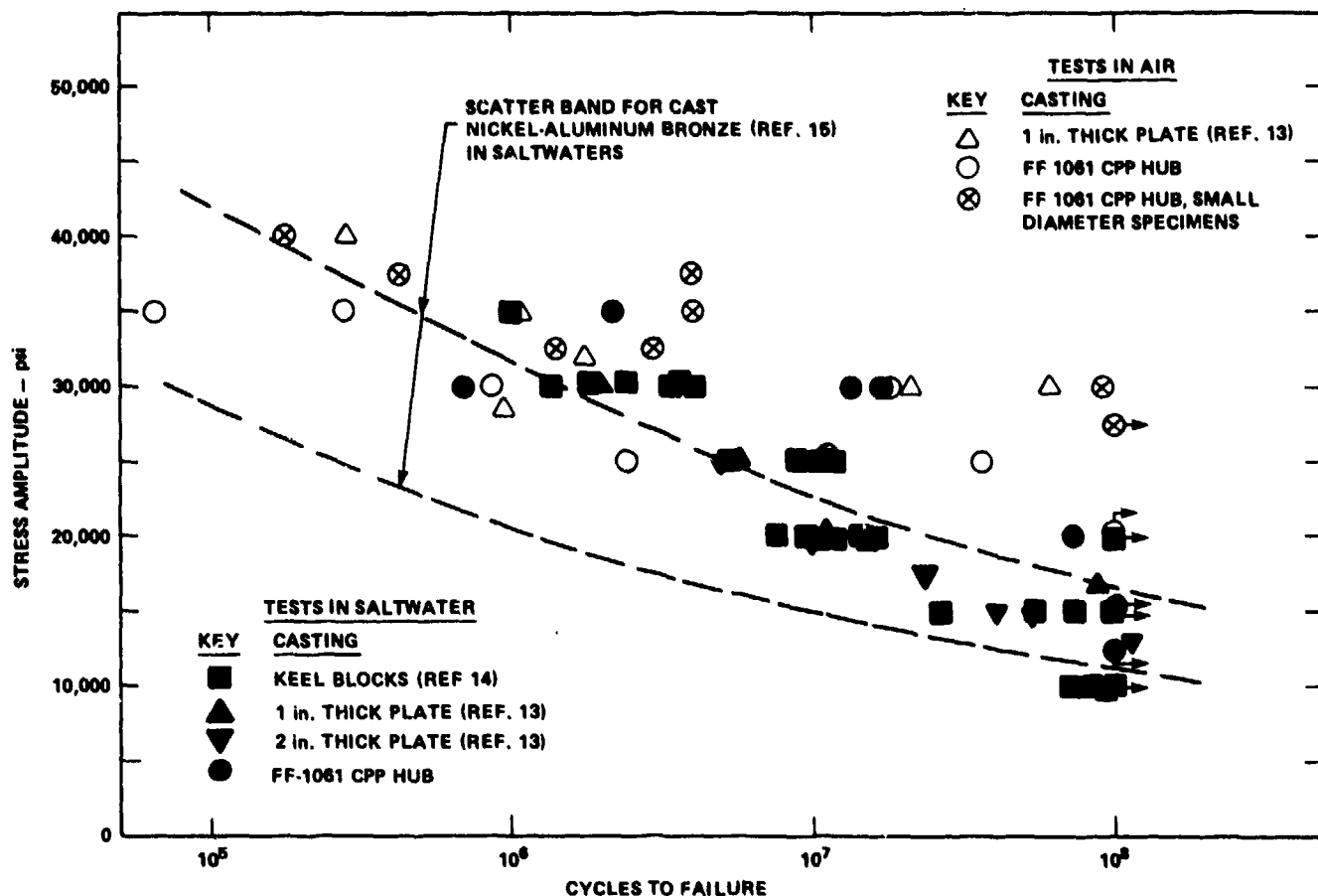
Figure 2 – Rotating Beam Fatigue Test Results for Smooth Specimens
of Cast Nickel-Aluminum Bronze (MIL-B-21230A, Alloy 1)

environments. The effects of weldments and notches are given in Figures 3 and 4, respectively. In Figures 2 through 4, the results are compared to the scatter band for results of a comprehensive "state-of-the-art" report[15] in which all available fatigue information on cast propeller bronzes including Ni-Al bronze was gathered and reviewed. The results for weldments do not appear to be significantly different from the as-cast material. These results, demonstrated also by others,[6] might be anticipated because both are cast metal structures.

As shown in Figure 4, cast Ni-Al bronze is not very notch sensitive. For these tests, the results indicate a fatigue notch reduction factor of about 1.5 for a notch with a theoretical stress concentration factor of 3.0. Tests of small and large specimens of cast Ni-Al bronze with stress concentration factors[16] ranging

249
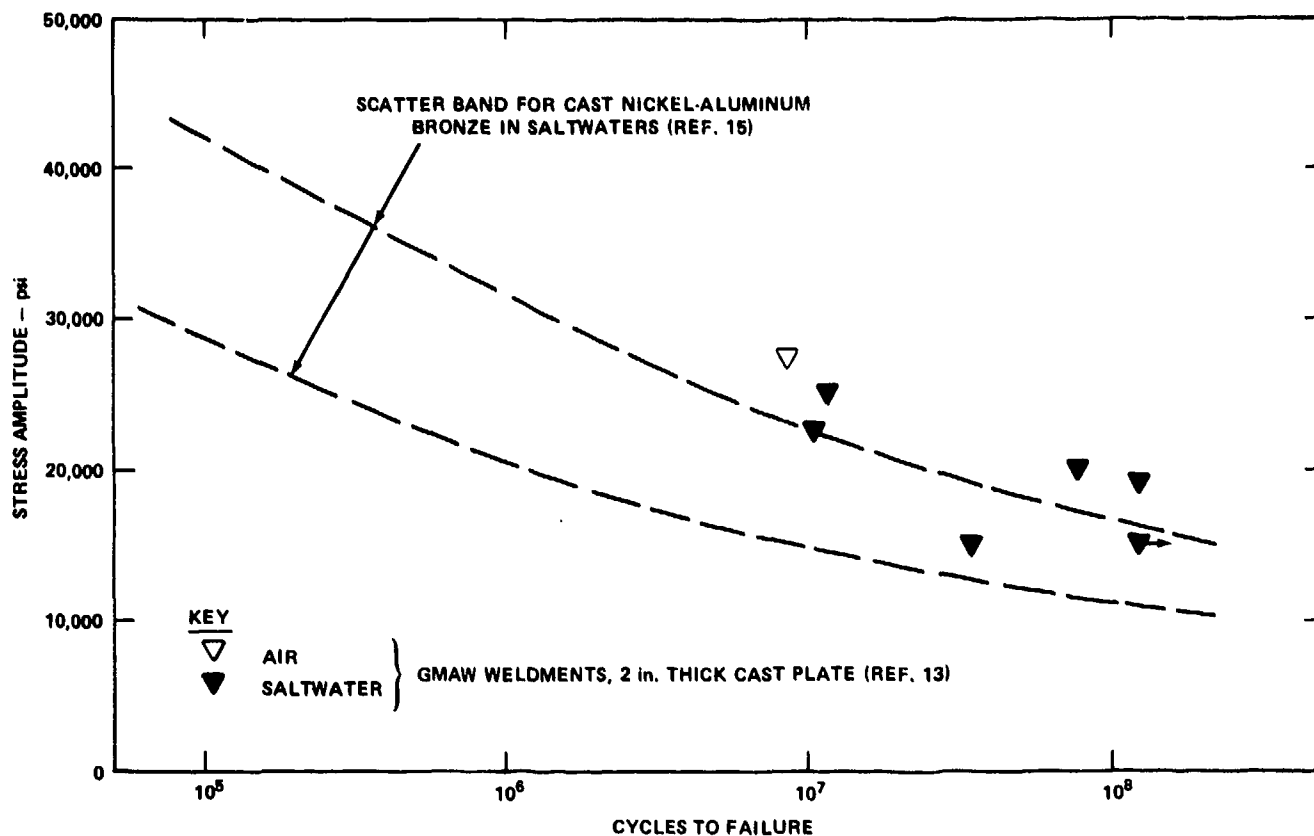
Figure 3 - Rotating Beam Fatigue Test Results for Smooth Specimens
of Welded Cast Nickel-Aluminum Bronze

from 2.5 to 9.7 showed that fatigue notch reduction factors were between 1.2 and 1.5, again demonstrating insensitivity to machined notches in a material inherently full of small, sharp defects.

It should be noted that in all cases the results of specimens removed from the CP propeller hub showed extreme scatter. Specimens containing large defects or porosity on the test section were rejected, but casting defects were noted on several specimen fractures. These defects, existing in a satisfactory casting proven in service, were more relevant to the fatigue life of a test specimen than were intentional machined notches.
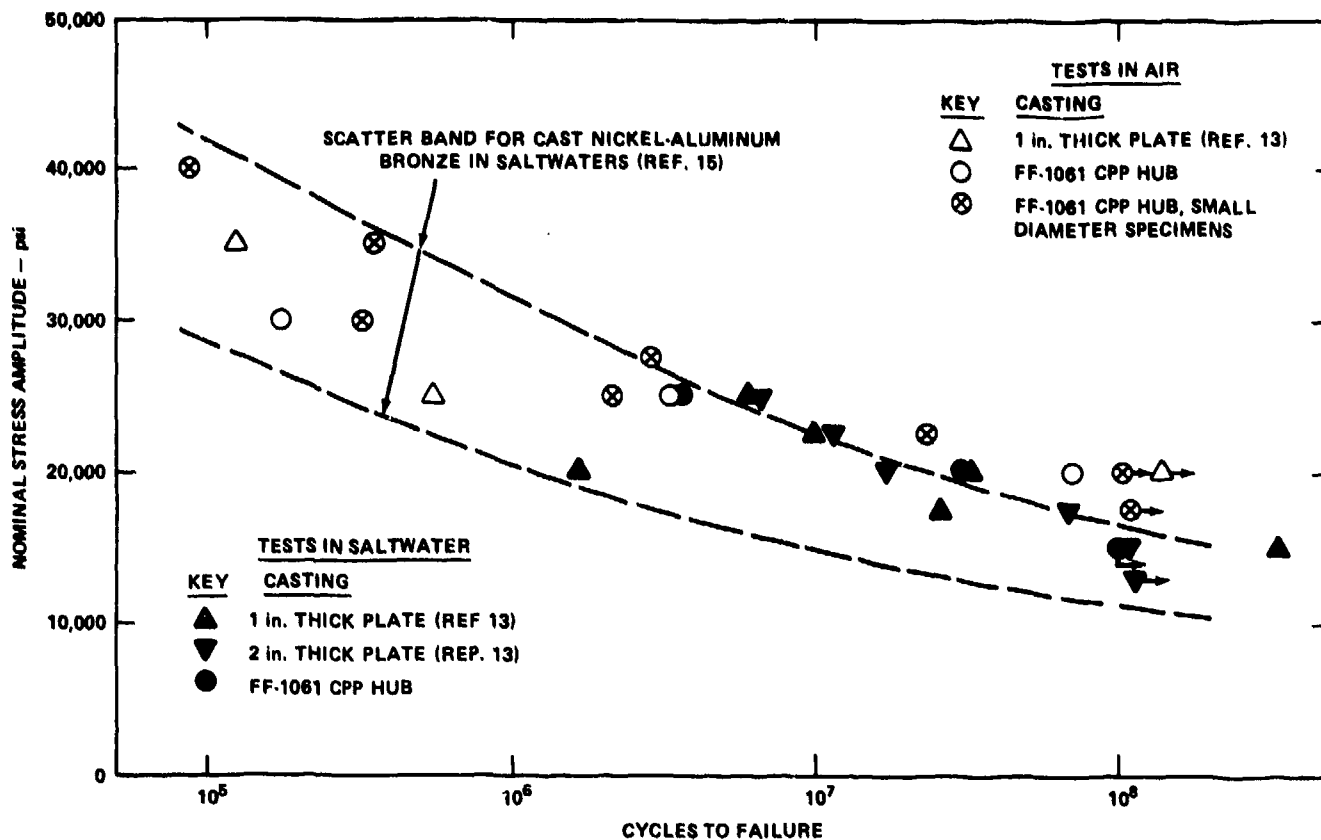
Figure 4 – Rotating Beam Fatigue Test Results for Notched (K_t=3) Specimens of Cast Nickel-Aluminum Bronze

In view of the insensitivity of cast Ni-Al bronze to notches in fatigue and the probability of porosity and defects in any massive casting, close attention to the design of fillet radii in bolt hole recess, blade fillet penetrations, etc., does not seem necessary beyond the prudent practice of avoiding sharp root radii.

REPAIRABILITY

Repairs to blades and hubs are necessary to rectify minor defects after casting or damage sustained in service from striking or cavitation erosion. These repairs consist of grinding, straightening, and welding. Repair by welding requires strict adherence to proper techniques and procedures specified by the Navy[17] and classification societies.[11,18-20] In all these documents, limitations are placed on the

251

extent of welding which may be performed in the critical zones of the propeller. These zones are where high mean and cyclic stresses occur in service: the blade area near the root, the blade flange, and the hub bridge. As previously noted, postweld stress relief heat treatment is essential for repairs in cast stainless steels, Mn bronze, and Mn-Al bronze to prevent local stress corrosion cracking which will subsequently grow by fatigue. Weld repairs in cast Ni-Al bronze are not required to be stress relieved for two reasons: (1) the alloy is immune to stress corrosion and (2) the alloy is hot short (has low ductility) in the temperature range 300°-500°C (570°-930°F).

Fatigue failures have occurred in service at repair welds in critical regions of Ni-Al bronze fixed pitch propellers and high residual welding stresses were suspect.[7] For repairs in the critical regions, it is recommended that postweld stress relief heat treatment be carried out after weld repairs to critical regions. Welding should be performed by the inert gas metal-arc (GMAW) process using matching electrodes. The welding parameters and procedures should be selected to minimize residual stresses, and finished welds should be smooth ground to eliminate stress raisers. The postweld heat treatment temperature must be above the hot short range, and heating up through the range must be as rapid as possible within the limits of good practice. Visual and dye penetrant inspections before and after the stress relief heat treatment are necessary.

Straightening of Ni-Al bronze propellers also requires attention to technique and temperature because of the hot short range. For minor straightening, temperatures must be below 200°C (400°F). Hot straightening requires that a temperature greater than 760°C (1400°F) be reached and maintained in the range 760°-950°C (1400°-1750°F) during the operation. The heat must be applied over a large area in the region to be plasticly bent during straightening by slowly applied uniform loading.

Although attention to procedures is necessary for effective repair of cast Ni-Al bronze propellers; in general, it is the good repairability which makes it the most attractive alloy for large propellers and CP propeller blades and hubs.

In summary, the investigation concluded that Ni-Al bronze is the optimum in presently available alloys for large U.S. Navy ship CP propeller blades and hubs. The castability; impact toughness; corrosion fatigue strength; insensitivity to notches; resistance to corrosion, stress corrosion, crevice corrosion, and cavitation

in seawater; repairability by welding without stress relief heat treatments for all but critical areas; and adequate strength render it less susceptible to the failure which have been experienced with other alloys in use. It is expected that Ni-Al bronze (MIL-B-21230, Alloy 1) will continue to be the sole propeller alloy for CP propeller blades and hubs in the near future.

BLADE CARRIER MATERIALS
(CRANK DISK, CRANK RING, TRUNNION)

The failure incident which precipitated the intensive Navy research and development program on CP propeller integrity was the previously noted catastrophic failure of the CP propeller of USS BARBEY (FF-1088). All five blades of the single screw installation, all bolts, and most of the crank disks were carried away. A metallurgical failure analysis[21] conducted on the remnants determined that the crank disks failed in brittle fracture. Laboratory tests of samples of the remnants verified the high strength but low fracture toughness of the crank ring material. Fatigue cracking from the internal thread at the blade bolt hole for the highest loaded bolt (near the trailing edge, pressure side) and in the crank disk fillet groove in that area was present in the Number 1 crank disk. Subsequent stress-measurement trials at sea[3] on BARBEY showed high mean and cyclic stress for the bolt and the fillet groove in that location (Bolt 6), especially during maneuvering.

Full-scale structural evaluation of the CP propeller blade attachment of SPRUANCE and PERRY Class installations was conducted as part of the R and D program in a laboratory test stand (Chapter V). During cyclic loading tests intended to determine the fatigue life of the bolts, a failure of the crank ring occurred after about one-million cycles. The failure was a result of fatigue initiating in the fillet groove at several locations near the highly loaded bolt (Bolt 8) on the pressure side and growing through to fracture. Within the Navy's experience, then, fatigue and fracture of crank rings and disks have occurred in high-powered CP propellers. Fatigue cracking in the fillet grooves of blade carriers (crank rings or disks) have also been experienced on merchant vessel CP propellers.[1] These primarily occurred in high-powered CP propellers where high loading was present and fillet radii were too small. In these cases, however, the maximum stresses in the component were low and fracture with loss of the blades did not occur.

The CP propeller designers, regardless of the pitch change mechanism used, generally provide a minimum working oil pressure in the hub cavity greater than the nominal external seawater pressure with the intent of preventing seawater leakage into the hub. Although extensive design measures to maintain the watertight integrity of the CP propellers hub are taken, instances of seawater intrusion into the system have occurred and have caused damages. Seawater or water-oil mixture not only causes corrosion of parts and accelerates wear, but also causes corrosion-fatigue cracking of unprotected steel blade carriers. Failures of crank rings and trunnions have occurred by corrosion fatigue where seawater has leaked into the hub.[1]

These three material problems: brittle fracture, fatigue, and corrosion fatigue were the focus of blade carrier material research.

BLADE CARRIER MATERIALS

The blade carriers of CP propeller mechanisms have been made from a variety of carbon steel, alloy steel, or bronze forgings. With a CP propeller of four or less blades, there is adequate room for a blade carrier of sufficient girth to carry the loads using a material of moderate strength and with a large margin of safety. The material selection for steel blade carriers, in general, followed the European practice for heavy section steel components of using medium carbon, low alloy steels in the annealed or normalized condition without tempering. Steels of Cr-Mo, Cr-Ni-Mo, and Ni-Mo, similar to AISI 4140 and 4340 types, are in extensive service with yield strengths from 50,000 psi to 60,000 psi and tensile strength of about 100,000 psi. At this strength level and in the normalized or annealed condition, the toughness characteristics would be more than adequate. In low-to-moderately stressed CP propellers, designed with a large margin of safety, it is not surprising that blade carrier fracture has not been experienced even in severe grounding and other impact incidents.

To meet the requirements of higher power levels, especially in a warship CP propeller of five blades, higher strength materials were required. Component sizes within a reasonably sized hub were limited. These higher strength requirements were satisfied by quenched and tempered alloy steel forgings of over 100,000 psi yield strength and 125,000 psi tensile strength. High strength steels are fatigue notch

254

sensitive and toughness adequate to resist fracture requires careful alloy and processing selection. The application of high strength steels in dynamically loaded machinery requires attention to fatigue and fracture design.

BLADE CARRIER FRACTURE TOUGHNESS

The objective of a toughness criteria as part of the materials selection for blade carriers is to provide a fracture-resistant component. In the current CP propeller investigation, it is apparent that relatively high engineering stress levels are developed in the fillet area of crank ring type blade carriers. The blade carrier contains many stress raisers such as section changes, fillets, threads, etc. In such a high strength component where cyclic loading occurs and exact local magnitudes may be unknown, fatigue cracks may develop. Should seawater enter the hub, corrosion fatigue may initiate cracks at even low stress levels.

The fracture toughness of the alloy influences the conditions for fracture; i.e. the critical crack size and the mode of fracture. With material of low toughness, fracture will be brittle and sudden and initiate from small cracks. While a tougher material, all else constant, may contain larger cracks and fail by a ductile mode with deformation, the latter case gives more opportunity for warning signs of a problem by vibration, oil leakage, jamming, etc.

This aspect of material selection has been made more quantitative through fracture mechanics technology[22,23] which defines three general levels of material behavior: (1) elastic plane-strain behavior, (2) elastic-plastic (plane-stress or mixed mode) behavior, and (3) plastic behavior or general yielding. Elastic plane-strain behavior is characterized by brittle fracture from small critical crack sizes at design stress levels. In elastic-plastic behavior, toughness levels are such that large plastic zones develop ahead of cracks with some amount of yielding prior to fracture. Tolerable flaw sizes can be quite large. Materials which fail in the plastic behavior mode exhibit ductile plastic fracture preceded by large deformations. Although fully plastic behavior would be a very desirable level of performance, it may be neither necessary nor economically or technically feasible for heavy-section components of high-strength materials. That is, for some components, a reasonable level of elastic-plastic behavior is often satisfactory to prevent initiation of brittle fracture provided the design, fabrication, and quality control are satisfactory.

255

Unfortunately, fracture mechanics technology is presently limited to quantitative analysis of linear elastic, plane-strain cases and does not provide the capability to quantify the fracture toughness requirements of a complex component, such as a crank ring under the complex loadings of the CP propeller hub assembly. However, it does provide the capability of identifying the toughness characteristics of steels for elastic-plastic to plastic behavior. The focus of this investigation was to use the available fracture mechanics technology to select a material fracture toughness criteria for blade carrier steel.

The objectives of the blade carrier fracture toughness criteria were to prevent brittle fracture under extreme loads, to render the blade carrier insensitive to small flaws and cracks (damage tolerance), and to influence failure mode. It becomes difficult to ensure fully plastic behavior in thick-section, high-strength steel forgings; but current technology can set criteria for elastic-plastic, mixed-mode fracture where the material's tolerance to flaws is increased. That is, the blade carrier material has adequate toughness to prevent failure of a catastrophic, brittle nature. In addition, the increased flaw tolerance and plastic deformation provide the probability of early warning of impending blade carrier failure by blade vibrations or increased torque required to change pitch, thereby avoiding the sudden catastrophic blade loss as occurred on BARBEY. The testing and analysis conducted to meet these objectives are detailed elsewhere[24] and are condensed herein. A brief discussion of the fracture mechanics basis for the fracture toughness criteria, the results of the experimental effort to characterize the fracture toughness of presently used and candidate blade carrier steels, and the consequent recommendations for selection of blade carrier materials are presented. The development of the blade carrier toughness criteria[24] was based on current fracture control design philosophies.[22,23] In summary, a ratio of fracture toughness (K_{IC}) to yield strength (S_y) was selected to be within the region of elastic-plastic fracture behavior. Correlation of fracture mechanics-type toughness measurements and Charpy V-notch (CVN) tests were then used to determine a minimum CVN value. The materials investigated were evaluated in regard to this criterion.

Fracture toughness is a function of the following: material, processing, strength level, section size, temperature, loading rate, and flaw (crack or defect) size. For conditions of maximum constraint, such as that in heavy sections, the basic relationships in fracture mechanics analyses (for a given temperature and

256

loading rate) show the critical flaw size to be proportional to the ratio K_{IC}/S_y. This expression is an indexing parameter for the toughness of materials. The problem in setting fracture criteria is selecting the magnitude of this toughness index necessary for a particular material to prevent brittle, plane-strain failure modes.

The following expressions relate section size to the toughness index for the three levels of fracture performance[22,23] previously discussed.

1. Elastic Plane-Strain Behavior (essentially brittle behavior)

$$\left(\frac{K_{IC}}{S_y}\right) < \left(\frac{t}{2.5}\right)^{1/2}$$

where t = section thickness.

2. Elastic-Plastic or Mixed-Mode Behavior

$$\left(\frac{t}{2.5}\right)^{1/2} < \left(\frac{K_{IC}}{S_y}\right) < \alpha(t)^{1/2}$$

where α may be unity[22] or as high as 2 or 3.[23]

3. General Yielding or Plastic Behavior

$$\left(\frac{K_{IC}}{S_y}\right) > \alpha(t)^{1/2}$$

The limitations of current fracture mechanics methodology are apparent in these three expressions. The methods are extensions of linear-elastic (plane-strain) mechanics into nonlinear (plane stress) mechanics. The bound between mixed-mode and general yielding behavior, hence, the quantity α, is not well established. The bound between mixed-mode and elastic, plane-strain behavior, $(t/2.5)^{1/2}$, was derived from the requirement for a section size, t, large enough to fully constrain the plastic zone ahead of a crack for linear-elastic behavior in the determination of K_{IC}, the plane-strain fracture toughness of a material.[22,23] It was shown that the requirement was conservative.[23] The section size t was strictly specimen or plate thickness, but was extended to minimum dimension under maximum stress for the general case.

The methods of linear elastic fracture mechanics to measure K_{IC}, the plane-strain fracture toughness of materials, are invalid in the elastic-plastic regime and other methods must be used. Correlations between Charpy V-notch[23] or dynamic tear[22] (DT) impact toughness shelf values and K_{IC} have been formulated for high-strength steels. Quantitative elastic-plastic fracture mechanics is an emerging research field and the J-integral method, an extension of linear elastic mechanics holds much promise. The material property J_{IC} characterizes the toughness of materials at or near the initiation of ductile crack extension. A J_{IC} value can be used to conservatively estimate K_{IC} for a material.[25] Thus, a determination of the toughness index (K_{IC}/S_y) can be made through estimation of K_{IC} from the impact and the J-integral tests by the following correlations:

1. K_{IC} and CVN in the upper shelf region;

$$\left(\frac{K_{IC}}{S_y}\right)^2 = \frac{5}{S_y}\left(CVN - \frac{S_y}{20}\right) \qquad \text{(Reference 23)}$$

2. K_{IC} and DT in the upper shelf region;

(Empirical, Graphical; References 24 and 26)

3. K_{IC} and J_{IC};

$$J_{IC} = \frac{K_{IC}^2}{E}(1-\mu^2) \qquad \text{(Reference 25)}$$

μ = Poisson's Ratio

Figure 5 is presented to provide an idea of expected toughness levels for various classes of steels. Also, Figure 5 gives an indexing of CVN and dynamic tear test (DT) shelf values, and corresponding K_{IC} values. The areas shown are general and apply to a thick plate from which most of the data were obtained. Chemical composition, melting practice, forging process, section size, and heat treatment all have marked effects on the toughness of the final forged product.

The conventional quenched and tempered (Q and T), low-alloy forged steels (AISI 4140 and 4340 types) used for high-strength blade carriers have relatively
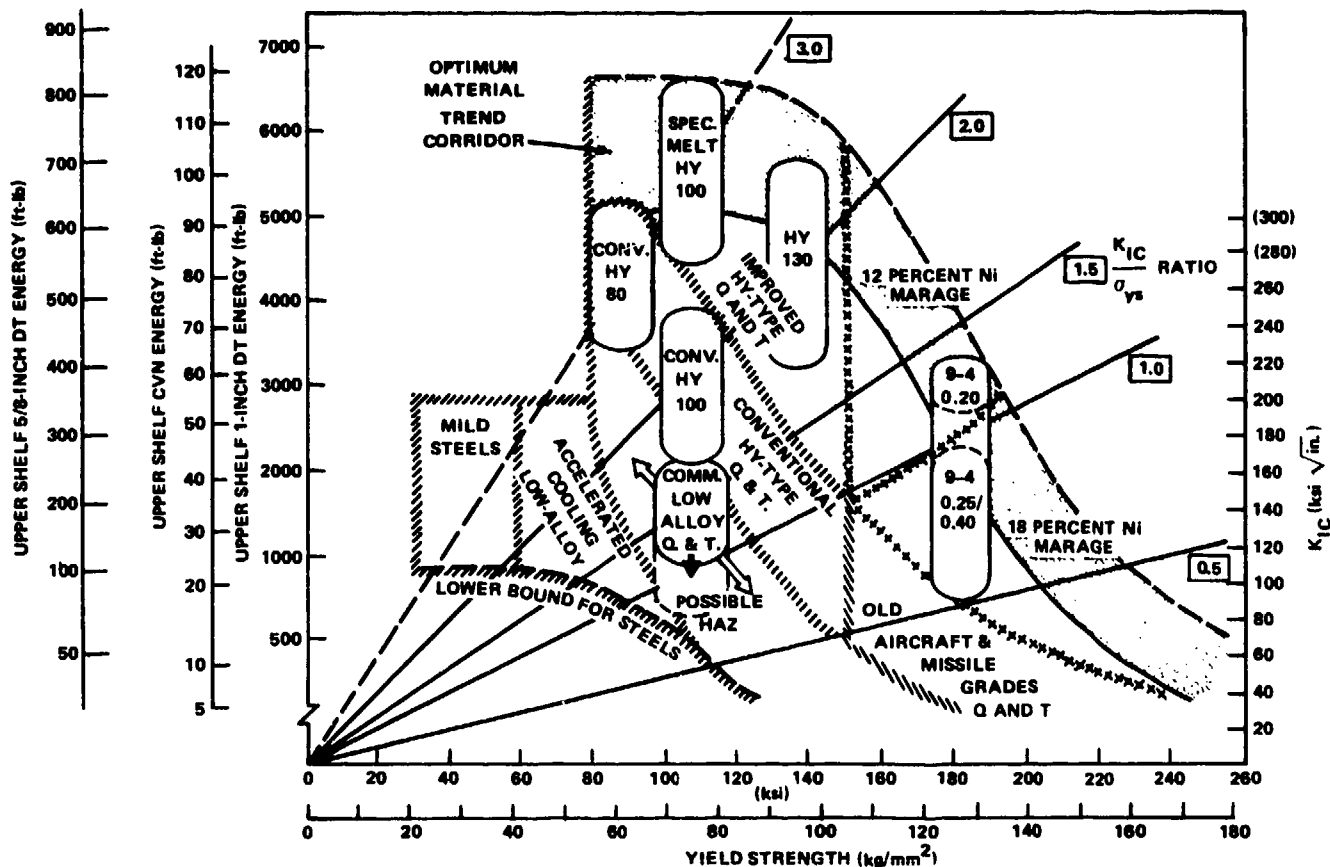
Figure 5 - Compendium Ratio Analysis Diagram Index for Generic
Classes of Steels (from Reference 22)

high carbon contents, 0.35 to 0.50, and low alloy content to meet the need for
increased yield strength at increased section size at minimum cost. The usual
criteria in selection of these steels is the specified minimum yield and tensile
strengths for the section size of the product. No toughness requirements are
usually given, for the achievable toughness bounds are limited as indicated in
Figure 5. In comparison with the commercial Q and T low alloy steels, the HY steels
developed for Navy use in submarine hulls are generally much higher in fracture
toughness. Special melting provides even greater assurance of a high level of
toughness.

The fracture toughness of crank rings used in Navy CP propellers and steels of
100 ksi yield strength or greater which would most likely satisfy the fracture and
fatigue requirements of blade carriers was evaluated.[24] Table 1 presents the
nominal composition and mechanical properties of the alloys which were evaluated

TABLE 1 – PROCESSING, CHEMICAL COMPOSITION, AND MECHANICAL PROPERTIES OF HIGH STRENGTH STEELS IN FRACTURE STUDY

Alloy Product (Specification)	Processing		Nominal Chemical Composition										Minimum Tensile Properties	
	Melting Practice	Heat Treatment*	C	Mn	P	S	Si	Ni	Cr	Mo	V	Co	Yield Strength (ksi)	Tensile Strength (ksi)
AISI 4340 Failed Barbey Crank Disk.	Open hearth air melt	Aust: 1600°F, OQ Tempered: 1250°F	0.40	0.70	0.040 max.	0.040 max.	0.30	1.80	0.80	0.25	-	-	113.5	128
AISI 4150H Original Spruance Crank Ring (ASTM A243 N)	Electric furn. air melt Vacuum degassed	Norm: 1650°F AC Aust: 1500°F OQ Tempered: 1000°F	0.50	0.90	0.030 max.	0.025 max.	0.25	0.10	1.00	0.20	-	-	115	140
HY-100, Replacement Barbey Crank Disk (MIL-S-23009A)	Electric furn. air melt	Aust: 1650°F WQ Tempered: 1150°F	0.20 max.	0.30	0.025 max.	0.025 max.	0.25	2.90	1.40	0.40	0.05	-	100	120**
ASTM A471 Class 6 Perry Crank Ring and Spruance Replacement	Electric furn. air melt Vacuum degassed	Norm: 1650°F AC Aust: 1600°F OQ Tempered: 1100°F	0.35	0.60	0.010	0.015	0.25	3.40	1.80	0.55	0.10	-	125	140
HY-130 Ring Forging (MIL-30-F/2)	Electric furn. air melt Vacuum degassed	Norm: 1600°F AC Aust: 1650°F WQ Tempered: 1000°F	0.10	0.80	0.005	0.010	0.30	5.00	0.60	0.50	0.06	-	130	150**
HP-9-4-20 Thick Plate***	Electric furn. Vacuum arc remelt	Norm: 1650°F AC Aust: 1550°F WQ Tempered: 1000°F	0.18	0.30	0.010 max.	0.010 max.	0.10	9.00	0.80	1.00	0.06	4.50	175	195
10 Ni (HY-180) Thick Plate	Vacuum induction melt Vacuum arc remelt	Aust: 1500°F WQ Tempered: 950°F WQ	0.12	0.06	0.005	0.005	0.03	10.00	2.10	1.00	-	8.00	180	195

*Norm-normalized, Aust-austenitized (hardening treatment), WQ-water quenched, OQ-oil quenched, AC-air cooled
**Not specified, for record only.
***Forgings under ASTM A579, Grade 81.

from forgings or heavy section plate when the former were not available or procurable within the limits of the program. In general, these are typically basic electric-furnace steels which are vacuum degassed, forged, quenched, and tempered. The ultrastrength HP 9-4-20 and 10Ni steels are produced by vacuum-arc-remelt of consumable electrodes of either air or vacuum induction melted metal. Therefore, they are costly and have largely been applied to aerospace forging requirements. In general, toughness is increased by processing which results in low gas, tramp element, and inclusion content. The compositions are low in carbon and gain strength with toughness from alloying content high in nickel, chromium, cobalt and molybdenum.

In Table 2 are summarized the fracture tests conducted on the high strength steels. Only the material from the 4340 and 4150H blade carriers gave valid plane-strain fracture toughness K_{IC} values. Included in the table are estimates of K_{IC} from the CVN and DT impact tests and the J-integral tests by the correlations previously given.

From these values an average value of K_{IC} for calculation of a fracture toughness index was selected for each alloy and given in Table 3. The index is compared to that for the limit of plane-strain fracture behavior

$$\left(\frac{K_{IC}}{S_y}\right) \; < \; \left(\frac{t}{2.5}\right)^{1/2}$$

Again, because of the complexity of the blade carrier, its loading, and analysis, the results in Table 3 must be viewed qualitatively. Note that the toughness index, when less than unity, results in relatively small section sizes for establishing plane-strain conditions and the risk of brittle behavior.

Higher material fracture toughness minimizes the risk of brittle fracture. It is one factor in the fracture resistance of the component; the others being stress, loading rate, operating temperature, flaw or defect size, and constraint (geometry and boundary conditions). A material of low fracture toughness index might perform satisfactorily where stresses are low, no defects or sharp stress raisers exist, or the conditions for plane-strain are never established. However, the blade carrier of a high-power CP propeller cannot be so precisely designed or manufactured and the use of a "safe" material is appropriate.

The material toughness requirement should be part of the material selection process for high-strength blade carriers. In preliminary design, the yield strength

TABLE 2 – SUMMARY OF FRACTURE TOUGHNESS TESTS ON HIGH STRENGTH STEELS

Alloy	4340	4150H	H7-100	A471, Cl 6	HY-130	HP 9-4-20	10 Ni (HY-180)
Average 0.2 Percent Offset Yield Strength, S_y (ksi)	102.8	112.5	100.6	125.6	141.6	175	180
Charpy V-Notch (CVN) Upper Shelf Value (ft-lb)	6-11*	7-11*	58-80	22-32	44-70	40-55	65-85
K_{I_C} **	20-55	28-55	163-194	99-127	162-213	165-201	224-260
5/8-Inch Dynamic Tear (DT) Upper Shelf Value (ft-lb)	45-85*	40-105*	160-210	330-400	620	370	490-580
K_{I_C} ***	60-80	55-90	110-135	170-195	250	200	220-240
Plane-Strain Fracture Toughness, K_{I_C} (ksi-in.$^{1/2}$)	80	55	not valid	95	not valid	135	135
Elastic-Plastic Fracture Toughness, J_{I_C} (in.-lb/in.^{2})	(Elastic fracture)	(Elastic fracture)	760	510	745	–	600
K_{I_C} †	–		140	115	(140)	–	(130)
Measured or (Estimated) K_{I_C} for Alloy (ksi-in.$^{1/2}$)	80	55	(140)	95	(140)	135	135

*Values for tests at room temperature, not upper shelf.

** $\left[\dfrac{K_{I_C}}{S_y} \right]^2 = \dfrac{5}{S_y} [CVN - \dfrac{S_y}{20}]$, Reference 23.

***Graphical estimate, Reference 26.

† $J_{I_C} = \dfrac{K_{I_C}^2}{E(1 - \mu^2)}$, Reference 25.

TABLE 3 - FRACTURE TOUGHNESS INDEX K_{IC}/S_y FOR HIGH STRENGTH STEELS INVESTIGATED

Alloy	0.2 Percent Yield Strength S_y (Minimum) (ksi)	Measured or (Estimated) K_{IC} (ksi-in.$^{\frac{1}{2}}$)	Fracture Toughness Index $\dfrac{K_{IC}}{S_y}$	Section Size t^* for Plane-Strain Limit (in.)
4340	100	80	0.80	1.6
4150H	115	55	0.48	0.6
HY-100	100	140	1.40	4.9
A471, Class 6	125	95	0.76	1.5
HY-130	130	140	1.08	2.9
HP 9-4-20	175	135	0.77	1.5
10 Ni (Hy-180)	180	135	0.75	1.4
Table IV-1		Table IV-2		

$^*t = 2.5 \left(\dfrac{K_{IC}}{S_y}\right)^2$, where "t" is minimum dimension under maximum stress; e.g., for crank ring-type blade carrier.
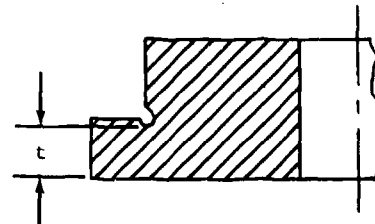
level and approximate dimensions are usually determined prior to selecting the blade
carrier material. The following simplified approach is recommended. Using the
yield strength, S_y, and approximate dimensions in the critical section of the blade
carrier, t, determine the fracture toughness, K_{IC}, to exceed plane-strain conditions;
i.e., $K_{IC} > S_y(t/2.5)^{1/2}$. Fracture toughness values inferred from correlations with
notch toughness tests or directly measured by fracture mechanics tests are readily
available. However, the most generally adopted industry criterion for the evaluation
of toughness of components is the CVN impact energy exhibited by the material at the
minimum expected operating temperature. The toughness requirements may be made on
this basis as related to more sophisticated fracture toughness tests. Correlations
of static fracture toughness and upper-shelf CVN have been extended down to steels
of yield strengths of 90 ksi.[23] The toughness requirement can be given as a CVN
impact toughness based on these correlations. Additional conservatism can be built
into the requirement by specifying the required CVN impact energy at a test temper-
ature of 0°F, whereas typical CP propeller hub operating temperatures may be near
the surrounding seawater temperature. Also, improved load estimation and strength
calculation should result in blade carrier peak local stresses well below the yield
strength level.

Because the toughness requirement derived from the preceding is based on many
simplifications and conservative assumptions, it must be regarded as guidance for
including a toughness requirement for blade carrier steels. It should not be a
limiting criterion, where a material selection is reasonable from other consider-
ations, such as cost, availability, and toughness that approaches the recommendation.
The criterion is intended to avoid high-strength steels of low toughness in the
material selection process.

FATIGUE PROPERTIES OF STEEL BLADE CARRIER FORGINGS

The fatigue properties of wrought steels are generally developed using tests of
small specimens subjected to fully reversed, constant amplitude stresses. These are
conducted to determine the "endurance limit" or the intrinsic fatigue strength of
the metal. It has been found that the endurance limit for a broad range of steels
in various product forms and heat treatments is a function of tensile strength.[26]
The endurance limit is approximately one-half of the ultimate tensile strength for
steels up to 150,000 psi tensile strength and less than 10 percent total alloy
content. Above these limits the ratio is less.[26]

264

There are a number of factors, however, which need to be considered before realistic designs are based on such values. Endurance limits developed as described above are dependent upon the following:

1. Specimen size--larger pieces have more gradual stress gradients and more flaws typical for the material

2. Condition of the metal--method of manufacture, heat treatment

3. Surface condition--polishing without scratches or working

4. Residual stresses--from specimen preparation

5. Test conditions--cyclic frequency and ambient environment

These conditions are controlled in laboratory studies, but may be quite different in the component to which the data are applied.

The fatigue properties of the alloy steels given in Table 1 were determined using conventional rotating beam tests.[27] The thick section forgings or plates of the alloys were used and lower endurance limits were expected due to the high tensile strength, product form, and alloy content of some of the materials. The results are given in Figure 6. For these materials, the ratio of the endurance limit to tensile strength from a best-fit curve to the data was from 0.40 to 0.45 as shown in Table 4.

A study of the directionality of fatigue properties in a large forging was conducted using material from the 4150H crank ring which had failed in the full-scale laboratory test.[28] Specimens were removed from the radial, circumferential (tangential), through-thickness, and 45 deg to the fillet groove (critical stress area) directions. The results fell within the band of scatter shown in Figure 7 with the specimens from the through-thickness (weakest) direction on the low end of the scatter band. The results from tests of other 4150H crank rings (SPRUANCE Class) determined, in some cases, with larger specimens (Figure 6) are included in Figure 7. Note that size effect, directionality, and material variability were not significant factors.[27]

The fatigue notch sensitivity of some of these steels was studied over a range of theoretical stress concentration factors (K_t) from 1.2 to 3.0. The results of the fatigue tests are included in Figure 6. The fatigue notch reduction factors (K_f) and the notch sensitivity (q) were determined[29] and are shown in Table 5. In summary, the notch sensitivity was near unity in most cases; indicating fatigue

Figure 6 – Fatigue Test Results for High Strength Steels, Rotating
Beam Fatigue Tests in Air

(Slashed Symbols for Thick Plate; else Forging)

Figure 6 (Continued)

D. HY-130

○ SMOOTH, K_t = 1
△ NOTCHED, K_t = 3

STRESS AMPLITUDE – ksi

CYCLES TO FAILURE

E. HP 9-4-20

○ SMOOTH, K_t = 1
△ NOTCHED, K_t = 3

STRESS AMPLITUDE – ksi

CYCLES TO FAILURE

F. 10 Ni (HY-180)

○ SMOOTH, K_t = 1
△ NOTCHED, K_t = 3

STRESS AMPLITUDE – ksi

CYCLES TO FAILURE

267
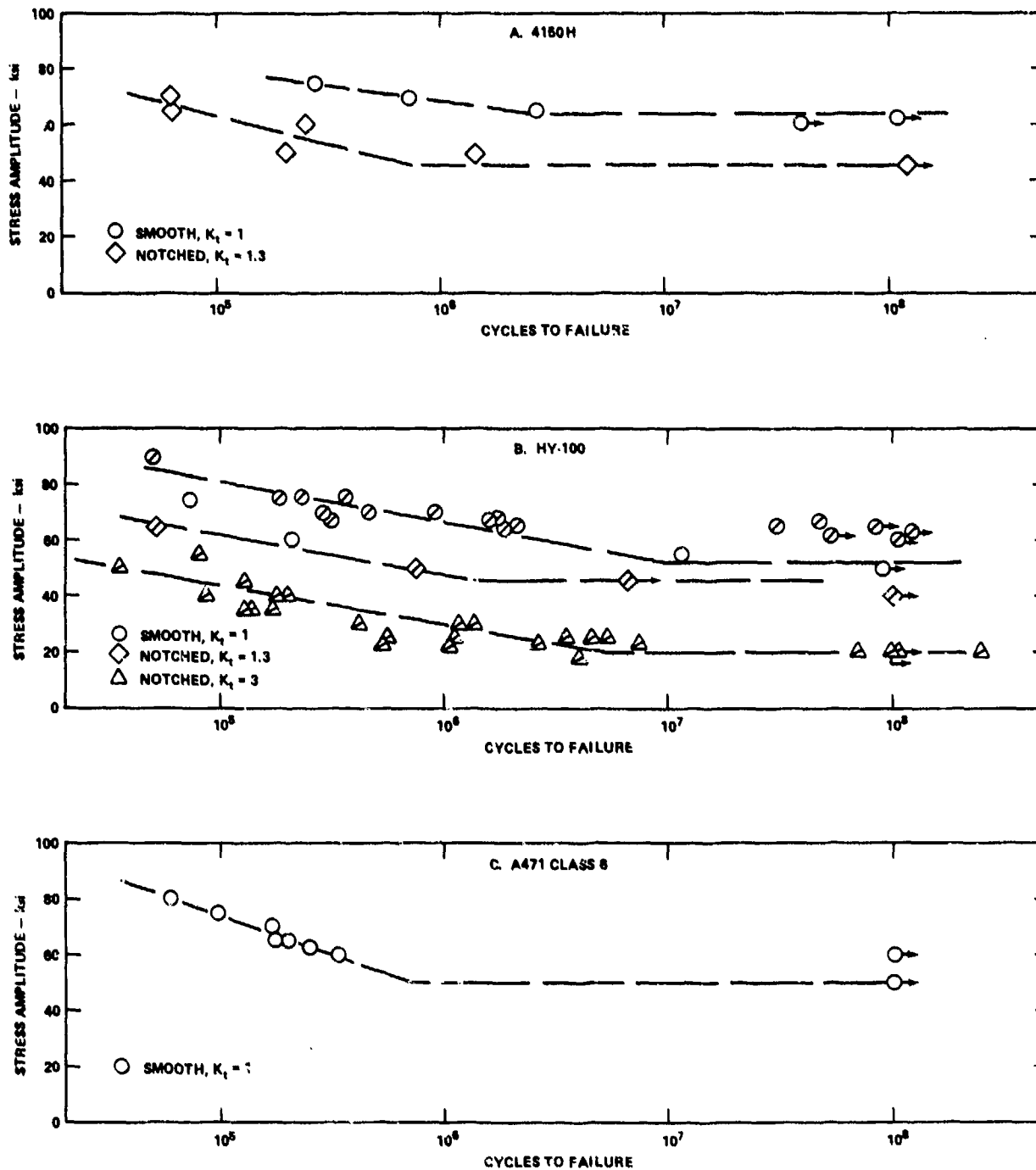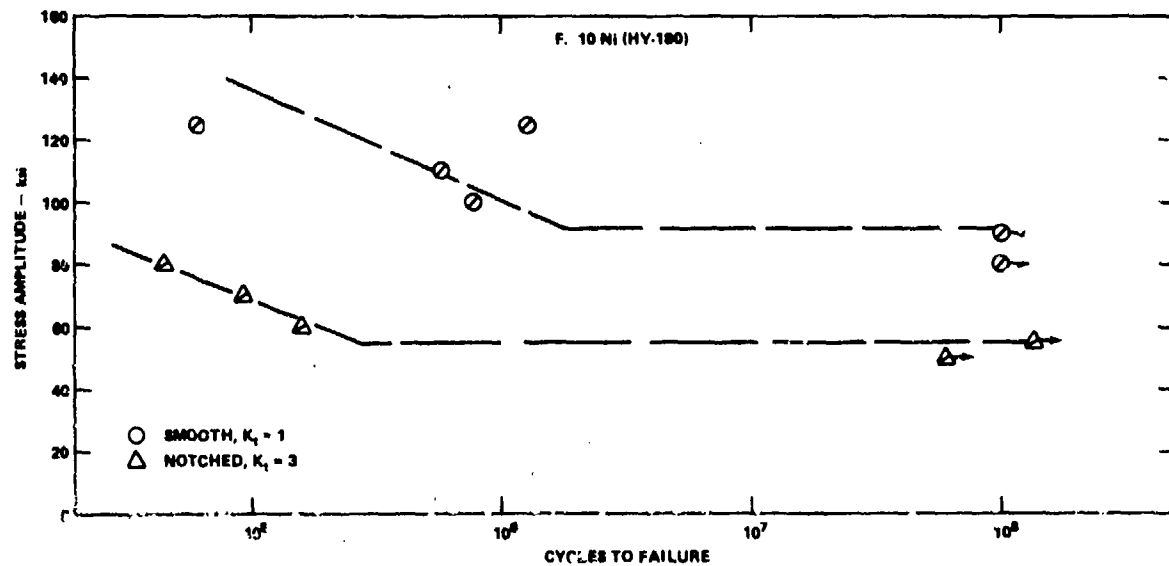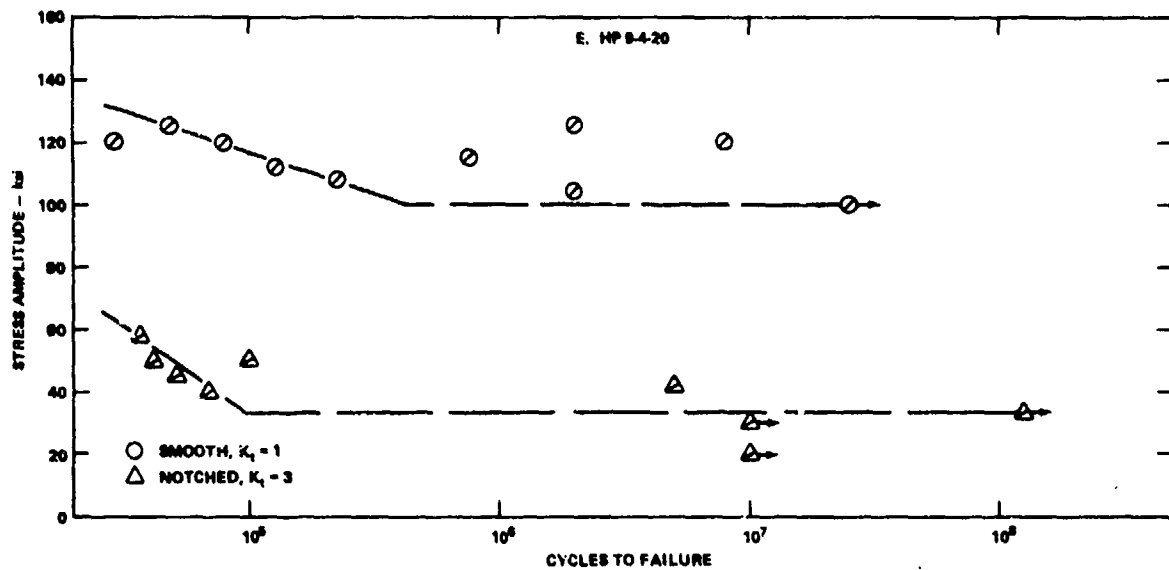
TABLE 4 - FATIGUE PROPERTY SUMMARY FOR HIGH STRENGTH STEELS

Alloy	Ultimate Tensile Strength, UTS (ksi)	Fatigue Strength at 10^8 Cycles, S_e (ksi)	Endurance Ratio $\dfrac{S_e}{UTS}$
4150H	146.3	60	0.41
HY-100	114.4	50	0.43
A471, Cl. 6	146.8	55	0.38
HY-130	149.2	55	0.38
HP 9-4-20*	195	100	0.51
10 Ni (HY-180)*	195	90	0.46

*Thick Plate
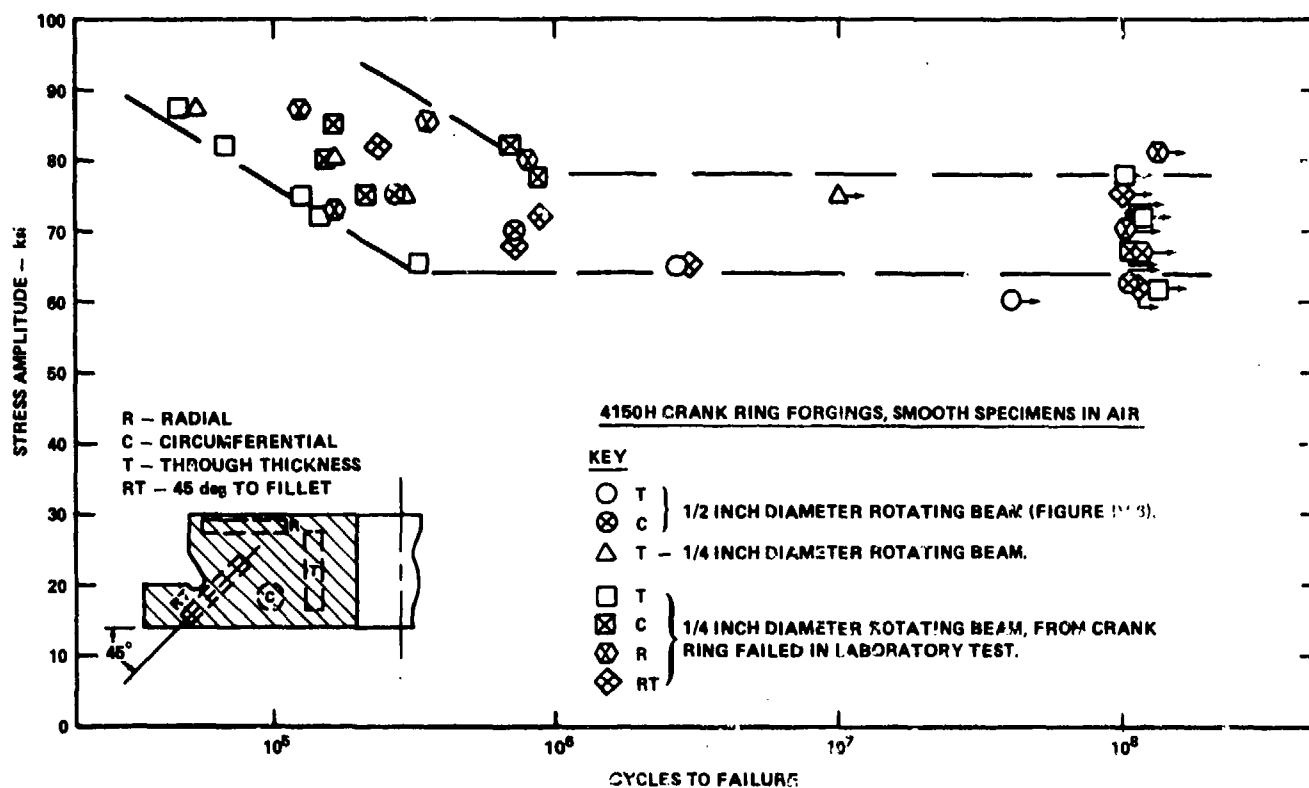
Figure 7 - Fatigue Test Results for 4150H Steel Crank Rings with Specimens Removed from Various Orientations within the Forgings

268

TABLE 5 — SUMMARY OF NOTCHED FATIGUE PROPERTIES AND NOTCH SENSITIVITY
OF HIGH STRENGTH STEELS

Alloy	Stress Concentration Factor K_t*	Fatigue Strength at 10^8 cycles (ksi)	Fatigue Notch Reduction Factor K_f***	Notch Sensitivity q+
4150H	1.0 1.3	60 45	– 1.3	– 1.0
HY-100	1.0 1.3 3.0	60 45 20	– 1.3 3.0	– 1.0 1.0
A471, Cl. 6	1.0	55	–	–
HY-130	1.0 3.0	70 40	– 1.8	– 0.4
HP 9-4-20	1.0 3.0	100 35	– 2.9	– 0.9
10 Ni (HY-130)	1.0 3.0	90 50	– 1.3	– 0.4

* Derived from Reference 29, K_t = 1.0 for smooth specimen.

** From Figure 6.

*** $K_f = \dfrac{\text{fatigue strength of smooth specimens}}{\text{fatigue strength of notched specimens}}$ at 10^8 cycles

+ $q = \dfrac{K_f - 1}{K_t - 1}$

reduction at nearly the full theoretical value. Fatigue notch sensitivity is expected to be high in high-strength materials.[29] For conservatism in designs, use of the full theoretical value, i.e., $K_f = K_t$, seems warranted.

Surface coatings and treatment applied for corrosion or wear resistance may affect the intrinsic fatigue strength of the metal. Cold working processes (shot peening, cold rolling) usually increase fatigue strength due to compressive residual stresses induced on the surface.[26] Both processes may only be applied to a limiting intensity beyond which they cause metallurgical or surface damage detrimental to fatigue strength. Studies of both cold-rolled and shot-peened 4150H and HY-100 steel forging were conducted[27] but showed little effect on fatigue strength, although applied by optimum parameters; see Figure 8. When applied to broad areas of high strength alloys, the level of compressive residual stress attainable on the surface is of a low order and may be ineffective relative to the high stress amplitudes
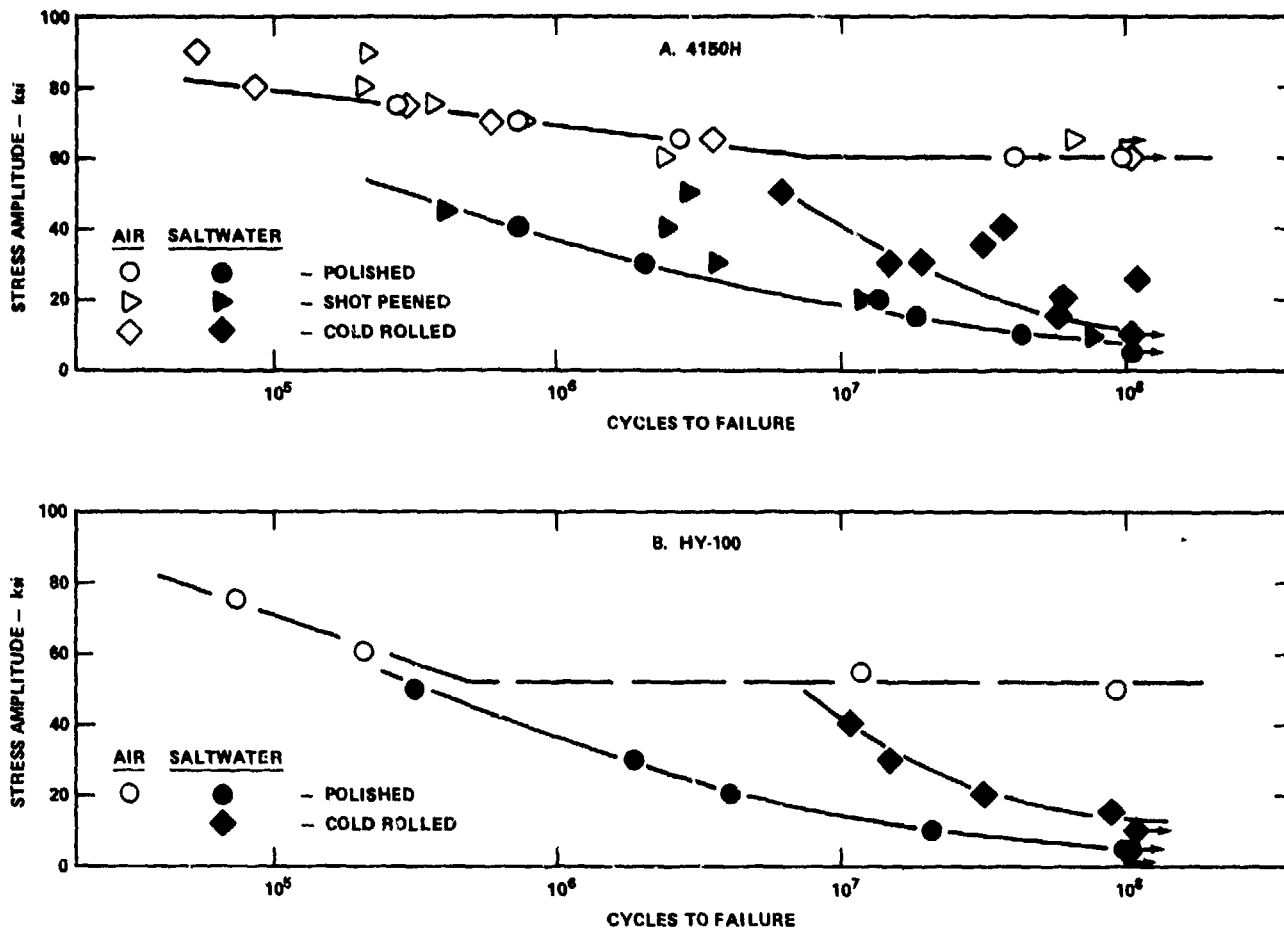
Figure 8 - Fatigue and Corrosion Fatigue Test Results for 4150H and HY-100
Steels Given Surface Cold Working Treatments

necessary for fatigue damage. However, that level of compressive residual stress
was sufficient to delay the onset of corrosion-fatigue crack initiation as discussed
in the next section. Platings, plasma-spray coatings, weld overlays and inlays,
and metallizing were known to cause damage to the substrate and thus decrease
intrinsic fatigue strength; these were not investigated.[27]

In designing again t fatigue in heavy machinery, ample safety factors are
conventionally used on the endurance limit of the steels determined by specimen
tests. A factor of 2 is typical[29] intended to cover size effect, material differ-
ences (grain flow and size, cleanliness, etc.), geometry effects (stress gradient,
shape factors, etc.), and surface finish. The factor is applied to both cyclic and
static stress components. It is generally accepted[26,29] that the modified Goodman

270

diagram (based on ultimate tensile strength) applies to steels as a conservative representation of the effect of mean stress on fatigue strength. Figure 9 presents the Goodman diagram for the 4150H steel crank ring based on the specimen data of
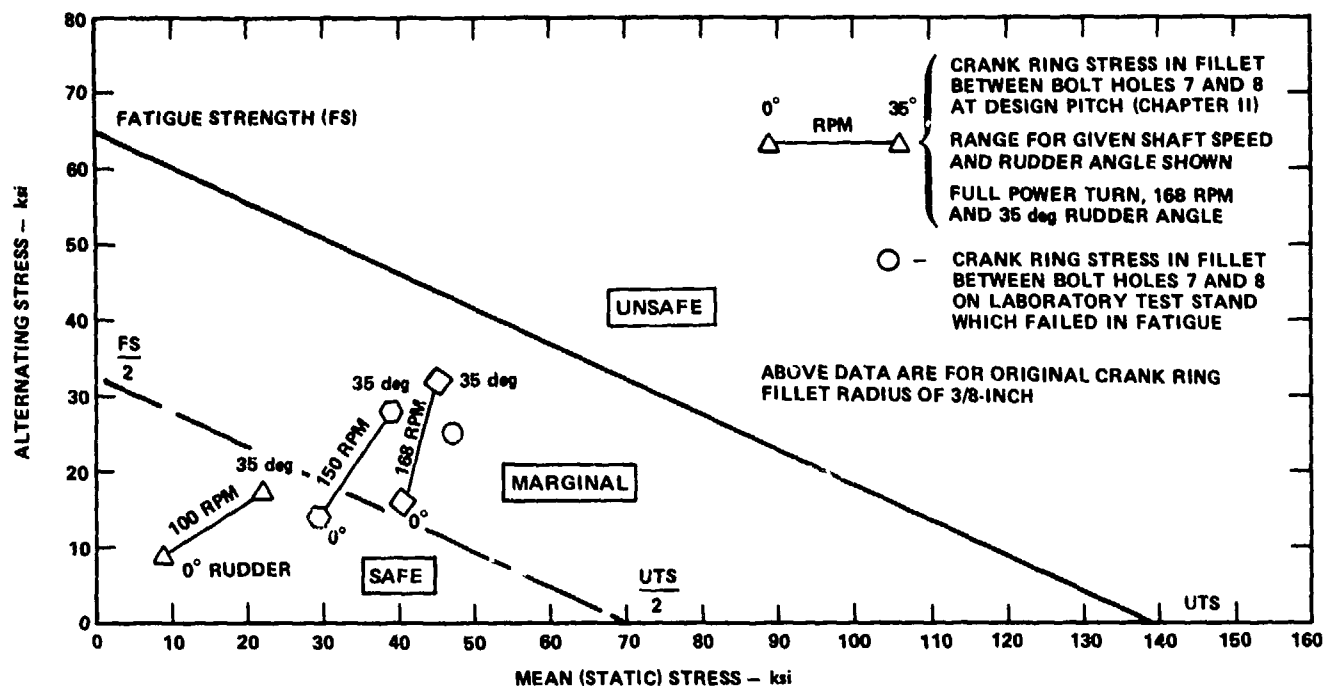
Figure 9 - Goodman Diagram for 4150H Steel Forging with Applied Safety
Factors Showing Stresses Measured on SPRUANCE Stress Trials and
Stress Applied in Laboratory Crank Ring Fatigue Failure

Table 4. The stresses measured on the SPRUANCE stress trials, Chapter II, and the laboratory test stand failure[28] are represented as points on the diagram. Note that the stress trial points for hard turns and the test stand failure lie within the marginal zone. Thus, the need to increase the crank ring fillet radius (reduce stress concentration factor) and the possibility of fatigue failure in the highly stressed crank ring are shown.

IMPROVEMENT OF STEEL BLADE CARRIER CORROSION-FATIGUE RESISTANCE

The fatigue strength of low and medium alloy steels is severly degraded by seawater to less than 10,000 psi (at 10^8 cycles) regardless of tensile strength.[26] Corrosion-fatigue tests in saltwaters were conducted on the high-strength steels given in Table 1 and the results are given in Figure 10. For all the steels,

271

Figure 10 - Corrosion Fatigue Test Results for High Strength Steels

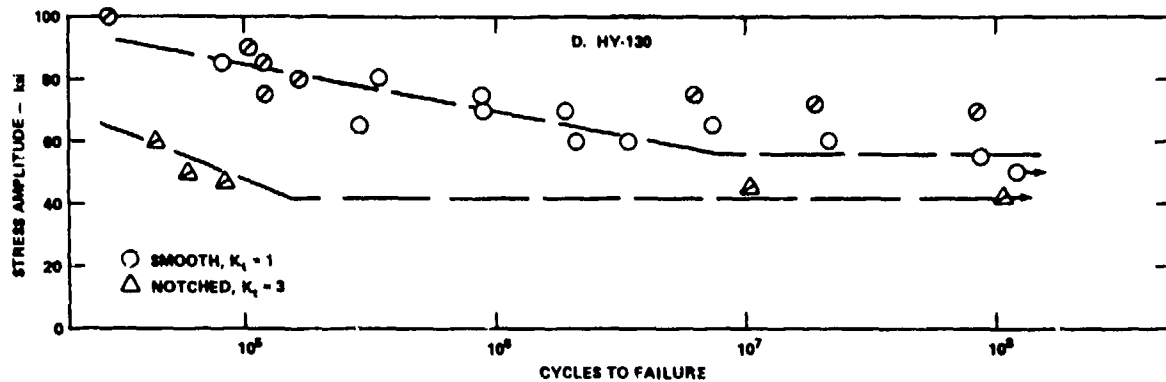(Slashed Symbols for Thick Plate; else Forging)

272

Figure 10 (Continued)

D. HP9-4-20

SMOOTH SEPCIMENS
○ — AIR
● — SALTWATER

E. 10 Ni (HY-180)

SMOOTH SPECIMENS
○ — AIR
● — SALTWATER
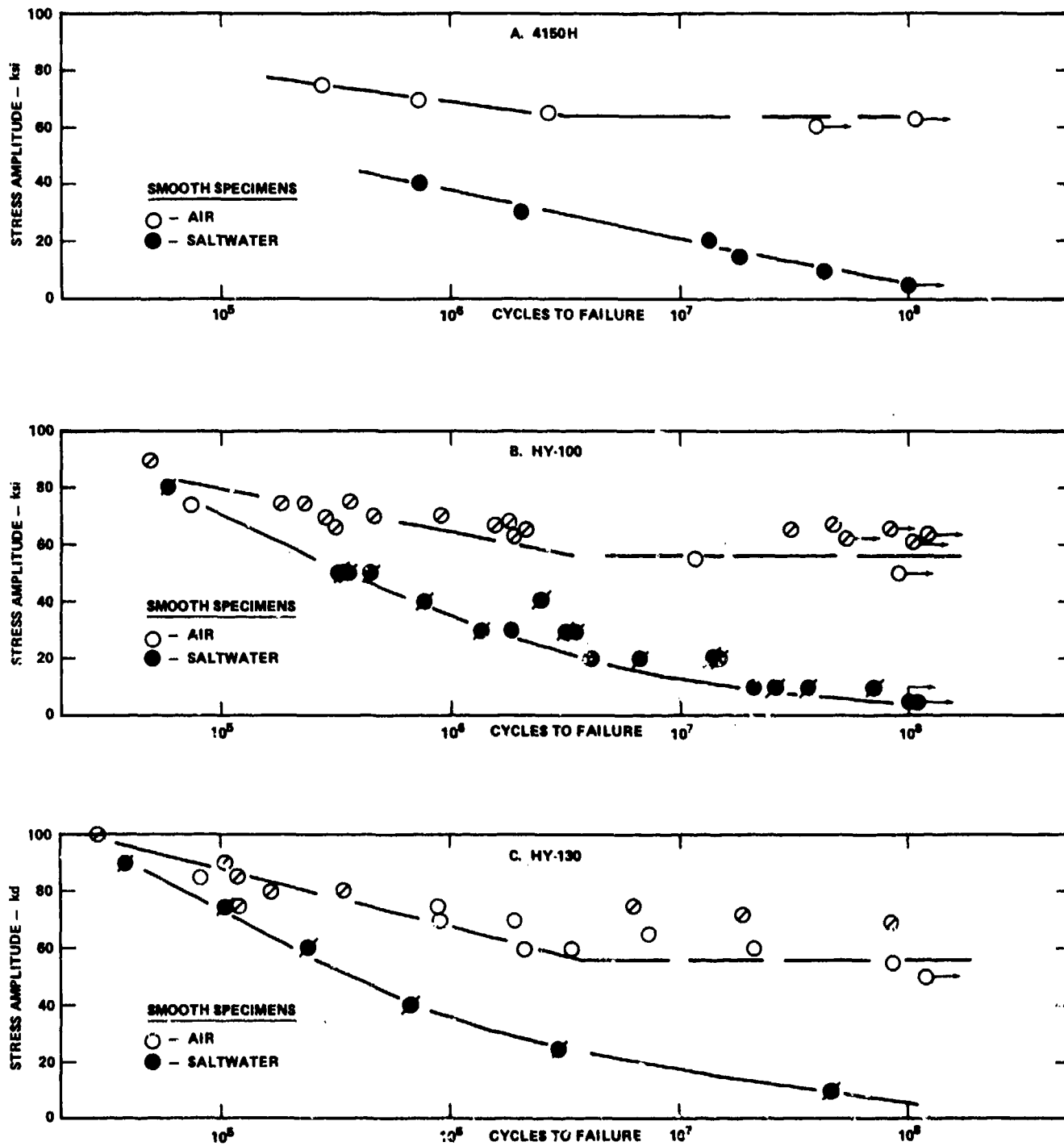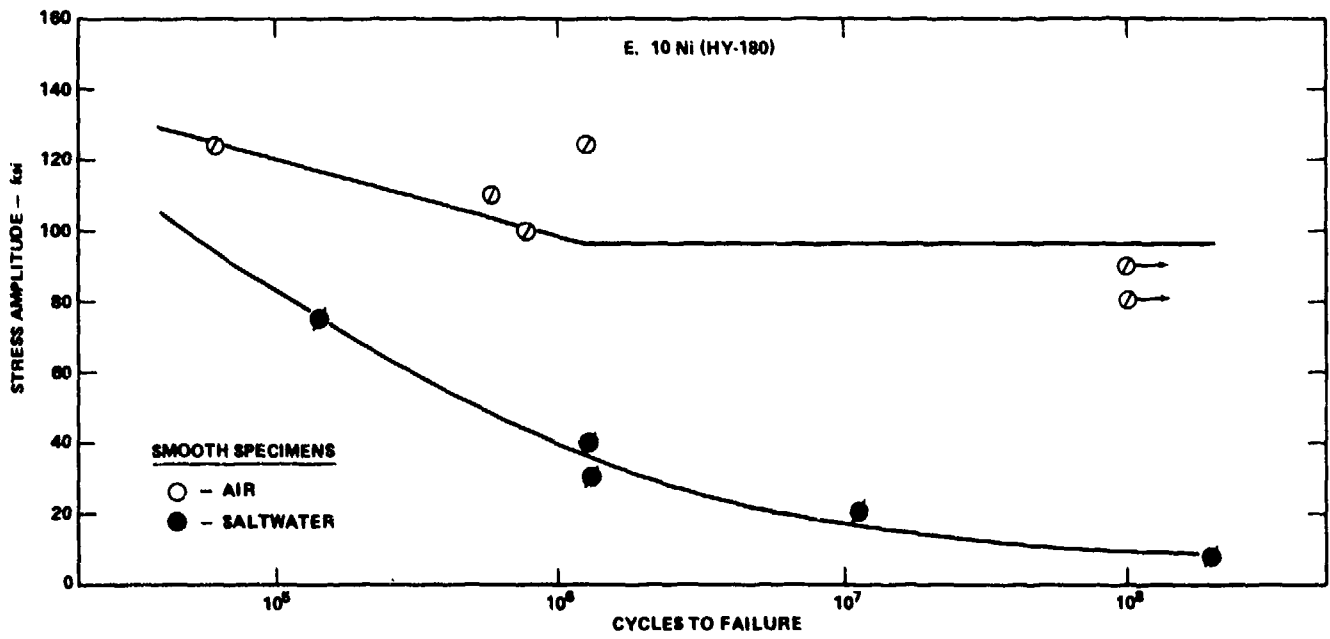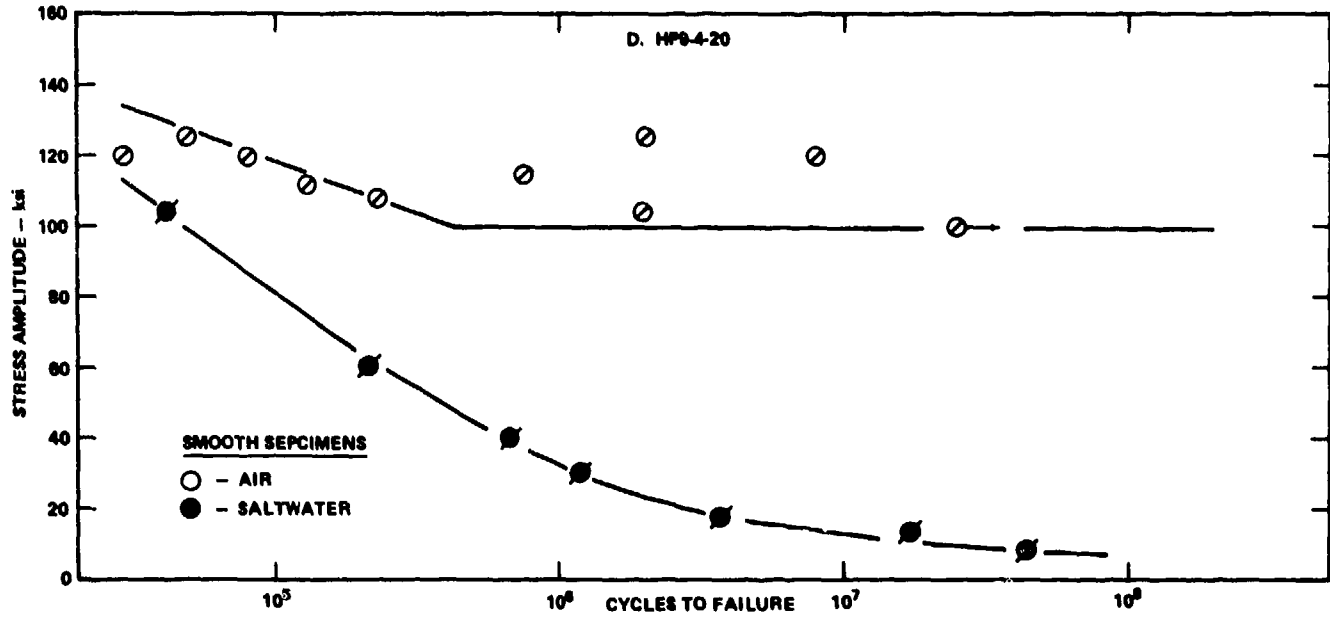
fatigue strength is drastically reduced by that environment. Even for the highly alloyed steels, fatigue strength in saltwater at 10^8 cycles was about 3 to 7 percent of the ultimate tensile strength of the steel.[27]

For the blade carrier application, the problem of seawater leakage into the hub and consequent contamination of the system oil must be addressed. Studies of the effect of seawater contamination of the 2190 TEP oil were conducted using small rotating beam tests of 4150H steel. The results are given in Figure 11 where a 50
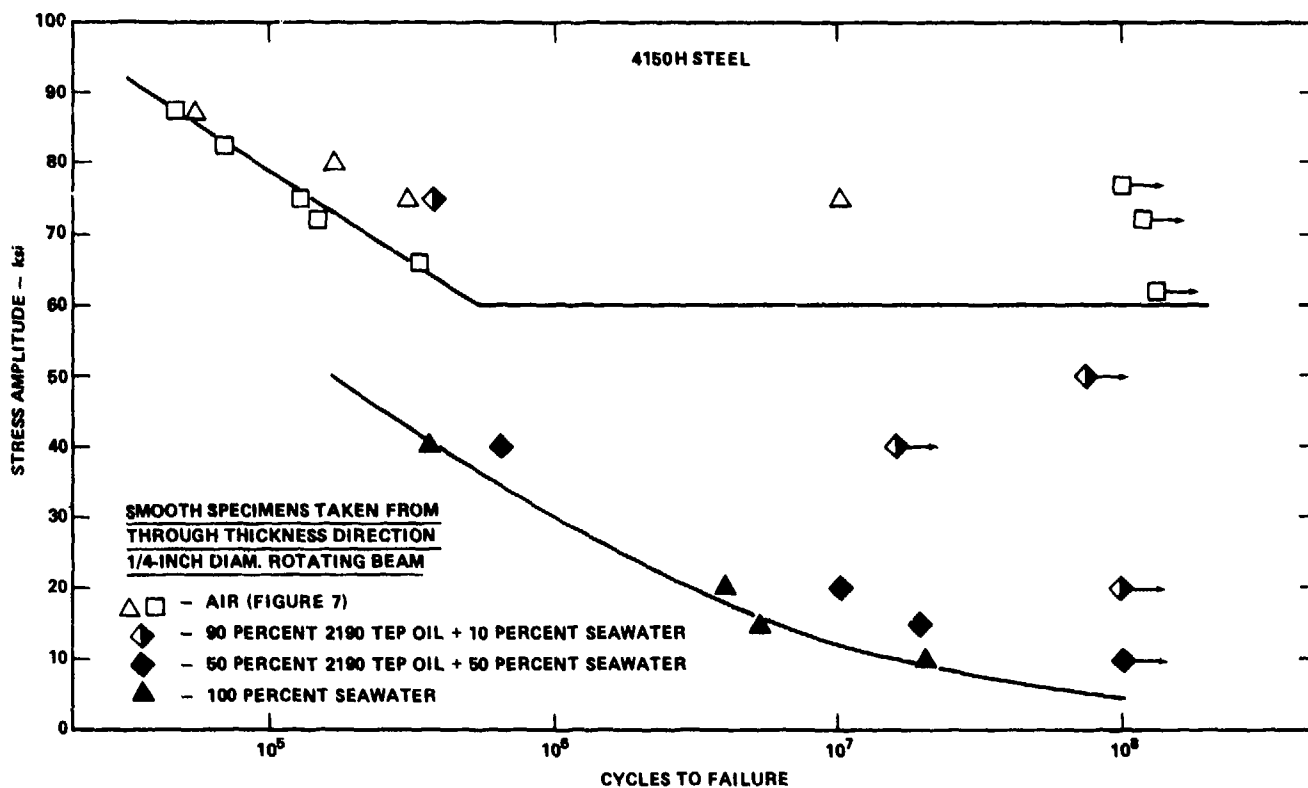
Figure 11 - Results of Rotating Beam Fatigue Tests of 4150H Steel Showing the Effect of Oil and Seawater Mixtures

percent oil and 50 percent seawater mixture was as severe as seawater. Results for a 90 percent oil and 10 percent seawater mixture were inconclusive,[27] but separation of the mixture at the specimen was suspected.

Corrosion fatigue studies using a fillet geometry were conducted to obtain a better representation of conditions in the high stress, fillet areas of crank ring

274

and crank disk type blade carriers. In these studies, the fatigue tests subjected several of the alloys under investigation to oil and seawater mixtures in a configuration and stress situation simulating service conditions.[27] A schematic description of the fillet fatigue test is given in Figure 12. The specimen was
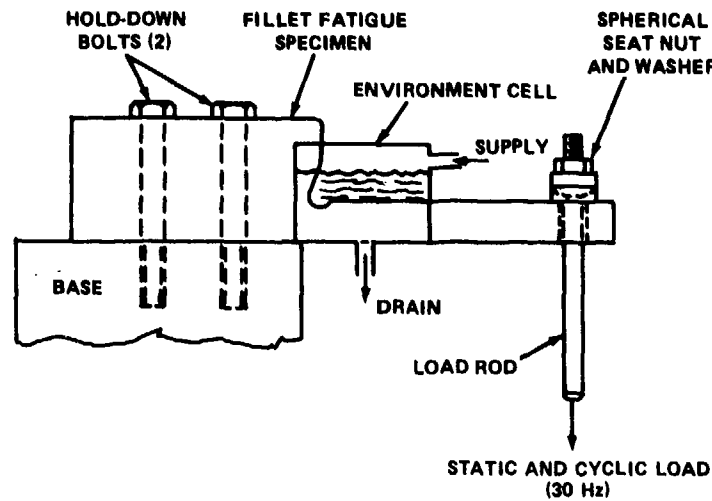
Figure 12a – Experimental Setup
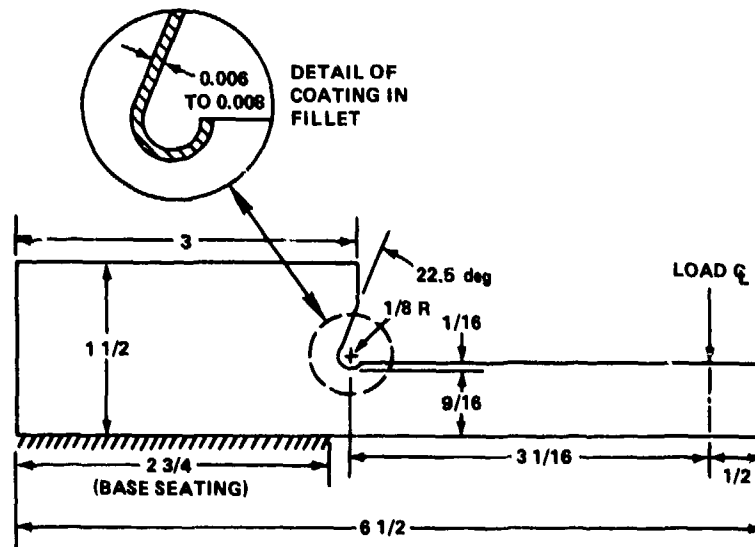
Figure 12b – Specimen (Nominal Dimensions in Inches)

Figure 12 – Schematic of Experimental Set-Up and Specimen for
Crank Ring Fillet Fatigue Test

approximately a one-third scale representation of the original SPRUANCE Class crank ring fillet geometry. The stress levels at which studies were conducted were similar to the mean and alternating stresses measured in the sea trials, Chapter II. An environmental chamber surrounded the test area through which 2190 TEP hydraulic oil, maintained at 120°F and contaminated with various volumes of seawater, was circulated.

Results for 4150H and HY-100 steel fillet studies are given in Table 6. Both

TABLE 6 – FILLET FATIGUE TEST RESULTS

Maximum Stress (ksi)	Mean Stress (ksi)	Cyclic Stress Amplitude (ksi)	100 Percent Oil (2190 TEP)		90 Percent Oil and 10 Percent Seawater	50 Percent Oil and 50 Percent Seawater	100 Percent Seawater		Coated Fillet* 100 Percent Seawater		Shot-Peened Fillet 100 Percent Seawater	
			4150H	HY-100	HY-100	HY-100	4150H	HY-100	4150H	HY-100	4150H	HY-100
102.6	56.0	46.6	1.26								0.38	
93.3	56.0	37.3	106.6**	30.0**	0.56		0.59		(E) 6.98***	(U)13.66***	23.21	
74.6	44.8	29.8						0.76				3.01
74.6	52.2	22.4					1.05		(E)11.27		4.67	
71.5	42.9	28.6				1.15			(U)41.89***			
70.9	51.0	19.9			2.54	1.23	4.87	2.74	(V)93.81**			
49.7	32.3	17.4					20.90		(U)75.55***	(E) 28.92	9.85	
49.7	39.8	9.9				17.83		22.22				
49.7	41.0	8.7					88.69		(E) 92.87**		52.97	
38.2	23.0	15.2				2.52		3.56				54.7**
38.2	24.9	13.3			19.10	8.55						41.41
28.6	17.4	11.2						53.16				
28.6	19.9	8.7						109.71**				
19.1	11.5	7.6						115.0**				

*Coating in fillet as follows: (E) epoxy, (U) urethane, (V) vulcanized rubber.

**Removed from test; did not fail.

***Failed outside of fillet in unprotected area.

steels performed similarly and demonstrated that even small volumes of seawater (10 percent) in hub oil can seriously degrade blade carrier fatigue strength.[27] Thus, in view of reported instances of seawater intrusion into CP propeller hubs,[1] it becomes imperative to consider methods for improving corrosion-fatigue resistance in highly stressed areas of blade carriers.

Surface cold-working is a convenient method for improving fatigue and corrosion fatigue strength in machine components.[30] Such processes (shot peening and cold

rolling) produce a surface layer of compressive residual stress which may delay the initiation of corrosion fatigue cracking. Studies were performed on rotating beam fatigue specimens of 4150H and HY-1' steels given shot peened and cold rolled test surfaces to optimum parameters for the materials.[27] The results of the corrosion fatigue tests as well as tests in air are given in Figure 8. The cold rolling increased fatigue life in saltwater by a factor of 2 for both alloys, while shot peening was ineffective. The compressive surface layer produced by shot peening was too thin and rapidly corroded. The layer from the cold rolling was deeper and required pitting and cracks to penetrate the layer prior to failure.[27] As previously noted, neither method of cold working affected fatigue life in air.

Surface protection methods such as plating, weld overlay and inlay, plasma spray, or metallizing, which decrease intrinsic fatigue strength, were not investigated. However, the application of three coating options were studied using the fillet fatigue test.[27] These were (a) epoxy coating, (b) urethane coating, and (c) vulcanized rubber; both (b) and (c) were applied as strain-gage protection on components in the instrumented trials, Chapter II. The results of the corrosion fatigue tests[27] showed that all three coating methods provided complete protection from seawater. In these studies the coatings were applied to conform to the fillet shape (thin layer) and terminate at the lip of the groove; see Figure 12. Failures occurred, however, when the maximum strain capability of the epoxy was exceeded and the coating cracked or due to faulty adhesion on one of the urethane coated items. Nondestructive examination of coatings applied in a fillet to detect poor adhesion or cracking is limited to visual inspection.

The advantages and disadvantages of each of the corrosion-fatigue improvement treatments considered are summarized in Table 7. Any of the coating treatments require application in the clean shop of an experienced vendor for optimum adhesion and properties. They are susceptible to damage in handling, and repairs also must be specially handled. However, a coating application is recommended (no type preference) over cold rolling in view of the special rigs, tooling, and process development required for cold rolling fillets.

CORROSION RESISTANT ALLOY BLADE CARRIERS

An alternative to methods of protecting or improving the corrosion-fatigue resistance of high strength steels was to consider alloys with inherent corrosion

277

TABLE 7 - STEEL CRANK RING FILLET AREA CORROSION FATIGUE IMPROVEMENT SUMMARY

Method	Advantage	Disadvantage
Cold Rolling	• Deep uniform compressive stress layer • Delays corrosion fatigue • Results in smooth surface finish	• Requires special tooling & jigging • Requires process development
Shot Peening	• Compressive stress surface layer • Easily applied to fillet areas • Delays corrosion fatigue	• Not as deep a compressive layer as cold rolling • Requires inspection for complete coverage
Urethane Coating	• Spray or brush application • Strippable with ease • Prevents corrosion fatigue if intact	• Visual inspection only for integrity • Possibly permeable at long exposure
Epoxy Coating	• Easily applied to fillet area • Not permeable • Prevents corrosion fatigue if intact	• Brittle coating, cracks at high strains • Not easily strippable • Visual inspection only for integrity
Vulcanized Rubber Coating	• Good adhesion • Field service proven • Prevents corrosion fatigue if intact	• Requires molds & curing in autoclave • Not easily strippable • Visual inspection only for integrity
Weld Inlay/Overlay	• Corrosion fatigue strength better than steel	• Low fatigue strength in oil/air compared to steel substrate • Possibility of weld defects, NDT unreliable for interface flaws
Plasma Spray Coating (Metal and Nonmetal)		• Require grit blast of substrate for adhesion • Porous coatings generally result • Little corrosion fatigue data

resistance. Forged bronzes, primarily Mn-Al bronze, have been used in some crank ring type CP propeller systems but strength of the material is limited.[1] For the high-power naval CP propeller, the selection of a nonferrous crank ring required a material with a yield strength of at least 100,000 psi and a toughness comparable to that required for steels of the same strength level. Primarily, the corrosion fatigue strength and corrosion resistance should be superior to steel.

A survey of alloys capable of meeting the requirements of steel forgings for crank rings but exceeding steels in corrosion fatigue strength was conducted. It was concluded that Alloy 718 (Inconel 718) was the best candidate to meet these requirements and was selected for further investigation.[31]

A thick-section disk forging of Alloy 718 was procured. Heat treatment studies were conducted to determine the optimum treatment to obtain the best combination of strength and toughness. The selected treatment and the properties obtained are given in Table 8, where they are compared to those established for steel forgings discussed in the preceeding section.

TABLE 8 - HEAT TREATMENT, MECHANICAL PROPERTIES, AND FRACTURE TOUGHNESS
OF INCONEL 718 FORGING

Inconel 718 Forging Heat Treatment

Solution Anneal: 1910°F, 1 hr, Air Cooled

Aging: 1320°F, 8 hr, Furnace Cooled to
1150°F, 10 hr, Air Cooled

Property	Inconel 718	4150H	HY-130
0.2 Percent Offset Yield Strength (ksi)	144.2	112.5	141.6
Ultimate Tensile Strength (ksi)	171.6	146.3	149.2
Upper Shelf Charpy V-Notch Impact Toughness (ft-lb)	40-80	7-11	44-70
5/8 Inch Dynamic Tear Toughness (ft-lb)	410	40-105	620
Elastic-Plastic Fracture Toughness, J_{IC} (in.-lb/in.^{2})	855	(115)*	795

*Estimated from K_{IC} value, Table 2.

Fatigue and corrosion-fatigue tests in saltwater were conducted in both smooth and notched conditions (K_t=1.3), and the results are shown in Figure 13. Fatigue strength in air and saltwater was below that expected for the alloy. In the heat treatment to optimize toughness, large grain size (about 0.20 mm average) developed in thick sections. The high cycle fatigue strength of Alloy 718 has been shown to
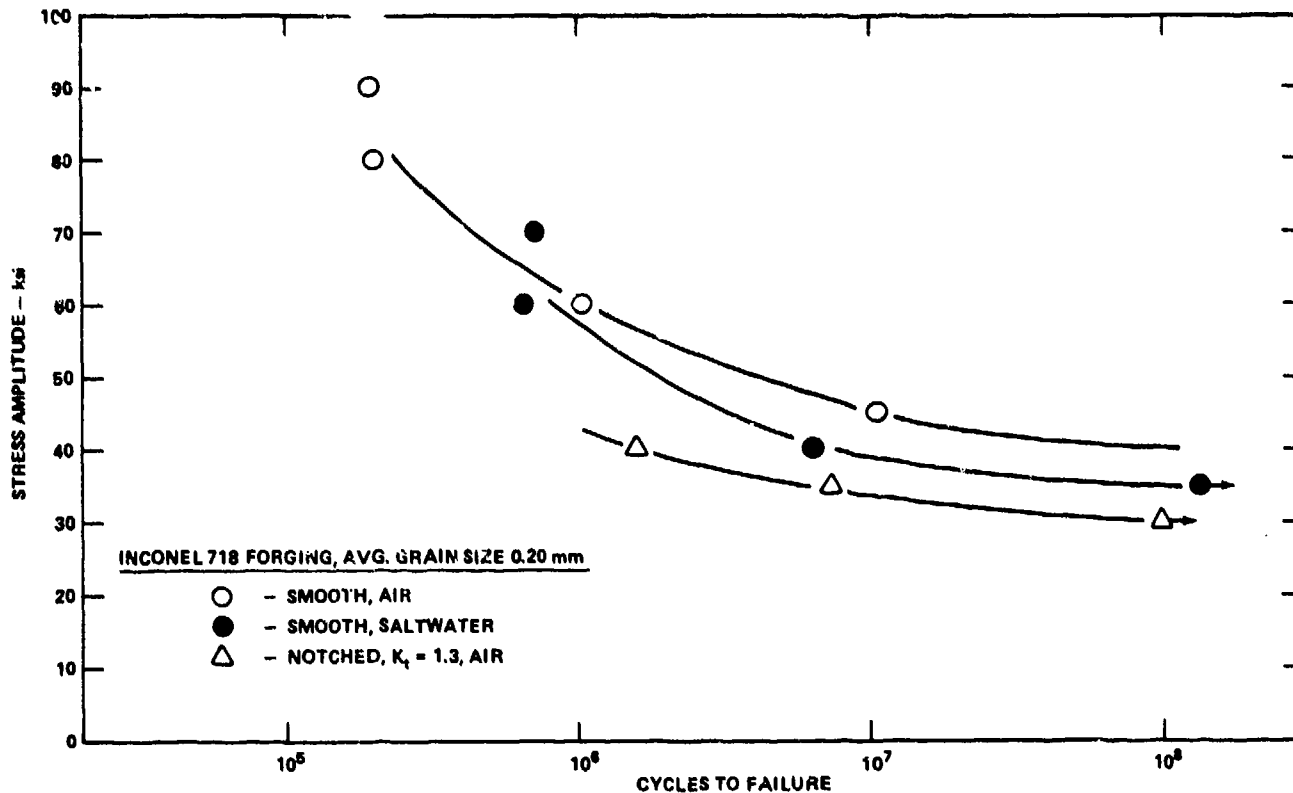
Figure 13 – Rotating Beam Fatigue and Corrosive Fatigue Test Results
for Inconel 718 Ring Forging

decrease significantly with increasing grain size.[31] The high-cycle fatigue pro-
perties of the Alloy 718 forging are compared to those of the steels investigated
in Table 9.

In summary, Alloy 718 satisfied the strength and toughness goals, but fatigue
strength at 10^8 cycles was only about 23 percent of the tensile strength as com-
pared to 40 to 45 percent of the tensile strength obtained with steel forgings.
Corrosion fatigue resis ince was significantly better than the steels; 20 percent
of the tensile strength compared to about 3 percent for steels. Of greater concern,
the cost of Alloy 718 was estimated to be near 10 times that of a low-alloy steel
forging. Use of the alloy could not be cost-effective when protected steels should
give acceptable durability.

TABLE 9 - COMPARISON OF HIGH-CYCLE FATIGUE AND CORROSION FATIGUE
PROPERTIES OF INCONEL 718 FORGING AND STEEL FORGINGS

	INCONEL 718	4150 H	HY-130
Ultimate Tensile Strength (ksi) - UTS	171.6	146.3	149.2
Fatigue Strength in Air at 10^8 Cycles (ksi) - FS	40	64	56
Ratio, FS/UTS	0.23	0.44	0.40
Fatigue Strength in Saltwater at 10^8 Cycles (ksi) - CFS	35	5	5
Ratio, CFS/UTS	0.20	0.03	0.03

BLADE BOLT MATERIALS

The CP propeller installation on BARBEY suffered fatigue cracking of the blade attachment bolts after approximately 1000 hours of operation. The 17-4 PH stainless steel bolts had failed in fatigue in the first two threads and all were located on the thrust side of the blade flange.[2,3] Subsequent stress trials on the BARBEY and SPRUANCE, Chapter II, showed that bolt load distribution on the thrust side of the blade flange (tension on the bolts) was nonuniform. Most of the load was carried by a single bolt; the location of failure in BARBEY. Investigation and discussion of the interaction of the blade fillet shape, blade palm thickness, and bolt location on the load and stress distribution on blade bolts is contained in Chapter V.

Bolt failures have also been reported[1] in other CP propeller service. Usually the inadequate application of preload or pretorque in bolt installation resulting in excessive cyclic load in the bolt was given as the reason for failure. Leakage past blade bolt O-rings[4] and bolt corrosion has occurred.[1] Corrosion fatigue failures of bolts are known but have not been documented.

BLADE BOLT MATERIALS

In general, CP propeller designers have chosen bolt alloys similar to the blade and hub alloy, i.e., bronze with bronze, stainless with stainless. However,

the strength of the best forged bronze bolts is insufficient for highly loaded propellers, such that the bolt size required is too large for practical assembly (torquing) or practical blade flange size. Stainless steels are prevalent in European CP propeller blade attachments, where wrought equivalents of the blade and hub cast alloys are used. Precipitation hardening 17-4 PH stainless has been used on BARBEY, ASHEVILLE Class, and WHEC 715 Class cutters. Low or medium alloy high strength steels have been used (initially on SPRUANCE) and require a protective capping system to prevent seawater penetration. Such systems may be unreliable.[1]

The initial selection of the blade bolt material is based on strength and corrosion resistance. Because the bolt must experience some level of cyclic loading (on the thrust side), the fatigue and corrosion fatigue strength must also be considered.

FATIGUE AND CORROSION FATIGUE PROPERTIES OF BLADE BOLT ALLOYS

For high-powered naval CP propeller designs, it is evident that high-strength bolt alloys will continue to be required, because the use of low-strength alloys would require large sizes or large numbers of bolts where installation, sizing, and load distribution problems develop. For the investigation, high-performance bolt materials of yield strength greater than 100,000 psi, high fatigue and corrosion fatigue strength, good seawater corrosion resistance, availability in diameters from 2 to 6 inches, and some fastener experience were surveyed.[32] The following alloys were selected for further study: K-Monel (Monel K-500), Inconel 718, 17-4 PH stainless steel, AF 1410 steel, titanium alloy 6A1-4V, and limited tests of 4140 steel (original SPRUANCE Class bolt alloy) for comparison. The properties of these alloys are given in Table 10.

These alloys were procured in large diameter bar for mechanical property and fatigue testing. As noted in studies of Alloy 718 forging for blade carriers, fatigue properties of nickel-base alloys are a function of grain size. Thus it was important to evaluate the K-Monel and Inconel 718 alloys in section sizes typical for the application. Fatigue and corrosion fatigue tests were conducted on smooth and notched rotating beam-type specimens. The notch used in these studies was a machined, circumferential V-groove to result in a theoretical stress concentration factor of $K_t = 3$. The stress concentration for machined screw threads of standard

TABLE 10 - COMPOSITION AND PROPERTIES OF BLADE BOLT ALLOYS

Alloy Common Name	Nominal Composition	Modulus of Elasticity (10^6 psi)	Yield Strength (ksi)	Ultimate Tensile Strength, UTS (ksi)	Fatigue Strength (FS) at 10^8 Cycles (ksi)	FS/UTS	Corrosion Fatigue Strength (CFS) at 10^8 Cycles (ksi)	CFS/UTS	Comments
AISI 4140*	Fe-0.40 C-1 Cr-0.2 Mo	29	90	125	70	0.56	8	0.06	Used in original Spruance Class CP propeller
Wrought Ni-Al Bronze	Cu-10 Al-5 Ni-3 Fe-1 Mn	17	50	100	35	0.35	30	0.30	Low strength, used in Newport Class CP propeller
17-4 PH H1150	Fe-17 Cr-4 Ni-4 Cu	29	100	135	65	0.48	20	0.15	Used in Barbey CP propeller
K Monel*	Ni-29 Cu-3 Al-1 Fe-0.5 Ti	26	100	160	40	0.25	20	0.13	Used in Spruance and Perry Classes, widely used for marine fastener applications
Inconel 625	Ni-22 Cr-9 Mo-4 Cb-3 Fe	30	60	120	55	0.46	45	0.37	Lower strength, no fastener experience
Ti-6 Al-4V*	Ti-6 Al-4V	16.5	125	135	55	0.41	50	0.37	Used in aerospace fastener applications
Inconel 718*	Ni-19 Cr-17 Fe-5 Cb-3 Mo-0.8 Ti-0.6 Al	30	180	200	80	0.40	60	0.30	Marine fastener and bolt experience
17-4 PH H925*	Fe-17 Cr-4 Ni-4 Cu	29	165	170	80	0.47	35	0.20	High strength heat treatment, representative of high strength PH steels
René 41	Ni-19 Cr-11 Co-10 Mo-3 Ti-1.5 Al	31.5	120	175	65	0.37	35	0.20	High temperature fasteners and bolt applications
AF 1410*	Fe-14 Co-10 Ni-2 Cr-1 Mo	29	150	210	80	0.38	5	0.02	Ultra strength steel for aerospace applications
MP 35 N	35 Ni-35 Co-20 Cr-10 Mo	33.5	255	285	100	0.35	50	0.17	Fastener alloy used on SES-100B CP propeller, costly. No large diam. experience

*Included in Blade Bolt Material Investigations.

form has been determined to be between 3 and 4.[33] The results are given in Figure 14 in which the fatigue notch sensitivity for the alloys is also shown.

Of particular note was the low fatigue strength of the K-Monel alloy in large section size. As noted earlier, the strength and fatigue properties of K-Monel are dependent upon the processing to obtain bar of a given section size.[32] Large diameter K-Monel bar must be hot-finished, whereas smaller bar is cold drawn. As a consequence, less work and larger grain size resulted in lower fatigue properties. Subsequent investigation of work hardened threads for K-Monel bolts was undertaken. The results for the high-strength alloys; Inconel 718, Ti-6Al-4V, AF-1410, and 17-4 PH-H900 demonstrate the high notch sensitivity of these materials. Such sensitivity makes it difficult to effectively use the high strength of such alloys. Therefore, studies into methods of improving the fatigue behavior of threaded bolts were performed.

In corrosion fatigue, the nickel alloys (K-Monel and Inconel 718) and Ti-6Al-4V are superior to the steels. Low corrosion fatigue strength was expected for the low alloy AISI 4140, but the high alloy content of 17-4 PH and AF-1410 was not effective in increasing corrosion fatigue resistance.

WORK HARDENED THREADS FOR BLADE BOLTS

Cold-roll formed or roll-worked threads have long been a method of obtaining fatigue resistant fasteners. The mechanism (involving work hardening, compressive residual stress, geometric factors, i.e., stress concentration factor) was not understood; therefore, it was not clear as to what properties make a material amenable to the process or how to optimize the process.

An investigation of cold rolling of threads using slipline field and finite element analyses was undertaken with experimental fatigue studies of roll-formed notches in K-Monel and Inconel 718 to verify analytical conclusions.[32,34] In the analytical study, the residual stress distribution around a plastically formed

Figure 14 - Fatigue and Corrosion Fatigue Properties of Blade Bolt Alloys

Figure 14 (Continued)

C. TI-6AI-4V

○ — SMOOTH, AIR
● — SMOOTH, SALTWATER
△ — NOTCHED, K_t = 3, AIR
▲ — NOTCHED, K_t = 3, SALTWATER

AT 10^8 CYCLES, K_f = 1.8, q = 0.4

SMOOTH, SALTWATER
SMOOTH, AIR
NOTCHED, AIR

STRESS AMPLITUDE — ksi

CYCLES TO FAILURE

D. INCONEL 718

○ — SMOOTH, AIR
● — SMOOTH, SALTWATER
△ — NOTCHED, K_t = 3, AIR
▲ — NOTCHED, K_t = 3, SALTWATER

SLASHED SYMBOLS FOR SPECIMENS FROM LARGE DIAM. BARS

AT 10^8 CYCLES, K_f = 3.2, q = 1.0

SMOOTH, AIR
SMOOTH, SALTWATER
NOTCHED, AIR

STRESS AMPLITUDE — ksi

CYCLES TO FAILURE

286
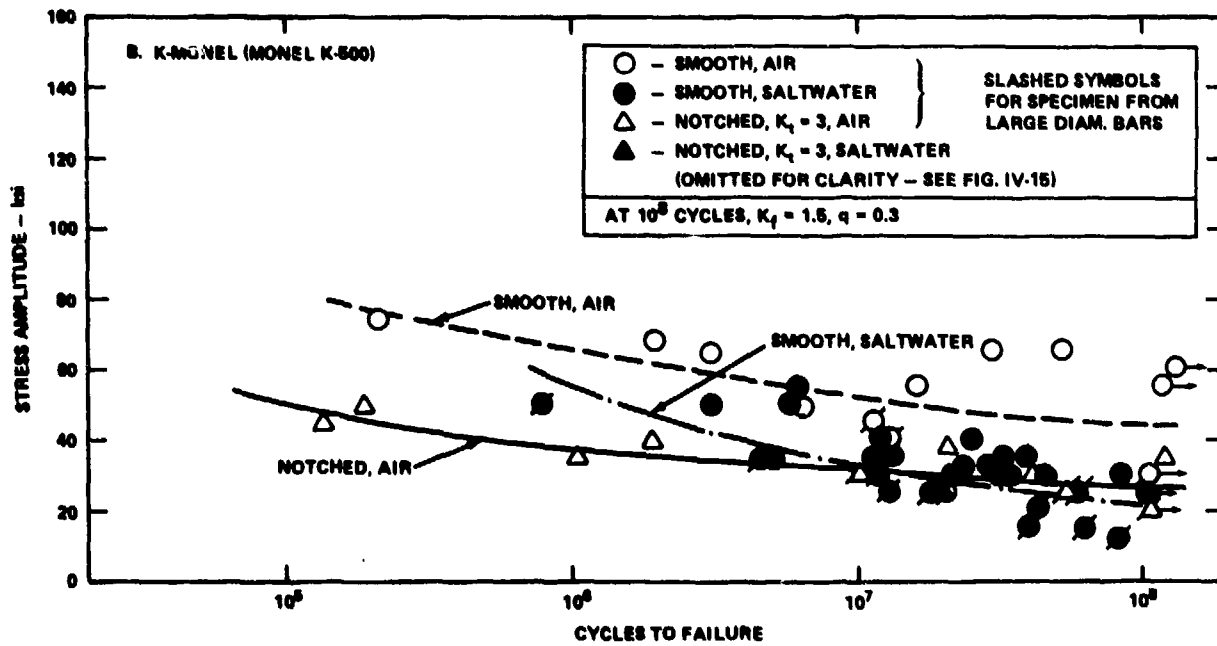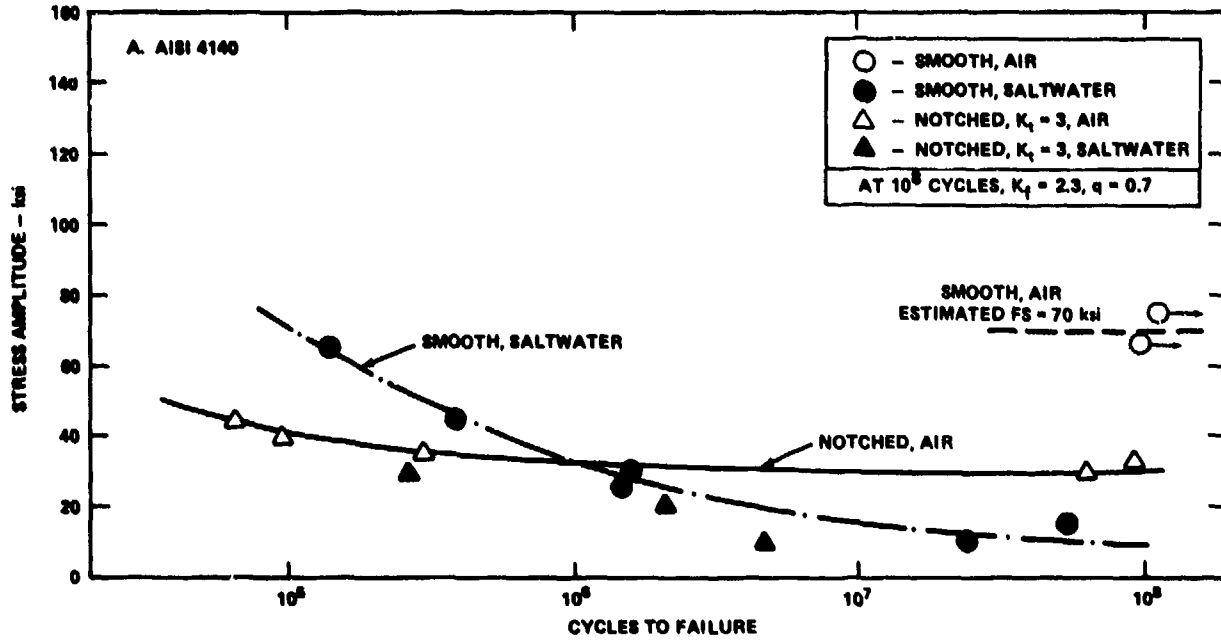
Figure 14 (Continued)

thread was mapped and showed an intense ....pressive region below the thread root
compensated by a region of tensile residual stress to the side of the thread.
Fatigue tests were conducted using specimens with cold-roll formed notches of the
same dimensions and profile as machined notches. The results of the fatigue tests
of rolled versus machined notches in K-Monel and Inconel 718 are shown in Figure 15.

Figure 15 - Fatigue and Corrosion Fatigue of K-Monel and Inconel 718
with Machined and Roll-Formed Notches

The path of fatigue crack growth in the rolled notches was not perpendicular to the
specimen axis with crack origin at the notch root as in the machined notches.

288
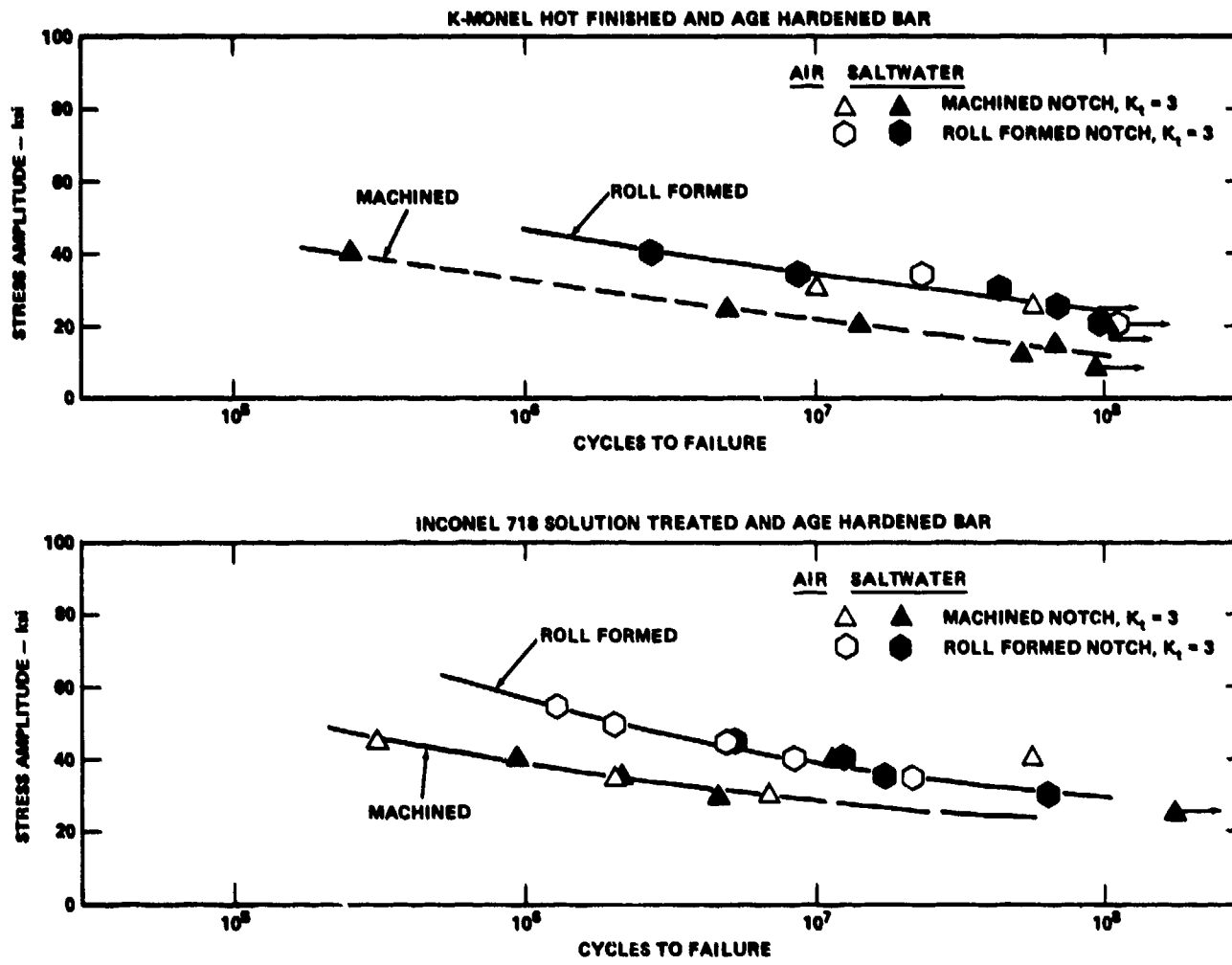
Instead, initiation and growth was altered by the residual stress pattern predicted.
Fatigue cracks initiated in the wall of the rolled notches (the region of tensile
residual stress) and grew at an angle to the specimen axis. This crack path
resulted in considerably longer fatigue lives for the rolled notch. The pattern of
fatigue crack origin and growth noted in the analytical and specimen studies were
also observed in the fracture of CP propeller bolts with rolled threads subjected
to fatigue tests.[32,35] The stress pattern, crack path, and failures of specimens
are shown in Figure 16.
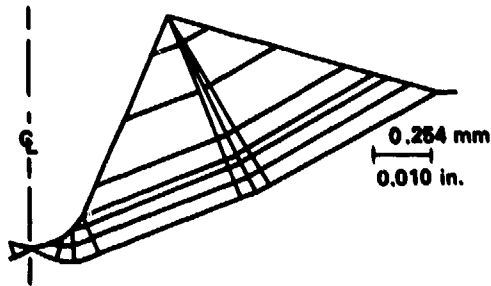
Figure 16a - Slip-Line Field
for Notch Indentation
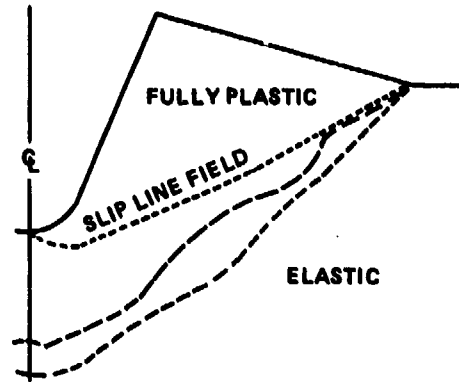
Figure 16b - Metallic State Resulting
from Notch Rolling Elastic--Stress
Below Proportional Limit
Plastic--Stress Greater
than Yield Stress
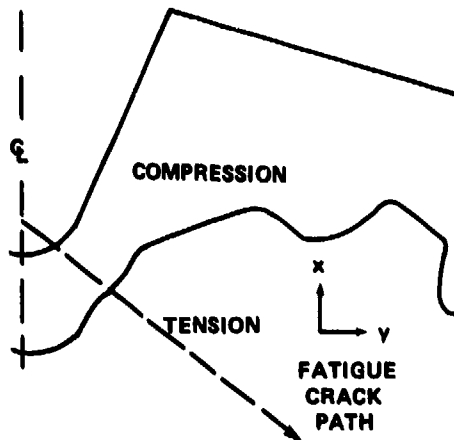
Figure 16c - Residual Stresses in the
Longitudinal Direction Resulting
from Notch Rolling
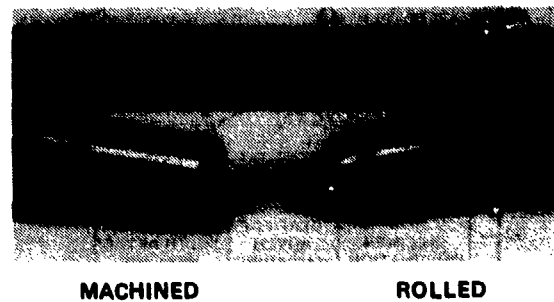
Figure 16d - Fracture Surfaces of
Notched Rotating Cantilever
Fatigue Specimens

Figure 16 - Analytical Development of Residual Stress State at Root of a
Roll-Formed Notch (A through C) and Fractures Typical of Fatigue
Specimen Failures with Machined and Roll-Formed Notches (D)

It was concluded that the process of roll forming of threads can be applied to any metal with a capacity for plastic flow. Fasteners with roll-formed threads are routinely made in titanium alloys, ultra high-strength steels, and superalloys such as MP35N.[32]

Although work-hardening of the metal and improved geometry contribute to the improved fatigue resistance of roll-formed threads, the residual stress distribution is the primary factor. Thread forming by this process is beneficial to the optimum only if performed after all heat treatments necessary to obtain the required material properties. Thus, for materials of very high strength, considerable power and tooling development may be required.

For materials of limited ductility, roll-forming of full, deep threads may cause microcracking in the surface layers and degrade fatigue resistance. Root rolling of high-strength, difficult to work metals was an option considered in the study.[32] Fatigue tests of partially machined and root-rolled-to-size notched specimens of Inconel 718 were conducted. The results, shown in Figure 17 indicate that fatigue
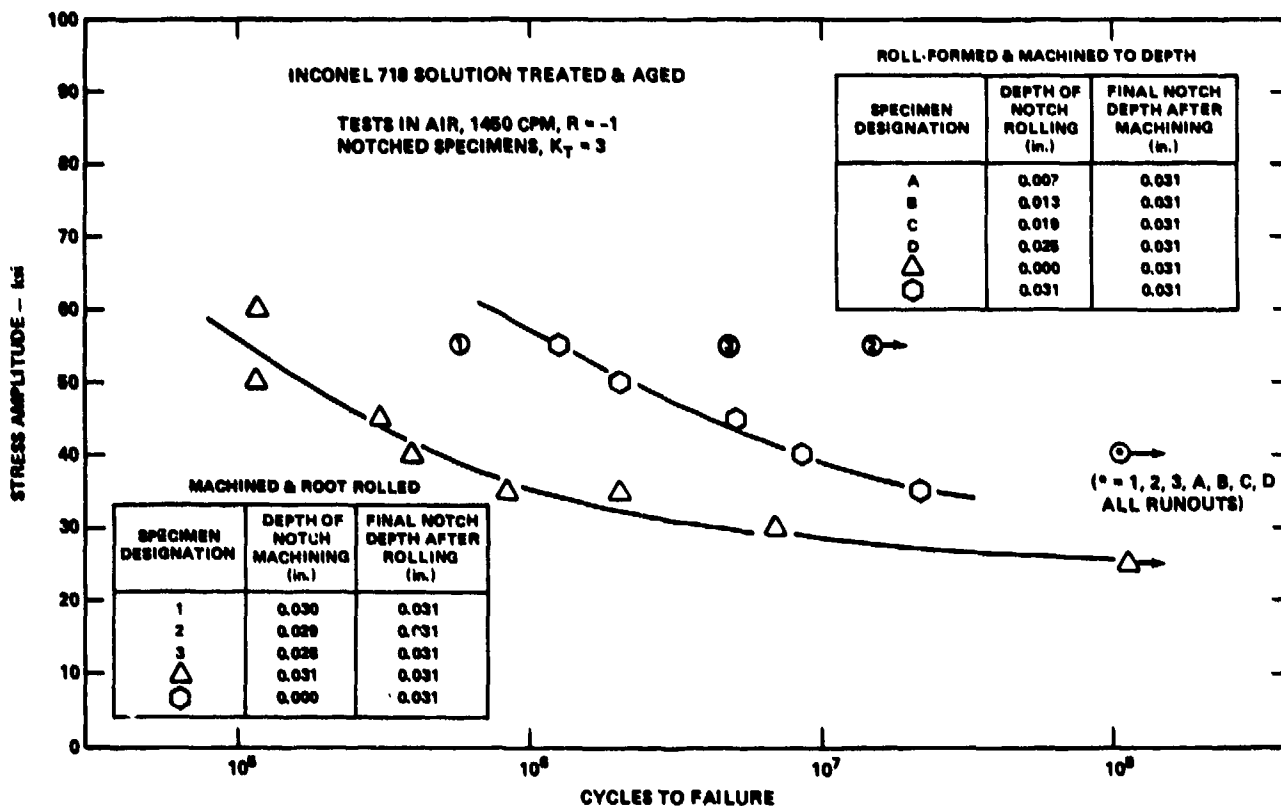
Figure 17 - Results of Fatigue Tests of Inconel 718 Specimens with Partially
Rolled and Machined Notches Compared to Fully Machined
and Fully Roll-Formed Notches

290

performance is better than for fully roll-formed notches. Such a process for bolt production would require development of parameters for different materials and thread sizes. Also, more steps in production are required. However, the results may provide the optimum for fatigue strength.

It is cautioned that fatigue tests with notched specimens are essentially qualitative, to compare various alloys, environmental factors, notch sensitivity, etc. The results may not be directly applicable in evaluating the performance of a full size bolt. Nevertheless, correlations of specimen data with full size bolt fatigue tests[35] have produced useful results.

GALVANIC COMPATIBILITY OF BOLT AND BLADE

The exposed bolt heads in a bolted-on CP propeller blade are but one part of a series of galvanic couples in the aft of a ship in the vicinity of the propeller. As a minimum, the zinc anodes are coupled to the steel hull, especially in the propeller vicinity to protect the steel. Current in this wet cell battery passes from the zincs through seawater to the blade and hub with bolts, through the shaft which is grounded to the hull to which the zincs are attached. The galvanic corrosion of the exposed bolt heads is of concern on the CP propeller. Such corrosion may cause deterioration of the bolt or of the blade flange in the local area surrounding the bolt head. Galvanic corrosion considerations were included for study in the research program[36] and are discussed in the following.

Basic material selection rules for seawater service are: (1) where possible use only one metal or alloy for all exposed components, (2) when not possible make the key components more noble (protected), and (3) expect and allow for corrosion on the less noble metal by providing a large area. The galvanic series in seawater indicates general tendencies to form galvanic cells. A series including the alloys considered for blades and bolts is given in Table 11 based on collected sources.[36] The alloys are grouped in the table, because within a given group there is little tendency to produce galvanic corrosion. The coupling of two metals distant from each other and in different groups may result in accelerated corrosion of the metal higher on the list.

The galvanic series only indicates the tendency of alloys to set up conditions for galvanic corrosion. Actual corrosion cannot proceed unless there is a flow of

291

TABLE 11 - ARRANGEMENT OF METALS AND ALLOYS IN GALVANIC SERIES IN SEAWATER

CORRODED END (ANODIC OR LEAST NOBLE)

Zinc

Aluminum Alloys

Steel and Iron

12 to 16 Percent Cr Martensitic Stainless Steels (Active)
and PH Stainless Alloys (Active)

18-8 Cr-Ni Austenitic Stainless Steel (Active)

$$\left\{\begin{array}{c} \text{Brasses} \\ \text{Bronzes} \\ \text{Nickel Aluminum Bronze} \\ \text{Copper-Nickel Alloys} \\ \text{Monel and K-Monel} \end{array}\right\}$$

12 to 16 Percent Cr Martensitic Stainless Steels (Passive)
and PH Stainless Alloys (Passive)

18-8 Cr-Ni Austenitic Stainless Steels (Passive)

$$\left\{\begin{array}{c} \text{Inconel 718} \\ \text{Titanium Alloys} \end{array}\right\}$$

Platinum

PROTECTED END (CATHODIC OR MOST NOBLE)

current. The factors involved are (1) conductivity of the circuit, (2) potential between the anode and cathode, (3) polarization of the surfaces, (4) relative anode and cathode surface areas, (5) geometrical relationship between the dissimilar metal surfaces, and (6) contact between the metals. In CP propeller systems the bolt and blade are intimately coupled, and the area ratio is in favor of the blade and hub alloy on the order of several hundred to one. Table 12 lists potential blade and

292

TABLE 12 - GALVANIC COMPATIBILITY OF POTENTIAL CONTROLLABLE PITCH
PROPELLER BLADE AND BLADE BOLT ALLOYS*

Blade Bolt Alloy	CPP Blade and Hub Alloy		
	Manganese Bronze	Stainless Steel (12-16 Percent Cr)	Nickel-Aluminum Bronze
Low Alloy High Strength Steel	U	U	U
12-14 Percent Cr Stainless Steel (AISI 410 or 416)	U	U	U
16-18 Percent Cr Stainless Steel (AISI 430)	U	U	U
Ni Al Bronze	Q	U	C
18-8 Cr-Ni Stainless Steel (3XX Types)	U	U	U
Monel	C	U	C
K Monel	C	U	C
18 Cr-12 Ni-Mo Stainless (316, 317)	Q	U	C
Inconel 625	C	U	C
Inconel 718	C	U	C
Titanium Alloys	C	U	C

*Metals in seawater over range of 40°-80°F, area ratio of blade to
bolt is very large, moderate seawater velocities

    U = Unfavorable, increased corrosion of one component
    Q = Questionable, uncertain
    C = Compatible

bolt combinations in which the area ratio largely in favor of the blade is recog-
nized. The combinations are rated as to galvanic compatibility.[36]

Although the bronze propeller alloys may be unfavorable in a one-to-one couple
with a noble alloy, as suggested in Table 11, the spreading of the galvanic effect
in seawater (an electrolyte of high conductivity) acts. The large area over which
to draw corrosion current minimizes deterioration of the large anode (blade and
hub) in the corrosion cell to protect the cathode (bolt heads) of the noble alloy.
In no case should the bolt head be anode to the blade, e.g., low alloy steel bolts
in a bronze blade.

Factors which also influence galvanic corrosion but are not apparent in a simplified look at bolt and blade alloys are (1) the effect of velocity and (2) the effect of the cathodic protection supplied by the zincs on the hull in the stern area. Studies of these variables were on-going for couples to Ni-Al bronze and the results were reviewed.[36]

In a study of the effect of velocity,[37] Ni-Al bronze was coupled to Monel 400, Inconel 625, and Ti-6Al-4V in 1-to-1 and 4-to-1 area ratios at seawater velocities from 0 to 13 ft/sec. It was concluded that the increased velocity led to more rapid polarization of the noble alloy. Corrosion rates in the Ni-Al bronze were less at higher velocity. Galvanic corrosion was more intense at low flow or stagnant conditions.

Studies of the effects of cathodic protection from -0.55V to -0.85V (zinc anode is about -1V) on couples of Ni-Al bronze to Monel 400 and Ti-6Al-4V in area ratios of 3-to-1 and 6-to-1 were conducted.[38] Except for the lowest level, where protection was incomplete, all other levels provided corrosion protection for the Ni-Al bronze in all coupled situations.[38]

The zinc anodes in the stern located to protect the hull from accelerated corrosion in the vicinity of the propeller drive a large current into the propeller, as evidenced by propeller fouling. Some slight corrosion of copper alloys with the release of copper ions is necessary for antifouling properties. This cathodic protection overides the simple galvanic couples considered. Stainless steel bolts have been successfully used with bronze propellers because the cathodic protection keeps the alloys in the passive state.[36]

In summary, the selection of any alloy which lies in the group of the blade and hub alloy or more noble in the galvanic series in seawater is a suitable bolt alloy from a corrosion standpoint. No adverse effect on the blade material from a more noble bolt alloy can be expected. In no case should an alloy higher in the series than the blade material be considered for bolts unless protection ·s provided.

BLADE BOLT AND BLADE CARRIER THREAD FRICTION

Four variables are involved in the torque-tension relationship or tightening characteristics of a bolt in a nut: (1) the thread surfaces, (2) lubrication, (3) the materials of the two rubbing surfaces, and (4) conditions under the bolt head seating. Whether torque or turn angle are used in setting preload, the combination of the variables, i.e., joint friction, may be of concern in highly preloaded joints

of high strength alloys. Use of stainless steels, titanium alloys, or high nickel
alloys may cause seizing or galling in the threads with repeated use.

Galling (also termed scoring, seizing, scuffing) is adhesive wear in the
extreme. It occurs when two mating metallic surfaces slide against each other under
pressure. Microscopic projections bond at the sliding interface. Subsequently,
the sliding forces fracture the bonds and tear metal from one surface and transfer
it to the other. Galling of titanium threaded fasteners in airframe construction
has required the use of steel nuts and special treatments of the threads.[36]

No standard tests are used to evaluate galling resistance. For the candidate
bolt alloys in this investigation, joint friction was evaluated using the torque-
tension test (similar to SAE procedure J174). The slope of the torque-tension
line was determined for various conditions and inspection of the representative
bolts was conducted after the test runs. Test conditions and materials are given
in Table 13, with the results of the three runs of torque-tension measurement for

TABLE 13 - RESULTS OF TORQUE-TENSION TESTS FOR JOINT FRICTION

Thread Lubrication	Test Nuts (2) \ Test Bolts (1)	Mean Slope of Torque-Tension on Loading, in.-lb/lb (3 Runs, Nickel-Aluminum Bronze Washers)				
		AISI 4140 Steel	17-4 PH H1150	K-Monel	Inconel 718	Titanium 6Al-4V
Unlubricated	AISI 4150H	0.171	0.203	0.267	0.247	0.200
	HY-100	0.098	0.194	0.203	0.252	0.206
	Inconel 718	0.190	0.206	0.293	0.283	0.282
Lubricated Molycote "G"	AISI 4150H	0.104	0.080	0.076	0.095	0.170
	HY-100	0.092	0.094	0.082	0.118	0.158
	Inconel 718	0.092	0.133	0.097	0.192	0.212
Polysulphide Sealant "PRC-1421" [MIL-S-880 Class B]	AISI 4150H	0.170	0.154	0.157	0.143	0.185
	HY-100	0.114	0.191	0.125	0.181	0.173
	Inconel 718	0.165	0.191	0.218	0.158	0.153
Theoretical Slope for Steel Bolt, Nut, & Washer (Coefficient of Friction, Steel Against Steel = 0.12)		0.103				
Theoretical Slope Zero Friction		0.017				

(1) 5/8 - 11 UNC 2A Hex Cap Screw.
(2) 5/8 - 11 UNC 2B Hex Thick Nut.

each set of variables. In these tests, a low slope (tension load induced per unit torque) indicated high joint friction, as compared to a theoretical zero friction line.

In the tests, all bolts were of the same size (5/8-11 NC) and finish with no special treatments used on the threads or nuts. Lubrication effects were studied as was the use of a polysulphide sealant on the threads. The latter was considered as a measure to prevent water entry to the internal threads of a steel blade carrier should seawater enter the hub.[36] In addition to varying bolt alloy, nuts representing three possible blade carrier alloys were used. Nickel-aluminum bronze washers were used to represent seating against a blade flange bolt hole.

The torque-tension tests were conducted to a limit equivalent to 75 percent of the bolt material yield strength in tension in the shank. No galling of the threads was observed. However, the high joint friction developed in the titanium alloy bolt with various nuts and the nickel alloy (Inconel 718 and K-Monel) bolts in the Inconel 718 nuts.

PITCH-CHANGE BEARING MATERIALS

During a full-scale fatigue test of a SPRUANCE Class CP propeller hub using service measured loads (discussed in Chapter V), degradation of the bearing surface between the crank ring blade carrier and internal bearing ring was found after one million cycles of load near those measured in a full power turn.[27] Deterioration of the Al-bronze overlay on the bearing ring and a transfer on the steel mating surface about 1 mm thick occurred. The test was conducted with the blade fixed, and no sliding under load, as occurs in pitch change, was performed.

Subsequent inspection of SPRUANCE after one year service showed similar but less severe transfer of bronze to the steel crank ring.[1] Also, after BARBEY operated 1400 hr limited to a maximum of 90 percent full power, inspection after removal of the CP propeller revealed transfer of bronze from the hub body (no separate bearing rings) to the steel crank disk.[2] Generally, degradation of both bearing and crank ring mating surfaces occurred on those LST 1179 class hubs where seawater had entered the hub oil. In mild cases, remachining of the bearing surfaces is required; replacement of the crank rings is required in extreme cases.[1,4]

Bearing wear in commercial service has been described as a problem in highly loaded hubs or in trawlers where frequent, continuous pitch-changing is required for station-keeping.[1] Increased wear due to seawater intrusion into the hub has been reported by others and bronze blade carriers are promoted for harsh service.

Thus, two bearing related problems were studied: (1) bearing bronze transfer and buildup as a consequence of a highly-loaded CP propeller operating at fixed pitch, and (2) high wear rate overall where seawater had entered the hub oil.

BEARING MATERIALS

Two practices are used by designers of CP propeller mechanisms for pitch change bearings. One is to use the hub body directly with no separate bearings, while others use separate bearing rings or pieces. The latter method may use a separately cast or wrought piece of bronze alloy for the bearing surface or an overlay of bronze alloy on a substantial bearing ring of steel. Where no separate bearings are used, the hubs are bronze. The use of separate bearing pieces seemed to be the practice of designers whose hub and blade alloys were commonly cast stainless steel.[1]

In any case the pitch change bearings are generally bronze against steel blade carriers or bronze against bronze blade carriers. No use of special or composite bearing materials being used in CP propeller pitch change mechanisms is known. Steel blade carrier bearing surfaces, however, are sometimes nitrided or otherwise specially hardened.

The loading of the pitch change bearing under the usual, ahead condition is reaction against the blade carrier to the propulsive forces. This is a combined static and cyclic load. When bolt load distribution is nonuniform, load distribution along the bearing surface will be nonuniform.[28] The pitch change is a high load, low speed operation. It is required that the bearing, with hub oil as a lubricant, provide smooth rotation of the blades without adding substantial resistance to the spindle torque which the hydraulic system must move.

Bearing deterioration and transfer (buildup) on the bearing surface to a degree which would cause overpressure or problems in the hydraulic system due to increased friction or seizure of the mechanism must be prevented.

297

The designers of CP propeller systems attempt to limit the bearing pressure. The values reported, however, vary from 3500 psi to 7000 psi.[1] Peak transient pressure may be two or three times greater in magnitude.

SMALL-SCALE FRICTION AND WEAR STUDIES

Preliminary small-scale friction and wear studies were conducted using a conventional wear tester (constant unidirectional speed) on materials used in the bearings of BARBEY and SPRUANCE Class CP propellers.[39] These tests did not include steady plus unsteady load or reciprocating motion and, therefore, were not representative of service conditions. A speed of 1.8 in./sec was used with lubrication by a 2190 TEP fluid at bearing pressures ranging from 4700 psi to 8600 psi. The results indicated that Ni-Al bronze, high-tin bronze, and Al bronze weld overlay against steel (HY-100 or AISI 4340) were all satisfactory. The coefficient of friction ranged from 0.10 to 0.15, and the surface finish of the steel was found to be an important factor. Rougher finish (35 to 50 CLA) showing the highest friction coefficient; approaching 0.20.[39]

Another small-scale wear test directed to CP propeller material selection has been reported[40] where Ni-Al bronze or Mn-Al bronze against steel and Mn-Al bronze against itself were evaluated. Contact pressures of 5,000, 10,000, 15,000, and 20,000 psi were used at a speed of 0.8 in./sec in hub oil. Normal pitch change speeds in service are less than 1.4 in./sec. The nature of the wear behavior was a break-in period followed by a steady-state condition. Based on the wear results (weight loss), the best combination was Mn-Al bronze against itself. Nickel-aluminum bronze against steel ranked second, and lastly Mn-Al bronze against steel. However, Ni-Al bronze tended to seize in these tests at 15,000 psi and above. The other pairs did not seize under any conditions of test.

Small-scale tests as described are useful for investigation of wear mechanisms and to provide a means of ranking the friction and wear (tribological) characteristics of bearing material combinations. A bench-scale simulator was developed for this purpose suited to studies of CP propeller pitch change bearings.[41] A schematic of the apparatus and the bearing pair specimens are shown in Figure 18 where the test variables are also described.

Figure 18a – Schematic Diagram of Small-Scale Bearing Tester
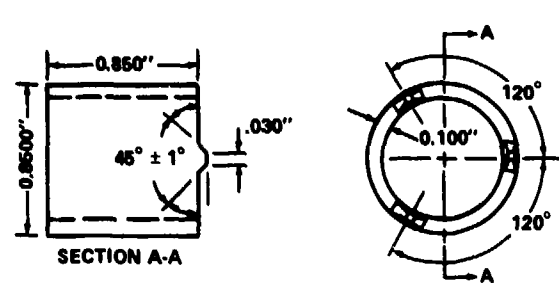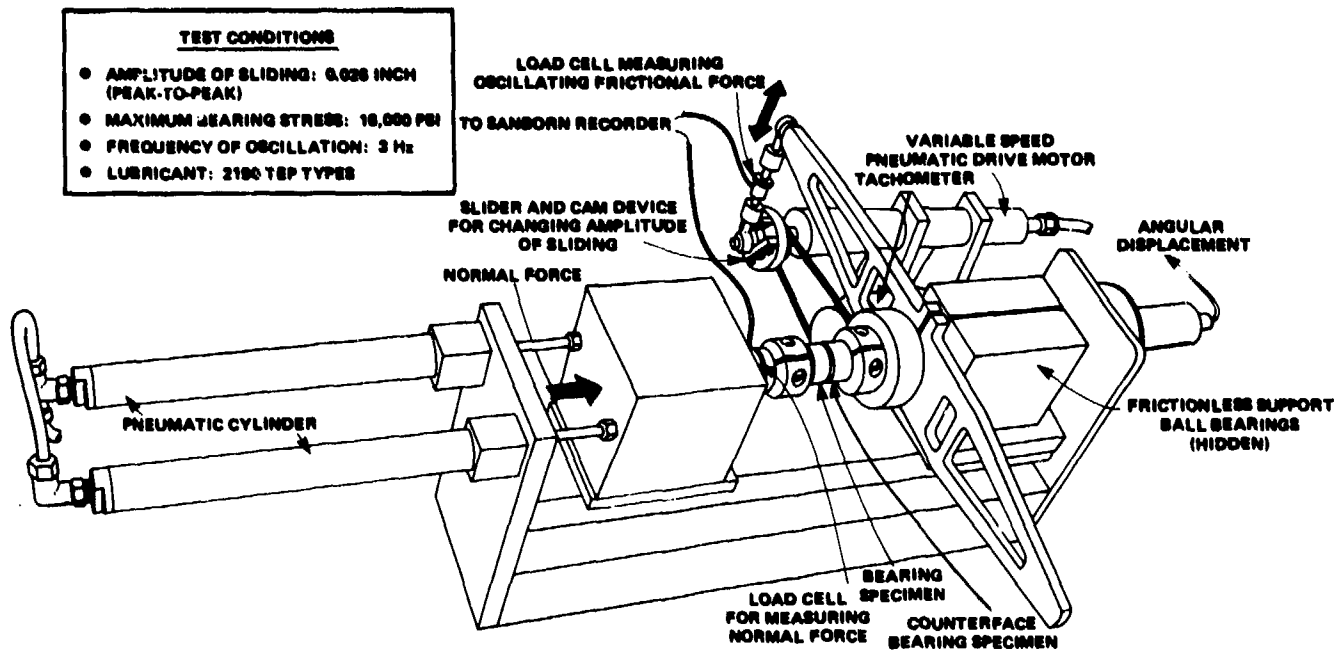
MATERIALS

AL BRONZE WELD OVERLAY
CAST AL BRONZE
CAST NI AL BRONZE
CAST HIGH TIN BRONZE
CAST MN AL BRONZE
DU(B) COMPOSITE/BRONZE BACKED
AL BRONZE – FORGED
LEADED TIN BRONZE

Figure 18b – Bearing Material Specimen
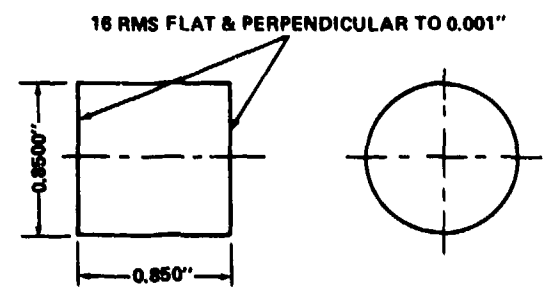
MATERIALS

AISI 4150H STEEL
INCONEL 718
HY-100 STEEL
MN AL BRONZE
AL BRONZE – FORGED
4150H STEEL – NITRIDE

Figure 18c – Blade Carrier (Crank Ring)
Material Specimen

Figure 18 – Small-Scale Controllable Pitch Propeller Bearing
Tester and Test Specimens

In tests conducted with the bench-scale simulator, bronze bearing alloys against steels typically showed a wear mechanism in which four stages were evident.[41] These are described in the following and are graphically shown in Figure 19 where
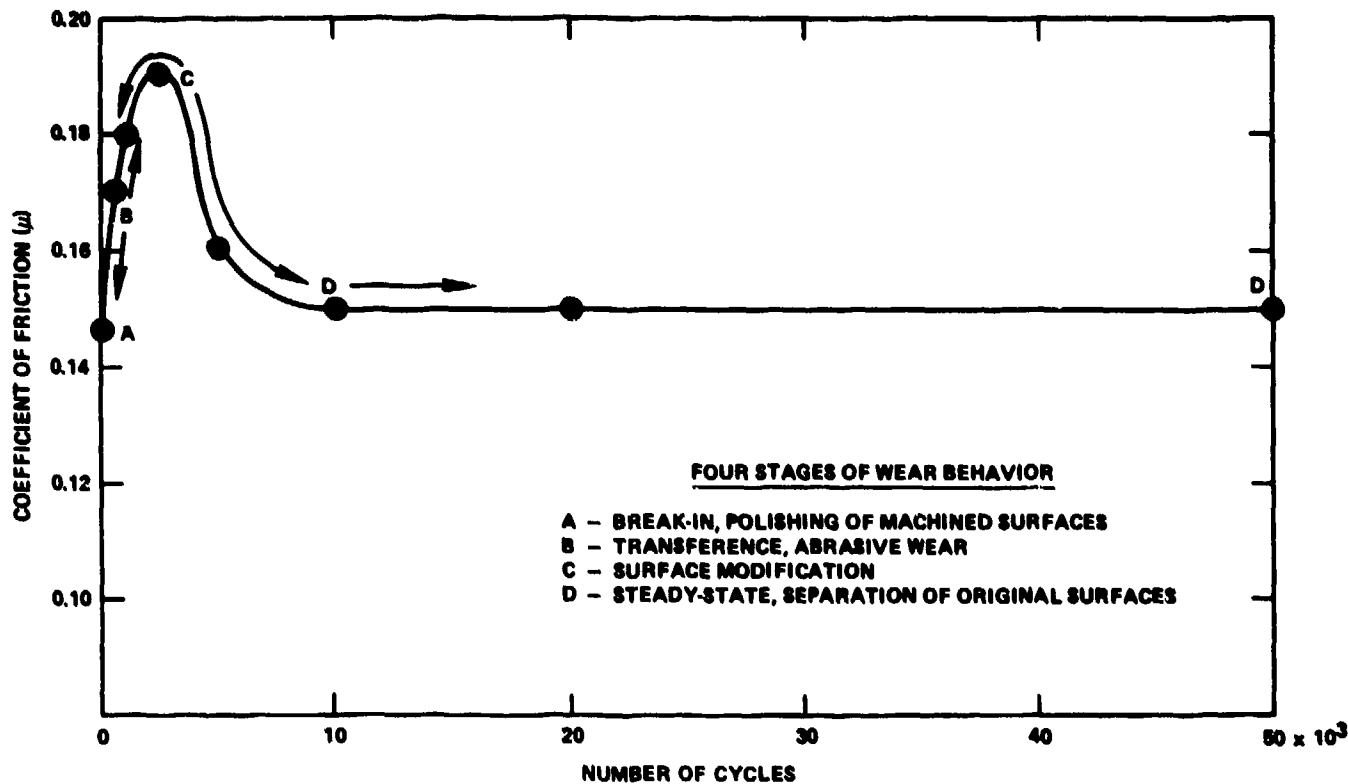
Figure 19 - Typical Friction versus Cycles of Wear for Bronze Against Steel Sliding Couples Showing Four Stages of Wear, Small-Scale Tester

coefficient of friction is plotted versus wear cycles:

A. An initial wear process which may be described as a "polishing" of the initial surfaces;

B. A transference stage in which bronze attaches to the steel counterface by adhesion and/or mechanical interlocking with an increase in coefficient of friction;

C. Rubbing of bearing bronze against transfer particles of bronze attached to the counterface steel in (B) eventually leading to a complete separation of the original surfaces (surface modification stage);

300

D. A steady-state region of lower friction and wear rate with enhanced
lubrication and smooth sliding.

During the transference stage (B), localized abrasive wear predominates on the steel
surfaces surrounding the transfer particles. The steel counterface at this stage
is shown in the scanning electron micrograph as in Figure 20. When transference
progresses to complete surface modification (C), the coefficient of friction peaks
and drops as the abrasive process ceases.

The change in coefficient of friction with accumulated cycles and the wear of
the bearing alloy measured by weight loss is shown in Figure 21 for the Al-bronze
overlay against 4150H steel sliding couple. Note the early achievement of steady-
state conditions and the low wear rate. Photomicrographs of the bearing and counter-
face surfaces during the stages of wear in the bench-scale tester are given in
Figure 22. (Note the polishing of machined surfaces, followed by transference of
bronze to adhesive wear particles on the steel counterface, and the eventual buildup
of bronze on the counterface.)

Studies of bronze against bronze sliding couples showed that the stages of
transference and surface modification (B and C) were not present. The initial
stage of friction rise and wear occurs when the as-machined surfaces are polishing;
then, steady-state conditions are established which are the same as the latter stage
of the bronze on steel couple. The behavior of the bronze against bronze couples
is shown in Figure 23.

Surface finish had a large influence on relative initial wear (break-in) of the
bronze against steel bearing pairs. Rougher bearing material surfaces caused
higher bearing alloy weight losses and total wear for a given cyclic life than
smoother initial surfaces. However, after the steady-state stage was achieved, the
coefficient of friction and wear rate were the same; independent of initial surface
finish.[41]

Table 14 summarizes the parameters measured in the bench-scale studies and the
sliding couples tested. Note that the high-tin and leaded tin bronzes offer low
coefficients of friction as do DU(B) and Karon, composite surfacing materials to be
discussed later in this section.

An investigation of Al-bronze overlay bearing against HY-100 steel sliding
couple with various base oils was conducted. All the oils qualified under the 2190

301

A — ABRADED STEEL SURFACE
B — AGGLOMERATION OF ABRADED STEEL DEBRIS
C — ALUMINUM BRONZE TRANSFERRED PARTICLE
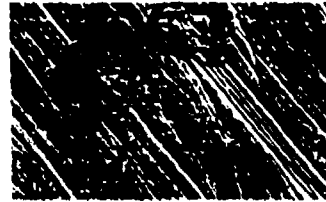
200X

2000X

Figure 20 – Scanning Electron Photomicrograph of Steel Counterface
at Transference Stage (B) in Wear Against Aluminum Bronze
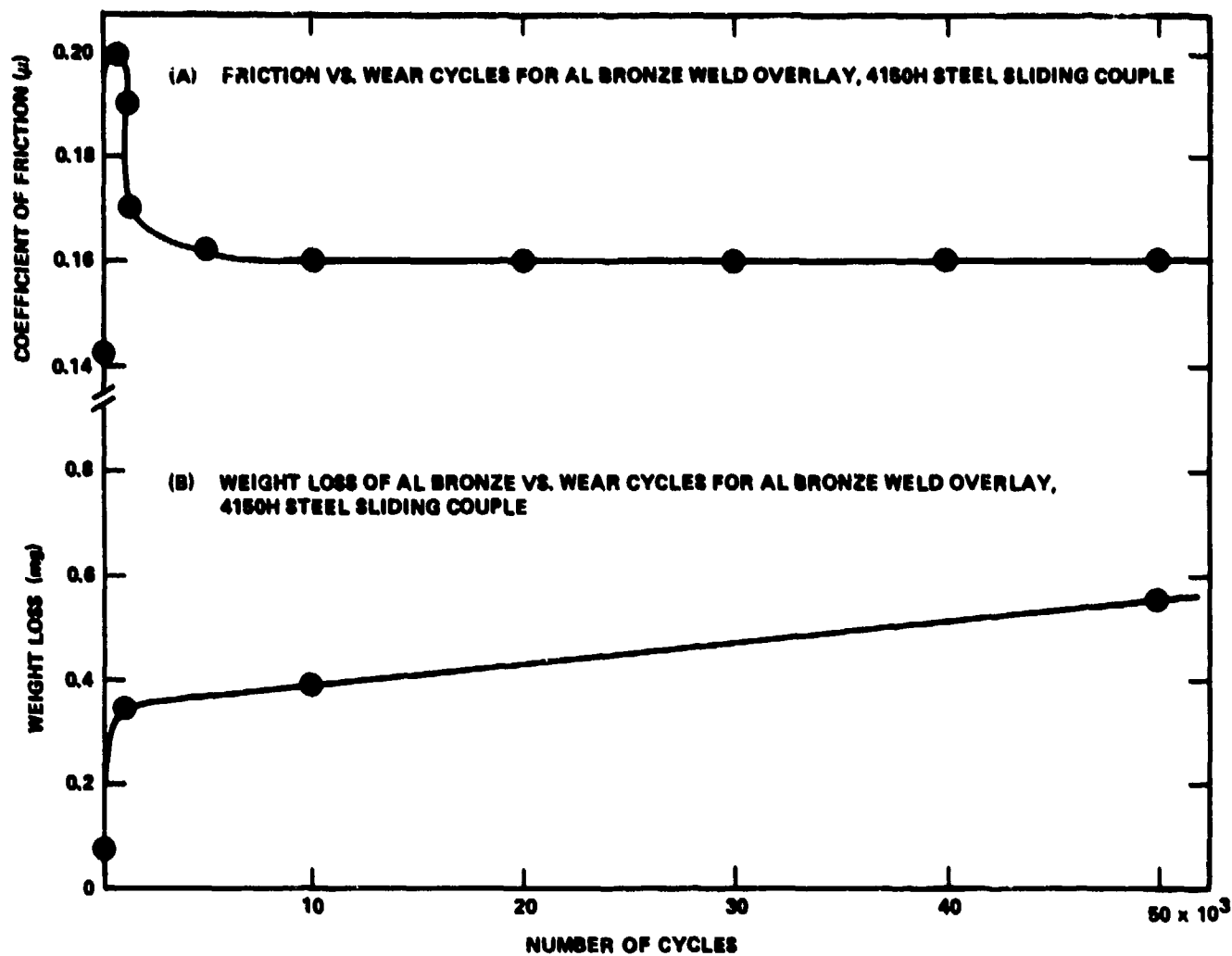
Figure 21 - Change in Coefficient of Friction and Weight Loss in Bearing
During Small-Scale Bearing Test of Aluminum Bronze Weld
Overlay Against 4150H Steel Sliding Couple

TEP classification. The results showed negligible differences among the lubricants
used. More reactive oils, those containing surface active additives, produced a
slightly greater weight loss and coefficient of friction than an inert oil such
as mineral oil.[41] Studies of the effect of water contamination were unsuccessful,
because oil and water separated leaving only bearing oil on the small bearing
surfaces.

ALUMINUM BRONZE (WELD OVERLAY) FACE, 200×

INITIAL A (10² cycles) B (10³ cycles) C (10⁴ cycles) D (0.5×10⁵ cycles)
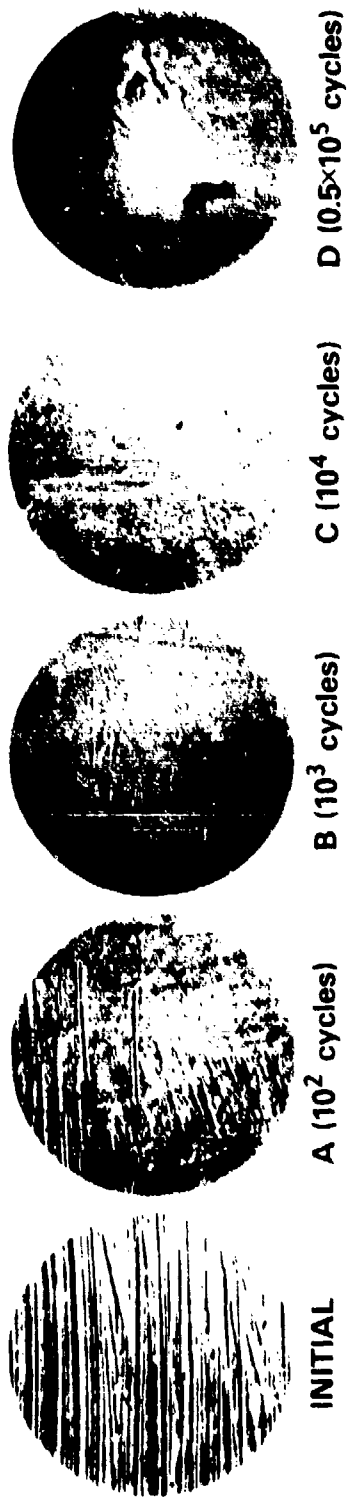
STEEL COUNTERFACE, 200×
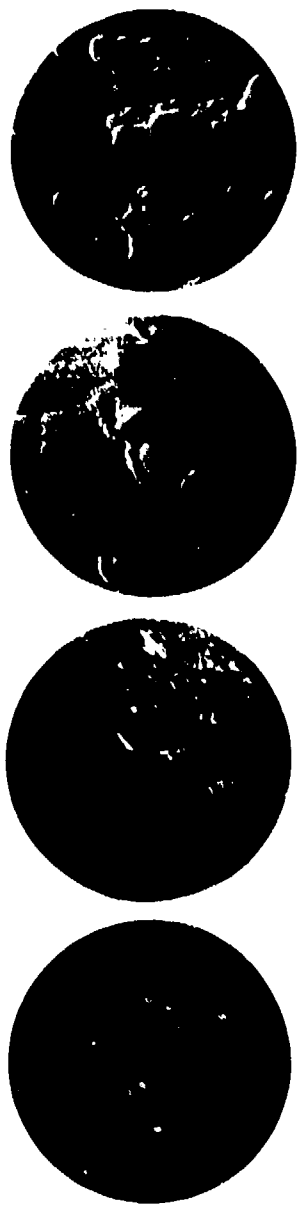
Figure 22 – Scanning Electron Photomicrographs of Aluminum Bronze Bearing and Steel Counterface for Wear Stages A, B, C, and D

304
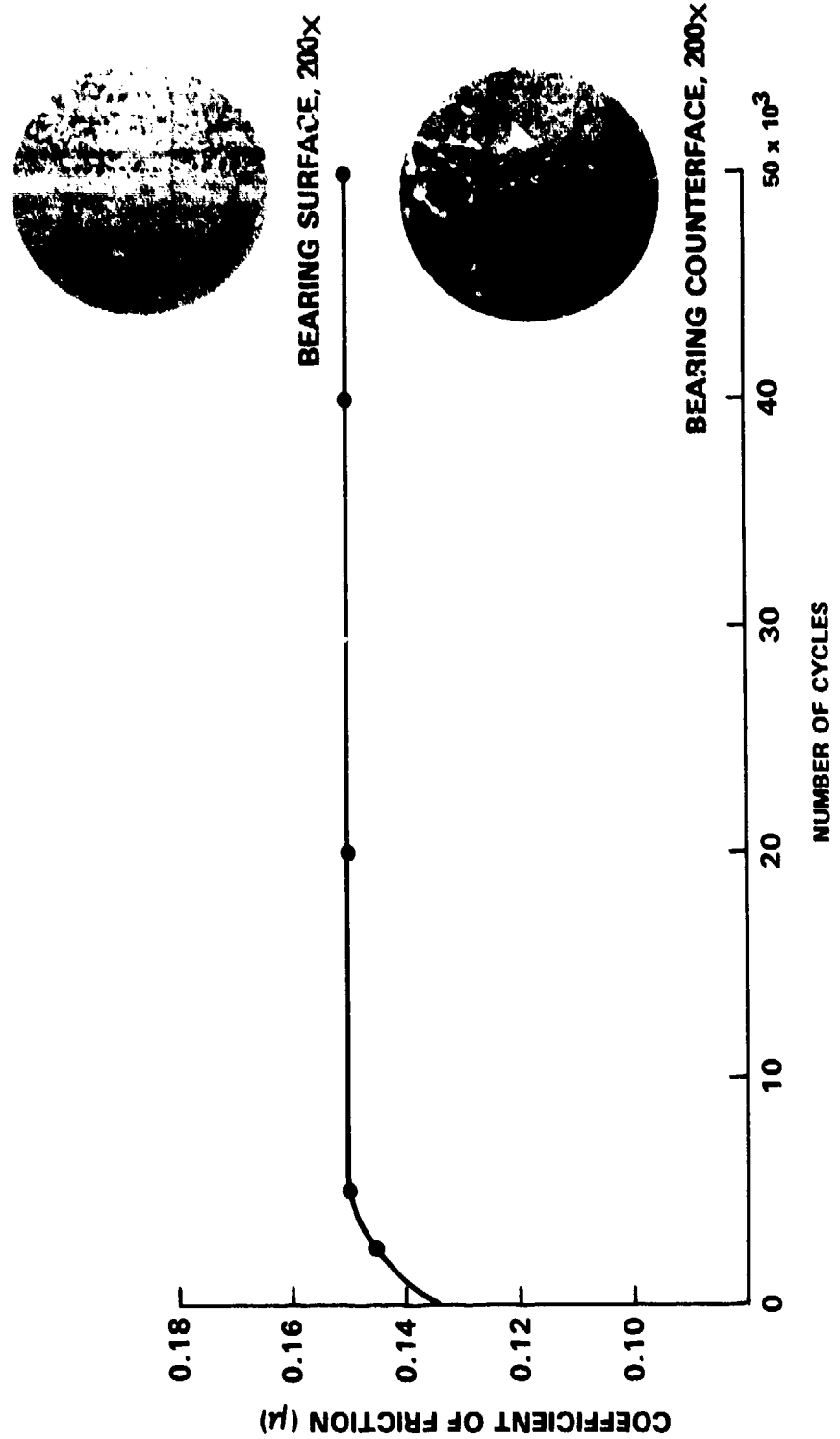
Figure 23 — Friction versus Wear Cycles for Aluminum Bronze versus Aluminum Bronze Sliding Couple

TABLE 14 - RESULTS OF SLIDING COUPLE FRICTION AND WEAR TESTS
IN SMALL-SCALE TESTER

Bearing Material	Counterface Material	Maximum Coefficient of Friction* (Break-In)	Steady-State Coefficient of Friction*	Steady-State Wear Rate ($mg/cycle \times 10^{-6}$)
Al Bronze Overlay	4150H Steel	0.20	0.16	1.32
Forged Al Bronze		0.21	0.16	1.32
High Tin Bronze		-	0.12	0.42
Leaded Tin Bronze		-	0.13	0.58
High Tin Bronze	Nitrided 4150H	-	0.12	0.42
Al Bronze Overlay	HY-100 Steel	0.20	0.16	1.32
Forged Al Bronze		0.18	0.16	1.32
Mn-Al Bronze		0.22	0.17	1.68
High Tin Bronze		-	0.12	0.42
OFHC Copper		-	0.24	6.60
DU(B)		0.06	0.06	Nil
Al Bronze Overlay	Forged Al Bronze	0.15	0.15	1.02
Al Bronze Overlay	Al Bronze Overlay	0.15	0.15	1.02
Mn-Al Bronze	Mn-Al Bronze	0.15	0.15	1.02
Al Bronze Overlay	Inconel 718	0.22	0.20	3.20
DU(B)	Inconel 718	0.06	0.06	Nil
OFHC Copper	Inconel 718	-	0.32	21.0
KARON	HY-100	0.07	0.07	Nil

*Reproducible to ± 10%

Lubricant: 2190 TEP (Texaco VSI Oil)
Duration of Tests: 50,000 Cycles
Bearing Pressure: 16,000 psi
Surface Finish of Bearing: 16 rms or Less
Surface Finish of Counterface: 32 rms or Less

LARGE-SCALE BEARING PERFORMANCE STUDIES

In order to more closely simulate the loads (contact stresses), motions (contact strains), and lubricant environment present in-service in CP propeller bearing operation, a large-scale simulator was constructed.[42] Dimensions of specimens and applied loads were approximately one-third scale with reference to the SPRUANCE Class pitch change bearing. A schematic of the large-scale test rig is shown in Figure 24. Two loading conditions were used based on (1) full power ahead loads

306

NORMAL (STEADY) LOAD

BALL JOINT LOCATION
(HIDDEN)

FORCE
TRANSDUCER
(TO RECORDER)

UPPER BEARING
SPECIMEN
(CRANK RING)

TOTAL BEARING LOAD
CELL/FRICTIONAL
TORQUE
(TO RECORDER)

LOWER BEARING
SPECIMEN

CYCLIC
(HYDRODYNAMIC)
LOAD

FORCE
TRANSDUCER
(TO RECORDER)

FLEXIBLE JOINT
(RUBBER)

ROTARY
DISPLACEMENT
CONTROLLER

ROTARY
ACTUATION
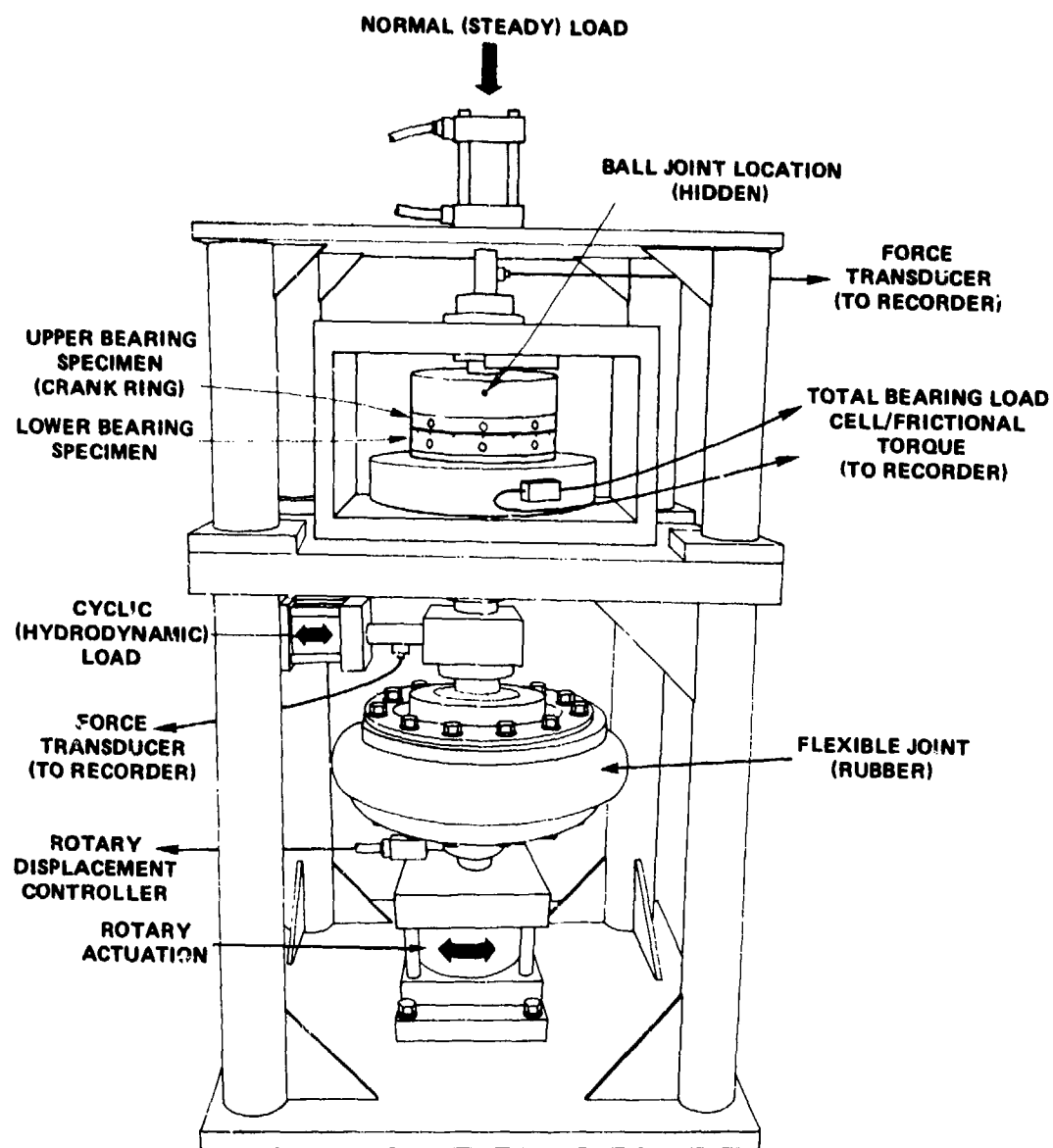
Figure 24 - Schematic Drawing of Large-Scale Controllable Pitch Propeller
Bearing Test Rig

and (2) the normal loading condition where pitch changes are made (excepting crash
ahead and crash astern). The loading conditions used in the large-scale investi-
gations are given in Table 15.

Initial studies were conducted with Al-bronze overlay bearing against HY-100
steel. The coefficient of friction was measured under the action of the vertically
applied load alone and under the resultant of horizontal and vertical components

307

TABLE 15 - TEST CONDITIONS USED IN LARGE-SCALE CONTROLLABLE PITCH PROPELLER BEARING SIMULATOR

Large-Scale (1/3rd Scale) CP Propeller Friction and Wear Test Conditions	Load Condition (Est. Spruance Class)*	
	Full Power Ahead (180 rpm)	Pitch Change (60 rpm)
Applied Vertical Load, lb	22,800	3,800
Applied Cyclic Horizontal Load, lb (±)	7,600	1,300
Resultant Total Load, lb	23,000	3,900
Relative Bearing Motion(Angular),deg	±10	±10
Total Travel per 10 deg, in.	0.75	0.75
Cyclic Frequency (Horizontal Load), Hz	3	1
Mean Velocity, in./min.	6	6
Maximum Stress Based on Wear Track Area, psi	7,700	4,900
Lubrication	Texaco VSI (MIL-L-24467)	Same

*Vertical load represents centrifugal load on bearing, and horizontal load represents hydrodynamic (thrust) load result on bearing from crank ring. Loads estimated to give applied to full-scale bearing in Spruance class laboratory test (Reference 28).

combined (representing the resultant of thrust load and centrifugal blade load on the bearing). The results, given in Table 16, indicate that the forces applied are

TABLE 16 - INITIAL FRICTION TESTS ON LARGE-SCALE TESTER FOR CALIBRATION AND DUPLICATION OF BREAK-IN STICK-SLIP MOTION

Bearing	Counterface	Lubricant
Al Bronze Weld Overlay	HY-100 Steel	Mobil DTE (Heavy)

Initial Cycling Conditions (Friction Tests)

	Total Bearing Load lb	Coefficient of Friction	Type of Motion	Relative Amplitude of Noise Signal
Combined Vertical & Horizontal (Resultant)	3,700	0.18	Stick-slip	1
	8,600	0.14		2
	20,100	0.155	↓	8
	29,900	0.15		20
Vertical Only	3,900	0.13	Stick-slip	1
	8,700	0.14		2
	20,600	0.15	↓	8
	29,900	0.15		20

308

transmitted to the bearing pair, with a relatively constant coefficient of friction
being measured, regardless of the manner of load application. The stick-slip type
of motion and noise sometimes generated during break-in of CP propeller systems was
duplicated in the large-scale tester during pitch change motion under load. Stick-
slip noise was a function of applied load.[42]

The friction and wear characteristics of the Al bronze overlay against steel in
the large scale studies showed the same behavior noted in the bench-scale studies,
i.e., four stages in which initial surfaces are polished; transference of bronze
particles to steel counterface, with the subsequent abrasion of the steel counter-
face; rubbing of bronze transfer particles; and eventual separation of original
surfaces with steady state conditions. A typical result of coefficient of friction
versus cycles is given in Figure 25. Again, the bronze against bronze sliding
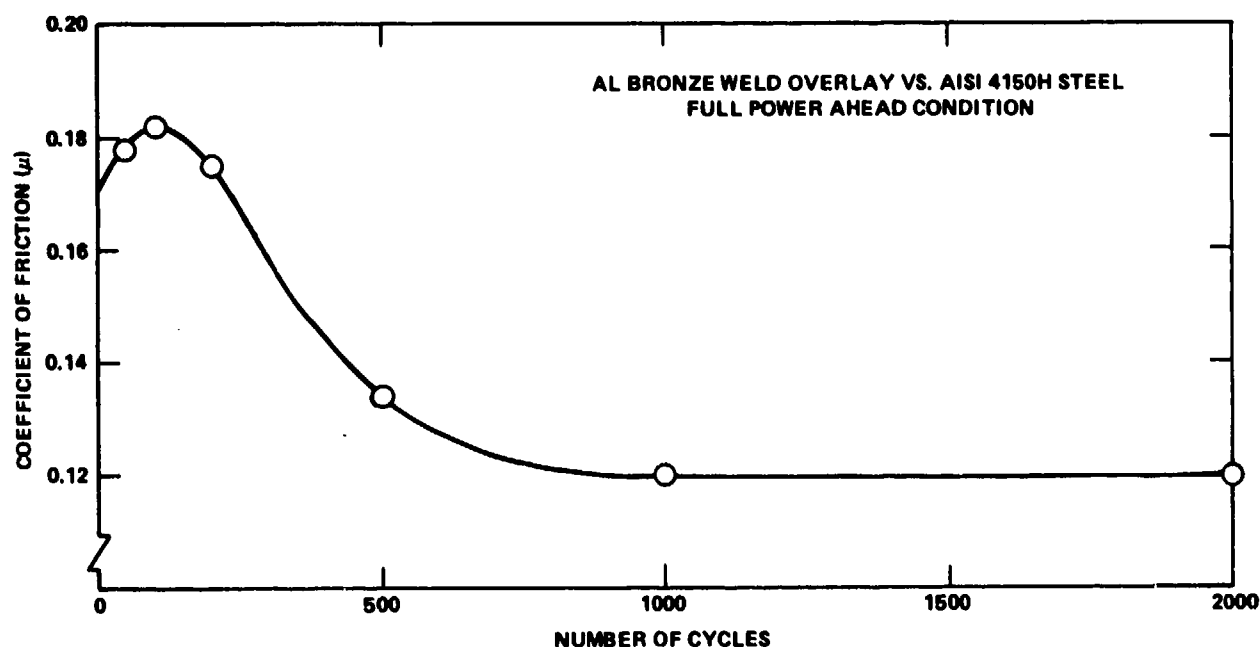
Figure 25 - Friction versus Wear Cycles for Aluminum Bronze Weld Overlay
Against 4150H Steel Sliding Couple in Large-Scale Bearing Tester

couple showed no transference or buildup, but a steady coefficient of friction
which was nominally the same as that achieved in bronze against steel after steady-
state conditions were established (see Figure 26).
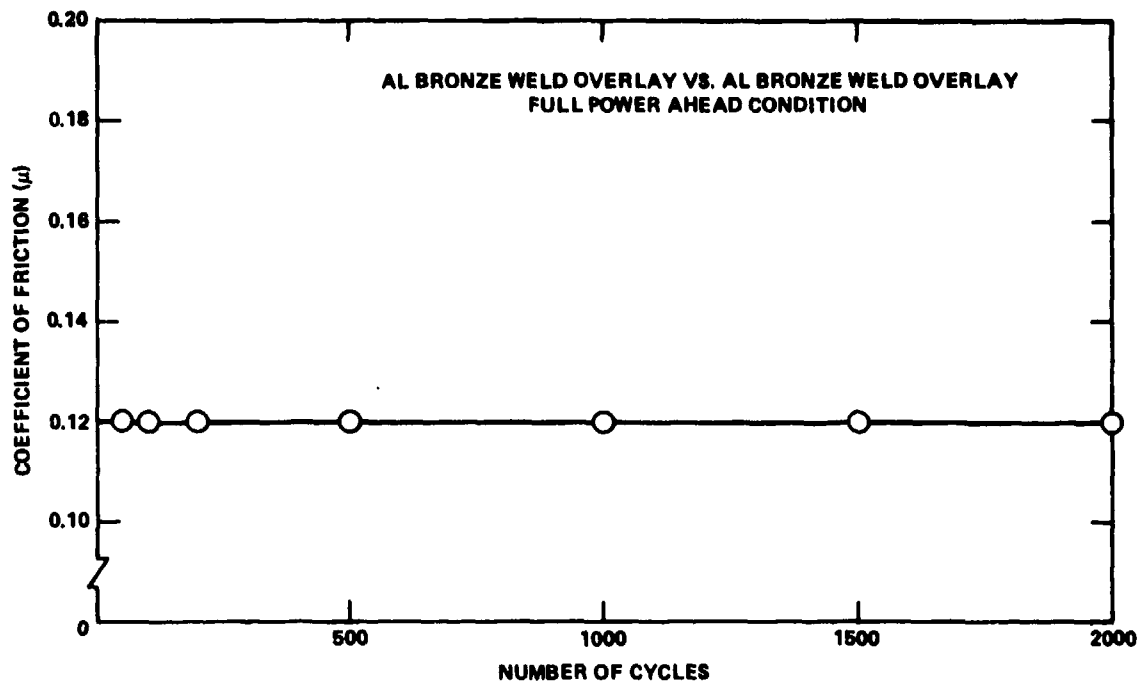
Figure 26 - Friction versus Wear Cycles for Aluminum Bronze Weld Overlay
Against Aluminum Bronze Weld Overlay Sliding Couple,
Large-Scale Bearing Tester

The results for the large-scale friction and wear tests of sliding couples of CP
propeller bearing materials are given in Table 17 for full power ahead load condi-
tions, and in Table 18 for the pitch change load conditions. In general, the charac-
teristics of bronzes against steel are similar in friction and wear performance.
In no case did a buildup of bronze occur to such a degree as to take up all the
internal clearance. It had been speculated that extensive buildup might result in
a deterioration of the frictional properties and possible seizure of the mechanism.
The high-tin bronze (CDA 911) exhibited lower friction than other metallic bearing
alloys. Excellent frictional characteristics were exhibited by the composite
bearing materials.

The DU(B) material is a composite of PTFE (Teflon) and lead powders impregnated
into the pores of sintered bronze powder matrix. It was supported on a bronze
backing strip and required segmented sections to be attached to the face of the
bearing by fasteners. The material showed low friction coefficient (0.1 or less)

310

TABLE 17 – RESULTS OF FRICTION AND WEAR STUDIES IN LARGE-SCALE
CONTROLLABLE PITCH PROPELLER BEARING TESTER,
FULL POWER AHEAD LOAD CONDITIONS

Bearing Material	Counterface Material	Maximum Coefficient of Friction (Break-In)	Steady-State Coefficient of Friction		
			2,000 Cycles	4,000 Cycles	10,000 Cycles
Al Bronze Overlay	4150H Steel	0.19	0.12	0.12	
Mn Al Bronze	4150H Steel	0.18	0.13		
High Tin Bronze	Nitrided 4150H	0.12	0.10		
Al Bronze Overlay	HY-100 Steel	0.19	0.13	0.12	0.12
Mn Al Bronze		0.17	0.13		
Forged Al Bronze		0.16	0.13		
DU (B)		0.04	0.06	0.08	0.10
Karon		0.07	0.07	0.07	
High Tin Bronze	Nitrided HY-100	0.13	0.10		
Al Bronze Overlay	Al Bronze	0.12	0.12	0.12	
Al Bronze Overlay	Inconel 718	0.18	0.15	0.15	0.15
DU (B)	Inconel 718	0.03	0.06		

Note: Lubricant: 2190 TEP Type, Texaco VSI Oil

TABLE 18 – RESULTS OF FRICTION AND WEAR STUDIES IN LARGE-SCALE
CONTROLLABLE PITCH PROPELLER BEARING TESTER,
PITCH CHANGE LOAD CONDITIONS

Bearing Material	Counterface Material	Maximum Coefficient of Friction (Break-In)	Steady-State Coefficient of Friction		
			2,000 Cycles	4,000 Cycles	10,000 Cycles
Al Bronze Overlay	4150 H Steel		0.14	0.14	0.14
Al Bronze Overlay	HY-100 Steel		0.12	0.12	0.12
DU (B)	HY-100 Steel		0.07	0.07	0.07
High Tin Bronze	HY-100 Steel				
Al Bronze Overlay	Al Bronze		0.12		
Al Bronze Overlay	Inconel 718		0.14	0.14	0.14
DU (B)	Inconel 718				
DU (B)	4150 H Steel				
High Tin Bronze	Inconel 718				

Note: Lubricant: 2190 TEP Type, Texaco VSI Oil

311

and low wear. Karon is a polymer composite (thickness about 20 mils) which was processed directly on the bearing surface or backing and thus provides a continuous bearing surface. Its friction and wear properties were comparable to DU(B).

Due to the thin coating of composite material involved, under the highest load condition, wear of the DU(B) was through the layer at about 10,000 cycles. Once worn away, the couple behaves as a bronze (backing) against the counterface. Thus, in the extreme load case, the DU(B) serves to delay the wear of the bronze bearing material.

The friction and wear of bronze bearing alloys against Inconel 718 was higher than that found for steels in both large-scale and bench-scale studies. Base oil studies were also conducted with the Al-bronze overlay against HY-100 steel counterface in large-scale to investigate the effect of additives. Results showed minimal effect.[42]

A comparison of the volume of bronze transfer in wear obtained after 10,000 cycles of full load condition for the following material pairs is shown in Figure 27: (1) Al bronze overlay against HY-100 steel, and (2) Al bronze overlay against Inconel 718. The higher wear of Al bronze against Inconel 718 is evident.

For three of the sliding couples: (1) Al bronze overlay against HY-100 steel, (2) Al bronze overlay against Inconel 718, and (3) DU(B) against HY-100; studies were conducted with 20 percent and 50 percent by volume seawater contamination in the Texaco VSI oil. In those studies with steel counterface, the coefficient of friction was increased to approximately 0.25 and wear rate was high. The rust (iron oxide particles) formed by corrosion of the steel set up a condition of continuing abrasive wear.[42] The couple with Inconel 718 counterface performed as with uncontaminated lubricant. The restoration or replacement of steel crank rings of LST 1179 Class CP propellers has been required because of bearing surface degradation from seawater intrusion.[1,4] Means of detecting seawater entry to the hub oil are deemed necessary to prevent prolonged operation in a contaminated condition.

SUMMARY

The research and development program on materials for CP propeller blade attachment components assessed related CP propeller damage and failure experience in order to identify material problem areas and assist in determining guidelines for selection

312
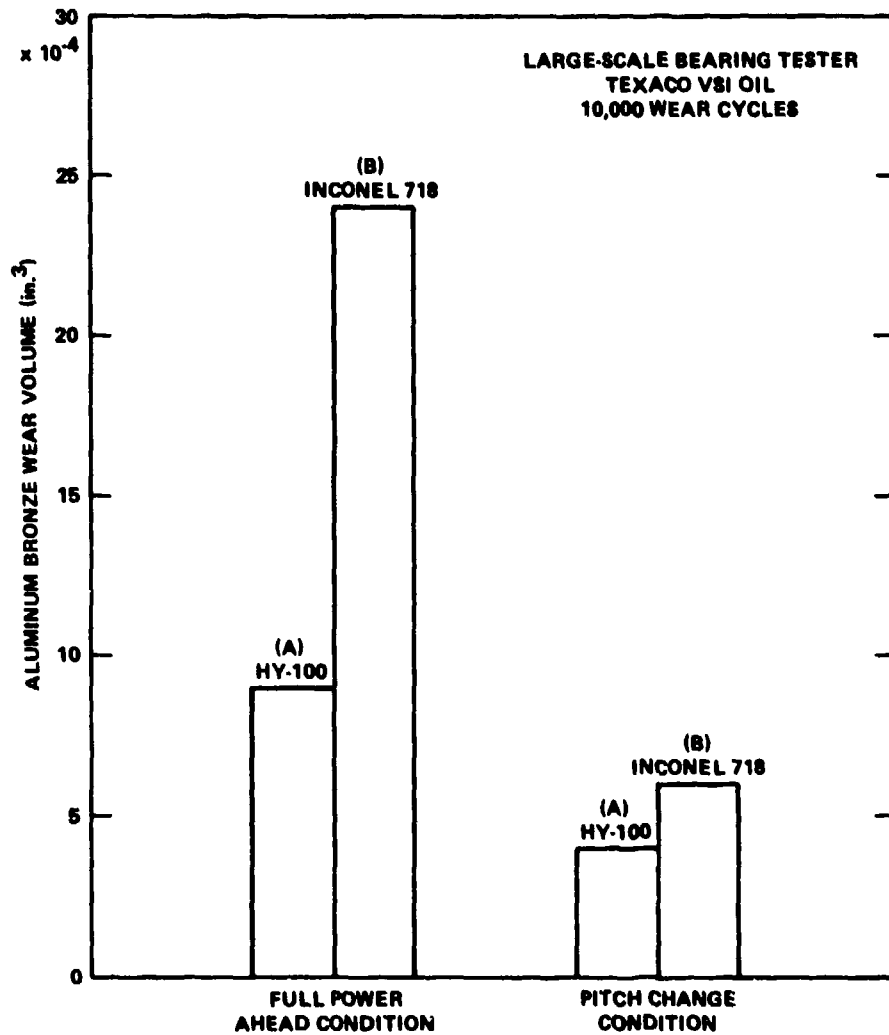
Figure 27 – Comparison of Aluminum Bronze Bearing Wear Volume After 10,000
Wear Cycles Against (A) HY-100 and (B) Inconel 718 Counterfaces

of materials for Navy CP propeller components. The following material areas were of
concern:

Blade and Hub Materials

Blade Carrier Materials

Blade Bolt Materials

Pitch Change Bearing Materials

Studies were conducted in each of the identified problem areas, and the results and
findings are summarized in the following discussion.

CONTROLLABLE PITCH PROPELLER DAMAGE AND FAILURE EXPE   .CE

1. The majority of CP propeller problems have been in control systems and hydraulics, not in blade attachment components.

2. In the category of blade attachment failures of CP propeller systems, propeller blade failures were most prevalent; the majority in cast stainless steel blades.

3. Failure rates increased with increased power (shp). Increased number of blades compounded reliability problems.

4. With experience in designing for a given power level, failure rates in CP propeller hub and mechanisms dropped but blade failure rates remained the same and similar to those of fixed pitch propellers of the same material.

BLADE AND HUB MATERIALS

1. Cast Ni-Al bronze (MIL-B-21230A, Alloy 1) is the best available material for large CP propeller blades and hubs.

2. Corrosion fatigue properties for the alloy are well established for design against fatigue.

3. The fatigue notch sensitivity of cast Ni-Al bronze was demonstrated to be low.

4. Cast stainless steels for large propellers involve a risk of cracking and distortion in the casting process, a heat treatment requirement, a requirement of intentional and maintained cathodic protection for corrosion resistance, and stringent repair procedures with post repair heat treatment required. They are not recommended for large Navy CP propellers.

BLADE CARRIER MATERIALS

1. Blade carriers for high-powered, large CP propeller mechanisms require the use of high yield strength alloys. A fracture toughness level, optimum for the strength and thickness of the component, must be specified and controlled to prevent brittle fracture.

2. High strength, high toughness steels were evaluated. These alloys require special melting and processing and contain high alloy content. Conventional low alloy, quenched, and tempered steels may not obtain sufficient toughness in heavy

314

sections to render a high-powered CP propeller immune to brittle fracture and tolerant of small cracks and defects from service.

3. Fatigue properties for large high strength steel forgings were examined. Endurance strength was between 40 percent and 45 percent of tensile strength, decreasing to the lower value as strength increased emphasizing the need for detailed design against fatigue in high performance systems.

4. Seawater contamination of hub oil, even at low levels, reduces the fatigue strength of steels to low levels.

5. Surface treatment by cold rolling delays initiation of corrosion fatigue cracks but shot peening was ineffective. Surface coating of critical areas with epoxy coatings, urethane, or vulcanized rubber can prevent corrosion fatigue cracking if coatings remain intact.

6. Inconel 718 was selected as a candidate corrosion resistant alloy having strength and toughness comparable to the high strength steels considered for the application but resistant to corrosion fatigue. Evaluation of an Inconel 718 forging showed that fatigue strength was not comparable to those steels (only 25 percent of the tensile strength) due to the large grain size developed in the item. Use of the alloy was not considered cost effective.

BLADE BOLT MATERIALS

1. In most applications CP propeller designers and producers use blade bolts of corrosion resistant alloys (bronzes, nickel alloys, stainless steels) compatible with blade and hub alloys. Use of low alloy steels requires complicated capping and sealing arrangements which may be unreliable in preventing corrosion and corrosion fatigue.

2. The fatigue and corrosion fatigue properties of several high performance bolt alloys were investigatied. Nickel alloys, Inconel 718 and K-Monel, and titanium 6Al-4V showed superior fatigue and corrosion fatigue strength relative to tensile strength. However, the fatigue strength of the Ni alloys was dependent upon section size (grain size) of the stock.

3. Notch sensitivity of the alloys in fatigue increased with strength level. Machined threads (K_t=3 to 4), therefore, reduce the intrinsic fatigue strength of high strength alloys to levels not different than lower strength materials.

4. Cold roll forming of threads after all thermal treatments offers the best option for fatigue and corrosion fatigue strength in a threaded fastener. Studies determined that compressive residual stresses at the root of the thread result from the roll forming operation and inhibit fatigue crack propagation.

5. Root rolling of partially cut machined threads offers the same or greater benefits in fatigue strength as full roll forming in difficult, work hardening high strength alloys.

6. Exposed bolt heads constitute a small exposed area in relation to blade and hub area. Any alloy near or more noble than the propeller alloy in the galvanic series in seawater should perform satisfactorily. The cathodic protection applied in the stern area protects the propeller from selective attack when more noble blade bolts attach the blade.

PITCH CHANGE BEARING MATERIALS

1. Severe wear of pitch change bearings has only occurred in highly loaded CP propeller systems or in instances where seawater has entered the hub and contaminated the oil.

2. A small-scale tester was developed to evaluate the tribological characteristics of sliding couples of the materials used in CP propeller bearings; primarily bronze bearing surfaces against steel or bronze crank rings.

3. A large-scale tester was constructed to simulate performance of the bearing pairs under service type loadings. The results for both testers were correlated and gave similar ranking in friction and wear performance for the same materials.

4. For steel surfaces against bronze at high bearing stresses, four stages of wear were identified. However, the most important was a final steady-state achieved after transference of bronze to the steel surface. This stage showed a low wear rate and friction coefficient similar to bronze against bronze.

5. Surface finish and hardness of steel surfaces were found to only influence initial, break-in stages and not the steady-state characteristics.

6. High tin bronze (CDA 911) was found to be the best of the bronzes in friction and wear performance.

7. Composite materials DU(B) and Karon may be applied to bronze backing and offer very low friction and wear characteristics. These materials may be back-fitted if problems with conventional bronzes have occurred.

316

8. Additives in the oil exert a minor influence on the friction and wear properties of the bronze against steel sliding couple.

9. Seawater contamination of the oil causes increased friction and high wear rates.

RECOMMENDATIONS

Specific recommendations based on findings of the materials R and D program are as follows:

BLADE AND HUB MATERIALS

1. Cast Ni-Al bronze (MIL-B-21230A, Alloy 1) remains the best alloy for large CP propeller blades and hubs. The selection of another alloy must be shown to be equal or superior to Ni-Al bronze in properties, castability, and ease of repair.

2. Cast stainless steels of the high Cr-Ni-Mo types require deliberate cathodic protection to prevent both crevice corrosion and stress corrosion cracking of repairs, and to raise corrosion fatigue strength. It is recommended that these alloys not be used for Navy CP propeller blades.

3. Detailed fatigue analysis should be performed in CP propeller blade and hub design. Sufficient fatigue data, stress trials data, and load prediction capability exist for highly refined designs against blade and hub fatigue without overly conservative safety factors.

4. U.S. Navy propeller repair guidance should be revised to include CP propeller blades and hubs, defining critical regions.

BLADE CARRIER MATERIALS

1. A material fracture toughness requirement should be determined for blade carriers of high-strength steels to be part of the material specification.

2. Detailed fatigue analysis of the blade carrier should be performed based on data for the material used and conservative factors applied.

3. The full theoretical stress concentration factor should be used as the fatigue notch reduction factor in fatigue design.

4. Protection of steel blade carriers by nonmetallic coatings applied in high stress areas, such as fillets and grooves, is recommended for corrosion fatigue resistance.

317

BLADE BOLT MATERIALS

1. Corrosion-resistant alloys with properties documented for the stock size intended for bolt manufacture should be used.

2. For maximum fatigue strength, the bolts should be manufactured with rolled threads and head fillet. Roll forming of the threads must be performed after all strengthening and stress relieving heat treatments are complete.

3. Root rolling of partially cut machined threads should be used for the manufacture of blade bolts of difficult to work materials. The manufacturing techniques and details, however, need to be developed and properties demonstrated for each particular case of material and fastener size.

4. The alloy should have corrosion fatigue strength in seawater and should be the basis of the blade bolt fatigue design.

5. The alloy should be near to or more noble than the alloy used as blade and hub in the galvanic series in seawater.

6. Alloys susceptible to galling should not be used in blade bolt applications.

PITCH CHANGE BEARING MATERIALS

1. A limiting bearing pressure should be established for the sliding couples involved in the pitch change bearing and a calculation procedure established.

2. Of the bearing bronzes evaluated, tin bronze (CDA 911) is recommended where separate bearing rings are used.

3. Composite materials DU(B) and Karon offer a means of reducing friction and wear in highly loaded systems. These materials are recommended for facing the bronze bearings in such systems to reduce maintenance required to refinish surfaces after bronze transfer and buildup.

4. Seawater intrusion into the hub can cause degradation of the blade carrier, bearings, hydraulic, and control components. Indicators which warn of seawater leakage into the hub must be provided to prevent prolonged operation with seawater within the hub.

REFERENCES

1. Czyryca, E.J., "A Review of Controllable Pitch Propeller Damage and Failure Experience," DTNSRDC Report (in preparation).

2. Angelo, J.J. et al., "U.S. Navy Controllable Pitch Propeller Programs," paper presented at Joint Meeting of Amer. Soc. of Naval Eng. and Soc. Naval Arch. and Marine Eng., Wash., D.C. (19 Apr 1977).

3. Noonan, C. et al., "The BARBEY Report, An Investigation into Controllable Pitch Propeller Failures from the Standpoint of Full-Scale Underway Propeller Measurements," DTNSRDC Report 77-0080 (Aug 1977).

4. Gatzoulis, J. and D. Woyowitz, "Reliability Study and Fixit Programs for Major Navy Controllable Pitch Propeller Systems," NAVSEA Journal, Vol. 23, No. 11, p. 2 (Nov 1974).

5. Czyryca, E.J., "An Investigation of Controllable-Pitch Propeller Blade and Hub Alloys," DTNSRDC Report (in preparation).

6. Meyne, K.J., "Propeller Manufacture-Propeller Materials-Propeller Strength," International Shipbuilding Progress, Vol. 22, No. 247 (Mar 1975).

7. LaQue, F.L., "Propellers," Chapter 9 of "Marine Corrosion, Causes and Prevention," John Wiley and Sons, New York (1975).

8. Bedford, G.T. and M.R. Gross, "High Performance Propellers, A Materials/Applications Survey," NSRDC Report 3909 (Oct 1972).

9. Denny, S.B. et al., "Hydrodynamic Design Considerations for the Controllable-Pitch Propeller for the Guided Missile Frigate," Naval Engineers Journal, p. 72 (Apr 1975).

10. Boswell, R.J., "Experimental Determination of Mean and Unstead Loads on a Model CP Propeller Blade for Various Simulated Modes of Ship Operation," presented at the 11th ONR Symposium on Naval Hydrodynamics, London, United Kingdom (28 Mar-2 Apr 1976).

11. Guidance Manual for "Inspection and Repair of Steel Propellers," Det Norske Veritas, Classification Note 4.2 (Aug 1977).

12.   Hersh, S. and R.D. Rockwell, "A Strength Assessment of Screwed-In and Trunnion Type Controllable Pitch Propeller Blade Attachments," DTNSRDC Report SD-79-2 (Sep 1978).

13.   Czyryca, E.J. and R.B. Niederberger, "Mechanical, Fatigue, and Corrosion Properties of Propeller Bronzes," "Propellers '75," SNAME Publication S-4, Paper 8 (1976).

14.   May, T.P., "Corrosion Fatigue of Large Ship Propeller Alloys" "Propellers '75," SNAME Publication S-4, Paper 10 (1976).

15.   Prager, M., "The Properties of Cast Alloys for Large Marine Propellers," "Cast Metal for Structural and Pressure Vessel Containment Application," G.V. Smith (edit.), MPC-11, Amer. Soc. Mech. Eng., N.Y. (1979).

16.   Tokuda, S. et al., "Fatigue Failure in Marine Propeller Blades," "Propellers '78," SNAME Publication S-6, Paper 5 (1979).

17.   "Repair of Bronze Ship Propellers, Straightening and Welding," NAVSHIPS Report 0991-023-300 (Jun 1965).

18.   "Guidance Manual for Making Bronze Propeller Repairs," American Bureau of Shipping, New York (1972).

19.   "Lloyds Provisional Rules and Guidance Notes," Chapter R(H), pp. 695-697 London, U.K. (July 1972).

20.   "Guidance Manual for Inspection and Repair of Bronze Propellers," Det Norske Veritas, Classification Notes 4.1 (1974).

21.   Czyryca, E.J., "Metallurgical Failure Analysis of Crank Disks from the Controllable Pitch Propeller System of USS BARBEY (DE-1088)," DTNSRDC Report TM-28-74-262 (Oct 1974).

22.   Pellini, W.S., "Principles of Structural Integrity Technology," Office of Naval Research (1976).

23.   Rolfe, S.T. and J.M. Barsom, "Fracture and Fatigue Control in Structures, Applications of Fracture Mechanics," Prentice-Hall, Inc., Englewood Cliffs, N.J. (1977).

24. Czyryca, E.J. et al., "Toughness Criteria for High Strength Blade Carrier Forgings for CP Propeller Systems," DTNSRDC Report (in preparation).

25. Landes, J.D. and J.A. Begley, "Recent Developments in J_{IC} Testing," "Developments in Fracture Mechanics Test Method Standardization," ASTM STP 632, pp. 57-81 (1977).

26. Lange, E.A. and F.J. Loss, "Dynamic-Tear Energy--A Practical Performance Criterion for Fracture Resistance," "Impact Testing of Metals," ASTM STP 466, pp. 241-258 (1970).

27. Czyryca, E.J. and S. Hersh, "Fatigue and Corrosion-Fatigue Resistance of High Strength Steels for Controllable Pitch Propeller Blade Carrier Applications," DTNSRDC Report (in preparation).

28. Rockwell, R. and S. Hersh, "Full-Scale Structural Evaluation of the USS OLIVER HAZARD PERRY (FFG-7) Controllable Pitch Propeller Blade Attachment, Phase 1-- Application of FFG-7 Blade Forces to the USS SPRUANCE (DD-963) Propeller," DTNSRDC- 80/066 (Jun 1980).

29. Peterson, R.E., "Stress Concentration Factors," John Wiley and Sons, New York (1974).

30. Horger, O.J., ed., "Metals Engineering Design," ASME Handbook, McGraw-Hill Book Co., Inc., New York (1953).

31. Czyryca, E.J. and S. Hersh, "Corrosion Resistant Alloys for Controllable Pitch Propeller Crank Rings," DTNSRDC Report (in preparation).

32. Czyryca, E.J. et al., "High Performance Bolt Alloys for Controllable Pitch Propeller Applications," DTNSRDC Report (in preparation).

33. Faires, V.M., "Design of Machine Elements," MacMillan Company, Third edition, New York (1955).

34. Vassilaros, M. and H. Kuhn, "Analysis of the Residual Stresses Resulting from Cold-Rolling of Threads and Their Effect on Fatigue Behavior," Proc. 7th North American Metalworking Research Conference (May 1979).

35. Phyillaier, W. and R. Rockwell, "Fatigue Behavior of Blade-Attachment Bolts of Different Materials for High-Horsepower Controllable Pitch Propellers," DTNSRDC Report 80/043 (Jun 1980).

36. Czyryca, E.J. et al., "Galvanic and Mechanical Compatibility Studies of Blade Bolt Alloys for Controllable Pitch Propellers," DTNSRDC Report (in preparation).

37. Hack, H.P., "Corrosion of Materials for SSN-688 Class Submarine Main Seawater Valves," DTNSRDC Report SME-79/9 (Feb 1979).

38. Vreeland, D.C., "Corrosion Protection for Axial Flow Pump, Mk17, Mod 0 Turbine Pump Ejection System," DTNSRDC Report SME-80/25 (Jul 1980).

39. Karpe, S., "The Friction and Wear Characteristics of Six Bearing-Material Combinations for Use in the Controllable Pitch Propellers of USS BARBEY (DE-1088) and USS SPRUANCE (DD-963)," DTNSRDC Report TM-28-75-103 (Jun 1975).

40. May, E.R., Cdr. and K. Brownlie, "An Advanced Design of British Controllable Pitch Propeller," Technical Paper 14, Stone Manganese Marine, Ltd., London, United Kingdom (Mar 1974).

41. Karpe, S. and E. White, "Investigation of the Friction and Wear Characteristics of Bearing Materials for CP Propeller Systems," DTNSRDC Report (in preparation).

42. White, E. and S. Karpe, "Full-Scale Laboratory Simulation of CP Propeller System Bearing Performance and Material Characterization," DTNSRDC Report (in preparation).

CHAPTER V

STRENGTH OF CONTROLLABLE PITCH PROPELLERS

TABLE OF CONTENTS

LIST OF FIGURES

LIST OF TABLES

INTRODUCTION

The structural design and analysis of high power controllable pitch (CP) propellers present complex problems in the blade attachment primarily because of the Navy's desire to keep the propeller hub diameter small in the interest of (1) keeping their hydrodynamic efficiency high and (2) keeping the overhung load on the propeller shaft small. The large blades and large forces associated with the high power, and the dynamic character of these forces have caused major structural problems with the otherwise attractive small diameter hubs.

In spite of the many mechanical and control complexities presented by CP propellers, service experience indicates that their design and manufacture has generally been adequate. However, there is also ample evidence that the incidence of structural problems has been increasing as shaft horsepower has been increasing, especially in five-bladed applications. Statistical evidence of Roren et al.,[1*] as well as experience with large shaft horsepower applications in the U.S. Navy[2] demonstrate this trend.

Unsteady hydrodynamic forces on a propeller blade as it rotates through the ship's wake has been shown by Keil et al.[3] to be as large as ± 84 percent of steady forces for operations at zero degree rudder. In high seas and in high power turns and pitch changes, which are particularly important for military application, the unsteady forces may be even higher.

The structural complexity of the CP propellers make a completely theoretical stress analysis just about impossible. The intent in this chapter is to provide a semiempirical approach which can be used as an aid in design and analysis of future CP propellers in sizes whose power ranges up to 60,000 to 70,000 hp capacity. Confidence in results of analyses, particularly in high horsepower applications, of designs using different physical arrangements or proportions, would require some experimental confirmation; the more deviation from past design, probably the more elaborate the experimental effort.

It has been identified that the limiting structural problem areas are the crank ring and blade bolts of the blade attachment; see Figure 1. As the increased power levels are considered, it is well to note that for similar designs, stress in the blade attachment due to the hydrodynamic force will vary as the applied bending moment divided by the section modulus. The section modulus or bending strength of

---

*A complete listing of references for this chapter is given on page 415.
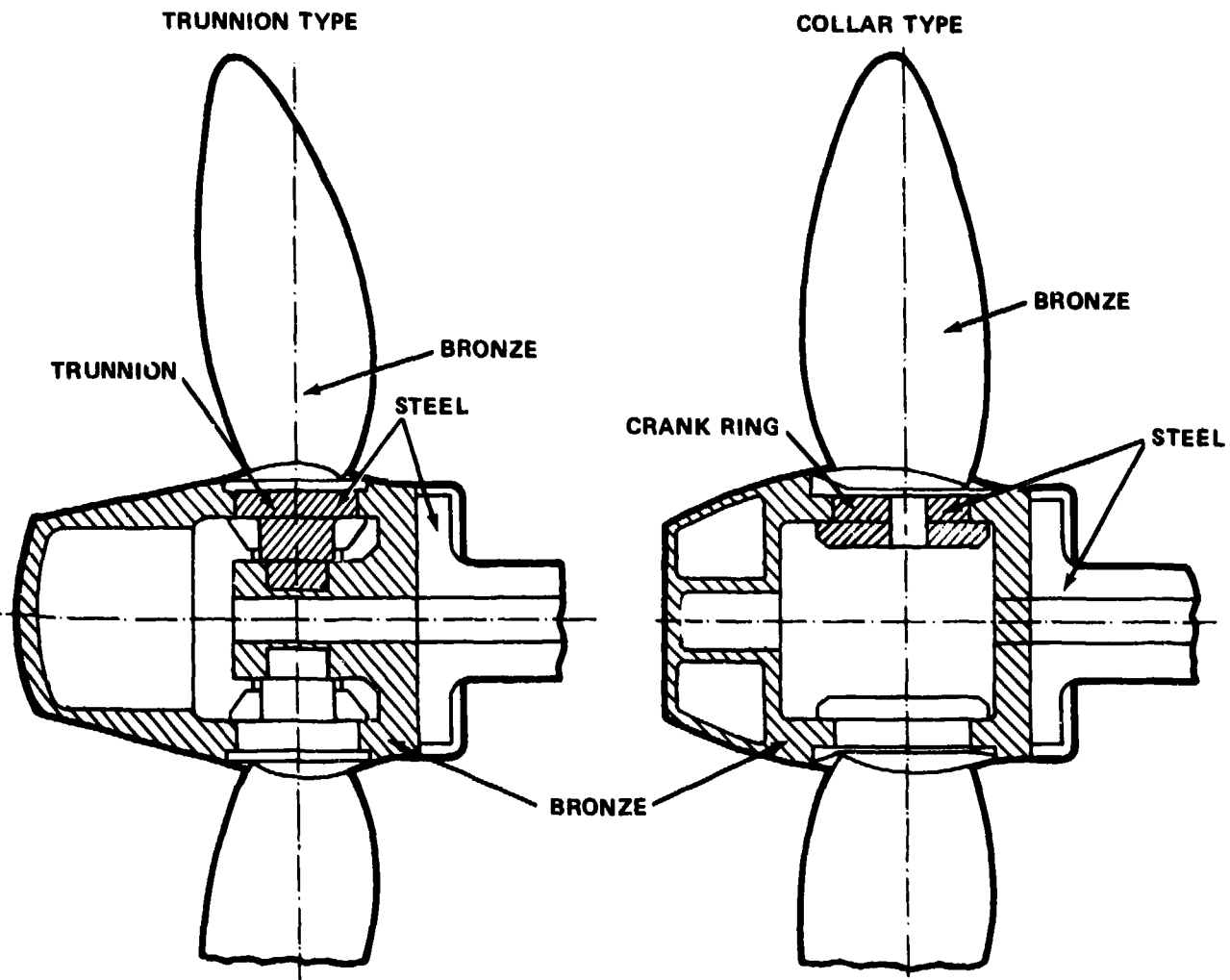
Figure 1 – Two Types of Blade Carrier Arrangements

the blade attachment will vary with the cube of the attachment diameter. The applied bending momen   ill vary with blade force and blade diameter, both of which depend upo   how the increased horsepower is used related to ship speed. For example, it might be used to power a larger ship with no change in ship speed, or it might be used to increase the speed of a ship of the same size. Both examples will be discussed.

Example 1: Larger ship with no change in ship speed. In this case, blade diameter will increase and if propeller rpm is not changed, the propeller blade

force will tend to vary with blade area so that the applied bending moment will vary with the cube of the blade diameter. Therefore, blade attachment stress will remain constant so long as the ratio of hub diameter to blade diameter remains constant. In equation form,

$$\text{stress} = \frac{M}{Z} \propto \frac{(F \times L)}{L^3} \propto \frac{L^3}{L^3}$$

where M = applied bending moment $\propto (F \times L)$

F = blade force $\propto L^2 \propto$ shp

Z = section modulus $\propto L^3$

shp = shaft horsepower

L = blade diameter $\propto$ shp$^{1/2}$

Example 2: Increased ship speed for same size ship. In this case, for example, in the extreme, for a constant propeller diameter, propeller rpm would be increased (likely requiring transcavitating or supercavitating blades). More blade force would be applied to the same size blade and hub, and blade attachment stress would increase. In equation form,

$$\text{stress} = \frac{M}{Z} \propto F$$

where M = applied bending moment $\propto (F \times L)$

L = constant = blade diameter

Z = section modulus = constant

F = blade force $\propto V^2$, so $V \propto F^{1/2}$

shp = shaft horsepower $\propto V^3$, so $V \propto$ (shp)$^{1/3}$

F $\propto$ (shp)$^{2/3}$

For a 50 percent increase in shaft horsepower, the blade attachment stress would increase by a factor of $(1.5)^{2/3}$ or 1.31.

CONTROLLABLE PITCH PROPELLER BLADE ATTACHMENTS

Two basic types of blade carriers used in the industry are the trunnion type and the collar type where the collar is known by various names such as the crank

ring or crank ring disk. Both are shown schematically in Figure 1. Each type has its inherent advantages and disadvantages as indicated in References 4 and 5, but both types have been used successfully in high horsepower applications with five blades.

Both types of CP propellers usually have bolted attachments for blades in high horsepower applications. This arrangement simplifies handling of the large blades and allows use of different materials for the blade and the blade carrier. It also accommodates the use of a coverplate between the blade and blade carrier thereby providing for the possibility of emergency underwater blade replacement by sealing hub internals from contamination underwater; see Figure 2. Coverplates are currently in use on the SPRUANCE and PERRY Class propellers and underwater blade changes have been made.

Another approach to attaching the blade to the blade carrier involves the use of a large buttress-threaded extension at the base of the blade where it is screwed into a socket in the blade carrier as shown in Figure 3. The historical development of this approach is described in Reference 6. The 35,000 shp USS PATTERSON (FF 1061) CP propeller operated successfully for 7000 hr with such an arrangement, but it has no apparent strength advantage over a bolted-on blade.* There is currently no CP propeller manufacturer using the buttress thread arrangement.

Integrated trunnions, in which the blade and blade carrier or trunnion are a one piece casting, are used in the propellers of the U.S. Coast Guard's POLAR STAR and POLAR SEA ice breakers. This arrangement eliminates a potential blade attachment bolt strength problem but requires use of high strength stainless steel material because of high stress levels which develop in the blade and trunnion when impacting ice. Stainless steel is not normally used in U.S. Navy propellers because it is susceptible to corrosion fatigue cracking and requires heat treatment after repair. In the above mentioned strength assessment of the USS PATTERSON CP propeller, it was also concluded that stresses in a Ni-Al-Bronze integrated trunnion would be un-acceptably high in a five bladed, highly loaded CP propeller with a hub-to-blade-tip diameter ratio of about 0.3 which is the ratio of interest here.

---

*A strength assessment of the screwed-in bronze blade of the USS PATTERSON reported informally by Hersh and Rockwell used blade forces determined from measurements at sea on the USS BARBEY (FF 1088), a sister ship of the PATTERSON. It was concluded that the screwed-in PATTERSON blade had inadequate fatigue life because of high stresses in the buttress threads.

330

	DESCRIPTION	MATERIAL
1	BLADE SEAL BASE RING	CAST BRONZE
2	SPRING, COMPRESSION	STEEL
3	PIN, DOWEL	STEEL AISI C 1042
4	CAP SCREW	SILICON BRONZE
5	COVER, BLADE PORT	Ni-Al-BRONZE MIL-B-21230A
6	PROPELLER BLADE	Ni-Al-BRONZE MIL-B-21230A
7	BOLT-PROPELLER BLADE	K-MONEL
8	BEARING RING	DU BEARING ON AISI 4130
9	HUB BODY ASSEMBLY	Ni-Al-BRONZE MIL-B-21230A
10	BEARING RING LOCK PIN	DRILL ROD (STEEL) AISI SAE
11	CRANK PIN RING	A471-70 CLASS 6 STEEL

Figure 2 - Typical Bolted Blade Attachment Assembly

Figure 3 - Two Methods of Attaching Blade to Blade Carrier

PROBLEM AREAS

The work summarized in this chapter has been directed mostly towards strength analysis of the bolted blade-crank ring combination because that is how current U.S. Navy CP propellers are made and where difficulties have been experienced. Structural problems which occur in CP propellers are generally found in the blade attachment region where blade attachment bolts and crank ring or disk type carriers have failed in service at regions of high stress. Other potential problem areas including the hub and bearings have been examined, but the bolts and crank ring are the limiting problems. For example, measurements on the SPRUANCE hub collar, which retains the crank ring in the hub, indicated that the peak stresses at the minimum cross section between blades were low, less than 10,000 psi at maximum full-power turn loadings. In the remainder of the chapter both the crank ring and the crank disk types of blade carriers will be referred to as crank rings. A very limited discussion of the trunnion-type blade carrier is included in the section on Closed Form Equations for Blade Carriers. Shock loadings are not considered because there is no evidence that current shock requirements have caused design problems. However, the importance of high fracture toughness in the presence of shock is notable.

Blade Bolts

Both hydrodynamic and centrifugal blade loads are transmitted to the crank ring or trunnion through the blade bolts. The basic design assumption used by the U.S. Navy CP propeller contractors was that the bolts were loaded by forces whose

magnitude was directly proportional to their distance from an axis which was perpendicular to the hydrodynamic force and, in one case, was near the circumference of the palm, while in another case it intersected the blade spindle axis. It was also assumed that the bolts were loaded in pure tension--that there were no bending moments applied to the bolts. There was no calculation of cyclic loads on the bolts and no specification requirement for a fatigue analysis. Even if there had been such a requirement, the basic bolt design assumption and the poor definition of cyclic blade forces would have led to an indication that bolt forces were well below specified bolt preload and that, therefore, bolt maximum and fatigue stresses were low.

Measurements in the laboratory and during sea trials demonstrated that most of these bolt design assumptions are not reasonable. Often one bolt carries much more force than the others. In addition, there are significant bending stresses in the bolts which are equal to or even greater in magnitude than the average tensile bolt stresses above prestress. Fatigue stress cycles of the preloaded bolts become increasingly important as the magnitude of the bolt forces approaches and exceeds preload. The combination of uneven bolt force distribution and bolt bending along with high unsteady blade loads and consequently unsteady bolt forces leads to high bolt stresses and potential bolt fatigue failures as have occurred at sea on both military (BARBEY, five blades) and commercial (Chevron tanker, four blades) vessels. Discussions with ship classification societies and CP propeller manufacturers verify that these design assumptions are not unusual. Typically, when blade bolt fatigue failures have occurred, inadequate bolt preload has been blamed as the probable cause of failure; inadequate design may have been an important contributor.

Crank Ring

Crank rings transmit blade spindle torque, centrifugal forces, and the bending moments due to hydrodynamic forces to the hub. No problems are known to have occurred in the crank ring pin or arm which transmits torque, but fatigue and fracture have occurred in other locations on the crank ring. A fracture of the BARBEY crank ring initiated at a fatigue crack at the base of the tapped hole for the most highly loaded blade bolt as shown in Figure 4a. The crack had initiated in the bottom bolt hole thread and had grown through the wall of the crank ring, which was only about 0.25 in. (6 mm) thick, to the 0.375 in. (9.5 mm) radius groove

333

FORWARD

MOST HIGHLY
LOADED BOLT

RADIAL
CROSS-
SECTION

AREA OF FATIGUE
CRACK PRIOR TO
BRITTLE FRACTURE

← 6 mm (1/4 IN.)

LOCATION OF FATIGUE CRACK AT HIGHLY LOADED BOLT POSITION
BETWEEN BOTTOM THREAD AND 9.5 mm (3/8 IN.) RADIUS GROOVE
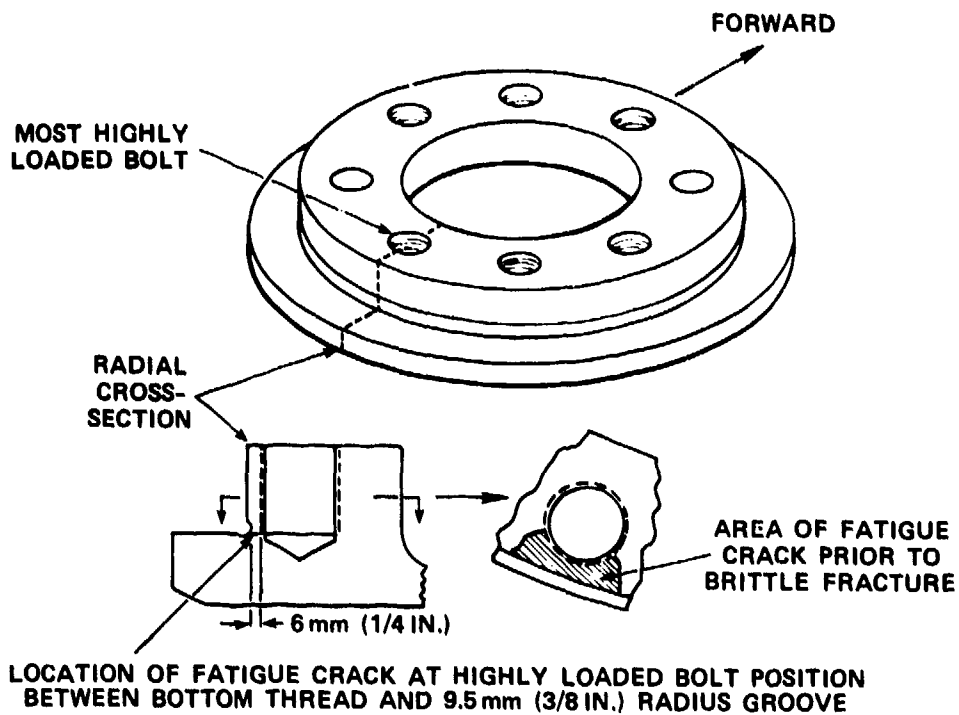
Figure 4a - Fatigue Failure in USS BARBEY Crank Ring

FORWARD

RADIAL
CROSS-
SECTION

JAGGED LINE INDICATES LOCATION
OF THE THREE CRACKS AT UPPER
SURFACE OF CRANK RING

DOTTED LINE INDICATES LOCATION OF THREE
CRACKS AT LOWER SURFACE OF CRANK RING
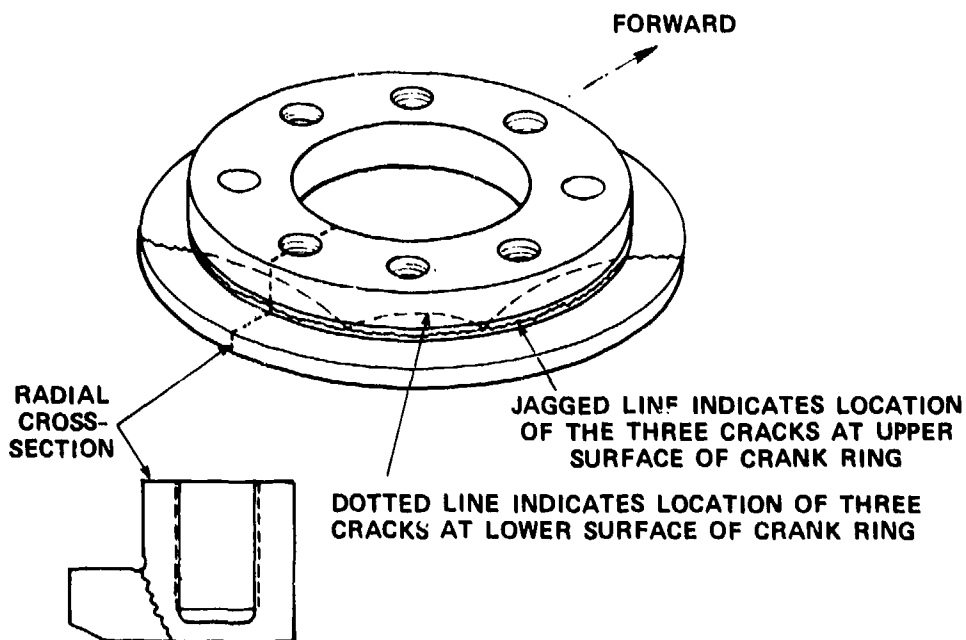
Figure 4b - Fatigue Failure in Steel Crank Ring of High Toughness

Figure 4 - Examples of Crank Ring Failures

334

or fillet at the crank ring flange. Another crank ring fatigue failure, shown in Figure 4b, was identified during discussions by Czyryca and Rockwell with Det Norske Veritas. Three cracks initiated in the 0.315 in. (8 mm) radius fillet at the crank ring flange and grew through the flange. The large cracks were constrained without fracture of this crank ring which was fabricated of a steel with high fracture toughness, but failure was evident when the propeller jammed and would not change pitch.

NATURE OF STRENGTH ASSESSMENT

In the present context, two stress criteria must be satisfied in order for the bolts and blade carrier to be considered to be adequate. The maximum stress must be less than the material's yield stress (except at thread roots, a special case) and the spectrum of fatigue stresses must be within the material's endurance capacity for the required life. The magnitudes of the safety factors to be applied during design and design assessment depend upon confidence levels in the methods of stress analysis used and in the available input data such as material physical character-istics and the magnitudes of forces applied.

Requirements for Stress Analysis Methods

Stress analyses of the bolts and crank rings of the bolted-on type blade attachments are complicated by their involvement of preloaded parts in contact and the complex deformation patterns of the palm, crank ring, and hub making rigorous analyses difficult and expensive. Simplifying assumptions can be made but the sub-sequent limitations in results must be recognized and evaluated.

A number of experimental methods are available for determining stresses in structural elements. They include use of small-scale metal or photoelastic models to full-scale measurements in the laboratory or under service conditions at sea. These were applied to the blade attachment problem during the DTNSRDC investigations, all in a generally successful manner. These experimental approaches provide the means for verification checks of numerical predictions, but are frequently too time consuming, expensive, or impractical to use during the design process. This is particularly true of full-scale experiments.

As noted earlier, the numerical methods for stress analysis of blade bolts which were used by designers of U.S. Navy CP propellers have been found during the

335

CP propeller research and development (R and D) program at DTNSRDC to be unreliable. A much more accurate determination of bolt forces and stresses was clearly needed. Therefore, the subject has received much attention. It is recognized that simple approximate methods are required for use during early design stages, but more complex methods may be required for analyses of final designs.

A series of three numerical stress analysis methods of varying complexity was developed for the blade bolts. The most sophisticated and most accurate of the numerical methods involves a three-dimensional finite element analysis of the blade, bolts, crank ring, and portions of the hub body. Stresses including bolt bending are determined. Results from this analysis can be used in conjunction with two-dimensional finite element analyses to obtain representations of stress in regions of stress concentration, in the crank ring or bolt head fillets, for example.

A somewhat more complex method for obtaining bolt forces and average bolt stresses is based on two-dimensional finite element analyses of the blade and blade palm or flange at slices perpendicular to the blades and through the bolt holes, as in Figure 5. This method eliminates the simplistic assumption of bolt force distribution and provides improved accuracy. It is neither difficult nor expensive to use, and with it, appropriate changes in blade fillet geometry can be identified to improve the distribution of bolt forces.

The simplest method for blade bolts might be called an "indicator of bolt force level" as it facilitates comparison of the level of forces through the bolts with similar data for a number of both successful and unsuccessful CP propellers. No consideration is given to bending stresses. This method is suitable only in initial stages of strength assessment.

Stresses in the crank ring and trunnion are dependent upon hub body deformations under load which affect pressure distributions at bearing surfaces between the carriers and the hub. The direct equations traditionally used by designers have been found to be adequate only in conjunction with conservative assumptions of pressure distribution and when the distance between the crank ring fillet and the bolt threads is above a certain minimum. These limitations will be discussed in detail later in the chapter.

336
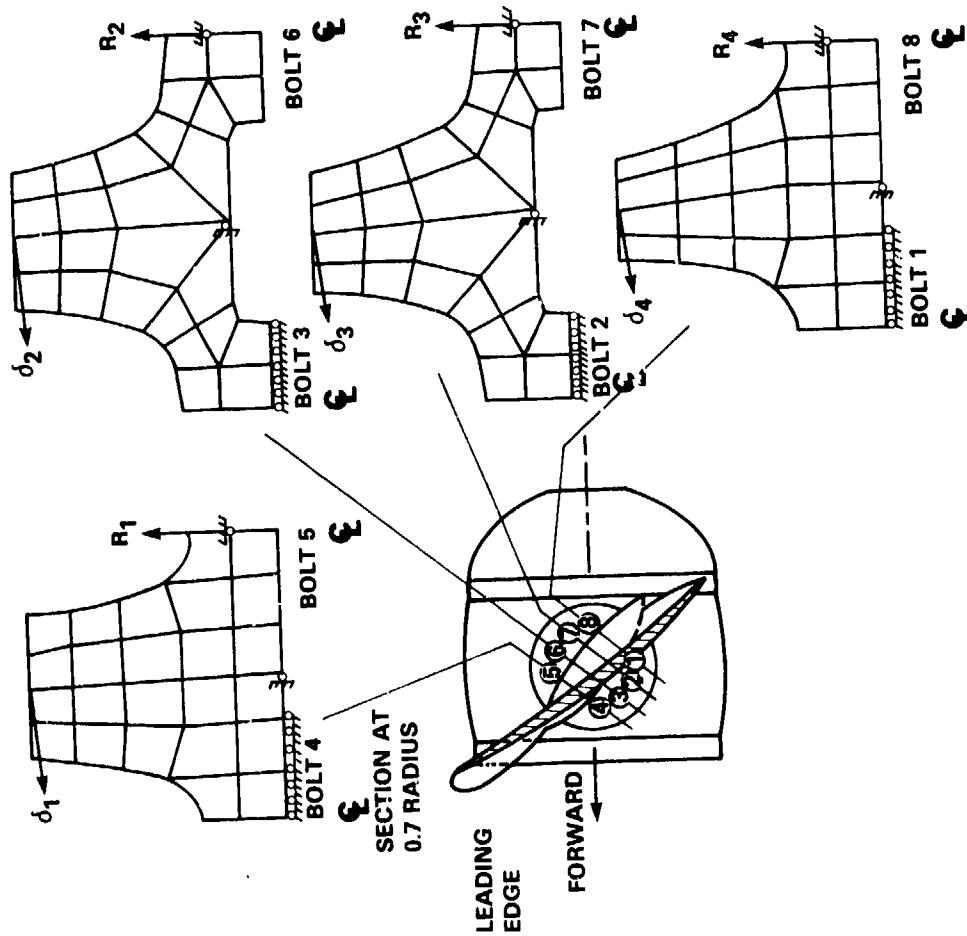
Figure 5 — Two-Dimensional Finite Element Slices on the USS OLIVER HAZARD PERRY Blade

337

Requirements for Fatigue Analysis

The complexity of the necessary fatigue analysis depends upon the magnitude of fatigue stresses compared with the fatigue endurance stresses in the various component parts. It is usually desirable to design components for infinite fatigue life. However, in some ship applications it might be necessary to allow fatigue stresses to exceed the endurance strength, in which case some other standard would be used such as a "life of ship" or a "life between overhaul" standard.

Fatigue life calculations involved in CP propeller design require knowledge of the ship operating profile and the resultant blade forces under all operating conditions which could limit fatigue life. Determination of the blade forces is discussed in Chapter III. Throughout the profile, fatigue stresses on various components such as blades, bolts, and blade carriers must be determined.

Knowledge of the fatigue characteristics of the material in each of the highly stressed regions is also required. Fatigue data for small, smooth specimens are needed along with data demonstrating the effect on fatigue of notches, surface treatments, size, etc., as discussed in Chapter IV. Where such data are not available, safety margins must be increased appropriately. In any case, it may be necessary in some instances to perform fatigue tests on components, or on a full hub assembly with an overload as described in Reference 7 in order to demonstrate fatigue performance.

CHAPTER ORGANIZATION

The rest of this chapter is arranged in three sections. First, all of the laboratory techniques which have been applied to the CP propeller strength problem at DTNSRDC are described. The numerical stress analysis methods which were applied are defined in sufficient detail to allow reproduction of the capability and duplication of results. Then the predictions of stress so obtained are compared with laboratory experimental data and with presently available data obtained during sea trials. Several methods which have been identified to help reduce stress levels are described. Finally, the sequential process of strength assessment is discussed in detail.

A number of methods are available for determining the structural response of the bolted blade attachment. These include the numerical technique of finite elements and closed form equations as well as use of both model and full-scale experiments.

In Table 1, the methods used during the DTNSRDC investigations are listed and are compared on the basis of cost and accuracy in determining stresses in the crank

TABLE 1 - COMPARISON OF STRUCTURAL MODELING TECHNIQUES

Estimates of Relative Cost*/Accuracy** for Most Simple Analysis or Experiment	Stress in Blade Carrier	Average Stress in Blade Bolts	Bending Stress in Blade Bolts
Numerical			
Finite Element			
- Three-dimensional	9/6.5	10/7	10/7
- Three- and two-dimensional	9.5/7.5	11/7	11/7.5
- Two-dimensional and closed form	1.0/7	1/6	--
Closed Form	0.5/6	0.5/3.5	--
Experimental			
Full-Scale			
- In lab.	25/8	25/8	25/8
- At sea	75/10***	75/10***	75/10***
Model Scale			
- Metal	10/6	10/7	10/7
- Photoelastic	8/3	8/3	8/3

   *Cost estimates are dependent upon DTNSRDC capabilities and facilities. Advances in technology, such as computer capacity or telemetry, may significantly change the estimates.

   **Numbers given for accuracy are subjective judgments of the relative overall accuracy based on comparison with results from measurements at sea. Blade loads for this purpose were inferred from the at-sea measurements.

   ***In general, there is no substitute for measurements at se. where the many factors such as blade loads, friction, tolerances, vibration, load-structure interaction, etc., which directly affect structural response, are all involved in an operational environment.

ring and blade bolts. The comparisons are somewhat subjective and, further, they are based on the numerical and experimental analysis capabilities at DTNSRDC including personnel and facilities.

The accuracy of the stress analysis methods is determined wherever possible by comparison with results from measurements at sea. Blade loads for this purpose have been inferred from the at-sea measurements. Differences in experimental data between at sea and laboratory measurements are probably due to differences in applied forces, gage locations, boundary conditions, number of blades loaded, friction effects, etc.

EXPERIMENTAL METHODS

In general, there is no substitute for accurate strain measurements at sea where the many factors such as blade loads, friction, tolerances, vibration, load and structure intera.... etc., which directly affect structural response, are all involved in an operational environment. In the course of the DTNSRDC investigations, strain meas....nents were made at sea on the CP propellers of four Navy ships: the single-screwed BARBEY,[3] with hub designed by Liaan, Inc., and built by Propulsion Systems, Inc.; the twin-screwed SPRUANCE, with hubs designed by Kamewa and built by Bird Johnson Company; the single-screwed PERRY[8] with virtually the same hub as the SPRUANCE, but different blades; and the twin-screwed R/V ATHENA (formerly PG-84) with hubs designed by Liann, Inc., and built by Propulsion Systems, Inc. Details of these at-sea experiments are provided in Chapter II. Confidence in interpreting results of the less expensive methods is gained through comparison with data from measurements at sea.

As indicated in Table 1, experimental methods on a model scale are much less costly than full-scale experiments at the expense of accuracy. The three-dimensional photoelastic model experiment shown in Figure 6 obtained good qualitative results; the tensile stresses due to bolt bending are indicated near the bolt head on the blade side of the bolt and in the threads on the opposite side of the bolt. This effect has been noted throughout the DTNSRDC investigations. In these experiments with three-dimensional photoelasticity, it was not possible to accurately model materials with different moduli. Young's modulus for bronze (blade and hub) is nearly one-half that for steel (crank ring); both must be modeled before accurate stresses can be obtained. In addition, only one load condition is possible with

340
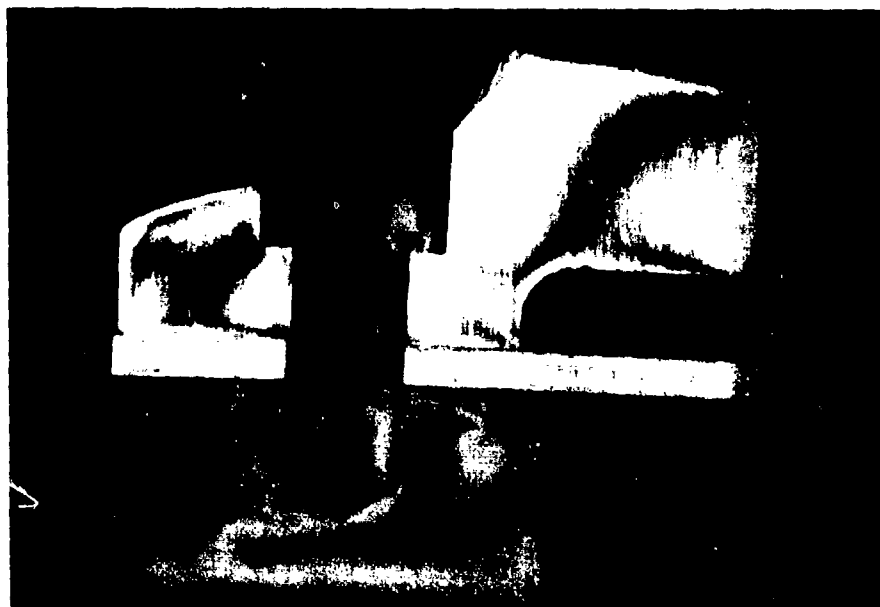
Figure 6 - Cross-Section of USS SPRUANCE Photoelastic Model
at Bolt 8

three-dimensional photoelasticity, although strain gage measurements for various
conditions can be made prior to the photoelastic experiment.

The one-third scale metal model in Figure 7 was used to determine the effect of
blade palm and blade fillet shape on bolt stresses. This work[9] led to a new blade
fillet shape for the SPRUANCE and TICONDEROGA Class propellers[10] which will sub-
stantially reduce bolt and crank ring stresses. Comparisons shown in Figure 8 based
on measurements of strain in the blade attachment bolts on the one-third-scale model
of the original SPRUANCE propeller and on the actual propeller indicate that the
model was a good simulation. Strains obtained from the model scale in the stress
concentration region of the crank ring did not compare as well because of limited
space in the small radius fillet and the need to place a strain gage at the point of
peak strain.

Much of the expense of either the three-dimensional photoelastic or metal
models is in the manufacture of the modular parts. Either model requires machining
a number of pieces including the blade, bolts, crank ring, dowel pins, etc. In
addition, care must be taken to simulate actual boundary conditions by modeling a
dummy hub with stiffness equivalent to that of the actual hub.

341

Figure 7 - One-Third-Scale Model

The accuracy of the experimental data is also dependent upon simulations of the actual hydrodynamic and centrifugal forces. The magnitude and distribution of the hydrodynamic force across the blade is time-dependent and complex, making duplication in the laboratory impractical. Figure 9 illustrates the manner in which blade forces were applied in the laboratory. One force simulated the hydrodynamic blade force at the predicted center of pressure near the 70 percent radius. The other force simulated the centrifugal blade force acting through the blade center of gravity. A comparison of the distribution of blade strains near the hub based on experiments with these vector forces and based on computations with distributed pressures is shown in Figure 10 (from Reference 11) with good agreement.

Several full-scale experiments in the laboratory were reported in References 10, 11, and 12. Figure 11 (from Reference 11) shows the setup for the PERRY propeller ready for test. As indicated in Table 1, these full-scale experiments are the best and the most expensive laboratory simulations. In Figure 12, good agreement
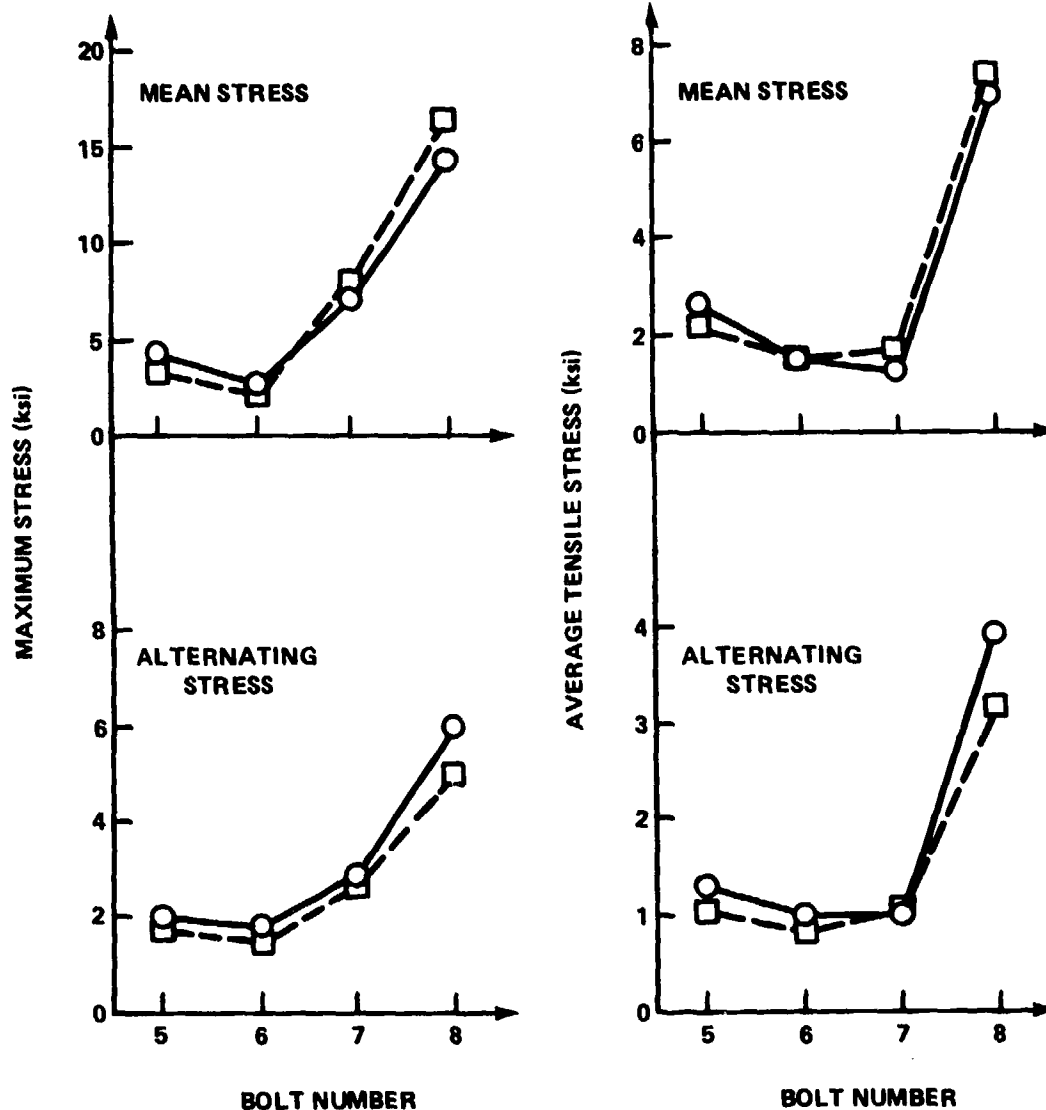
NOTE: BOLT PRELOAD WAS ABOUT 125 TO 130 kip IN ALL BOLTS. STRESSES FOR BOLTS 5 AND
6 ARE AT MIDSHANK, WHILE STRESSES FOR BOLTS 7 AND 8 ARE NEAR THE BOLT HEAD.

Figure 8 – Bolt Stresses at Blade Forces for Full–Power
Full–Rudder Operation
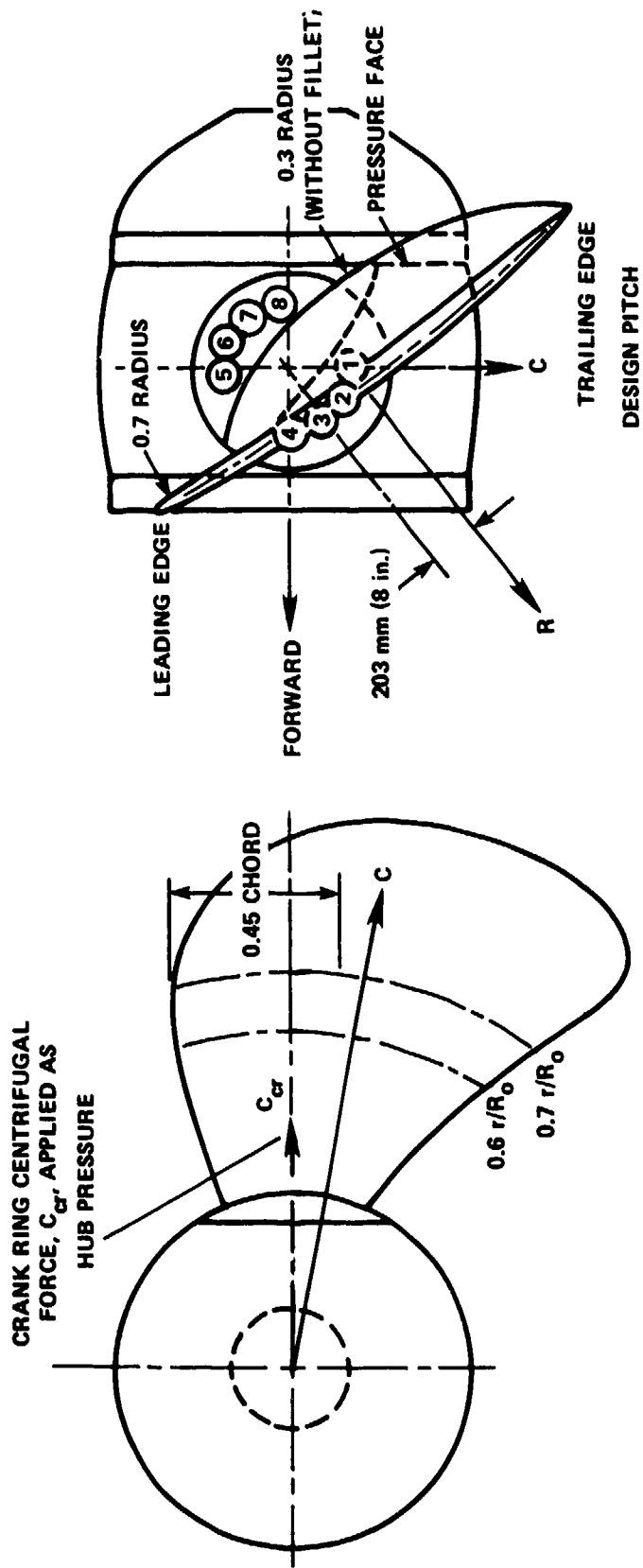
Figure 9 – Propeller Blade Showing Load Vectors Applied in Test

344
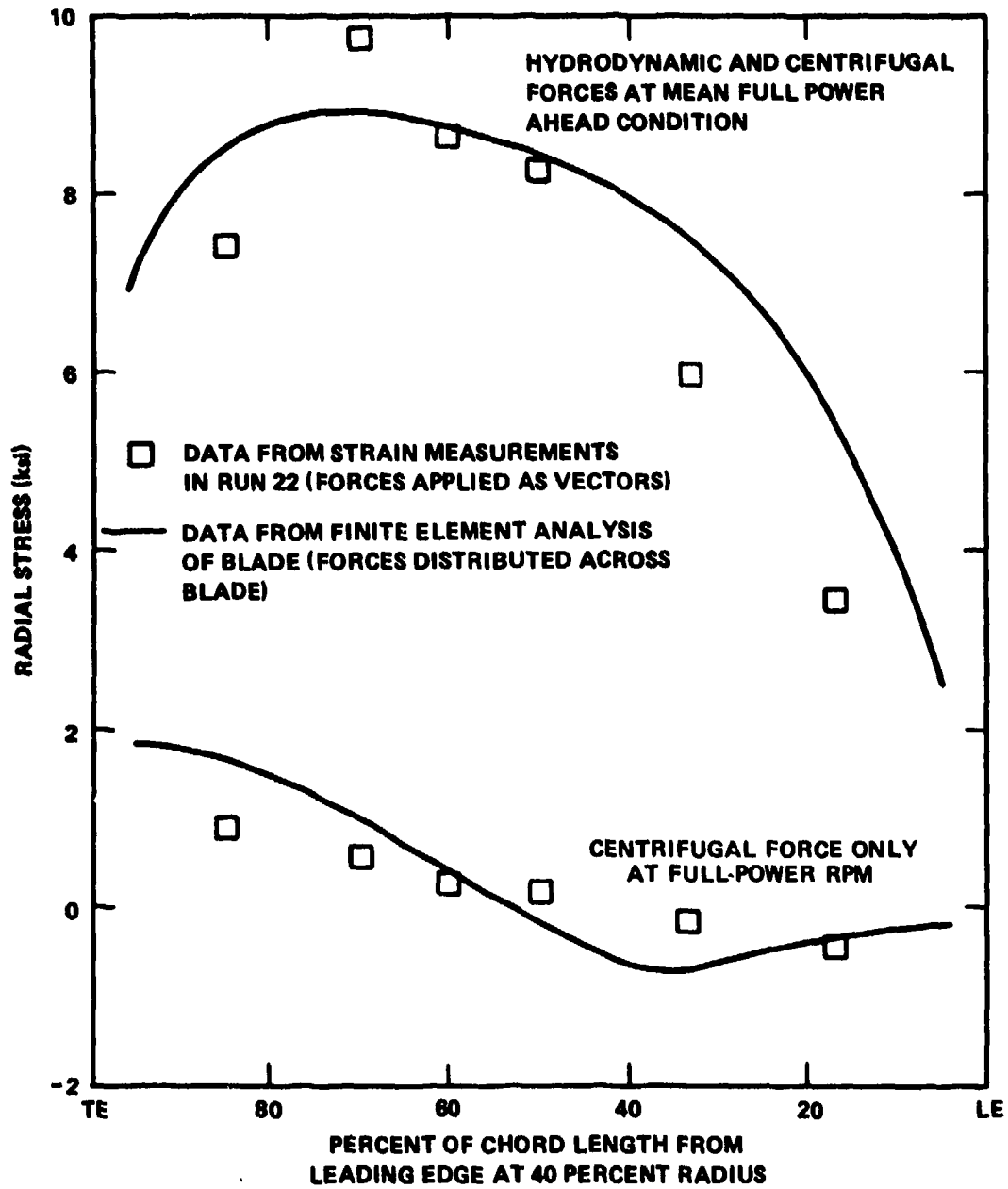
Figure 10 — Comparison of Measured and Computed Blade Stresses

Figure 11 - Propeller Blade Attached to Hub in Laboratory
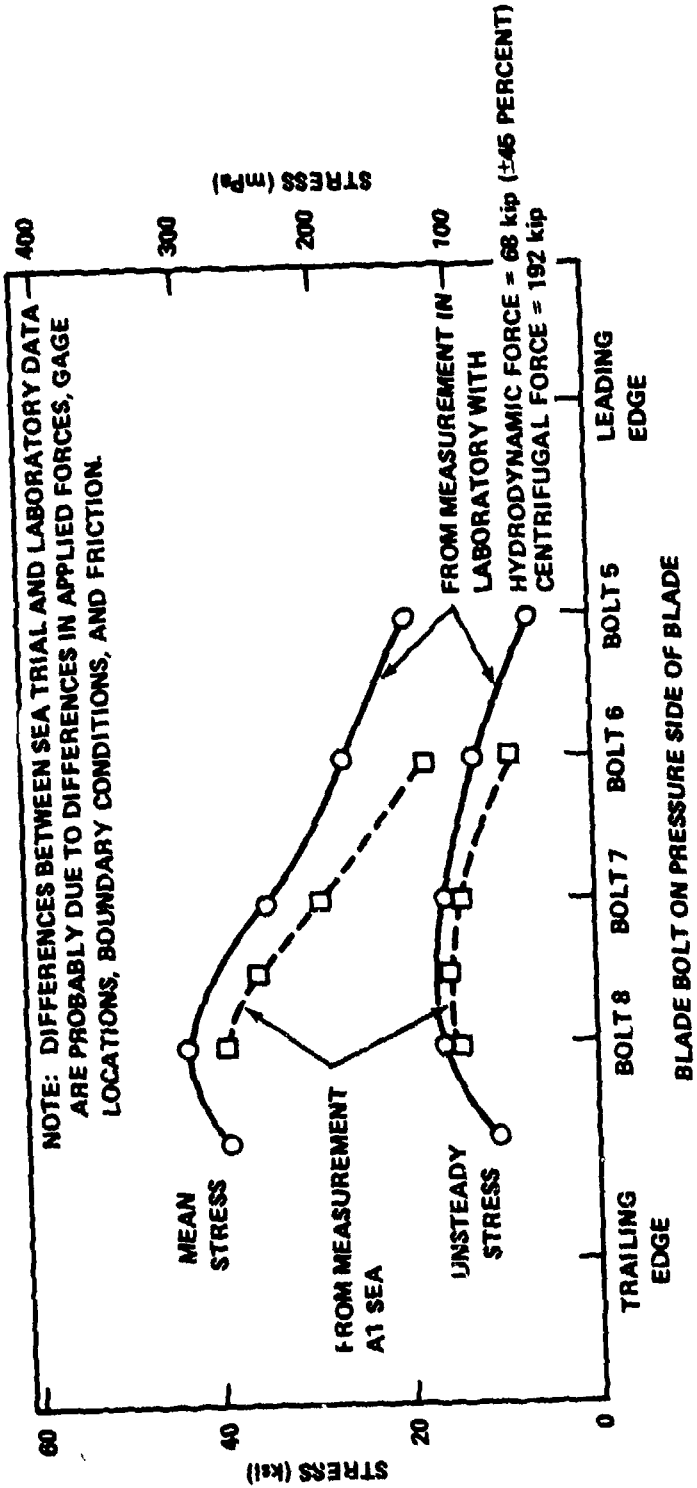
Figure 12 - Stress in Groove at Crank Ring Flange, Ahead Condition, USS SPRUANCE Controllable Pitch Propeller

347

is evident between strains on the crank ring measured at sea and in the laboratory on the SPRUANCE propeller. Similar agreement shown in Figures 13 and 14 occurred in measured strains on the blade bolts. It was found that due to friction effects, strains had to be measured while blade forces were applied dynamically. The hydraulic jack simulating the hydrodynamic force was cycled in a sine wave at 2 to 3 Hz (similar to shaft frequency) while strains were constantly monitored. These friction effects were more pronounced in the blade bolts than they were in the crank ring.

A tendency is evident in Figures 13 and 14 for the full-scale laboratory simulation represented by Figures 9 and 11 to increase the stresses at bolt 8 and decrease the stresses at bolt 5. A detailed discussion of three apparent causes of this discrepancy is given in Reference 11: (1) the effect of different boundary conditions in the laboratory because hydrodynamic blade forces were applied at one blade only, (2) friction effects, and (3) the manner in which centrifugal blade forces were applied in the laboratory.

As discussed in the section on the Strength Assessment Process, it may be necessary to perform full-scale fatigue tests of components to verify adequacy of a design. Reference 12 reports such tests which were conducted on a SPRUANCE hub assembly with one blade at strain levels greater than those measured at sea during full-power, zero-rudder operations but less than those measured during high power turns. These tests were discontinued when the most highly loaded blade bolt failed in fatigue. Later inspection of the crank ring revealed that it, too, had developed a fatigue crack. Additional, more definitive data for the bolts and crank rings were obtained in a number of fatigue tests of individual, full-size bolts[13] and portions of full-size crank rings[14] in which the stresses obtained at sea were reproduced. All these fatigue data strongly influenced decisions to make the design modifications described in References 10 and 15.

Conclusions from Reference 13 related to the use of AISI 4140-steel, K-Monel, and titanium 6A1-4V bolts are as follows based on results of 2.75-in. diameter bolt fatigue experiments:

"1. K-Monel bolts with rolled threads perform much better than AISI 4140 steel bolts with cut threads. The K-Monel has a lower elastic modulus than steel, and K-Monel bolts with rolled threads will perform slightly better in air than will steel bolts with rolled threads. The K-Monel is more corrosion resistant than steel. As
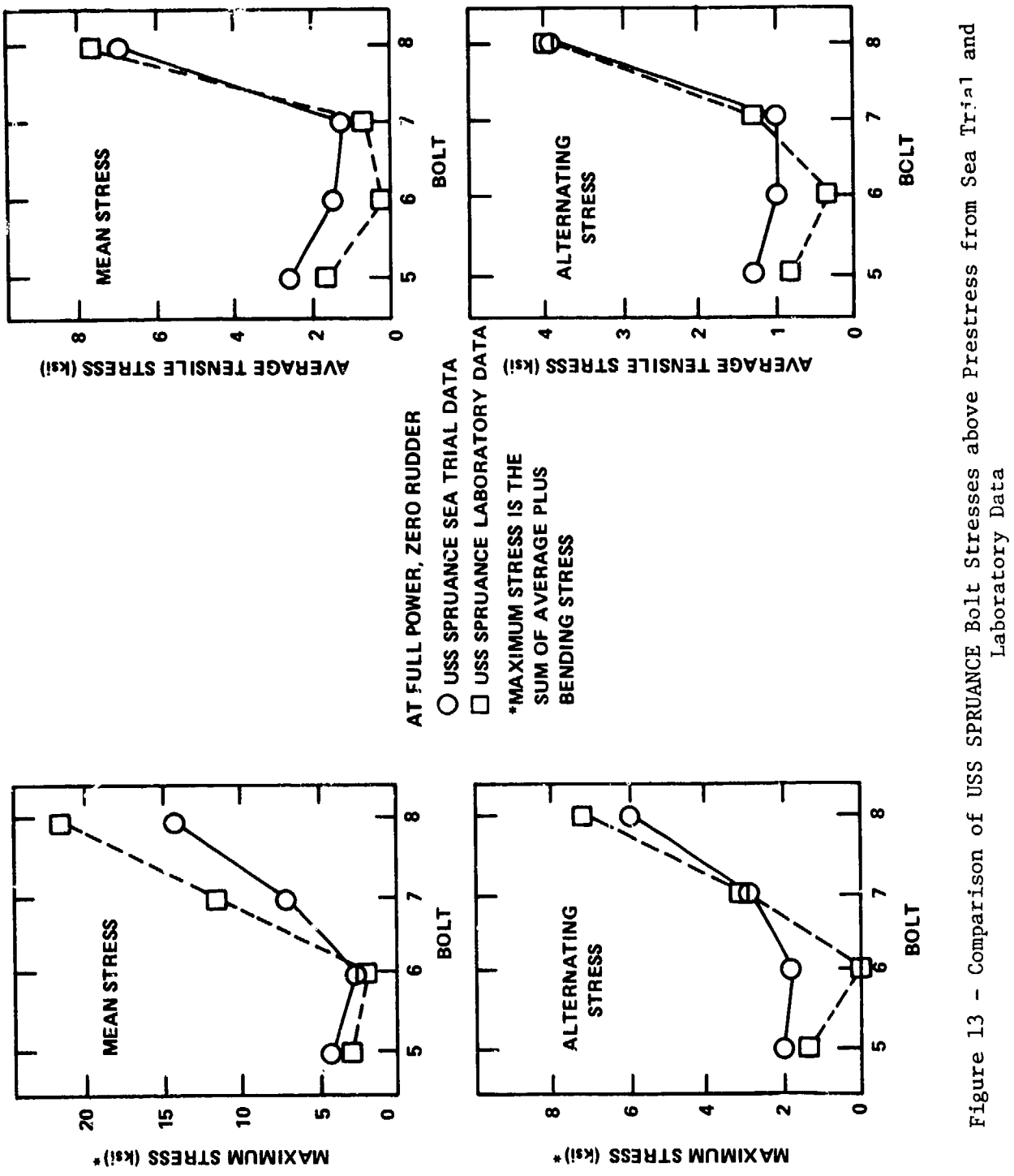
Figure 13 - Comparison of USS SPRUANCE Bolt Stresses above Prestress from Sea Trial and Laboratory Data
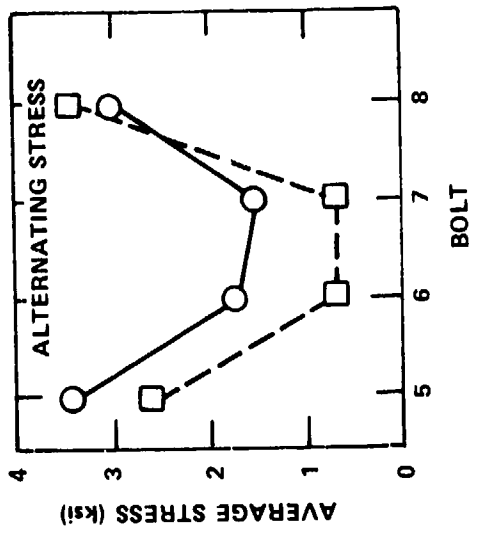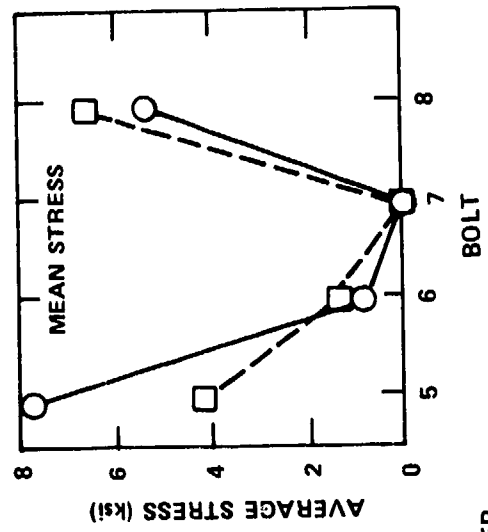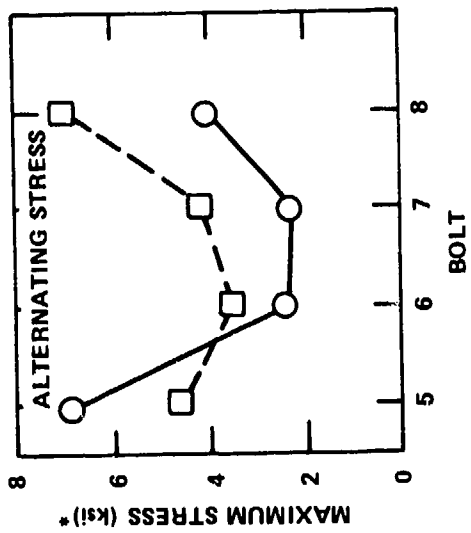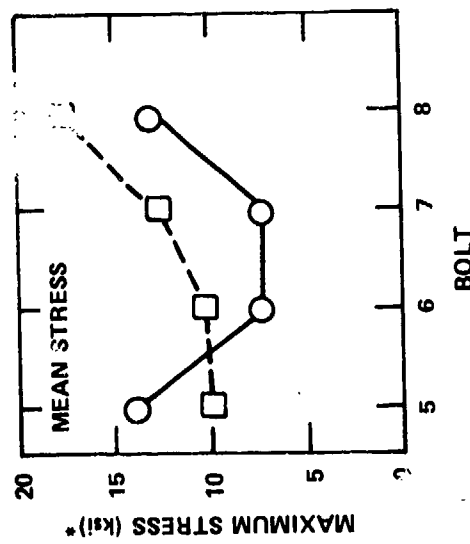
349

Figure 14 – Comparison of USS OLIVER HAZARD PERRY Bolt Stresses above Prestress from Sea Trial and Laboratory Data

there is some possibility propeller bolts may be exposed to seawater in service, K-Monel (K-500 alloy) is a better material than AISI 4140 steel for blade bolts.

"2. In air, titanium 6Al-4V bolts with rolled threads have fatigue lives comparable to AISI 4140 steel bolts with rolled threads. Titanium is more corrosion resistant, and it may be a good material for blade bolts. However, the test data for titanium bolts are too limited to demonstrate whether titanium is superior to either steel or K-Monel.

"3. Data show that the fatigue life of K-Monel blade bolts on the SPRUANCE can be increased by using prestresses as great as 150 percent of the presently specified prestress. A higher prestress should be used only if the operational stresses are known well enough to give confidence that the stresses in the bolt shank and in the blade palm under the bolt head will not exceed the material yield strength.

"4. The service life of K-Monel blade bolts with rolled threads should be significantly greater than the original AISI 4140 steel bolts with cut threads used on the SPRUANCE. Results of a small number of experiments of cumulative fatigue damage done at full-scale have indicated that failure will occur earlier than predicted by the theory of linear cumulative damage. The value $\Sigma n_i / N_i = 0.6$, where n_i = number of applied cycles at stress level i and N_i = cycles to failure at stress level i, should continue to be used to estimate blade-bolt fatigue life.

"5. For design purposes, a fatigue strength-reduction factor of 4.0 is conservative for steel or K-Monel blade bolts with cut threads, and a fatigue strength-reduction factor of 3.0 is conservative for steel or K-Monel blade bolts with rolled threads. The design procedure of Snow and Langer[16] is conservative enough for blade bolts of either AISI 4140 steel or K-Monel; design curves for the two materials are presented in Figures 15 and 16."

Reference 13 also reported that, although test results for Inconel 718 had been inconclusive due to bolt manufacturing problems, properly rolled Inconel 718 bolts might prove to be satisfactory because of their high strength and corrosion resistance. Fatigue tests of 1-in. diameter Inconel 718 bolts with rolled threads and a yield stress of 120,000 psi are currently being conducted at DTNSRDC with the preliminary indication that they may have an endurance strength as much as two times that of the K-Monel bolts with rolled threads. The effect of size on these Inconel 718 bolts has not been evaluated, but Equation (3-17) from Reference 17 for high

351
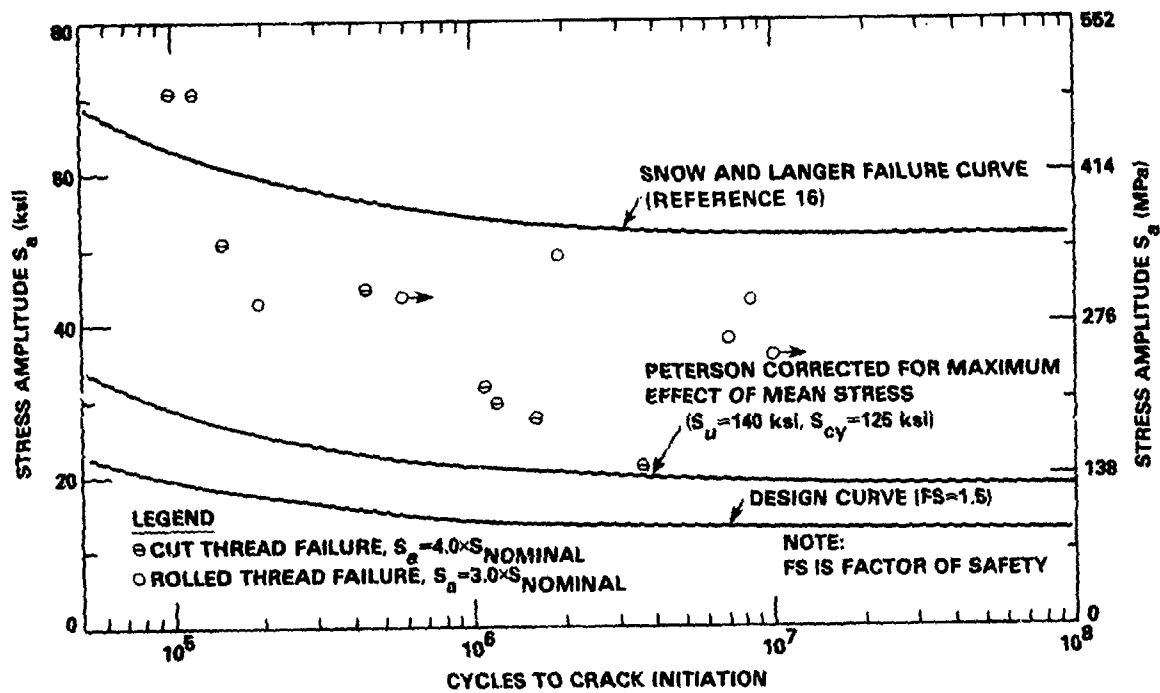
Figure 15 — Fatigue-Failure Curve for High-Strength Steel, Corrected for
Maximum Effect of Mean Stress, Design Curve, and
Experimental Results
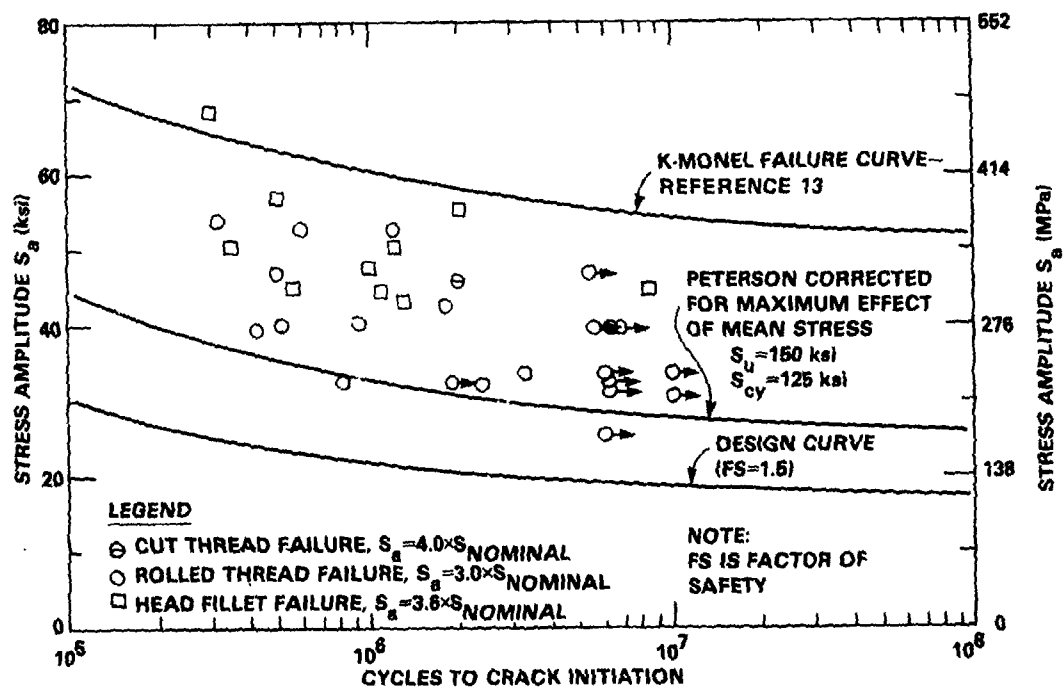
Figure 16 — Fatigue-Failure Curve for K-Monel, Corrected for
Maximum Effect of Mean Stress, Design Curve, and
Experimental Results

strength steel indicates that 3-in. diameter bolts would have about 90 percent of the fatigue limit of 1-in. diameter bolts with the same steel and stress distributions.

The work by Garala[14] on fatigue tests of portions of full-size crank rings was summarized as follows:

"In order to identify the cause of an unexpected fatigue failure in an ASTM A243-64 Cl N steel crank ring of the SPRUANCE CP propeller, fatigue tests were conducted on full-sized fillet specimens (30-deg wedge segments) cut from actual crank rings. The crank ring had failed during laboratory testing at an effective alternating stress level which simulated a full power turn condition and which was less than 30 percent of the ultimate strength of the material. Cracks had initiated at brittle nonmetallic inclusions which are inherent in large forgings even of high quality. Small specimen tests of the crank ring material had previously indicated that the endurance stress was greater than 40 percent of the ultimate strength. Fatigue tests were carried out on 13 full-sized wedge specimens. No cracks occurred in the highly stressed fillet area even at 150 percent of the original stress level except at an inclusion in one of two such specimens which had been cut from the opposite side of the failed crank ring. These tests demonstrated that it is possible for an inclusion of sufficient size to exist in the crank rings and to act as an initial crack if it is unfortunately located and oriented in a high stress field. The combined mean and alternating crank ring stresses in high power turns should not exceed the desired limit of 50 percent of the fatigue limit which is customary for large, heavy-sectioned high strength steel forgings. For the SPRUANCE, the planned substitution of crank ring material to A471 steel provides the opportunity to improve fracture toughness to reduce stresses by increasing the fillet radius."

NUMERICAL METHODS

The numerical techniques listed in Table 1 include two-dimensional and three-dimensional finite element (FE) methods and closed form equations. These approaches have been applied singly and in combination to predict stresses in the crank ring and blade attachment bolts. In all cases, involvement of the more expensive FE methods increases accuracy of the results.

Three-Dimensional Finite Element Method

Use of the three-dimensional (FE) method involves numerical modeling of the structure in three-dimensions. Careful attention is required at the interface between the blade palm and crank ring with this method because the local separation which occurs under load makes the bolt stress problem nonlinear. The cost of this method for blade attachments is fairly high--currently about the same as for metal model experiments. The reason for the high cost is that modeling all the structure necessary to obtain good predictions, including the blade, bolts, crank ring, and portions of the hub body leads to a large number of degrees of freedom. This, in turn, causes large amounts of computer time to be used during the iterative solution of the nonlinear problem.

In Figure 17, bolt stress predictions from a three-dimensional FE analysis of the BARBEY blade attachment are compared with stresses from measurements at-sea for the mean, full power, ahead condition. Good agreement is evident. This analysis was completed using eight noded brick finite elements in the MARC-CDC General Purpose Finite Element Analysis Program.[18] Approximately 1700 elements and 3000 nodes were used to model the blade, bolt, crank ring, and part of the hub with 1300 degrees of freedom. It was shown that the bolt stresses were nonlinear with respect to increasing blade force due to the increasing separation of the blade-palm-crank-ring interface. The interface was modeled with tied nodes and the separation was taken into account by releasing ties. Three iterations were necessary to obtain the results in Figure 17. A similar analysis indicating similar nonlinear behavior was carried out by Chu and McLaughlin[19] who used the SAP IV computer program. The major conclusion of these efforts was that the three-dimensional FE method, although costly, provides an important design tool for CP propellers.

An unsuccessful and abandoned attempt to reduce the costs of the three-dimensional FE method application to blade attachments is described by Martin[20] in which an elastic foundation of "equivalent spring stiffness" was used to model the crank ring and hub body. The increasing separation of the blade-palm-crank-ring interface was modeled by releasing elements in the blade palm from the elastic foundation. Using this approach, the distribution of forces among the bolts was predicted with good accuracy and the area of separation at the interface was determined. However, the reliability of the bolt stresses from this analysis was

THREE-DIMENSIONAL
FINITE ELEMENT
MESH
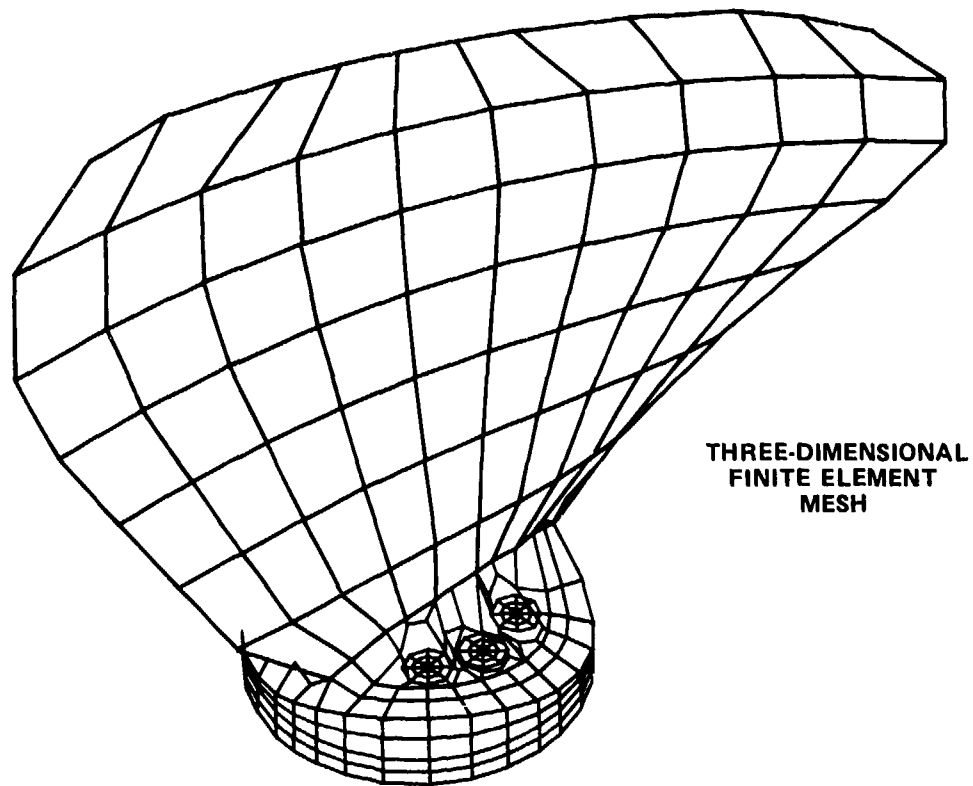
BOLT NUMBER	MEASURED STRESS (ksi) SEA TRIALS		CALCULATED STRESS (ksi)	
	AVERAGE TENSION	MAX.	AVERAGE TENSION	MAX.
6 (TRAILING EDGE)	7.8	14.0	5.8	12.0
2	0.2	—	1.5	2.7
4 (LEADING EDGE)	1.0	—	2.3	5.0

BOLT PRESTRESS NOT INCLUDED.

Figure 17 - Calculated versus Measured Bolt Stress above Prestress for
USS BARBEY Mean Full-Power Ahead Condition

limited because of uncertainties in the "equivalent spring stiffness" upon which the stresses depend, and because crank ring deflections and deformations under load, which affect bolt bending, were not modeled.

Combined Three-Dimensional and Two-Dimensional
Finite Element Methods

In the three-dimensional FE analysis, stresses are computed inside an element at "integration points," but not at the surface of the element. These integration point stresses can be extrapolated to the surface, but accuracy is lost in regions of stress concentration.

As indicated in Table 1, the stress predictions from the three-dimensional FE analysis can be enhanced by combining it with two-dimensional FE analyses. For example, nodal displacements from the three-dimensional analysis can be applied to a two-dimensional FE model of a slice through the crank ring as shown in Figure 18 which is taken from Reference 20. In this manner, detailed examination of stresses at stress concentrations is possible as in Figures 19 and 20, which were obtained using the APES[21] computer program. In a similar manner, the behavior of the bolts including bending and the effects of stress concentrations can be identified. Although stress concentration factors (SCF) from handbooks such as Peterson[22] are available, none are based on cases of good comparability with crank rings. Also, the nominal stress level to which a handbook SCF would be applied is not apparent from a three-dimensional FE analysis.

Closed-Form Equations

Typical CP propeller blade attachment design calculations by blade manufacturers are based on simplifying assumptions which allow use of standard, straightforward handbook equations to compute stresses. The DTNSRDC investigations have shown that for the blade bolts, the assumptions are very nonconservative and lead to calculated bolt stresses which are much less than those determined from laboratory and at-sea measurements. A DTNSRDC derived set of closed-form equations provides substantially better results and is the basis for the closed-form equation entries in Table 1. The DTNSRDC equations are somewhat better for the crank rings than for the blade bolts. In both cases, improvements in predictions are possible by combining the

FILLET RADIUS = 0.375 in.
(0.009 m)
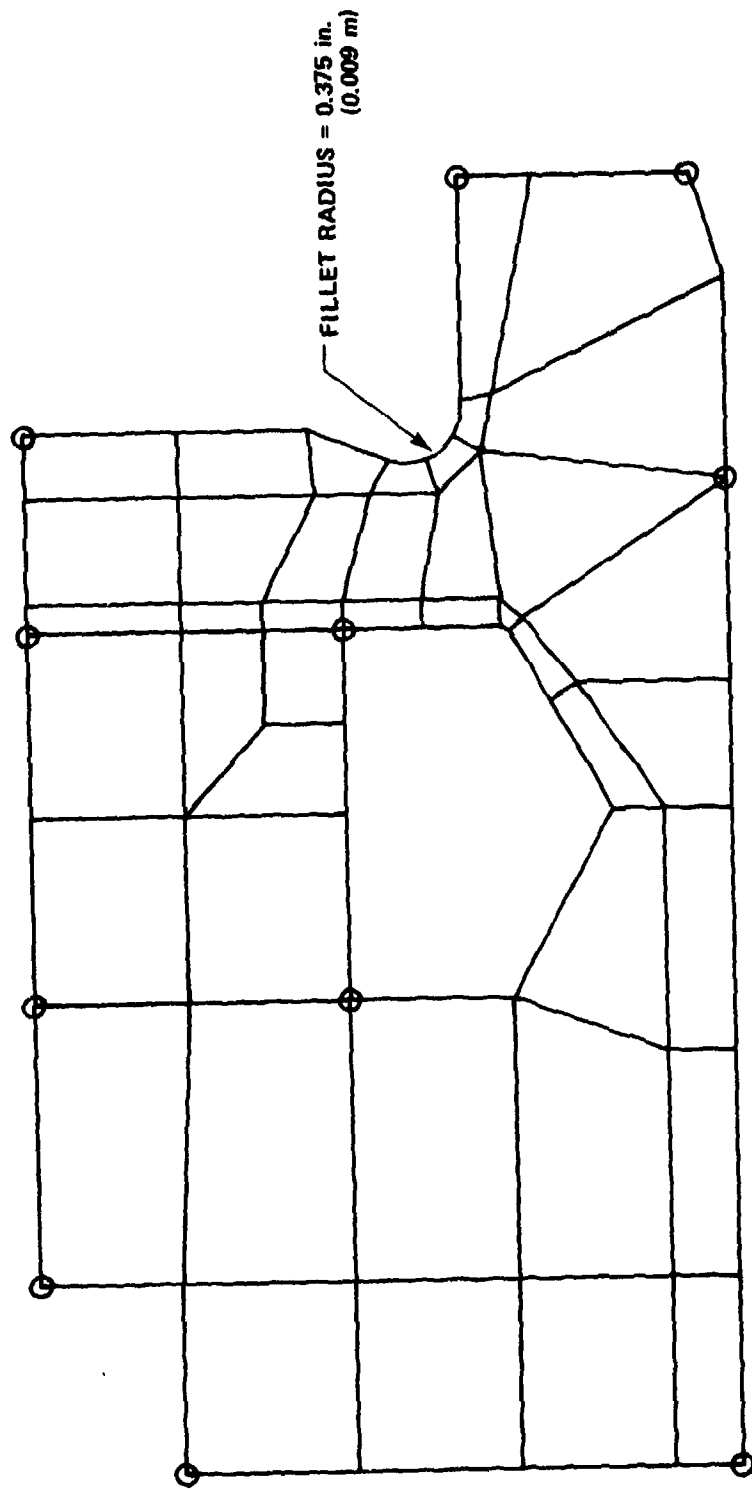
O NODES AT WHICH DISPLACEMENTS FROM A THREE-DIMENSIONAL ANALYSIS HAVE BEEN APPLIED

Figure 18 - Two-Dimensional Finite Element Crank Ring Slice

357

CONTOUR VALUES MAXIMUM PRINCIPAL STRESSES

1 — -70000.000
2 — -50000.000
3 — -30000.000
4 — -10000.000
5 — 10000.000
6 — 30000.000
7 — 50000.000
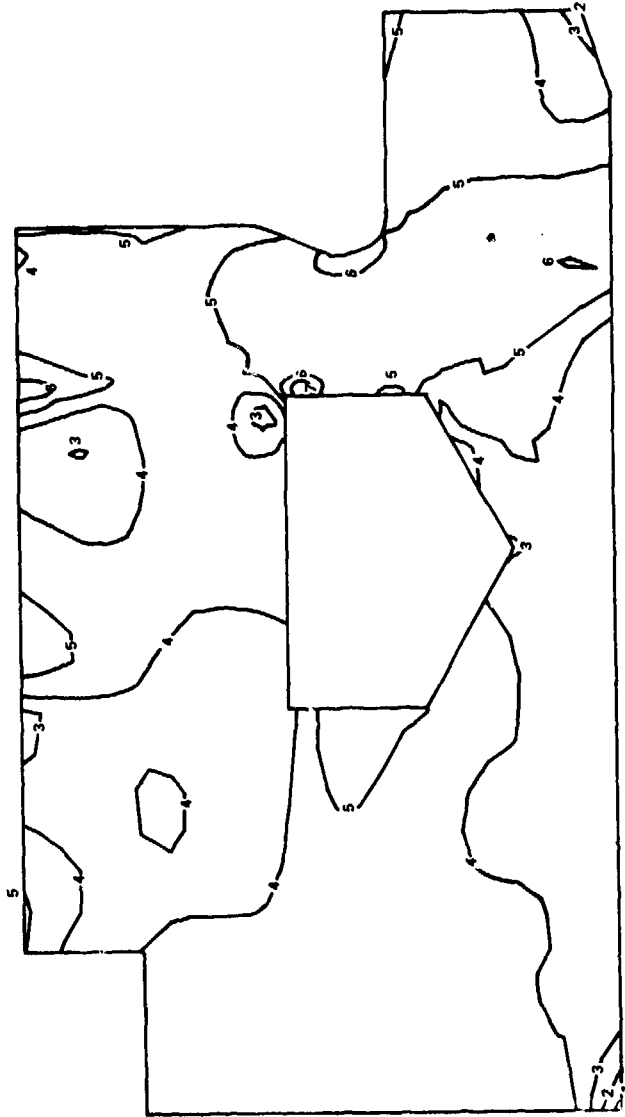
Figure 19 - Maximum Principal Stress for Crank Ring Slice with 0.375 Inch (0.009 Meter) Fillet

CONTOUR VALUES MAXIMUM PRINCIPAL STRESSES

1 — -20000.000
2 — -10000.000
3 —   0.000
4 — 10000.000
5 — 20000.000
6 — 30000.000
7 — 40000.000
8 — 50000.000
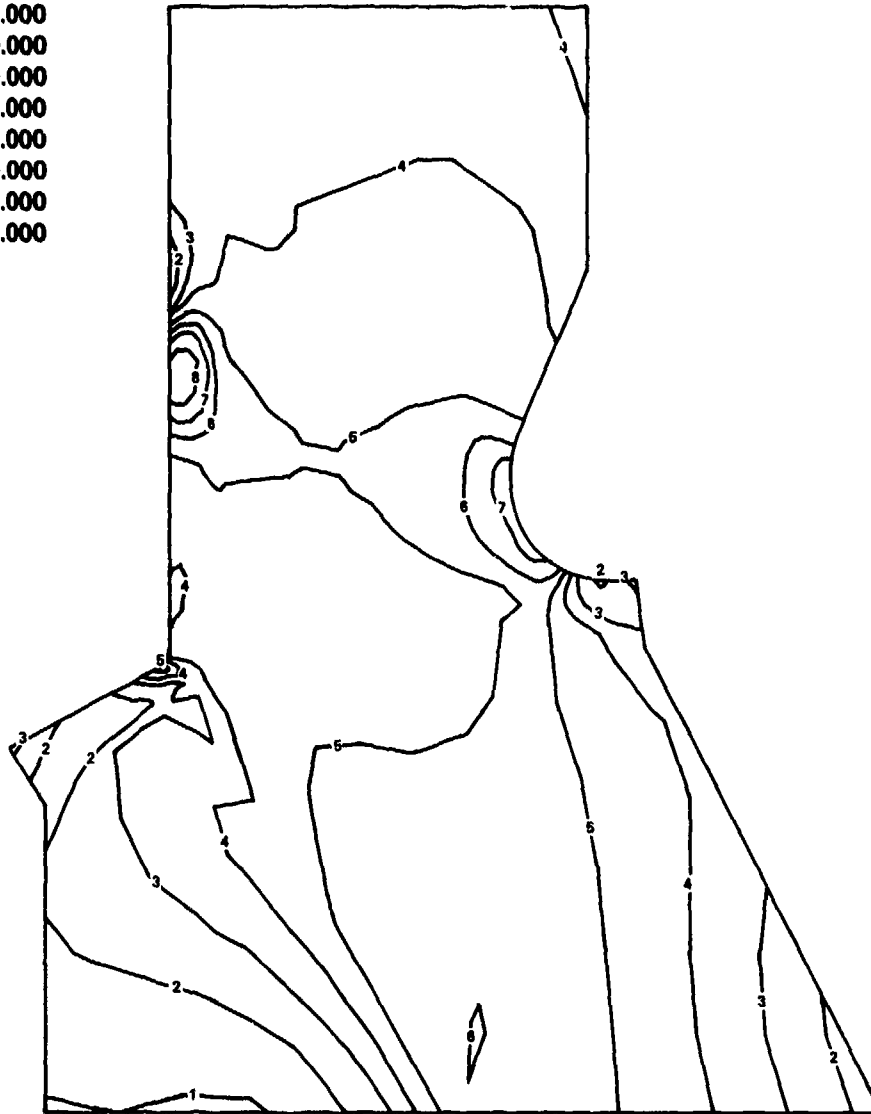
Figure 20 — Maximum Principal Stress near Crank Ring Fillet with
0.375 Inch (0.009 Meter) Fillet

359

equations with results of two-dimensional finite element analyses as described below. It is important to note that the amount of bolt bending is not predicted with these approaches.

Typical Designer Approach for Blade Bolts. Typical CP propeller blade bolt design calculations by blade manufacturers are based on the supposition that bolt forces are purely tensile, that they are distributed in a simplistic manner, and that there is no bolt preload.* That is, the force in a bolt is directly proportional to its distance from an assumed neutral bending axis. The location of the neutral axis has been assumed to be parallel to the nose-tail line at the 0.7 radius and either to intersect the blade palm at its center or near its forward edge; see Figure 21. The former assumption was used in designing the SPRUANCE blade bolts while the latter assumption, which leads to about 25 percent smaller calculated bolt forces, was used for the BARBEY. With either assumption, an equation for bolt force is written:

$$F_{bolt\ i} = \frac{C}{n} + \left[M \times \frac{y_i}{\sum\limits_{all\ i} y_i^2} \right] \tag{1}$$

where $F_{bolt\ i}$ = the force at bolt i

C = applied centrifugal force

M = bending moment

y_i = the distance from the bolt center of bolt i to the assumed neutral bending axis

n = the number of bolts

In some cases, the value of y in the numerator is replaced with the value, $y_{max} + r$ where r is the bolt radius and y_{max} is the distance to the bolt furthest from the neutral axis. The data F_1 in Table 2 for ahead loads at design pitch were obtained using Equation (1) with the more conservative assumption that the neutral axis inter-sects the blade palm at its center and with $y_{max} + r$ in the numerator. The alter-nating forces listed for F_1 were found using the second term of Equation (1) with the predicted alternating bending moment.

---

*The term "bolt force" in this and the following discussions means force at a bolt location, some of which is applied to increase the force in the bolt and some to decrease precompression or preload in the joint.
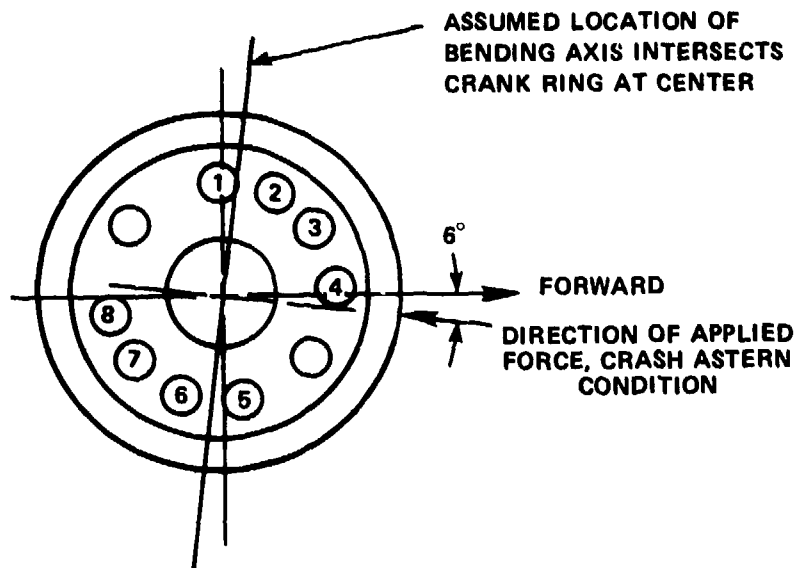
Figure 21a — USS SPRUANCE Crank Ring
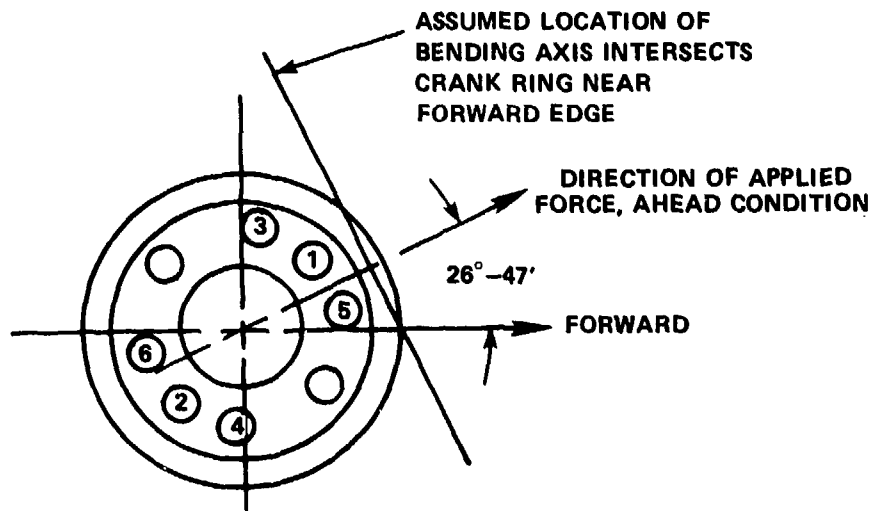
Figure 21b — USS BARBEY Crank Ring

Figure 21 — Assumed Location of Bending Axis for Design of
Blade Attachment Bolts

TABLE 2 - BOLT FORCES COMPUTED WITH EQUATIONS (1) THROUGH (6)

Ship	Centrifugal Force, C (kip)	Number of Bolts, n	Bending* Moment, (in. kip)	F_1** (kip)	F_2*** (kip)	F_6† (kip)
USS SPRUANCE	192.0	8	3.15×10^3 $\pm 1.42 \times 10^3$	88.4 ± 29.0	112.4 ± 34.8	125.6 ± 38.3
USS OLIVER HAZARD PERRY	188.0	8	3.18×10^3 $\pm 1.59 \times 10^3$	88.3 ± 32.4	113.3 ± 37.4	116.1 ± 40.4
R/V ATHENA	64.7	6	2.18×10^3 $\pm 1.09 \times 10^3$	26.5 ± 7.9	32.9 ± 9.4	29.4 ± 7.7
USS BARBEY	236.3	6	2.83×10^3 $\pm 1.27 \times 10^3$	126.8 ± 39.3	146.4 ± 47.2	134.9 ± 43.2

*Mean $\pm$ alternating bending moments at the top of the crank ring based on measurements at sea during full power, zero rudder operations.

**Computed with Equation (1), F_1 is the force in the bolt furthest from the neutral axis on the pressure side.

***Computed with Equation (2), F_2 is similar to F_1 except that C/4 replaces C/n in Equation (2) and for computing alternating, not mean, forces, the moment M is increased empirically by a factor of 1.2.

†Computed with Equations (3) through (6), F_6 is the force in the most highly loaded bolt in tension.

Empirical Modification to Designer Approach for Blade Bolts. Table 2 also contains F_2 data based on another approach to obtaining the maximum bolt forces; F_2 is based on Equation (2) which is the same as Equation (1) but with empirical modifications. The term C/n is replaced with C/4 and, when computing alternating, not mean, forces, the moment term is increased by a factor of 1.2. These empirical modifications to Equation (1) were made on the basis of sea-trial measurements so that it would provide a better indication of the maximum bolt force in any bolt. The basic irrationality of the approach remains--it assumes that the most highly loaded bolt is located furthest from the neutral bending axis while measurements indicate that the

bolt nearest the leading edge or trailing edge of the blade is the most highly loaded. They are probably not the same. Also, important bolt bending stresses are not considered. Using the term C/4, regardless of the number of bolts, distributes the centrifugal force equally among the four bolts which are closest to the body of the blade. This is probably more correct than using equal distribution among all the bolts and the error would be small for a symmetrical blade. With the modifications and allowing for the alternating bending moment, Equation (1) becomes

$$F_{bolt\ i} = \frac{C}{4} + \left[M_{mean} \times (1.0 \pm a \times D) \times \frac{(y_{max} + r)}{\sum\limits_{all\ i} y_i^2} \right] \qquad (2)$$

where C   = applied centrifugal force

M_{mean} = mean hydrodynamic bending moment

D   = an empirical constant equal to 1.2

y_{max} = the maximum distance of any bolt on the pressure side of the blade from the bolt center to the assumed neutral bending axis

a   = the ratio of alternating to mean bending moment

r   = the bolt radius

y_i = the distance from the center of bolt i to the assumed neutral bending axis

Combined Two-Dimensional Finite Element Methods and Closed-Form Equations for Blade Bolts. A major problem with the approach of the typical designer in computing bolt stresses is that the actual distribution of bolt forces caused by the varying stiffness of the blade palm, the effect of bolt preload, and bolt bending are ignored. Measurements at-sea and in the laboratory have demonstrated that the bolts in the stiffer portions of the palm near the leading and trailing edges of the blade are more highly loaded and there is significant bolt bending. The following discussion shows that if the stiffness distribution can be included along with bolt bending and bolt preload, then closed form equations can lead to reasonable bolt stress predictions.

Measured average tensile strains above prestrain at the shanks of the BARBEY and SPRUANCE blade bolts are shown in Table 3 for the mean and unsteady blade forces

363

TABLE 3 – MEASURED BLADE BOLT STRAINS FOR THE USS SPRUANCE AND
USS BARBEY CONTROLLABLE PITCH PROPELLERS AT THE
FULL–POWER AHEAD CONDITION

Ship	Bolt Number	Bolt Location, Fwd or Aft Side, Leading Edge (LE) or Trailing Edge (TE) of Blade	Average Measured Bolt Strain Above Prestrain*	
			Mean (Microstrain)	Unsteady (Microstrain)
USS SPRUANCE**	1	Fwd (TE)	–70	$\overline{+}$ 35
	2	Fwd	–27	$\overline{+}$ 10
	3	Fwd	–18	$\overline{+}$ 7
	4	Fwd (LE)	–45	$\overline{+}$ 20
	5	Aft (LE)	50	± 19
	6	Aft	5	± 5
	7	Aft	18	± 10
	8	Aft (TE)	237	± 94
USS BARBEY***	3	Fwd (TE)	–28	$\overline{+}$ 32
	1	Fwd	0	$\overline{+}$ 18
	5	Fwd (LE)	– 7	$\overline{+}$ 21
	4	Aft (LE)	39	± 25
	2	Aft	7	± 14
	6	Aft (TE)	274	±109

*For the measurements in this table, prestrain was 1160 micro-strain for the AISI 4140 steel bolts of the SPRUANCE and 1930 micro-strain for the 17–4 PH stainless steel bolts of the BARBEY.

**Measurements shown for the SPRUANCE were obtained in the laboratory.

***Measurements shown for the BARBEY were obtained at sea.

at the full-power ahead operating condition. Because the strains are negative on one side of the blade and positive on the other, the neutral bending axis must lie between them. Note also that the strains in the bolts at the trailing edge on the pressure (aft) sides of the blades are much higher than in the others.

Because the bolt strains in Table 3 are additions to bolt prestrain, the magnitude of the force that is actually being carried by each bolt is not clear. However, the bolt forces can be estimated by combining the strains in Table 3 with information showing bolt force versus strain relationships in Figures 22 and 23. These figures are experimentally based. In addition, once the actual bolt forces have been so estimated, a "balance" can be carried out in which the magnitude of the bolt forces are examined to determine the degree to which they balance the applied forces and moments. Such a procedure is demonstrated in Table 4 for the unsteady or peak variation in load. As an example, the load data in Table 4 for bolt 8 of the SPRUANCE was obtained in the following manner. The mean and cyclic strain from Table 3 was plotted in Figure 22 as Δ_1. Then the peak to peak variation in bolt load, F, and the associated mean load were determined from Figure 22.

Figure 24 shows that the neutral axes were assumed to lie perpendicular to the applied bending moment and 2 in. on the suction side of center of the blade palm. The 2-in. shift of the neutral axis from the center of the blade palm was made because this was consistent with the appearances of the crank ring and bearing interfaces after fatigue testing of the SPRUANCE hub. This assumption leads to a fairly good balance for both ships. For the SPRUANCE, the applied bending moment of 89.6 ft-lbf (121.5 kNm), which is computed in the bottom portion of Table 4, is balanced by a resisting moment of 83.5 ft-lbf (113.2 kNm). For the BARBEY, the respective values are 113.4 ft-lbf (153.7 kNm) and 98.3 ft-lbf (133.3 kNm). However, it seems appropriate to ignore the 2-in. shift because of simplicity and conservatism in that decreasing the assumed bolt moment arms would increase calculated bolt forces. The location of the neutral axis in future designs is unknown so assuming the more conservative centerline location is appropriate.

The force distribution at the joint for a bolted on CP propeller blade can be obtained from an analysis using two-dimensional finite elements. Parallel slices through bolt centers and extending from the bottom of the blade palm up to the fillet-blade intersection are idealized with two-dimensional elements as shown in Figure 5. A displacement is applied to each slice to the node at the center of the

365
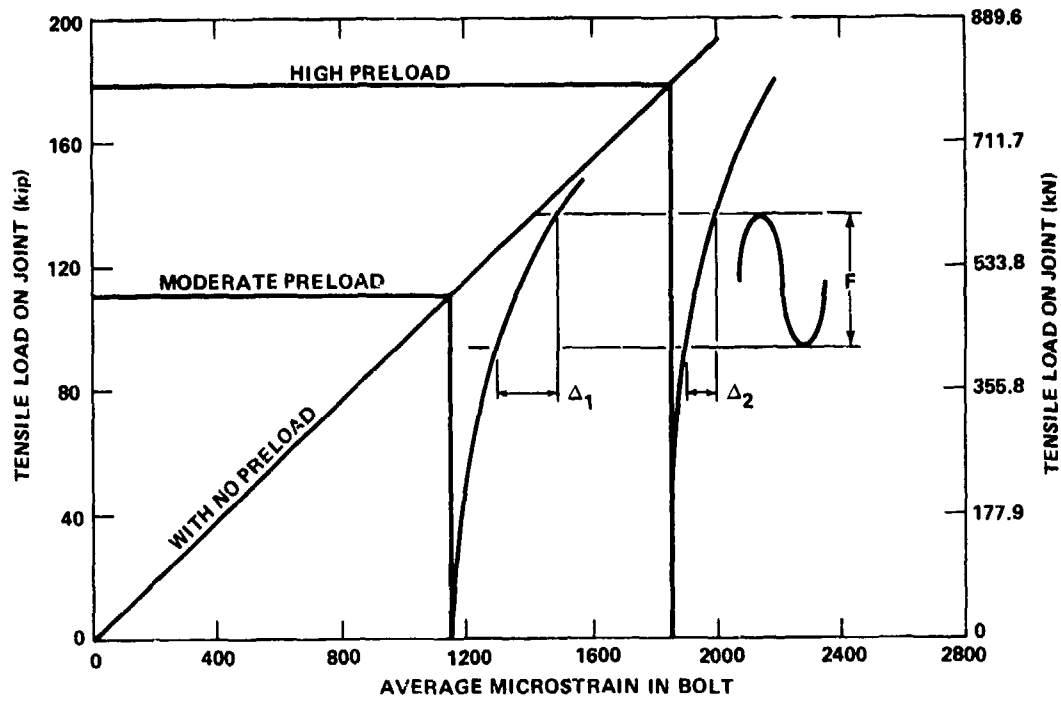
Figure 22 — Effect of Bolt Preload on Bolt Strain, AISI 4140 Steel
Bolts of the USS SPRUANCE Controllable Pitch Propeller
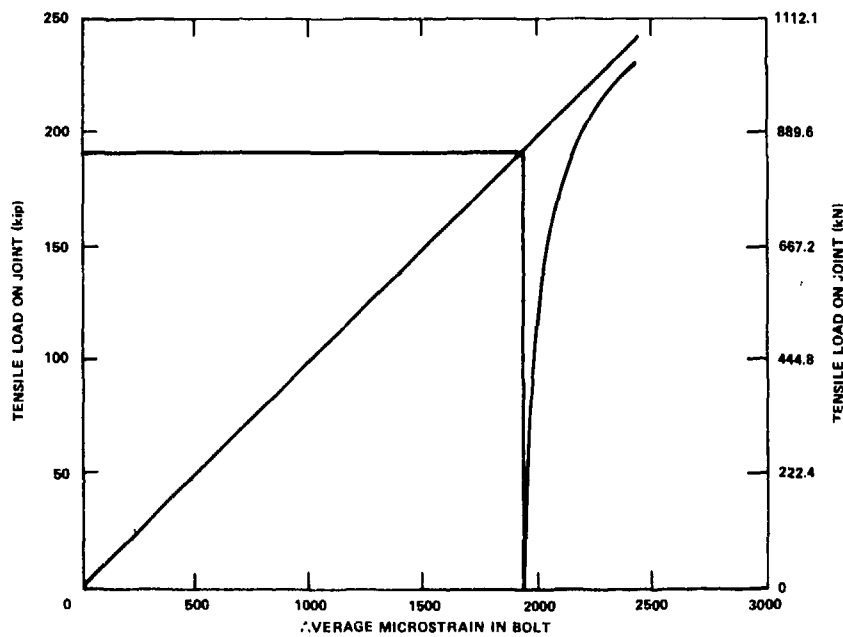
Figure 23 — Effect of Bolt Preload on Bolt Strain, 17-4 PH Stainless
Steel Bolts of the USS BARBEY Controllable Pitch Propeller

366

TABLE 4 - BLADE BOLT FORCES FOR THE FULL-POWER AHEAD CONDITION

Ship	Bolt Number	Mean Bolt Force (kN)	Peak to Peak Bolt Force F (kN)	Distance from Bolt to Neutral Axis, y (m)	Peak to Peak Bending Moment, Fxy (kNm)
USS SPRUANCE	5	222.4	137.9	0.164	22.6
(from	6	22.2	40.0	0.26	10.4
measurements in	7	80.1	93.4	0.3	28.0
laboratory)	8	520.4	191.3	0.273	52.2
					113.2
USS BARBEY	4	258.0	351.0	0.158	55.5
(from	2	44.5	124.6	0.241	30.0
measurements at sea)	6	889.6	186.8	0.256	47.8
					133.3

peak to peak variation in applied bending moment,

$$BM = H \times a \times r \times C$$

where H = mean hydrodynamic load on blade at 0.7 radius

a = moment arm between 0.7 radius and bolt head

r = peak to peak variation in H as a ratio of H

C = 0.5 accounts for one-half the bending moment which is resisted on each side of the blade palm neutral axis

Ship	H (kN)	a (m)	r	BM (kNm)
USS SPRUANCE	302.5	1.148	0.7*	121.5
USS BARBEY	311.4	1.097	0.9**	153.7

*As actually applied in laboratory experiment.

**Inferred from blade strains measured at sea.

367

ASSUMED LOCATION
OF NEUTRAL AXIS

DIRECTION OF APPLIED
LOAD, AHEAD CONDITION

35°

FORWARD

51 mm (2 in.)

y
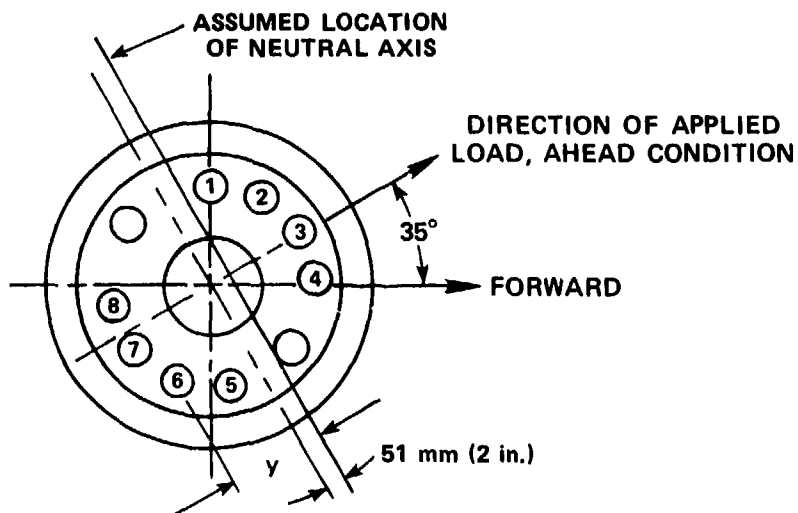
DD-963 CRANK RING

Figure 24a - USS SPRUANCE Crank Ring

ASSUMED LOCATION
OF NEUTRAL AXIS

DIRECTION OF APPLIED
LOAD, AHEAD CONDITION

26° -47'

FORWARD

51 mm (2 in.)

y
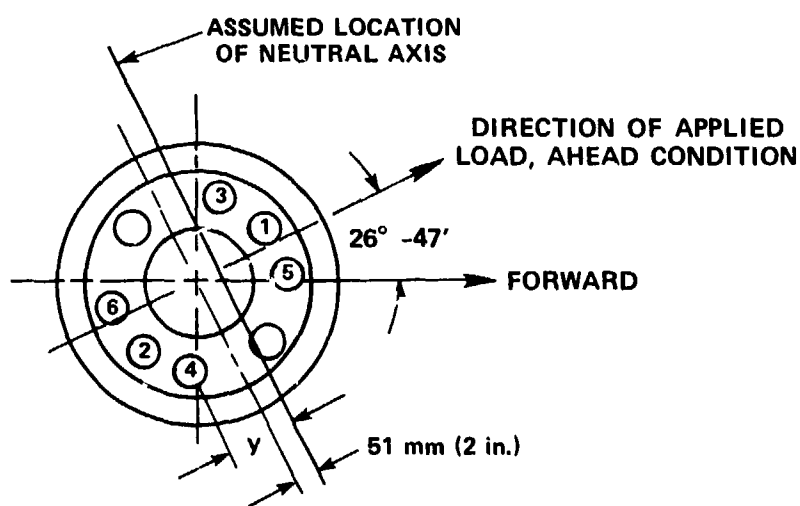
FF-1088 CRANK RING

Figure 24b - USS BARBEY Crank Ring

Figure 24 - Assumed Location of Bending Axis for Load Balance

368

line connecting the suction and pressure side fillet-blade intersection points. Usually these applied displacements at the design condition of the blade would have already been determined by a three-dimensional FE analysis, with either solid or shell elements, of the blade alone--a normal step in the U.S. Navy blade design process. Boundary conditions are as shown in Figure 5. The computer program APES[21] was used for the slice analyses described here. The reaction forces at the bolt hole centers R_i, which are output from APES,[21] are used to obtain the bolt force distribution among the bolts on the pressure side of the blade; see Figure 5. For a particular blade joint,

$$P_i = \text{percent at bolt i of total force} = \frac{R_i}{\sum\limits_{\text{all i}} R_i} \times (100) \qquad (3)$$

These joint percentages, P_i, can be combined with the simple Equations (4) through (7) which are programmable on a hand-held calculator, to provide estimates for the average tension stresses in the bolts. They consider the equilibrium of the overall forces and moments and the local bolted joint nonlinearity. In the first of these steps, the component of the total of all bolt forces resulting from the mean component of hydrodynamic force, F_{Rmean}, is found,

$$F_{Rmean} = \frac{M}{\sum\limits_{\text{all i}} \left(\frac{P_i}{100} \times y_i \right)} \qquad (4)$$

where M $\quad= R_{mean} \times 0.5 \times d$

R_{mean} = mean hydrodynamic force vector

d $\quad=$ the distance from the top of the crank ring to the 70 percent radius of the blade

0.5 $\quad=$ portion of M resisted on tensile side of neutral axis

P_i $\quad=$ percent at bolt i of total forces (from Equation (3))

y_i $\quad=$ distance from the center of bolt i to the assumed neutral axis

369

Similarly, the component of the total of all bolt forces resulting from the alternating component of hydrodynamic force, F_{Ralt}, is,

$$F_{Ralt} = a \times F_{Rmean} \qquad (5)$$

where a is the ratio of the alternating hydrodynamic force to the mean hydrodynamic force. The neutral axis is assumed to pass through the spindle axis and to be parallel to the nose-tail line of the blade at the 70 percent radius. One-half of the centrifugal force, C, must be added to F_{Rmean} to give the total mean force for the bolts on the pressure side of the blade. The total mean force and the alternating force are combined to give the total minimum and total maximum forces. For each value of total force (minimum, mean, and maximum), a set of individual bolt forces is calculated using the values of P_i obtained from the two-dimensional FE analyses assuming that the distribution of centrifugal forces among the bolts is the same as that for the hydrodynamic forces. At the mean force condition the force at bolt i is given by

$$F_{bolt\ i} = \frac{P_i}{100} \times \left(F_{Rmean} + \frac{C}{2} \right) \qquad (6)$$

In the second step, bolted joint nonlinearity is accounted for with the equation

$$\frac{S_{bolt\ i}}{S_{prestress}} = 0.2 \times \left(\frac{F_{bolt\ i}}{F_{preload}} \right)^{1.6} \qquad (7)$$

where $S_{bolt\ i}$ = average tensile stress at bolt i above prestress

$S_{prestress}$ = bolt prestress

$F_{bolt\ i}$ = total force at bolt i for a particular load condition

$F_{preload}$ = bolt preload

0.2 and 1.6 = constants describing curve shown in Figure 25

$$\frac{\sigma_{BOLT}}{\sigma_{PRESTRESS}} = 0.2 \left(\frac{F_{JOINT}}{F_{PRELOAD}}\right)^{1.60} + 1.0$$
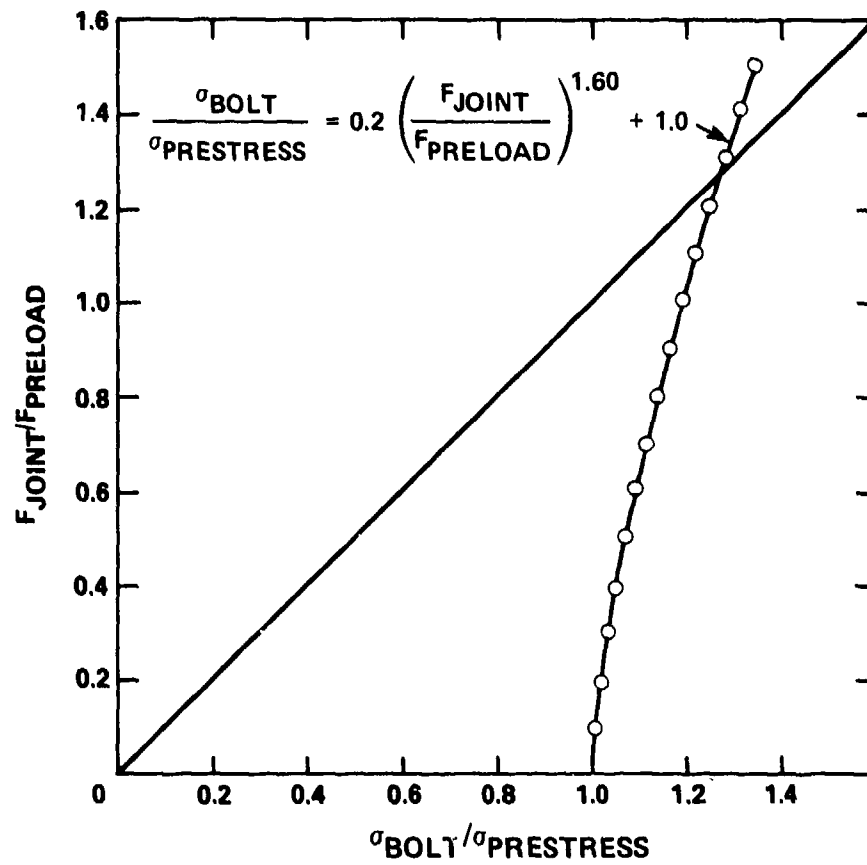
Figure 25 – Relationship Between Joint Force and Average
Tension Bolt Stress

This equation was chosen to fit experimental data for a K-Monel bolt in a SPRUANCE blade attachment and is plotted in Figure 25. Because of the coefficient 0.2, the bolt stress above prestress from Equation (7) is equal to 20 percent of bolt pre-stress when the bolt force is equal to bolt preload. Although, the value 0.2, was chosen on the basis of SPRUANCE experimental data, it can also be calculated, approx-imately, as the ratio of bolt stiffness to bolted joint stiffness for these mate-rials. If an experimentally derived curve is not available for other combinations of materials and geometries, then modifying the coefficient 0.2 to agree with the calculated stiffness ratio might be appropriate. In that case, the coefficient 1.6 might also be changed, perhaps by maintaining the point at which the curve of Equation (7) crosses the straight line (no preload case). This point is, approxi-mately, at a value of bolt force divided by bolt preload of 1.3.

Average bolt stresses obtained with this approach are compared in Figure 26 with stresses based on at-sea measurements. Agreement is very good for the SPRUANCE and PERRY for which Equation (7) applies. For the BARBEY and R/V ATHENA, agreement is not as good, but materials and geometries are different and, therefore, Equation (7) is not as good a simulation. Nevertheless, the highly loaded bolt and distri-bution are indicated.

The assumed location of the neutral bending axis also effects these predictions. The actual location is dependent upon several variables, with blade palm and fillet stiffness apparently being among the more important. The stiff blade palm material of the R/V ATHENA (stainless steel, Young's Modulus = 30×10^6 psi, versus bronze in the other blades, Young's Modulus = 15×10^6 psi) has probably caused the neutral axis to be further away from the bolts in tension; hence, the alternating bolt stresses are overpredicted for ATHENA.* The shift is small, however. When the neutral axis is assumed to shift less than 10 percent of the bolt circle diameter (less than 0.72 in.), the stresses at bolt 6 are then underpredicted slightly.

The values F_{bolt}, used in Equation (7) to obtain the stresses in Figure 26 are included as F_2 and F_6 in Table 2. Comparison of the values F_2 and F_6, in con-junction with stresses shown in Figure 26 for F_2 and F_6 indicates the following:

---

*Mean stresses which include effects of both centrifugal and hydrodynamic forces also tend to be overpredicted except at the most highly loaded bolt. Apparently the distribution of bolt forces due to centrifugal force is different from the distri-bution due to hydrodynamic force. Experimental evidence and additional discussion of this point is provided late in the section, Methods to Reduce Stress Levels - Blade Fillet Shape.

372

Figure 26 - Comparison of Computed Average Bolt Shank Stresses
with Sea Trial Results

O SEA TRIAL
△ TWO DIMENSIONAL FEM AND CLOSED-FORM ANALYSIS
□ CLOSED-FORM EQUATIONS (2) AND (7)

Figure 26 (Continued)
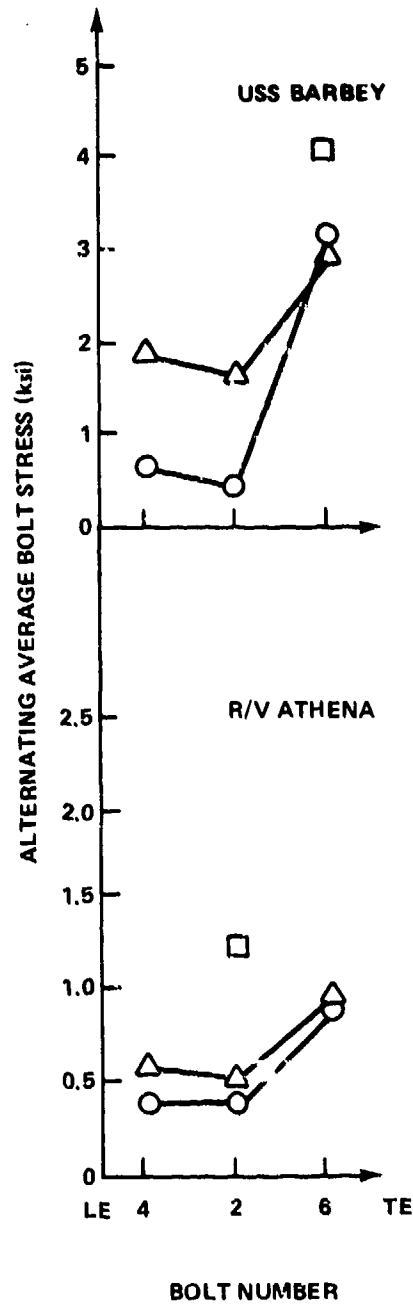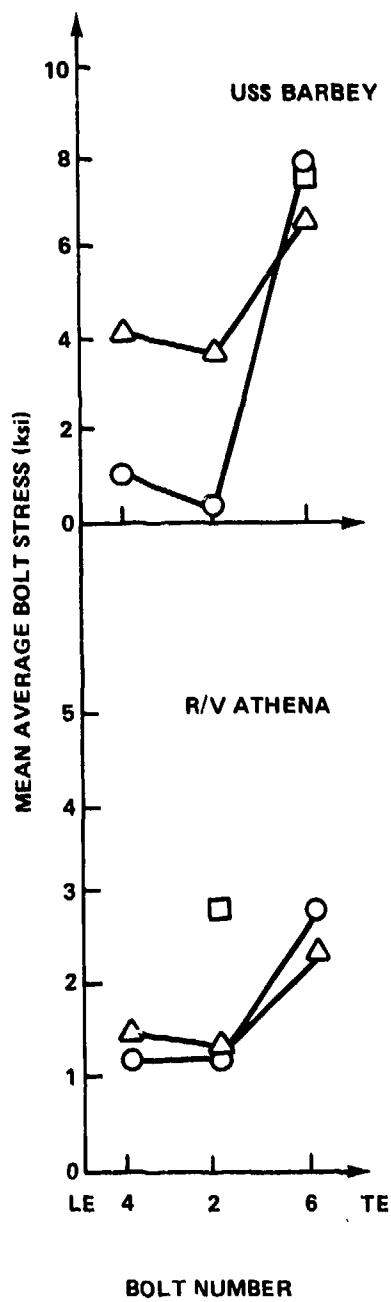
1. Use of Equation (2) with Equation (7) provides an indication of the average tensile stress in the most highly loaded bolt, within about 30 percent of experimental data. However, Equation (2) erroneously assumes that the most highly loaded bolt is furthest from the neutral bending axis.

2. A better indication of the average tensile stresses in the most highly loaded bolt, within about 15 percent, can be found by combining two-dimensional finite element analyses with Equations (3) through (7). This method also provides a good indication of the distribution of bolt forces.

3. Use of Equation (7) provides an adequate representation of the nonlinear bolt response. It is most appropriate for the case of a bronze blade attached to a steel blade carrier with K-Monel bolts, but it can apparently be used for the case of a stainless steel blade attached to a steel carrier with steel bolts like those on the R/V ATHENA.

Bolt bending stresses are not predicted with the above approaches. However, examination of Figures 13 and 17 shows that the bending stresses were about the same as the average stresses. In Table 5, maximum bolt stresses obtained using Equations (3) through (7) and a factor of 2.0 to account for bolt bending are compared with stresses based on at-sea measurements for the most highly loaded bolt. All predictions for the combined two-dimensional FE-closed form equation approach are within 10 percent of the experimental values. Predictions using Equation (2) with Equation (7) are not as consistently good.

Use of the factor 2.0 to account for bolt bending stress is based on measurements on the eight bolted SPRUANCE and PERRY propellers and the six bolted BARBEY and R/V ATHENA propellers, all having steel crank rings. The distribution of bolt forces was very uneven in all of these but the PERRY. These propellers were fairly highly loaded and had Ni-Al-bronze blades of relatively low stiffness, except for the lightly loaded R/V ATHENA propeller which had stainless steel blades of high stiffness. Blade attachment designs which are different from the above, such as those with trunnions rather than crank rings or those having more bolts, may have more, or less, bolt bending.

Simple Comparison Method for Blade Bolts. A simple comparison method has been developed which acts as an "indicator of bolt force level." Comparisons are made against bolt forces so derived for a number of both successful and unsuccessful CP

TABLE 5 - COMPARISON OF CALCULATED AND MEASURED MAXIMUM STRESS
(TENSION PLUS BENDING) IN MOST HIGHLY LOADED BOLT

Ship	Maximum Stress Based on Measurements at Sea (ksi)		Predictions Based on Two-Dimensional FE Analyses and Equations (3) through (7) (Average × 2.0 ksi)		Predictions Based on Equations (2) and (7) (Average × 2.0 ksi)	
	Mean	Alternating	Mean	Alternating	Mean	Alternating
Full-Power, Zero-Rudder (FPA)*						
USS SPRUANCE	16.0	7.0	16.0	7.4	13.4	6.3
USS OLIVER HAZARD PERRY	13.2	7.1	14.3	7.5	13.4	7.0
USS BARBEY	14.6	5.1	13.0	5.7	15.1	8.1
R/V ATHENA	6.1	N.A.**	4.7	1.9	5.6	2.5
Full-Power, Full-Rudder (FPT)*						
USS SPRUANCE	21.0	17.0	21.8	16.5	17.7	13.7
USS OLIVER HAZARD PERRY	15.8	10.8	16.9	11.8	15.2	10.8
USS BARBEY	19.9	13.1	18.0	12.5	20.5	15.7
R/V ATHENA	N.A.	N.A.	5.9	3.8	7.1	5.0

*Centrifugal forces, C, and hydrodynamic bending moments, M, for the full-power, zero-rudder condition (FPA) used in these calculations are those listed in Table 2. For the full-power, full-rudder condition (FPT), the following ratios, which were inferred from sea trial results, were applied to the forces and moments in Table 2.

**N.A. means not available.

Ship	$\dfrac{C_{FPT}}{C_{FPA}}$	$\left(\dfrac{M_{alt}}{M_{mean}}\right)_{FPA}$	$\dfrac{(M_{mean})_{FPT}}{(M_{mean})_{FPA}}$	$\left(\dfrac{M_{alt}}{M_{mean}}\right)_{FPT}$
USS SPRUANCE	0.96	0.45	1.27	0.75
USS OLIVER HAZARD PERRY	0.86	0.50	1.17	0.65
USS BARBEY	0.84	0.45	1.36	0.66
R/V ATHENA	0.96 (from USS SPRUANCE)	0.50	1.27 (from USS SPRUANCE)	0.75 (from USS SPRUANCE)

propellers. This method is based on several simplifying assumptions which are shown schematically in Figure 27. The moment due to the hydrodynamic force acting on the blade is assumed to be resisted by any one bolt in tension on the pressure side of the blade. This bolt is also assumed to resist 25 percent of the centrifugal force. The hydrodynamic force is assumed to act at the 70 percent radius and is calculated based on design shaft horsepower and speed. The centrifugal force is computed based on the mass of the blade and blade palm, the shaft speed, and the location of the center of gravity. The bending moment caused by the hydrodynamic force F, is assumed to be equivalent to a couple, F × d, where d is the distance between the blade palm-crank ring bolting face and the 70 percent radius. This couple, F × d, is resisted by a couple at the bolting face which is assumed to consist of two opposed forces separated by the bolt circle diameter. With the above assumptions, a total bolt force can be computed for the bolt in tension at the design horsepower level. Bolt stress associated with that force is then computed as force divided by shank area

C (CENTRIFUGAL FORCE)

(HYDRODYNAMIC FORCE)

F AT 0.7 R

d

TOTAL BOLT FORCE ASSUMED $= P + \dfrac{C}{4}$

WHERE $P = \dfrac{F \times d}{b}$

b = BOLT CIRCLE DIAMETER

F

P   P

$\dfrac{C}{2}$ $\dfrac{C}{2}$
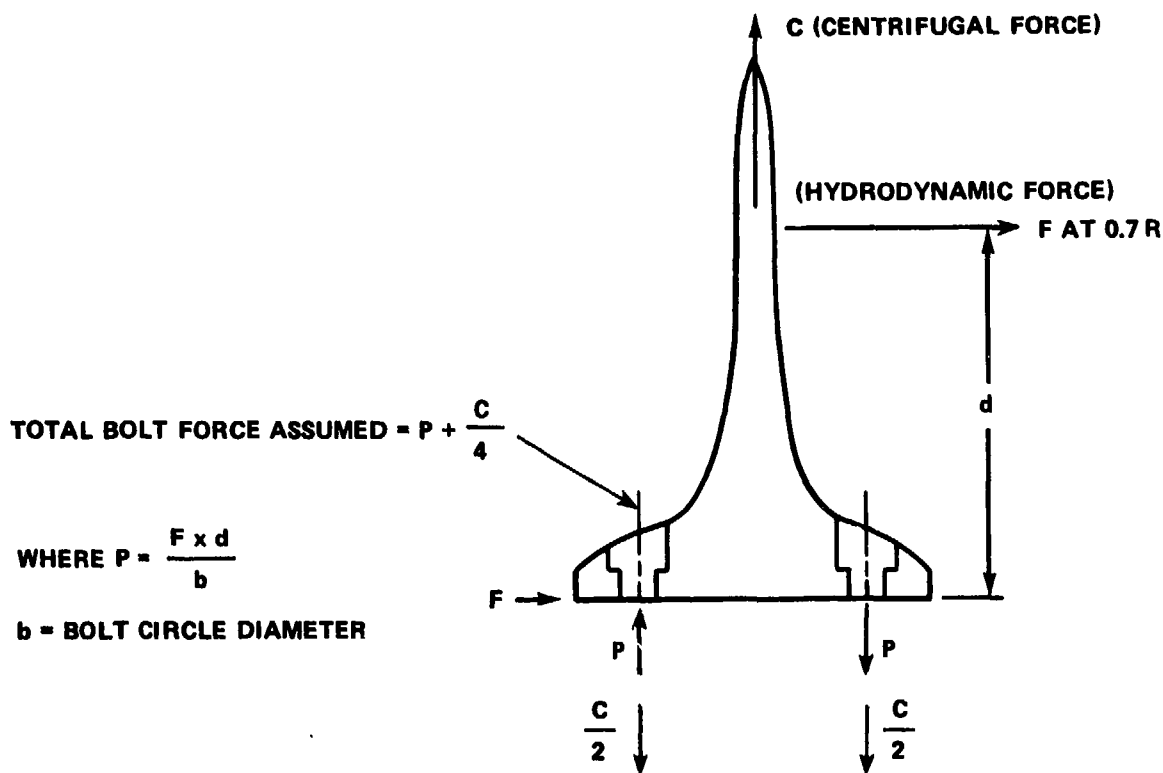
Figure 27 – Force Diagram on the Blade

and compared with bolt prestress. Because the actual prestress obtained during assembly is generally only poorly known, the comparisons are based on the designer specified prestress, where it is available, or on a prestress equal to 40 percent of the yield stress of the bolt material which appears to be a typical design value. Comparisons of the ratios of bolt stress divided by bolt prestress based on the above method for more than 30 propellers show that if the ratio is greater than 1.0, potential bolt fatigue problems exist. It must be noted that this simple method should not be used as a design criterion because the ratio could be greater than 2.0 for a satisfactory design if there is a good distribution of bolt forces.

<u>Closed-Form Equations for Blade Carriers</u>. High stresses in the blade carriers (trunnions or crank rings) occur at the abrupt changes in diameter, or notches, shown in Figure 1. Usually small radii are provided to ease the transitions and reduce stress concentrations.

The trunnion is, apparently, the simplest of the attachment structures to analyze. The blade-trunnion combination is an overhung beam whose attachment is stressed primarily in bending. However, the locations of the effective reactions at the hub bearings are not clear. They depend upon relative deformations of the trunnion and hub at the bearings. Not only are the deformations largely mutually independent, but the elastic behavior of the hub is difficult to quantify. It is important to note that the bolted-on trunnion arrangement has not been the subject of experimental evaluation during the CP propeller R and D program. The effects of bolts on trunnion stresses and vice versa have not been measured. The stresses at the fillet at the end of the small diameter section of the trunnion are sensitive to the location of the effective reaction at the inner bearing. The location of the other reaction is, relatively, much less important. The effects of variations in location of these reactions would require examination. The equation for nominal stress at any cross-section of the trunnion is the following, assuming that centrifugal force acts through the section and that the center of gravity is on the spindle axis.

$$\text{Stress} = \frac{C}{A} + \frac{M}{Z} \qquad (8)$$

where C = applied centrifugal force

M = bending moment

A = area of cross-section

Z = section modulus of cross-section

The value of stress obtained with Equation (8) must be increased by a stress concentration factor--from Peterson,[22] for example.

Predictions of stress for the crank ring type of blade carrier are more complex than for the trunnion type. As indicated in Figure 28, the crank rings, are relatively thick at the bolt circles, but have thinner flanges extending beyond the thick portion. The thick flanges engage bearing surfaces in the hub, thereby transmitting to the hub both the applied centrifugal forces of the blade, bolts, and crank ring, and the bending moment due to hydrodynamic forces. The forces are transmitted to the crank ring intermittently at bolts in a nonuniform manner and are passed through to the hub which varies in stiffness circumferentially around the crank ring. Closed-form equations and two-dimensional axisymmetric finite element analyses have been applied to this problem, but much of the asymmetry has necessarily been ignored in so doing. Stresses due to the centrifugal forces which are applied in a more-or-less axisymmetric manner have been computed assuming the problem to be axisymmetric as in Figure 28. Stresses due to the bending moment caused by hydrodynamic forces have been computed assuming either that the problem is axisymmetric or that trunnion bending (Figure 28) equations apply. Neither approximation determines the location of maximum stress to be where measurements on the SPRUANCE, PERRY, and BARBEY crank rings have indicated; see Figure 12.

Stress at the transition fillet between the thick portion of the crank ring and the flange due to the centrifugal force can be found using either an axisymmetric two-dimensional FE analysis such as APES[21] or a closed-form equation coupled with a stress concentration factor. In either case, uniform pressure reactions as in Figure 28 are used. In the latter case, stresses computed with the following equation from Roark[23] (Table 24, Case 21) must be multiplied by the appropriate stress concentration factor--from Peterson,[22] for example,*

---

*The difficulty in using information from Reference 22 for this purpose is discussed in the next to the last paragraph of this section.

$$P_C = \frac{C}{A} = \frac{C}{\pi \times (R_o^2 - R_b^2)}$$

$$P_M = \frac{R_o \times M}{I} = \frac{4 \times R_o \times M}{\pi \times (R_o^4 - R_b^4)}$$
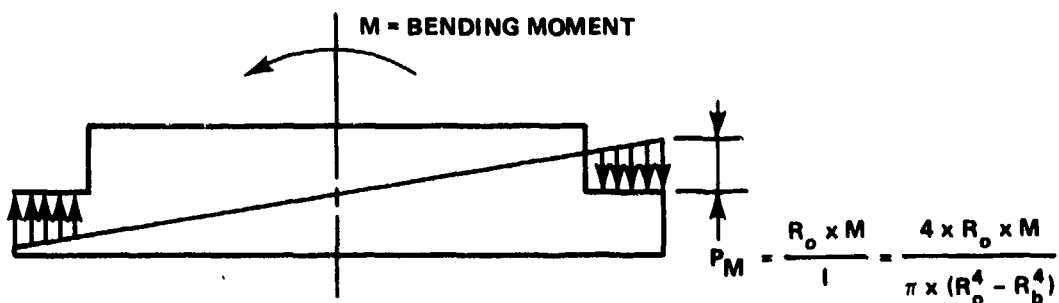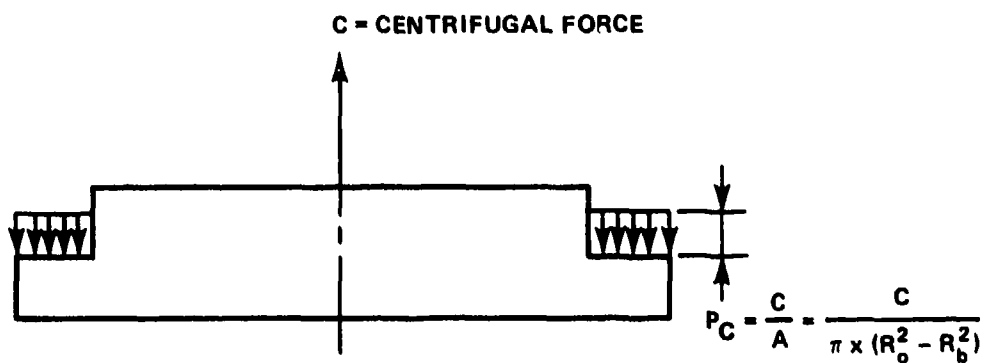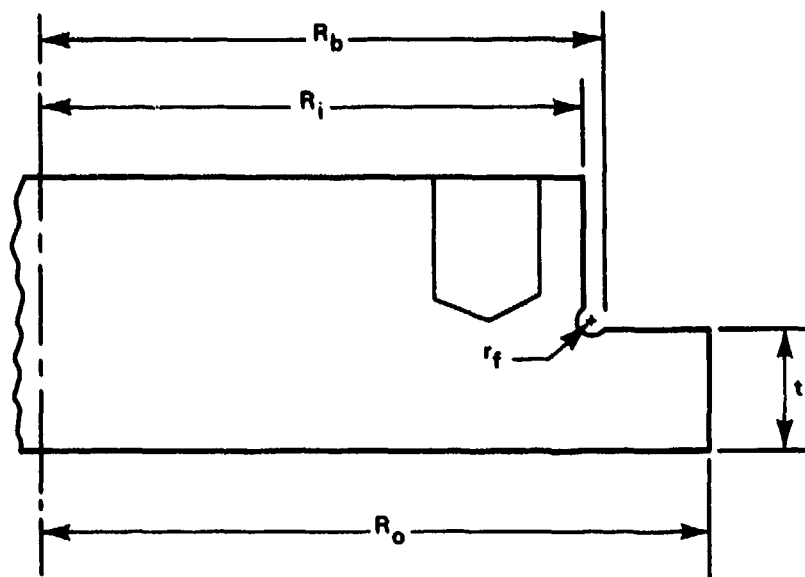
Figure 28 — Crank Ring Dimensions and Terminology

$$S_9 = \frac{6 \times P \times R_o^2}{t^2 \times C_8} \times \left[\frac{C_9}{2 \times R_o \times R_i} \times (R_o^2 - R_b^2) - L_{17} \right] \tag{9}$$

where P = C/A = uniform pressure

C = applied centrifugal force

A = area of bearing surface = $\pi \times (R_o^2 - R_b^2)$

t = flange thickness, Figure 28

R_i = radius of thick portion of crank ring, Figure 28

R_o = outer radius of flange of crank ring, Figure 28

R_b = inner radius of bearing surface under pressure, Figure 28

$$C_8 = \frac{1}{2} \times \left[1 + \nu + (1-\nu) \times \left(\frac{R_i}{R_o} \right)^2 \right] \tag{10}$$

$$C_9 = \left(\frac{R_i}{R_o} \right) \times \left\{ \frac{1+\nu}{2} \times \ln \frac{R_o}{R_i} + \frac{1-\nu}{4} \times \left[1 - \left(\frac{R_i}{R_o} \right)^2 \right] \right\} \tag{11}$$

$$L_{17} = \left(\frac{1}{4} \right) \times \left\{ 1 - \frac{1-\nu}{4} \times \left[1 - \left(\frac{R_b}{R_o} \right)^4 \right] - \left(\frac{R_b}{R_o} \right)^2 \times \left[1 + (1+\nu) \times \ln \left(\frac{R_b}{R_o} \right) \right] \right\} \tag{12}$$

ν = Poisson's ratio

S_9 = nominal stress in crank ring fillet

The distribution of forces in the crank ring resisting the bending moment due to the hydrodynamic force is asymmetric and no simple closed-form equation can be applied directly. Two approaches are described here. (1) Simulate the varying pressure in Figure 28, with a uniform pressure equal to P_M and then use one of the above methods for axisymmetric loadings. That is, make P in Equation (9) equal to P_M. (2) It is apparently better to start with approach (1) and then to modify the resulting stress to compensate for the asymmetric loading using the following ratio. Closed-form solutions are available both for trunnion bending with edges supported

and for axisymmetric loading with edges supported. A ratio is formed by dividing the result for the trunnion, edge-support case by the result for the axisymmetric edge-support case. This ratio is applied to the stress found in approach (1) either by using the axisymmetric finite element analysis or by using Equation (9). The equations from Roark[23] for the edge support cases are:

1. Nonsymmetric (trunnion) Edge Support (Table 24, Case 20),

$$S_{13} = B \times \frac{M}{(R_o \times t^2)} \tag{13}$$

where $B = 2.9375 \ g^2 - 7.315 \ g + 4.412125$ \hfill (14)

$$g = \frac{R_1}{R_o}$$

M = applied bending moment

R_1, R_o, t = same as in Equation (9) and in Figure 28

2. Axisymmetric Edge Support (Table 24, Case 11),

$$S_{15} = \frac{A \times R_o \times M}{I} \times \frac{3}{\pi \times t^2} \times \frac{R_o}{R_1} \times \frac{C_9}{C_8} \tag{15}$$

where \hfill $I = \left(\frac{\pi}{4}\right) \times (R_o^4 - R_b^4)$ \hfill (16)

and other variables are as defined for Equations (9) and (13).

Predictions made using Equation (9) modified with Equations (13) and (15) are compared with experimental data in Table 6 along with the results for the two-dimensional FE analysis, also modified with Equations (13) through (15). Fairly good agreement is evident for the SPRUANCE and PERRY data, but not for the BARBEY. The predictions based on two-dimensional FE analysis are generally better than those based solely on closed-form equations and handbook values for stress concentration factors. The two-dimensional FE analysis results are not limited by the simplifying assumptions of thin plate theory which does not account for any shear deflection.

TABLE 6 - COMPARISON OF CALCULATED AND MEASURED
STRESS IN FILLET AT CRANK RING FLANGE

	Full-Power Zero Rudder		Full-Power Full Rudder	
	Mean (ksi)	Alternating (ksi)	Mean (ksi)	Alternating (ksi)
USS SPRUANCE (0.375 in. radius fillet)				
Experimental	40.0	16.0	45.0	31.0
Closed Form	43.6	14.4	50.7	30.1
Two-Dimensional, Finite Element and Closed Form	40.9	13.5	47.6	28.3
USS OLIVER HAZARD PERRY (0.375 in. radius fillet)				
Experimental	42.3	14.4	42.3	20.8
Closed Form	45.6	17.4	48.7	25.5
Two-Dimensional, Finite Element and Closed Form	42.8	16.3	45.8	24.0
USS BARBEY				
Experimental (1)	44.8	11.5	53.8	18.1
Experimental (2)	58.0	11.6	69.6	18.1
Closed Form	24.8	7.4	28.5	13.3
Two-Dimensional, Finite Element and Closed Form	33.3	9.9	38.3	17.8

383

This is the probable explanation for the large difference in the two approaches to calculated values for the BARBEY which had a very thick flange compared to the SPRUANCE and PERRY and, therefore, a larger shear effect. Also, the two-dimensional FE method allows a close approximation of the fillet shape from which the stress concentration is accounted for directly. Handbook values of stress concentration factors (SCF) are questionable because they do not reflect crank ring geometry and loading. For example, the SCF values applied in Table 6 for the closed-form equation case are from Figure 78 of Peterson[22] for which the crank ring is represented as two coaxial cylindrical rods or shafts of very short length, with a shoulder fillet at their juncture, subjected to a bending moment.

The poor agreement in predicted and experimental data for the BARBEY is likely due to the fact that the bolts were close to the fillet in the crank ring and the strain gages were located adjacent to the bolts. Figure 63 of Reference 2 reporting the BARBEY measurements at-sea shows that the crank ring stress adjacent to the most highly loaded bolt was much higher, nearly twice as high as the stress at the next bolt. On the basis of the assumptions used for the calculated stresses, however, the stress at these two bolts would be nearly equal because the effect of the closeness of the most highly loaded bolt threads to the fillet is ignored. The limiting distance or wall thickness between the bolt threads and the fillet, less than which this effect becomes important, cannot be determined directly without use of the combined two- and three-dimensional FE analysis method discussed earlier. However, it appears that a crude limit can be established empirically for use of the closed-form Equations (9) through (16) by examining the ratio of wall thickness, t_{wall}, to bolt force as shown in Table 7. The estimate of bolt force from the "simple comparison method for blade bolts" which was described earlier is used here because it provides an indication of maximum bolt force level which can be consistently and simply applied to various geometries. In equation form, the ratio is

$$\text{ratio} = \frac{t_{wall}}{\text{force}}$$

where t_{wall} = minimum wall thickness between the bolt thread and crank ring fillet

force = $F \times \frac{d}{b} + \frac{C}{4}$ (see Figure 27)

TABLE 7 - COMPARISON OF RATIO OF WALL THICKNESS TO BOLT FORCE

Ship	Hydrodynamic Force, F (kip)	Centrifugal Force, C (kip)	d Figure 27 (in.)	b Figure 27 (in.)	t_{wall} (in.)	Force Figure 27 Equation (kip)	$t_{wall}/$Force ($\times 10^{-3}$)
USS SPRUANCE	68.0	192.0	45.2	19.625	1.25	204.6	6.1
USS BARBEY	74.3	236.3	41.6	16.25	0.241	249.3	0.97
USS BARBEY*	74.3	236.3	41.6	16.25	0.835*	249.3	3.35
USS OLIVER HAZARD PERRY	74.0	188.0	43.1	19.625	1.25	209.5	5.97

*As redesigned for instrumented sea trials.

385

F = hydrodynamic force

d = distance between blade palm at crank ring bolting
    face and 70 percent radius

b = blade bolt circle diameter

C = centrifugal force

The ratios in Table 7 for both the SPRUANCE and PERRY are about 6.0, while for the BARBEY the ratio is 3.6. Because predictions from Equations (9) through (16) were good for the SPRUANCE and PERRY compared with experimental data, but only poor (and nonconservative) for the BARBEY, use of the equations should be limited to cases where the ratio is 6.0 or better. For geometries with lower ratios, the state of stress between the bolt threads and crank ring fillet should be examined with the combined two- and three-dimensional FE analysis method, or experimentally to demonstrate that the effect of closeness of the bolt is not significant.

METHODS TO REDUCE STRESS LEVELS

High strains which have been measured in the blade bolts and in the crank ring can be reduced by relatively simple design changes. They include changing the shape of the blade fillet to better distribute bolt forces, increasing bolt preload, and increasing the radii in way of stress concentrations.

BLADE FILLET SHAPE

Full-scale and one-third scale model laboratory measurements demonstrate that the distribution of bolt forces is dependent upon the shape of the blade fillet and blade palm. For example, cross-sections through the highly loaded bolt for two different blades are shown in Figure 29. Although power ratings, hub, and crank rings are virtually the same (both for 40,000 shp), the blades and blade fillets are different. The PERRY blade in Figure 29 is described in Reference 24 as having been designed for balanced skew to minimize blade spindle torque, so the midchords of blade sections between the hub and about 70 percent of the tip radius are located forward of the blade spindle axis. This leads to a smaller blade fillet near the bolt 8 than the SPRUANCE blade fillet, while the opposite is true near bolt 5. Measurements from full-scale laboratory experiments indicate that when the same blade loads are applied, maximum mean and alternating bolt stresses at bolt 8 for

LEADING EDGE

SECTION AT 0.7 RADIUS

FORWARD

USS SPRUANCE BLADE

FORWARD

USS OLIVER HAZARD PERRY BLADE

*0.3 RADIUS WITHOUT FILLET

AT BOLT 8 ON USS SPRUANCE AND BOLT 5 ON
USS OLIVER HAZARD PERRY

AT BOLT 5 ON USS SPRUANCE AND BOLT 8 ON
USS OLIVER HAZARD PERRY

CROSS SECTIONS AT
BOLTS 5 AND 8
SECTION A-A
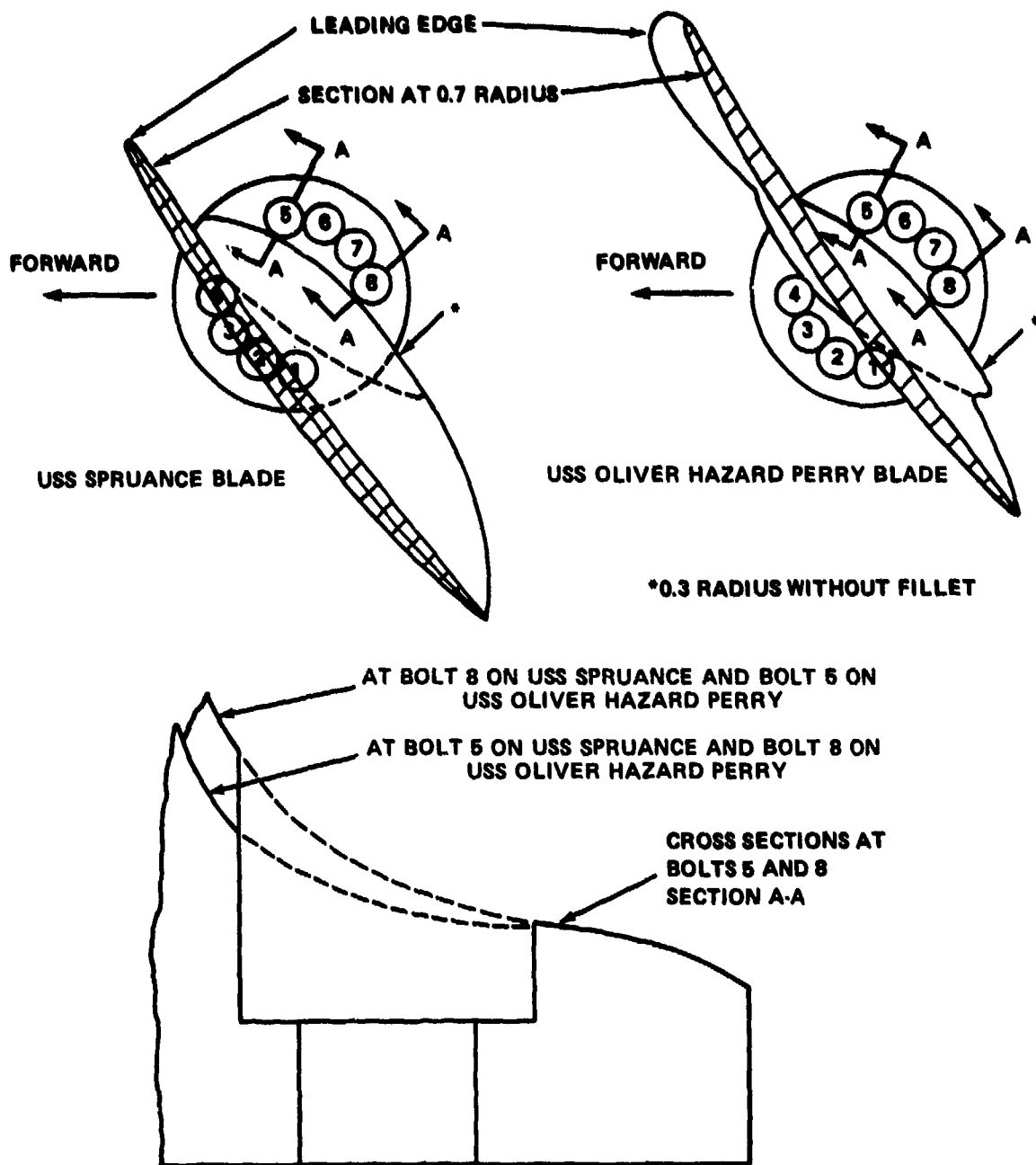
Figure 29 - Comparison of the USS SPRUANCE and USS OLIVER HAZARD PERRY
Blade Fillets

387

the PERRY blade fillet are about 80 to 85 percent of those for the SPRUANCE blade fillet, while at bolt 5 the stresses for the PERRY are nearly double those for the SPRUANCE.

Similar indications were found during experiments with a one-third scale model in which the blade fillet geometry was systematically varied in order to identify the improved blade fillet shape for the SPRUANCE shown in Figures 30 and 31. Material was added to the fillet near the more lightly loaded bolts 5 and 6 while material was removed near the heavily loaded bolt 8. Smoothness in the fillet-palm
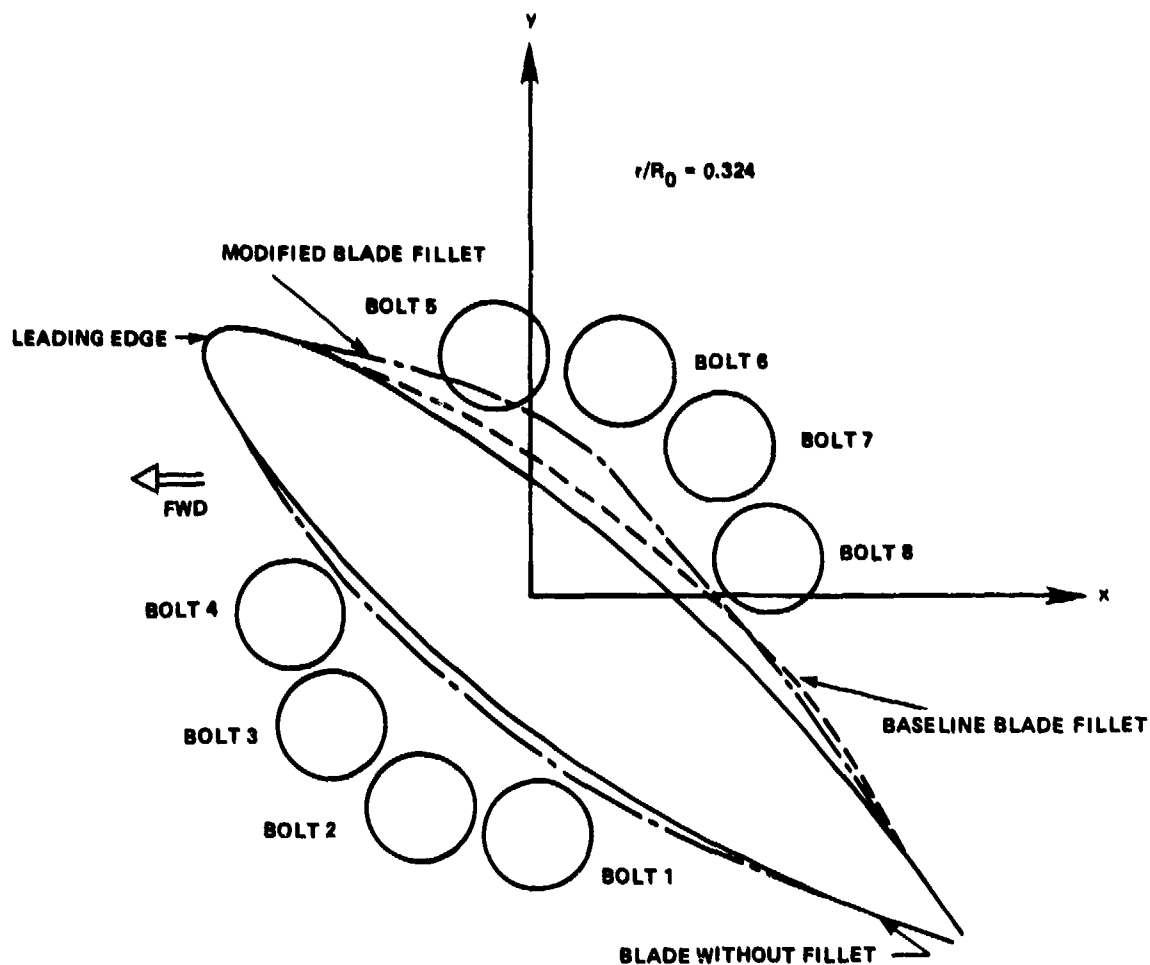
Figure 30 - Projection of Baseline and Modified Blade Fillets at r/R_o = 0.324

NOTE: MODIFIED BLADE FILLET IS
THE SAME AS BASELINE
BLADE FILLET

BOLT 1   BOLT 8

Figure 31a - Bolts 1 and 8

——————— MODIFIED BLADE FILLET
- - - - - BASELINE BLADE FILLET

BOLT 4   BOLT 5
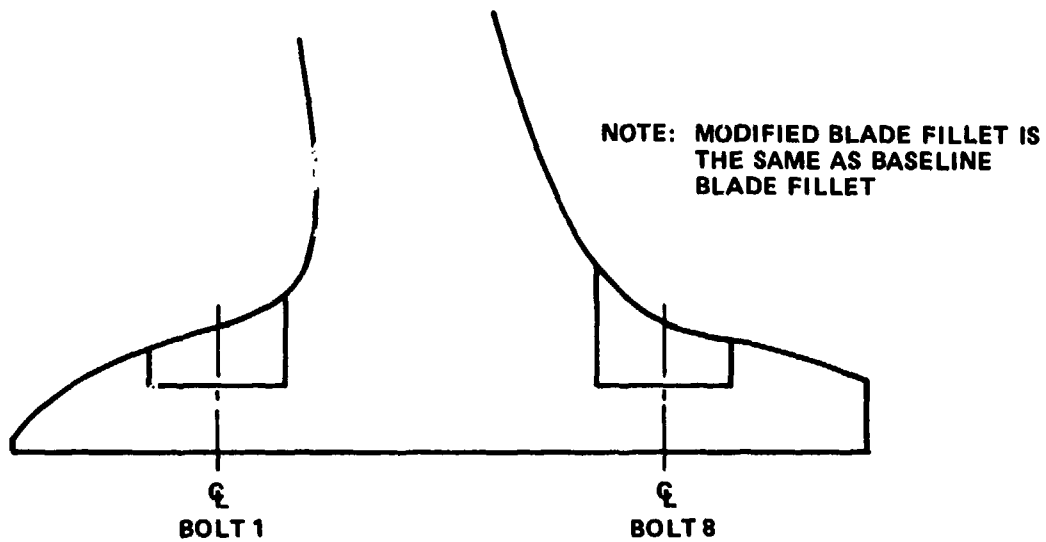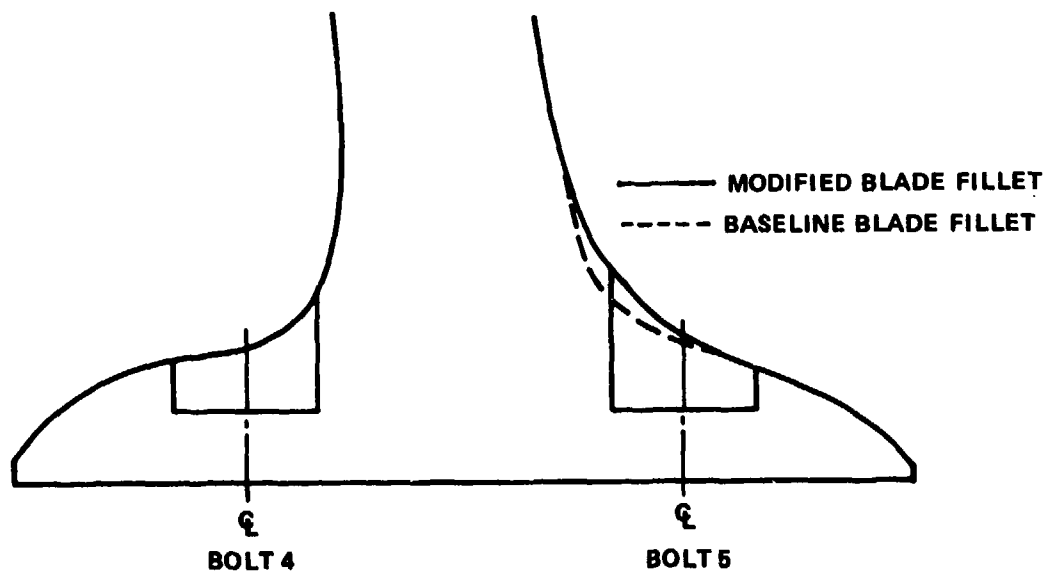
Figure 31b - Bolts 4 and 5

Figure 31 - Planar Cuts of Baseline and Modified Blade Fillets for the
USS SPRUANCE Blade

region and data for machining were obtained using the methods of Gorman.[25] Full-scale verification tests[10] of the significant reductions in bolt stress were carried out using the experimental setup of Figure 9. Figure 32 shows that the maximum

USS SPRUANCE CP PROPELLER

LEGEND

○ – BASELINE FILLET, BRONZE COVERPLATE (RUN 1)

□ – MODIFIED FILLET, BRONZE COVERPLATE (RUN 2)

FULL-POWER TURN—DYNAMIC RUN, END OF CYCLE
GAGES ON BOLT THREAD
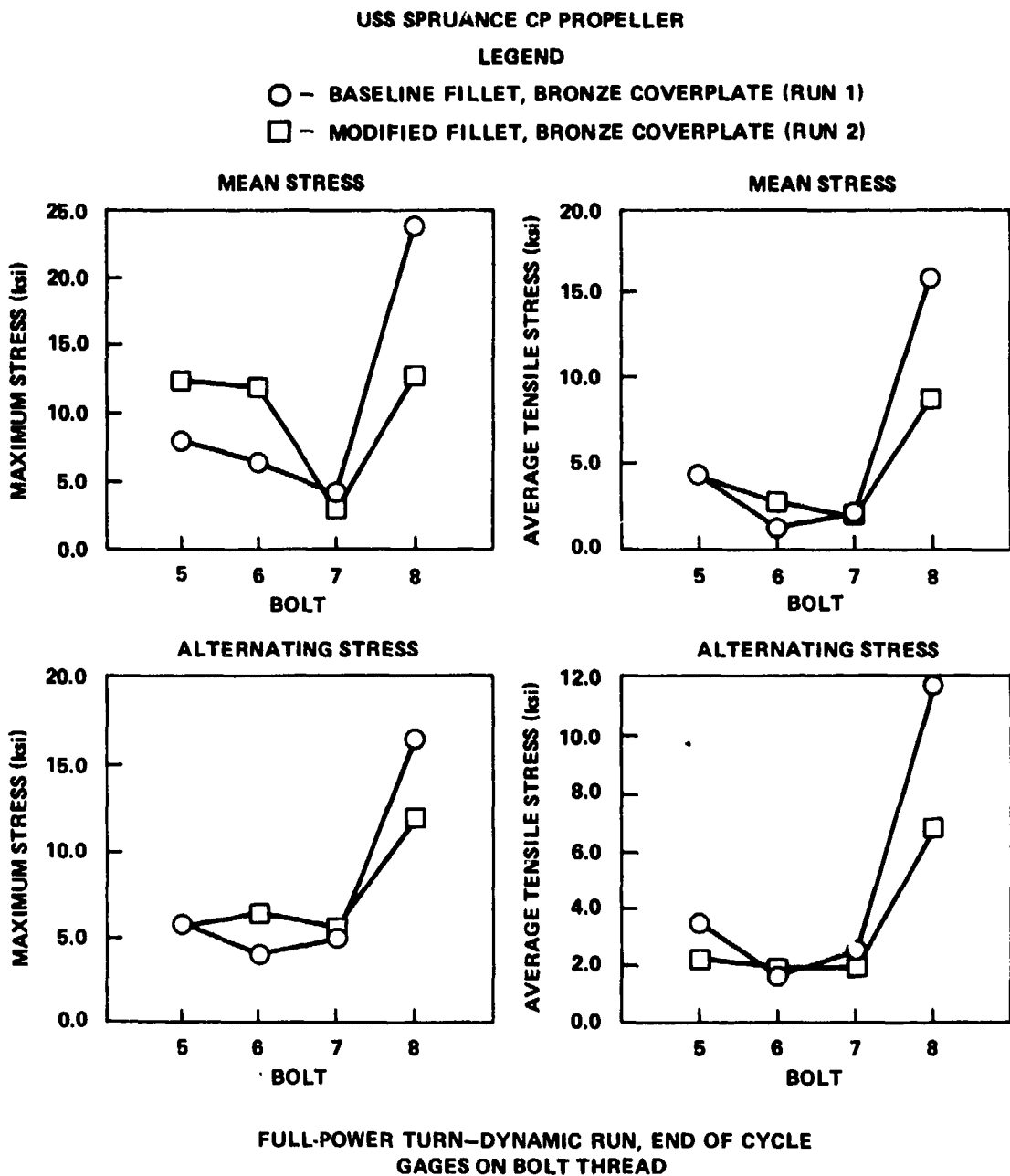
Figure 32 – Comparison of Blade Bolt Thread Stresses with the Baseline and Modified Blade Fillets and with a Bronze Coverplate

390

alternating stress at the highly loaded bolt was reduced by about 30 percent. In addition, as shown in Figure 33, the alternating stress in the crank ring was reduced by about 15 percent probably because the neutral bending axis shifted when palm stiffness was increased. Further indication of the effect of palm stiffness on the location of the overall bending axis was discussed earlier in relation to Figure 26 for the R/V ATHENA. It was supposed that the higher modulus stainless steel blade
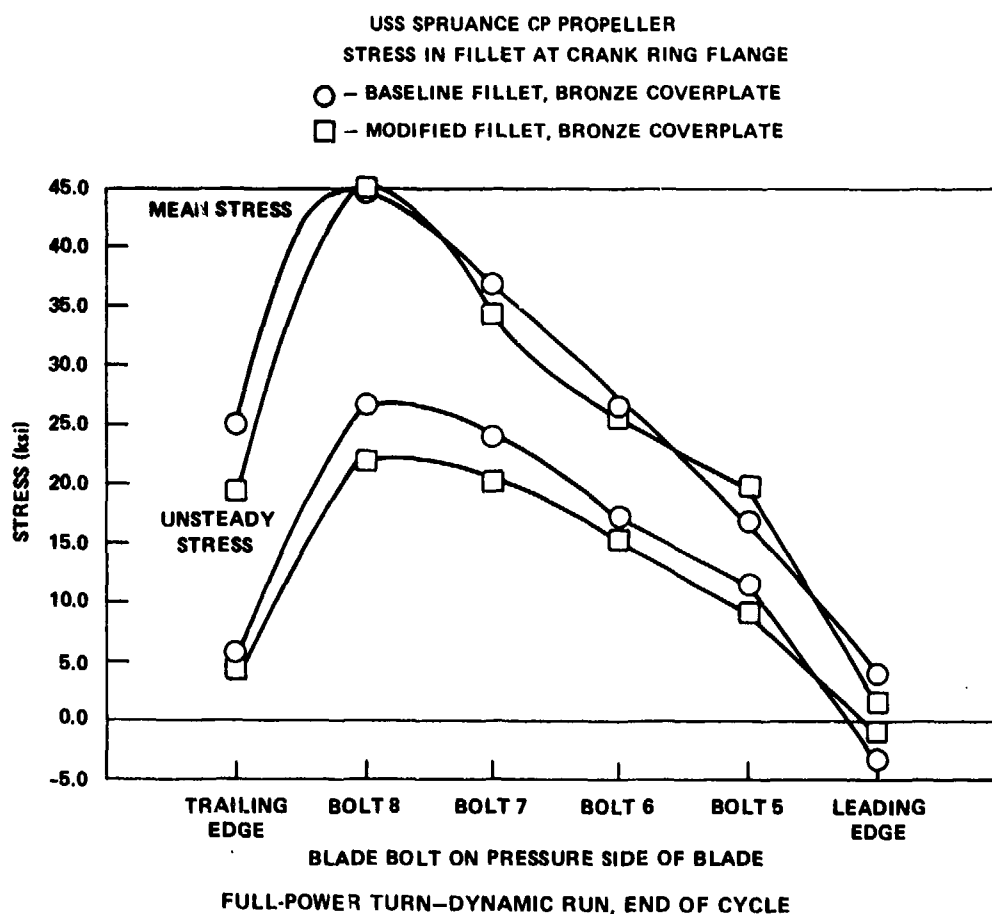
Figure 33 - Comparison of Crank Ring Fillet Stresses with the Baseline and Modified Blade Fillets and a Bronze Coverplate

palm on the R/V ATHENA caused the neutral axis to be located further from the bolts in tension than assumed for the calculations; hence the calculated stresses were somewhat high. There appears to be no change in the mean stress in Figure 33 due to the new blade fillet. However, as indicated in Figure 34, this is due to a shift in the location of the maximum stress due to centrifugal force. The effect of the new

USS SPRUANCE CP PROPELLER
STRESS IN FILLET AT CRANK RING FLANGE
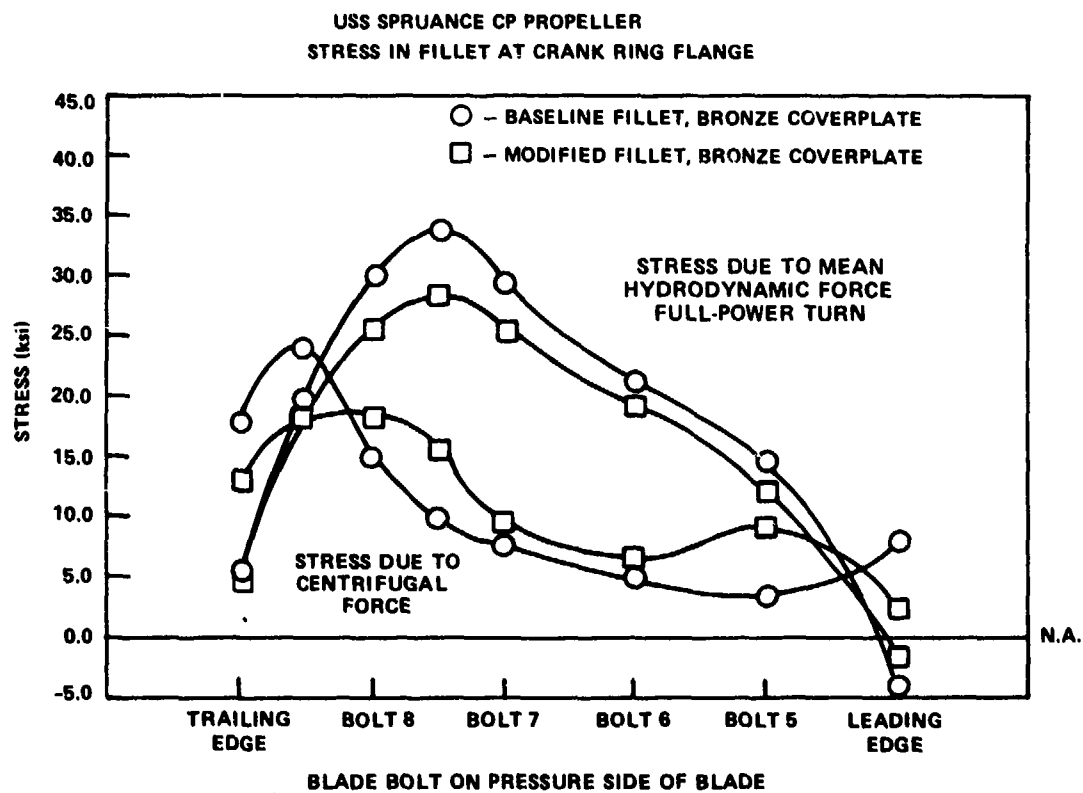
Figure 34 – Comparison of Crank Ring Fillet Stresses with the Baseline and Modified Blade Fillets and a Bronze Coverplate

blade fillet on crank ring stress due to mean hydrodynamic force was the same as for the alternating hydrodynamic force, a reduction of about 15 percent. This reduction is masked by stresses due to centrifugal force.

Modifications to the traditional shape of the blade fillet must be accompanied by a reexamination of stresses in the blade fillet. The traditional shape fillet has been virtually trouble free from a structural viewpoint but any modifications might increase stresses and cause problems. The combined two- and three-dimensional FE analysis method described earlier for the crank ring (see Figures 19 and 20) has also been successfully applied to blade fillets.

BOLT PRELOAD

Cyclic blade bolt stress can be reduced at the expense of higher mean stress by increasing bolt preload. At least two CP propeller manufacturers limit bolt preload by limiting the average stress under the bolt head due to bolt preload to a percentage (90 percent) of the blade palm material yield stress. Where relatively low-strength nickel-aluminum bronze is used in the blade (yield stress = 35 ksi or 241 MPa), this design procedure may lead to an unnecessary limitation of the effectiveness of bolt preload. In Figure 22, measured values of bolt strain were plotted against forces applied to a bolted joint for two values of bolt preload. The lower value of bolt preload is that used for the SPRUANCE Class CP propeller. These data were obtained using an experimental setup[16] for fatigue testing SPRUANCE blade bolts one at a time. A single bolt was preloaded in a joint which included bronze plates equal to the blade palm and coverplate thickness and a portion of an actual steel crank ring. Bolt strains were measured. The applied forces were estimates of those which occur at the most highly loaded bolt at the full-power ahead condition. The approximate maximum variation in average tensile strain measured at sea on the SPRUANCE is indicated in Figure 22 as Δ_1. Because the distribution of bolt force between bolts is not much affected by bolt preload, as demonstrated in full-scale laboratory experiments,[11] the variation in average tensile strain which would result from use of the higher bolt preload is Δ_2, which is considerably smaller than Δ_1.

Because higher bolt preload may lead to stress over yield stress in the blade palm under the bolt head, there is concern that bolt preload would be reduced as yielding of the palm took place. However, measurements on the BARBEY CP

propeller indicate that the concern may be unfounded. Before strain measurements were made at-sea on the BARBEY, the bolts were prestressed to 55 ksi (379 MPa). This corresponded to a pseudoelastic* stress in the bronze of the blade palm of 37 ksi (255 MPa). During the stress trials, the maximum average tensile stress in the bolts reached about 70 ksi (482 MPa) at which point the pseudoelastic stress in the palm was 47 ksi (324 MPa). Measurements of residual prestrain, Noonan et al.,[2] which were made upon removal of the CP propeller after nine months of operation, showed that the loss in bolt preload was between 5 and 10 percent. Measurements in the laboratory during fatigue testing of large bolts having two different levels of preload[13] also indicate that prestrain falls off to about 90 percent of the installed value where it remains until removal. In some of these tests, the bearing stress under the bolt head was above the nominal yield stress in the bronze, up to 50,000* psi. It is evident that the bearing stress in the bronze palm under the bolt head can be allowed to exceed somewhat the 2 percent offset yield stress. Nickel-aluminum bronze has a high ultimate stress (80,000 psi) compared to yield stress (35,000 psi), and the bearing stresses occur in a small volume of material which is constrained by a relatively large volume of material in the elastic stress range. Nevertheless, measurable permanent deformation in this region did occur during a full-scale laboratory experiment with very high bolt preloads[11] in which the bearing stress in the bronze exceeded 60,000* psi on the side of the bolt where maximum bending occurred. In that short term experiment, the loss in bolt preload was about 10 percent and the preload bending pattern was changed. Because of the importance of obtaining desired bolt preload, it is apparent that for an otherwise acceptable design, the approach of increasing bolt preload to reduce cyclic bolt stress should be limited by the magnitude of bearing stress in the blade palm compared to yield stress. Where necessary, higher bearing stresses might be allowed, but experimental evidence should be obtained to identify the potential loss in bolt preload. Work hardening the bronze to effectively increase its yield stress to a level above the expected bearing stress might be accomplished by preloading the bolt to higher levels than finally intended and then backing off to the desired level.

While increasing the bolt prestress leads to reduced cyclic stress, it also leads to an increase in the mean stress. Limited fatigue data obtained during the

---

*Assumes that the material stress-strain curve remains linear above yield stress.

DTNSRDC investigations for large K-Monel bolts having rolled threads indicate that, for the bolts tested, the two effects are nearly in balance. The reduction in fatigue endurance stress, because of higher mean stress on these bolts, nearly counteracted a dramatic reduction in cyclic stress measured in the PERRY CP propeller due to a 150 percent increase in bolt preload. In that instance, only marginal improvement in fatigue performance would be obtained from increasing prestress. Nevertheless, higher bolt prestress should be considered wherever it can be shown that improved fatigue performance will result.

Preload assembly procedures must also be considered in determining the best level of bolt prestress in a particular application. There are two common methods of installation of blade bolts. In one, torque is applied with a torque wrench. In the other, separate devices under hydraulic pressure are used to stretch the bolt prior to insertion and seating, after which the pressure is released leaving a residual stretch. With these approaches, careful measurements of elongation or angle of turn give indications of preload attained, when correlation between elongation and stress has been predetermined under laboratory conditions using strain gage techniques. Both methods have been used successfully in large bolt applications. The shank of the torque-type bolt can be designed more appropriately to reduce the possibility of fatigue at the bolt head to shank fillet because it does not have to accommodate the piston associated with hydraulic loading devices; however, fatigue at the bolt threads is the same for both types of bolts. High levels of preload torque cause difficulties for bolts larger than about 2 in. in diameter. Also, underwater removal and installation under emergency condition become impracticable. The hydraulically loaded bolts have been successfully installed underwater, but a more skilled mechanic is needed whenever the hydraulic devices are used. The critical need to obtain the prescribed level of bolt prestress in order to limit alternating bolt stresses has been discussed in relation to Figures 22 and 25. Depth gages can be used with either of the above approaches to check that it has been obtained.

BOLT HEAD AND CRANK RING FILLET RADII

During the DTNSRDC investigations, the effect of changes in fillet radii in way of stress concentrations was closely examined. Strain gaged and photoelastic

models were used along with two-dimensional FE analyses to examine the effect of variations in fillet shape. In certain cases, there was room within the constraints of the existing design to increase fillet radii. Where this is possible, the machinist, who likes constant radius fillets, and the stress analyst, who likes low stresses, can both be satisfied. Clearly, careful attention to such design details can lead to significant and important stress reductions. While constant radius fillets are commonly used, it was found that compound radius fillets could reduce maximum stresses by as much as 25 percent.

STRENGTH ASSESSMENT PROCESS

Two stress criteria must be satisfied at all times during the useful life of the CP propeller in order for the bolts and blade carrier to be considered to be adequate. The maximum stress must be less than the material's yield stress (except at the thread roots, a special case, and bearing stress under the bolt head) and the spectrum of fatigue stresses must be within the material's endurance capacity.

The accuracy of the predicted stresses is not only dependent upon the accuracy of the stress analysis, but also upon the accuracy of the blade loads used in the analysis. As described in Chapter III on loading, methods for predicting blade loads range in accuracy from less than ± 5 percent of the true value to approximately ± 75 percent. The former applies to prediction of mean load at the steady-ahead, zero-rudder condition, while the latter applies to prediction of unsteady or periodic loads during a sharp turn in rough seas. Combined errors in the prediction of the maximum load in a turn might lead to its underprediction by as much as 60 percent. In addition to the inaccuracies in load predictions, there is always a certain degree of scatter in material properties, particularly those related to fatigue, which must be considered. Another important unknown is the operating profile. The number of high power turn operations, for example, may be a critical factor in determining fatigue life, but only poor estimates of this number are available.

The choice of the margins of safety to apply to the predicted stresses must be judgmental on a case by case basis depending upon confidence in the analyses used as well as the ship application. On the one hand, it is desirable for any new CP propeller design that strength criteria be satisfied with as small a hub as possible.

On the other hand, it is also desirable that costs and time associated with analyses and experiments required to demonstrate adequacy be limited especially in low horse-power applications for which the operating spectrum is mild.

Because of the above considerations and because there is an increasingly sophisticated and costly array of methods for predicting both blade loads and resulting stresses, the steps at DTNSRDC required for assessing the structural adequacy of a CP propeller are being formalized. The complexity of the process depends upon the magnitude of estimated stresses versus strength criteria at each of several possible decision points. Where all stresses are well below the criteria, factors of safety are inherently large and, therefore, only the more simple analysis methods for both loads and stresses are appropriate. In the other extreme, where stresses exceed the criteria, it may be possible to decrease stress levels through modifications as described earlier. Also, any perceived problems might be alleviated by changes in materials or manufacturing methods like rolling of bolt threads. In these cases, experimental verification of computed stresses might be required along with suitable fatigue tests. In addition, the most sophisticated blade load prediction techniques would probably be required.

The first step in the design process for U.S. Navy CP propellers is normally carried out jointly by NAVSEA and DTNSRDC. The blade beyond the blade fillet is sized in this step to meet requirements for ship powering, vibration, cavitation, etc. It is notable that balanced skew and forward rake of the blade will cause the blade mass center of gravity to be near or on the blade spindle axis, and thereby provide more uniform bolt loading due to centrifugal force. Further, it is currently planned to provide guidelines for blade fillet shape which will lead to a more even distribution of bolt forces. The blade design and the guidelines for blade fillet shape will be provided to competing CP propeller manufacturers for design of the fillet, blade attachment, hub, and pitch control systems. In the past, contractors have also been provided with the design forces, only at the mean, full-power, zero rudder condition. In the following discussion it is assumed that the manufacturers will also be provided either predictions or methods to predict blade loads for a spectrum of operating conditions to govern fatigue design.

After the components of the blade attachment and hub have been sized, materials selected, and the supporting design calculations have all been submitted by the

397

contractors, the initial phase of the U.S. Navy assessment process can be undertaken. First, the materials and material characteristics, such as yield, ultimate and fatigue strength, will be reviewed and related to availability, machinability, compatibility, reliability, toughness, etc., as has been discussed in Chapter IV on materials. Data for the stress analyses will first be listed as shown in Table 8 to

TABLE 8 - DIMENSIONAL COMPARISON OF BLADE ATTACHMENTS

	USS SPRUANCE	USS BARBEY		USS NEWPORT
Materials				
Blade	Ni-Al-Bronze	Ni-Al-Bronze		Ni-Al-Bronze
Blade Bolts	K-Monel	17-4 PH Steel		K-Monel
Blade Carrier	A471-70, Cl 6	HY-100		A243-64, Cl J
Hub	Ni-Al Bronze	Ni-Al-Bronze		Ni-Al-Bronze
General Description				
Hub type (Figure 35)	Cylinder	Cylinder		Cylinder
Blade carrier type	Crank ring	Crank ring		Crank ring
Number of bolts	8	6		6
Number of blades	5	5		4
Method of bolt preloading	Hydraulic	Torque		Torque
Coverplate?	Yes	No		No
Dimensions				
Blade tip radius, r_{blade}	102.0	90.0		69.0
Hub (Figure 35)				
Radius, r_{hub}	30.6	26.25		20.0625
Radius forward, r_{hf}	28.75	26.25		20.0625
Radius aft, r_{ha}	28.75	26.25		20.0625
Blade flange or palm (Figures 35 and 36)				
Radius, r_{flg}	15.375	14.125		12.219
Radius of bolt circle, r_{BC}	9.8125	8.125		7.188
Radius of counterbore, r_{CB}	2.219	2.125		2.188
Radius of through bolt hole, r_b	1.406	1.281		1.562
Radius of dowel pin, r_{dp}	1.625	1.375		1.062
Thickness of counterbore, t_{cb}	2.219	2.313		1.906
Distance to inner flange surface, a_{fl}	26.187	21.406		15.0
		(Original)	(Modified)	
Crank Ring (Figure 37)				
Outer radius, R_o	14.53	12.063	12.063	11.031
Inner radius, R_i	12.688	9.813	12.218	9.641
Fillet radius, r_f	0.375	0.375	0.375	0.219
Thickness of wall, t_{wall}	1.25	0.241	0.835	0.735
Thickness of lip, t	1.938	2.152	2.561	1.781
Maximum thickness, t_{max}	5.125	4.965	4.965	3.908
Distance to top bolt thread, x_t	+2.875	+2.251	+0.967	+1.814
Distance to bottom bolt thread, x_b	+0.875	+0.001	-1.408	+0.012
Blade Bolts (Figure 38)				
Bolt head radius, r_{bh}	2.031	1.938	1.938	2.0625
Bolt shank radius, r_{bs}	1.25	1.062	1.062	1.366
Bolt thread radius, r_{bt}	1.375	1.25	1.25	1.5
Length of threads, l_{bt}	2.0	2.25	2.375	1.8125
Length of shank, l_{bs}	3.594	2.875	3.75	2.219
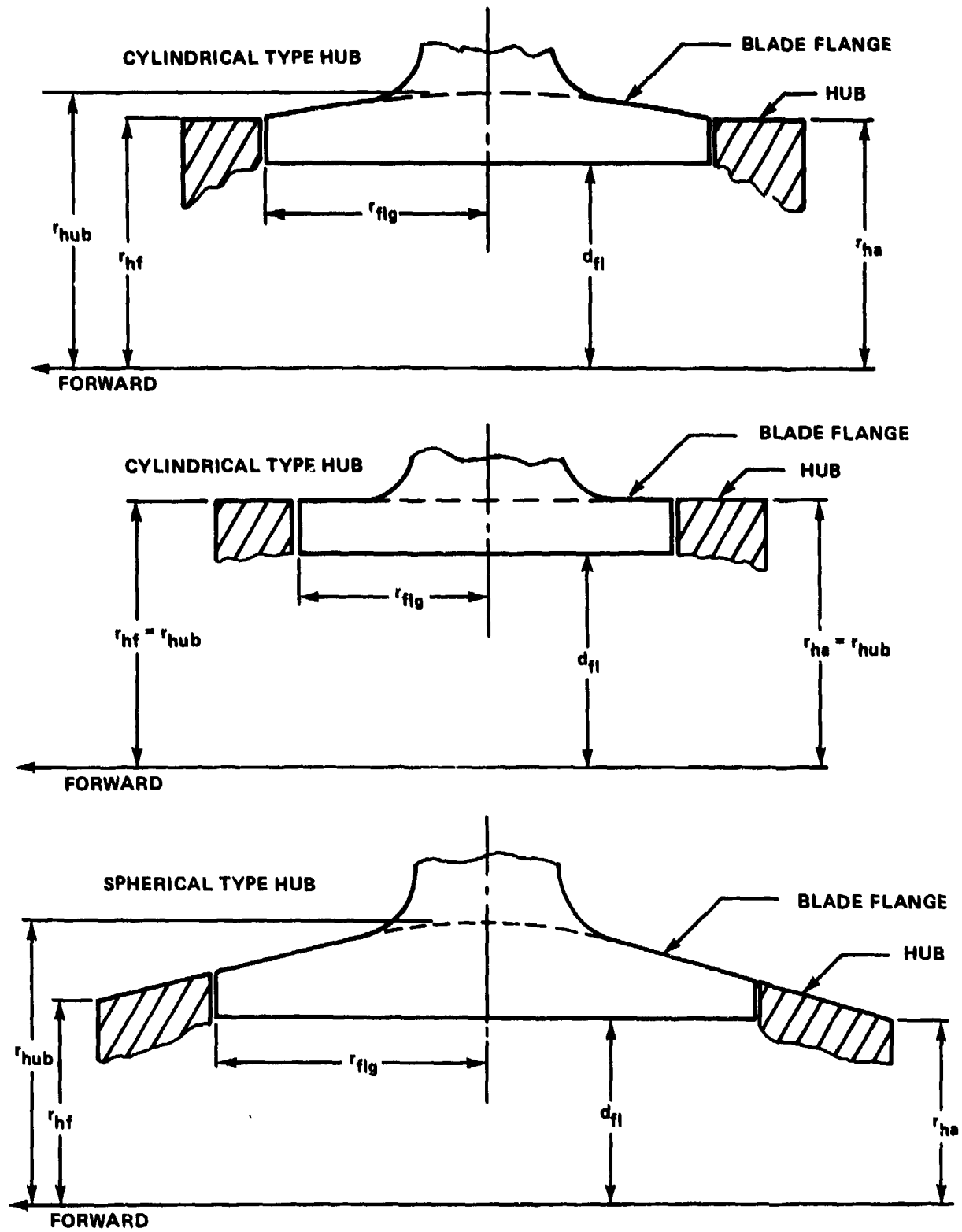
Figure 35 – Dimensions Used in Table 8 for Hub and Blade Flange
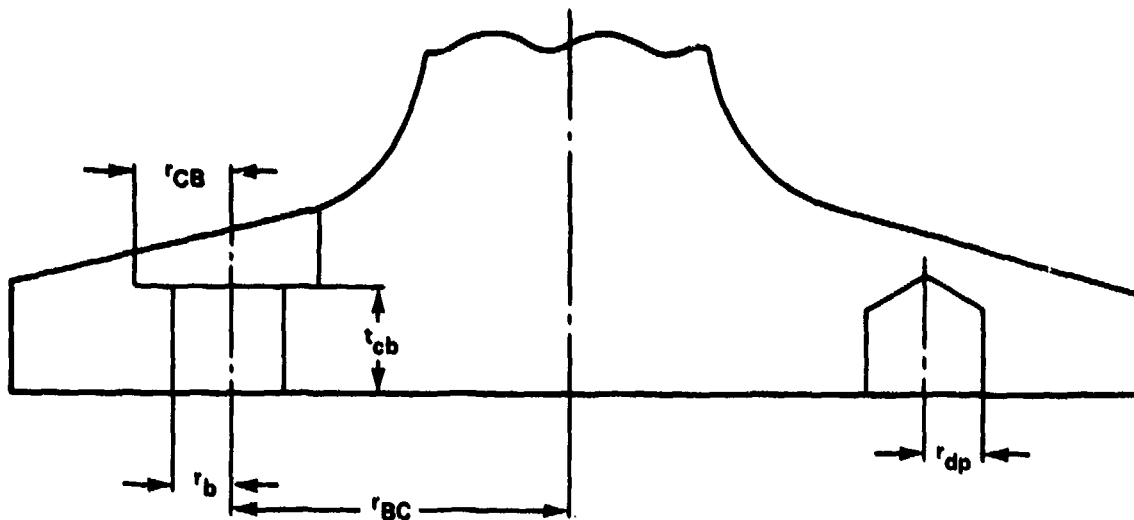
Figure 36 - Dimensions Used in Table 8 for Blade Flange

ensure completeness and then compared nondimensionally with previous experience as in Table 9. Deviations from previous experience may indicate where the designer is deviating from past practice and from the designs involved in the DTNSRDC investigations, and thereby possibly indicate potential problem areas.

The next step is to apply the "simple comparison method for blade bolts" and the closed-form stress analysis method to the blade attachment bolts and blade carrier. Again, comparisons with past practice should be made along the way taking into account any material changes from previous designs.

Initially, predicted stresses using the simple, closed-form methods should be related to the following criteria:

1. Bolt Shank Stress, $\qquad S_{B,max} \leq 0.67 \times SY_B$ (17)

2. Blade Carrier Stress, $\qquad S_{BC,max} \leq 0.5 \times SY_{BC}$ (18)

3. Average Stress Under Bolt Head, $\quad S_{BH,max} \leq 0.9 \times SY_{BL}$ (19)

4. Fatigue Stresses, $\qquad S_{EFF,max} \leq 0.4 \times S_{END}$ (20)

where SY_B, SY_{BC}, SY_{BL} = 0.2 percent offset yield stress of bolt, blade carrier and blade materials, respectively
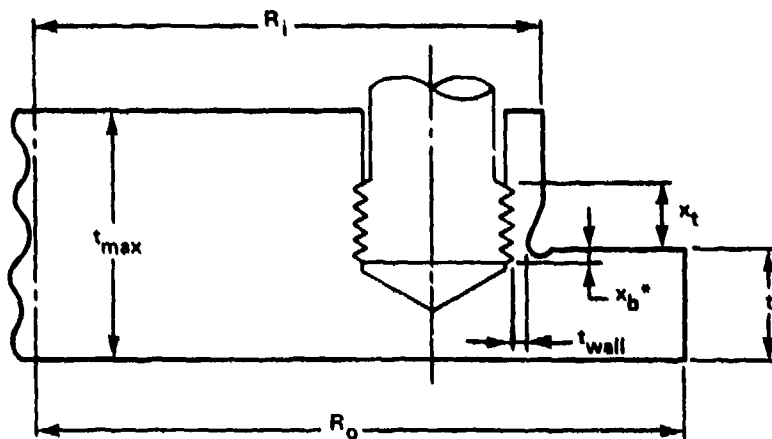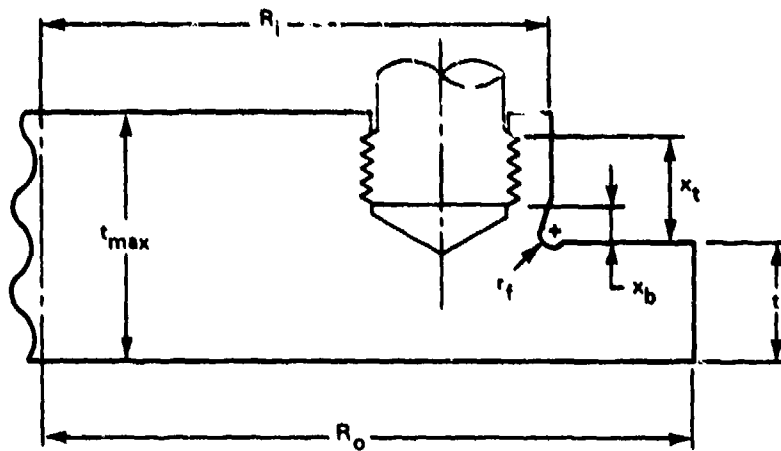
S_{END} = 0.4 × ultimate tensile strength of material

400

*NOTE: x_b AND x_t ARE NEGATIVE WHEN BOLT THREADS ARE DEEPER IN CRANK RING THAN FLANGE SURFACE.
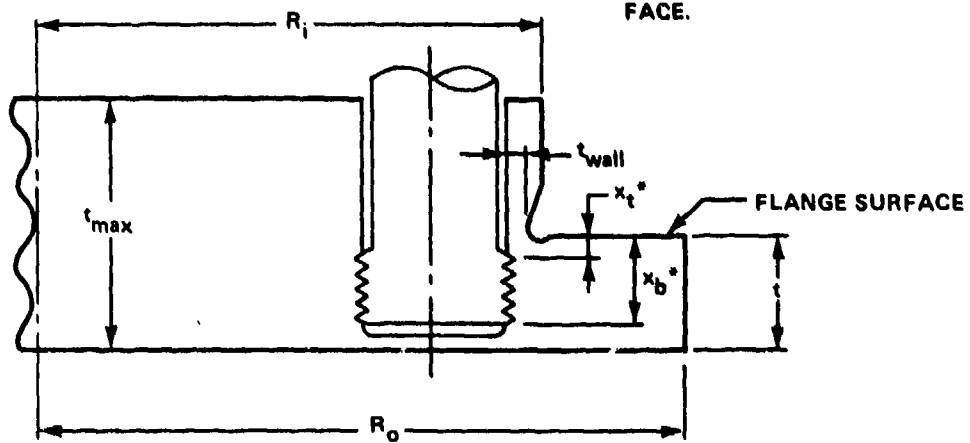
Figure 37 – Dimensions Used in Table 3 for Crank Ring
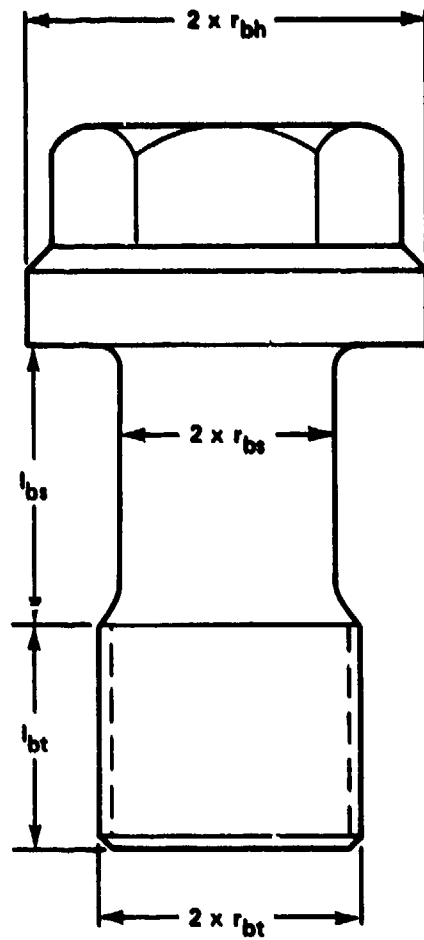
Figure 38 - Dimensions Used in Table 8 for Blade Bolts

TABLE 9 - NONDIMENSIONAL COMPARISON OF BLADE ATTACHMENTS

	USS SPRUANCE	USS BARBEY		USS NEWPORT
Hub				
r_{hub}/r_{blade}	0.30	0.292		0.291
r_{hf}/r_{blade}	0.282	0.292		0.291
r_{ha}/r_{blade}	0.282	0.292		0.291
Blade Flange or Palm				
r_{flg}/r_{hub}	0.502	0.538		0.609
r_{BC}/r_{flg}	0.638	0.575		0.588
r_b/r_{BC}	0.143	0.158		0.217
R_{CB}/r_{BC}	0.226	0.262		0.304
t_{cb}/r_b	1.578	1.806		1.220
r_{dp}/r_{BC}	0.166	0.169		0.148
d_{fl}/r_{hub}	0.856	0.815		0.748
		(Original)	(Modified)	
Crank Ring				
R_o/r_{hub}	0.475	0.460	0.460	0.550
R_i/R_o	0.873	0.813	0.847	0.874
r_{BC}/R_o	0.675	0.674	0.674	0.652
t_{wall}/r_{bt}	0.909	0.193	0.668	0.49
x_t/x_b	3.286	2251.0	−0.687	153.73
r_f/R_i	0.030	0.038	0.037	0.023
t/t_{max}	0.378	0.433	0.516	0.456
t_{max}/r_{hub}	0.167	0.189	0.189	0.195
Blade Bolts				
r_{bh}/r_{BC}	0.207	0.239	0.239	0.287
r_{bs}/r_{BC}	0.127	0.131	0.131	0.190
r_{bt}/r_{BC}	0.140	0.154	0.154	0.209
$(1_{bt}+1_{bs})/r_{bs}$	4.475	4.826	5.767	4.278
r_{bh}/r_{bt}	1.477	1.550	1.990	1.379

The maximum bolt shank stress, $S_{B,max}$, for Equation (17) is calculated as follows:

$$S_{B,max} = S_{prestress} \times \left[1.0 + 2.0 \times 0.2 \times \left(\frac{F_{bolt,max}}{F_{preload}} \right)^{1.6} \right] \qquad (21)$$

the constants, 0.2 and 1.6, are the same as in Equation (7), while the constant, 2.0, accounts for bolt bending due to applied loads

where $S_{prestress}$ = average bolt prestress

$$F_{bolt,max} = \frac{C_{max}}{4} + M_{max} \times \frac{(y_{max} + r_{bolt})}{\sum\limits_{all\ i} y_i^2} \qquad (22)$$

C_{max}, M_{max} = the maximum combination of centrifugal force and peak hydrodynamic bending moment (mean plus alternating) which the propeller will encounter. Usually, these occur during full-rudder, full-power turns, but the effect of rough seas during other operations should be considered

y_{max} = maximum distance of any bolt on the pressure side of the blade from the bolt center to the assumed neutral bending axis

y_i = distance from the center of bolt, i, to the neutral bending axis assumed to intersect the blade palm at its center

r_{bolt} = bolt radius

$F_{preload}$ = bolt preload

The maximum blade carrier stress, $S_{BC,max}$, for Equation (18) is calculated as follows:

$$S_{BC,max} = k_{BC} \times \left(\frac{C_{max}}{A} + \frac{M_{max}}{Z} \right) \quad \text{(for a trunnion)} \qquad (23)$$

at the cross-section giving the highest stress

where k_{BC} = stress concentration factor for blade carrier, from Peterson[22] for example

A, Z as defined for Equation (8)

404

$$S_{BC,max} = k_{BC} \times \left(S_{9,pc} + S_{9,pm} \times \frac{S_{13}}{S_{15}} \right) \qquad \text{(for a crank ring)} \qquad (24)$$

where $S_{9,pc}^*$ and $S_{9,pm}^*$ = stresses from Equation (9) for pressures P_C and P_M, in Figure 28 at the maximum loading as defined for Equation (22)

S_{13}, S_{15}^* = stress from Equations (13) and (15) at the maximum loading as defined for Equation (22)

The maximum average stress under the bolt head, $S_{BH,max}$, for Equation (19) is calculated as follows:

$$S_{BH,max} = F_{bolt,max}/A_{contact}$$

where $A_{contact}$ = area under the bolt head in contact with blade palm

The maximum fatigue stresses, S_{EFF}, for Equation (20) are calculated as follows:

S_{EFF} = maximum effective, fully reversed alternating stress for full-power turn loading, corrected for effect of mean stress

For Blade Carrier,

$$S_{EFF}^{**} = \frac{S_{BC,alt}}{1 - \dfrac{S_{BC,mean}}{SU_{BC}}} \qquad (25)$$

where $S_{BC,alt}$ and $S_{BC,mean}$ are obtained using Equations (23) or (24) with the alternating or mean bending moment and maximum centrifugal force for full power turn loading

SU_{BC} = ultimate tensile strength of blade carrier

For Blade Bolts,

---

*Assumes that the minimum distance between the bolt threads and fillet is large enough to keep the effect of bolt thread loading on fillet stress to an insignificant level.

**Modified Goodman mean stress correction.

$$S_{EFF}^* = \frac{k \times S_{B,alt}}{\left[1 - \frac{(SY_B - k \times S_{B,alt})}{SU_B}\right]} \quad (SU_B < 100{,}000 \text{ psi}) \tag{26}$$

$$S_{EFF}^{**} = \frac{7 \times k \times S_{B,alt}}{8 - \left[1 + \frac{(SY_B - k \times S_{B,alt})}{SU_B}\right]^3} \quad (SU_B \geq 100{,}000 \text{ psi}) \tag{27}$$

where $\quad k = 4$ for cut threads or 3 for rolled threads

$$S_{B,alt} = S_{prestress} \times 2.0 \times 0.2 \times \left[\left(\frac{F_{bolt,max}}{F_{preload}}\right)^{1.6} - \left(\frac{F_{bolt,min}}{F_{preload}}\right)^{1.6}\right] \tag{28}$$

$F_{bolt,max}$ and $F_{bolt,min}$ are obtained using Equation (22) with the centrifugal force and bending moments for full-power turn loading

SU_B = ultimate tensile strength of bolt

The criteria in Equations (17) through (20) are intentionally conservative when used in conjunction with the simple stress analysis methods. For example, the stresses for the SPRUANCE, PERRY, and BARBEY propellers listed in Tables 5 and 6 exceed the criteria of Equations (17), (18), and (20). If the criteria are satisfied, and the design is not too different from the designs on which these analyses are based, the blade and blade carrier should provide adequate structural performance.

If any of the criteria are exceeded using the simple analyses, it may be that use of more accurate methods for computing stresses, as listed in Table 1, or blade loads would indicate otherwise. For example, Equation (2) for computing bolt force is empirically based on data in which one bolt was highly loaded. But the two-dimensional FE method of Equations (3) through (7) might show that the distribution of bolt forces is more even. Or perhaps a model experiment would be appropriate to provide more accurate stress predictions. Possible design modifications might also be considered. Bolt forces can be reduced by modifying blade fillet shape, and

*Modified Goodman stress correction modified in accordance with Reference 7.

**Peterson mean stress correction modified in accordance with Reference 7.

fatigue stresses in bolts can be reduced by increasing bolt preload. Perhaps a material change in either the bolt or blade carrier would allow more preload or improve fatigue properties. Using rolled threads instead of cut threads would reduce the fatigue notch factor. Increasing the fillet radius in the blade carrier would reduce stresses. If such changes are made and then the criteria in Equations (17) through (20) are satisfied, the blade bolts and carrier stresses should be acceptable.

Special examination may be necessary at certain high stress areas where the normal criteria are exceeded. For example, it may be claimed that a particular type of bolt has excellent fatigue properties, exceeding those indicated by Equations (26) and (27). These claims would require corroboration with fatigue test data on actual hardware. References 13 and 16 provide examples of this kind of data for large K-Monel, AISI 4140, and AISI 4340 bolts. The data in Reference 16 was the basis for developing a widely used steel bolt design curve.[7]

Also, if the fatigue criterion is exceeded during high load operations which occur infrequently, it may be possible to demonstrate adequate fatigue strength through application of cumulative fatigue damage rules. Miner's rule was shown to be applicable in Reference 13 provided that the commonly applied summation factor of 1.0 be replaced with 0.6.

SUMMARY OF THE STRENGTH ASSESSMENT PROCESS FOR THE USS SPRUANCE, USS OLIVER HAZARD PERRY, AND USS TICONDEROGA CLASS PROPELLERS

The approach described above to the strength assessment process is intended to reduce, if not eliminate the need for expensive, large-scale testing in the laboratory and at-sea. Such tests were necessary for assessment of the SPRUANCE and PERRY Class propellers, but the analysis methods developed during that process and the lessons learned should provide a suitable basis for determining structural adequacy in future CP propellers of similar design. Lest we forget, the following, largely excerpted from Reference 15, is a summary of those extensive investigations which led to improved propellers on the SPRUANCE, PERRY, and TICONDEROGA (CG-47).

BACKGROUND

In 1974, while the fatigue life of the blade palm and bolts of the SPRUANCE CP propeller were under investigation at DTNSRDC, the CP propeller on USS BARBEY

experienced two separate occurrences of serious structural failures. The first failure involved blade bolts, the second failure involved improved blade bolts and also crank rings. It was then decided to conduct full-scale tests of an assembled SPRUANCE propeller* at DTNSRDC. Simultaneously, redesigned crank rings with improved blade bolts were installed on BARBEY and instrumented sea trials[2] were conducted during which unacceptably high stresses were recorded in high-speed turns. The BARBEY CP propeller was then replaced with a fixed pitch propeller.

It had become apparent that there was insufficient information available concerning design loads, structural response, and material properties for CP propeller hub components, thereby raising serious fundamental questions concerning the adequacy of the CP propellers then being procured for the SPRUANCE Class, and of those which would be required in future gas turbine propelled ships. The NAVSEASYSCOM, therefore, sponsored a program to determine the adequacy of the CP propellers then under procurement for the SPRUANCE Class (later extended to the PERRY and TICONDEROGA Classes) and an R and D program to improve the technology base in design loads, strength analysis, and material selection of CP propeller hub components for future procurement. The entire efforts, both the R and D portion and the portion which was directed specifically to support the ongoing ship construction projects, made important contributions to the resolution of the SPRUANCE, PERRY, and TICONDEROGA Class CP propeller problems.

STRUCTURAL PROBLEM

The two basic questions in the blade attachment structural problem were: what are the forces imposed by the blades during the variety of ship operating conditions, and how does the extremely complex hub structure respond to the pulsating and multibladed forces in a "ship-at-sea" environment? Answers to these questions were required in order to be confident of judgments which could be reached on the basis of any laboratory experiments and analyses.

---

*Reported informally by R. Rockwell and S. Hersh as Enclosure (1) (Full Scale Structural Evaluation of the USS SPRUANCE (DD-963) Controllable Pitch Propeller Blade Attachment - Phase 1, Application of Maximum Loads at Design Pitch) to DTNSRDC letter Serial 75-172-129 of 14 July 1976.

Blade Forces

When this effort began, the mean component of blade force was known quite well for only calm sea, steady ahead operations. Until the BARBEY instrumented sea trials, blade forces for destroyer type hulls under other operating conditions could be estimated only poorly--so poorly that they were not considered in the structural design of the blades. Blades were designed structurally to limit stresses under the mean load for steady-ahead, calm sea operation to an arbitrarily but judiciously selected value based on long experience.

The BARBEY trials demonstrated that the blade forces and particularly the fatigue critical alternating components were considerably higher than expected. Because the BARBEY is a single screw ship and the SPRUANCE a twin screw ship, it was anticipated that the magnitude of the alternating components in SPRUANCE would be larger and would be more difficult to estimate. The high stresses which were being obtained from full-scale laboratory experiments on an assembled SPRUANCE CP propeller hub (and which are discussed in other sections of this report) clearly indicated the need for reliable information on the magnitude of blade forces. Therefore, instrumented trials were conducted on the SPRUANCE. Later, after the failure of a blade bolt in a fatigue test[12] during which the higher forces estimated for PERRY were applied to the SPRUANCE hub assembly, instrumented sea trials were also conducted on the PERRY, a single screw ship. On both ships, measurements were made during a variety of maneuvers in relatively calm seas. In the SPRUANCE trials, blade forces and the resultant blade bolt and crank ring stresses were inferred from strain measurements on the blades, and crank rings while in the later PERRY trials, only bolt strains were obtained.

Structural Response

In the two-year interval between the BARBEY failures and PERRY sea trials, the previously mentioned series of full-scale laboratory experiments were conducted on a complete propeller hub assembly which was configured first with a single SPRUANCE and then with a single PERRY blade. The hydrodynamic component of blade force was applied at the one blade while the centrifugal component was applied at all five blade ports. It became apparent quickly that the stresses in the blade bolts and crank ring were much higher than those which had been computed by the vendor during their design: the blade attachment was not behaving in the neatly distributed

manner which had been assumed. Using the SPRUANCE blade under loads simulating ahead operations, bolt forces above preload were concentrated in bolt 8 and the crank ring stresses peaked near bolt 8. In the later tests with the PERRY blade, bolts 5 and 8 carried, approximately, equal loads, while very little was carried by bolts 6 and 7. A similar distribution was obtained in the crank ring. A large bending component which was not considered in the design analyses was found in bolt stresses both at assembly and under load.

Crank Ring Stress. Excessive crank ring stresses were recorded in the first labora-tory experiments using the full-scale SPRUANCE blade, and in the SPRUANCE sea trials. The combined mean and alternating crank ring stresses in high-power turns exceeded the desired limit of 50 percent of the endurance limit which is customary for large, heavy-sectioned high strength steel forgings. The excessive stresses were very localized. They were primarily the result of high stress concentrations in the small radius in the fillet and secondarily the result of a poor distribution of forces into the crank ring which was caused by the poor bolt force distribution. The crank ring problem was confirmed in the previously mentioned fatigue test[12] when the crank ring, which had 0.375 in. radius fillet, developed a fatigue crack after about 1 million cycles of high-power turn stresses.

Bolt Stress. In view of the disturbingly high stresses which were being recorded for the bolts, NAVSEASYSCOM accepted the DTNSRDC recommendation* that the vendor be directed to reduce the tolerance in bolt hole angularity, thereby eliminating bolt read bending as a potential problem for all future production. In addition, the fu. scale bolt fatigue tests[13] were undertaken in order to develop reliable in-for cion on the fatigue life of bolts of potential interest under the conditions of use in the propellers: (1) bending stress under load, approximately, equal to the average tensile stress above prestress because of bending in both the blade palm and the crank rings, and (2) compressing a bronze flange. Several bolt mate-rials, designs, and fabrication techniques were tested under a range of preloads and at stress levels which spanned the bolt stresses measured in all of the sea

---

*Reported informally by J. Sickles as Enclosure (1) (Propeller Blade Bolt Bending as a Result of Bolt Hole Misalignments in the Crank Rings of the USS SPRUANCE (DD-963) Controllable Pitch Propeller) to DTNSRDC letter Serial 75-178-77 of 10 Sep 1975.

trials. The tests also included runs intended to determine a reasonable value for the summation factor to be used in Miner's rule in estimating the cumulative damage associated with the varying stress levels which would be characteristic of propellers on these ships. The results of these tests were used directly in arriving at the blade bolt life determinations.

DESIGN MODIFICATIONS

It became apparent in surveying the BARBEY and SPRUANCE designs that the crank rings in both propellers were made of steel alloys that had very little fracture toughness and, therefore, were susceptible to brittle fracture. A material with much more fracture toughness was needed as protection against rapid, catastrophic fracture in the presence of material flaws, fatigue cracks, or corrosion pits. Therefore, it was recommended, and accepted, that the crank ring material be changed from AISI 4150H to A471 Class 6, a fracture tough material of equivalent strength. At the same time, several steps were taken to relieve the fillet stresses. One was to increase the fillet radius from 0.375 to 0.50 in. for production of initial PERRY crank rings. This was a sufficient change for PERRY because the alternating blade forces in high-power turns were determined (by measurements at sea) to be lower than the SPRUANCE blade forces and because of the more favorable distribution of bolt forces. An increase in the fillet radius to 0.60 in. was recommended for initial production of TICONDEROGA crank rings and for replacement crank rings for the SPRUANCE.

The first of several design modifications related to blade bolts was made because of high bolt bending stresses due to bolt preload alone. The NAVSEASYSCOM accepted the DTNSRDC recommendation that the vendor be directed to reduce the tolerance in bolt hole angularity, thereby eliminating bolt preload bending as a potential problem in future procurements.

The distribution of bolt forces on an operational propeller is influenced strongly by the shape of the blade fillet and palm. This was recognized early in the SPRUANCE blade attachment investigation at DTNSRDC. In experiments using a crude, flat "dummy hub" as a blade support, bolt 8 nearest the trailing edge of the blade, pressure side, resisted a much larger share of the applied blade forces. The apparent reason was the heavier section of palm at bolt 8 than at the other bolts. A similar effect was seen in the later experiments and sea trials on both

411

the SPRUANCE and PERRY. The relative thickness of the palm at bolt 5 and at bolt 8 is reversed on the PERRY compared to the SPRUANCE, and these bolts carried nearly equal shares of the forces.

More favorable distribution of bolt forces and the smaller alternating component of the measured blade forces in high-speed turns on the PERRY than on the SPRUANCE enabled the PERRY bolt problem to be resolved by a shift from AISI 4140 steel bolts with cut threads to K-Monel bolts with rolled threads and fillets and increased head to shank fillet radii. The series of full-scale bolt fatigue tests[13] had demonstrated the inadequacy of the original AISI 4140 steel bolts as well as the improved fatigue life of the replacement K-Monel bolts. By itself, however, this change would not have been adequate for the SPRUANCE and TICONDEROGA Classes.

Therefore, a series of 1/3-scale model experiments[9] was conducted to evaluate the effects on bolt stresses due to changes in blade fillet geometry and in the modulus of elasticity of the coverplate between the crank ring and the blade palm. The strong influence of fillet geometry was demonstrated in these experiments and a new fillet geometry for SPRUANCE and TICONDEROGA blades was developed to more nearly equalize the forces in the bolts. The beneficial effect of increasing the modulus of the coverplate material was also demonstrated by comparative tests using Ni-Al bronze (the standard material), a steel plug insert in the bronze around the bolt hole, and a steel coverplate. The experimental results were confirmed by analytical investigations.[20] Then full-scale verification experiments[10] were conducted in the laboratory on the SPRUANCE propeller using a blade with the proposed fillet, the standard coverplate, and an Inconel 625 coverplate. Inconel 625 was used in place of steel because it is noncorrosive and yet has the same high elastic modulus. The laboratory data were modified to allow for the differences between the laboratory and at-sea data which had been observed in the earlier experiments using the original components. The major improvement in fatigue life, which resulted from the changes, led to acceptance of the recommended changes in blade fillet geometry for initial production of blades for the TICONDEROGA Class and for backfit on the SPRUANCE Class. Inconel plug inserts in the bronze coverplate were substituted for Inconel coverplate because they would be nearly as effective and much less expensive.

SUMMARY AND CONCLUSIONS

This chapter addresses the strength assessment of the blade attachment. The limiting structural problem areas were identified as the blade attachment bolts and crank ring to which the blade is attached. Stress analyses of the blade attachment are complicated by their involvement with preloaded parts in contact and the complex deformation patterns of the blade palm, crank ring, and hub which make rigorous analyses difficult and expensive. Simplifying assumptions can be made, but the subsequent limitations in results must be recognized and evaluated.

Stress analysis methods described in this chapter include model and full-scale experiments in the laboratory as well as the numerical methods of three-dimensional and two-dimensional finite elements (FE) along with closed form equations. The accuracy of the stress analysis methods is determined, wherever possible, by comparison with results from measurements at sea.

Experimental methods on a model scale are much less costly than full-scale experiments at the expense of accuracy. However, 1/3-scale metal models provided a good simulation for determining stress levels and the effect of design changes on the SPRUANCE propellers.

The numerical methods were applied singly and in combination to predict stresses in the crank ring and blade attachment bolts. In all cases, involvement of the more expensive FE methods increased accuracy of the results. For example, use of a semi-empirical closed-form equation provided an indication of the average tensile stress in the most highly loaded bolt within about 30 percent of experimental data. Improved predictions, within about 15 percent, were found by combining two-dimensional FE analyses with closed-form equations. The best numerical stress predictions were made using three-dimensional FE analyses, but the total blade attachment including part of the hub must be included in order to properly account for the bolted joint nonlinearities and hub and crank ring deformations. At this time, this full three-dimensional analysis is very time consuming and expensive. An attempt to reduce the costs by replacing the crank ring and hub with an elastic foundation of "equivalent spring stiffness" was limited by uncertainties in the "equivalent spring stiffness," and because crank ring deformations under load, which effect bolt bending, were not included.

A method is presented for predicting crank ring fillet stresses which is based on closed-form equations. Comparisons of predictions with experimental data show

413

that this method provides reasonable accuracy if the minimum distance between the bolt threads and fillet is large enough to keep the effect of bolt thread loading on fillet stress to an insignificant level. A crude empirical method for determining this distance is described.

Methods to reduce stress levels were identified including modifying the shape of the blade fillet and palm, changing the magnitude of bolt preload, and increasing radii in a way of stress concentrations. The geometry of the blade fillet and palm was shown to directly affect the distribution of forces in the blade attachment bolts. The severely skewed distribution which caused fatigue problems in the BARBEY propeller can be much improved by changing the blade fillet shape. Increasing bolt preload decreases unsteady bolt stresses at the expense of increased mean stress in the bolt and in the blade palm counterbore area under the bolt head. While lower unsteady bolt stresses improve bolt fatigue performance, higher mean stress degrades it. Also, as preload is increased, the problem of yielding in the low strength bronze under the bolt head must be faced.

Two stress criteria must be satisfied at all times during the useful life of a CP propeller in order for the bolts and crank ring to be considered adequate. The maximum stress must be less than the material's yield stress (except at the thread roots, a special case, and under the bolt heads) and the spectrum of fatigue stresses must be within the material's endurance capacity. Examination of these criteria is referred to as the strength assessment process. Uncertainties in input to the process include the areas of blade load and stress prediction, and the characterization of material properties. The amount of uncertainty can be reduced in each area by using more sophisticated and more expensive methods to obtain the desired data. The choice of margins of safety are dependent upon which methods are used. It is desirable for any new CP propeller that strength criteria be satisfied with as small a hub as possible, but it is also desirable that costs and time associated with analyses and experiments required to demonstrate adequacy, be limited.

The approach described herein to the strength assessment process is intended to reduce, if not eliminate the need for expensive, large-scale testing in the laboratory and at sea. Such tests were necessary for assessing the SPRUANCE and PERRY Class propellers. The much less expensive analysis methods developed during this program and the lessons learned should provide a suitable basis for determining structural adequacy in future CP propellers of closely similar designs.

414

REFERENCES

1. Roren, E.M.Q. et al., "Marine Propeller Blades - Allowable Stresses, Cumulative Damage and Significance of Sharp Surface Defects," Second Lips Propeller Symposium, Drunen, Holland (May 1973).

2. Noonan, C. et al., "The BARBEY REPORT, An Investigation into Controllable Pitch Propeller Failures from the Standpoint of Full-Scale, Underway Propeller Measurements," DTNSRDC Report 77-0080 (Aug 1977).

3. Keil, H.G. et al., "Stresses in the Blades of a Cargo Ship Propeller," Journal of Hydronautics, Vol. 6, No. 1, p. 2 (Jan 1972).

4. Wuhrer, W., "CP Propeller Design Considerations in Respect of Vibratory Loads," The Institute of Marine Engineers, London (1977).

5. Koyama, M. et al., "Development of Semi-Integrated Trunnion for Heavily Loaded CP Propeller Blade," Propellers '78 Symposium, Society of Naval Architects and Marine Engineers, New York (1978).

6. Boatwright, G. and J. Strandell, "Controllable Pitch Propellers," Naval Engineers Journal (Aug 1967).

7. "ASME Boiler and Pressure Vessel Code, Section III, Nuclear Power Plant Components," 1974 Edition.

8. Schauer, R.E. and C. Noonan, "Full-Scale, Underway Controllable Pitch Propeller Stress Trials on USS OLIVER HAZARD PERRY (FFG-7)," DTNSRDC Report 80/114 (Dec 1980).

9. Garala, H., "One-Third Scale Model Structural Evaluation of the USS SPRUANCE (DD 963) Controllable Pitch Propeller Blade Attachment," DTNSRDC Report 80/099 (Sep 1980).

10. Gorman, R.W., "Full-Scale Verification of Reduced Stresses in the Blade Attachment of the DD 963 and CG 47 Controllable Pitch Propellers through Modification of the Blade Fillet and Coverplate," DTNSRDC Report 80/081 (Nov 1980).

11. Rockwell, R.D., "Full-Scale Structural Evaluation of the USS OLIVER HAZARD PERRY (FFG 7) Controllable Pitch Propeller Blade Attachment, Phase II--Application of FFG 7 Blade Forces to the FFG 7 Propeller," DTNSRDC Report 80/067 (Jun 1980).

12. Rockwell, R. and S. Hersh, "Full-Scale Structural Evaluation of the USS OLIVER HAZARD PERRY (FFG 7) Controllable Pitch Propeller Blade Attachment, Phase I-- Application of FFG 7 Blade Forces to the USS SPRUANCE (DD 963) Propeller," DTNSRDC Report 80/066 (Jun 1980).

13. Phyillaier, W. and R. Rockwell, "Fatigue Behavior of Blade Attachment Bolts of Different Materials for High-Horsepower Controllable Pitch Propellers," DTNSRDC Report 80/043 (Jun 1980).

14. Garala, H.J., "Fatigue Strength Evaluation of Crank Ring Fillets for the DD 963, FFG 7 and CG 47 Controllable Pitch Propellers Based on Full-Sized Fillet Specimens," DTNSRDC Report 80/107 (Sep 1980).

15. Rockwell, R. and S. Hersh, "DD 963, FFG 7 and CG 47 Class Propellers - Strength of Blade Bolts and Crank Rings and Overview of Investigations," DTNSRDC Report 80/068 (Jun 1980).

16. Snow, A.L. and B.F. Langer, "Low Cycle Fatigue in Large Diameter Bolts," Journal of Engineering for Industry (Feb 1967).

17. "Fatigue Design Handbook," edited by James A. Graham, Society of Automotive Engineers, Inc. (1968).

18. MARC-CDC User Information Manual, General Purpose Finite Element Analysis Program, Control Data Corporation, Minneapolis, Minnesota (1974).

19. Chu, T.Y. and D.W. McLaughlin, "Contributions to the Development of Design Criteria for Controllable Pitch Propellers," Mechanical Technology Incorporated Report MTI 76TR45 (Jun 1976).

20. Martin, D.L., "Numerical Methods for Investigating Stresses in Controllable Pitch Propeller Blade Attachments," DTNSRDC Report 80/085 (Aug 1980).

21. Gifford, L.N., Jr., "APES-Second Generation Two-Dimensional Fracture Mechanics and Stress Analysis by Finite Elements," NSRDC Report 4799 (Dec 1975).

22. Peterson, R.E., "Stress Concentration Factors," John Wiley and Sons, Inc. (1974).

23. Roark, R.J. and W.C. Young, "Formulas for Stress and Strain," McGraw Hill Book Company (1975).

24. Denny, S.B. et al., "Hydrodynamic Design Considerations for the Controllable Pitch Propeller for the Guided Missile Frigate," Naval Engineers Journal (Apr 1975).

25. Gorman, R.W., "General Mathematical Definition of Propeller Blade Fillet Geometry," DTNSRDC Report 79/053 (Aug 1979).

CHAPTER VI

SPECIFICATIONS

TABLE OF CONTENTS

Propeller specification requirements can take two forms:

1. The procrustean approach sets arbitrary fixed limits irrespective of any other considerations. An example of this is the requirement for a Charpy impact of 30 ft/lb minimum at 0°F for all propeller blade attachments. This approach is simple to administer and assures the reliability of any propeller (assuming the limits are properly chosen). However, in many cases it unnecessarily restricts the manufacturer, results in a less than optimum propeller, and is insensitive to advances in the state-of-the-art.

2. The flexible approach permits limits to vary with each application. This permits greater flexibility of design, optimization, and possible savings in material costs. On the other hand, this approach requires that the manufacturer prove to the satisfaction of the buyer that the limits chosen in each case result in a reliable and suitable propeller design.

From an optimal design standpoint, the flexible approach should be used throughout, limited only by the operating requirements of the finished product. However, this greatly complicates the design and design review processes. In the controllable pitch (CP) propeller area, a case by case determination of each limit would require much more research cost and time than could be justified. Hence, fixed limits will always be necessary in some areas.

At the start of the program, we were aware that not only did we not have the analytical tools to use the flexible approach in many areas, we did not even know the proper magnitudes for such basic propeller features as propeller blade bolt loads and alternating blade stresses.

The basic ordering document for CP propellers is Military Specification DOD-P-24562. This specification was issued 28 December 1977 and is designed to be suitable

for CP propellers of all power ranges, sizes, and types. Some criteria developed early in the program and included in the specifications are:

1. Charpy impact strength requirements for propeller blade attachment components (page 7, Table I, Note 1).

2. Minimum fatigue life requirements for propeller blade attachments (page 10, paragraph 3.3.2.3).

3. Requirements to torque propeller blade bolts under controlled conditions (page 11, paragraph 3.3.8).

4. Requirements to calculate stresses in the propeller blade attachments assuming that 90 percent of the forces on the blade are transmitted through any bolt in tension, that fatigue studies be prepared, and that blade alternating stresses shall be a minimum of 40 percent (page 30, paragraphs 3.22.1 and 3.22.1.1).

Improvements in this specification resulting from the program will mostly lie in the areas of stress calculations and fatigue analysis.

STRESS CALCULATIONS

Calculations of stresses in hub components have always been performed ignoring the effects of deformations of the hub casting and the blade attachment components. As discussed in Chapter V, this approach results in calculated stresses which are considerably lower than actual stresses. A more sophisticated analysis is necessary to properly estimate their magnitude.

Another reason for needing accurate knowledge of propeller blade attachment component stresses is that these stress levels affect the hub diameter which, in turn, affects propeller efficiency.

Guidance and acceptance criteria for conducting the propeller blade attachment stress analysis must be provided, e.g., the components to be so analyzed, treatment of boundary conditions, configuration of elements, etc.

One result of the program was the finding that the distribution of stresses among the blade bolts and, hence, the maximum blade bolt stress, depends upon the "stacking" of the blade sections relative to the spindle axis. Significant stress reduction can be obtained by changes in stacking. Guidance for optimizing blade bolt stress distribution by proper stacking must be provided whenever the manufacturer of the propeller provides the hydrodynamic design of the propeller blades.

FATIGUE CALCULATIONS

Fatigue analyses of propeller hub components had not been performed prior to the start of the program because the stress levels in hub components, as they had been calculated, were well below safe fatigue limits. Also, alternating stress magnitudes had been grossly underestimated.

To properly calculate the fatigue life of propeller hub components, the following must be known:

1. Fatigue life curves for the materials used. Obtaining this information is the responsibility of the contractor. The safety factor to be applied to the curves must be specified. Reduction in the safety factor is possible in cases where fatigue tests of the actual component have been conducted.

2. Mean stresses on the propeller blades. Mean propeller blade stresses can be accurately calculated using methods known prior to the initiation of this program.

3. Alternating stresses on the propeller blades. A method of calculating alternating propeller blade forces was developed under the program and is described in Chapter III. This information must be provided to the propeller designer so that alternating propeller blade stresses can be calculated.

4. The relationship between alternating stress, shaft rpm, and rudder angle in each operating mode. The effect of rudder angle on mean and alternating blade stresses was also studied under the program. This information must be provided to the propeller designer.

5. The operating profile of the ship, so that the number of cycles (shaft turns) at each increment of alternating stress magnitude can be determined. The operating profile is unique to each ship class and is normally developed as part of each ship design.

6. The number, duration, and magnitude of rudder angle shifts at each speed increment. Because maximum blade stresses occur during ship turns, this information is essential for proper calculation of fatigue life.

7. The fatigue calculations must invoke that variant of Miner's rule which has been found to provide the best estimate of fatigue life.

Items 5 and 6 can never be accurately predicted because they depend upon the predilections of the individual ship operators and future ship uses and missions. The only realistic way to ensure that fatigue limits will not be exceeded is to require that maximum stresses not exceed the fatigue endurance limit for each material

involved. This would decrease the effort necessary to verify adequate fatigue strength, and provide greater assurance of propeller reliability.

CHAPTER VII

GUIDELINES AND PROCEDURES FOR EVALUATION OF BLADE ATTACHMENT STRENGTH

TABLE OF CONTENTS

LIST OF FIGURES

LIST OF TABLES

INTRODUCTION

One of the first steps taken by the U.S. Navy following the USS BARBEY (FF-1088) Controllable Pitch (CP) propeller failures in 1974 was to initiate several independent stress analyses of the BARBEY blade attachment using state-of-the-art methods. The accuracy of those analyses was generally poor when stress results were compared with actual stresses obtained later through measurements at sea. The reasons for the inaccuracies included both underprediction of blade loads and use of inappropriate stress analysis methods.

Extensive efforts to determine the cause of the BARBEY failures and their importance with respect to the new propellers for the USS SPRUANCE (DD-963) and USS OLIVER HAZARD PERRY (FFG-7) Classes have led to development of a series of blade load and stress prediction methods of increasing accuracy. In addition, more suitable materials have been identified than were used in BARBEY and an awareness of important material selection parameters has been generated. Chapters II through V of this report summarize those efforts. There are some limitations. Because the new blade load prediction methods are based on work concerning high speed ships with transom sterns and exposed shafts and struts, use of these methods for other ship types should be made with caution. The new stress prediction methods were verified experimentally only on "bolted-on" blade attachments having six or eight bolts attached to crank rings. Confidence in results using these stress methods on designs having different physical arrangements or proportions would require some experimental confirmation.

Because of the complexity of the overall problem of evaluating CP propeller strength, there are a number of different prediction methods which might be used. These are described in Chapters III and V. Because cost and accuracy vary for each of the methods, some judgement must be applied in the evaluation process in selecting from among the several methods which may be applied. The intent of this chapter is to describe the strength evaluation process as it now exists for blade attachments of U.S. Navy CP propellers. The necessary guidelines for appropriately using the several load and stress prediction methods are provided along with guidelines for examining material properties. Details for use of each method are given in Appendixes A and B or are available in specified references.

STRENGTH CRITERIA

Two stress criteria must be satisfied at all times during the useful life of the CP propeller in order for the bolts and blade carrier to be considered to be adequate. The maximum stress must be less than the material's yield stress (except at the thread roots, a special case, and bearing stress under the bolt head) and the spectrum of fatigue stresses must be within the material's endurance capacity.

The accuracy of the predicted stresses is dependent not only upon the accuracy of the stress analysis, but also upon the accuracy of the blade loads used in the analysis. As described in Chapter III on loading, methods for predicting blade loads range in accuracy from less than ± 5 percent of the true value, to approximately ± 75 percent. The former applies to the prediction of mean load at the steady-ahead, zero-rudder condition, while the latter applies to the prediction of unsteady or periodic loads during a sharp turn in rough seas. Combined errors in the prediction of the maximum load in a turn might lead to its underprediction by as much as 60 percent. In addition to the inaccuracies in load predictions, there is always a significant degree of scatter in material properties, particularly those related to fatigue, which must be considered. Another important unknown is the operating profile. The number of high-power turn operations, for example, may be a critical factor in determining fatigue life, but only poor estimates of this number are available.

The choice of the margins of safety to apply to the predicted stresses must be judgmental on a case by case basis depending upon the ship application and the confidence in the analyses used. On the one hand, it is desirable for any new CP propeller design that strength criteria be satisfied with as small a hub as possible. On the other hand, it is also desirable that costs and time associated with analyses and experiments required to demonstrate adequacy be limited, especially in low horsepower applications for which the operating spectrum is mild.

The following strength criteria are established as a baseline for use during initial evaluation of blade attachments or for use with the "simple"* load and stress prediction methods. These criteria are intentionally conservative as are the simple stress methods; when any one of the criteria is exceeded, additional evaluation of the blade attachment strength is required:

_____

*The simple load and stress prediction methods are identified in the following section of this chapter.

426

1. Maximum bolt shank stress including prestress is to be less than two-thirds of the bolt material yield stress;

2. Maximum blade carrier stress is to be less than one-half of the blade carrier material yield stress;

3. Maximum average bearing stress under the bolt heads is to be less than 90 percent of the blade material yield stress; and

4. Maximum fatigue stresses in the bolts and the blade carrier are to be less than 40 percent of the materials' endurance stress.

STRENGTH EVALUATION PROCESS

The above considerations related to strength criteria and the increasingly sophisticated and costly array of methods for predicting both blade loads and resulting stresses have made it desirable to formalize the steps at DTNSRDC required for evaluating the structural adequacy of a CP propeller blade attachment. The complexity of the process depends upon the magnitude of estimated stresses versus strength criteria at each of several possible decision points. Where all stresses are well below the previously noted criteria, factors of safety are inherently large and, therefore, only the more simple prediction methods for both loads and stresses would normally be appropriate. Where stresses exceed those criteria, the use of more accurate load and stress prediction techniques would probably be required, possibly along with experimental verification of computed stresses and suitable fatigue tests. It would also be reasonable to consider the possibility of decreasing stress levels through design modifications such as changes in blade fillet shape or increased radii at stress concentrations. Alternatively, strength problems might be alleviated by changes in materials or manufacturing methods such as rolling of bolt threads. As confidence in predictions is increased through the use of more accurate analysis methods, the previously noted strength criteria can be relaxed somewhat, on a case by case basis.

The strength evaluation process begins after design of the propeller blades and hub. The blades (not the blade attachment and hub) of U.S. Navy propellers are normally designed jointly by the Naval Sea Systems Command (NAVSEASYSCOM) and DTNSRDC to meet requirements for ship powering, vibration, cavitation, etc. In the future design of CP propellers, it is important to note that balanced skew and forward rake

of the blade will cause the blade mass center of gravity to be near or on the blade spindle axis and, thereby, provide more uniform bolt loading due to centrifugal force. Further, it is possible to design blade fillet shapes which will lead to a more even distribution of bolt forces. The blade design and the guidelines for blade fillet shape will be provided to competing CP propeller contractors for their information in their design of the fillet, blade attachment, hub, and pitch control systems.

In the past, contractors have been provided blade loads at the design condition.* These time-average loads under steady-ahead operation in a calm sea can be predicted to a high degree of accuracy by any one of several methods. These methods include: (1) routine model powering experiments, (2) the propeller design calculations, (3) theoretical predictions based on inverse propeller theory, and (4) a combination of these methods. They are described in detail in Appendix A.

In the future, contractors will generally be provided with additional information on blade loads including: (1) unsteady loads at the design condition, (2) mean and unsteady loads in a full-power, full-rudder turn, and (3) an estimate of the effect of rough seas.

STEP ONE--EXAMINE DIMENSIONS AND MATERIAL PROPERTIES

The DTNSRDC evaluation process is undertaken after the components of the blade attachment and hub have been sized, materials selected, and the supporting design calculations have all been submitted by the designers. In step one, the materials and material characteristics (such as yield, ultimate, and fatigue strength, and toughness, listed as in Table 1) are reviewed and related to availability, machinability, compatibility, reliability, etc., as has been discussed in Chapter IV on Materials. Also, data for the stress analyses are listed as shown in Table 2 and then, as appropriate, compared nondimensionally with previous experience as in Table 3. Deviations from previous experience may indicate where the designer is departing from past practice and from the designs involved in the DTNSRDC investigations, and thereby indicate potential design problem areas.

_____

*The design condition is defined as the steady-ahead condition in calm water at which the detailed design of the propeller blades is conducted. This condition generally corresponds to a specified speed or delivered power, and a specified propeller rotational speed.

TABLE 1 - MATERIALS AND MATERIAL CHARACTERISTICS

Crank Ring	USS SPRUANCE (DD-963)	USS OLIVER HAZARD PERRY (FFG-7)	USS BARBEY (FF-1088)	USS NEWPORT (LST-1179)
Material	Steel A471-70, Cl 6	Steel A471-70, Cl 6	Steel HY-100	Steel A243-64, Cl J
Yield Stress (ksi)	130(min)	130(min)	100	60 (min)
Ultimate Strength (ksi)	140(min)	140(min)	-	90 (min)
Fatigue Strength (ksi)	55	55	50	-
Toughness (Minimum Charpy-V, ft-lb)	40(RT)	40(RT)	30(120 deg F)	-

Blade Bolts				
Material	K-Monel	K-Monel	Steel 17-4PH	K-Monel
Yield Stress (ksi)	100	100	100	100
Ultimate Strength (ksi)	160	160	135	160
Fatigue Strength (ksi)	40	40	65	40
Toughness	21	21	20	21

TABLE 2 - DIMENSIONAL COMPARISON OF BLADE ATTACHMENTS

	USS SPRUANCE	USS BARBEY		USS NEWPORT
MATERIALS				
Blade	Ni-Al-Bronze	Ni-Al-Bronze		Ni-Al-Bronze
Blade Bolts	K-Monel	17-4 PH Steel		K-Monel
Blade Carrier	A471-70, Cl 6	HY-100		A243-64, Cl J
Hub	Ni-Al-Bronze	Ni-Al-Bronze		Ni-Al-Bronze
GENERAL DESCRIPTION				
Hub type (Figure 1)	Cylinder	Cylinder		Cylinder
Blade Carrier type	Crank ring	Crank ring		Crank ring
Number of bolts	8	6		6
Number of blades	5	5		4
Method of bolt preloading	Hydraulic	Torque		Torque
Cover plate?	Yes	No		No
DIMENSIONS				
Blade tip radius, r_{blade}	102.0	90.0		69.0
Hub (Figure 1)				
Radius, r_{hub}	30.6	26.25		20.0625
Radius forward, r_{hf}	28.75	26.25		20.0625
Radius aft, r_{ha}	28.75	26.25		20.0625
Blade Flange or Palm (Figures 1 and 2)				
Radius, r_{flg}	15.375	14.125		12.219
Radius of bolt circle, r_{BC}	9.8125	8.125		7.188
Radius of counterbore, r_{CB}	2.219	2.125		2.188
Radius of through bolt hole, r_b	1.406	1.281		1.562
Radius of dowel pin, r_{dp}	1.625	1.375		1.062
Thickness of counterbore, t_{cb}	2.219	2.313		1.906
Distance to inner flange surface, d_{fl}	26.187	21.406		15.0

Crank Ring (Figure 3)		(Original)	(Modified)	
Outer radius, R_o	14.53	12.063	12.063	11.031
Inner radius, R_i	12.688	9.813	10.218	9.641
Fillet radius, r_f	0.375	0.375	0.375	0.219
Thickness of wall, t_{wall}	1.25	0.241	0.835	0.735
Thickness of lip, t	1.938	2.152	2.561	1.781
Maximum thickness, t_{max}	5.125	4.965	4.965	3.908
Distance to top bolt thread, x_t	+2.875	+2.251	+0.967	+1.814
Distance to bottom bolt thread, x_b	+0.875	+0.001	-1.408	+0.012
Blade Bolts (Figure 4)				
Bolt head radius, r_{bh}	2.031	1.938	1.938	2.0625
Bolt shank radius, r_{bs}	1.25	1.062	1.062	1.366
Bolt thread radius, r_{bt}	1.375	1.25	1.25	1.5
Length of threads, l_{bt}	2.0	2.25	2.375	1.8125
Length of shank, l_{bs}	3.594	2.875	3.75	2.219
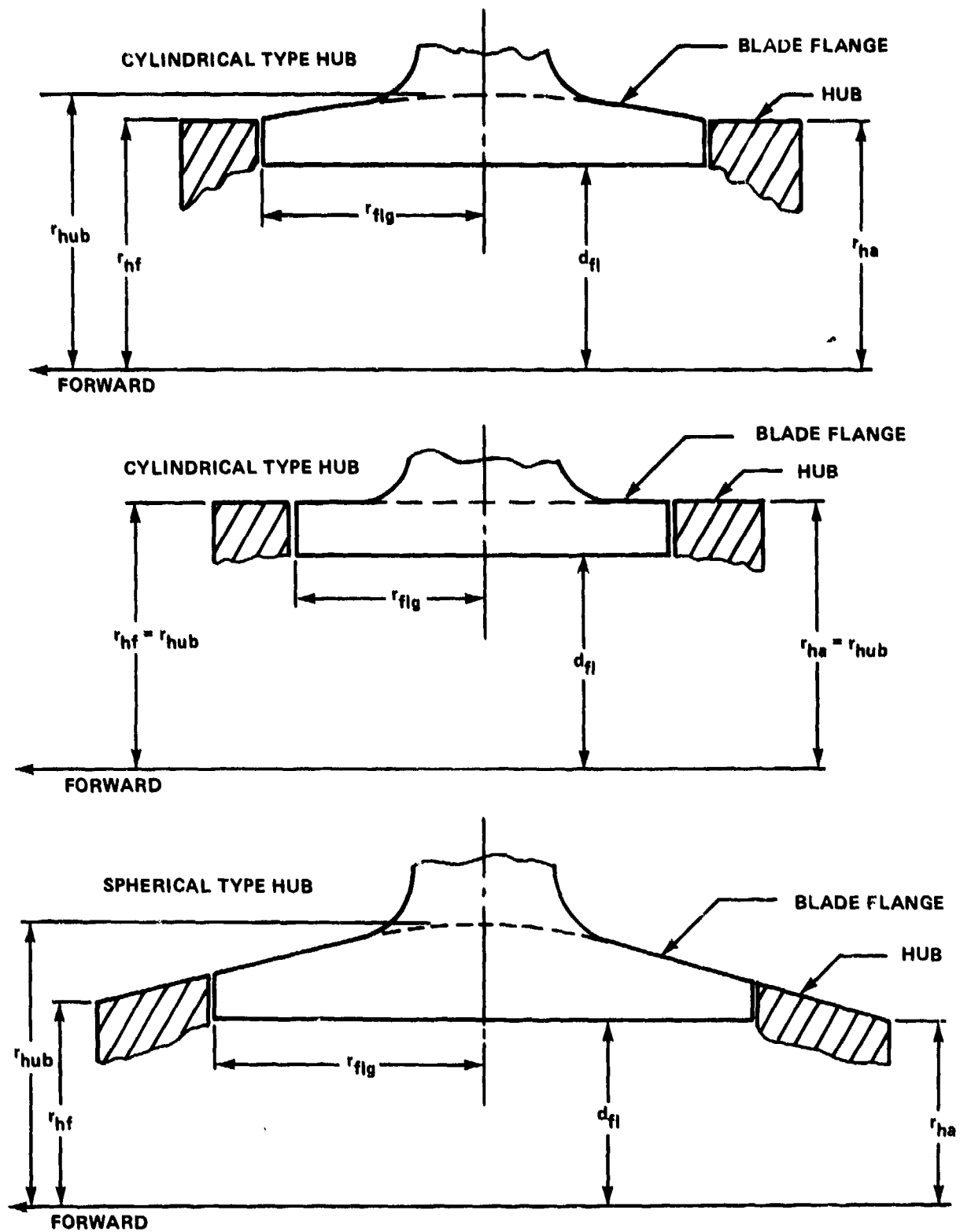
Figure 1 - Dimensions Used in Table 2 for Hub and Blade Flange

431
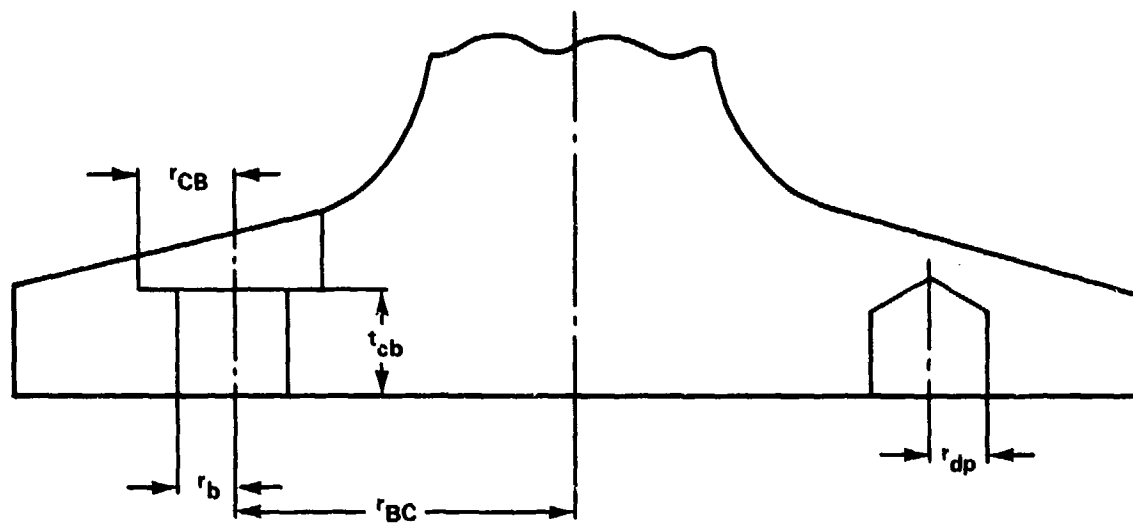
Figure 2 - Dimensions Used in Table 2 for Blade Flange
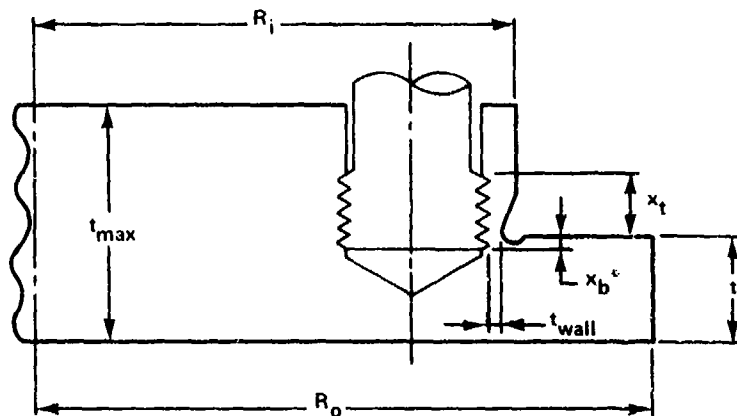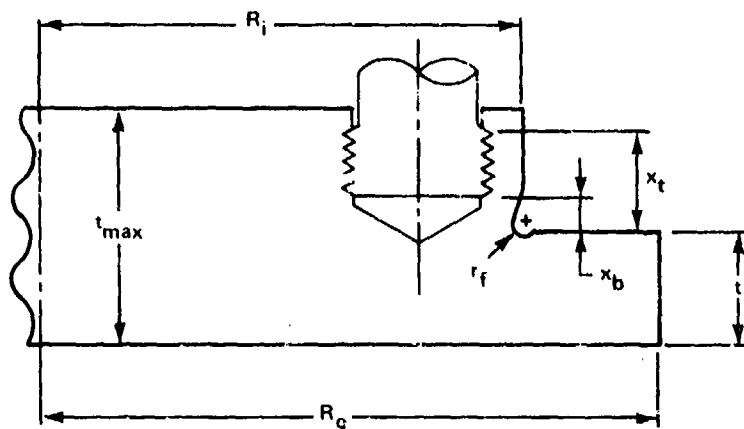
432

*NOTE: x_b AND x_t ARE NEGATIVE WHEN BOLT THREADS ARE DEEPER IN CRANK RING THAN FLANGE SURFACE.
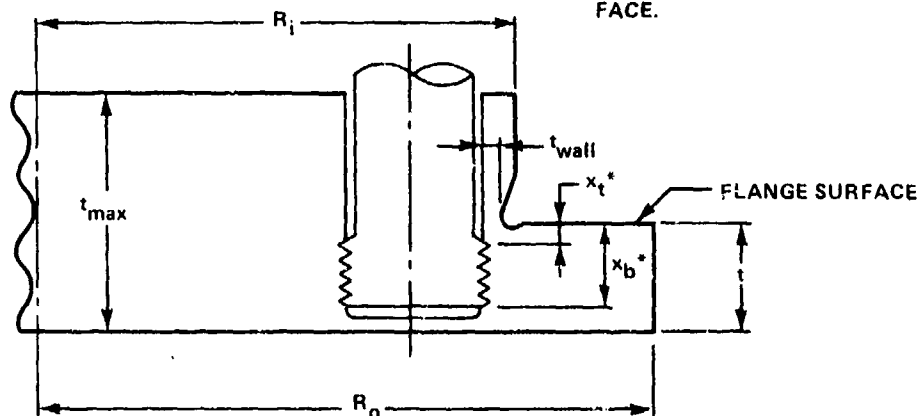
Figure 3 - Dimensions Used in Table 2 for Crank Ring

433
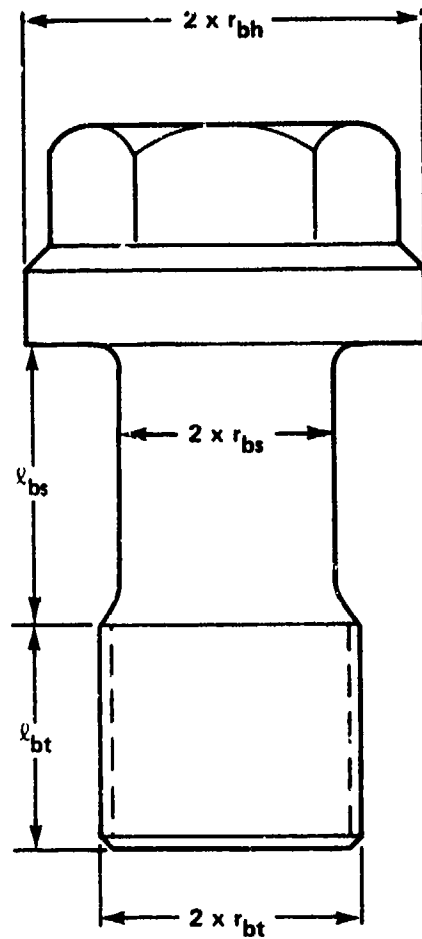
Figure 4 - Dimensions Used in Table 2 for Blade Bolts

TABLE 3 - NONDIMENSIONAL COMPARISON OF BLADE ATTACHMENTS

	USS SPRUANCE	USS BARBEY		USS NEWPORT
Hub (Figure 1)				
r_{hub}/r_{blade}	0.30	0.292		0.291
r_{hf}/r_{blade}	0.282	0.292		0.291
r_{ha}/r_{blade}	0.282	0.292		0.291
Blade Flange or Palm (Figure 1 or 2)				
R_{flg}/r_{hub}	0.502	0.538		0.609
r_{BC}/r_{flg}	0.638	0.575		0.588
r_b/r_{BC}	0.143	0.158		0.217
R_{CB}/r_{BC}	0.226	0.262		0.304
t_{cb}/r_b	1.578	1.806		1.220
r_{dp}/r_{BC}	0.166	0.169		0.148
d_{fl}/r_{hub}	0.856	0.815		0.748
Crank Ring (Figure 3)		(Original)	(Modified)	
R_o/r_{hub}	0.475	0.460	0.460	0.550
R_i/R_o	0.873	0.813	0.847	0.874
r_{BC}/R_o	0.675	0.674	0.674	0.652
t_{wall}/r_{bt}	0.909	0.193	0.668	0.49
x_t/x_b	3.286	2251.0	-0.687	153.73
r_f/R_i	0.030	0.038	0.037	0.023
t/t_{max}	0.378	0.433	0.516	0.456
t_{max}/r_{hub}	0.167	0.189	0.189	0.195
Blade Bolts (Figure 4)				
r_{bh}/r_{BC}	0.207	0.239	0.239	0.287
r_{bs}/r_{BC}	0.127	0.131	0.131	0.190
r_{bt}/r_{BC}	0.140	0.154	0.154	0.209
$(l_{bt}+l_{bs})/r_{bs}$	4.475	4.825	5.767	4.278
r_{bh}/r_{bt}	1.477	1.550	1.990	1.379

An additional part of step one is the application of the Simple Comparison Method for Blade Bolts, which is described in Appendix B. This simple method, which requires about one man-day, provides a preliminary overview and indication of bolt force level through comparisons with similar calculations for a number of successful and unsuccessful designs. Blade loads at the full-power steady-ahead operation in calm water (the design condition) are used. Results from this analysis only indicate whether bolts are relatively highly loaded requiring close examination, or lightly loaded.

STEP TWO--APPLY SIMPLE LOAD AND STRESS PREDICTION METHODS

Step two of the strength evaluation process is the application of the closed-form stress analysis methods to the blade attachment bolts and blade carrier. These methods were described, in detail, in Chapter V of this report and are repeated in Appendix B of this chapter. Predictions of maximum and periodic blade loads are needed so that predictions can be made of maximum stresses and fatigue stresses in the blade attachment. The stresses are then compared with the strength criteria described earlier.

Blade loads and subsequent stresses vary as indicated in Figure 5, whether the ship is operating at zero rudder in a calm sea or at full rudder in rough seas.
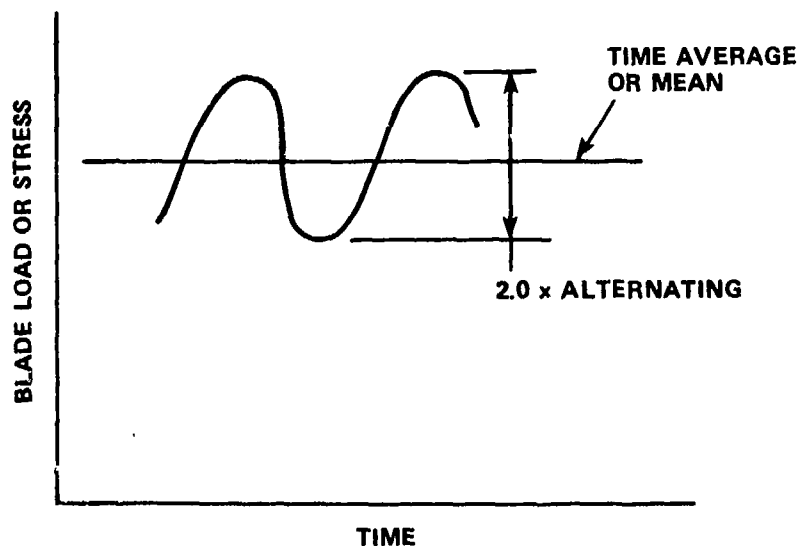
Figure 5 - Blade Load and Stress Variation with Time

436

The time-average or mean loads at zero rudder are already available for step two. In most cases a model wake survey and calculation of the periodic loads under full-power steady-ahead operation in calm water (the design condition) are conducted as part of the design of the propeller blades. For these cases, these periodic loads should be used. If no wake survey is available, then the periodic loads under steady-ahead operation in calm water can be estimated by judicious use of statistical data, such as that listed in Table 4, following guidelines provided in Chapter III of this report and in Appendix A of this chapter.

The peak blade loads (the maximum blade loads considering the time-average, transient, and periodic contributions) generally occur during full-power, full-rudder turns in a calm sea or during high speed operation in rough seas, depending upon the operating characteristics of the ship. The peak and periodic blade loads during a turn in a calm sea can be estimated by judicious use of statistical data following guidelines provided in Chapter III of this report and in Appendix A of this chapter. This requires a general knowledge of the mode of operation of the CP propeller control system. The effect of rough seas on peak and periodic blade loads can be readily estimated by a method which is described in Chapter III and in Appendix A of this chapter.

The predicted maximum and fatigue stresses from step two are now compared with the criteria described earlier in this chapter to determine if additional evaluation is required. These criteria are thought to be conservative because stresses for the structurally adequate PERRY blade attachment based on both experimental data and the prediction methods described here for step two exceed the criteria. Therefore, if the criteria are satisfied, and the design is not very different from the designs on which these analyses are based, then the blade and blade carrier would be judged to be capable of providing adequate structural performance.

STEP THREE--APPLY MORE ACCURATE LOAD AND STRESS PREDICTION METHODS IF NEEDED

If any of the initial criteria are exceeded in step two using the simple analyses, then it is necessary to proceed to more accurate predictions of blade loads and stresses in step three or to modifications to the design in step four, or both. More accurate prediction of periodic blade loads under steady-ahead operation in a calm sea than those obtained in step two can be obtained by direct measurement of

TABLE 4 - STATISTICAL DATABASE FOR BLADE LOADS

Ship	Source	At 0 Degrees Rudder			Remarks
		Average Stress tons/in.^{2} (kg/mm^2)	Fluctuation in Stress tons/in.^{2} (kg/mm^2)	Percent Fluctuation	
VIANA	Wereldsma, International Shipbuilding Progress Vol. 133, 1964	2.93 (4.61)	+0.84 (1.32)	±29	42,000-ton tanker
USS FRANKLIN D. ROOSEVELT	Antonides DTNSRDC Report 2562, 1968	3.88 (6.11)	+1.61 (2.54)	±47*	Aircraft Carrier quadruple screw
NEUENFELS	Keil et al., Journal of Hydronautics, 1972	1.79 (2.82)	+1.50 (2.36)	±84	Cargo ship (two failures in class)
FLINDERS BAY	Chirila, Shipping World and Shipbuilder, 1971	1.91 (3.01)	+0.76 (1.12)	±40	Container ship
MICHIGAN	Brewer, J. SESA, 1971	4.68 (7.37)	+2.61 (4.11)	±56	Fast cargo ship (five failures in class)
GOLAR NICHU	Sontvedt et al., RINA Symp, 1973	4.00 (6.30)	+1.40 (2.20)	±3	Ducted propeller
SEIUN MARU	Ueta et al., Mar. Eng. Soc. Japan, 3/74	5.85 (9.21)	+2.76 (4.35)	±46	Training ship
HAKANO MARU	Nakano, Shipbuilding Research Assoc., R.A. Japan No. 172, 1972	3.62 (5.70)	+1.33 (2.09)	±37	Container ship
**	Conolly, Trans. Royal Inst of Naval Architects, 1960			±43	Twin-screw destroyer
USS BARBEY	Noonan, C.J. et al., DTNSRDC 77-0080, 1977	4.8 (7.56)	+1.9 (2.99)	±45*	Single-screw frigate
USS SPRUANCE	Antonides, G.P. DTNSRDC SAD-164E-1962, 1977	4.68 (7.38)	+1.77 (2.79)	±45*	Twin screw destroyer
R/V ATHENA USS OLIVER HAZARD PERRY	Noonan et al., DTNSRDC, 1977,1978; 80/114 (Dec 1980)			±50* ±50*	Twin-screw gunboat Single-screw frigate

*Test results have been modified to exclude centrifugal loads.
**Ship name not given.

Ship	$\dfrac{C_{FPT}}{C_{FPA}}$	$\left(\dfrac{M_{alt}}{M_{mean}}\right)_{FPA}$	$\dfrac{(M_{mean})_{FPT}}{(M_{mean})_{FPA}}$	$\left(\dfrac{M_{alt}}{M_{mean}}\right)_{FPT}$
USS SPRUANCE	0.96	0.45	1.27	0.75
USS OLIVER HAZARD PERRY	0.86	0.50	1.17	0.65
USS BARBEY	0.84	0.45	1.36	0.66

NOTE: The ratios of full-power, full-rudder (FPT) loads and full-power, zero rudder (FPA) loads are available for three ships. C represents centrifugal force and M represents hydrodynamic bending moment.

these loads on a scale model using procedures described in Chapter III of this report. These measurements should be cross-checked with theoretically calculated periodic blade loads based on the wake measured in the plane of the propeller behind the model hull.

More accurate prediction of the peak and periodic blade loads during high speed turns in a calm sea than those obtained in step two can be obtained by conducting model wake surveys in simulated turns. The periodic and peak loads can then be theoretically calculated based on these wake surveys using methods described in Chapter III of this report and Appendix A of this chapter.

More accurate prediction of the increase in peak, transient, and periodic blade loads due to the influence of a rough sea than those obtained in step two can be obtained by direct measurement of these loads on a scale model using procedures described in Chapter III of this report.

More accurate predictions may show that stresses are lower, and that the initial criteria are not exceeded. For example, the method in step two for computing bolt force is empirically based on data for propellers in which one bolt was highly loaded. But use of the two-dimensional finite element (FE) slice method for determining bolt stresses, which is described in Chapter V and in Reference 1,* might show that the distribution of bolt forces is more even.

The full three-dimensional FE analysis of the blade, bolts, blade carrier, and portions of the hub is the most complex of the numerical stress prediction methods, but it is also the most accurate. As described in Reference 1, this method can be combined with two-dimensional FE method to closely examine stresses in fillets such as the crank ring fillet or the bolt head to shank fillet. This three-dimensional method also provides a prediction of the amount of bolt bending which is not possible with the simple analyses of step two nor with the two-dimensional slice method for bolt stresses mentioned above. These simpler methods use an empirical factor of 2.0 to account for bolt bending which may be too large, thereby leading to excessive conservatism.

A structural model experiment might also be appropriate to provide more accurate stress predictions. Reference 2 describes such an experiment.

As indicated earlier, the evaluation of structural adequacy must be judgmental on a case by case basis. The sophisticated blade load and stress prediction methods

---

*A complete listing of references is given on page 475.

addressed under step three would have to be used in the evaluation process for the blade attachment of a new CP propeller for a class of ships with significantly higher horsepower than the SPRUANCE Class. On the other hand, the simpler prediction methods would probably be adequate for a new 10,000 shaft horsepower design provided it was similar to the PERRY, SPRUANCE, or BARBEY designs, and the criteria described earlier were satisfied.

STEP FOUR--MODIFY DESIGN IF NEEDED

Possible design modifications might also be considered if stresses are too high. Bolt forces can be reduced by modifying blade fillet shape. Fatigue stresses in bolts can be reduced by increasing bolt preload. Perhaps a material change in either the bolt or blade carrier would allow more preload or improve fatigue properties. Using rolled threads instead of cut threads in the bolts would reduce the fatigue notch factor. Increasing the fillet radius in the blade carrier would reduce stresses. If such changes are made and the strength criteria are satisfied, the blade bolts and carrier stresses should be acceptable.

Special examination may be necessary in certain high stress areas where the normal criteria are exceeded. For example, it may be claimed that a particular type of bolt has excellent fatigue properties, exceeding those indicated by Equations (7) and (8) in Appendix B. These claims would require corroboration with fatigue test data on actual hardware. References 3 and 4 provide examples of this kind of data for large K-Monel, AISI 4140, and AISI 4340 bolts. The data in Reference 4 were the basis for developing a widely used steel bolt design curve.[5]

As noted earlier, increased confidence in predictions made with the sophisticated blade load and stress analysis methods, might enable a relaxation of the initial strength criteria. For example, if the fatigue criterion is exceeded during high load operations which occur infrequently, it may be possible to demonstrate adequate fatigue strength through application of cumulative fatigue damage rules. Miner's Rule was shown to be applicable in Reference 3 provided that the commonly applied summation factor of 1.0 be replaced with 0.6.

SUMMARY OF STRENGTH ASSESSMENT PROCESS FOR THE
USS SPRUANCE, USS OLIVER HAZARD PERRY, AND
USS TICONDEROGA CLASS PROPELLERS

The approach to the strength assessment process, described previously, is intended to reduce, if not eliminate the need for expensive, large-scale testing in the laboratory and at sea. Such tests were necessary for assessment of the SPRUANCE and PERRY Class propellers, but the analysis methods developed during that process and the lessons learned should provide a suitable basis for determining structural adequacy in future CP propellers of similar design. Lest we forget, the following, largely excerpted from Reference 6, is a summary of those extensive investigations which led to improved propellers on the SPRUANCE, PERRY, and TICONDEROGA.

BACKGROUND

In 1974, while the fatigue life of the blade palm and bolts of the SPRUANCE CP propeller were under investigation at DTNSRDC, the CP propeller on BARBEY experienced two separate occurrences of serious structural failures. The first failure involved blade bolts, the second failure involved improved blade bolts and also crank rings. It was then decided to conduct full-scale tests of an assembled SPRUANCE propeller* at DTNSRDC. Simultaneously, redesigned crank rings with improved blade bolts were installed on BARBEY and instrumented sea trials[7] were conducted during which unacceptably high stresses were recorded in high-speed turns. The BARBEY CP propeller was then replaced with a fixed pitch propeller.

It had become apparent that there was insufficient information available concerning design loads, structural response, and material properties for CP propeller hub components, thereby raising serious fundamental questions concerning the adequacy of the CP propellers then being procured for the SPRUANCE Class, and of those which would be required in future gas turbine propelled ships. The NAVSEASYSCOM, therefore, sponsored a program to determine the adequacy of the CP propellers then under procurement for the SPRUANCE Class (later extended to the PERRY and TICONDEROGA Classes) and an R and D program to improve the technology base in design loads,

---

*Reported informally by R. Rockwell and S. Hersh as Enclosure (1) (Full-Scale Structural Evaluation of the USS SPRUANCE (DD-963) Controllable Pitch Propeller Blade Attachment – Phase 1, Application of Maximum Loads at Design Pitch) to DTNSRDC letter Serial 75-172-129 of 14 July 1976.

strength analysis, and material selection of CP propeller hub components for future procurement. The entire effort, both the R and D portion and the portion which was directed specifically to support the ongoing ship construction projects, made important contributions to the resolution of the SPRUANCE, PERRY, and TICONDEROGA Class CP propeller problems.

STRUCTURAL PROBLEM

The two basic questions in the blade attachment structural problem were: what are the forces imposed by the blades during the variety of ship operating conditions, and how does the extremely complex hub structure respond to the pulsating and multi-bladed forces in a "ship-at-sea" environment? Answers to these questions were required in order to be confident of judgments which could be reached on the basis of any laboratory experiments and analyses.

Blade Forces

When this effort began, the mean component of blade force was known quite well for only calm sea, steady-ahead operations. Until the BARBEY instrumented sea trials, blade forces for destroyer type hulls under other operating conditions could be estimated only poorly--so poorly that they were not considered in the structural design of the blades. Blades were designed structurally to limit stresses under the mean load for steady-ahead, calm sea operation to an arbitrarily but judiciously selected value based on long experience.

The BARBEY trials demonstrated that the blade forces and particularly the fatigue critical alternating components were considerably higher than expected. Because the BARBEY is a single screw ship and the SPRUANCE is a twin screw ship, it was anticipated that the magnitude of the alternating components in SPRUANCE would be larger and would be more difficult to estimate. The high stresses which were being obtained from full-scale laboratory experiments on an assembled SPRUANCE CP propeller hub (and which are discussed in other sections of this report), clearly indicated the need for reliable information on the magnitude of blade forces. Therefore, instrumented trials were conducted on the SPRUANCE. Later, after the failure of a blade bolt in a fatigue test,[8] during which the higher forces estimated for PERRY were applied to the SPRUANCE hub assembly, instrumented sea trials were

442

also conducted on the PERRY, a single screw ship. On both ships, measurements were made during a variety of maneuvers in relatively calm seas. In the SPRUANCE trials, blade forces and the resultant blade bolt and crank ring stresses were inferred from strain measurements on the blades, blade bolts, and crank rings, while in the later PERRY trials, only bolt strains were obtained.

Structural Response

In the two year interval between the BARBEY failures and PERRY sea trials, the previously mentioned series of full-scale laboratory experiments were conducted on a complete propeller hub assembly which was configured first with a single SPRUANCE and then with a single PERRY blade. The hydrodynamic component of blade force was applied at the one blade while the centrifugal component was applied at all five blade ports. It became apparent quickly that the stresses in the blade bolts and crank ring were much higher than those which had been computed by the vendor during their design: the blade attachment was not behaving in the neatly distributed manner which had been assumed. Using the SPRUANCE blade under loads simulating ahead operations, bolt forces above preload were concentrated in Bolt 8, and the crank ring stresses peaked near Bolt 8. In the later tests with the PERRY blade, Bolts 5 and 8 carried approximately equal loads while very little was carried by Bolts 6 and 7, and a similar distribution was obtained in the crank ring. A large bending component which was not considered in the design analyses was found in bolt stresses both at assembly and under load.

Crank Ring Stress. Excessive crank ring stresses were recorded in the first laboratory experiments using the full-scale SPRUANCE blade, and in the SPRUANCE sea trials. The combined mean and alternating crank ring stresses in high-power turns exceeded the desired limit of 50 percent of the endurance limit which is customary for large, heavy-sectioned high strength steel forgings. The excessive stresses were very localized. They were primarily the result of high stress concentrations in the small radius in the fillet and secondarily the result of a poor distribution of forces into the crank ring which was caused by the poor bolt force distribution. The crank ring problem was confirmed in the previously mentioned fatigue test[8] when the crank ring, which had 0.375 in. radius fillet, developed a fatigue crack after about 1 million cycles of high-power turn stresses.

Bolt Stress. In view of the disturbingly high stresses which were being recorded for the bolts, NAVSEASYSCOM accepted the DTNSRDC recommendation* that the vendor be directed to reduce the tolerance in bolt hole angularity, thereby eliminating bolt preload bending as a potential problem for all future production. In addition, the full-scale bolt fatigue tests[3] were undertaken in order to develop reliable information on the fatigue life of bolts of potential interest under the conditions of use in the propellers: (1) bending stress under load, approximately, equal to the average tensile stress above prestress because of bending in both the blade palm and the crank rings, and (2) compressing a bronze flange. Several bolt materials, designs, and fabrication techniques were tested under a range of preloads and at stress levels which spanned the bolt stresses measured in all of the sea trials. The tests also included runs intended to determine a reasonable value for the summation factor to be used in Miner's Rule in estimating the cumulative damage associated with the varying stress levels which would be characteristic of propellers on these ships. The results of these tests were used directly in arriving at the blade bolt life determinations.

DESIGN MODIFICATIONS

It became apparent in surveying the BARBEY and SPRUANCE designs that the crank rings in both propellers were made of steel alloys that had very little fracture toughness and, therefore, were susceptible to brittle fracture. A material with much more fracture toughness was needed as protection against rapid, catastrophic fracture in the presence of material flaws, fatigue cracks, or corrosion pits. Therefore, it was recommended, and accepted, that the crank ring material be changed from AISI 4150H to A471 Class 6, a fracture tough material of equivalent strength. At the same time, several steps were taken to relieve the fillet stresses. One was to increase the fillet radius from 0.375 to 0.50 in. for production of initial PERRY crank rings. This was a sufficient change for PERRY, because the alternating blade forces in high-power turns were determined by measurements at sea to be lower than

---

*Reported informally by J. Sickles as Enclosure (1) (Propeller Blade Bolt Bending as a Result of Bolt Hole Misalignments in the Crank Rings of the USS SPRUANCE (DD-963) Controllable Pitch Propeller) to DTNSRDC letter Serial 75-178-77 of 10 Sep 1975.

the SPRUANCE blade forces and because of the more favorable distribution of bolt forces. An increase in the fillet radius to 0.60 in. was recommended for initial production of TICONDEROGA crank rings and for replacement crank rings for the SPRUANCE.

The first of several design modifications related to blade bolts was made because of high bolt bending stress due to bolt preload alone. The NAVSEASYSCOM accepted the DTNSRDC recommendation that the vendor be directed to reduce the tolerance in bolt hole angularity, thereby eliminating bolt preload bending as a potential problem in future procurements.

The distribution of bolt forces on an operational propeller is influenced strongly by the shape of the blade fillet and palm. This was recognized early in the SPRUANCE blade attachment investigation at DTNSRDC. In experiments using a crude, flat "dummy hub" as a blade support, Bolt 8 nearest the trailing edge of the blade, pressure side, resisted a much larger share of the applied blade forces. The apparent reason was the heavier section of palm at Bolt 8 than at the other bolts. A similar effect was seen in the later experiments and sea trials on both the SPRUANCE and PERRY. The relative thickness of the palm at Bolt 5 and at Bolt 8 is reversed on the PERRY compared to the SPRUANCE, and these bolts carried nearly equal shares of the forces.

That more favorable distribution of bolt forces and the smaller alternating component of the measured blade forces in high-speed turns on the PERRY than on the SPRUANCE enabled the PERRY bolt problem to be resolved by a shift from AISI 4140 steel bolts with cut threads to K-Monel bolts with rolled threads and fillets and increased head to shank fillet radii. The series of full-scale bolt fatigue tests[3] had demonstrated the inadequacy of the original AISI 4140 steel bolts as well as the improved fatigue life of the replacement K-Monel bolts. By itself, however, this change would not have been adequate for the SPRUANCE and TICONDEROGA Classes.

Therefore, a series of 1/3-scale model experiments[2] was conducted in which the effects on bolt stresses due to changes in blade fillet geometry and in the modulus of elasticity of the coverplate between the crank ring and the blade palm were evaluated. The strong influence of fillet geometry was demonstrated in these experiments and a new fillet geometry for SPRUANCE and TICONDEROGA blades was

developed to more nearly equalize the forces in the bolts. The beneficial effect of increasing the modulus of the coverplate material was also demonstrated by comparative tests using nickel-aluminum (Ni-Al) bronze (the standard material), a steel plug insert in the bronze around the bolt hole, and a steel coverplate. The experimental results were confirmed by analytical investigations.[1] Then, full-scale verification experiments[9] were conducted in the laboratory on the SPRUANCE propeller using a blade with the proposed fillet, the standard coverplate, and an Inconel 625 coverplate. Inconel 625 was used in place of steel because it is noncorrosive and yet has the same high elastic modulus. The laboratory data were modified to allow for the differences between the laboratory and at sea data, which had been observed in the earlier experiments using the original components. The major improvement in fatigue life, which resulted from the changes, led to acceptance of the recommended changes in blade fillet geometry for initial production of blades for the TICONDEROGA Class and for backfit on the SPRUANCE Class. Inconel 625 plug inserts in the bronze coverplates were substituted for Inconel coverplates because they would be nearly as effective and much less expensive.

APPENDIX A

METHODS OF PREDICTING BLADE LOADS

This appendix summarizes the available techniques for predicting blade loads under various operating conditions using, in part, the results and procedures developed under the R and D program on CP propellers as discussed in Chapter III. As discussed in Chapter III, the blade loading transmitted to the hub can be represented as three force components and three moment components along a set of orthogonal axes. The coordinate systems shown in Figure A.1 are used in the present

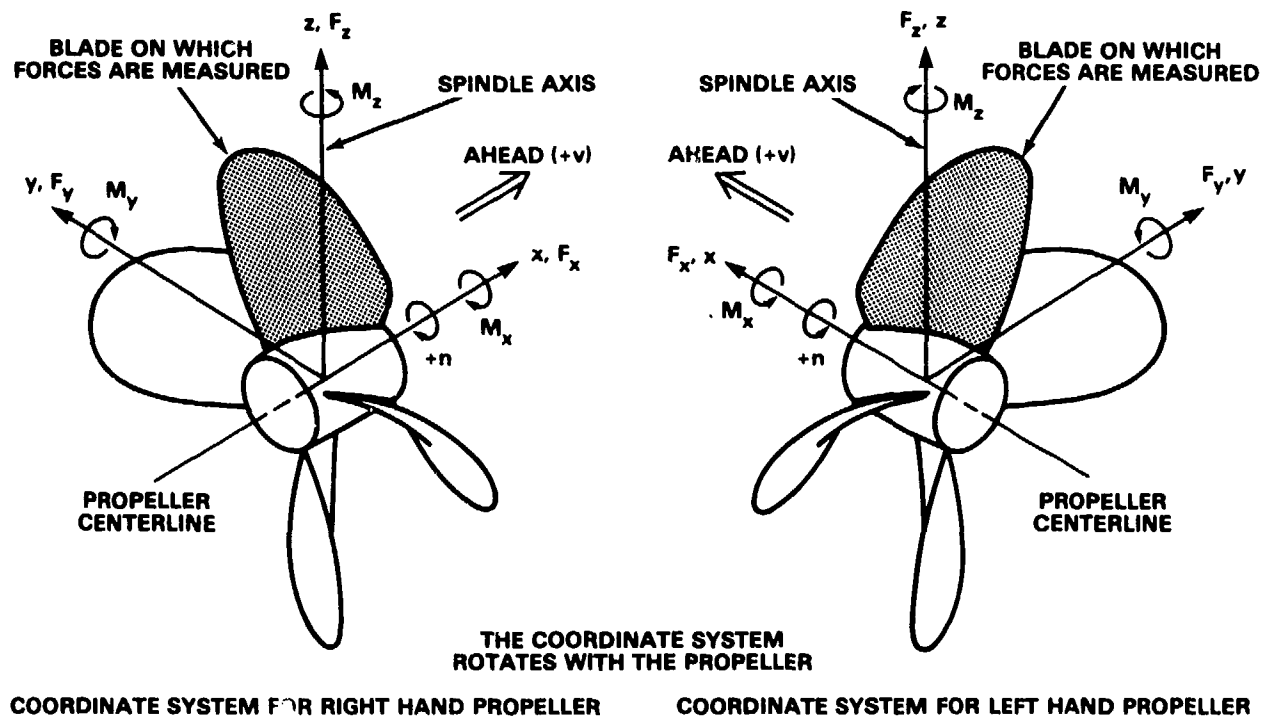**COORDINATE SYSTEM FOR RIGHT HAND PROPELLER** **COORDINATE SYSTEM FOR LEFT HAND PROPELLER**

Figure A.1 – Components of Blade Loading

report. The F_x, M_y, F_y, and M_x components (see Figure A.1) can also be resolved into the magnitude and direction of a force and bending moment about some reference radius such as the average radius of the crank ring. For hydrodynamic loads, the

447

directions of these force and moment vectors are, approximately, perpendicular and parallel, respectively, to the blade pitch line at the 70 percent radius for all operating conditions except crashback maneuvers. The spindle torque M_z, is in general, substantially less than the bending moments M_x and M_y. Spindle torque M_z is important from considerations of controlling the blade pitch, and may, depending upon the blade skew, significantly contribute to high stresses in various components of the hub mechanism. The role of skew in minimizing M_z is discussed in the section on Guidelines for Minimizing Blade Loads.

CENTRIFUGAL AND GRAVITATIONAL LOADS

The centrifugal loading, which is a function only of the blade geometry, blade density, and propeller rotational speed, has only time average and transient components and can be readily calculated. This is generally calculated during the propeller blade design process, when the propeller blade is structurally analyzed by finite element methods.

Centrifugal loading can be represented as a concentrated radial force through the blade centroid, and transmits primarily an $F_{z,c}$* component to the hub; see Figure A.1. However, depending upon the blade rake and skew, centrifugal loads can also produce substantial bending moment components $M_{y,c}$ and $M_{x,c}$. The propeller blade designer has essentially no control over the value of $F_{z,c}$ after the prelimi- nary design stage in which propeller diameter and rpm are fixed; however, the designer can control $M_{y,c}$, and to a lesser extent $M_{x,c}$, by the proper selection of blade rake and skew. It is desirable to minimize the total (hydrodynamic plus centrifugal) values of loading components, and the hydrodynamic portion $M_{y,H}$* is inherently positive (see Figure A.1 for sign convention) and is the largest moment component for all operating conditions except deceleration and backing. Therefore, it is desirable to have $M_{y,c}$ negative, which can be achieved by placing the blade centroid forward of the spindle axis. This requires negative rake or skew.

Requirements to minimize propeller-induced vibratory forces and spindle torque under steady-ahead operation dictate a balanced skew with forward skew at the inner radii and aft skew at the outer radii. This inherently places the blade centroid near the spindle axis for an unraked blade so that $M_{y,c}$ and $M_{x,c}$ are small. Blade

---

*The subscript c denotes centrifugal loads; H denotes hydrodynamic loads.

rake has no influence on $M_{x,c}$, but $M_{y,c}$ varies directly with rake for all other parameters held constant. Therefore, it is desirable to apply as much forward (negative) rake as practical from considerations of clearances, design theory, and total blade geometry. In summary, balanced skew and forward rake are recommended from considerations of centrifugal blade loads.

The gravitational loading, which is a function only of the blade geometry and blade density, occurs primarily as a first harmonic of blade angular position and can be readily calculated.

The gravitational loads can be represented as a constant downward force (the weight of the blade in water) applied at the centroid of the blade. The magnitude and point of application of the blade weight are generally calculated during the propeller design process. The blade weight is generally an order of magnitude less than the time-average thrust under full-power steady-ahead operation. The blade weight has a constant F_x component, $F_{x,g}$,* and a first harmonic component of F_y, F_z, M_x, M_y, and M_z relative to a coordinate system rotating with the propeller blade. Force component $\overline{F}_{x,g}$** is negligible relative to $\overline{F}_{x,H}$ for realistic shaft inclination angles. The amplitudes of $(M_y)_{1,g}$*** and $(M_z)_{1,g}$, which are essentially the product of the weight of the blade and the x coordinate of the blade centroid relative to the spindle axis, are negligible relative to the respective hydrodynamic components. The amplitude of $(F_z)_{1,g}$ is essentially the weight of the blade which is, in general, less than three percent of $\overline{F}_z$ which is essentially the centrifugal force on the blade. Therefore, $(F_z)_{1,g}$ can be neglected. Components $(F_y)_{1,g}$ and $(M_x)_{1,g}$ are, in general, approximately 180 degrees out of phase with and smaller than the respective components of hydrodynamic loading for wakes behind high-speed transom sterns with exposed struts and shafting, i.e., for wakes of the type encountered on surface combatants. On the SPRUANCE and R/V ATHENA these components of centrifugal loading reduced the maximum bending moment about the hub by less than 7 percent of the hydrodynamic moment for steady-ahead operation. Therefore, the neglect of these components results in a slightly conservative prediction of the maximum periodic

---

*The subscript g denotes gravitational loads.

**The superscript – denotes time-average loads.

***The notation $(\ )_1$ denotes the first harmonic of $(\ )$.

blade bending moment. In summary, the gravitational loads may be completely neglected without a significant loss in accuracy of the predicted total loads.

HYDRODYNAMIC LOADS

In this section, the use of available techniques, for determining hydrodynamic loads as they are applicable to CP propeller design, and their associated accuracies and costs, is discussed. The available techniques which were developed under the R and D program on CP propellers were discussed earlier in this chapter. The estimated accuracies and costs are summarized in Table A.1.

The blade loading transmitted to the palm is represented as the three force components and three moment components shown in Figure A.1. For the radial force component F_z, the hydrodynamic loads are relatively unimportant because essentially all of the time average and transient portions of F_z arise from centrifugal force, and most of the periodic portion of F_z which is quite small, arises from gravitational loads.

Steady-Ahead in a Calm Sea

Time-Average Loads. Time-average loads under steady-ahead operation in a calm sea can be predicted to a high accuracy by any one of several methods. These methods include: (1) routine model powering experiments, (2) propeller design calculations, (3) propeller inverse theory, and (4) a combination of these methods.

1. Routine model powering experiments. Routine model powering experiments yield predictions of time-average thrust and torque over the speed range. Blade bending moments about any desired radius equal to or less than the radius of the blade palm can be calculated from these measured quantities by assuming a radial point of application of thrust $\bar{F}_x$ and transverse force $\bar{F}_y$. An estimate of the radial points of application of these force components can be obtained from propeller design or analysis calculations, or, if these are unavailable, it is reasonable to assume that these force components are applied at the 0.7 radius. The true radial centers of these force components are generally within ± 2 percent of the 0.7R; therefore,

TABLE A.1 – SUMMARY OF DESIGN TOOLS AND ESTIMATED ACCURACY AND
COST FOR PREDICTING PROPELLER BLADE LOADS

	Time-Average and Transient Loads	Accuracy ± Percent [1]	Estimated Cost [2] ($k)	Periodic Loads [3]	Accuracy ± Percent [1]	Estimated Cost [2] ($k)
Steady-ahead in a calm sea	Design calculations	5	2	Model blade loading experiments	15	100
	Model powering experiments	8	2	Theory plus empirical factor	20	10
	Theory	10	5	Statistical data	30	3
Acceleration and deceleration in a calm sea	Computer simulation[4]	15	150	Theory plus empirical factor	25	10
	Statistical data	40	10	Statistical data	40	5
Turning maneuvers in a calm sea	Computer simulation[4]	20	150	Theory plus empirical factor with model wake survey in turn	30	30
	Statistical data	40	10	with estimated wake in turn	40	10
				Statistical data with model wake survey in turn	45	25
				with estimated wake in turn	60	5
Steady-ahead in rough water	Model experiments in rough water[5]	15	40	Semi-empirical theory[4,7]	30	5
	Statistical data[5]	25	5			
	Semi-empirical theory[4,6]	20	5			

All accuracies are ± "true" value in percent.

[1] Accuracies shown apply to the F_x, M_y, F_y, and M_x component, the deviations from "true" values for M_z are approximately twice the values shown.

[2] All estimated costs are rough approximations for conducting the work in FY 1980. It is assumed that the usual information for designing the propeller and evaluating the hull and propeller, without regard to blade loads, is available. This includes model hull and propellers, model resistance, propulsion, maneuvering, and seakeeping experiments, and steady-ahead wake surveys. The cost of special experiments, useful primarily for predicting blade loads, are included in the estimates quoted. Actual costs may vary substantially.

[3] Assumes that the most accurate method listed was used to predict time-average or transient loads.

[4] Requires same supporting model experiments.

[5] Time-average values.

[6] Transient values.

[7] Assumes that the most accurate method listed was used to predict periodic loads in calm sea.

451

errors resulting from assuming that these radial centers are locat.. at 0.7R can result in an error of ±5 percent in the moment arms at the crank ring (at approximately 0.25R). These experiments predict thrust and torque to within approximately ±3 percent, and blade bending moments at the crank ring to within approximately ±8 percent. These experiments yield no information on spindle torque M_z. The estimated cost of these predictions is approximately $2000.*

2. **Propeller design calculations.** The distribution of hydrodynamic loads over the blade at the design condition** is specified during the process of designing the propeller blades. This yields the F_x, F_y, M_x, and M_y components to an accuracy of approximately ±5 percent and the M_z component to an accuracy of approximately ±10 percent at an estimated cost of approximately $1000. The predicted spacial distributions of loading are applicable only at the design advance coefficient J; however, the radial distributions of these loads are insensitive to J over the range of J encountered by a surface combatant under steady-ahead operation in a calm sea. Therefore, the blade bending moments over the speed range can be readily calculated using the radial centers of thrust and transverse force from the design calculations, and the thrust and torque as a function of speed from routine model powering experiments, as discussed in the preceding paragraph. The estimated cost of these predictions is approximately $2000.

3. **Propeller inverse theory.** The distribution of time-average hydrodynamic loads over a propeller blade can be calculated by propeller lifting-surface theory[10] for given propeller geometry, radial distribution of inflow, and operating conditions. This yields the F_x, F_y, M_x, and M_y components to an accuracy of approximately ±10

---

*All estimated costs are rough approximations for conducting the work in FY-1980. It is assumed that the usual information for designing the propeller and evaluating the hull and propeller, without regard to blade loads, is available. This includes model hull and propellers, model resistance, propulsion maneuvering, seakeeping experiments, and steady-ahead wake surveys. The cost of special experiments useful primarily for predicting blade loads are included in the estimates quoted. Actual costs may vary substantially.

**The design condition is defined as the steady-ahead condition in calm water at which the detailed design of the propeller blades is conducted. This condition generally corresponds to a specified speed or delivered power, and a specified propeller rotational speed.

percent and the M_z component to an accuracy of approximately ±20 percent at an estimated cost of approximately \$3000. The primary use of this method is for applications in which the design calculations are unavailable or unsuitable, such as off-design conditions. The predicted radial centers of F_x and F_y from this method can also be used with the thrust and torque predicted from routine powering experiments to more accurately calculate the blade bending moments, as discussed previously. The estimated cost of these predictions is approximately \$5000.

Periodic Loads. Periodic blade loads under steady-ahead operation in a calm sea can be predicted by one of several methods. These methods include: (1) model blade loading experiments on the propeller-hull configuration under consideration, (2) analytical calculations on the propeller-hull configuration under consideration plus an appropriate empirical factor, and (3) estimates from the existing statistical database of model and full-scale blade loading experiments.

1. Model experiments. The most accurate, but also the most expensive and time consuming, method of predicting periodic blade loads on a new propeller-hull configuration is to measure the six components of blade loading on a model of the propeller-hull configuration under consideration using the experimental techniques developed under the R and D program on CP propellers. This yields the periodic portions of F_x, F_y, M_x, and M_y components to an accuracy of approximately ±15 percent of their true values, and the periodic portion of M_z to an accuracy of approximately ±30 percent of its true value, at an estimated cost of approximately \$100,000.

2. Analytical calculations. The periodic blade loads can also be analytically calculated using the method of Kerwin[11] together with an empirical factor derived from extensive correlations between this method and experimental data obtained under the R and D program on CP propellers. A wake survey conducted behind the model hull is a necessary input to this calculation. This method yields $\tilde{F}_x$, $\tilde{F}_y$, $\tilde{M}_x$, and $\tilde{M}_y$* to an accuracy of approximately ±20 percent of their true values, and $\tilde{M}_z$ to an accuracy of approximately ±40 percent of its true value, at an estimated cost of approximately \$10,000. This method is substantially cheaper and quicker, but somewhat less accurate, than measuring the periodic blade loads behind the model hull.

---

*The superscript $\tilde{}$ denotes the periodic portion of loads.

453

3. _Statistical data._ The periodic blade loads on a new propeller-hull config-
uration can also be estimated directly from the existing statistical database of
model and full-scale measurements of periodic blade loads. This method is substan-
tially cheaper, quicker, but less accurate than either model experiments or analyti-
cal calculations. The accuracy of estimates using this procedure depends upon the
degree of similarity between the new configuration including propeller geometry,
wake, and operating conditions and the configurations in the database, and upon the
physical insight of the person making the estimates. For a new configuration which
is somewhat similar to the configurations in the database, a person with reasonable
insight into the problem could probably estimate F_x, F_y, M_x, and M_y to an accuracy
of approximately ±30 percent of their true values, and M_z to an accuracy of ±60
percent of its true value, at an estimated cost of approximately \$3000.

For a new propeller-hull configuration, which is significantly different from
an existing configuration, it is recommended that blade loads be predicted by both
model measurements of the six components of blade loading and by the unsteady lifting
surface theoretical method of Kerwin[12] supplemented by the appropriate empirical
factor. This provides two independent predictions that can be cross-checked. These
predictions should be further checked by comparison with the existing statistical
database.

Maneuvers
Transient Loads

1. _Computer dynamic simulation._ Transient loads during maneuvers, including
acceleration, deceleration, and various types of turning maneuvers, depend strongly
upon the instantaneous values of ship speed, propeller rotational speed, propeller
pitch, and propeller-hull interaction coefficients. The transient loads, or time-
average loads per revolution, appear to be insensitive to the time rate of change
of the aforementioned variables, based on limited experimental data and physical
arguments. Therefore, if the time histories of the aforementioned variables through
a maneuver are known, then the time-average loads can be estimated from routine
propeller model thrust and torque characteristics in uniform flow (propeller open
water characteristics) and propeller inverse lifting-surface theory[13] as described
in the preceding section for steady-ahead operation.

The time histories of ship speed, propeller rotational speed, propeller pitch, and propeller-hull interaction coefficients during a specific maneuver depend, in a complex manner, upon interactions between the characteristics of the propeller, hull, prime mover, and control system. For a new ship design the best method of predicting the time histories of the aforementioned variables is a computer dynamic simulation of the complete propulsion system and ship response, such as those described in References 14 through 18. These dynamic simulations require accurate knowledge of the individual characteristics of the propeller, hull, propeller-hull interaction, prime mover, and control system.

The individual characteristics of the propeller, hull, and propeller-hull interactions over the pertinent range of conditions likely to be encountered during maneuvers, must be obtained from systematic model experiments on the propeller and hull under consideration. These experiments include open-water characterization of the propeller and associated blade spindle torque measurements over a range of conditions including ahead and astern velocities, each over a range of positive and negative pitches, determining the pertinent maneuvering coefficients of the hull, and determining the propeller-hull interaction coefficients over the pertinent range of conditions likely to be encountered during maneuvers.

The accurate determination of the propeller-hull interaction coefficients over the pertinent range of conditions is probably the most difficult and weakest part of the simulation. There exist very few reliable measurements of these interaction coefficients under conditions likely to be encountered during maneuvers. These interaction coefficients are inherently difficult to determine accurately, and they are very sensitive to small changes in many parameters so that it is difficult to interpolate or extrapolate them, as is necessary in the dynamic simulation process, without further loss of accuracy. This is a particularly difficult problem for turning maneuvers due to the large number of pertinent parameters in turns. In addition to those listed previously, these include roll, drift angle, rudder angle, unbalances between the two propellers for twin-screw ships, and complex interactions between the various parameters.

Another problem in simulating turning maneuvers is that the path and orientation of the hull, which have a very significant influence on the loads, must be predicted. These can be predicted using four-degrees-of-freedom maneuvering simulation programs

455

for the hull which use the pertinent maneuvering coefficients of the hull, as determined from model experiments. Usually, four-degrees-of-freedom programs are designed to predict ship motion characteristics for constant power maneuvers with no regard to propeller thrust and torque.[19,20] Recently Carroll and Harper[21] modified the ship motion equations in the four-degrees-of-freedom simulation to include propeller thrust and torque as a function of propeller rotational speed, ship velocity, and ship orientation. With this refinement, the influence of the path and orientation of the hull can be incorporated into the dynamic simulation of the system including the propeller, hull, propeller-hull interaction, prime mover, and control system.

The use of computer dynamic simulations, supported by the necessary model experiments on the propeller and hull under consideration, yields predictions of the maximum transient values of the F_x, F_y, M_x, and M_y components of blade loading to an accuracy of approximately ± 15 percent for acceleration and deceleration maneuvers, and to an accuracy of approximately ± 20 percent for turning maneuvers, at an estimated cost of approximately \$150,000. The deviations from the true values for M_z are approximately twice the percentages for the other components. If the computer dynamic simulations use propeller, hull, or propeller-hull interaction coefficients approximated from hulls or propellers that are different from the final configuration, then the inaccuracies in predicting the blade loads become somewhat greater.

2. <u>Statistical data</u>. The transient blade loads on a new propeller-hull control system configuration can also be estimated directly from the existing statistical database of full-scale measurements and computer dynamic simulations on previous ships. The method is substantially cheaper, quicker, but less accurate then the use of computer dynamic simulations, supported by the necessary model experiments, on the control system, hull, and propeller under consideration. The accuracy of estimates using this procedure depends upon the degree of similarity between the new configuration including propulsion control system, stern geometry, propeller geometry, and types of maneuvers and the configurations in the database, and upon the physical insight of the person making the estimates. For a new configuration, which is somewhat similar to the configurations in the database, a person with reasonable insight to the problem could probably estimate the maximum values of F_x, F_y, M_x, and M_y to an accuracy of approximately ± 40 percent of their true values, and the maximum

value of M_z to an accuracy of ±100 percent of its true value for acceleration, deceleration, and turning maneuvers, at an estimated cost of approximately $10,000. For a new configuration, which is significantly different from an existing configuration, the inaccuracies in predicting transient blade loads from the statistical database become somewhat greater.

Periodic Loads

1. _Analytical calculations_. The periodic loads during maneuvers, including acceleration, deceleration, and various types of turning maneuvers, depend upon the same parameters as discussed in the preceding paragraphs for transient loads, except that the dependence upon the propeller-hull interaction coefficients may not be as strong. However, unlike the transient loads, the periodic loads depend critically upon the spacial distribution of the wake velocity components in the propeller at a given time in a maneuver. Therefore, two basic inputs are required for predicting periodic blade loads in a maneuver:

(a) A time-history of the maneuver that may be estimated as described in the preceding paragraphs, and

(b) An estimate of the wake velocity components in the propeller plane at a given time in the maneuver.

For acceleration and deceleration maneuvers, the nondimensional wake velocity components for ahead speed $V > 0$ is approximately the same as it is for steady-ahead operation.[22,23] For astern speed $V < 0$, the periodic loads are, in general, small due to the relatively low magnitudes of V and rotational speed n under these conditions, so that it is not usually necessary to accurately estimate the wake velocity components. If desirable, model wake surveys can be conducted under astern operation simulated in a quasi-steady manner, i.e., $V < 0$, $\dot{V} = 0$.

For turning maneuvers, the circumferential variation of the wake velocity components in the propeller becomes more severe than it is for steady-ahead operation due to the large drift angle; i.e., the angle between the local undistributed direction of motion and the hull centerline. This drift angle is, in principle, equivalent to the inclination angle of the flow relative to the propeller shaft for steady-ahead operation, except that it occurs in the horizontal plane. Therefore, this drift angle produces a large first harmonic tangential wake, and thereby produces large first harmonic periodic loads.

457

Wake surveys conducted on models of the SPRUANCE and BARBEY[24] during simulated steady turns showed that the circumferential variation of the wake is dominated by the drift angle at the propeller plane. Further, these wake surveys indicated that the peak to peak circumferential variation of the velocity components of the wake of a high-speed transom stern configuration, with exposed shafting and struts in a turning maneuver, can be estimated within approximately ± 20 percent from the known wake velocity components under steady-ahead operation, the drift angle at the propeller plane, and the location of the propeller in the turn; i.e., inboard, outboard, or centerline.

Alternatively, a more accurate estimate of the wake velocity components can be obtained from a model wake survey conducted on a model of the hull of interest at the conditions existing at a given time in the maneuver simulated in a quasi-steady manner; i.e., constant values of ship speed, drift angle, turning radius, roll, etc. This model wake survey would be run for conditions at which nearly maximum values of periodic loads are predicted based on more approximate wake velocity components. The estimated cost of conducting a model wake survey in turns is approximately $20,000.

Once the time-history of the maneuver including the wake velocity components is estimated, the periodic loads at any time during the maneuver can be calculated using the same procedures as for steady-ahead operation as described in the preceding subsection "Steady-Ahead in a Calm Sea" of this section of Appendix A. For preliminary estimates to determine at what conditions the largest peak and periodic loads occur, the periodic loads can be estimated from the calculated or measured periodic loads under steady-ahead operation, adjusted for operating conditions and wake patterns using trends of the data presented in References 10, 22, and 25 through 30 as a guide.

If the time-history of the maneuver is predicted by the best available methods, as discussed in the preceding section, then the maximum values of the $\tilde{F}_x$, $\tilde{F}_y$, $\tilde{M}_x$, and $\tilde{M}_y$ components during acceleration and deceleration maneuvers can be predicted by theoretical calculations[12] plus an empirical factor to an accuracy of approximately ± 25 percent at an estimated cost of approximately $10,000. Similarly, the maximum values of the $\tilde{F}_x$, $\tilde{F}_y$, $\tilde{M}_x$, and $\tilde{M}_y$ components during turning maneuvers can be calculated to an accuracy of approximately ± 30 percent if model wake surveys during simulated turns are conducted, and to an accuracy of approximately ± 40 percent if the wake patterns during the turns are approximated from the drift angle and the

458

wake data during steady-ahead operation or the statistical wake data in the literature. The estimated cost is approximately $30,000 if a model wake survey in turns is conducted, and $10,000 if no such wake survey is conducted. The deviations from the true values for the M_z component are approximately twice the percentages for the other components.

2. Statistical data. The periodic blade loads on a new propeller-hull configuration can also be estimated directly from the existing statistical database of model and full-scale measurements and theoretical calculations of periodic blade loads. This method is somewhat cheaper but less accurate than analytical calculations. The accuracy of estimates using this procedure depends upon the degree of similarity between the new configuration including propeller geometry, wake, and operating conditions and the configurations in the database and upon the physical insight of the person making the estimates. If the time-history of the maneuver is predicted by the best available methods, as discussed in the preceding section, then, for a new configuration that is somewhat similar to the configurations in the database a person with reasonable insight into the problem could probably estimate the maximum values of F_x, F_y, M_x, and M_y to an accuracy of ± 40 percent of their true values for acceleration and deceleration maneuvers, to an accuracy of ± 45 percent for turning maneuvers using measured wakes on the configuration under consideration in simulated turns, and to an accuracy of ± 60 percent for turning maneuvers using estimated wakes in turns. The deviations from the true values for the M_z component are approximately twice the percentages for the other components. The estimated cost of predicting these periodic loads in maneuvers based on the statistical data is approximately $5000.

Influence of Rough Seas

When a ship operates in rough seas, the ship speed and propeller rotational speed at a given delivered power decrease from the corresponding values in calm water due to increased resistance of the hull and change in the propulsion coefficients (involuntary speed loss).[31-33] Furthermore, in rough seas the delivered power is often reduced from the calm water value (voluntary speed loss).[32,34] Therefore, the difference in blade loads between operation in calm seas and operation in rough seas can be represented as being made up of two major parts:

1. Differences in loads resulting from the difference in ship speed and propeller rotational speed between calm seas and rough seas, and

2. Increases in loads due to the direct influence of waves and ship motions at a given value of ship speed and propeller rotational speed.

Time-Average Loads. The changes in the time-average* propeller rotational speed, speed of advance, thrust, and torque at a given delivered power due to operation in rough seas can be estimated experimentally or theoretically using methods or data summarized by Oosterveld,[32] Day et al.,[33] and Lloyd and Andrew.[34] The most accurate approach is to conduct model experiments on the propeller-hull configuration of interest using the experimental procedures summarized by Day et al.[33]

For a given operating condition and time-average thrust and torque, the time-average values of the various components of blade loading can be calculated using the pertinent procedures as described previously for steady-ahead operation in a calm sea.

Using these procedures based on a model experiment on the propeller-hull configuration of interest, the F_x, F_y, M_x, and M_y components can be calculated to an accuracy of ± 30 percent at a cost of approximately \$40,000 including the model experiment.

Alternatively, using these procedures, based on statistical data, the F_x, F_y, M_x, and M_y components can be calculated to an accuracy of ± 25 percent, and the M_z component to an accuracy of ± 50 percent at a cost of approximately \$5000.

Transient and Periodic Loads. For given time-average ship speed and propeller rotational speed, the increase in transient and periodic loads** due to the influence of waves and ship motions can be estimated from the experimental data obtained under the R and D program on CP propellers as discussed previously. It is reasonable to disregard any transient variation in ship speed and propeller rotational speed n.

---

*Time-average quantities are defined here as quantities averaged over a length of time that is much greater than the period of any significant component of the wave or ship motion of interest.

**Transient portion of quantities is defined here as the variations of time-average values per propeller revolution with local sea conditions and ship motions, and the periodic portion is defined as the variation with blade angular position.

In practice, there is a small transient variation in V and n, the variation in n for a gas turbine propulsion system being dependent upon the propulsion control system.

As discussed previously, the increase in transient loads is controlled primarily by the axial component of the orbital wave velocity at the propeller, and the increase in the periodic loads is controlled primarily by the vertical component of the orbital wave velocity at the propeller, as modified by the presence of the hull, and by the vertical velocity of the propeller due to ship motions.

For a given sea spectrum, the orbital wave velocities can be calculated directly from orbital wave theory.[35,36] McCarthy et al.[35] gives equations for averaging the orbital wave velocities over the propeller disk. However, this refinement is not justified in light of the various approximations that are required for predicting loads in a rough sea. Therefore, it is recommended that the orbital wave velocities be calculated at the depth of the propeller centerline.

The vertical velocity of the propeller due to ship motions depends upon the sea spectrum and the response of the hull in the pitch, heave, and roll modes. The response of the hull is best predicted by seakeeping experiments on a model of the hull under consideration. These experiments give information on the amplitudes and phases of the various components of hull response as functions of the lengths and orientations of the various wave components.

Therefore, the maximum transient loads in a rough sea $\bar{L}_{max,\zeta,\psi}$* for ships with high-speed transom sterns and exposed shafts and struts may be calculated as follows:

1. Calculate the minimum axial velocity at the shaft centerline from orbital wave theory for the assumed or specified sea spectrum, $V_A + V_{\zeta A,min}$ where V_A is the time-average axial velocity of advance derived from a thrust identity from the predicted powering performance in the rough sea and $V_{\zeta A,min}$ is the minimum axial velocity due to the waves ($V_{\zeta A,min}$ is negative so that $V_A + V_{\zeta A,min} < V_A$).

2. Calculate the maximum transient loads $\bar{L}_{max,\zeta,\psi}$ from quasi-steady theory[37] based on $V_A + V_{\zeta A,min}$ and the time-average n that is predicted in the rough sea.

The maximum periodic loads in a rough sea $\hat{L}_{max,\zeta,\psi}$ for ships with high-speed transom sterns and exposed shafts and struts may be calculated as follows:

1. Calculate the periodic blade $\hat{L}$ that would occur if the ship were operating in a calm sea at the values of V and n that are predicted to occur in a rough sea.

---

*The subscript ζ denotes the direct influence of the waves, and the subscript ψ denotes the influence of ship motions.

This may be estimated from the values calculated for steady-ahead operation in a calm sea, with adjustment for the differences in V and n between operation in a calm sea and in a rough sea, using the trends of the data in Reference 30.

2. Calculate the maximum upward orbital wave velocity component V_ζ at the shaft centerline from orbital wave theory in the absence of the hull for the assumed or specified sea spectrum.

3. Calculate the maximum increase in periodic blade loads due to wave velocities from the corresponding loads that would occur if the ship were operating in calm water without ship motions at the same V and n as follows:

$$\Delta \tilde{L}_{max,\zeta} = \frac{0.5 \, V_\zeta}{(V_{t0.7})_1} \tilde{L}$$

where $\Delta \tilde{L}_{max,\zeta}$ = maximum increase in periodic loads with waves over the values in calm water at the values of V and n that occur in a rough sea

$\tilde{L}$ = periodic blade loads in calm water at the values of V and n that occur in a rough sea

V_ζ = maximum vertical component of the orbital wave velocity in the propeller plane neglecting the influence of the hull

$(V_{t0.7})_1$ = first harmonic of the tangential wake at the 0.7 radius in calm water at the values of V and n that occur in a rough sea.

The 0.5 is an empirical factor to account for the influence of the hull boundary in reducing the upward orbital velocity to below its calculated value in the absence of the hull.

4. Calculate the maximum downward vertical velocity of the propeller from the pitch, heave, and roll modes of ship motions for operation in the assumed or specified sea spectrum.

5. Calculate the maximum increase in periodic blade loads due to ship motions from the corresponding loads that would occur if the ship were operating in calm water without ship motions at the same V and n as follows:

$$\Delta \tilde{L}_{max,\psi} = \frac{0.6 \, V_\psi}{(V_{t0.7})_1} \tilde{L}$$

where $\Delta\tilde{L}_{max,\psi}$ = maximum increase in periodic loads with ship motions over the values in calm water without ship motions at the values of V and n that occur in a rough sea

$\tilde{L}$ = periodic blade loads in calm water without ship motions, at the values of V and n that occur in a rough sea

V_ψ = maximum vertical velocity of the propeller due to ship motions

$(V_{t0.7})_1$ = first harmonic of the tangential wake at the 0.7 radius in calm water without ship motions at the values of V and n that occur in a rough sea.

The 0.6 is an empirical factor to account for the displacement effect of the hull above the propeller. This displacement effect induces a velocity at the propeller so that the velocity of the propeller relative to the local fluid particles is only 60 percent or less of the vertical velocity of the propeller.

6. Calculate the maximum periodic blade loads assuming that the increase in periodic loads due to wave velocities and due to ship motions occur simultaneously and, therefore, add in phase:

$$\tilde{L}_{max,\zeta,\psi} = \tilde{L} + \Delta\tilde{L}_{max,\zeta} + \Delta\tilde{L}_{max,\psi}$$

The assumption that these two increases add directly in phase is justified by results from the R and D program on CP propellers as discussed previously, and any error in this assumption is conservative.

The maximum value of the peak loads, including both transient and periodic contributions, may then be calculated assuming that the maximum values of the periodic loads and transient loads occur simultaneously and, therefore, add in phase as:

$$L_{peak,\zeta,\psi} = \overline{L}_{max,\zeta,\psi} + \tilde{L}_{max,\zeta,\psi}$$

The assumption that these two values add directly in phase is justified by the results from the R and D program on CP propellers as discussed previously, and any error in this assumption is conservative.

463

If ship motions and time-average conditions and loads in a rough sea are predicted, based on experiments on a model of the hull and propeller under consideration, and if loads under steady-ahead motion in a calm sea are predicted by the best available methods, then the maximum values of $\overline{F}_x$, $\overline{F}_y$, $\overline{M}_x$, and $\overline{M}_y$ due to operation in a rough sea can be predicted to an accuracy of approximately ± 20 percent using the procedures described here. Similarly, the maximum values of $\tilde{F}_x$, $\tilde{F}_y$, $\tilde{M}_x$, and $\tilde{M}_y$ can be predicted to an accuracy of ± 30 percent, and the maximum values of $\overline{F}_x + \tilde{F}_x$, $\overline{F}_y + \tilde{F}_y$, $\overline{M}_x + \tilde{M}_x$, and $\overline{M}_y + \tilde{M}_y$ can be predicted to an accuracy of ± 25 percent. The deviations from the true values for the M_z components are approximately twice the percentages for the other components. If ship motions or time-average conditions and loads in a rough sea are estimated from hulls or propellers that are different from the final configuration, then the inaccuracies in predicting transient and periodic blade loads in a rough sea become somewhat greater. The estimated cost of calculating the influence of a rough sea on blade loads is approximately $5000.

APPENDIX B

COMPARISON METHOD FOR BLADE BOLTS AND CLOSED FORM STRESS
ANALYSIS METHODS FOR BLADE BOLTS AND BLADE CARRIER

SIMPLE COMPARISON METHOD FOR BLADE BOLTS

The simple comparison method for blade bolts is very inexpensive. In this method, comparisons are made of blade attachments with blade bolts which have had either successful or unsuccessful operating experience. Bolt forces are calculated based on several simplifying assumptions shown schematically in Figure B.1. The
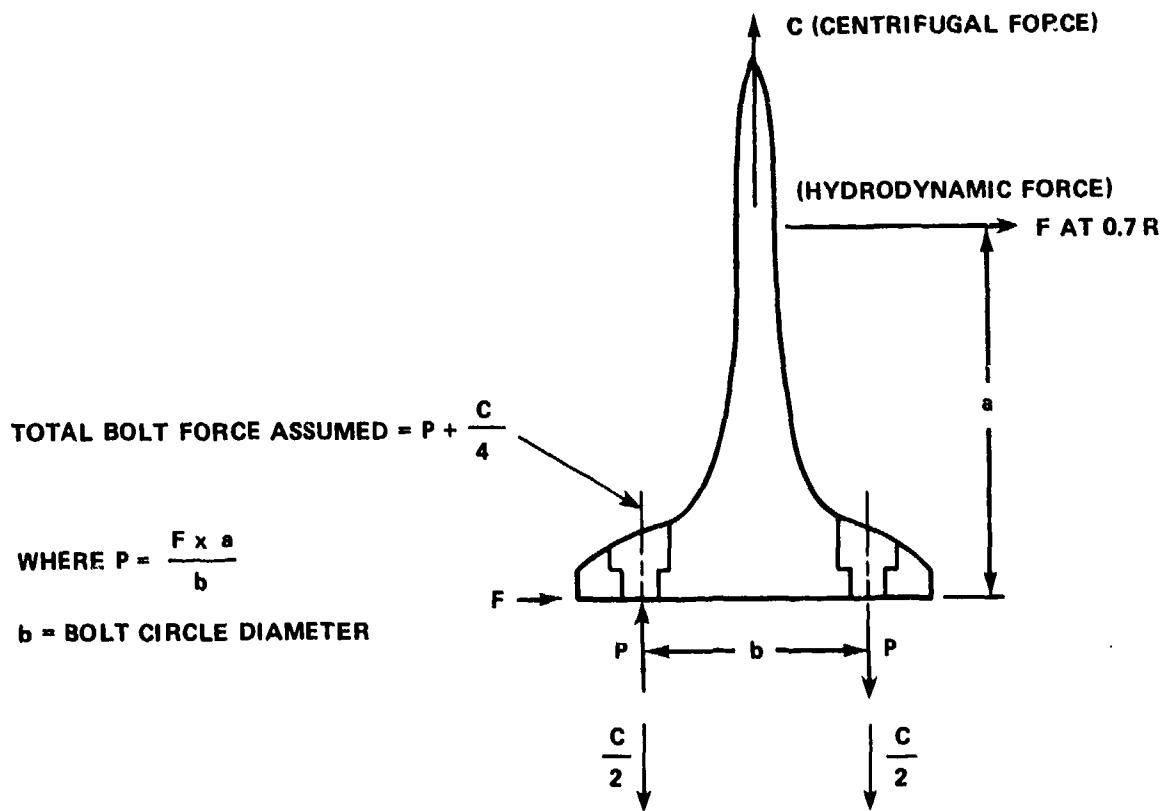

Figure B.1 - Assumptions for Comparison Method for Blade Bolts

moment due to the hydrodynamic force acting on the blade is assumed to be resisted by one bolt in tension on the pressure side of the blade. The bolt is also assumed to resist 25 percent of the centrifugal force. The applied forces and moments are balanced as indicated in Figure B.1.

The hydrodynamic force is assumed to act at the 70 percent radius and is calculated based on design shaft horsepower and rotational velocity. The centrifugal force is computed based on the mass of the blade and blade palm, the rotational velocity, and the location of the blade center of gravity.

The bending moment caused by the hydrodynamic force F is assumed to be equivalent to a couple, $F \times a$, where a is the distance between the crank ring face and the 70 percent radius. This couple, $F \times a$, is resisted by a similar couple, $P \times b$, where P is the resisting force in the bolt and b is the bolt circle diameter.

With the above assumptions, a total bolt force can be computed which is an indication of the maximum possible bolt force at the design horsepower level. Bolt stress associated with that force is then computed as force divided by shank area and compared with bolt prestress. Because the actual prestress obtained during assembly is generally only poorly known, the comparisons are based on the designer specified prestress, where it is available, or on a prestress equal to 40 percent of the yield stress of the bolt material which appears to be a typical design value. Comparisons of the ratios of bolt stress divided by bolt prestress based on the above method for more than 30 propellers show that if the ratio is greater than 1.0, potential bolt fatigue problems exist. It must be noted that this simple method should not be used as a design criterion because the ratio could be greater than 2.0 for a satisfactory design if there is a good distribution of bolt forces.

CLOSED FORM STRESS ANALYSIS METHODS FOR BLADE BOLTS

There are three strength criteria for use with the closed-form stress analysis methods for blade bolts. In equation form these are:

1. Maximum bolt shank stress — $S_{B,max} \leq 0.67 \times SY_B$ (1)

2. Maximum average stress under bolt head -- $S_{BH,max} \leq 0.9 \times SY_{BL}$ (2)

3. Maximum fatigue stress - $S_{EFF,max} \leq 0.4 \times S_{END}$ (3)

where SY_B, SY_{BL} = 0.2 percent offset yield stress of bolt and blade materials, respectively

S_{END} = 0.4 × ultimate tensile strength of material

The <u>maximum bolt shank stress</u>, $S_{B,max}$, for Equation (1) is calculated as follows:

$$S_{B,max} = S_{prestress} \times \left[1.0 + 2.0 \times 0.2 \times \left(\frac{F_{bolt,max}}{F_{preload}}\right)^{1.6}\right] \quad (4)$$

where $S_{prestress}$ = Average bolt prestress

$$F_{bolt,max} = \frac{C_{max}}{4} + \left[M_{max} + \frac{(Y_{max} + r_{bolt})}{\sum\limits_{all\ i} y_i^2}\right] \quad (5)$$

C_{max}, M_{max} = The maximum combination of centrifugal force and peak hydrodynamic bending moment (mean plus alternating) which the propeller will encounter. Usually, these occur during full-rudder, full-power turns, but the effect of rough seas during other operations should be considered.

0.2 and 1.6 = Constants describing curve shown in Figure B.2

2.0 = Constant accounting for bolt bending due to applied loads

y_{max} = Maximum distance of any bolt on the pressure side of the blade from the bolt center to the assumed neutral bending axis.

y_i = Distance from the center of bolt i to the neutral bending axis assumed to intersect blade palm at its center

r_{bolt} = Bolt radius

$F_{preload}$ = Bolt preload

The <u>maximum average stress under the bolt head</u>, $S_{BH,max}$, for Equation (2) is calculated as follows:

$$S_{BH,max} = \frac{F_{bolt,max}}{A_{contact}} \quad (6)$$

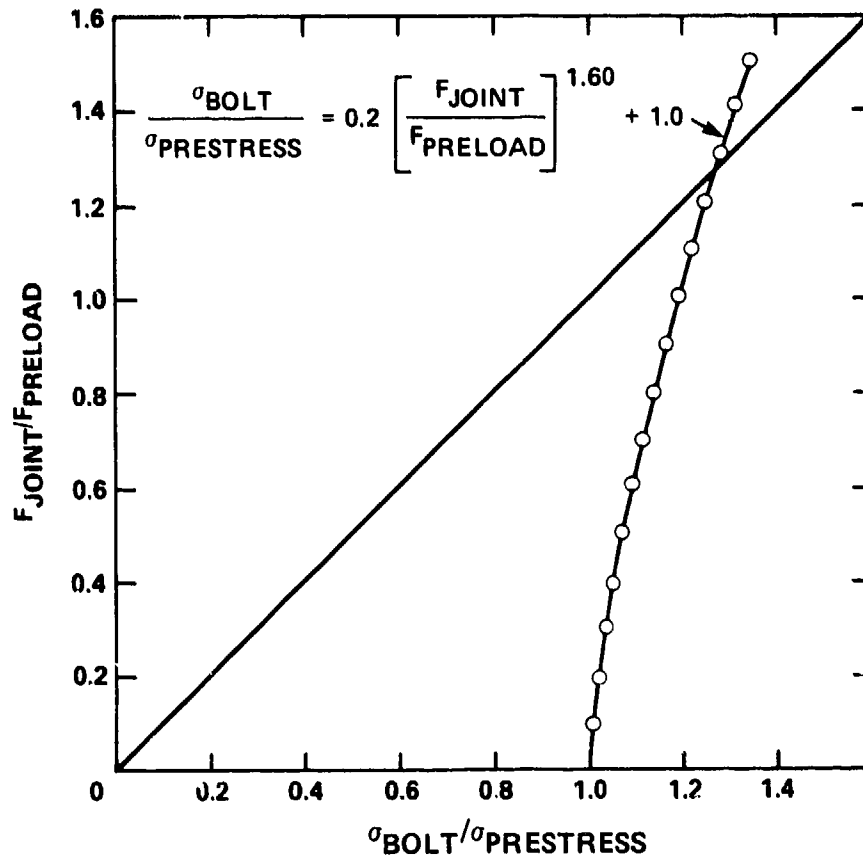where $A_{contact}$ = Area under the bolt head in contact with blade palm

467

Figure B.2 — Relationship between Joint Force and Average Tension Bolt Stress

The maximum fatigue stress, $S_{EFF,max}$, for Equation (3) is calculated as follows:

$S_{EFF,max}$ = Maximum effective, fully-reversed alternating stress for full-rudder, full-power turn loading, corrected for effect of mean stress

for bolts with SU_B < 100,000 psi

$$S_{EFF}* = \frac{k \times S_{B,alt}}{1 - \frac{(SY_B - k \times S_{B,alt})}{SU_B}} \tag{7}$$

for bolts with $SU_B \geq 100,000$ psi

$$S_{EFF}** = \frac{7 \times k \times S_{B,alt}}{8 - \left[1 + \frac{(SY_B - k \times S_{B,alt})}{SU_B}\right]^3} \tag{8}$$

where k = Fatigue notch factor equals 4 for cut threads or 3 for rolled threads

$$S_{B,alt} = S_{prestress} \times 2.0 \times 0.2 \times \left[\left(\frac{F_{B,max}}{F_{preload}}\right)^{1.6} - \left(\frac{F_{B,min}}{F_{preload}}\right)^{1.6}\right] \tag{9}$$

$$F_{B,max} = \frac{C_{FPT}}{4} + \left[M_{FPT,max} \times \frac{(y_{max} + r_{bolt})}{\sum\limits_{all\ i} y_i^2}\right] \tag{10}$$

$$F_{B,min} = \frac{C_{FPT}}{4} + \left[M_{FPT,min} \times \frac{(y_{max} + r_{bolt})}{\sum\limits_{all\ i} y_i^2}\right] \tag{11}$$

$M_{FPT,min}$ = Difference of mean minus alternating bending moment in full-rudder full-power turn due to hydrodynamic blade loads

---

*Modified Goodman mean stress correction.

**Peterson mean stress correction.

$M_{FPT,max}$ = Sum of mean plus alternating bending moment in full-rudder, full-power turn due to hydrodynamic blade loads

C_{FPT} = Centrifugal force of blade, blade palm and bolts in full-power, full-rudder turn

SU_B = Ultimate tensile strength of bolt

CLOSED FORM STRESS ANALYSIS METHODS FOR BLADE CARRIER

There are two strength criteria for use with the closed form stress analysis methods for the crank ring or trunnion type of blade carrier. In equation form, these are:

1. Maximum stress –
$$S_{BC,max} \leq 0.5 \times SY_{BC} \tag{12}$$

2. Maximum fatigue stress – $S_{EFF,max} \leq 0.4 \times S_{END}$ (13)

where SY_{BC} = 0.2 percent offset yield stress of crank ring or trunnion material

S_{END} = 0.4 × ultimate tensile strength of crank ring or trunnion material

$S_{BC,max}$ = Maximum stress in the crank ring or trunnion as computed with Equation (14) or (26)

$S_{EFF,max}$ = Maximum effective, fully-reversed alternating stress for full-power, full-rudder turn loading, corrected for effect of mean stress, as computed with Equation (27).

The maximum stress for a crank ring, $S_{BC,max}$, for Equation (12) is calculated as follows:

$$S_{BC,max} = k_{BC} \times \left(S_{9,pc} + S_{9,pm} \times \frac{S_{13}}{S_{15}} \right) \tag{14}$$

where $S_{9,pc}$ and $S_{9,pm}$ = Nominal stress in crank ring fillet from Equation (15) for pressures, P_c and P_m, in Figure B.3 at the maximum loading as defined for Equation (5). See Reference 38, Table 24, case 21.

S_{13}, S_{15} = Stresses from Equations (16) and (17) at the maximum loading as defined for Equation (5). See Reference 38, Table 24, cases 20 and 11.

k_{BC} = Stress concentration factor in crank ring fillet from Peterson[39] for example.
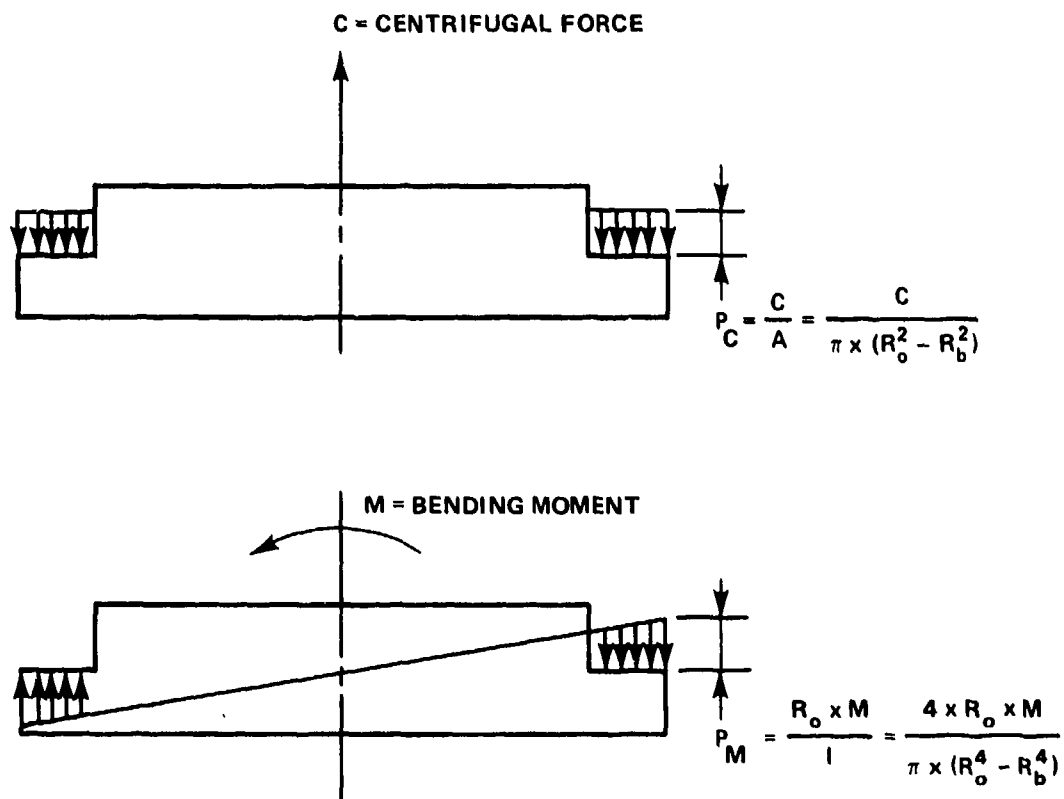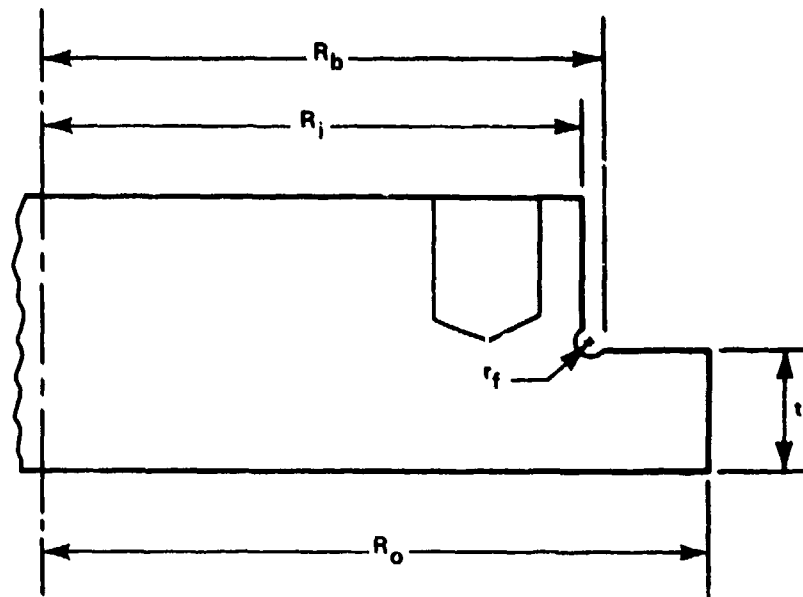
470

Figure B.3 – Crank Ring Dimensions and Terminology

$$S_9 = \frac{6 \times P \times R_o^2}{t^2 \times C_8} \times \left[\frac{C_9}{2 \times R_o \times R_i} \times (R_o^2 - R_b^2) - L_{17} \right] \qquad (15)$$

$$S_{13} = \frac{B \times M_{max}}{(R_o \times t^2)} \qquad (16)$$

$$S_{15} = \frac{A \times R_o \times M_{max}}{I} \times \frac{3}{\pi \times t^2} \times \frac{R_o}{R_i} \times \frac{C_9}{C_8} \qquad (17)$$

where, P = $\dfrac{C_{max}}{A}$ = uniform pressure

C_{max} = Applied centrifugal force at maximum loading (same as for Equation (5))

A = Area of bearing surface = $\pi \times (R_o^2 - R_b^2)$

t = Flange thickness, Figure B.3

R_i = Radius of thick portion of crank ring, Figure B.3

R_o = Outer radius of flange of crank ring, Figure B.3

R_b = Inner radius of bearing surface under pressure, Figure B.3

$$C_8 = \frac{1}{2} \times \left[1 + \nu + (1-\nu) \times \left(\frac{R_i}{R_o} \right)^2 \right] \qquad (18)$$

$$C_9 = \left(\frac{R_i}{R_o} \right) \times \left\{ \frac{1+\nu}{2} \times \ln \frac{R_o}{R_i} + \frac{1-\nu}{4} \times \left[1 - \left(\frac{R_i}{R_o} \right)^2 \right] \right\} \qquad (19)$$

$$L_{17} = \left(\frac{1}{4} \right) \times \left\{ 1 - \frac{1-\nu}{4} \times \left[1 - \left(\frac{R_b}{R_o} \right)^4 \right] - \left(\frac{R_b}{R_o} \right)^2 \times \left[1 + (1+\nu) \times \ln \left(\frac{R_o}{R_b} \right) \right] \right\} \qquad (20)$$

ν = Poisson's Ratio

$$B = 2.9375\, g^2 - 7.315 + 4.412125 \qquad (21)$$

$$g = \frac{R_i}{R_o} \qquad (22)$$

M_{max} = Applied bending moment at maximum loading (same as for Equation (5))

$$I = \frac{\pi}{4} \times (R_o^4 - R_b^4) \tag{23}$$

Use of Equations (15), (16), and (17) to predict crank ring fillet stresses should be limited to geometries in which the minimum distance between the bolt threads and fillet is large enough to keep the effect of bolt thread loading on fillet stress to an insignificant level. A crude method for estimating this limiting distance was established empirically in Chapter V of this report. In equation form,

$$(t_{wall})_{limit} \geq 6.0 \times 10^{-3} \times \text{bolt force} \tag{24}$$

where $(t_{wall})_{limit}$ = limiting distance between bolt threads and fillet

$$\text{bolt force} = F \times \frac{a}{b} + \frac{C}{4} \quad \text{(See Figure B.1)} \tag{25}$$

F = Hydrodynamic force at design condition

a = Distance between blade palm at crank ring bolting face and 70 percent blade radius

b = Blade bolt circle diameter

C = Centrifugal force at design condition

The maximum stress for a trunnion, $S_{BC,max}$, for Equation (12) is calculated as follows:

$$S_{BC,max} = k_{bc} \times \left[\left(\frac{C_{max}}{A} \right) + \left(\frac{M_{max}}{Z} \right) \right], \quad \begin{array}{l} \text{for a trunnion at the cross section} \\ \text{giving the highest stress} \end{array} \tag{26}$$

where k_{bc} = Stress concentration factor in trunnion fillet from Peterson,[39] for example

C_{max} and M_{max} as defined in Equation (5)

A = Area of cross section

Z = Section modulus of cross section

473

The maximum effective, fully-reversed alternating stress for either the crank ring or the trunnion for Equation (13), $S_{EFF,max}$, is found with the modified Goodman mean stress correction as follows:

$$S_{EFF,max} = \frac{S_{BC,alt}}{1 - \dfrac{S_{BC,mean}}{SU_{BC}}} \tag{27}$$

where $S_{BC,alt}$ is obtained using Equations (14) or (26) with the alternating bending moment for full-power turn loading

SU_{BC} = Ultimate tensile strength of the crank ring or trunnion material

$S_{BC,mean}$ is obtained using Equations (14) or (26) with the mean bending moment for full-power turn loading

REFERENCES

1. Martin, D. L., "Numerical Methods for Investigating Stresses in Controllable Pitch Propeller Blade Attachments," DTNSRDC Report 80/085 (Aug 1980).

2. Garala, H., "One-Third Scale Model Structural Evaluation of the USS SPRUANCE (DD-963) Controllable Pitch Propeller Blade Attachments," DTNSRDC Report 80/099 (Sep 1980).

3. Phyillaier, W. and R. Rockwell, "Fatigue Behavior of Blade Attachment Bolts of Different Materials for High-Horsepower Controllable Pitch Propellers," DTNSRDC Report 80/043 (Jun 1980).

4. Snow, A. L. and B. F. Langer, "Low Cycle Fatigue in Large Diameter Bolts," Journal of Engineering for Industry (Feb 1967).

5. "ASME Boiler and Pressure Vessel Code, Section III, Nuclear Power Plant Components," 1974 Edition.

6. Rockwell, R. and S. Hersh, "DD 963, FFG 7 and CG 47 Class Propellers - Strength of Blade Bolts and Crank Rings and Overview of Investigations," DTNSRDC Report 80/068 (Jun 1980).

7. Noonan, C. et al., "The BARBEY REPORT, An Investigation into Controllable Pitch Propeller Failures from the Standpoint of Full-Scale, Underway Propeller Measurements," DTNSRDC Report 77-0080 (Aug 1977).

8. Rockwell, R. and S. Hersh, "Full-Scale Structural Evaluation of the USS OLIVER HAZARD PERRY (FFG 7) Controllable Pitch Propeller Blade Attachment, Phase 1--Application of FFG 7 Blade Forces to the USS SPRUANCE (DD 963) Propeller," DTNSRDC Report 80/066 (Jun 1980).

9. Gorman, R. W., "Full-Scale Verification of Reduced Stresses in the Blade Attachment of the USS SPRUANCE (DD-963) and TICONDEROGA (CG-47) Controllable Pitch Propellers through Modification of the Blade Fillet and Coverplate," DTNSRDC Report 80/081 (Nov 1980).

10. Jessup, S. D. et al., "Experimental Unsteady and Time Average Loads on the Blades of the CP Propeller on a Model of the DD-963 Class Destroyer for Simulated Modes of Operation," DTNSRDC Report 77-0110 (Dec 1977).

475

11. Schwanecke, H. and R. Wereldsma, "Strength of Propellers Considering Steady and Unsteady Shaft and Blade Forces, Stationary and Nonstationary Environmental Conditions," Proceedings of the Thirteenth International Towing Tank Conference, Report of the Propeller Committee, Appendix 2B, Vol. 2 (1972).

12. Kerwin, J. E., "The Effect of Trailing Vortex Asymmetry on Unsteady Propeller Blade Forces," Massachusetts Institute of Technology Report on Contract N0014-77-C-0810, MIT OSP 85871 (May 1979).

13. Kerwin, J. E. and C. S. Lee, "Prediction of Steady and Unsteady Marine Propeller Performance by Numerical Lifting Surface Theory," Transactions of the Society of Naval Architects and Marine Engineers, Vol. 86, pp. 218-253 (1978).

14. Rubis, C. J., "Acceleration and Steady State Propulsion Dynamics of a Gas Turbine Ship with Controllable-Pitch Propeller," Transactions of the Society of Naval Architects and Marine Engineers, Vol. 80, pp. 329-360 (1972).

15. Rubis, C. J., "CRP Propeller Ship-Propulsion Dynamics," DTNSRDC Report 3238 (Feb 1971).

16. Rubis, C. J. and T. R. Harper, "Propulsion Dynamics Simulation of the DD-963 Class Destroyer," Propulsion Dynamics, Inc. Report 74RDIB (Jan 1975).

17. Rubis, C. J. and T. R. Harper, "Gas Turbine Ship Propulsion Control Systems Research, Phase I," Propulsion Dynamics, Inc. Report 443-1, Vol. II - Propulsion and Control System Dynamics (Oct 1977).

18. Rubis, C. J. and T. R. Harper, "Reversing Dynamics of a Gas Turbine Ship with Controllable-Pitch Propeller," Proceedings of the Fifth Ship Control Systems Symposium, Sponsored by DTNSRDC, Annapolis, Md (Oct-Nov 1978).

19. Abkowitz, M. A., "Stability and Motion Control of Ocean Vehicles," The MIT Press (1972).

20. "A Digital Computer Technique for Prediction of Standard Maneuvers of Surface Ships," DTMB Report 2130 (Dec 1965).

21. Carroll, L. C. and T. R. Harper, "DD-963 Class Destroyer Four Degree-of-Freedom Maneuvering Simulation," Propulsion Dynamics, Inc. Report 4443-3 (Jul 1979).

22. Boswell, R. J. et al., "Mean and Unsteady Loads on a CP Propeller Blade on a Model of the FF-1088 for Simulated Modes of Operation (U)," DTNSRDC Report SPD-C-011-17 (Jun 1976) CONFIDENTIAL.

23. Tsakonas, S. et al., "Documentation of a Computer Program for the Pressure Distribution, Forces and Moments on Ship Propellers in Hull Wakes," (In Four Volumes), Stevens Institute of Technology, Davidson Laboratory Report SIT-DL-76-1863 (Jan 1976) revised (Apr 1977).

24. Remmers, D. D. and A. L. Hendrican, "Analyses of Wake Surveys in the Port Propeller Plane During Starboard and Port Turns for the DDG-47 Class Destroyer Represented by Model 5265-1B (U)," DTNSRDC Report SPD-C-558-05 (Jun 1976) CONFIDENTIAL.

25. Boswell, R. J. et al., "Experimental Determination of Mean and Unsteady Loads on a Model CP Propeller Blade for Various Simulated Modes of Ship Operation," The Eleventh Symposium on Naval Hydrodynamics, Sponsored Jointly by the Office of Naval Research and University College, London, Mechanical Engineering Publication Limited, London and New York, pp. 789-823, 832-834 (Apr 1976).

26. Boswell, R. J. et al., "Experimental Unsteady and Mean Loads on a CP Propeller Blade of the FF-1088 for Simulated Modes of Operation," DTNSRDC Report 76-0125 (Oct 1976).

27. Boswell, R. J. et al., "Experimental Time Average and Unsteady Loads on the Blades of a CP Propeller Behind a Model of the DD-963 Class Destroyer," Propellers '78 Symposium, The Society of Naval Architects and Marine Engineers Publication S-6, pp. 7-1 through 7-22 (May 1978).

28. Boswell, R. J. et al., "Experimental Unsteady and Time-Average Loads on the Blades of the CP Propeller on a Model of the R/V ATHENA (PG 84 Class) for Simulated Modes of Operation," DTNSRDC Report 81/086 (Nov 1981).

29. Jessup, S. D. and R. J. Boswell, "Experimental Unsteady and Time-Average Loads on the Blades of DTNSRDC Propellers 4402 and 4661 Operating in Simulated Tangential Longitudinal Wakes," DTNSRDC Report 81/085 (Nov 1981).

30. Boswell, R. J. et al., "Periodic Single-Blade Loads on Propellers in Tangential and Longitudinal Wakes," DTNSRDC Report 81/054 (Jun 1981); also, Propellers '81 Symposium, the Society of Naval Architects and Marine Engineers Publication S-7, pp. 181-202 (May 1981).

31. Tasaki, R., "Propulsion Factors and Fluctuating Propeller Loads in Waves," Proceedings of the Fourteenth International Towing Tank Conference, Report of Seakeeping Committee, Appendix 7, Vol. 4, pp. 224-236 (1975).

32. Oosterveld, M. W. C. (Editor), "Report of the Seakeeping Committee," Fifteenth International Towing Tank Conference, The Netherlands Ship Model Basin, Wageningen, The Netherlands pp. 55-114 (1978).

33. Day, W. G. et al., "Experimental and Prediction Techniques for Estimating Added Power Requirements in a Seaway," Proceedings of the Eighteenth American Towing Tank Conference, U.S. Naval Academy, Annapolis, MD, Vol, I, pp. 121-141 (1977).

34. Lloyd, A. R. J. M. and R. N. Andrew, "Criteria of Ship Speed in Rough Weather," Proceedings of the Eighteenth American Towing Tank Conference, U.S. Naval Academy, Annapolis, MD, Vol. II, pp. 541-565 (1977).

35. McCarthy, J. H. et al., "The Performance of a Fully Submerged Propeller in Regular Waves," DTMB Report 1440 (May 1961).

36. Lewis, E. V., "Motion of Ships in Waves," Chapter IX, Principles of Naval Architecture, Edited by J. P. Comstock, The Society of Naval Architects and Marine Engineers, pp. 607-717 (1967).

37. McCarthy, J. H., "On the Calculation of Thrust and Torque Fluctuations of Propellers in Nonuniform Wake Flow," DTMB Report 1533 (Oct 1961).

38. Roark, R. J. and W. C. Young, "Formulas for Stress and Strain," McGraw Hill Book Company (1975).

39. Peterson, R. E., "Stress Concentration Factors," John Wiley and Sons, Inc. (1974).

ACKNOWLEDGMENTS

INITIAL DISTRIBUTION

Copies		Copies	
1	NAVMAT/08T23	1	NAVSHIPYD PHILA
1	NRL/2627 (Library)	1	NAVSHIPYD PTSMH
1	USNA	2	SUPSHIP BATH
1	NAVPGSCOL (Library)	2	SUPSHIP PASCAGOULA
1	USNROTC & NAVADMINU, MIT	2	DTIC
1	NSWC (White Oak)	1	U.S. COAST GUARD/G-ENE-4/64
1	NOSC (Library)		

CENTER DISTRIBUTION

Copies	NAVSEA			Copies	Code	Name
35	NAVSEA					
	1	SEA 03D3				
	1	SEA 3213		1	11	
	1	SEA 05B				
	1	SEA 05E2		1	15	
	1	SEA 05H				
	1	SEA 05R		1	1506	A.M. Reed
	1	SEA 05R15		1	152	
	1	SEA 52				
	1	SEA 52B		1	1521	W.G. Day
	1	SEA 52G		1	1528	K. Remmers
	1	SEA 52P				
	1	SEA 521		1	154	
	3	SEA 524		1	1544	
	1	SEA 5241 (J. Allan)		2	1544	R.J. Boswell
	1	SEA 92		1	1544	S.D. Jessup
	1	SEA 93				
	1	PMS 307		1	17	
	5	PMS 389		1	1706s	(m)
	1	PMS 392				
	5	PMS 399		1	172	
	5	PMS 400		5	1720.6	R.D. Rockwell
1	NAVSHIPYD BREM			1	173	
1	NAVSHIPYD CHASN			1	177	
				1	177.7	(m)
1	NAVSHIPYD LBEACH			1	19	
1	NAVSHIPYD MARE			1	1962	
				2	1962	C.J. Noonan
1	NAVSHIPYD NORVA					
1	NAVSHIPYD PERL			1	27	
				1	272	

481

Copies	Code	Name
1	28	
1	281	
1	2814	
2	2814	E.J. Czyryca
1	2832	
1	2832	S.A. Karpe
10	5211.1	Reports Distribution
1	522.1	Unclassified Lib (C)
1	522.2	Unclassified Lib (A)

DTNSRDC ISSUES THREE TYPES OF REPORTS

1. DTNSRDC REPORTS, A FORMAL SERIES, CONTAIN INFORMATION OF PERMANENT TECH-
NICAL VALUE. THEY CARRY A CONSECUTIVE NUMERICAL IDENTIFICATION REGARDLESS OF
THEIR CLASSIFICATION OR THE ORIGINATING DEPARTMENT.

2. DEPARTMENTAL REPORTS A SEMIFORMAL SERIES, CONTAIN INFORMATION OF A PRELIM-
INARY, TEMPORARY, OR PROP. ETARY NATURE OR OF LIMITED INTEREST OR SIGNIFICANCE.
THEY CARRY A DEPARTMENTAL ALPHANUMERICAL IDENTIFICATION.

3. TECHNICAL MEMORANDA, AN INFORMAL SERIES, CONTAIN TECHNICAL DOCUMENTATION
OF LIMITED USE AND INTEREST. THEY ARE PRIMARILY WORKING PAPERS INTENDED FOR IN-
TERNAL USE. THEY CARRY AN IDENTIFYING NUMBER WHICH INDICATES THEIR TYPE AND THE
NUMERICAL CODE OF THE ORIGINATING DEPARTMENT. ANY DISTRIBUTION OUTSIDE DTNSRDC
MUST BE APPROVED BY THE HEAD OF THE ORIGINATING DEPARTMENT ON A CASE-BY-CASE
BASIS.

DEPARTMENT OF THE NAVY
NAVAL SURFACE WARFARE CENTER
CARDEROCK DIVISION

CARDEROCK DIVISION HEADQUARTERS
DAVID TAYLOR MODEL BASIN
9500 MACARTHUR BOULEVARD
WEST BETHESDA, MD 20817-5700

Errata

IN REPLY REFER TO:
5605
506 Ser 94
1 9 NOV 1998

From: Commander, Carderock Division, Naval Surface Warfare Center
To: Distribution

Subj: CHANGE IN DISTRIBUTION STATEMENT

1.   DTNSRDC-81/065 Report entitled, " Summary Report of the Control and Pitch Propeller Research Program," has been approved for public release.

2.   Please change the distribution on you copy of the report to read as follows:

Approved for Public Release;
Distribution Unlimited

Wm. B. MORGAN
By Direction

Distribution:
DTIC
NRL/2627 (Library)
USNA
NAVPGSCOL (Library)
NAVSEA
03H
03R
92
93
PMS 307
PMS 389
PMS 392
PMS 399
PMS 400
NAVSHIPYD BREM
NAVSHIPYD NORVA
NAVSHIPYD PERL
NAVSHIPYD PTSMH
SUPSHIP BATH
SUPSHIP PASCAGOULA
U.S. COAST GUARD/G-ENE-4/64

Completed
15 may 2000